

**Evaluating phosphorus incorporation into belemnite calcite as  
an environmental proxy**

Ailsa Connon Roper



**UNIVERSITY OF LEEDS**

Submitted in accordance with the requirements for the degree of Doctor of Philosophy

The University of Leeds

School of Earth and Environment

Earth Surface Science Institute

**September 2023**

I confirm that the work submitted is my own and that appropriate credit has been given where reference has been made to the work of others.

This copy has been supplied on the understanding that it is copyright material and that no quotation from the thesis may be published without proper acknowledgement.

The right of Ailsa Connon Roper to be identified as author of this work has been asserted by Ailsa Connon Roper in accordance with the Copyright, Designs and Patents Act 1988.

## Acknowledgements

There are many people who deserve thanks for their help and support, without whose backing this project wouldn't have been possible.

I would like to thank North York Moors National Park (NYMNP) and Anglo American for the funding which allowed this project to go ahead. I am also grateful to my amazing supervision team: Robert Newton, Crispin Little, Paul Wignall, Simon Poulton and Clemens Ullmann for their advice, expertise, and guidance throughout. I would also like to thank everyone who has helped me to acquire the samples, including Briony Fox at NYMNP and David Warburton, Phil Johnson and Asher Haynes at Anglo American, as well as Ivan Savov and Lubo Metodiev for all their help with the Bulgarian material. A very special thanks also to the amazing technical staff at the University of Leeds, and everyone who has helped with my lab work including Harri Wyn Williams, Andy Hobson, Stephen Reid, Lesley Neve, Robert Jamieson, Gary Keech, Tianchen He and Yijun Xiong. And to Ben Mills for his help with coding and biogeochemical modelling.

I would like to thank my incredible family and friends for their unwavering belief and patience over the last four years, with special thanks to my mum (for the cakes) and dad (for the many cups of tea and 'helpful' suggestions). Finally, I would like to give a huge thank you to Marc, for being the best sounding board and my biggest supporter throughout this journey, and to Frankie, for never failing to make me smile.

## Abstract

Phosphorus is the ultimate limiting nutrient for marine primary productivity over geological timescales and plays a key role in modulating several geochemical cycles. Established methods for investigating phosphorus do not provide direct evidence of water-column phosphorus cycling, but recent work on carbonate associated phosphorus has shown potential to record dissolved phosphorus concentrations. This project developed a method to extend the application of carbonate associated phosphorus measurements to belemnites and quantify the variability of phosphorus and other elements within and between belemnites. This technique was applied to samples from across the Early Jurassic, in particular the Pliensbachian and Toarcian. Samples analysed were from three locations in the Laurasian Seaway, the Moesian Basin (Bulgaria), the Cleveland Basin (Yorkshire, UK) and the Cardigan Bay Basin (North Wales, UK).

Carbonate associated phosphorus was found to vary coherently through time, with similarities between the records generated for each study location. When carbonate associated phosphorus records were compared to different established geochemical proxies, different regional controls on P/Ca values were identified including redox conditions and temperature. This suggests that carbonate associated phosphorus can record water column phosphorus concentrations, but the controls on dissolved phosphorus concentrations are complex. Correlation between P/Ca and Mg/Ca was also identified, which was unrelated to temperature variations, and suggested potential mineralogical control on phosphorus incorporation. Na/Ca records were also investigated and were found to show clear stratigraphic variation. Na/Ca changes were shown to be unrelated to temperature or salinity changes, but also showed evidence of mineralogical control on sodium incorporation.

This work indicates that belemnites may be a promising record of carbonate associated phosphorus, but also emphasises the importance of holistic analysis of belemnite calcite in the interpretation of geochemical proxies.

# Table of Contents

<b>1. Project Rationale and overview</b>	<b>1</b>
1.1. Importance of phosphorus	1
1.2. The ocean phosphorus cycle	1
1.3. Methods of investigating phosphorus	4
1.4. Phosphorus in belemnites	6
1.5. Early Jurassic	8
1.6. Sodium and other elements in belemnites	11
1.7. Thesis Aims	12
1.8. Other work	12
<b>2. Phosphorus extraction and quantification</b>	<b>14</b>
2.1. Introduction	14
2.2. Experimental Design	16
2.3. Materials	21
2.3.1. Bulk samples	21
2.3.2. Sample variability	22
2.3.3. Modern analogue samples	24
2.3.4. Standards	24
2.4. Methods	25
2.4.1. Weighing and Cleaning	25
2.4.2. Acidification	26
2.4.3. Analysis	27
2.4.4. Iodine analysis	28
2.4.5. Statistical tests	29
2.4.6. Diagenetic screening protocol	29
2.5. Results	30
2.5.1. Impact of calcium concentrations	30
2.5.2. Impact of cleaning method	32
2.5.3. Impact of dissolution method	39
2.5.4. Impact of sample size	41
2.5.5. Investigating variability	41
2.6. Discussion	47

2.6.1.	Impact of cleaning method	47
2.6.2.	Impact of dissolution method	54
2.6.3.	Impact of sample mass	56
2.6.4.	Implications for other CAP studies	56
2.6.5.	Variability	58
2.7.	Conclusion	61
<b>3.</b>	<b>Extraction and quantification of other elements</b>	<b>63</b>
3.1.	Introduction	63
3.2.	Materials and methods	67
3.2.1.	Carbon and oxygen isotope analysis	68
3.3.	Results	68
3.3.1.	Elemental ratios with analytical issues	69
3.3.2.	Impact of cleaning method	73
3.3.3.	Impact of dissolution method	78
3.3.4.	Impact of sample size	82
3.3.5.	Investigating variability	82
3.4.	Discussion	90
3.4.1.	Impact of a cleaning method	90
3.4.2.	Impact of dissolution method	92
3.4.3.	Impact of sample size	94
3.4.4.	Variability	94
3.4.5.	Effect of P/Ca protocol	100
3.5.	Conclusion	101
<b>4.</b>	<b>Early Jurassic P/Ca records in a stratigraphic context</b>	<b>103</b>
4.1.	Introduction	103
4.2.	Materials	107
4.2.1.	North Wales	108
4.2.2.	North Yorkshire	110
4.2.3.	Bulgaria	115
4.3.	Methods	119
4.3.1.	Sampling	119

4.3.2.	Carbonate analyses	120
4.3.3.	Sediment analyses	121
4.4.	Results	123
4.4.1.	Screening	123
4.4.2.	Carbonate-associated phosphorus ratios	125
4.4.3.	CAP variation with redox	129
4.4.4.	CAP variation with temperature	134
4.4.5.	CAP variation with magnesium	138
4.5.	Discussion	146
4.5.1.	Impact of diagenesis	146
4.5.2.	CAP records	146
4.5.3.	Redox	147
4.5.4.	Temperature	148
4.5.5.	Magnesium	154
4.6.	Conclusions	161
	<b>5. Na/Ca records in a stratigraphic context</b>	<b>164</b>
5.1.	Introduction	164
5.2.	Materials and methods	165
5.3.	Results	165
5.3.1.	Screening for Diagenesis	165
5.3.2.	Sodium in belemnites through time	169
5.3.3.	Sodium and temperature	172
5.3.4.	Observations from El/Na ratios	174
5.4.	Discussion	178
5.4.1.	Factors affecting Na concentrations	178
5.4.2.	Ratio to sodium	194
5.4.3.	What information might Na values contain?	196
5.5.	Conclusions	200
	<b>6. Conclusions and further work</b>	<b>202</b>
6.1.	Impacts of preparative methods	202
6.2.	Natural variability of elements	203

6.3.	Stratigraphic variation of El/Ca and relationships between elements	204
<b>7.</b>	<b>References</b>	<b>207</b>
<b>8.</b>	<b>Appendix</b>	<b>241</b>
8.1.	Bulk Samples analysis	241
8.2.	Variability Samples analysis	249
8.3.	Modern Analogue Samples analysis	267
8.4.	Stratigraphic Samples	270
8.5.	XRD analysis	296
8.6.	Sediment analysis	298

## List of figures

Figure 1 - Illustration of the phosphorus cycle	2
Figure 2 - CAP in various carbonates	5
Figure 3 - Labelled diagram of a belemnite	6
Figure 4 - Schematic for method development tests	17
Figure 5 - Schematic for variability tests	19
Figure 6 - Schematic for modern analogue tests	20
Figure 7 - Ratios of P to mass for Bulk 1, 2 and 3 samples	31
Figure 8 - Ratios of Ca to mass for Bulk 1, 2 and 3 samples	32
Figure 9 - Mean P/Ca values for preparative methods tested on Bulk samples	33
Figure 10 - P/Ca ratios for Variability Samples cleaned with water and hydrogen peroxide	34
Figure 11 - P/Ca values for samples of cuttlefish cleaned with hydrogen peroxide or water	35
Figure 12 - CVs for P/Ca from Bulk Samples for different preparative methods	37
Figure 13 - Fe/Ca values against Mn/Ca values for all Variability Sample analyses	42
Figure 14 - P/Ca against the distance along the belemnite rostrum from the apex	44
Figure 15 - P/Ca values for Variability Samples showing differences between individuals, species and levels	44
Figure 16 - P/Ca values for aragonite samples from cuttlebones cleaned with water	46
Figure 17 - P/Ca values for samples from <i>S. spirula</i> shells cleaned with water	47
Figure 18 - Plot of El/Ca against the distance along the belemnite rostrum from the apex	84
Figure 19 - El/Ca values for the Variability Samples showing differences between individuals, species and levels	87
Figure 20 - Seawater palaeotemperatures for the Early Jurassic	104
Figure 21 - Palaeogeographic map of the Western Tethys and Laurasian Seaway	108
Figure 22 - Llanbedr borehole log with carbon isotopes, temperature and redox summary	109
Figure 23 - Correlation and sample distribution for Dove's Nest Core and Yorkshire Coast	111
Figure 24 - Log of the Dove's Nest borehole with carbon isotope record	113
Figure 25 - Map of the modern locations of Yorkshire sections	114
Figure 26 - Map of modern locations Bulgarian sections	116
Figure 27 - Correlation between Dove's Nest Core and Yorkshire Coast including sample distribution, lithology, OAE occurrences and carbon and oxygen isotope curves	118
Figure 28 - Plot of Fe/Ca and Mn/Ca for samples from all sites	124
Figure 29 - Stratigraphic P/Ca record for each study location	127
Figure 30 - Stratigraphic record of redox proxies compared to P/Ca record for Dove's Nest	130
Figure 31 - U/Al against $Fe_{HR}/Fe_{TOT}$ for sediment samples from Dove's Nest	132
Figure 32 - Mo/Al against $Fe_{Py}/Fe_{HR}$ for sediment samples from Dove's Nest	133

Figure 33 - $Fe_{HR}/Fe_{TOT}$ from sediment against P/Ca from belemnites from Dove's Nest	134
Figure 34 - $Fe_{PY}/Fe_{HR}$ from sediment against P/Ca from belemnites from Dove's Nest	134
Figure 35 - Stratigraphic P/Ca record alongside $\delta^{18}O$ values for each study location	135
Figure 36 - Crossplot of $\delta^{18}O$ against P/Ca values	137
Figure 37 - Stratigraphic P/Ca ratios alongside Mg/Ca values for each study location	139
Figure 38 - Cross-plot of P/Ca values against Mg/Ca values	140
Figure 39 - Cross-plot of $\delta^{18}O$ against Mg/Ca values	141
Figure 40 - Pie chart of the proportions of measured $2^+$ ions (Ca, Mg, Mn, Sr, Ba)	142
Figure 41 - Pie chart of the proportions of substituted ions (all measured ions except Ca)	142
Figure 42 - Diagram of a pure calcite unit cell	143
Figure 43 - Cross-plot of belemnite Mg/Ca values and unit cell parameter a in angstroms	144
Figure 44 - Cross-plot of belemnite Mg/Ca values and unit cell parameter c	144
Figure 45 - Cross-plot of belemnite Mg/Ca values and unit cell volume	145
Figure 46 - Cross-plot of belemnite Sr/Ca against Na/Ca values	168
Figure 47 - Stratigraphic Na/Ca record for each study location	170
Figure 48 - Cross-plot of belemnite $\delta^{18}O$ compared to Na/Ca	173
Figure 49 - Cross-plot of belemnite Mg/Ca against Na/Ca	174
Figure 50 - Cross-plot of belemnite Mg/Ca against Sr/Ca	175
Figure 51 - Cross-plot of belemnite Mg/Na against Sr/Na	175
Figure 52 - Cross-plot of belemnite Mg/Na against P/Na ratios	176
Figure 53 - Cross-plot of belemnite $\delta^{18}O$ against Mg/Na values	177
Figure 54 - Fe/Ca and Mn/Ca values for samples from this study and previous studies	183
Figure 55 - Fe/Ca and Na/Ca values for samples from this study and previous studies	184
Figure 56 - Mn/Ca and Na/Ca for samples from this study and previous studies	184
Figure 57 - Sr/Ca and Na/Ca values for samples from this study and previous studies	185
Figure 58 - Sr/Ca against Na/Ca for McArthur <i>et al.</i> (2007a)	187
Figure 59 - Fe/Ca against Mn/Ca for McArthur <i>et al.</i> (2007a)	188
Figure 60 - Na/Ca values for different VPI values for samples from Li <i>et al.</i> (2012)	189
Figure 61 - Sr/Ca values for different VPI values for samples from Li <i>et al.</i> (2012)	189
Figure 62 - Na/Ca against Sr/Ca for samples from Li <i>et al.</i> (2012), for VPI values	190
Figure 63 - Na/Ca against $\delta^{18}O$ values for samples from this study and previous studies	191
Figure 64 - Mg/Ca against $\delta^{18}O$ values for samples from this study and previous studies	192
Figure 65 - Mg/Ca against Na/Ca for samples from this study and previous studies	193
Figure 66 - Mg/Ca values for altered and unaltered samples from McArthur <i>et al.</i> (2007a)	194
Figure 67 - Mg/Na against Sr/Na values for samples from this study and previous studies	194
Figure 68 - Mg/Ca against Sr/Ca for samples from this study and previous studies	195



## List of Tables

Table 1 - Sample information (location, species, ammonite zone) for Variability Samples	23
Table 2 - Certified and informational values for JCP-1 standard reference material	25
Table 3 - LOD, LOQ and percentage uncertainties for ICP-MS analyses	28
Table 4 - LOD, LOQ and percentage uncertainties for ICP-OES analyses	28
Table 5 - Example LOD, LOQ and percentage uncertainties for ICP-MS analysis of iodine.	29
Table 6 - CV <sub>ind</sub> for P/Ca values two cuttlebones and one <i>S. spirula</i> shell	38
Table 7 - t-tests results for P/Ca values of Bulk Samples with different preparative methods	40
Table 8 - R <sup>2</sup> of Variability Samples for relationship between P/Ca and either Mn/Ca or Fe/Ca	42
Table 9 - Summary of differences in magnitude and variance of P/Ca ratios	48
Table 10 - Mean values and standard deviations for EMA Carrara Marble	68
Table 11 - t-test results for Mg/Ca and Sr/Ca between cleaning methods for two belemnites from the Variability Samples	74
Table 12 - t test results for Mg/Ca and Sr/Ca in Modern Analogue Samples	76
Table 13 - t test results for Mg/Ca and Sr/Ca and Na/Ca between Bulk Samples cleaned with different methods	77
Table 14 - t-test results demonstrating the differences in Mg/Ca and Sr/Ca between Bulk Samples dissolved in different acids	80
Table 15 - R <sup>2</sup> values for Fe/Ca and Mn/Ca and other El/Ca ratios for Variability Samples	82
Table 16 - R <sup>2</sup> values for distance from the apex and El/Ca ratios Variability Samples	85
Table 17 - CV <sub>M</sub> values indicating the variability of El/Ca values for Variability Samples	86
Table 18 - t-test results for differences in El/Ca ratios between Modern Analogue Samples	89
Table 19 - Summary of the differences in El/Ca ratios between different cleaning methods for different sample materials and dissolution methods	90
Table 20 - Summary of the differences in El/Ca ratios between different dissolution methods for different sample materials and cleaning methods	93
Table 21 - R <sup>2</sup> values for Fe/Ca and Mn/Ca; Fe/Ca and P/Ca and Mn/Ca and P/Ca for samples from different locations	124
Table 22 - Average, maximum and minimum and the standard deviation of measured values of unit cell parameters a and c and unit cell volume	145
Table 23 - Comparison between high measured P/Ca values in the Early Toarcian and predicted P/Ca based on the relationships between CAP and temperature/pH	152
Table 24 - Study summarising the locations, time periods and important palaeoenvironmental factors in a subset of previous studies which have compared Mg/Ca and $\delta^{18}\text{O}$	159
Table 25 - R <sup>2</sup> values for Fe/Ca and Mn/Ca; Fe/Ca and Na/Ca and Mn/Ca and Na/Ca for samples from different locations	167

Table 26 - R <sup>2</sup> values for the correlation between Mg and P as ratios to Na or to Ca in the different locations included in this study	176
Table 27 - Summary of samples and methodologies used by this study and some previous studied which measured Na concentrations in belemnite calcite	179
Table 28 - Summary of R <sup>2</sup> values for relationships between key elemental and isotopic ratios relating to sodium in each of the studies included in this chapter	199
Table 29 - Main elemental results for analysis of Bulk Samples	241
Table 30 - Supplemental elemental results for analysis of Bulk Samples	245
Table 31 - Main elemental and isotopic results for analysis of Variability Samples	249
Table 32 - Supplemental elemental results for analysis of Variability Samples	258
Table 33 - Elemental results for analysis of Modern Analogue Samples	267
Table 34 - Main elemental and isotopic results for analysis of stratigraphic samples from the Yorkshire Coast	270
Table 35 - Main elemental and isotopic results for analysis of stratigraphic samples from the Dove's Nest core	279
Table 36 - Main elemental and isotopic results for analysis of stratigraphic samples from the Llanbedr core in North Wales	285
Table 37 - Main elemental and isotopic results for analysis of stratigraphic samples from the Bulgarian outcrops	291
Table 38 - XRD results for samples from the Llanbedr Borehole, North Wales	296
Table 39 - Results of the total digest sediment analysis	298
Table 40 - Results of the iron-speciation sediment analysis	300

## List of Equations

Equation 1 - Calculation of CV values	36
Equation 2 - Calculating percentage distance along the rustrum	43
Equation 3 – Percentage difference of unit cell parameters compared to literature values	145

## Abbreviations

BGS	British Geological Survey
CAP	Carbonate-associated phosphorus
CV	Coefficient of variation
CV <sub>ind</sub>	Coefficient of variation within individual specimens
CV <sub>lvl</sub>	Coefficient of variation within stratigraphic levels
CV <sub>rep</sub>	Coefficient of variation within replicate samples
df	Degrees of freedom
El	Element
EMA	Elemental Microanalysis
ETME	Early Toarcian Mass Extinction
ETNCIE	Early Toarcian negative carbon isotope excursion
EXAFS	Extended X-ray Absorption Fine Structure
Fe <sub>Carb</sub>	Carbonate-associated iron
Fe <sub>HR</sub>	Highly reactive iron
Fe <sub>Mag</sub>	Magnetite
Fe <sub>Ox</sub>	Iron oxides
Fe <sub>Py</sub>	Iron pyrite
Fe <sub>TOT</sub>	Total iron
ICP-MS	Inductively coupled plasma mass spectrometry
ICP-OES	Inductively Coupled Plasma Optical Emission spectroscopy
LIP	Large igneous province
LOD	Limit of detection
LOQ	Limit of quantification
LPE	Late Pliensbachian Event
MBA	Marine Biological Association
mOD	Meters below ordinance datum (sea-level)
NIGPAS	Nanjing Institute of Geology and Palaeontology, Chinese Academy of Sciences
NMR	Nuclear Magnetic Resonance
OAE	Ocean anoxic event
P <sub>Apt</sub>	Crystalline apatite-bound phosphorus
P <sub>Aut</sub>	Detrital (authigenic) phosphorus
P <sub>Fe</sub>	Iron-bound phosphorus
P <sub>Org</sub>	Organic phosphorus

P <sub>Reac</sub>	Reactive phosphorus
P <sub>TOT</sub>	Total phosphorus
RSD	Relative standard deviations
TOAE	Toarcian Ocean Anoxic Event
UCC	Upper continental crust
VPDB	Vienna Pee-Dee Belemnite
XANES	X-ray Absorption Near-Edge Structure
XRD	X-ray diffraction

# 1. Project Rationale and overview

## 1.1. Importance of phosphorus

Phosphorus is an essential nutrient for life, used in all living organisms to build cell membranes, RNA, DNA, and hard tissues. Phosphorus, alongside bioavailable nitrogen, is also a key nutrient control for marine primary productivity (e.g., Delaney, 1998; Tyrrell, 1999; Paytan and McLaughlin, 2007; Filippelli, 2008). Over geological timescales, biological fixation of N<sub>2</sub> can address deficiencies, meaning phosphorus is considered the ultimate limiting nutrient on these timescales (Tyrrell, 1999). In deep time, understanding phosphorus cycling is vital to understand the coevolution of the environment and life on our planet, as phosphorus availability directly controls the rate of production of photosynthetic oxygen, contributing to the redox state of the oceans and atmosphere and even impacting the rate of evolution (e.g., Van Cappellen and Ingall, 1996; Lenton and Watson, 2000; Bjerrum and Canfield, 2002; Papineau, 2010; Planavsky *et al.*, 2010; Lenton *et al.*, 2012; Reinhard *et al.*, 2017; Alcott *et al.*, 2022).

Excess bioavailable phosphorus can also affect environmental conditions by eutrophication, where high levels of bioavailable phosphate cause spikes in primary productivity comprised of large algal blooms (Schindler *et al.*, 2006). When these blooms die, microbial decomposition depletes dissolved oxygen in the water column, leading to dysoxic or anoxic 'dead zones', which have insufficient oxygen to support life. In the modern Earth system, dead zones are found seasonally in many freshwater lakes (e.g., Lake Erie: Arend *et al.*, 2011), and in marine coastal environments, particularly close to large nutrient-rich rivers (e.g., Mississippi River and the Gulf of Mexico; Susquehanna River and the Chesapeake Bay) (Chislock *et al.*, 2013). These dysoxic-anoxic events are considered to be at least partially anthropogenic, with high levels of nutrients in the water column related to sewage and fisheries waste or run-off from agriculture (Schindler *et al.*, 1974). Eutrophication has also occurred naturally throughout Earth's history and high concentrations of nutrients have been suggested as a driver of ocean anoxic events and coincident extinctions at several points in history (e.g., Monteiro *et al.*, 2012; Schobben *et al.*, 2020; Hülse *et al.*, 2021; Qiu *et al.*, 2022). Overall, ocean phosphate availability is an important driving force for periods of environmental and evolutionary change throughout Earth's history.

## 1.2. The ocean phosphorus cycle

The marine phosphorus cycle is formed of a complex set of processes which regulate the ocean concentration of phosphorus (Figure 1). The total inventory of phosphorus in the oceans is

regulated by the balance between continental inputs and the net burial flux at the seafloor (e.g., Ruttenberg, 2002; Paytan and McLaughlin, 2007; Wallmann, 2010). The largest input of phosphorus into the oceans is from continental weathering, with particulate and dissolved phosphorus transported to the ocean in river-run off, and accounts for over 80 % of the present-day phosphorus flux into the ocean (Savenko, 2010; Baturin, 2003) (Figure 1). Small amounts of phosphorus are also deposited into the ocean from aerosols, mineral dust, or volcanic ash, which is a significant source of phosphorus for the open ocean as the majority of riverine particulate phosphorus is deposited in the shelf (e.g., Ruttenberg, 2002; Paytan and McLaughlin, 2007). In the modern ocean, the average phosphorus content is  $70\text{--}72 \mu\text{g L}^{-1}$ , but this is variable with values of  $< 1 \mu\text{g L}^{-1}$  in surface layers where it is being actively used by biota, and maximum concentrations in the intermediate layer, which occurs at different depths in different basins (Ruttenberg, 2002).

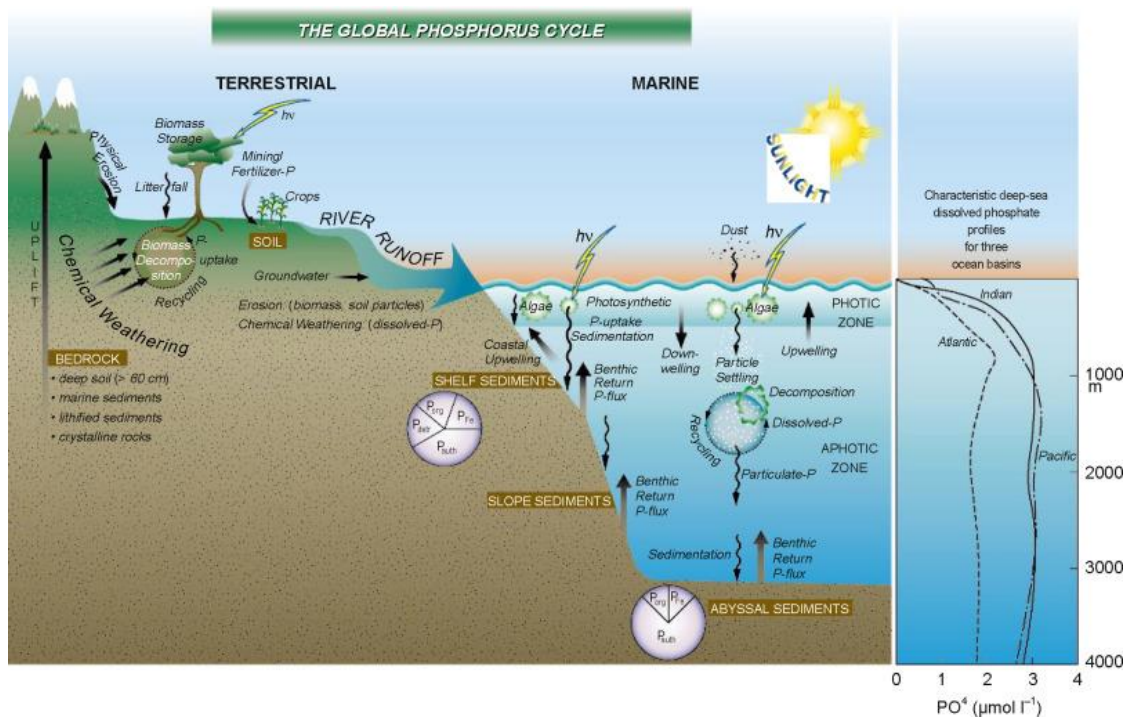


Figure 1 - Cartoon illustration of the major reservoirs and fluxes of phosphorus taken from Ruttenberg (2001)  $P_{Org}$  = organic phosphorus;  $P_{Fe}$  = iron-bound phosphorus;  $P_{Detr}$  = detrital apatite;  $P_{Aut}$  = authigenic/biogenic apatite. The  $P_{Org}$ ,  $P_{Fe}$ , and  $P_{Aut}$  reservoirs represent potentially reactive phosphorus pools.

Phosphorus in the ocean is comprised of both dissolved phosphorus and particulate phosphorus. Dissolved phosphorus is predominantly comprised of orthophosphate ( $-\text{PO}_4^{3-}$ ) and organic phosphorus compounds, while particulate phosphate can be comprised of many forms of phosphorus including plankton, phosphorus mineral precipitates, particulate-

absorbed phosphate. Both organic and inorganic particulate, and dissolved phosphorus undergo continuous transformation as they are assimilated and transformed by biota such as phytoplankton (Paytan and McLaughlin, 2007). The primary loss of phosphorus from the continuous cycling by biota is by sinking particulate phosphorus. Sinking particulate phosphorus is comprised of particulate organic phosphorus (~40%), authigenic particulate inorganic phosphorus (~25% [formed from remineralized phosphorus reprecipitated as calcium fluorapatite]), labile particulate inorganic (21%), and nonreactive detrital P (~13%) (Kolowitz *et al.*, 2001; Faul *et al.*, 2005). The vast majority of phosphorus is remineralized within the water column, with only around 1 % of phosphorus in sinking particulate matter reaching the sediment (Broecker and Peng, 1982).

In marine sediments, the dominant forms of phosphorus which are deposited and buried are non-reactive particulate phosphorus from riverine inputs, and reactive particulate phosphorus, primarily comprised of organic matter associated phosphorus, but also comprises iron-oxide adsorbed phosphorus (Delaney, 1998; Faul *et al.*, 2005). Redox conditions in the pore-waters and at the sediment water interface affect the retention of phosphorus in marine sediments (e.g., Paytan and McLaughlin, 2007; Alcott *et al.*, 2022). In oxic sediments much of the organic matter is mineralised in the sediment, but the released phosphorus is generally retained in the pore water or on surface adsorption sites with eventual conversion to apatite. (Sundby *et al.*, 1992; Faul *et al.*, 2005). Some is still removed from the sediment by bacterial mining of the detrital organic matter, though this fraction is relatively small, and often phosphorus binds to minerals such as iron (oxy)hydroxides, which act as a phosphorus sink, before it can be recycled into the water column (Slomp *et al.*, 1996; Algeo and Ingall, 2007). In anoxic environments, anaerobic bacterial communities on the seabed preferentially mine sedimentary organic matter for nutrients such as phosphorus and releasing them from the sediment (e.g., Paytan and McLaughlin, 2007; Alcott *et al.*, 2022). Where sulfidic pore-waters are present close to the sediment-water interface, the released phosphorus is predominantly released back into the water column, as free hydrogen sulfide removes phosphorus sinks such as iron (oxy)hydroxides (e.g., Alcott *et al.*, 2022). Sulfidic bottom waters are most commonly associated with euxinic environments, though ferruginous conditions with small amounts of added sulfide can have the same effect (e.g., Alcott *et al.*, 2022). This means that different redox conditions impact not only the cycling of phosphorus, but also phosphorus signals which could be preserved by both sediments and water column proxies.

This indicates that there are several factors which can affect the cycling of phosphorus in the ocean, including the concentration of phosphorus in the water column and sediments. This includes changes in the inputs of phosphorus to the ocean (such as the intensity of weathering

or changes in volcanic ash inputs), changes in the biota (which recycle phosphorus in the water column and affect fluxes of phosphorus to the sediment), and changes in the redox conditions which control recycling of phosphorus from the sediment.

### 1.3. Methods of investigating phosphorus

Despite the environmental importance of phosphorus cycling, measuring changes in phosphorus cycling through Earth's history has proved challenging. Unlike some other nutrient elements, phosphorus has only one natural stable isotope, so isotope mass balances cannot be used to track changes in phosphorus fluxes in the same way as nitrogen, carbon, or oxygen. Established methods of investigating phosphorus cycling throughout Earth's history, such as phosphorus speciation (Ruttenberg, 2003; Thompson *et al.*, 2019), P/Fe ratios of iron formations (Bjerrum and Canfield, 2002; Planavsky *et al.*, 2010), and bulk rock phosphorus concentrations (Reinhard *et al.*, 2017), have been successful in providing some constraints on the distributions and cycling of phosphorus in the past, but have their own limitations (e.g., Dodd *et al.*, 2021). For example, phosphorus speciation provides valuable insight into phosphorus cycling in the sediment, which is one factor which can affect oceanic phosphorus concentrations, but it can only provide inferences about phosphorus cycling in the water column (Ruttenberg, 2003). Simple bulk rock phosphorus content also cannot give information about the water-column phosphorus concentration, as redox and primary producers can alter the ratios of retained and recycled phosphorus (Ingall *et al.*, 1993; Ingall and Jahnke, 1997; Algeo and Ingall, 2007; Reinhard *et al.*, 2017). This demonstrates a need for the development of a direct water-column phosphorus concentration proxy, which could be used to complement existing sediment data to better understand the phosphorus cycle (Dodd *et al.*, 2021).

Recent work, predominantly focussed on corals, has indicated that the phosphorus content of carbonates is related to the concentration of phosphorus in the solution the carbonate precipitates in (e.g., Dodge *et al.*, 1984; Shotyk *et al.*, 1995; Kumarsingh *et al.*, 1998; Montagna *et al.*, 2006; LaVigne *et al.*, 2008; 2010; Anagnostou *et al.*, 2011; Mallela *et al.*, 2013; Chen *et al.*, 2013; Ingalls *et al.*, 2020; Dodd *et al.*, 2021; Ingalls *et al.*, 2022; Dodd *et al.*, 2023). This indicates the potential for carbonate-associated phosphorus (CAP) to be used as a proxy for water-column phosphorus. So far CAP has been investigated in a range of modern and ancient carbonates, including biotic carbonates such as foraminifera (Dodd *et al.*, 2021), gastropods (Dodd *et al.*, 2021), Ophiocomidae bioclasts (brittle stars) (Dodd *et al.*, 2021), and corals (Dodge *et al.*, 1984; Shotyk *et al.*, 1995; Kumarsingh *et al.*, 1998; Montagna *et al.*, 2006; LaVigne *et al.*, 2008; 2010; Anagnostou *et al.*, 2011; Mallela *et al.*, 2013; Chen *et al.*, 2013; Dodd *et al.*, 2021), as well as natural abiotic carbonates such as dolomites and ooids (Ingalls *et*

*et al.*, 2020; Dodd *et al.*, 2021; 2023), and synthetic lab-grown carbonates (Dodd *et al.*, 2021). These investigations have also covered large periods of Earth's history, with samples from as early as the Neoproterozoic (Ingalls *et al.*, 2022) to the Ediacaran (Dodd *et al.*, 2023) to the modern day (e.g., Dodge *et al.*, 1984; Dodd *et al.*, 2021).

Dodd *et al.* (2021) investigated the impact of solution phosphorus concentrations, as well as other environmental factors on CAP (Figure 2). This demonstrated that CAP varied with multiple environmental factors including temperature, pH, as well as the mineralogy of the carbonates, with aragonites and calcites giving different CAP values for the same solution phosphorus concentration (Figure 2). Dodd *et al.* (2021) suggested that the magnitude of changes in CAP likely to be caused by pH changes or temperature changes in the ocean are likely to be small – as the changes in pH and temperature which were used to investigate the variations in CAP were large. For example, CAP increased less than two-fold over a temperature change of 20 °C and decreased around five-fold with a pH increase of 2 points; both of which would be very large environmental changes in a natural ocean system (Figure 2).

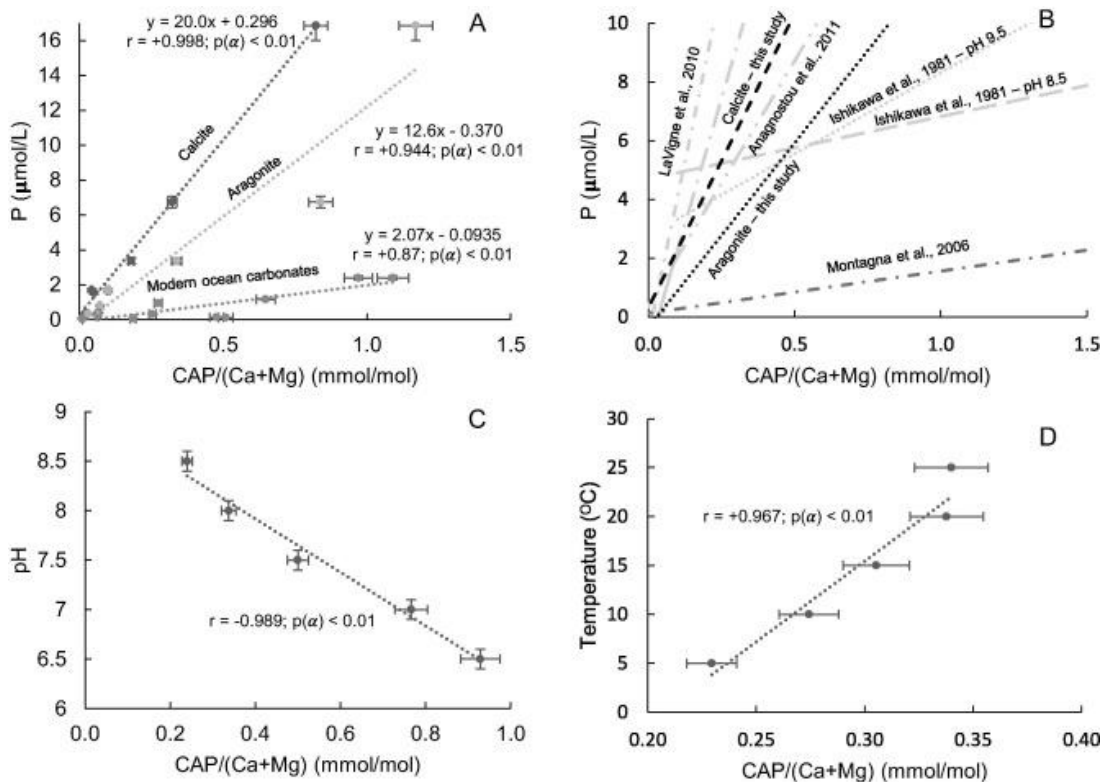


Figure 2 - CAP in various carbonates, compared to other environmental proxies. **a.** CAP in synthetic aragonite and calcite and modern ocean carbonates as a function of solution phosphate concentration; **b.** Comparison of CAP relationships with solution phosphate in other published work; **c.** CAP in synthetic aragonite as a function of solution pH; **d.** CAP in synthetic aragonite as a function of solution temperature. All CAP values are normalized to Ca + Mg concentrations in their corresponding decarbonated solutions. Plot taken from Dodd *et al.* (2021).

Overall, the work by Dodd and others suggests that, despite other factors affecting phosphorus incorporation into carbonates, CAP in natural carbonates may be a suitable proxy for water-column phosphorus concentration in modern and ancient oceans. This project seeks to investigate the potential expansion of this proxy to other forms of carbonate, more specifically to calcite from belemnite rostra.

#### 1.4. Phosphorus in belemnites

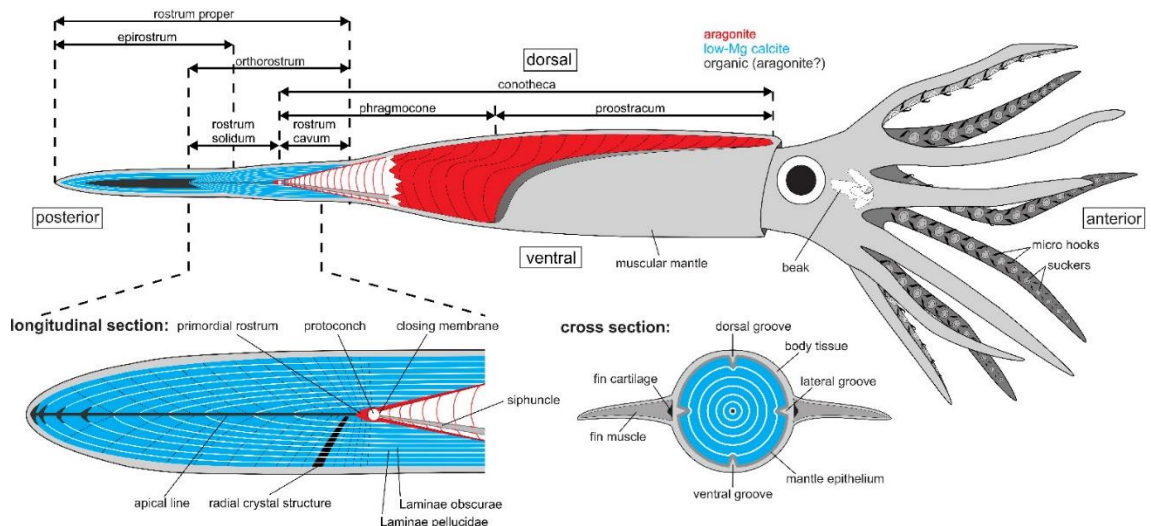


Figure 3 – Labeled diagram of a belemnite, as it would have looked when alive. The rostrum is commonly preserved and subject to geochemical analyses. The phragmocone region is occasionally also preserved, but is commonly replaced by secondary minerals, and sediment. The soft parts of the belemnite are rarely preserved, and only known from a small number of specimens. Image taken from Hoffmann and Stevens, 2020.

Belemnites are an extinct order of coleoid cephalopods, similar to modern day cuttlefish or ram's horn squid (*Spirula spirula*), which had a hard internal rostrum comprised of low-Mg calcite (e.g., Hoffmann *et al.*, 2016; Hoffmann and Stevens, 2020 and references therein). The belemnite rostrum is a commonly studied geochemical material as they are relatively abundant in the fossil record, retain geochemical signals from their time of formation and are at least somewhat resistant to diagenetic alteration (Figure 3) (e.g., Ullmann *et al.*, 2015). Other regions of the belemnite may also be preserved, such as the phragmocone region, though these are usually comprised of diagenetic material, secondary minerals or infilled sediment so are not used for geochemical analyses (Figure 3) (e.g., Ullmann *et al.*, 2015).

Belemnites were widely distributed, and survived for a significant portion of the Mesozoic, from the Late Triassic to the end of the Cretaceous (over 130 million years), making them an ideal candidate for geochemical analyses to examine nutrient changes through time (Iba *et al.*, 2011; 2012). Belemnites were among the first carbonates to be used in the oxygen-isotope

palaeotemperature estimation method and have been used as a key record of geochemical information ever since (e.g., Urey, 1948; Urey *et al.*, 1951; Lowenstam and Epstein, 1954). There has been some debate as to the exact habitat of belemnites, but it is generally believed they likely inhabited the outer-shelf areas, with some species also living closer to the shore (e.g., Stevens, 1965; Stevens and Clayton, 1971; Christensen, 1976; Jarvis, 1980; Doyle and Bennet, 1995; Stevens *et al.*, 2014; Hoffmann and Stevens, 2020).

Whilst belemnite rostra are commonly used for geochemical analysis, there is some uncertainty in the interpretation of geochemical information from belemnites due to poorly constrained understanding of belemnites palaeobiology, ecology, distribution, and lifespans (e.g., McArthur *et al.*, 2002; Li *et al.*, 2012; Hoffmann *et al.*, 2016; Stevens *et al.*, 2017; Hoffmann and Stevens, 2020 and references therein). There is also evidence of differences in elemental and isotopic ratios between individuals and species of belemnite, indicating that small differences in habitat or species-specific vital effects may be important to understand belemnite geochemistry (e.g., McArthur *et al.*, 2007a; b; Li *et al.*, 2012; Stevens *et al.*, 2017).

Phosphorus in belemnite calcite has rarely been investigated, and even where phosphorus values have been recorded, they were usually not the primary focus of the studies (Longinelli *et al.*, 2002; 2003; Gröcke *et al.*, 2003; Doguzhaeva *et al.*, 2013; Hoffmann *et al.*, 2016; Hoffmann and Stevens 2019). There is enough previous research to indicate that phosphorus is present in belemnite calcite in small but variable amounts, with Longinelli *et al.* (2003) demonstrating that phosphate made up less than 0.3 % of belemnite calcite.

As phosphorus in belemnites has not been routinely measured before, in order to robustly investigate carbonate associated phosphorus in belemnites, a method had to be developed to reliably quantify phosphorus in belemnites. Alongside this, the variability of phosphorus within individual belemnite rostra, as well as between individuals of the same and different species within stratigraphic levels.

In order to determine the potential of belemnite CAP to record water-column phosphorus, P/Ca records were generated and compared to established proxies for other environmental factors such as temperature and redox. The time period selected for this investigation was the Early Jurassic, with samples used mostly taken from the Pliensbachian and Toarcian, with some samples from the earlier Sinemurian and the later Aalenian and Bajocian in the Middle Jurassic. Belemnites occur frequently in the fossil record throughout the Early Jurassic making it possible to examine changes in belemnite CAP through time. Additionally, the Early Jurassic encompasses a period of substantial environmental change which is likely to impact nutrient cycling and ocean phosphorus concentrations.

## 1.5. Early Jurassic

The Early Jurassic is a period encompassing multiple significant changes to the climate and ocean systems, affecting nutrient cycling and biota. These changes are distributed throughout the Early Jurassic, with the most extreme environmental perturbations occurring in the Toarcian, marked by widespread ocean anoxia, elevated global temperatures, marine mass extinction and perturbations to the global carbon cycle.

At the end of the Triassic, the super continent Pangea began to break apart. This process continued into the Early Jurassic, as the continental plates continues to drift apart forming two major landmasses: Laurasia and Gondwana (Golonka and Ford, 2000; Golonka, 2007). The Panthalassa Ocean and the Tethys Ocean became connected in the North-Western corner of the Tethys by an epicontinental seaway, referred to henceforth as the Laurasia Seaway. As well as palaeogeographic changes, the Early Jurassic was also an interval of recovery from the Triassic-Jurassic mass extinction, which resulted in the loss of over 24 % of marine families (Hallam and Wignall, 1997). The Early Jurassic is also a period with marked temperature perturbations throughout, including oscillations between ice-house and green-house conditions, as well as fluctuations in the carbon isotope record, biodiversity, the intensity of the hydrological cycle and the ocean redox state (e.g., Sælen *et al.*, 1996; McArthur *et al.*, 2000; Bailey *et al.*, 2003; Jenkyns, 2003; Rosales *et al.*, 2004; Gómez *et al.*, 2008; Metodiev and Koleva-Rekalova, 2008; Suan *et al.*, 2008; 2010; Dera *et al.*, 2009a; b; 2010; 2011; Gómez and Goy, 2011). CAP has the potential to record changes in nutrient cycling across these events, allowing it to add crucial information to the understanding of these periods in Earth's history.

Samples in this study are predominantly from the Pliensbachian and Toarcian stages in the Early Jurassic. Studies demonstrate variable geochemical and climate conditions throughout the Pliensbachian, with warming events at the Early-Late Pliensbachian Boundary and near the end of the Pliensbachian (Jenkyns and Clayton, 1986; van de Schootbrugge *et al.*, 2005; Suan *et al.*, 2010; Korte and Hesselbo, 2011; Gómez and Goy, 2011;). Both of these periods are associated with warmer, wetter climates, and are associated with  $\delta^{13}\text{C}$  excursions (Jenkyns and Clayton, 1986; van de Schootbrugge *et al.*, 2005; Suan *et al.*, 2010; Korte and Hesselbo, 2011; Gómez and Goy, 2011). In the latter of these two intervals, known as the Late Pliensbachian Event (LPE), the positive carbon isotope excursion (2 ‰) was followed by a negative shift in  $\delta^{13}\text{C}$  which coincided with an increase in  $\delta^{18}\text{O}$  (2 ‰) indicative of a period of global cooling (e.g., Rosales *et al.*, 2004; Dera *et al.*, 2009a; b; Suan *et al.*, 2010; Korte and Hesselbo, 2011; Gómez and Goy, 2011). The causes of the LPE and concomitant CIE are debated but thought to be related to enhanced marine carbon burial (e.g., Hesselbo and Jenkyns, 1994; Suan *et al.*, 2010; Korte and Hesselbo, 2011).

The Toarcian stage encompasses more dramatic changes in climate and geochemical cycling, as well as periods of biotic crisis. The most significant event is the Early Toarcian Negative Carbon Isotope Excursion (ETNCIE) in the *tenuicostatum-falciferum* ammonite zones. The ETNCIE has been attributed to the release of isotopically light carbon into the atmosphere, potentially from the coincident eruption of the Karroo Ferrar Large Igneous Province (LIP), or the release of methane from marine clathrates (Hesselbo *et al.*, 2000; McElwain *et al.*, 2005; Svensen *et al.*, 2007; Kemp *et al.*, 2011). Concomitant to the ETNCIE was a period of global warming and marine mass extinction (the early Toarcian Mass Extinction [ETME]) as well as widespread ocean anoxia (the Toarcian Ocean Anoxic Event (TOAE) (Schlanger and Jenkyns, 1976; Pancost and Boot., 2004; McArthur *et al.*, 2007a; 2008; Jenkyns, 2010; Monteiro *et al.*, 2012). During this time the increased global temperatures resulted in a strengthened hydrological cycle and increased continental weathering, which also potentially increased nutrient flux to the ocean (McArthur *et al.*, 2000; Cohen *et al.*, 2004; Hermoso and Pellenard, 2014; Brazier *et al.*, 2015; Percival *et al.*, 2016; Fu *et al.*, 2017). There is a disconnect between the knowledge of a general increase in weathering, and evidence of increased fluxes of nutrients to the ocean for this event and similar events through Earth's History, which provides motivation for this project to provide a way to resolve this disconnect. This is particularly important as it has been suggested that the high levels of nutrients in the ocean caused an increase in primary productivity, which eventually led to eutrophication and wide-spread oxygen-depleted conditions, particularly in some of the restricted basins of the Laurasian Seaway and other marginal basins around the world (Zempolich, 1993; Tremolada *et al.*, 2005; Fantasia *et al.*, 2019). This interval of widespread dysoxic-anoxic, the TOAE, is evidenced in multiple locations, though with differing extents and durations, suggesting regional influences on the expression of the TOAE (Schlanger and Jenkyns, 1976; Pancost and Boot., 2004; McArthur *et al.*, 2007a; 2008; Jenkyns, 2010; Monteiro *et al.*, 2012).

Widespread ocean anoxia is suggested as one of the potential kill mechanisms for the concomitant mass extinction, the ETME, a second order mass extinction responsible for the loss of 5 % of marine invertebrate families, with shallow marine molluscs particularly affected (e.g., Jenkyns, 1988; Little and Benton, 1995; Wignall *et al.*, 2006; Mailliot *et al.*, 2006; Mattioli *et al.*, 2009; Caswell *et al.*, 2009). The ETME is likely to have been a two-pulsed extinction event, with one pulse occurring around the Pliensbachian-Toarcian boundary and another occurring later in the Early Toarcian, around the top of the *tenuicostatum-falciferum* zone boundary (e.g., Arias *et al.*, 1992; Bassoullet and Baudin, 1994). Other potential kill mechanisms for the ETME have been suggested as warming (Gómez and Goy, 2011), sea level change (Jenkyns 1988) or ocean acidification (Hermoso *et al.*, 2012; Trecalli *et al.*, 2012). The

ETNCIE is recognised as a period of significant sea-level change, with world-wide rapid transgression which may have caused extinction in its own right, or contributed to extinction through the development of anoxia as the proposed sea-level changes are coeval with the onset of dysoxic/anoxic facies in northern Europe (Jenkyns 1988). Ocean acidification events have also been recorded during the during the ETNCIE and ETME, as well as biocalcification crises, though the duration and geographical extent of the acidification are poorly constrained (Hermoso *et al.*, 2012; Trecalli *et al.*, 2012).

The Early Jurassic, and particularly the Early Toarcian present a good opportunity to investigate the potential of belemnite CAP to record water-column phosphorus concentrations. During the Early Jurassic and the ETNCIE specifically, changes in multiple environmental conditions such as temperature, weathering, and ocean redox may be expected to influence nutrient cycling and alter ocean phosphorus concentrations. It is possible that comparison of a belemnite CAP record with other environmental proxies from this time period may indicate factors affecting water column phosphorus and belemnite CAP.

This study presents P/Ca records for the Early Jurassic from three different basins in the Laurasian Seaway – the Cleveland Basin, the Cardigan Bay Basin and the Moesian Basin (represented by samples from modern day Yorkshire, North Wales, and Bulgaria respectively). These basins were chosen, as together they provide Early Jurassic records from basins which experienced different expressions of the TOAE and had different degrees of water mass restriction. During the Early Jurassic, the Moesian Basin was proximal to the open Tethys Ocean, and has minimal evidence of anoxia, and likely good ocean circulation (Pugh, 2018). At the other end of the spectrum, the Cleveland Basin was likely to be extremely restricted during the Early Jurassic, and the organic-rich, laminated black shales present in this basin indicate strong local anoxic conditions during the TOAE. The Cardigan Bay Basin represents an intermediate environment between these two extremes, and the Mochras borehole also presents the most expanded Early Jurassic sequence in the UK, with a thickness three times that of any similarly aged strata in the UK (Hesselbo *et al.*, 2013). Belemnite CAP records from each location are compared to each other, and to established proxies, including proxies for temperature and redox, to investigate factors affecting the incorporation of phosphorus into belemnite calcite. Each of these locations represents slightly different palaeoenvironments, with different extents and expressions of the TOAE at each site, and different degrees of restriction from the open ocean. This means that comparisons can be made between locations with different redox histories, and different levels of water-mass exchange with the open Tethys Ocean.

## 1.6. Sodium and other elements in belemnites

As well as analysing belemnite phosphorus concentrations, several other elemental ratios were also measured. In interpreting the phosphorus results, it became clear that concentrations of phosphorus, and other elements are at least somewhat interlinked, as substituting elements can have impacts on the carbonate environment, which in turn affects other substituted elements and so on. This suggests that evaluating the concentrations of multiple elements in belemnites is important to the interpretation of both the belemnite phosphorus ratios and belemnite chemistry as a whole. As the importance of investigating belemnite chemistry in a holistic way became clear, the impacts of different preparative methods, and the natural levels of intra- and inter-belemnite variability were examined for other elements. This includes both commonly measured elements, such as Mg and Sr, as well as little-studied elements such as Na.

In this study, method and variability data is presented for a range of elements including Sr, Mg and Na and stratigraphic data for Na in each study location is also investigated. Na was chosen for closer stratigraphic interpretation, as sodium is a major component of belemnite calcite, yet, unlike Mg and Sr, minimally studied. While several previous studies have measured Na concentrations in belemnites, the majority have measured it as an additional element in a multi-element study, and the factors affecting Na incorporation in belemnite calcite have rarely been discussed in detail (McArthur *et al.*, 2000; 2004; Wierzbowski, 2004; McArthur *et al.*, 2007a; Wierzbowski and Rogov, 2011; Li *et al.*, 2012; 2013; Wierzbowski *et al.*, 2013; Wierzbowski, 2015; Wierzbowski *et al.*, 2017; 2018). As it was determined that examining belemnite chemistry holistically was important to validate any potential palaeoenvironmental interpretations, investigating the factors affecting the concentration of sodium was determined to be important. Previous studies have suggested that sodium in belemnites may be a proxy for temperature, due to its apparent covariation with  $\delta^{18}\text{O}$  in some sample sets (McArthur *et al.*, 2000; 2004), or a proxy for diagenetic alteration (Brand and Veizer, 1980; Veizer, 1983; McArthur *et al.*, 2007a; Wierzbowski and Rogov, 2011; Li *et al.*, 2012; 2013; Wierzbowski *et al.*, 2013; 2017; 2018). In other carbonates, some studies have suggested that sodium concentration may reflect salinity (White, 1978; Ishikawa and Ichikuni, 1984; McArthur *et al.*, 2007a; Wit *et al.*, 2013; Mezger *et al.*, 2016; Bertlich *et al.*, 2018; Gray *et al.*, 2023) or water column calcium ion concentration (Evans *et al.*, 2018; Hauzer *et al.*, 2018; Evans *et al.*, 2020; Zhou *et al.*, 2021; Gray *et al.*, 2023; Nambiar *et al.*, 2023). Na/Ca records were generated for each location studied, and the records were compared to a range of palaeoenvironmental proxies to investigate the relationship between environmental factors and sodium.

## 1.7. Thesis Aims

Study aims were identified based on the knowledge gaps established surrounding the applicability of CAP to phosphorus in belemnites, as well as outstanding questions regarding phosphorus in belemnites and belemnite chemistry more widely. The following broad aims were established for this study, and each aim is addressed in the corresponding chapter:

- Chapter 2     Develop a method to extract and quantify phosphorus in belemnite calcite and assess the natural levels of variability of P/Ca within and between belemnites, including between different species.
  
- Chapter 3     Investigate the impact of different preparative methods on the quantification of other elements in belemnite calcite, including commonly studied elements such as Mg and Sr, as well as less frequently studied elements such as Na.
  
- Chapter 4     Prepare records for CAP for multiple sites in the Early Jurassic and compare these records to records of existing proxies to investigate the factors affecting phosphorus incorporation into belemnites.
  
- Chapter 5     Prepare records for Na/Ca ratios for the same locations and compare to existing proxies to investigate factors affecting sodium concentrations in belemnites.

## 1.8. Other work

As part of this project, time was also spent developing a model simulation to investigate the impact of water mass restriction on the development of ocean anoxia. The aim was to simulate conditions in epicontinental basins using different degrees of water-mass restriction and varying concentrations of nutrients to investigate the impact on ocean redox conditions. This was completed during Covid-19 enforced lab shutdowns and involved the adaptation of the COPSE model, a biogeochemical model predicting the histories of O<sub>2</sub>, CO<sub>2</sub>, and ocean composition through the Phanerozoic (e.g., Lenton *et al.*, 2018), to partition the 'ocean' model box into 'shelf' and 'open' ocean boxes. Due to time constraints for this project, based on the quantity of lab-work required after labs reopened, this work wasn't completed as the model was not applied to a time period or problem relevant to this study. The completed model adaptations have subsequently been adapted into a different biogeochemical model with spatial representation (SCION; Mills *et al.*, 2021). This has resulted in co-authorship of a publication investigating radiations of major animal phyla that occurred in concert with

repeated carbon and sulfur isotope excursions during the early Cambrian (Zhang *et al.*, *in review*).

## 2. Phosphorus extraction and quantification

### 2.1. Introduction

Recent work has sought to investigate the potential for carbonate-associated phosphorus (CAP) in biogenic carbonates to be used as a proxy for water column phosphorus, both in the modern ocean and in the past (Dodge *et al.*, 1984; Shotyk *et al.*, 1995; Kumarsingh *et al.*, 1998; Montagna *et al.*, 2006; LaVigne *et al.*, 2008; 2010; Anagnostou *et al.*, 2011; Mallela *et al.*, 2013; Chen *et al.*, 2013; Ingalls *et al.*, 2020; Dodd *et al.*, 2021; Ingalls *et al.*, 2022). Experiments have been conducted on many types of carbonates including lab-grown synthetic carbonates, bulk rock carbonates, stromatolites, micrites, and biogenic carbonates from coral and foraminifera (Ishikawa and Ichikuni, 1981; Dodge *et al.*, 1984; Shotyk *et al.*, 1995; Kumarsingh *et al.*, 1998; Montagna *et al.*, 2006; LaVigne *et al.*, 2008; 2010; Anagnostou *et al.*, 2011; Chen *et al.*, 2013; Mallela *et al.*, 2013; Sugiura *et al.*, 2019; Ingalls *et al.*, 2020; Dodd *et al.*, 2021; Ingalls *et al.*, 2022). It has been shown that in these media, CAP varies with water column phosphorus concentration, but is affected by a number of other factors such as temperature, pH, and mineralogy of the carbonates (Dodd *et al.*, 2021). This project sought to build on this work and investigate the potential to extend the use of CAP to investigate past ocean water column phosphorus concentrations using calcite from belemnites.

Previous studies of phosphorus in belemnites have been extremely scarce, and even in studies where it has been recorded it is rarely the primary focus (Longinelli *et al.*, 2002; 2003; Gröcke *et al.*, 2003; Doguzhaeva *et al.*, 2013; Hoffmann *et al.*, 2016; Hoffmann and Stevens, 2020). A study by Longinelli *et al.* (2003) found that phosphorus made up a small (less than 0.3 %) and variable fraction of belemnite calcite and suggested that it was either linked with primary phosphate and indicative of well-preserved calcite or released from the breakdown of organic matter introduced by early diagenetic fluids.

In order to investigate CAP in belemnite calcite, it was necessary to develop a method to extract and quantify the phosphorus in belemnite calcite. Different methods for cleaning and dissolving powdered belemnite calcite were tested on homogenised bulk samples to allow methods to be compared. Belemnite calcite contains phosphorus in a range of forms, such as carbonate-bound phosphate and calcium phosphate, as well as small but variable levels of organic-bound phosphorus which is concentrated in the apical line and dark regions in the growth bands (Veizer, 1974; Longinelli *et al.*, 2002; 2003; Gröcke *et al.*, 2003; Dunca *et al.*, 2006; Hoffmann *et al.*, 2016; Stevens *et al.*, 2017; Hoffmann and Stevens, 2020). Belemnite calcite can also contain contamination from diagenetic minerals and sediments, including

more organic material, varying levels of clay minerals or salts, as well as pyrite and hydroxy-, fluor- chlor- and carbonate apatite and iron-oxides (such as ferrihydrite or goethite), which phosphorus can bind to (e.g., Sælen, 1989; Ruttensberg *et al.*, 1992; Ullmann *et al.*, 2015; Ullmann and Korte, 2015; Hoffmann *et al.*, 2016; Stevens *et al.*, 2017; Hoffmann and Stevens, 2020; Thompson *et al.*, 2019).

The various forms of phosphorus in the samples are likely to respond to different cleaning methods in different ways. Previous studies of elemental ratios in biogenic carbonates, including previous CAP studies and studies on belemnites, have used different methods to clean carbonate powders, from no cleaning step at all, to cleaning with ultra-pure water to oxidative cleaning with hydrogen peroxide or sodium hypochlorite (e.g., Shotyk *et al.*, 1995; Penkman *et al.*, 2008; Zhang *et al.*, 2020; Riding, 2021 and references therein). Analysing the carbonates with no cleaning method simplifies the preparative method and avoids CAP ratios being affected by different solubilities of the various phosphorus and calcium containing minerals. However, soluble contaminants such as clays, salts and some organics would also be analysed, which can disrupt analysis by inductively coupled plasma mass spectrometry (ICP-MS) analysis. Soluble impurities such as clays, salts and soluble organics will be removed by both water and oxidative cleaning. Oxidative cleaning will oxidise and break down organic matter and may also partially oxidise and remove small fractions of other components including CAP, calcium phosphate, apatite, and other minerals – through etching. The free dissolved phosphorus could then either be removed with the oxidant or adsorbed to the surface of the remaining powder (e.g., Ruttensberg, 1992). In previous studies, the degree of this dissolution of apatite was shown to be small, and oxidative cleaning had the benefit of removing organic phosphorus which can be beneficial for measuring CAP. For this study, three different cleaning methods were tested: water, sodium hypochlorite and hydrogen peroxide.

Different forms of phosphorus may also respond differently to different dissolution methods. Previous studies of biogenic carbonates, including studies on belemnites and CAP studies in other carbonates, have used strong acids, such as nitric acid and hydrochloric acid (e.g., Shotyk *et al.*, 1995; Kumarsingh *et al.*, 1998; Penkman *et al.*, 2008), as well as weak acids, such as acetic acid (e.g., Ingalls *et al.*, 2020; Dodd *et al.*, 2021; Ingalls *et al.*, 2022). Previous studies by Ingalls *et al.* (2020; 2022) on bulk rock carbonates, as well as Neoproterozoic stromatolites, micrites, and crystal fans have shown that dissolution in strong acids such as nitric acid and hydrochloric acid gives higher P/Ca values than dissolution with acetic acid. It is suggested that stronger acids are more able to leach phosphorus from organic matter and other phosphorus containing minerals, such as different forms of apatite, as well as dolomite, which can be associated with iron-oxides in the sample and can cause over estimations of CAP due to the

dissolution of iron-oxide bound phosphorus (Sælen, 1989; Ingalls *et al.*, 2020; 2022). As CAP studies have not been investigated on belemnite calcite before, hydrochloric and nitric acid were still trialled, in addition to acetic acid, to determine which method was most suitable for belemnite calcite.

It was also necessary to investigate the variability in CAP within and between belemnites, and to investigate the effect of factors such as size and species on CAP. Previous work on belemnites has demonstrated that concentrations of some elements vary within and between individuals (McArthur *et al.*, 2007a; Li *et al.*, 2013; Ullmann *et al.*, 2015). Several studies have shown differences in some elemental ratios such as Mg/Ca between different species of belemnite, but some elemental ratios seem unaffected by species (such as Na/Ca, Sr/Ca) (e.g., McArthur *et al.*, 2007a; Li *et al.*, 2013; Ullmann *et al.*, 2015). Other studies have shown differences in elemental ratios within a belemnite rostrum, including variations between darker areas of calcite which represent more organic-rich growth rings, and variation long the length of the rostrum for elements, such as Mg/Ca and Sr/Ca (McArthur *et al.*, 2007a; Ullmann *et al.*, 2015).

## 2.2. Experimental Design

Initial tests to determine the best method for quantifying CAP were conducted on homogenised bulk samples. These samples were derived from whole crushed and powdered belemnite rostra to allow sufficient material for a range of methods to be evaluated with replicate analyses. Three bulk samples were used from levels which were predicted to have different water-column phosphorus concentrations, based on different palaeotemperatures during the time periods, to investigate the impact of different methods on samples with different amounts of phosphorus (Figure 4). In one of the samples, infilled material from the alveolar region of the belemnite, where the phragmocone would have originally been located, were included in the sample. This is a region of the belemnite rostra with an elevated level of infilled diagenetic minerals and sediment, so not removing it prior to sampling created a contaminated bulk sample, which could be used to investigate the impacts of different preparative methods on samples containing elevated levels of phosphorus in diagenetic minerals such as apatite, pyrite, and iron-bound phosphorus (Figure 4). Three different cleaning methods and three different dissolution methods were tested on each bulk sample.

Oxidative and non-oxidative cleaning methods were trialled on each of the three bulk samples: NaOCl, H<sub>2</sub>O<sub>2</sub> and water on the contaminated bulk; H<sub>2</sub>O<sub>2</sub> and water on the uncontaminated bulks. For each sample, 5 mg of cleaned calcite was taken, and three different acids were evaluated for dissolution (acetic, hydrochloric, and nitric). Different sample masses (2 and 10

mg) were also investigated to determine the minimum quantity of material needed to give reliable results, whilst minimising destructive sampling (Figure 4). For these additional sample masses, only one preparative method was trialled to avoid adding unnecessary analyses – so 2 mg and 10 mg sample masses were cleaned with H<sub>2</sub>O<sub>2</sub> and dissolved in acetic acid (Figure 4).

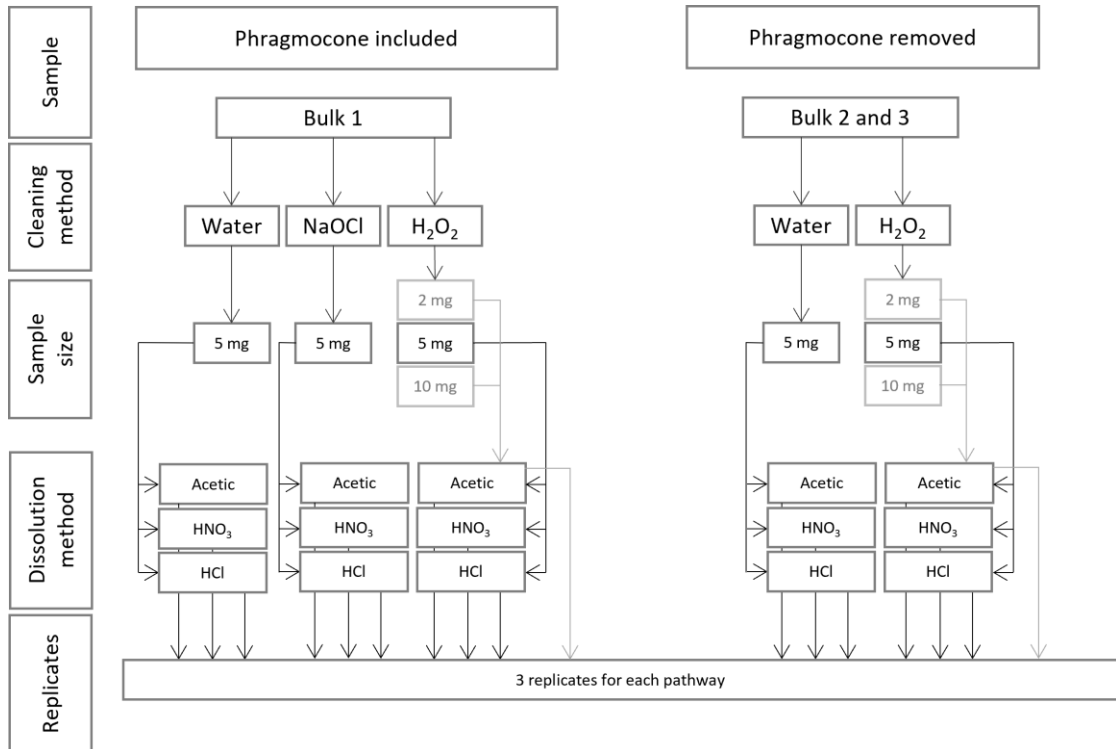


Figure 4 - Schematic for method development tests conducted using Bulk 1, Bulk 2, and Bulk 3. Bulk 1 contained the phragmocone region of the belemnite, whereas this was removed for Bulks 2 and 3. Three different cleaning methods were trialled on Bulk 1 (H<sub>2</sub>O<sub>2</sub>, NaOCl and water) and two different methods were conducted on Bulks 2 and 3 (H<sub>2</sub>O<sub>2</sub> and water). For each cleaning method, 5 mg samples of cleaned powder were weighed out and three different dissolution methods were tested for each Bulk Sample (acetic, nitric, and hydrochloric acid). Additional tests were conducted on 2 mg and 10 mg samples cleaned with H<sub>2</sub>O<sub>2</sub>, which were dissolved in acetic acid. For each combination of Bulk, cleaning method, dissolution method and sample size, three replicate samples were analysed.

Tests were also conducted to investigate the variability of CAP within belemnites and between belemnites. Within belemnites, CAP might vary by sampling position on the rostrum or growth rate. Between belemnites CAP could be affected by factors such as species, age, size, sex or differences in behaviour such as slightly different habitats or diets. There is also a requirement to examine variability of P/Ca values within belemnites and between belemnites. CAP could also be affected by contamination with sediment of phragmocone material, or by diagenetic alteration of the calcite. To investigate these factors, samples were analysed from ten belemnites across five species from two stratigraphic levels in the Pliensbachian. Specimens were chosen from the same bedding plane to ensure they were from the same stratigraphic level. Each belemnite was sampled six times along the length of the rostrum to investigate variation in CAP values within individuals, and trends with sampling position (Figure 5).

Differences in P/Ca between belemnites were also investigated to examine effects of belemnite species and size (Figure 5). Due to limited material and to avoid unnecessary analyses, samples were cleaned with water and dissolved in acetic acid as this method showed the least variability in initial tests. Where there was sufficient material, samples from each sampling site on each individual were analysed in triplicate (Figure 5). Where there was remaining material after triplicate analyses, additional samples were oxidatively cleaned with H<sub>2</sub>O<sub>2</sub> to determine if oxidative cleaning affected the measured intra- and inter- belemnite P/Ca variability (Figure 5). Hydrogen peroxide should oxidise and remove most organic phosphorus. Several studies have demonstrated the presence of organic matter in belemnite rostra, mostly concentrated within the apical line but also associated with the dark concentric growth bands (Bettencourt and Guerra, 2000). Very few studies have investigated the type or amount of organic matter in belemnites. After death, microbial and diagenetic processes breakdown most organic matter to amino acids or simple hydrocarbons, though some studies have reported finding components with peptide and saccharide properties, and even amino acids (Westbroek *et al.*, 1979; Collins and Gernaey-Child, 2001). Oxidatively treating belemnite samples with hydrogen peroxide should remove the phosphorus associated with any remaining primary organic matter and any contaminant organic matter, potentially reducing variability within and between belemnites.

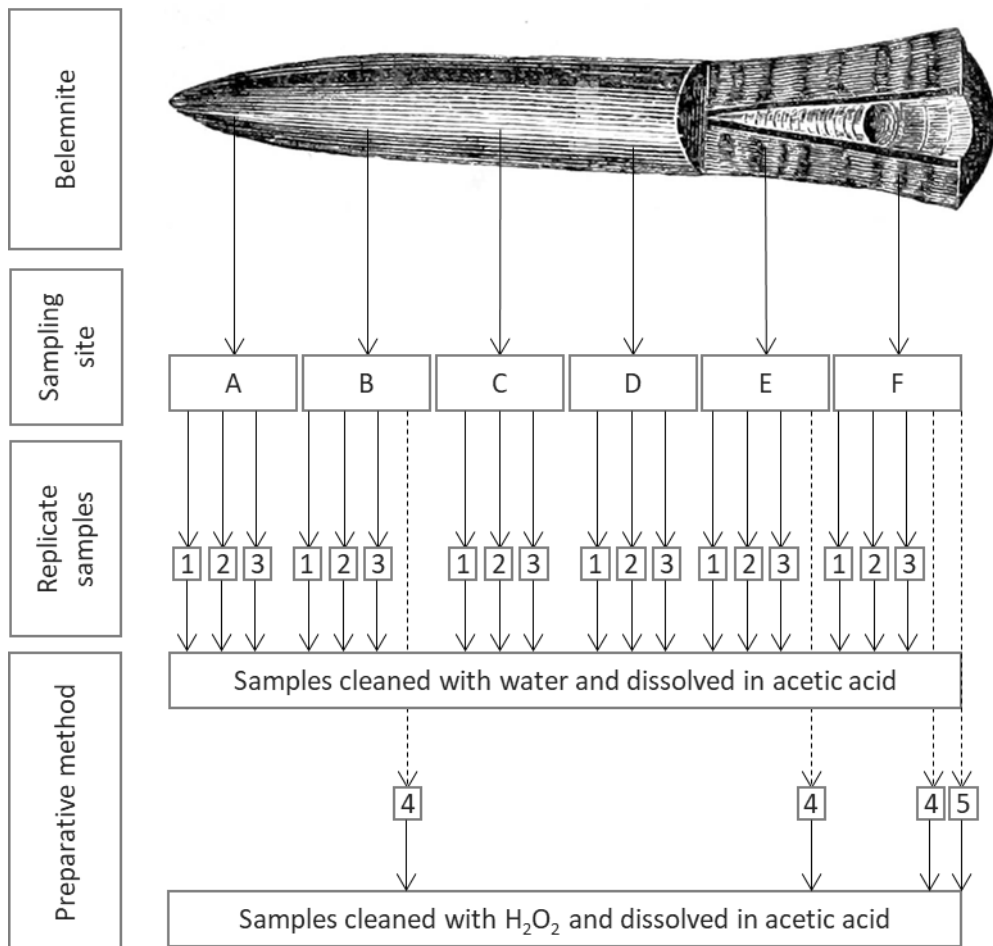


Figure 5 - Schematic for variability tests which were conducted on ten belemnites from five different species across two stratigraphic levels. The schematic describes the process which each belemnite underwent. Each belemnite was sampled at six sampling sites along the length of the rostrum. At each sampling site, where there was sufficient material, three replicate samples were taken and cleaned with water before dissolution in acetic acid. Where sampling sites had additional remaining material, further samples were taken which were cleaned with hydrogen peroxide before dissolution in acetic acid (belemnite picture taken from alamy.com; Image ID: JYJKF6; accessed 04/23)

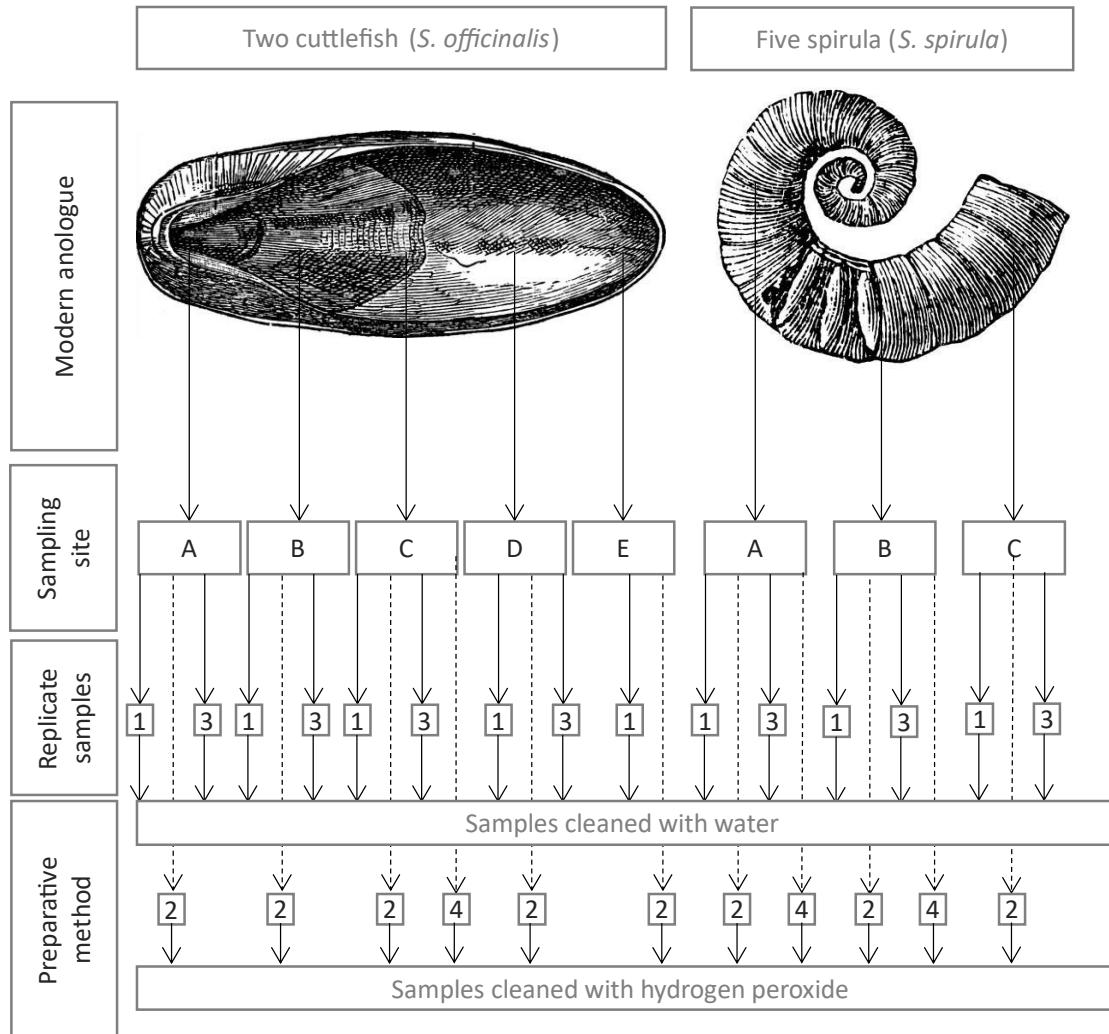


Figure 6 - Schematic for modern analogue tests, which were conducted on two cuttlebones (*Sepia officinalis*) and five Spirula shells (*Spirula spirula*). Each cuttlebone was sampled at a maximum of five sampling sites. Each *S. spirula* shell was sampled at a maximum of three sampling sites. At each sampling site a maximum of four replicate samples (indicated by, 1, 2, 3 and 4 numbers on diagram) were taken. Half of the replicate samples were cleaned with water; the remaining samples were cleaned with hydrogen peroxide. All samples were then dissolved in acetic acid for analysis. (Cuttlebone image from alamy.com, Image ID: 2BTH6DD; *S. Spirula* from <https://www.istockphoto.com/vector/spirula-peronii-gm1143463844-307081975> accessed 04/23)

Belemnites are extinct, so all analyses of belemnite rostra were conducted on fossils which are likely to have been diagenetically altered to some extent. Additional tests were conducted on modern analogues of belemnites – cuttlefish (*Sepia officinalis*) and ram's horn squid (*Spirula spirula*), which will have no diagenetic phosphorus-containing minerals and higher concentrations of organic material compared to belemnite carbonate. *S. officinalis* and *S. spirula* are considered to be among the closest extant relatives of belemnites (e.g., Rexfort and Mutterlose, 2006; Price *et al.*, 2009; Rexfort and Mutterlose, 2009). Similar to belemnites they are both are cephalopods and members of the subclass Coleoidea, with internal skeletons formed of calcium carbonate. In both *S. spirula* and cuttlefish, the internal skeleton is comprised of aragonite, rather than the calcite which forms belemnite rostra.

For this test, two cuttlefish *S. officinalis* cuttlebones and five *S. spirula* shells were analysed (Figure 6). For the larger cuttlefish, the cuttlebone was sampled at five sampling sites along the cuttlebone's length, and the smaller cuttlebone was sampled three times (Figure 6). For the *S. spirula*, some of the shells were incomplete and comprised only a few shell chambers – the shells were sampled at as many sites as possible, with a maximum of three and a minimum of one (Figure 6). For each sampling site 2-4 replicate samples were taken (Figure 6). Half of these replicates were cleaned with hydrogen peroxide, and the remaining half with water, then all the samples were dissolved in acetic acid (Figure 6). This will give potentially useful insight into how different forms of phosphorus respond to different preparative methods.

As well as providing a way to assess the impacts of different preparative methods on carbonates with no diagenetic material and high concentrations of organic phosphorus, studying modern analogues of belemnites also allows us to investigate how different environmental factors may be affecting elemental ratios in biogenic carbonates. Elemental ratios in carbonates can be affected by many factors, such as temperature, pH, mineralogy and for biogenic carbonates biological factors such as species, age, and sex as well as behavioural factors such as habitat and diet can all alter elemental concentrations in the carbonate (e.g., McArthur *et al.*, 2002; Li *et al.*, 2012; Hoffmann *et al.*, 2016; Stevens *et al.*, 2017; Hoffmann and Stevens, 2020 and references therein). Analyses of modern carbonates can help investigate the impact of these factors on P/Ca ratios and may suggest factors which are likely to have impacted P/Ca ratios in the past. Both cuttlebones (*S. officinalis*) were donated from The Marine Biological Association (MBA), who provided information on the environment in which the individuals were raised (including pH, salinity, temperature and the concentrations of ammonia, nitrate, and phosphate), which may allow for comparison between the elemental ratios of the cuttlebone carbonate and environmental conditions. Five *S. spirula* shells were collected from beaches in New Zealand, so have no accompanying environmental information. *Spirula* is monospecific, which eliminates the possibility of interspecific differences in P/Ca ratios. Other factors may cause differences in P/Ca ratios between individuals, such as sex, age or differences in behaviour including different habitats or feeding preferences.

## 2.3. Materials

### 2.3.1. Bulk samples

Bulk samples were generated from three Lower Jurassic belemnites collected from the Yorkshire coast. Belemnites were selected based on size to ensure there was enough material to generate a substantial bulk sample, which could be used to test multiple preparative method with replicates. Care was also taken to ensure belemnites were visually well

preserved, with predominantly pale-brown, translucent material, with minimal cracks and secondary mineral formation (Sælen and Karstang 1989; McArthur *et al.*, 2000; Ullmann *et al.*, 2015). Belemnites were selected from different stratigraphic levels which might have been expected to have different water column phosphorus concentrations as they were represented by different palaeotemperatures based on understanding of climate fluctuations in the Lower Jurassic. These specimens were used to examine the effect of different methods on calcite with potentially different concentrations of phosphorus. The bulk samples were named Bulk 1, Bulk 2, and Bulk 3 – and will be referred to collectively as Bulk Samples (Figure 4).

Bulk 1 was created from a from a large (29 g) Lower Toarcian belemnite identified as *Passaloteuthis bisulcata*. The belemnite was collected from the *Dactylioceras tenuicostatum* ammonite zone of the Grey Shale Member of the Whitby Mudstone Formation at Runswick Bay, North Yorkshire. The exterior of the belemnite was abrasively removed by wet grinding on a 75 µm full faced diamond grinding disc (8 inch/200mm) on an ATM Saphir 330 grinding machine, but the alveolar region was not removed. This region contains infilled and diagenetic material which is higher in many elements such as iron, manganese, phosphorus, and magnesium than the surrounding calcite. These elements can be in a range of diagenetic precipitates and minerals from infilled sediment including pyrite, barite, sphalerite, calcite, apatite, chalcopyrite, and silty mud. Including the alveolar region in this bulk means that Bulk 1 can be considered a ‘contaminated’ bulk sample, spiked with high concentrations of diagenetic minerals, including higher concentrations of elements of interest. The interior was crushed by hand in a steel pestle and mortar and sieved to ensure a grain size of < 180 microns. The resulting powder is referred to as Bulk 1 (Figure 4).

Bulk 2 was created from a large Lower Toarcian belemnite identified as *Acrocoelites oxyconus*. The belemnite was collected from the *Dactylioceras commune* ammonite subzone of the Alum Shale Member, Whitby Mudstone Formation at Ravenscar, North Yorkshire.

Bulk 3 was created from a large Upper Pliensbachian belemnite identified as *Passaloteuthis pessula*. This belemnite was collected from the *Amaltheus stokesi* ammonite subzone at the Cowbar Nab section in Staithes, North Yorkshire. For both Bulks 2 and 3 belemnite rostra, the exterior was abrasively removed in the same way as Bulk 1, along with the infilled alveolar region, which is considered to be an area contaminated with diagenetic and sediment minerals.

### 2.3.2. Sample variability

Tests were conducted to examine the variability in P/Ca within and between belemnites of the same and different species, and within and between stratigraphic levels. This could not be

tested using the Bulk Samples, as they were from different stratigraphic levels and were homogenised samples which could not indicate variability within belemnites (Figure 4; Figure 5).

Multiple Pliensbachian belemnites were collected from two stratigraphic levels from the Yorkshire coast. The genus, and where possible the species, of each belemnite was determined using descriptions by Doyle (1990). Ten belemnites which had been identified to at least genus level were selected based on visual markers for well-preserved calcite (pale brown, translucent calcite with minimal cracks and secondary mineral formation), as well as larger size to allow multiple samples to be taken (Sælen and Karstang, 1989; McArthur *et al.*, 2000; Ullmann *et al.*, 2015) (Figure 5).

Six belemnites of three different species were selected from the Penny Nab section at Staithes, North Yorkshire which corresponds to the *Amaltheus gibbosus* ammonite subzone in the Upper Pliensbachian (Table 1). Four individuals of two different species were selected from the Wine Haven section at Robin Hood's Bay and correspond to the *Phricodoceras taylori* ammonite subzone in the Lower Pliensbachian (Table 1). Within each stratigraphic level, specimens were collected from the same bedding plane to ensure they were as contemporaneous as possible.

*Table 1 - Table of sampling locations, ammonite zones, belemnite species and number of individuals tested for specimens used in the variability tests to examine inter- and intra- belemnite variability.*

Sampling Location	Ammonite subzone	Belemnite species	Number of individuals
Penny Nab, Staithes	<i>Amaltheus gibbosus</i>	<i>Bairstowius</i> sp.	1
		<i>Parapassaloteuthis</i> sp.	3
		<i>Passaloteuthis pessula</i>	2
Wine Haven, Robin Hood's Bay	<i>Phricodoceras taylori</i>	<i>Passaloteuthis pessula</i>	1
		<i>Nannobelus delicatus</i>	3

Each belemnite rostrum was sampled six times along the length of the rostrum using an abrasive diamond tipped Dremel drill bit (Figure 5). Attempts were made to minimise inclusion of contaminants and diagenetically altered material by applying best sampling practice, including avoiding sampling the belemnite exterior, phragmocone and apical line as well as targeting visually clear calcite (Ullmann *et al.*, 2015). In most cases the resulting powder was extremely fine (< 180 µm) but for some samples additional powdering was completed by hand

using an agate pestle and mortar. Collectively samples used in the variability tests will be referred to as Variability Samples (Figure 5).

### 2.3.3. Modern analogue samples

Two *S. officinalis* cuttlebones were donated by the MBA. The individuals were raised together, so differences in environmental conditions are expected to be minimal. The key difference between both specimens is lifespan. Though neither individual can be considered fully mature, one specimen lived for 8 months, primarily over winter (September-May) and the second specimen lived for 13 months (September-following October). As the water the *S. officinalis* were raised in is extracted from the Plymouth Sound, it follows the natural variation in temperature and other environmental conditions as the Plymouth Sound seawater and records for these variations were maintained by the MBA. This means the second individual will have experienced a higher average temperature than the younger cuttlefish, as well as any other seasonal changes.

The cuttlebones were removed from the deceased individuals by the Marine Biological Association (MBA) and frozen before donation. They were then defrosted and dried in an oven at 70 °C for 72 hours to remove moisture. The exterior was removed using a scalpel, revealing the porous interior. Samples were taken using a scalpel across the width of the cuttlebones but avoiding the apical line. Each sample incorporated multiple growth rings providing an averaged signal throughout the aragonite growth. Samples were then powdered using an agate pestle and mortar.

*S. spirula* have an aragonitic, open planispiral internal chambered shell. For each of the five *S. spirula* shells, sections were removed beginning from the outer end of the open planispiral shell. In the case of fragments, a determination was made as to which end was most likely the outer end. Each section was powdered using an agate pestle and mortar.

### 2.3.4. Standards

A minimum of five samples of JCp-1 certified reference material were prepared and run for every set of analyses conducted. JCp-1 is a reference material of coral *Porites* sp. prepared by the Geological Survey of Japan. The certified and informational values for the concentrations of different components of JCp-1 are detailed in Table 2.

For variability tests and modern analogue tests, five replicate samples of either Bulk 2 or Bulk 3 were analysed in every run as an additional standard, though they are not certified reference materials (CRMs).

Table 2 - certified and informational values for JcP-1 standard reference material, adapted from GSI CRM JcP-1 Coral Geochemical Reference Material Technical Information sheet.

Component	Certified value (mass fraction %)
CaO	53.50 ± 0.28 (mg / kg)

Certified values (mg / kg)		Information values (mg / kg)	
Element	Certified value	Element	Information values
Ba	10.3 ± 0.5	Al	490, 480
Fe	29 ± 2	B	47.7
K	185 ± 8	Cd	0.028, 0.032
Mg	972 ± 8	Cl	584
Mn	1.0 ± 0.1	Li	1.3
Na	4350 ± 30	Mo	0.08, 0.07
P	4.1 ± 0.9	Total S	1920
Sr	7240 ± 70	Zn	0.5

## 2.4. Methods

### 2.4.1. Weighing and Cleaning

10-20 mg samples of all samples, including Bulk Samples, Variability Samples, Modern Samples, and samples of a reference material (JcP-1) were cleaned using different cleaning methods. Three cleaning methods were trialled on Bulk 1 samples: ultrapure water, hydrogen peroxide (H<sub>2</sub>O<sub>2</sub>) and sodium hypochlorite (NaOCl) (Figure 4). H<sub>2</sub>O<sub>2</sub> and water were also trialled on samples of Bulk 2, Bulk 3 and the JcP-1 reference material – NaOCl was not included in these tests as initial measurements showed cleaning with NaOCl gave similar results to cleaning with hydrogen peroxide (Figure 4). For each Bulk Sample and reference material, sufficient samples were weighed to provide triplicate analysis for each preparative method – including investigating the impact of sample size (Figure 4). This meant that for Bulk 1, 33 samples were weighed out, and for Bulk 2 and 3 and the reference material 24 samples were weighed out (Figure 4).

For Variability Samples, samples were weighed in triplicate where there was sufficient calcite (Figure 5). Samples were cleaned using water only, as initial tests suggested this method introduced the least variability in P/Ca ratios, and limited material from each sampling site prohibited trialling multiple preparative methods (Figure 5). For some sampling sites, where there was remaining material after triplicate analysis with water-only cleaning, additional samples were weighed out to be cleaned using hydrogen peroxide (Figure 5). This was to

determine if oxidative cleaning reduced variability between different sampling sites on the same belemnite, or between belemnites of different or the same species at the same stratigraphic level – for instance if the variability were caused by different amounts of organic phosphorus which could be removed by oxidative treatment. Where there was sufficient material, replicate samples for cleaning with H<sub>2</sub>O<sub>2</sub> samples were also weighed out (Figure 5).

For the Modern Analogue samples, for each sampling site of each *S. spirula* shell or *S. officinalis* cuttlebone, 10-20 mg samples of powder were weighed out, with up to four replicates for each sampling site where there was sufficient quantity of powder (Figure 6). Half the replicates were cleaned with ultra-pure water (Figure 6). The remaining samples were cleaned using H<sub>2</sub>O<sub>2</sub> to remove any organic material which may be more prevalent in modern biogenic carbonates than in belemnite calcite (Figure 6).

#### 2.4.1.1. Water only

Ultrapure water (2 mL) was added to the samples and reference material and sonicated for 15 minutes. Samples were centrifuged and the supernatant was pipetted off. This was repeated a further four times to ensure removal of soluble contaminants. Samples were covered to avoid contamination with dust, and air dried in a fume cupboard for at least 48 hours.

#### 2.4.1.2. Bleaching with hydrogen peroxide

Hydrogen peroxide (H<sub>2</sub>O<sub>2</sub>) (2 mL, 9.8 M, trace metal grade) was added to each sample and reference material and left for 72 hours on a shaker table, to ensure the powder is completely exposed to the H<sub>2</sub>O<sub>2</sub>. Samples were centrifuged (10 minutes, 10,000 rpm), and the supernatant pipetted away. The samples were rinsed five times with ultrapure water using the same method as samples which were cleaned with water only (2.4.1.1).

#### 2.4.1.3. Bleaching with sodium hypochlorite

Sodium hypochlorite (NaOCl) (2 mL, 12 %, trace metal grade) was added to each sample, and left for 48 hours on a shaker table, to ensure the powder was completely exposed to the NaOCl. Samples were centrifuged (10 minutes, 10,000 rpm), and the supernatant liquid pipetted away. Samples were rinsed with water and methanol using the same method as samples cleaned with H<sub>2</sub>O<sub>2</sub> (2.4.1.2). Samples were covered to avoid contamination with dust, and air dried in a fume cupboard for at least 48 hours.

### 2.4.2. Acidification

For all samples and standards, the cleaned and dried belemnite powders were accurately weighed into approximately 5-6 mg samples.

For Bulk Samples, either HCl (1 mL, 1 M, trace metal grade), nitric acid (1 mL, 0.7 M, trace metal grade) or acetic acid (1 mL, 5 M, trace metal grade) was added to ensure the hydronium ions were in excess. Once the addition was complete, the samples were placed in an ultrasonic bath for 15 minutes to ensure complete dissolution, then sealed and centrifuged (10 minutes, 10,000 rpm). To investigate the impact of sample size on P/Ca ratios, additional powders from of Bulks 1, 2 and 3, which were cleaned using the H<sub>2</sub>O<sub>2</sub> method, were accurately weighed into samples of approximately 2 mg and 10 mg. These samples were dissolved in acetic acid (1 mL, 5 M, trace metal grade) following the same procedure as the 5-6 mg powders. Multiple preparative methods were not trialled on samples of different sizes, as this would have resulted in a large number of additional analyses which would be unnecessary in the investigation of the impact of sample size. For each combination of sample material, cleaning method dissolution method, sample size samples were prepared and analysed in triplicate.

For Variability and Modern Analogues Samples only one dissolution method was used to reduce the number of analyses and ensure sample material was conserved where possible. Acetic acid dissolution was used as it showed the most promise in initial testing. Cleaned and dried powders of belemnite, *S. officinalis* and *S. spirula* carbonates were accurately weighed into approximately 5-6 mg samples. These samples were dissolved in acetic acid (1 mL, 5 M, trace metal grade) following the same procedure as the Bulk Samples. For Variability Samples, triplicate samples were prepared for each sampling site where there was sufficient material. For Modern Analogues Samples, for each combination of sampling site and cleaning method, samples were analysed in duplicate where material allowed.

Some studies have used repeat high salinity washes to remove adsorbed phosphate from any remaining material not dissolved in acid, such as the MgCl<sub>2</sub> washes used in the SEDEX phosphorus speciation method (Ruttenberg *et al.*, 1992; Thompson *et al.*, 2019) and the NaCl washes used in the analysis of bulk rock samples in Dodd *et al.* (2021). Belemnite samples are almost entirely soluble calcite, compared to a lower percentage of soluble material in bulk rock samples – including carbonates. For most samples there was no visible material left after dissolution, so it was determined that high salinity washes were not necessary.

### 2.4.3. Analysis

For each sample, 0.3 mL of the supernatant liquid was added to a matrix solution (HNO<sub>3</sub>, 8.6 mL, 0.1 M, trace metal grade) and an internal standard (Y, 0.1 mL, 10 ppb, 0.1 M HNO<sub>3</sub> matrix).

Samples and blanks were analysed on a Thermo Scientific iCAPQc ICP-MS for Li, B, Na, Al, K, Ba and U concentrations and a Thermo Scientific iCAP 7400 Radial ICP-OES for Ca, Mg, P, Fe, Mn, S and Sr concentrations in the Cohen Laboratory at the University of Leeds. For each run, the

limits of detection (LOD), limits of quantification (LOQ) and analytical percentage uncertainties were calculated for each element analysed. LOD is the concentration below which the analyte element cannot be detected, defined as three times the standard deviations of six blank measurements. LOQ is the concentration below which the analyte element cannot be accurately quantified and was defined as ten times the standard deviation of six blank measurements. The percentage uncertainty is the calculated 95 % confidence interval (two standard deviations) of six repeated quality control standard measurements. Example LOD values, LOQ values and percentage uncertainties for each element from representative ICP-MS and ICP-OES runs are reported in Table 3 and Table 4 respectively. Full results of elemental analysis of Bulk, Variability and Modern Analogue Samples can be found in the appendix (8.1; 8.2; 8.3).

*Table 3 - Example limits of detection (LOD), limits of quantification (LOQ) and percentage uncertainties for an individual ICP-MS run for Li, B, Na, Al, K, Mn, Ba and U. LOD and LOQ values are calculated as 3 times and 10 times the standard deviation of six blank samples respectively. The percentage uncertainty is the calculated 95 % confidence interval of 6 repeated quality control standard measurements.*

	<b>Li</b>	<b>B</b>	<b>Na</b>	<b>Al</b>	<b>K</b>	<b>Ba</b>	<b>U</b>
<b>LOD / mg L<sup>-1</sup></b>	2.5E-06	1.7E-03	1.6E-02	5.9E-04	6.6E-02	1.5E-05	1.0E-06
<b>LOQ / mg L<sup>-1</sup></b>	8.2E-06	5.6E-03	5.2E-02	2.0E-03	2.2E-01	5.0E-05	3.5E-06
<b>% Uncertainty</b>	2.48	3.12	1.69	1.34	8.72	0.88	1.58

*Table 4 - Example limits of detection (LOD), limits of quantification (LOQ) and percentage for an individual ICP-OES run for Ca, Mg, P, Fe, Mn, S and Sr. LOD and LOQ values are calculated as 3 times and 10 times the standard deviation of six blank samples respectively. The percentage uncertainty is the calculated 95 % confidence interval of 6 repeated quality control standard measurements.*

	<b>Ca</b>	<b>Mg</b>	<b>P</b>	<b>Fe</b>	<b>Mn</b>	<b>S</b>	<b>Sr</b>
<b>LOD / mg L<sup>-1</sup></b>	1.8E-01	1.3E-03	1.9E-03	5.9E-04	8.4E-04	2.2E-04	2.4E-02
<b>LOQ / mg L<sup>-1</sup></b>	5.9E-01	4.2E-03	6.3E-03	2.0E-03	2.8E-03	7.3E-04	8.1E-02
<b>% Uncertainty</b>	0.93	0.29	0.49	1.34	1.54	0.25	6.64

#### 2.4.4. Iodine analysis

For Bulk Samples from Bulk 2 and 3 samples and samples of the JCP-1 reference material and Variability Samples, concentrations of iodine were also measured using a method adapted from He *et al.* (2022). For each sample 0.5 mL of the supernatant was added to ammonium hydroxide (0.5 mL, 2 M, trace metal grade) to stabilise the iodine. For each stabilised solution an amount of solution required dilute into a 5 mL solution containing  $50 \pm 5 \mu\text{g mL}^{-1}$  of calcium

was made up to 4.9 mL with a matrix solution of ammonium nitrate to stabilise iodine (0.1 M nitric acid, 0.3 M ammonium hydroxide, 3 % methanol) and an internal standard was added (Te, 0.1 mL, 10 ppb, 0.1 M HNO<sub>3</sub> matrix). Samples and blanks were analysed on a Thermo Scientific iCAPQc ICP-MS in the Cohen Laboratory at the University of Leeds. An example of an LOD value, LOQ value and percentage uncertainty for an ICP-MS run for iodine is reported in Table 5. Full results of iodine analysis of Bulk, Variability and Modern Analogue Samples can be found in the appendix (8.1; 8.2; 8.3).

*Table 5 - Example of limit of detection (LOD), limit of quantification (LOQ) and percentage uncertainty for an individual ICP-MS run analysing iodine. LOD and LOQ values are calculated as 3 times and 10 times the standard deviation of six blank samples respectively. The percentage uncertainty is the calculated 95 % confidence interval of 6 repeated quality control standard measurements.*

	I
<b>LOD / mg L<sup>-1</sup></b>	3.11E-05
<b>LOQ / mg L<sup>-1</sup></b>	1.04E-04
<b>% Uncertainty</b>	0.94

#### 2.4.5. Statistical tests

Where comparisons were made different between samples or preparative methods, an independent two-sample t test assuming unequal variance was conducted with a 95 % confidence interval to determine if any differences were statistically significant. In some cases, as multiple t tests have been performed on the same datasets, it is possible that statistically significant results with P values close to the threshold (0.05) are false positive results, and there are no statistically significant differences between the cleaning methods. This may be addressed using a family-wise correction to adjust the threshold used to indicate statistically significant results, which may improve the reliability of the data, though this has not been attempted in this study.

For each t test conducted, the mean and standard deviation of each dataset compared are given, along with the P value, t value and degrees of freedom.

#### 2.4.6. Diagenetic screening protocol

Differences in P/Ca values between different parts of the belemnite rostrum, or between belemnites may be attributable to different levels of diagenetic alteration in the calcite sampled. Previous studies on belemnites have used various techniques to differentiate between well-preserved and poorly preserved material, including visual inspection, cathode luminescence and Mn and Fe enrichment.

Visual inspection and cathode luminescence are applied to specimens prior to sampling to determine the best regions of calcite to sample. For visually inspected samples (either by eye

or by microscope), well-preserved calcite is honey-coloured and translucent with no obvious cracks (e.g., Brand and Veizer, 1980; Ullmann *et al.*, 2015). Poorly preserved calcite is usually darker in colour and opaque as well as often containing visible cracks (e.g., Ullmann *et al.*, 2015). Some studies use visual markers to assign a preservation index number to the samples (a number between 1 and 5 reflecting the preservation conditions) (e.g., Li *et al.*, 2012), whereas other studies group the samples into only 'altered' and 'well-preserved' categories (e.g., McArthur *et al.*, 2004; 2007).

Cathode luminescence is often applied to samples to assess altered material, as unaltered material is characterised by blue intrinsic luminescence, and altered material shows a dull violet to orange luminescence (e.g., Ullmann *et al.*, 2015). This technique has shown to have good agreement with geochemical proxies for alteration, especially Mn/Ca (e.g., Brand and Veizer, 1980; Ullmann *et al.*, 2015).

Geochemical screening techniques are applied to data after samples have been analysed to remove results with high levels of diagenetic overprint. Progressively more altered samples display decreased decreasing  $\delta^{13}\text{C}$ ,  $\delta^{18}\text{O}$  and Sr/Ca, and increasing Mn/Ca and Fe/Ca (e.g., Ullmann *et al.*, 2015). Fe/Ca and Mn/Ca are the most used, as  $\delta^{13}\text{C}$ ,  $\delta^{18}\text{O}$  are often targets of environmental interpretation, and Sr/Ca can vary within and between species and through time (e.g., Korte and Hesselbo, 2011; Li *et al.*, 2012; Ullmann *et al.*, 2013; Ullmann and Korte, 2015; Ullmann *et al.*, 2015). Variable screening limits of Fe/Ca and Mn/Ca have been applied in previous studies, as the concentrations of Mn and particularly Fe in calcite vary between different basins and also vary based on differing physiochemical conditions during alteration (Ullmann *et al.*, 2015), for example, upper screening limits of Mn/Ca in previous studies have varied from 50-640  $\mu\text{mol mol}^{-1}$  (Ullmann and Korte, 2015 and references therein).

In this study, an attempt was made to predominantly sample well-preserved calcite based on visual inspection, though no formal categorisation protocol was applied to the samples.

Geochemical screening was applied to variability samples and stratigraphic samples (from Chapters 4 and 5) to identify altered and unaltered samples. Limits of Fe/Ca < 600  $\mu\text{mol mol}^{-1}$  and Mn/Ca < 300  $\mu\text{mol mol}^{-1}$  were used to screen samples, though these could be refined further by choosing different limits for each basin depending on the conditions.

## 2.5. Results

### 2.5.1. Impact of calcium concentrations

After analysing multiple elements, measurements were converted into ratios to calcium (E/Ca). All E/Ca values throughout this study are given in  $\mu\text{mol mol}^{-1}$ , as this allows for comparison of concentrations between elements, as well as between samples. The impact of

different methods P/Ca ratios are discussed in this chapter, alongside the impact of natural variation of P/Ca within and between belemnites. The impact of different preparative methods on other El/Ca ratios (e.g., Mg, Sr, Na, Ba, B, S, I) is discussed in Chapter 3, alongside their natural variability within and between belemnites.

For several El/Ca ratios (including P/Ca, Na/Ca, Mg/Ca, and Sr/Ca) it was demonstrated that El/Ca ratios were highest for Bulk 1, followed by Bulk 3 then Bulk 2. It was shown that for Na, Mg and Sr values as ratios to the sample mass, Bulk 1 gave the lowest El/mass ratio followed by Bulk 2 with Bulk 3 giving the highest – which is different to the order of the measured El/Ca ratios (3.3.2.1). This was different for P/Ca ratios, where Bulk 1 gave the highest P/mass ratio, followed by Bulk 3, then Bulk 2 (Figure 7). This was the same as the order for P/Ca ratios in  $\mu\text{mol mol}^{-1}$ , suggesting that differences in Ca concentration between the three bulks had less of an effect on P/Ca ratios than on other El/Ca ratios (Figure 7; Figure 9). For Ca values given as ratios to the mass, Bulk 1 gave mean values of around  $3.5 \mu\text{mol mg}^{-1}$  – less than half the values obtained for Bulk 2 and Bulk 3 ( $\bar{x} \approx 10 \mu\text{mol mg}^{-1}$ ) (Figure 8). There was no statistically significant difference in Ca / mass values between Bulk 2 ( $\bar{x} = 10.0 \mu\text{mol mg}^{-1}$ ,  $s = 0.29 \mu\text{mol mg}^{-1}$ ) and Bulk 3 ( $\bar{x} = 9.8 \mu\text{mol mg}^{-1}$ ,  $s = 0.49 \mu\text{mol mg}^{-1}$ );  $t(28) = 2.048$ ,  $p = 0.121$  (Figure 8). Interestingly,  $10 \mu\text{mol mg}^{-1}$  corresponds to pure calcite – suggesting that Bulk 2 and 3 are formed almost completely of calcium carbonate. For these samples, the standard deviations ( $0.29$  and  $0.49 \mu\text{mol mg}^{-1}$  for Bulks 2 and 3 respectively) likely indicate the uncertainty in the method process as a whole – including weighing, processing, and analysis – though as these values re calculated across all methods trialled, they do not provide much information in this instance.

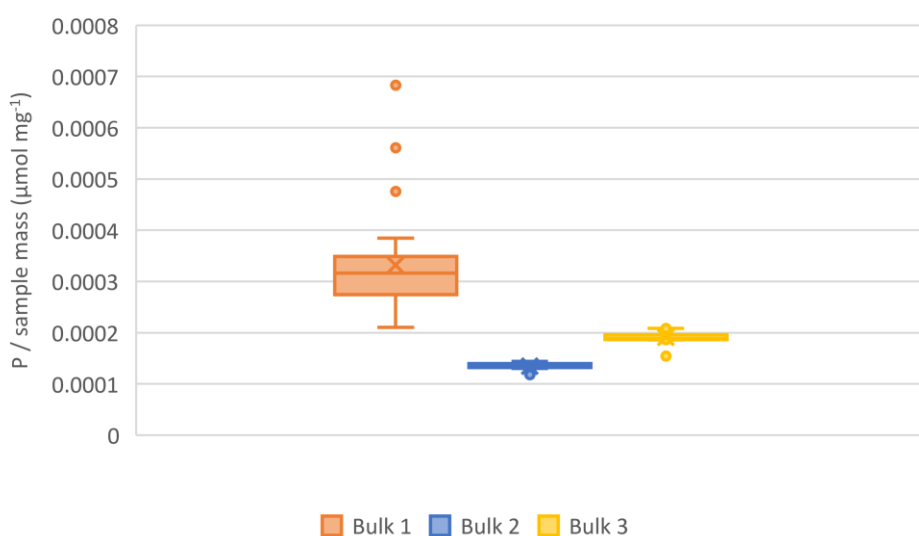


Figure 7 - Ratios of P to mass for Bulk 1, 2 and 3 samples. Samples for all preparative methods are included for each Bulk Sample.

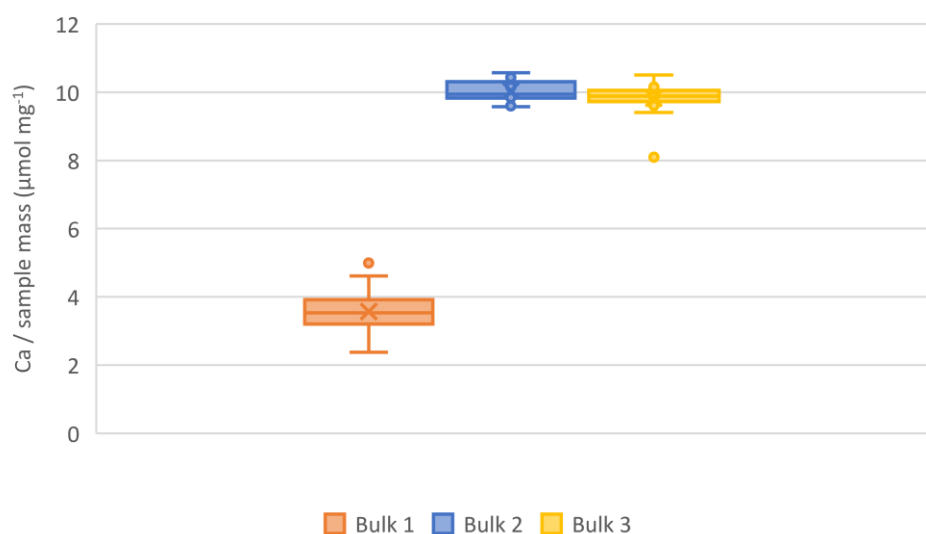


Figure 8 - Ratios of Ca to mass for Bulk 1, 2 and 3 samples. Samples for all preparative methods are included for each Bulk Sample.

## 2.5.2. Impact of cleaning method

### 2.5.2.1. Magnitude

ICP-OES and ICP-MS results for phosphorus and calcium were converted into molar ratios to calcium. The magnitude of P/Ca ratios in each Bulk Sample for each preparative method were compared.

For Bulk Samples, the magnitude of the P/Ca ratios were compared to investigate the impact of different cleaning methods. For all preparative methods, there were differences in P/Ca values between Bulk 2 (mean ( $\bar{x}$ ) = 787  $\mu\text{mol mol}^{-1}$ , standard deviation ( $s$ ) = 20  $\mu\text{mol mol}^{-1}$ ) and Bulk 3 ( $\bar{x}$  = 1,112  $\mu\text{mol mol}^{-1}$ ,  $s$  = 40  $\mu\text{mol mol}^{-1}$ );  $t(25) = 2.06$ ,  $p = 3.40\text{E-}21$  (Figure 9). Within Bulk 2 and 3, different cleaning methods did not affect the P/Ca ratio. For example, in Bulk 2, a  $t$  test showed that there was no difference between samples cleaned with hydrogen peroxide

( $\bar{x} = 790 \mu\text{mol mol}^{-1}$ ,  $s = 23 \mu\text{mol mol}^{-1}$ ) when compared to samples cleaned with water ( $\bar{x} = 785 \mu\text{mol mol}^{-1}$ ,  $s = 16 \mu\text{mol mol}^{-1}$ );  $t(15) = 2.13$ ,  $p = 0.59$ .

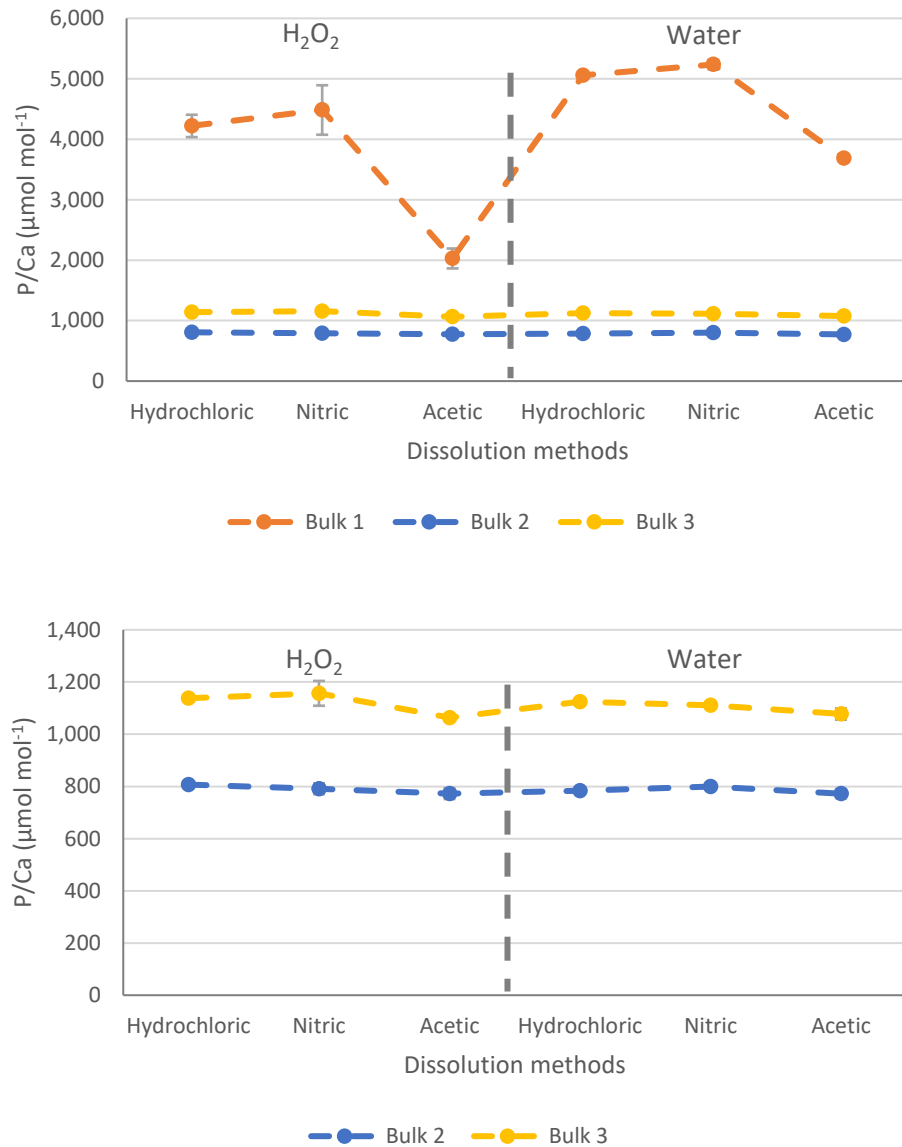


Figure 9 - Mean P/Ca values for preparative methods used in the preparation of calcite powders from Bulks 1, 2 and 3 powders, including two different cleaning methods (H<sub>2</sub>O<sub>2</sub> and water) and three different methods of dissolution (hydrochloric acid, nitric acid, and acetic acid). Error bars represent one standard deviation about the mean. Dashed lines are added for clarity of comparison, though the data is non-continuous. For each data-point  $n=3$ .

For Bulk 1, the magnitude of the P/Ca values was much larger, and more variable between preparative methods, with P/Ca values ranging from around 2,000 to 5,200  $\mu\text{mol mol}^{-1}$ . The higher P/Ca ratio for Bulk 1 is likely to be because the phragmocone was included in Bulk 1, and not in Bulks 2 and 3. The phragmocone is rich in infilled diagenetic material, which has high concentrations of phosphorus, iron, manganese, and other elements. For Bulk 1, for all dissolution methods, cleaning with H<sub>2</sub>O<sub>2</sub> ( $\bar{x} = 3,578 \mu\text{mol mol}^{-1}$ ,  $s = 1,135 \mu\text{mol mol}^{-1}$ ) gave lower P/Ca ratios than cleaning with ultrapure water ( $\bar{x} = 4,661 \mu\text{mol mol}^{-1}$ ,  $s = 694 \mu\text{mol mol}^{-1}$ )

and the difference was statistically significant based on a t test;  $t(13) = 2.16$ ,  $p = 0.04$  (Figure 9). In Bulk 1 for all dissolution methods, there was no statistically significant difference between cleaning with NaOCl ( $\bar{x} = 4,399 \mu\text{mol mol}^{-1}$ ,  $s = 774 \mu\text{mol mol}^{-1}$ ) and cleaning with hydrogen peroxide ( $\bar{x} = 3,578 \mu\text{mol mol}^{-1}$ ,  $s = 1,135 \mu\text{mol mol}^{-1}$ );  $t(14) = 2.15$ ,  $p = 0.11$  (Figure 9).

As well as Bulk Samples, different cleaning methods were tested on the Variability Samples to investigate the impact of oxidative cleaning on the variability of P/Ca ratios within and between belemnites. A subset of Variability Samples were oxidatively cleaned with hydrogen peroxide, and the P/Ca ratios for these samples were compared to P/Ca ratios for samples cleaned with water. Due to limited material, there were not enough oxidatively cleaned replicates within a single sampling site on a belemnite to compare to water-cleaned replicates from the same site. Instead of comparing replicates from within a sampling site, P/Ca values for oxidatively cleaned samples from each individual belemnite were compared to water-cleaned samples from the same belemnite.

As with Bulk 1, there were differences in P/Ca ratios between samples prepared with different cleaning methods – but unlike Bulk 1, samples cleaned with water gave lower values than samples cleaned with hydrogen peroxide (Figure 10). For example, in the *Passaloteuthis pessula* belemnite from the *Phricodoceras taylori* ammonite subzone, samples cleaned with hydrogen peroxide ( $\bar{x} = 793 \mu\text{mol mol}^{-1}$ ,  $s = 56 \mu\text{mol mol}^{-1}$ ) had statistically higher P/Ca ratios than samples cleaned with water ( $\bar{x} = 595 \mu\text{mol mol}^{-1}$ ,  $s = 62 \mu\text{mol mol}^{-1}$ );  $t(7) = 2.37$ ,  $p = 4.20\text{E}-04$  (Figure 10). Comparable results were obtained for other belemnites.

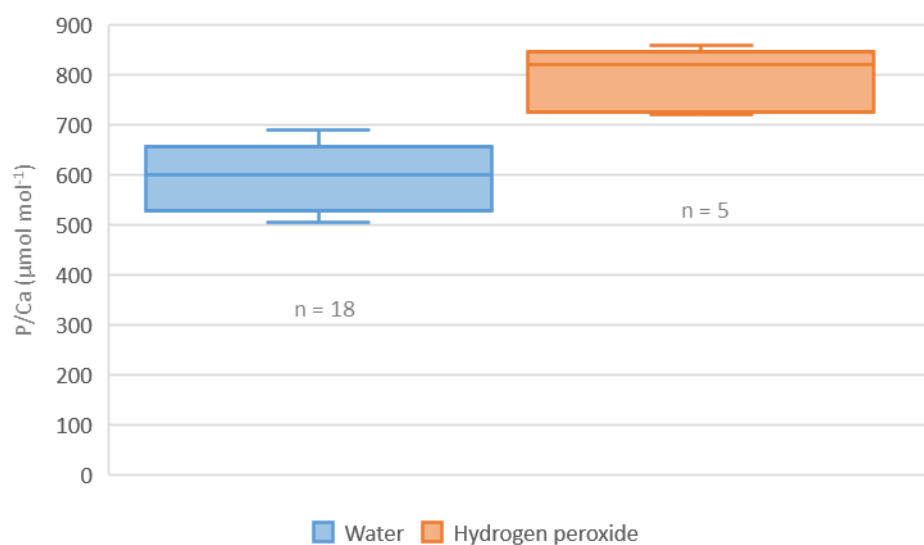


Figure 10 - P/Ca ratios for samples from a *Passaloteuthis pessula* belemnite from the *Phricodoceras taylori* ammonite zone, collected from the Wine Have section in Robin Hood's Bay, North Yorkshire. Samples in the blue box were cleaned using the water method with  $n=18$ . Samples in the orange box

were cleaned with hydrogen peroxide with  $n=5$ . This plot is representative of P/Ca plots for other individuals.

Different cleaning methods were also trialled on Modern Analogue samples of *S. officinalis* cuttlebone and *S. spirula* shell. This allowed comparison between oxidative and non-oxidative cleaning in samples with no diagenetically sourced phosphorus, but a higher percentage of organic-bound phosphorus, compared with their belemnite counterparts. As with the Variability Samples, limited sample material meant that there were not enough replicate samples from each sampling site to compare between oxidative and non-oxidative cleaning.

For both *S. officinalis* and *S. spirula*, non-oxidative cleaning with water gave substantially lower P/Ca ratios than cleaning with  $H_2O_2$  (e.g., Figure 11). Cuttlefish samples cleaned with water gave average P/Ca values of around  $500 \mu\text{mol mol}^{-1}$ , compared to average values around  $8,300 \mu\text{mol mol}^{-1}$  for samples cleaned with hydrogen peroxide – a difference of nearly 17 times (Figure 11). *S. spirula* samples cleaned with water gave average P/Ca value around  $700 \mu\text{mol mol}^{-1}$  compared with around  $3,200 \mu\text{mol mol}^{-1}$  for samples cleaned with hydrogen peroxide, a factor of five difference.

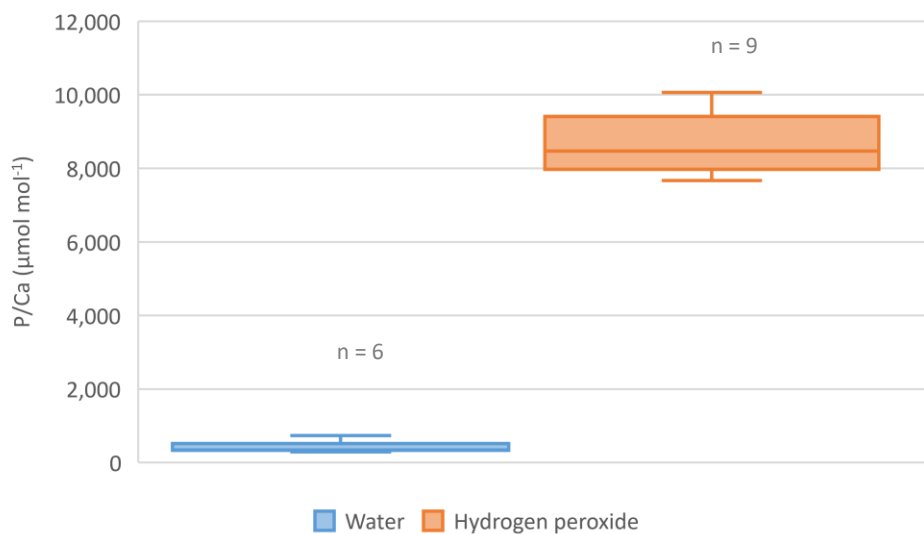


Figure 11 - P/Ca values for samples of cuttlefish (*Sepia officinalis*) aragonite cleaned with either hydrogen peroxide (orange;  $n = 6$ ) or ultrapure water (blue,  $n = 9$ ). Cuttlebone was from a 13-month-old individual raised at the MBA. The  $n$  number for the number of samples included in each box is displayed.

### 2.5.2.2. Variance

As well as the magnitude, the variance within replicate samples was evaluated. Coefficient of variation (CV) values were used as a measure of variance, as using a ratio to of the standard deviation to the mean allows datasets with different means to be compared. This allows for

comparison between different Bulk Samples with different P/Ca ratios, as well as between ratios for different elements.

For replicate analyses of the same Bulk Sample with the same preparative method, CV values were calculated from standard deviation ( $s$ ) and the mean ( $\bar{x}$ ) of the replicate analyses (Equation 1). These CV values can be compared to determine preparative methods which gave the lowest intra-sample variability.

$$CV = \frac{s}{\bar{x}} \times 100 \quad \text{Equation 1}$$

For Bulk 1, cleaning with ultrapure water had a lower CV for P/Ca ratios than either of the oxidative cleaning method, with CV values for water-only cleaning below 2 % (Figure 12). For oxidatively cleaned Bulk 1 samples, the CV values were much higher. For samples cleaned with H<sub>2</sub>O<sub>2</sub>, no dissolution methods gave CV values below 4 %. For samples cleaned with NaOCl, only dissolution with nitric acid gave CV values below 2 %, with CV values of around 3 % for dissolution with hydrochloric acid and 11 % for dissolution with acetic acid (Figure 12). For samples cleaned with water-only, there was only a 0.7 % difference between the P/Ca CV values for the different dissolution methods trialled (Figure 12). For oxidatively cleaned samples, there were larger differences between the P/Ca CV values of different dissolution

methods – for example in samples cleaned with H<sub>2</sub>O<sub>2</sub> exhibited P/Ca CV values between 4.4 % (dissolution in hydrochloric acid) and 9.1 % (dissolution in nitric acid) (Figure 12).

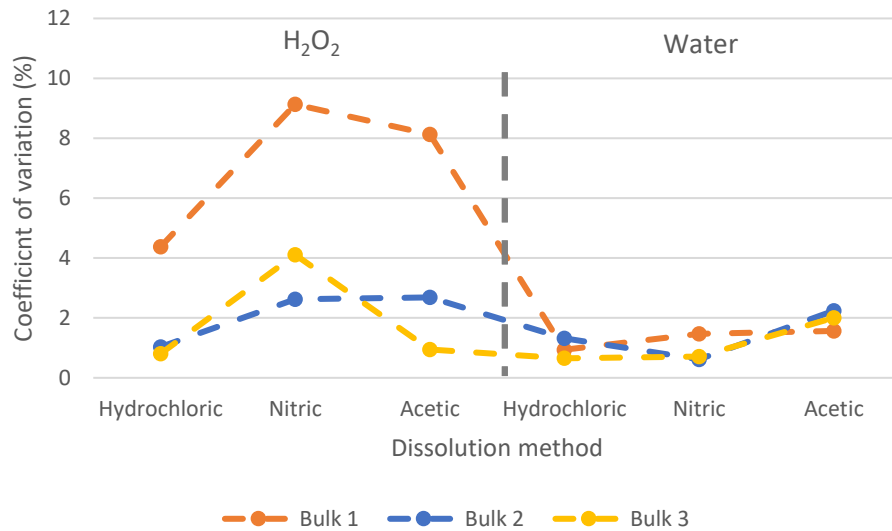


Figure 12 - coefficient of variation (%) for P/Ca values calculated from analysis of calcite powder from Bulks 1,2 and 3 using two different cleaning methods (H<sub>2</sub>O<sub>2</sub> and water) and three different methods of dissolution (hydrochloric acid, nitric acid, and acetic acid). The dashed lines are added to emphasise trends, though the data is non-continuous. For each data-point n=3.

For Bulks 2 and 3, cleaning with NaOCl was not tested, but the P/Ca ratio CV for H<sub>2</sub>O<sub>2</sub> and water with each dissolution method was compared across all Bulk Samples (Figure 12). The CV values for P/Ca in Bulks 2 and 3 were similar to the values in Bulk 1 (Figure 12). In all bulks, cleaning with ultra-pure water, in most cases, gave lower CV values for P/Ca than for oxidative cleaning with hydrogen peroxide (Figure 12). The CV values for P/Ca in all samples cleaned with water were below 2.5 % (Figure 12). As with Bulk 1, there were also smaller differences in the CV values between dissolution methods in the Bulk Samples cleaned with water than in the oxidatively cleaned samples (Figure 12).

The differences in CV values of P/Ca between Bulk Samples were more pronounced in samples cleaned with H<sub>2</sub>O<sub>2</sub> than in samples cleaned with ultra-pure water only. For samples cleaned with hydrogen peroxide, the CV values for P/Ca in Bulk 1 were larger than in Bulks 2 and 3, and in some cases by over four times.

CV values for oxidatively and non-oxidative cleaned Variability Samples were also investigated. In the Variability Samples cleaned with ultrapure water, material from each sampling site on the belemnites was analysed in triplicate whenever there was sufficient material. This allowed CV values for P/Ca ratios within sampling sites to be calculated using these replicate analyses and is referred to as CV<sub>rep</sub>. For oxidatively cleaned samples, limited sample material meant only

samples from a subset of sampling sites from each belemnite were cleaned with H<sub>2</sub>O<sub>2</sub>, and none of these were analysed in triplicate. Instead, CV values were calculated for whole individual belemnites – referred to as CV<sub>ind</sub>, and belemnites with fewer than three oxidatively cleaned samples were excluded. CV<sub>ind</sub> values were also calculated for samples cleaned with water. For water-cleaned samples, it was shown that CV<sub>rep</sub> values ( $\bar{x}_{CV} = 1.5\%$ ;  $s_{CV} = 1.0$ ;  $n = 33$ ) were lower than the CV<sub>ind</sub> values ( $\bar{x}_{CV} = 6.5\%$ ,  $s_{CV} = 3.2$ ,  $n = 10$ ), though both were low enough to be considered highly reproducible. The CV<sub>rep</sub> samples for water-cleaned Variability Samples were similar to the CV values obtained for Bulk Samples, indicating the different sampling method used for the Variability Samples (precision sampling with a drill rather than powdering an entire belemnite) did not introduce extra variability in the P/Ca value. Oxidatively cleaned samples gave lower CV<sub>ind</sub> than water cleaned samples ( $\bar{x}_{CV} = 3.3\%$ ;  $s_{CV} = 2.5$ ;  $n = 5$ ) indicating reduced variability in samples within the same belemnite when samples were cleaned using hydrogen peroxide.

For Modern Analogue samples there were also not enough replicate analyses for each combination of sampling site and cleaning method to generate CV values for each sampling site. CV values were instead calculated from P/Ca ratios for all samples within each individual *S. officinalis* cuttlebone or *S. spirula* shell – CV<sub>ind</sub>. Individuals with fewer than three samples cleaned with hydrogen peroxide, or fewer than three samples cleaned with water were excluded – so CV<sub>ind</sub> values were only calculated for both *S. officinalis* cuttlebones and one *S. spirula* shell (Table 6).

Table 6 – CV<sub>ind</sub> values (CV values calculated from all samples taken from an individual *S. officinalis* cuttlebone or *S. spirula* shell) for P/Ca values of calcium carbonate from two cuttlebones and one *Spirula* shell.

Species	Individual	Value with H <sub>2</sub> O <sub>2</sub>		Value with water	
		CV <sub>ind</sub>	n	CV <sub>ind</sub>	n
<i>S. officinalis</i> (cuttlefish)	1	13.30	3	34.77	3
	2	9.20	6	32.37	9
<i>S. spirula</i>	1	13.24	5	2.71	6

For both *S. officinalis* cuttlebones analysed, cleaning with H<sub>2</sub>O<sub>2</sub> gave lower CV<sub>ind</sub> values for P/Ca ratios than cleaning with water (Table 6). For the *S. spirula* shells, where CV<sub>ind</sub> values for cleaning with hydrogen peroxide and water could be calculated the opposite was true; cleaning with water gave lower CV<sub>ind</sub> values than cleaning with H<sub>2</sub>O<sub>2</sub> (Table 6). For *S. spirula*, the CV values were all low (< 20) indicating a high reproducibility of P/Ca ratios within individual shells. In *S. officinalis* cuttlebones, the CV<sub>ind</sub> for samples cleaned with water were

higher suggesting this method of cleaning gives less reproducible P/Ca results for cuttlebone samples.

### 2.5.3. Impact of dissolution method

#### 2.5.3.1. Magnitude

For Bulk Samples, in addition to trialling different cleaning methods, three different acids were used for dissolution: acetic acid, hydrochloric acid and nitric acid. The impact of the different dissolution methods within each Bulk Sample and preparative method was examined, and a series of t tests were carried out, to investigate any significant differences between the different dissolution methods (Table 7). For Bulks 2 and 3, there were no significant differences between the dissolution methods for any cleaning method (Table 7). For Bulk 1, there were no statistically significant differences in P/Ca values between samples dissolved in nitric acid and samples dissolved in hydrochloric acid, for any of the cleaning methods (Table 7). For Bulk 1, both hydrochloric and nitric acid gave consistently higher P/Ca ratios than samples dissolved in acetic acid by a factor of around 1.5, and these differences were shown to be statistically significant (Table 7).

Table 7 - Results of t tests conducted on P/Ca values from replicate analyses of Bulk Samples with different preparative methods, which were used to investigate differences in P/Ca values as a result of different acids used for dissolution of the carbonate. All values are calculated from triplicate analyses with each method ( $n = 3$ ). Mean ( $\bar{x}$ ) and standard deviation ( $s$ ) are given for each preparative method and sample combination. Independent two sample t tests assuming unequal variance were performed with a 95 % confidence limit, comparing results of dissolution with nitric acid and hydrochloric acid, and nitric acid with acetic acid. For each t test, degrees of freedom ( $df$ ), two-tail P values ( $P$ ) and two-tail t critical values ( $t$ ) are reported for each t test. P results which are statistically significant differences are highlighted in pale green.

Sample material	Cleaning method	Hydrochloric		Nitric		Acetic		Hydrochloric and nitric			Nitric and acetic		
		$\bar{x}$	$s$	$\bar{x}$	$s$	$\bar{x}$	$s$	$df$	$P$	$t$	$df$	$P$	$t$
Bulk 1	Water	5,058	48	5,236	77	3,690	58	3	6.78E-02	3.18	4	2.20E-05	2.78
	NaOCl	4,794	143	5,038	88	3,365	369	3	1.32E-01	3.18	2	2.47E-02	4.30
	H <sub>2</sub> O <sub>2</sub>	4,220	185	4,484	409	2,028	165	3	4.66E-01	3.18	3	4.27E-03	3.18
Bulk 2	Water	783	10	799	5	772	17	3	1.38E-01	3.18	2	1.66E-01	4.30
	H <sub>2</sub> O <sub>2</sub>	807	8	791	21	773	21	3	3.94E-01	3.18	4	4.19E-01	2.78
Bulk 3	Water	1,124	7	1,112	8	1,077	22	4	1.76E-01	2.78	3	1.26E-01	3.18
	H <sub>2</sub> O <sub>2</sub>	1,138	9	1,157	48	1,064	10	2	6.44E-01	4.30	2	1.14E-01	4.30

### 2.5.3.2. Variance

The CV for P/Ca values from replicate analyses of each combination of Bulk Sample, cleaning method and dissolution method were calculated to give an idea of the reproducibility of each method (Figure 12). For different Bulk Samples and cleaning methods, there was no dissolution method which consistently gave the lowest CV values. All of the calculated CV values were below 15 % which is considered a good level of reproducibility for this method (Figure 12).

### 2.5.4. Impact of sample size

Different sample masses gave similar magnitudes for P/Ca values. For example, for Bulk 3, 2 mg ( $\bar{x} = 1104$ ,  $s = 19$ ), 5 mg ( $\bar{x} = 1063$ ,  $s = 10$ ) and 10 mg ( $\bar{x} = 1025$ ,  $s = 18$ ) samples cleaned with hydrogen peroxide and dissolved in acetic acid all gave similar P/Ca values.

For all Bulk Samples, CV values were calculated for each of the different sample mass. For Bulk 3, all of the sample masses gave similar CV values of around 1.7 %. For Bulk 3, 5 mg and 10 mg samples gave similar CV values and the CV value for 2 mg samples could not be detected as phosphorus fell below the limit of detection for two of the three replicate samples. For Bulk 1, 2 mg samples had the highest CV value of 12.7 %, followed by 5 mg samples with 8.1 % and then 10 mg samples with 2.6 %.

### 2.5.5. Investigating variability

As well as examining differences in P/Ca ratios between different methods, differences in P/Ca ratios within and between belemnites was examined. The Variability Samples allowed us to examine differences in P/Ca within different regions of the belemnite rostra, between belemnites of the same species, between belemnites of different species, and between stratigraphic levels.

#### 2.5.5.1. Screening for diagenesis

High Mn/Ca and Fe/Ca were used as exclusionary criteria to screen out samples with high levels of diagenetic alteration. Mn/Ca and Fe/Ca showed a positive correlation in both stratigraphic levels with  $R^2$  values of 0.77 and 0.98 for samples from Penny Nab and Wine Haven respectively (Figure 13).

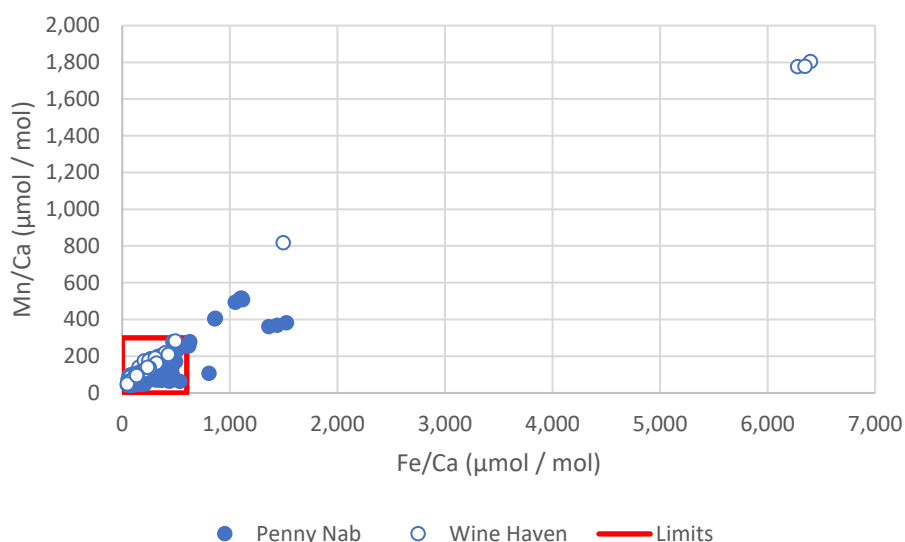


Figure 13 – Fe/Ca values against Mn/Ca values for all Variability Sample analyses of belemnites from both the *Amaltheus gibbosus* ammonite subzone from the Penny Nab section (filled blue) and belemnites from the *Phricodoceras taylori* ammonite subzone from the Wine Haven section (outline blue). Also indicated are the limits Mn/Ca > 300 and Fe/Ca > 600 which were subsequently applied to exclude samples with higher levels of diagenetic alteration.

Limits of Fe/Ca < 600  $\mu\text{mol mol}^{-1}$  and Mn/Ca < 300  $\mu\text{mol mol}^{-1}$  were applied, for the Variability Samples this excluded just over 10 % of samples. These limits are similar to limits set in previous studies of belemnite calcite, though these limits vary from study to study (Ullmann and Korte, 2015; Stevens *et al.*, 2022). It was found that for samples which met the iron and manganese screening criteria there was still a correlation between Mn/Ca and Fe/Ca – particularly in the samples from the Wine Haven section, with  $R^2$  values of 0.39 and 0.93 for samples from the Penny Nab section and Wine Haven section, respectively. This indicates that these samples have still undergone a degree of diagenetic alteration, so correlations between iron and manganese and phosphorus were investigated to ensure that the diagenetic alteration was not impacting the P/Ca ratios.

Table 8 –  $R^2$  values indicating correlation between P/Ca and either Mn/Ca and Fe/Ca for Variability Samples from the Penny Nab and Wine Haven sections, which either had no screening criteria applied, or which had been screened to remove samples with a high level of diagenetic alteration (using Mn/Ca < 300  $\mu\text{mol mol}^{-1}$  and Fe/Ca < 600  $\mu\text{mol mol}^{-1}$ ).

Data	Penny Nab section		Wine Haven section	
	Fe	Mn	Fe	Mn
All data	1.0E-01	1.9E-01	6.5E-03	4.1E-02
Screened samples	3.0E-05	3.6E-02	4.4E-01	4.2E-01

Even for samples which had not been screened, the correlation between P/Ca and either Fe/Ca and Mn/Ca was low with the highest  $R^2$  value (0.19) observed for correlation between P/Ca and Mn/C in Penny Nab samples (Table 8). After screening conditions had been applied, the  $R^2$

value for correlation between P/Ca and both Fe/Ca and Mn/Ca decreased in samples from Penny Nab but increased for samples from Wine Haven (Table 8). The highest R<sup>2</sup> value was for correlation between Fe/Ca and P/Ca in screened samples from Wine Haven, with an R<sup>2</sup> value of 0.44 – which is reasonably high (Table 8). This suggests that the screening criteria used here was successful in eliminating samples where diagenesis is influencing P/Ca ratios for samples from Penny Nab, but lower limits may be needed for samples from Wine Haven. For screened samples from Wine Haven, it should be considered that P/Ca values may still be impacted by diagenesis.

#### 2.5.5.2. Variability within a belemnite

After screening for diagenesis, P/Ca values were used to determine the CV<sub>ind</sub> for each belemnite rostrum (as described in Section 2.5.2.2). The CV<sub>ind</sub> for each belemnite ( $\bar{x}_{CV} = 6.5\%$ ,  $s_{CV} = 3.2$ ,  $n = 10$ ) was low, with a highest value of 11 %, indicating a high level of reproducibility of P/Ca ratios within each belemnite.

Trends in P/Ca ratios along the length of the belemnite rostra were examined. For each sample, the distance along the rostrum from the apex was converted to a percentage of the total rostrum length (Equation 2).

$$\begin{aligned} \text{Distance along rostrum (\%)} & \qquad \qquad \qquad \text{Equation 2} \\ & = \frac{\text{Distance from apex to sampling site (cm)}}{\text{Total rostrum length (cm)}} \times 100 \end{aligned}$$

The percentage distance along each rostrum was compared to the average P/Ca ratios for each sampling site from each belemnite. For most individuals, P/Ca values were found to be slightly elevated towards the apex of the rostrum (Figure 14). This was seen in all of the *Nannobelus delicatus* belemnites from Wine Haven, but not in the *Passaloteuthis* sp. belemnite from the same section (Figure 14). For each *Nannobelus delicatus* belemnite there was a negative correlation between the distance along the rostrum, and the P/Ca ratio – with R<sup>2</sup> values for each individual above 0.55 (Figure 14). For belemnites from the Penny Nab section, similar trends were seen for samples from *Bairistowius* sp. belemnite and one of the *Parapassaloteuthis* belemnites with R<sup>2</sup> values of 0.312 and 0.564, respectively. For the other belemnites from Penny Nab, no coherent trend in P/Ca ratios with distance along the rostrum was observed.

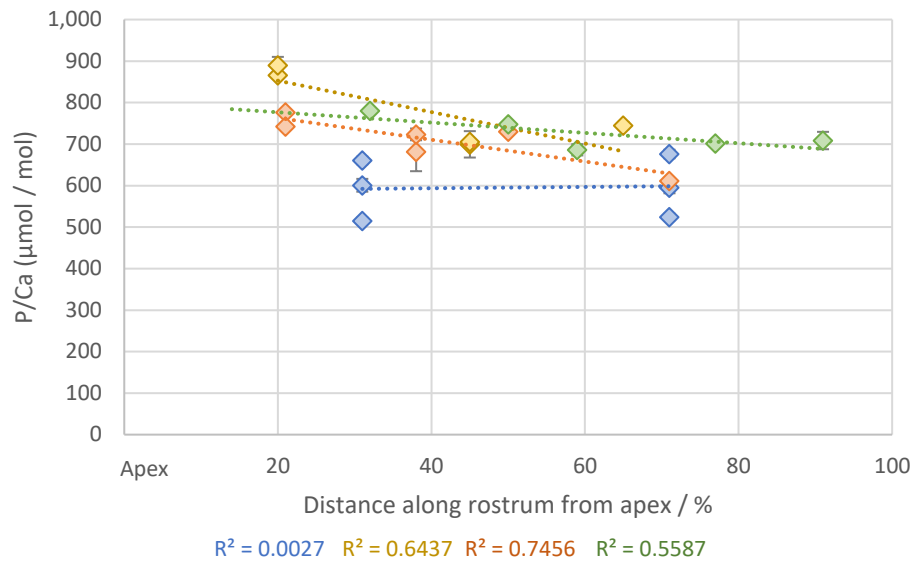


Figure 14 – P/Ca against the distance along the belemnite rostrum from the apex for four individual belemnites collected from Wine Haven, North Yorkshire. These belemnites are from the *Phricodoceras taylori* ammonite zone in the Lower Pliensbachian. Each colour represents a different individual belemnite. The sample in blue is *Passaloteuthis* sp. And the other three samples are *Nannobelus delicatus*. Each data point is the average of triplicate sample analysis and error bars depict one standard deviation about the mean where  $n=3$ .  $R^2$  values for each line are indicated in the colour matching the points.

### 2.5.5.3. Between belemnites

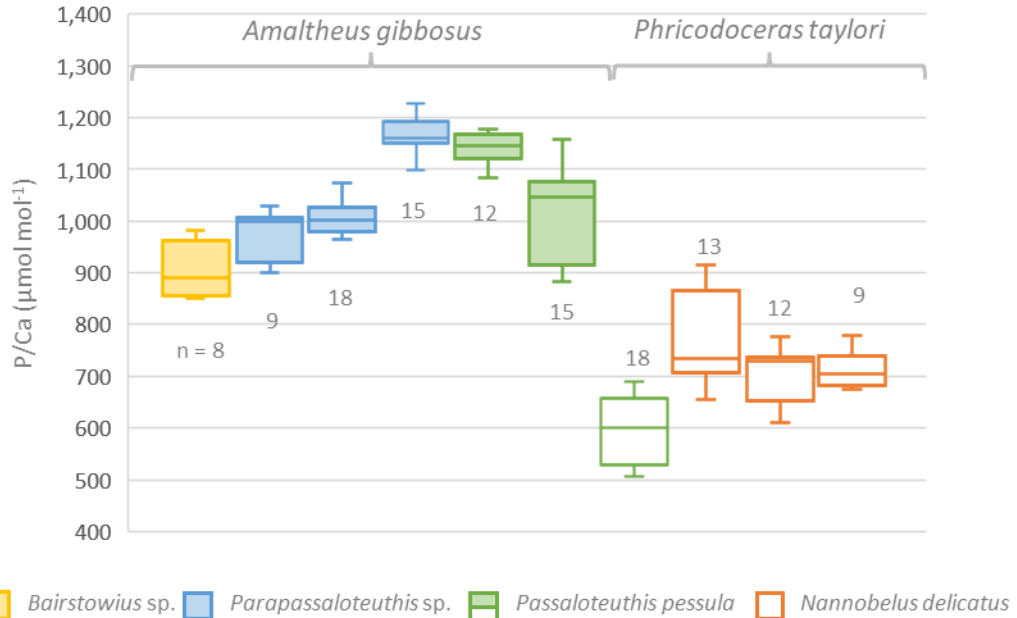


Figure 15 – P/Ca values for 10 belemnites from two different stratigraphic heights collected from the Yorkshire coast. Each box represents one individual belemnite. Each colour represents a belemnite species. Each individual was sampled six times along the length of the rostrum, and where material was available each sample was analysed in triplicate. Filled boxes indicate samples collected from Penny Nab in Staithes from the *Amaltheus gibbosus* ammonite subzone in the Upper Pliensbachian. Unfilled boxes indicate samples collected from Wine Haven in Robin Hood's Bay from the *Phricodoceras taylori* ammonite subzone in the Lower Pliensbachian. The  $n$  number for the number of samples included in each box is displayed.

The variance in P/Ca between belemnites is larger than the variance within each specimen (Figure 15). For each stratigraphic level studied, a CV value was calculated ( $CV_{M}$ ) to give an indication of the variability of P/Ca ratios between belemnites from the same stratigraphic level. For samples from the *Amaltheus gibbosus* ammonite subzone, the  $CV_{M}$  value was 10.2 % ( $n = 77$ ); for samples from the *Phricodoceras taylori* ammonite subzone, the  $CV_{M}$  value was 13.5 % ( $n = 52$ ). These CV values are higher than the  $CV_{ind}$  values for variability of P/Ca values within individual belemnites ( $\bar{x}_{CV} = 6.5$  %,  $s_{CV} = 3.2$ ,  $n = 10$ ) but are still low and indicate high reproducibility of P/Ca values within a stratigraphic level.

The impact of taxonomy on the P/Ca values within a stratigraphic level was investigated. A t test showed that there was no significant difference between P/Ca values in samples from *Parapassaloteuthis* sp. ( $\bar{x} = 1054$ ,  $s = 89$ ) and samples from *Passaloteuthis pessula* ( $\bar{x} = 1070$ ,  $s = 97$ ) in samples from the *Amaltheus gibbosus* ammonite subzone);  $t(51) = 0.666$ ,  $p = 0.508$ . Therefore, no significant taxonomic effect was in determining P/Ca ratios for these species.

The largest difference observed was between individuals from different stratigraphic levels. A further t test was performed to compare P/Ca values between the stratigraphic levels. There was a significant difference in P/Ca values between samples from the *Amaltheus gibbosus* ammonite subzone ( $\bar{x} = 1042$ ,  $s = 106$ ) and samples from the *Phricodoceras taylori* ammonite subzone ( $\bar{x} = 684$ ,  $s = 92$ );  $t(119) = 20.12$ ,  $p = 4.10E-40$ .

The impact of the size of belemnites on P/Ca ratios were also investigated. The sizes of the belemnites studied varied from 3.5 to 6.8 cm long. For every P/Ca ratio there was no significant correlation with rostrum length and element ratios to calcium. This may have been affected by the sample selection criteria for the variability test, where larger samples which were able to be sampled multiple times were selected preferentially.

#### 2.5.5.4. Variability in modern analogues

##### 2.5.5.4.1. Within individuals

$CV_{ind}$  values were calculated to assess the variability of P/Ca within individual *S. officinalis* cuttlebones and *S. spirula* shells, as described in Section 2.5.2.2 (Table 6).  $CV_{ind}$  values for *S. officinalis* cleaned with water were considerably higher than the comparable results for belemnites ( $\bar{x}_{CV} = 6.5$  %,  $s_{CV} = 3.2$ ,  $n = 10$ ), and were all over 30 %, we would consider this level of variability too high for robust determination of P/Ca values for these species (Table 6; Figure 16). For *S. officinalis* cuttlebone samples cleaned with hydrogen peroxide, the  $CV_{ind}$  values were 9 % and 13 % for each cuttlebone, which is closer to the  $CV_{ind}$  values obtained for belemnites, though still quite a lot higher (Table 6; Figure 16). For *S. spirula*,  $CV_{ind}$  values could only be calculated for one individual – for this individual the  $CV_{ind}$  values were around 3 % for

samples cleaned with water and around 13 % for samples cleaned with hydrogen peroxide, which is similar to the  $CV_{ind}$  values obtained from belemnites ( $\bar{x}_{CV} = 6.5 \%$ ,  $s_{CV} = 3.2$ ,  $n = 10$ ) (Table 6; Figure 17).

#### 2.5.5.4.2. *Between individuals*

A t test was conducted to compare P/Ca values from the modern cuttlebones of different s. The t test showed that in samples cleaned with water, there was no statistically significant difference in P/Ca values between samples from the younger cuttlefish ( $\bar{x} = 733$ ,  $s = 255$ ) and samples from the older cuttlefish ( $\bar{x} = 418$ ,  $s = 135$ );  $t(2) = 4.30$ ,  $p = 0.23$  (Figure 16).

Comparable results were found for samples cleaned with hydrogen peroxide.

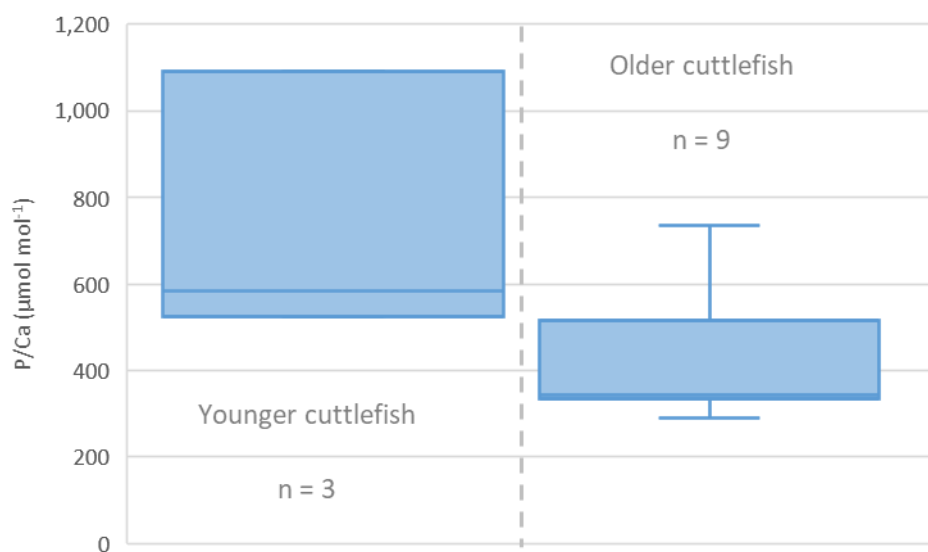


Figure 16 – P/Ca values for aragonite samples from two different *S. officinalis* cuttlebones cleaned with ultrapure water. The younger cuttlefish was aged 8 months at death and the older was aged 13 months. Both cuttlebones were from individuals raised at the MBA. Each box represents analysis of samples from one individual, and the n number for the number of samples included in each box is displayed.

A further t test was conducted to compare P/Ca values from the shells from two different *S. spirula* specimens. Specimens were selected for comparison on the basis there was enough material for a minimum of three samples from each shell which could be compared. The t test showed that between the specimens examined, there was a statistically significant difference in P/Ca ratios, with the one specimen ( $\bar{x} = 768$ ;  $s = 21$ ;  $n = 6$ ) giving higher P/Ca values than the other specimen ( $\bar{x} = 640$ ,  $s = 50$ ,  $n = 4$ );  $t(4) = 2.78$ ,  $p = 0.0137$ .

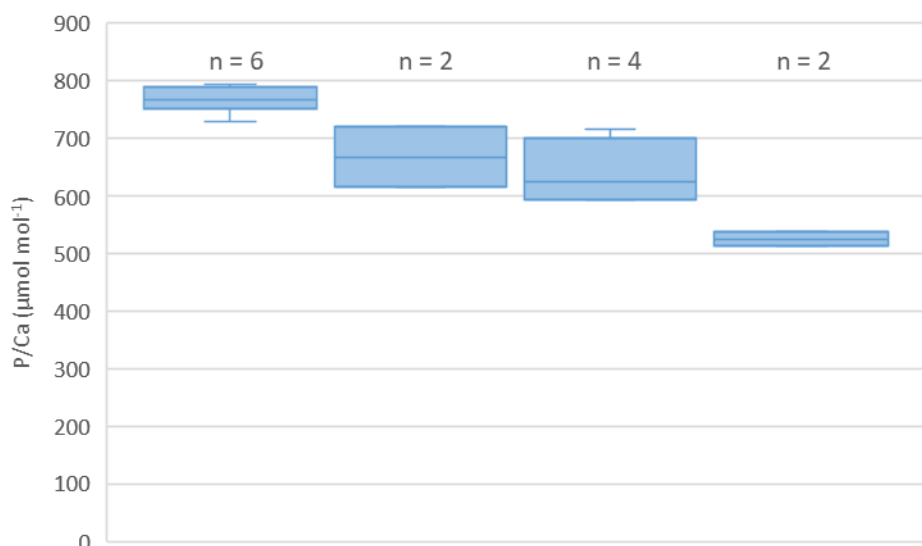


Figure 17 - P/Ca values for samples from four individual aragonitic *S. spirula* shells collected from the New Zealand coastline. Samples were prepared with water-only cleaning (blue). Each box represents analysis of samples from one individual, and the n number for the number of samples included in each box is displayed.

## 2.6. Discussion

### 2.6.1. Impact of cleaning method

Oxidative and non-oxidative cleaning methods were tested on Bulk Samples, Variability Samples and Modern Analogue samples. The different cleaning methods had different impacts on the magnitude and variability of P/Ca ratios for each of the materials tested (summarised in Table 9). This is likely to relate to the different forms of phosphorus present in the samples, which will be present in different proportions (Table 9).

Despite the range of different preparative methods, almost all combinations of sample, cleaning method and dissolution method gave high reproducibility of results between replicate samples and within individuals. Although the variability between replicates and within individuals was generally very low, there were some differences in the CV for some samples and cleaning methods, as well as differences in the magnitude of P/Ca values. These differences were most pronounced for the Modern Analogue samples but were also notable in samples from Bulk 1 (Table 9). This is likely due to both Modern Analogue samples and Bulk 1 containing elevated levels of 'contaminant phosphorus' – such as diagenetic minerals including secondary calcite and aragonite, authigenic phosphorus, apatite, and organic bound phosphorus. Different components of the samples will respond differently to each of the preparative steps, which can explain the differences between them.

Table 9 - Summary of differences in magnitude and variance of P/Ca ratios of different sample materials with different cleaning methods

Sample	Features of sample	Magnitude	Variability
<b>Bulk 1</b>	Whole belemnite powdered; contains phragmocone – high concentration of diagenetic material	Cleaning with water gave slightly higher P/Ca values than cleaning with either NaOCl or H <sub>2</sub> O <sub>2</sub> . No difference between cleaning with NaOCl and H <sub>2</sub> O <sub>2</sub> (Figure 9).	Samples cleaned with H <sub>2</sub> O <sub>2</sub> gave higher CV values (increased variability) in P/Ca ratios compared to samples cleaned with water (Figure 12). All CV values were still low enough to indicate good reproducibility.
<b>Bulk 2 and 3</b>	Whole belemnite powdered; phragmocone removed – some diagenetic material likely	No difference in the magnitude of P/Ca values between samples cleaned with H <sub>2</sub> O <sub>2</sub> and samples cleaned with water (Figure 9).	Samples cleaned with H <sub>2</sub> O <sub>2</sub> gave slightly higher CV values (increased variability) in P/Ca ratios compared to samples cleaned with water (Figure 12). All CV values were still low enough to indicate good reproducibility.
<b>Variability</b>	Belemnite calcite selectively sampled to avoid visually altered calcite – smaller amounts of diagenetic material likely	Cleaning with H <sub>2</sub> O <sub>2</sub> gave slightly higher P/Ca values than cleaning with water (Figure 10).	Differences in cleaning methods for CV <sub>rep</sub> values could not be examined due to limited sample material – CV <sub>ind</sub> examined instead. Samples cleaned with water gave higher CV values (increased variability) in P/Ca ratios compared to samples cleaned with H <sub>2</sub> O <sub>2</sub> (2.5.2.2). All CV <sub>ind</sub> and CV <sub>rep</sub> values were still low enough to indicate good reproducibility.
<b><i>S. spirula</i> shells</b>	<i>S. spirula</i> shell aragonite. Modern, so no diagenetic alteration. Likely elevated	Cleaning with H <sub>2</sub> O <sub>2</sub> gave much higher P/Ca values than cleaning with water –	Differences in cleaning methods for CV <sub>rep</sub> values couldn't be examined due

	levels of organic-bound phosphorus.	by a factor of nearly 5 times (2.5.2.1).	to limited sample material – CV <sub>ind</sub> examined instead. Samples cleaned with H <sub>2</sub> O <sub>2</sub> gave higher CV values (increased variability) in P/Ca ratios compared to samples cleaned with water (2.5.2.2). All CV <sub>ind</sub> values were still low enough to indicate good reproducibility.
<b><i>S. officinalis</i> cuttlebones</b>	Porous cuttlebone aragonite. Modern, so no diagenetic alteration. Likely very high levels of organic-bound phosphorus from material trapped in the pores.	Cleaning with H <sub>2</sub> O <sub>2</sub> gave much higher P/Ca values than cleaning with water – by a factor of nearly 17 times (Figure 11).	Differences in cleaning methods for CV <sub>rep</sub> values could not be examined due to limited sample material – CV <sub>ind</sub> examined instead. Samples cleaned with water gave much higher CV values (increased variability) in P/Ca ratios compared to samples cleaned with H <sub>2</sub> O <sub>2</sub> (2.5.2.2). All CV <sub>ind</sub> values for samples cleaned with water were high enough to indicate poor reproducibility, samples cleaned with H <sub>2</sub> O <sub>2</sub> gave CV values low enough to indicate good reproducibility.

Although phosphorus in belemnites has not been well studied, in other modern biogenic carbonates such as corals, phosphorus is mostly present in the skeleton in an inorganic form such as hydrogen, di-hydrogen or hydrogen phosphate, along with some organic-bound phosphorus and hydroxyl-apatite (Ishikawa and Ichikuni, 1981; House and Donaldson, 1986; Mason *et al.*, 2011; Dodd *et al.*, 2021). Assuming similar forms of phosphorus are present in primary belemnite calcite, the Variability Samples are likely to contain mostly inorganic phosphorus, as they were sampled to avoid visually altered calcite and the results were

screened for diagenesis (2.4.6; 2.5.5.1). Bulks 2 and 3 were generated from whole powdered belemnites, and the data was not screened for diagenetic alteration, so there is likely to be a slightly higher quantity of diagenetic minerals, such as altered calcite, aragonite, and apatite. Bulk 1 contains the phragmocone of the belemnite, which is known to be high in infilled sediment and diagenetic minerals, making it a contaminated Bulk. Bulk 1 will likely have much higher concentrations of a range of minerals from sediment and diagenetic processes, mixtures of clays, quartz, and feldspars from the burial sediments; crystalline apatite and authigenic phosphate minerals from organic matter decomposition and the reduction of iron oxides and iron containing minerals such as pyrite and iron oxides (e.g., Ruttenberg, 1992; Thompson *et al.*, 2019). Due to a mixture of minerals present, the phragmocone is known to have high concentrations of iron, manganese, phosphorus, and other elements. This is the reason Bulk 1 samples gave higher P/Ca ratios compared to samples from Bulks 2 and 3.

Modern samples of *S. officinalis* cuttlebone and *S. spirula* shell aragonite contain no diagenetically altered material, and higher concentrations of organic-bound phosphorus. *S. officinalis* cuttlebones have an organic matter content of 3-4.5 %, mostly comprised of a chitin-protein complex from the network of organic membranes within the pores of the carbonate structure (Birchall and Thomas, 1983; Checa *et al.*, 2015). *S. spirula* also have a thin organic matter rich membrane comprised of conchiolin between the prismatic layers of the conch wall (Mutvei, 1964; Florek *et al.*, 2009; Hoffmann *et al.*, 2018; Checa *et al.*, 2022). Quantification of *S. spirula* shells organic matter has not been conducted, but the shells of the similar chambered nautilus (*Nautilus pompilius*) have an organic matter content of around 1 % (Petrochenkov *et al.*, 2016). Due to this, it is likely that the cuttlebone has a higher concentration of organic matter than *S. spirula* shells – though values for *S. spirula* would need to be obtained to demonstrate this definitively.

Different preparative methods will have impacted these different pools of phosphorus in different ways. For organic matter, oxidative cleaning will have broken down any organic-bound phosphorus to form free phosphate this it was able to access. Despite this, Modern Analogue samples with high levels of organic-bound phosphorus gave higher P/Ca ratios with oxidative cleaning than with water. This is likely due to the tendency of phosphate to adsorb to the surface of powders, preventing it from being removed with the oxidative agent or subsequent water washes (Ruttenberg, 1992). Phosphate is readily adsorbed to the surface of powders, with different minerals adsorbing phosphate more or less strongly, with reactive iron phases such as iron (oxy)hydroxides adsorbing phosphate most readily (Ruttenberg, 1992). The amount of phosphate which is able to be adsorbed depends on the distribution of the iron phases, as well as the surface area as determined by the crystallinity and grain size of the

powder (Ruttenberg, 1992). Powders with higher concentrations of reactive iron, as well as lower crystallinity and smaller grain sizes, have a higher surface area so provide more adsorption sites for phosphate to adhere to, allowing more phosphate to be retained adsorbed to the powder (Ruttenberg, 1992). In samples cleaned with water only, the organic material is not broken down and phosphate is not released. In this case, the organic-bound phosphorus is either removed in the water washes (in the case of water-soluble organic material) or remains undissolved in the acid – giving lower P/Ca ratios. A small fraction may also be dissolved in the acid (in the case of acid-soluble and water-insoluble organic matter), though acetic acid is a weak acid which is less able to dissolve large, complex organic molecules such as the chitin-protein complexes found inside cuttlebones (Checa *et al.*, 2015).

For *S. officinalis* cuttlebones, the variability was higher ( $CV_{ind}$  values > 30 %) in samples cleaned with water than in samples cleaned with hydrogen peroxide ( $CV_{ind}$  values  $\approx$  11 %). This may be due to either variable amounts of the water-soluble organic matter being removed by the water washes, or different amounts of organic matter being dissolved by the acid, or some combination of the two. In hydrogen peroxide-cleaned cuttlefish samples, the adsorbed phosphate from the high concentration of broken-down organic matter may have saturated the adsorption sites on the remaining calcium carbonate powder. Any remaining free phosphate would have been removed, with the remaining phosphate correlating with the availability of adsorption sites (and therefore other factors such as grain size and homogeneity of the powder) which may have decreased the measured variability in P/Ca ratios. *S. spirula*, on the other hand, showed lower variability in samples cleaned with hydrogen peroxide compared to those cleaned with water (Table 6). This may be a result of potential differences in concentration of organic matter between *S. spirula* shells and cuttlebones. *S. officinalis* cuttlebones have an organic matter content of 3-4.5 %, from membranes trapped in the pores of the aragonite (Birchall and Thomas, 1983; Checa *et al.*, 2015). *S. spirula* are likely to have a lower organic matter content than this, potentially similar to the organic content of chambered nautilus (*Nautilus pompilius*) which has an organic matter content of around 1 % (Mutvei, 1964; Petrochenkov *et al.*, 2018; Checa *et al.*, 2022). The variability for oxidatively cleaned *S. spirula* shell samples ( $CV_{ind} \approx$  13 %) was similar to oxidatively cleaned *S. officinalis* cuttlebone samples ( $CV_{ind} \approx$  11 %), but for *S. spirula* the variability for water cleaned samples was much lower ( $CV_{ind} \approx$  3 %) (Table 6). One explanation for this is that different forms of organic matter are present in the *S. spirula* shells compared to the organic matter in the porous *S. officinalis* cuttlebones, which may exhibit different solubilities in water. It is possible that the conchiolin organic in *S. spirula* shells is less soluble in water than the chitin-protein complexes found in the pores of *S. officinalis* cuttlebones, and the P/Ca values for *S. spirula*

shells are more reflective of inorganic phosphorus. It is also possible that the lower  $CV_{ind}$  values for water-cleaned *S. spirula* compared to water cleaned *S. officinalis* cuttlebones are due to a less variability in P/Ca ratios between different sampling sites on the individual, though this doesn't fully account for the similar  $CV_{ind}$  values of oxidatively cleaned samples.

In belemnites, organic-bound phosphorus is expected to represent a smaller proportion of the phosphorus than carbonate-associated phosphorus. Any primary organic-bound phosphorus is likely to have been converted by early diagenesis and microbial breakdown of the organic matter in belemnite soft tissue and sediment to other forms of phosphorus, such as apatite (Hoffmann *et al.*, 2016). This is supported by the differences in P/Ca values between the modern analogues and the belemnite samples. In Modern Analogue samples, cleaning with hydrogen peroxide gave substantially higher P/Ca values than cleaning with water due to the breakdown and release of organic-bound phosphorus and its adsorption as phosphate. In belemnite samples, differences in P/Ca values between samples cleaned with each method were much smaller. In Variability Samples, cleaning with hydrogen peroxide gave only slightly higher P/Ca values than cleaning with water (Figure 10); in Bulks 2 and 3 there was no difference in the magnitude of P/Ca values between oxidatively cleaned samples and samples cleaned with water (Figure 9). Bulk 1 gave an opposite trend to Modern Analogue Samples, with water cleaned samples giving slightly higher P/Ca values than samples cleaned with hydrogen peroxide (Figure 9; Figure 11). This suggests that, compared to modern samples, the breakdown of organic matter and release and adsorption of phosphate is much less prominent in analysis of belemnite calcite, if present at all, so organic-bound phosphorus is not likely to be a major fraction of phosphorus. If future studies were to examine inorganic phosphorus in *S. officinalis* cuttlebone or *S. spirula* carbonates without the influence of the organic fraction, one solution may be to oxidatively clean the samples with hydrogen peroxide, then rinse the samples with magnesium chloride ( $MgCl_2$ ) to remove adsorbed phosphate (e.g., Thompson *et al.*, 2019). If magnesium is also of interest, rinses with other high-salinity solutions, such as sodium chloride (NaCl) could also be used (e.g., Dodd *et al.*, 2021).

As well as organic matter, varying quantities of other forms of phosphorus will impact the P/Ca results, as different forms will respond differently to different preparative methods. Belemnite calcite may contain a range of diagenetic and contaminant minerals such as apatite, authigenic phosphate and pyrite (Sælen, 1989; Ruttenberg *et al.*, 1992; Ullmann *et al.*, 2015; Ullmann and Korte, 2015; Hoffmann *et al.*, 2016; Stevens *et al.*, 2017; Thompson *et al.*, 2019; Hoffmann and Stevens, 2020). Bulk 1 is likely to have a higher concentration of these contaminant minerals, as it contains the phragmocone region which is would have been infilled with sediment and diagenetic fluids in the early stages of diagenesis (Sælen, 1989; Ruttenberg *et al.*, 1992;

Ullmann *et al.*, 2015; Ullmann and Korte, 2015; Hoffmann *et al.*, 2016; Stevens *et al.*, 2017; Thompson *et al.*, 2019; Hoffmann and Stevens, 2020). In Bulk 2 and 3, the magnitude of the P/Ca ratios was unchanged regardless of preparative method (Figure 9). For Bulk 1, cleaning with water gives the highest P/Ca values for each dissolution method, slightly above P/Ca values for NaOCl and H<sub>2</sub>O<sub>2</sub> (Figure 9). Despite the differences between the two oxidative cleaning methods trialled, H<sub>2</sub>O<sub>2</sub> being slightly acidic and a less persistent oxidant, and sodium hypochlorite being strongly alkaline and more strongly oxidising, there was no statistical difference between samples cleaned with NaOCl and H<sub>2</sub>O<sub>2</sub>. The higher P/Ca values for Bulk 1 samples cleaned with water suggest that oxidative cleaning with both these agents does remove a form of contaminant phosphorus, such as apatite or iron-oxide bound phosphorus. An alternative explanation is the differences arise from differences in the solubility of the different forms of phosphorus in the oxidative treatments compared to in water washes. It has been shown that both oxidising agents show dissolution of carbonates, with H<sub>2</sub>O<sub>2</sub> dissolving calcite more strongly than NaOCl (Chaduteau *et al.*, 2021). It is possible that a form of phosphorus such as apatite or authigenic phosphorus was preferentially dissolved and removed in oxidative cleanings compared to water cleanings, creating slightly lower P/Ca values.

Different cleaning methods also resulted in different variabilities in P/Ca ratios for different samples. In Bulk Samples, oxidative cleaning gave higher variability in the P/Ca ratios compared to cleaning with water, and this difference was largest for Bulk 1 samples (Figure 12; Table 9). This increased variance may be a result of variable amounts of diagenetic phosphorus (iron-bound, apatite, etc.) being removed by the oxidative agent (H<sub>2</sub>O<sub>2</sub> or NaOCl) either by oxidation and removal, or by dissolution. Though the same sample methods were applied, and the Bulk Sample was homogenised, slight differences in the method applied to each sample (such as how thoroughly each sample was exposed to the oxidative agent) could have affected the oxidation and removal or dissolution of organic or diagenetic material and caused greater variance. This effect could be amplified in samples with higher concentrations of P, such as the phragmocone-containing Bulk 1, especially where different forms of phosphorus, such as iron oxide bound phosphorus, are more likely to be present. In Variability Samples, samples cleaned with water gave slightly higher CV<sub>ind</sub> values than samples cleaned with H<sub>2</sub>O<sub>2</sub> – the opposite was observed in Bulk Samples. This may be a result of the smaller test masses used in the Variability Samples, or variability within the whole belemnite being slightly reduced by the use of an oxidative agent, but all CV<sub>ind</sub> values were low enough to indicate a high degree of reproducibility regardless of cleaning method. Alternatively, it is possible that the differences between the Bulk Samples and the Variability Samples was caused by a difference in the

oxidising power of the hydrogen peroxide used in the preparation. The Bulk Samples were prepared with an older bottle of hydrogen peroxide, which had potentially been incorrectly stored, making it less strongly oxidising than the hydrogen peroxide used with the Variability Samples and Modern Analogue samples. This may explain why there was a difference in samples cleaned with H<sub>2</sub>O<sub>2</sub> in the Variability Samples, which was not seen in Bulks 2 and 3.

In the analysis of belemnite calcite both oxidative and non-oxidative cleaning methods gave consistently low variabilities, which indicates high reproducibility regardless of cleaning method. In Modern Analogue samples it was shown that oxidative cleaning increased the measured P/Ca ratio, likely by oxidising and breaking down organic matter which adsorbed to the remaining powder. Though the concentration of organic-bound phosphorus in belemnite calcite is lower than in the Modern Analogue samples, any remaining primary organic matter or organic matter from sediment contamination could increase the measured P/Ca. Ideally, only primary inorganic phosphorus would be measured, and measuring contaminant phosphorus from oxidised organics would be avoided. Going forwards, it is recommended that for P/Ca measurements, belemnite samples are cleaned with water only to avoid also measuring contaminant organic-bound phosphorus.

### 2.6.2. Impact of dissolution method

Different methods for dissolution were only evaluated on the Bulk Samples. Three dissolution methods were tested – dissolution in acetic acid, nitric acid, or hydrochloric acid. For all combinations of samples and dissolution methods, low CV<sub>rep</sub> values indicate a high level of reproducibility, and the variability did not seem to be affected by dissolution method. Different dissolution methods did give different magnitudes of P/Ca value, depending on the different types of phosphorus in the sample.

As with different cleaning methods, different dissolution methods are likely to impact different forms of phosphorus in belemnite samples calcite differently. For Bulk 1, there were no differences in magnitude of P/Ca ratios between samples dissolved in nitric acid and samples dissolved in hydrochloric acid (Figure 9; Table 7). Bulk 1 samples dissolved in acetic acid gave lower P/Ca values than Bulk 1 samples dissolved in either nitric or hydrochloric acid by a factor of over 2, and the difference was shown to be statistically significant (Figure 9; Table 7). Hydrochloric and nitric acid are both strong acids, which are better able to target and dissolve some forms of phosphorus, such as apatite, which are concentrated in the diagenetically altered phragmocone material. Acetic acid is a weak acid, meaning the dissociation of the acid to form the reactive hydronium ion is incomplete. It has been shown that as a weak acid, acetic acid is likely less able to target and dissolve apatite, and other forms of phosphorus

which are present in the phragmocone material (Ingalls 2020; 2022). As a result of this, the P/Ca values for Bulk 1 samples dissolved in acetic acid are more similar to samples from Bulk 2 and 3 than Bulk 1 samples dissolved in other acids, as less contaminant apatite has been dissolved.

Different dissolution methods were not tested on the organic-matter rich Modern Analogue samples, but it is likely that the different acids used would also affect organic matter dissolution. Organic-bound phosphorus present in the belemnite samples is less likely to be extracted by acetic acid dissolution than dissolution in strong acids. Previous studies have shown that a high proportion of organic matter found in belemnites has a high acid resistivity, particularly in regions of the belemnite which are organic-rich or diagenetically altered (high concentrations of iron and manganese) (Sælen, 1989). The organic matter with high acid resistivity is less soluble in weaker acids, such as acetic acid, compared to stronger acids such as nitric and hydrochloric acid. This may also partially account for the difference in P/Ca values between samples cleaned with hydrochloric and nitric acids, and samples cleaned with acetic acid in Bulk 1. If the phragmocone contained higher concentrations of organic matter (either primary, from infilled sediment during diagenesis, or from contamination during extraction and sampling of the belemnite) then this organic matter would have been less soluble in acetic acid compared to the strong acids, reducing the measured P/Ca.

In Bulk 2 and 3, levels of contaminant phosphorus from other diagenetic minerals were much lower compared to in Bulk 1. Bulks 2 and 3 both gave mean P/Ca values of around  $800 \mu\text{mol mol}^{-1}$  and  $1,100 \mu\text{mol mol}^{-1}$  respectively, and the values were unaffected by changes in dissolution method (Figure 9; Table 7). This is because the phragmocone was not included in Bulk Samples 2 and 3, so there were much lower levels of contaminant phosphorus from apatite or organic matter. The inorganic forms of phosphorus in unaltered calcite, such as calcium phosphate and carbonate associated phosphate are soluble even in weak acids such as acetic acid.

Ideally, diagenetically altered material should be avoided during sampling, but should some altered material be included, dissolution with acetic acid reduces the dissolution of some forms of contaminant phosphorus, such as organic-bound phosphorus and apatite, compared with dissolution by nitric or hydrochloric acid. Reducing the amount of contaminant phosphorus dissolved, reduces the impact of diagenesis or contamination on the results of the analysis and gives a signal more representative of the inorganic P/Ca from the primary belemnite calcite. It is therefore recommended that measurement of P/Ca values be conducted using acetic acid to reduce the impact of organic-bound phosphorus and apatite

phosphorus on the results of the analysis, and acetic acid was selected as the acid used for dissolution going forwards.

### 2.6.3. Impact of sample mass

Ideally, the smallest sample mass possible would be used to minimise the impact of destructive sampling and conserve material where possible for repeat analyses or future tests. Sample masses of 2 mg, 5 mg and 10 mg were compared to determine the optimum sample mass to give reproducible results while conserving material for future analyses.

For all sample masses, CV values for P/Ca ratios were below 20 % indicating good reproducibility. For each Bulk Sample, 5 and 10 mg samples gave very low CV values with similar magnitudes. For Bulk 2, 5 mg and 10 mg samples gave similar CV values and the CV value for 2 mg samples could not be detected as phosphorus fell below the limit of detection for two of the three replicate samples. For Bulk 1, 2 mg samples had the highest CV value of 12.7 %, followed by 5 mg samples with 8.1 % and then 10 mg samples with 2.6 %.

As 5 and 10 mg samples gave similar levels of variance, and 5 mg samples require much less material than 10 mg samples, 5 mg samples were determined to be the optimum sample mass. 2 mg samples gave a higher level of variance for some Bulk Samples, but the CV values were still low enough to indicate high reproducibility in P/Ca ratios. For some 2 mg samples phosphorus fell below the limits of detection or quantification, so are not preferred. Where a belemnite rostrum is only very small, or there is only a limited amount of sample remaining from a previous study, smaller samples may be used, and it is not expected that this would negatively impact the reproducibility of the P/Ca ratios.

### 2.6.4. Implications for other CAP studies

Ideally, CAP measurements would only encapsulate primary inorganic phosphorus, and other forms of phosphorus – from apatite to primary and contaminant organic phosphorus to iron oxide bound phosphorus – can be considered ‘contaminant phosphorus’. In the comparison of different preparative methods, the impact of different forms of contaminant phosphorus on CAP measurements was clear. Some preparative methods were able to partially mitigate the impact of contaminant phosphorus on CAP measurements. Cleaning with water rather than using oxidative cleaning methods minimised the oxidation of organic matter, preventing the release of free phosphate which could adsorb to the remaining powder. Dissolving with acetic acid rather than strong acids such as nitric or hydrochloric acid reduced the dissolution of apatite and acid resistant organic matter. However, in the most contaminated samples, even the optimal preparative method is not enough to prevent contaminant phosphorus from impacting the P/Ca ratio.

In Bulk 1 samples cleaned with water and dissolved in acetic acid, the P/Ca value was 1.4 times lower than samples dissolved in hydrochloric or nitric acid, demonstrating less contaminant phosphorus from sources such as apatite or even organic matter. Despite this, the P/Ca ratios recorded for Bulk 1 samples cleaned with water and dissolved in acetic acid ( $\bar{x} = 3690$ ;  $s = 58$ ) are four times higher than the average P/Ca for the equivalently treated samples from Bulks 2 and 3 ( $\bar{x} = 772$ ;  $s = 17$  and  $\bar{x} = 1077$ ;  $s = 22$  respectively) (Table 7). This shows that in analysis of samples with high concentrations of contaminant forms of phosphorus, such as organic matter, iron oxide bound phosphorus and organic phosphorus, it is likely that the P/Ca values will not be reflective of primary inorganic phosphorus from the carbonate.

This is most likely to be of concern for analysis of high organic modern carbonates, poorly preserved biogenic carbonates, as well as CAP analysis of bulk rock carbonate samples, which comprise of more forms of phosphorus than are often found in well-preserved biogenic carbonates. Previous studies on bulk rock carbonates (e.g., Ingalls *et al.*, 2020; Dodd *et al.*, 2021; Ingalls *et al.*, 2022) used acetic acid for dissolution which is likely to have reduced the dissolution of contaminant phosphorus, for example from apatite and organic matter, but may not have eliminated it. This suggests that the CAP ratios generated from previous studies for bulk rock carbonates may not be representative of primary inorganic carbonate bound phosphate, as phosphorus from other minerals will have been partially dissolved and included in the CAP total. These studies have used lower concentrations of acetic acid which may reduce the amount of apatite and organic matter dissolved, though not eliminate it (Ingalls *et al.*, 2020; Dodd *et al.*, 2021; Ingalls *et al.*, 2022). It is likely that more work needs to be done to design a method which eliminates the impact of contaminant forms of phosphorus on CAP ratios and enables the proxy to be confidently applied to samples with high concentrations of apatite, iron oxide-bound phosphorus and organic-matter bound phosphorus.

One further implication of this work for the analysis of bulk rock carbonates, is an illustration of the importance of high salinity washes on samples which leave a residue after dissolution. In the study by Dodd *et al.* (2021) successive washes with NaCl were used to ensure all phosphate dissolved by the acetic acid was freed from the remaining residue and added to the total CAP. The importance of this step for samples with substantial residues after dissolution was demonstrated here in the oxidative cleaning of the organic matter-rich Modern Analogue samples which demonstrated free phosphate was not removed when the hydrogen peroxide was removed, nor with subsequent water washes. In Dodd *et al.* (2021), phosphate from the NaCl washes accounted for up to 70 % of the total CAP recorded indicating the necessity of the washes to analyse all free phosphate. Other studies of bulk rock carbonates where remaining residues were not rinsed with high salinity solutions, such as MgCl<sub>2</sub> or NaCl (e.g., Ingalls *et al.*,

2020; 2022) may have failed to analyse a high proportion of phosphate freed in the dissolution process. If a method is developed to eliminate the impact of contaminant forms of phosphorus on CAP ratios, samples with remaining residue after acid dissolution will still need to be rinsed with high salinity solutions to ensure all free dissolved phosphate is analysed and included in the resultant CAP ratio. Other studies on carbonates where the concentration of organic matter is unknown, should take care to determine the TOC content or incorporate washes into their preparative procedure.

## 2.6.5. Variability

### 2.6.5.1. Sampling technique

The variability for Bulk Samples (from whole powdered belemnites) and Variability Samples (precision sampled and powdered with a drill) was compared to determine if sampling with a drill introduced variability, and to make sure the samples were suitably homogenised.

For samples cleaned with water and dissolved in acetic acid, the CV value of P/Ca ratios were similar between the Bulk Samples (all around 2 %) and the Variability Samples ( $\bar{x}_{CV} = 1.5\%$ ;  $s_{CV} = 1.0$ ;  $n = 33$ ). This suggests neither sampling technique increases variability in P/Ca ratios, and following best practice, sampling with a drill should be used going forwards to minimise the inclusion of visually altered calcite in samples.

### 2.6.5.2. Within belemnites

It was found that there was a higher level of variability between multiple samples from the same belemnite, than there was in replicate samples from the same sampling site on the specimen's rostra. In Variability Samples cleaned with water the CV value for replicate samples ( $\bar{x}_{CV} = 1.5\%$ ;  $s_{CV} = 1.0$ ;  $n = 33$ ) were lower than the CV values for the specimen as a whole ( $\bar{x}_{CV} = 6.5\%$ ,  $s_{CV} = 3.2$ ,  $n = 10$ ). This suggests that different regions of the belemnite calcite may have different concentrations of phosphorus. It was shown that in some individuals, there was a consistent trend in P/Ca ratios along the length of the rostrum (Figure 14). This trend was predominantly observed in *Nannobelus delicatus* individuals from *Phricodoceras taylori* ammonite subzone ( $R^2$  all above 0.55), which were collected from the Wine Haven section. In these samples, P/Ca values were highest towards the apex of the belemnite rostrum. The same trend was not observed in the *Passaloteuthis* sp. specimen, which was also from the Wine Haven section, though this may be due to the limited spread of the sampling sites in this individual.

In the samples from the *Amaltheus gibbosus* ammonite subzone from the Penny Nab section, the same trend is seen strongly in one of the *Parapassaloteuthis* sp. individuals ( $R^2 = 0.56$ ), and weakly in the one *Bairstowius* sp. individual ( $R^2 = 0.31$ ), though not at all in the remaining

*Parapassaloteuthis* sp. belemnites, or the *Passaloteuthis pessula*. Again, this may be due to differences in the distribution of sampling sites along the length of the rostrum, or it may be that variation in P/Ca along the length of the belemnite is species-specific, and the trend is more pronounced in some species, such as *Nannobelus delicatus*.

It also may be linked to growth rate or biological age of the individual, as sampling through the growth rings at different points along the rostrum could constitute a primitive growth study. Near the apex of the belemnite the growth bands in the calcite will be closer together, compared to further away from the apex. It has been shown that other element ratios such as Mg/Ca and Sr/Ca are affected by growth rate and growth bands, so it is likely that P/Ca will also be affected (Ullmann *et al.*, 2017).

To minimise the impact of the P/Ca variation within belemnite rostrums on the results going forwards, where possible sampling should be conducted at the sample point on each belemnite, as well as avoiding the apical line and the phragmocone. It should be noted that even taking into consideration the variations within individual belemnites, the CV values were low enough to indicate high reproducibility – so fragmented and broken belemnite material can still be used even when sampling site on the rostrum cannot be controlled for.

#### 2.6.5.3. Between belemnites

The differences in P/Ca ratios between belemnites were greater than the differences within individuals. For samples cleaned with water, low CV values were calculated for all samples from the *Amaltheus gibbosus* ammonite subzone ( $CV_{VI} = 10.2\%$ ,  $n = 77$ ) and the *Phricodoceras taylori* ammonite subzones ( $CV_{VI} = 13.5\%$ ,  $n = 52$ ). These values were higher than the CV values calculated from samples within the same belemnite, showing a higher level of variability between belemnites from the same stratigraphic level than within individuals. This is not surprising, as the belemnites were from a range of different species, and also may have been of different ages, sizes, or sexes. The specimens may also have occupied slightly different habitats during life, or been subjected to slightly different processes after death, which could increase the variability. The CV values within each stratigraphic level are still low, which indicates a high degree of reproducibility within stratigraphic levels, even from different individuals of different species.

The impact of some of the potential controlling factors on P/Ca ratios were investigated – namely species and size. It was shown that species did not have an effect on the P/Ca ratios between belemnites, for example in the *Amaltheus gibbosus* ammonite subzone, there was no statistical difference between samples from *Parapassaloteuthis* sp. and samples from *Passaloteuthis pessula* belemnites. This means that for investigation of P/Ca ratios, species is

not a factor which needs to be considered. This means that samples which cannot be assigned to a particular genus or species may still be used for analysis, including samples which are externally weathered, broken or fragmented. It was also shown that size did not have an effect on the P/Ca ratio, though this may be an artefact of the sample selection for the variability test, where larger individuals were selected in preference.

#### 2.6.5.4. Between modern analogues

Differences between individuals were also investigated in modern analogues of belemnite rostra – *S. officinalis* cuttlebones and *S. spirula* shells. In *S. officinalis* cuttlefish, there was found to be no statistically significant difference in P/Ca ratios between the two cuttlebones which were studied, potentially as the samples were from cuttlefishes living in similar environments (Figure 16). They were also of the same species and were raised in the same tank, with similar environmental conditions (similar ammonia, nitrate, phosphate levels and similar pH). One individual lived slightly longer than the other, with the younger cuttlefish living 8 months primarily over winter, and the older cuttlefish living 13 months (though neither of these cuttlefish can be considered fully grown). The older cuttlefish therefore experienced a higher average temperature as its lifespan included warmer summer conditions– but if that affected the P/Ca values in the aragonite, the difference was not statistically significant in this case.

For *S. spirula*, it was found that there was a statistically significant difference between in P/Ca values between the different shells studied (Figure 17). This may be due to greater natural variation in P/Ca ratios between individuals, related to differences in the individuals' behaviours. All of the *S. spirula* shells were found on beaches in New Zealand, suggesting similar habitats. As wild specimens however, they are likely to have had more environmental differences between individuals, such as differences in water column depth and location of habitat, which can lead to different average temperatures or different sources of food. They also potentially encompass a range of ages, sexes and sizes which cannot be fully determined by examining the shells alone, particularly as many of them are partial shells.

In this case the *S. spirula* shells are likely to be a better analogue for the belemnite rostra than the cuttlebone because the belemnites would have experienced a more natural range of environmental conditions and greater variation in biology. For example, they likely occupied a greater range of different habitats, had different and more varied feeding habits, and there would have been a greater range of different biological ages – as well as species differences which cannot be examined using the which is not variable in the mono-specific modern analogues.

## 2.7. Conclusion

Trialling different methods on carbonates with different quantities and types of contaminant forms of phosphorus, such as apatite and organic matter bound phosphorus, allowed the responses of different forms of phosphorus to different preparative methods to be examined. Oxidative cleaning methods can breakdown organic phosphorus to form phosphate, but the free phosphate re-absorbs to the powder unless rinsed with a high salinity solution. Adsorbed phosphorus is dissolved with the powder during dissolution, increasing the measured P/Ca values. Strong acids also dissolve organic matter bound phosphorus, as well as other forms of contaminant phosphorus such as apatite which also increases the P/Ca total. In order to ensure studies of CAP in other carbonates are constrained to only measure primary inorganic phosphate, contaminant forms of phosphorus in the carbonate should be identified and quantified where possible. Organic matter associated phosphate can be removed by use of an oxidising agent and high salinity washes, but other forms of contaminant phosphorus such as apatite and iron-oxide bound phosphorus are not removed by existing cleaning methods and are at least partially dissolved during acid dissolution. This limits the use of this method to carbonate samples with low levels of contaminant phosphorus, which fortunately includes well preserved belemnite calcite.

In order to measure the primary inorganic carbonate associated phosphate, water cleaning, followed by dissolution in acetic acid was determined to be the preferred preparative method. This method was shown to be highly repeatable for belemnite analysis, with low CV values within replicate samples (Variability Samples:  $\bar{x}_{CV} = 1.5\%$ ;  $s_{CV} = 1.0$ ;  $n = 33$ ), within belemnites (Variability Samples:  $\bar{x}_{CV} = 6.5\%$ ,  $s_{CV} = 3.2$ ,  $n = 10$ ) and within stratigraphic levels (*Amaltheus gibbosus* ammonite subzone:  $CV_{VI} = 10.2\%$ ,  $n = 77$ ; *Phricodoceras taylori* ammonite subzones:  $CV_{VI} = 13.5\%$ ,  $n = 52$ ). This means this method is appropriate for examining P/Ca in belemnite calcite and observing trends in P/Ca of belemnites through stratigraphic time. Some individuals showed consistent trends in P/Ca values along the length of the rostra, which may be linked to growth rate effects, though not all belemnites showed this so the effect may be species-dependant. To negate this, wherever possible belemnites should be sampled at consistent sites on each individual, and to reduce the impact of diagenesis sampling should also avoid the exterior, apical line and phragmocone. Neither species nor size of belemnite had a significant effect on P/Ca ratios, so broken and fragmented belemnites which cannot be easily measured or identified can be used for this analysis.

To fully interpret the impacts of different preparative methods on E/Ca ratios, in belemnites and other modern and ancient biogenic and abiogenic carbonates, it would be useful to

further quantify the different pools of each element in each type of sample analysed. For phosphorus, this could be achieved through a number of methods, including element mapping (to determine what elements phosphorus is spatially associated with), phosphorus speciation (to identify and quantify the different pools of phosphorus present), and less commonly applied techniques, such as phosphorus NMR (to identify what elements phosphorus is commonly bonded to). Applying further analysis to determine the forms and amounts of contamination would also be beneficial, such as iron speciation (to identify and quantify iron-bound phosphorus, and pyrite), and TOC analysis (to quantify organic carbon content and estimate the organic content of the carbonate). This would help to determine the forms of primary and contaminant phosphorus and be useful in explaining the differences between preparative methods, as well as potential changes between samples and through time.

### 3. Extraction and quantification of other elements

#### 3.1. Introduction

In order to investigate the ratio of different elements to calcium (El/Ca), the samples described in 2.3 (including the Bulk, Variability, and Modern Analogue Samples) were analysed for multiple elements to investigate the variability of different El/Ca ratios, and the impact of different preparative methods. In addition to measuring the concentration of P and Ca, concentrations of Mg, Fe, Mn, S, Sr, Li, B, Na, Al, K, Ba and U were recorded for all samples, and for Bulk 2 and Bulk 3 and the Variability Samples, iodine concentrations were also measured. As with P/Ca in Chapter 2, the impacts of different preparative methods on the variability of element concentrations within and between belemnites were assessed for the El/Ca ratios. Each of these elements can give different information about the samples, such as information about contamination (Al), ocean circulation (Ba), pH (B), weathering (Li), diagenetic alteration (Mn, Fe), as well as information about the redox state of the water column (I) and palaeotemperature (Sr, Mg).

Previous studies on belemnites have shown high intra-rostrum variability in elemental (including Mn, Mg, Fe, Sr, and Ca) and isotopic composition ( $\delta^{18}\text{O}$ ,  $\delta^{13}\text{C}$ ), even in well preserved rostra (Podlaha *et al.*, 1998; McArthur *et al.*, 2002; 2007; 2008; Li *et al.*, 2012; Sørensen *et al.*, 2015; Ullmann *et al.*, 2015; Stevens *et al.*, 2017; Ullmann *et al.*, 2017). Some authors have suggested this indicates belemnite rostra are a poor archive for palaeoenvironmental information (e.g., Hoffmann *et al.*, 2016; 2021), though some contend that belemnites provide a valuable palaeoenvironmental record as the variability in elemental ratios and isotopes is predictable and quantifiable (e.g., McArthur *et al.*, 2002; 2007; 2008; Ullmann *et al.*, 2017). With this work we aim to produce a full characterisation of the chemistry of belemnite rostra, by quantifying major ions substituted into the calcite belemnite chemistry. The most abundant cations and anions in belemnite calcite, aside from  $\text{Ca}^{2+}$  and  $\text{CO}_3^{2-}$ , are  $\text{Mg}^{2+}$ ,  $\text{Sr}^{2+}$ ,  $\text{Na}^+$ ,  $\text{PO}_4^{3-}$  and  $\text{SO}_4^{2-}$ . Additional trace element ions were analysed for their potential in recording palaeoenvironmental signals, as used in other palaeoenvironmental studies (such as barium ( $\text{Ba}^{2+}$ ), lithium ( $\text{Li}^+$ ), sodium ( $\text{Na}^+$ ), potassium ( $\text{K}^+$ ), boron (usually in the form of borate ions ( $\text{B}(\text{OH})_4^-$ )) and iodine (in the form of iodate ( $\text{IO}_3^-$ )). Aluminium ( $\text{Al}^{3+}$ ), iron ( $\text{Fe}^{2+}/\text{Fe}^{3+}$ ), and manganese ( $\text{Mn}^{2+}$ ) were measured as they were used to screen samples for contamination and diagenetic alteration, as was described in 2.5.5.1.

Magnesium and strontium incorporation into calcite is thermodynamically controlled, meaning both Sr/Ca and Mg/Ca covary with palaeotemperatures (Rosales *et al.*, 2004; McArthur *et al.*, 2007a; b; Armendáriz *et al.*, 2008; Li *et al.*, 2012). In belemnites, some studies have shown

reasonable correlation between oxygen isotopes and Mg/Ca (Rosales *et al.*, 2004; McArthur *et al.*, 2007a; b; Armendáriz *et al.*, 2008) and Sr/Ca ratios (McArthur *et al.*, 2007a; b; Li *et al.*, 2012), suggesting that both elements vary with temperature and could be used as palaeotemperature proxies. However, other studies have found no significant correlation between Mg/Ca ratios and oxygen isotopes records in belemnite rostra (Wierzbowski and Rogov, 2011; Li *et al.*, 2013; Stevens *et al.*, 2014). In addition, McArthur *et al.* (2007a) demonstrated that sexual dimorphism affected Mg/Ca ratios of some belemnites but found there was limited biological control on Sr/Ca ratios potentially making Sr/Ca a more appropriate elemental ratio for recording palaeotemperature changes. Overall, while both Sr/Ca and Mg/Ca are affected by a variety of factors, it is likely that temperature will still influence Mg/Ca and Sr/Ca values, and these ratios may be able to give us important palaeotemperature and other environmental conditions.

Barium is of interest as a further example of a divalent cation (in addition to Mg, Sr, etc.) which can substitute for the Ca lattice position. Previous work on Ba has seen it used as a proxy for ocean circulation and salinity in other biogenic carbonates, though it has not been applied to belemnite calcite (e.g., Boyle, 1981; Shen and Sanford, 1990; Lea and Boyle, 1993). Ba substitution into carbonate is proportional to its concentration in seawater, allowing it to record salinity changes (Lea and Boyle, 1989; 1991; Tudhope *et al.*, 1996; Torres *et al.*, 2001; McCulloch *et al.*, 2003; Sinclair and McCulloch, 2004; Gillikin *et al.*, 2006; 2008; Poulain *et al.*, 2015). Ba predominantly reaches ocean from runoff and riverine fluxes, so examining concentrations of Ba can differentiate saline samples from brackish estuarine samples (Carroll *et al.*, 1993; Guay and Falkner, 1997; 1998; Shaw *et al.*, 1998). There are also variations in Ba concentrations at different ocean depths driven by the precipitation of barite in the upper ocean and its dissolution at depth, allowing the potential to track upwelling of deeper waters (e.g., Tudhope *et al.*, 1996).

Sulfur was measured as sulfate is one of the most abundant anionic substitutions in calcite, alongside phosphate. Additionally, previous studies on S/Ca ratios in foraminifera have shown that they can be a proxy for water column sulfate concentrations, in the same way P/Ca ratios may represent water column phosphate (Paris *et al.*, 2014; Thaler *et al.*, 2023). In belemnites, sulfur isotope values in carbonate-associated-sulfate of belemnites have been used to investigate marine sulfur concentrations and marine sulfur cycling (e.g., Gill *et al.*, 2011; Newton *et al.*, 2011).

Lithium has been assayed, as both lithium isotopes and Li/Ca ratios, in belemnites and biogenic carbonates (e.g., Hathorne and James, 2006; Misra and Froelich, 2012; Pogge von Strandmann *et al.*, 2013; Ullmann *et al.*, 2013; Lechler *et al.*, 2015; Pogge von Strandmann *et al.*, 2017;

Dellinger *et al.*, 2018). Several studies conducted on a variety of sedimentary and biogenic carbonates have suggested that lithium isotopes and Li/Ca ratios can provide evidence of palaeo-weathering and hydrothermal activity, and Li/Mg ratios have also been suggested as a palaeotemperature proxy for some biogenic carbonates (Bryan and Marchitto, 2008; Case *et al.*, 2010; Montagna *et al.*, 2014; Rollin-Bard and Blamart, 2015; Fowell *et al.*, 2016; Dellinger *et al.*, 2018). Silicate weathering is the primary terrestrial source of lithium to the oceans, and silicate weathering causes strong fractionation in lithium isotopes, with  $^7\text{Li}$  being preferentially dissolved and  $^6\text{Li}$  being preferentially incorporated into clays (Chan *et al.*, 1992; Huh *et al.*, 1998; Pistiner and Henderson, 2003). This means that ocean lithium isotope ratios and Li concentrations can be used to reflect the intensity of silicate weathering (Pogge von Strandmann and Henderson, 2015). Carbonate Li/Ca and lithium isotope ratios have been shown to vary based on the concentration and isotopic ratios in the liquid they precipitate from, though other factors play a role, including temperature, salinity and mineralogy in inorganic calcite and biogenic carbonates, as well as growth rate and vital effects in biogenic calcites (Delaney *et al.*, 1985; Okumura and Kitano, 1986; Delaney *et al.*, 1989; Marriott *et al.*, 2004b; Gabitov *et al.*, 2011; Vigier *et al.*, 2015). In lab-based tests on inorganic calcite, as well as studies on brachiopods, Li/Ca ratios were shown to correlate with temperature. In biogenic carbonates more widely (including in corals and foraminifera), Li/Mg ratios were shown to vary with temperature – and have been suggested as a reliable proxy for ocean temperature (Bryan and Marchitto, 2008; Case *et al.*, 2010; Montagna *et al.*, 2014; Rollin-Bard and Blamart, 2015; Fowell *et al.*, 2016; Dellinger *et al.*, 2018). Lithium in belemnites has the potential to give palaeoenvironmental information on a range of conditions, such as weathering and temperature, changes in which would be expected to relate to changes in phosphorus and other nutrient cycling.

Boron concentration values were measured for each of the belemnite calcite samples analysed in this study. In previous studies of other carbonate systems, boron isotopes have shown potential value as an interesting palaeoenvironmental indicator for water-column pH, though this has not been trialled on belemnites. Dissolved boron in seawater is found in two major forms: borate ions ( $\text{B}(\text{OH})_4^-$ ) and boric acid ( $\text{B}(\text{OH})_3$ ), and there is isotopic fractionation between the two forms with heavier  $^{11}\text{B}$  preferentially incorporated in boric acid and lighter  $^{10}\text{B}$  incorporated preferentially into borate ions (Klochko *et al.*, 2006). The relative abundance of boric acid and borate is pH dependent, hence the isotopic ratio of dissolved boron in seawater is also pH dependent – with more positive isotopic boron values correlating to increasing pH. Borate is the dominant form of boron which is incorporated into calcite in synthetic and biogenic carbonates, and so carbonate boron isotopes in biogenic carbonates

can be used as a proxy for pH of past oceans (Hemming and Hanson, 1992; Sanyal *et al.*, 2000; Zeebe and Wolf-Gladrow, 2001). Additionally, as boric acid is less likely to be incorporated, there is the potential for B/Ca ratios to partially reflect pH. Biogenic carbonates such as corals and foraminifera have shown promise for the generation of species-specific bulk isotope records, but different species-effects in biogenic carbonates, and significant intra-individual variability in other organisms such as brachiopods has been reported (e.g., Hemming and Hanson, 1992; Sanyal *et al.*, 1996; Sanyal *et al.*, 2001; Lécuyer *et al.*, 2002; Joachimski *et al.*, 2005; Simon *et al.*, 2006; Krief *et al.*, 2010; Trotter *et al.*, 2011). Overall, there is the potential for boron isotopes in belemnites to be used as a palaeo pH proxy, depending on the impact of differing vital effects between species and variability within the belemnites. As such, assessing B/Ca ratios within the belemnites is of interest as a potential precursor to a more thorough boron isotope evaluation.

Sodium and potassium were both measured as these small cations may be important elements to make up the charge balance when other elements are incorporated into the calcite (e.g., Ishikawa and Ichikuni, 1984). Previously attributed to contamination with clay or salt water, both Na/Ca and K/Ca have been understudied in biogenic carbonates compared to elemental ratios of divalent cations (Mg, Sr, etc.). The limited studies which have been conducted on them have shown that they hold mineralogical significance, and sodium in particular may have a potential use as a palaeosalinity proxy (e.g., White, 1978; Ishikawa and Ichikuni, 1984; McArthur *et al.*, 2007a; Wit *et al.*, 2013; Mezger *et al.*, 2016; Bertlich *et al.*, 2018; Gray *et al.*, 2023). Other studies in foraminifera have demonstrated Na/Ca as a potential measure of Ca concentrations (Evans *et al.*, 2018; Hauzer *et al.*, 2018; Evans *et al.*, 2020; Zhou *et al.*, 2021; Gray *et al.*, 2023; Nambiar *et al.*, 2023). Na/Ca ratios in foraminifera have been shown to vary with solution  $[Ca^{2+}]$  at constant  $Na^+$  (Hauzer *et al.*, 2018). In the ocean,  $[Ca^{2+}]$  is thought to have varied more than  $Na^+$  concentrations during Earth history - providing the potential to reconstruct seawater  $Ca^{2+}$  concentrations when salinity is constant (e.g., Evans *et al.*, 2018; Hauzer *et al.*, 2018; Evans *et al.*, 2020; Zhou *et al.*, 2021; Nambiar *et al.*, 2023). Both sodium and potassium have been shown to occupy interstitial sites in calcite lattices, as opposed to substituting into the Ca lattice position (Ishikawa and Ichikuni, 1984). This gives both ions a high potential to balance charge differences caused by the substitution of other elements into Ca or  $CO_3^{2-}$  lattice positions. Previous studies of Na in sedimentary and biogenic calcites have shown correlation with Na and salinity (e.g., Gordon *et al.*, 1970; Veizer *et al.*, 1977; White, 1978; Ishikawa and Ichikuni, 1984). Ishikawa and Ichikuni (1984) found good correlation with Na in biogenic calcite and salinity up to 10 ‰ salinity, and weak correlation above 10 ‰ salinity which was attributed to differences in vital effects, organic-matter associated Na,

sample contamination with seawater and mineralogical effects of Mg on Na incorporation. McArthur *et al.* (2007a) provided Na/Ca ratios for belemnites, which were shown to be subject to only very limited vital effects. Together this suggests that Na/Ca in carefully prepared samples, with organic and modern sea-water contamination eliminated, have the potential to indicate salinity, or potentially to shed light on mineralogical effects of charge balance relationships.

Iodine was measured because I/Ca ratios in belemnites can be used as a water column redox proxy (Lu *et al.*, 2010). This was of particular interest as a method to determine if P/Ca in belemnites ratios vary with redox. Iodide ( $I^-$ ) and iodate ( $IO_3^-$ ) are thermodynamically stable and are the dominant forms of iodine in seawater (Wong and Brewer, 1977). The standard reduction potential of  $IO_3^-/I^-$  is very close to that of  $O_2/H_2O$  making it one of the first species to respond during ocean deoxygenation events (Rue *et al.*, 1997). Only iodate precipitates with carbonate, so the formation of carbonate-associated iodine requires an oxygenated water column (Lu *et al.*, 2010). I/Ca therefore correlates positively with the oxygenation of the water-column, and low I/Ca ratios can indicate dysoxia or anoxia (Lu *et al.*, 2010).

## 3.2. Materials and methods

As described in 2.4, all the samples for which P/Ca values were determined were also analysed for a suite of other elements. Samples were prepared by different methods to investigate the impact of different preparative methods on the EI/Ca results. Previous studies on biogenic carbonates have used a range of cleaning methods (oxidative and non-oxidative) to prepare samples, as well as different acids for sample dissolution (e.g., Shotyk *et al.*, 1995; Kumarsingh *et al.*, 1998; 1995; Penkman *et al.*, 2008; Zhang *et al.*, 2020; Riding, 2021 and references therein; Dodd *et al.*, 2021; Ingalls *et al.*, 2022). In this study we used the Bulk Samples to compare oxidative and non-oxidative cleaning methods (sodium hypochlorite, hydrogen peroxide or ultra-pure water), and three different dissolution methods (nitric acid, acetic acid, hydrochloric acid) (2.4).

Additionally, the Variability Samples were used to investigate the natural variance in EI/Ca ratios within a belemnite, between belemnites of the same species, between belemnites of different species and within and between stratigraphic levels (2.3.2). This was investigated using 10 belemnites from two different stratigraphic levels and six different species (2.3.2). Each belemnite was sampled six times at different points along the length of the rostra (Figure 5). A subset of these samples was prepared using an oxidative cleaning method to investigate the impact of oxidative cleaning on the intra- and inter- belemnite EI/Ca variability.

All samples were analysed for Li, B, Na, Al, K, Mn, Ba and U by ICP-MS and for Ca, Mg, P, Fe, Mn, S and Sr by ICP-OES. Except for Bulk 1 samples, all were also analysed to determine iodine concentration (2.4.4). The experimental method and details on method error, LOD and LOQ values are reported in (2.4.4). Statistical tests are conducted according to the same protocol set out in section 2.4.5. This allows the impact of different methods on different EI/Ca ratios of belemnite calcite and modern analogues to be assessed in the same way as for P/Ca. The same diagenetic screening protocol was applied to these samples, as described in 2.4.6. Full results of elemental analysis of Bulk, Variability and Modern Analogue Samples can be found in the appendix (8.1; 8.2; 8.3).

### 3.2.1. Carbon and oxygen isotope analysis

For Variability Samples which had remaining material after other analyses were performed, stable isotope analysis was conducted. For each sample 60-100 µg of uncleaned calcite were analysed using an Elementar IsoPrime Dual-Inlet Isotope Ratio Mass Spectrometer in the Cohen Geochemistry Laboratory, University of Leeds. The results are reported to the Vienna Pee Dee Belemnite (VPDB) scale using a standard of Elemental Microanalysis (EMA) Carrara marble (Table 10; EMA Technical Information Bulletin, Carrara Marble, 2016). Analytical precisions for  $\delta^{13}\text{C}$  and  $\delta^{18}\text{O}$  gave standard deviations better than 0.07 and 0.15 ‰ based on standard values for the EMA Carrara marble. Full isotopic results for the Variability Samples can be found in the appendix (8.2).

For all oxygen isotope measurements, temperature estimates are based on  $\delta^{18}\text{O}$  values using the equation of Anderson and Arthur (1983), and assuming an original  $\delta^{18}\text{O}$  of non-glacial seawater of -1 ‰ SMOW.

*Table 10 - Mean values and standard deviations of EMA Carrara Marble compared to Vienna Pee Dee Belemnite (VPDB) (EMA Technical Information Bulletin, Carrara Marble, 2016). Mean values are reported to 3 significant figures, standard deviations to one.*

	$\delta^{13}\text{C}_{\text{VPDB}}$	$\delta^{18}\text{O}_{\text{VPDB}}$
<b>Mean value (<math>\bar{x}</math>) / ‰</b>	+ 2.10	- 2.01
<b>Standard Deviation (s) / ‰</b>	0.07	0.1

## 3.3. Results

ICP-MS and ICP-OES results for other elements were converted into molar ratios to calcium to eliminate sample size effects. These EI/Ca ratios were compared to investigate the impacts of preparative methods and variability on elemental concentrations and their potential for investigating palaeoenvironmental changes.

### 3.3.1. Elemental ratios with analytical issues

Some elements which were analysed are excluded from the main results and discussion sections due to issues with their analysis - these are briefly described and discussed in this section and full tabulated results can be seen in the appendix (8).

#### 3.3.1.1. Trace element ratios with high variability and/or incomplete datasets

For some of the elements analysed, the methods did not produce reliable, reproducible data. This was due to variability in measured E/Ca ratios, or low concentrations of the measured element compared to the limits of detection (LOD) and quantification (LOQ).

Potassium and uranium consistently gave ICP-MS results below the LOD or LOQ values, with potassium only giving measurable results for the contaminated Bulk 1 samples. Slightly more samples gave values for uranium, though these results are likely to be artefacts of memory effects on the ICP-MS resulting from prior analysis of samples high in uranium.

Boron values were also usually below the LOD or LOQ, with no values recorded in the analysis of the Variability Samples and only one recorded value in the Modern Analogue Samples. To indicate variability, CV values were calculated. As in 2.5.2.2,  $CV_{rep}$  values indicate variance within replicates of the same sample (same individual, same site, same preparative method);  $CV_{ind}$  values indicate variance for multiple samples from different sampling sites along the rostra using the same preparative methods;  $CV_{IV}$  represent variability for samples from multiple sites on multiple individuals prepared with the same preparative method from the same stratigraphic level. In the Bulk Samples, B/Ca values could be calculated for some analyses – predominantly for Bulk 3 with  $CV_{rep}$  values ranging from 17.6 to 54.7 % for different preparative methods. This indicates poor reproducibility of B/Ca ratios for belemnite calcite – potentially due to levels of boron close to the LOD and LOQ ( $B/Ca \bar{x} = 23 \mu\text{mol mol}^{-1}$  averaged across all belemnite samples and preparative methods;  $n = 39$ ). B/Ca values were also recorded for the JCP-1 standard, which gave lower  $CV_{rep}$  values of between 1.0 and 8.1 % for different preparative methods. This is potentially due to higher concentrations of boron in the standard ( $B/Ca \bar{x} = 339 \mu\text{mol mol}^{-1}$  averaged across all preparative methods;  $n = 18$ ). This suggests accurate and reproducible results for B/Ca ratios could be obtained in samples with higher boron concentrations, or by adjusting the dilution factors used for ICP-MS analysis.

In many samples, sulfur was also commonly below the LOD or LOQ values. For Variability Samples only 32 % of samples and 58 % of Bulk Samples contained measurable quantities of sulfur – and no modern analogue had sulfur quantities above the LOD. The values which were obtained demonstrated reasonably small  $CV_{rep}$  values for both variability and Bulk Samples, with a maximum value of 17 %. The  $CV_{ind}$  values for S/Ca ratios were similar with a maximum  $CV_{ind}$  value of 19 %, showing high reproducibility within individuals.  $CV_{IV}$  values could not be

calculated for the Variability Samples as all samples from the Wine Haven section were below measurable limits for sulfur. The low  $CV_{rep}$  and  $CV_{Ivl}$  values indicate that this method is only appropriate for measuring S/Ca values in samples with high sulfur concentrations, but not samples with lower sulfur concentrations. A different analytical method, such as ion chromatography analysis of sulfate ions is suggested as an alternative method of measuring sulfur concentrations.

For barium, no variability or Bulk Sample fell below the LOQ or LOD however there was a high degree of variability in Ba/Ca ratios. For Ba/Ca the  $CV_{rep}$  values were high and variable (Bulk Samples:  $\bar{x}_{CV} = 26\%$ ,  $s = 28\%$ ; Variability Samples:  $\bar{x}_{CV} = 22$ ,  $s = 27$ ).  $CV_{rep}$  values for belemnite Bulk Samples were lowest when samples were cleaned with water and dissolved in acetic acid (Water cleaning and acetic acid dissolution: Bulk 1  $CV_{rep} = 11$ ; Bulk 2  $CV_{rep} = 23$ ; Bulk 3  $CV_{rep} = 4\%$ ). For water cleaned samples in all Bulk Samples, dissolving in acetic acid also gave the lowest magnitude of Ba/Ca ratios, similar to the pattern observed for P/Ca in Bulk 1 samples (e.g., for Bulk 2 water cleaned samples:  $\bar{x}_{HCl} = 15.4 \mu\text{mol mol}^{-1}$ ,  $s_{HCl} = 3.4 \mu\text{mol mol}^{-1}$ ,  $n_{HCl} = 3$ ;  $\bar{x}_{nitric} = 11.2 \mu\text{mol mol}^{-1}$ ,  $s_{nitric} = 0.6 \mu\text{mol mol}^{-1}$ ,  $n_{nitric} = 3$ ;  $\bar{x}_{acetic} = 3.7 \mu\text{mol mol}^{-1}$ ,  $s_{acetic} = 0.9 \mu\text{mol mol}^{-1}$ ,  $n_{acetic} = 3$ ). This suggests that barium may be present in the calcite in a form such as barium sulfate, which is not fully dissolved in a weak acid (i.e., acetic acid). Bulk 1 also contains higher magnitude of Ba/Ca ratios compared to Bulk 2 and Bulk 3 (Bulk 1 all preparative methods:  $\bar{x} = 27.2 \mu\text{mol mol}^{-1}$ ,  $s = 11.7 \mu\text{mol mol}^{-1}$ ,  $n = 27$ ; Bulk 2 and Bulk 3 all preparative methods:  $\bar{x} = 7.8 \mu\text{mol mol}^{-1}$ ,  $s = 5.1$ ,  $n = 31$ ), suggesting that contamination from the phragmocone affects Ba/Ca ratios with high concentrations of barium present in the phragmocone region, and also less  $\text{CaCO}_3$  – both of which contribute to the elevated Ba/Ca ratios in Bulk 1. The alveolar infills in belemnites collected from Yorkshire often contain fine macroscopic barite, so the elevated Ba in Bulk 1 is consistent with Ba originating from contamination. Although these results indicate a potential for reliable and reproducible Ba/Ca ratios using the water cleaning and acetic acid dissolution, the Variability Samples demonstrated high variability in Ba/Ca ratios within individual belemnites with high  $CV_{ind}$  values ( $\bar{x}_{CV} = 101$ ,  $s = 47$ ) indicating poor reproducibility. There was also poor reproducibility within the stratigraphic levels, with  $CV_{Ivl}$  values in Variability Samples of 215 % and 151 % for samples from the Penny Nab section and Wine Haven section respectively. For all Variability Samples, one standard deviation was larger than the average magnitude of the Ba/Ca ratios by a factor of 2 ( $\bar{x} = 43 \mu\text{mol mol}^{-1}$ ;  $s = 90 \mu\text{mol mol}^{-1}$ ). There were no apparent trends in Ba/Ca related to the size of the rostra or the sampling position, and a t test found no statistically significant differences between Ba/Ca values in samples from *Parapassaloteuthis* sp. ( $\bar{x} = 54.2 \mu\text{mol mol}^{-1}$ ,  $s = 129.7 \mu\text{mol mol}^{-1}$ ) and samples from *Passaloteuthis pessula* ( $\bar{x} = 33.5 \mu\text{mol mol}^{-1}$ ,  $s = 17.0 \mu\text{mol mol}^{-1}$ ) in samples from the

*Amaltheus gibbosus* ammonite subzone);  $t(44) = 2.015$ ,  $p = 0.312$ . This suggests that species is not an important factor in determining Ba/Ca ratios. There was also no statistically significant difference in Ba/Ca values between the two stratigraphic levels studied in the Variability Samples (*Amaltheus gibbosus* ammonite subzone:  $\bar{x} = 45.1 \mu\text{mol mol}^{-1}$ ,  $s = 97.5 \mu\text{mol mol}^{-1}$ ; *Phricodoceras taylori* ammonite subzone:  $\bar{x} = 30.7 \mu\text{mol mol}^{-1}$ ,  $s = 46.3 \mu\text{mol mol}^{-1}$ );  $t(118) = 1.980$ ,  $p = 0.266$ . The uneven distribution of Ba in belemnites and lack of statistically significant differences between stratigraphic levels mean it would be difficult to create a robust and reproducible stratigraphic record for Ba/Ca in belemnite calcite using the methods trialled here.

Similar issues were present in the analysis of Li/Ca ratios. The variability between replicate samples for Li/Ca values was low for both Bulk Samples ( $CV_{\text{rep}}: \bar{x}_{\text{CV}} = 4.7 \%$ ,  $s = 7.8 \%$ ) and Variability Samples ( $CV_{\text{rep}}: \bar{x}_{\text{CV}} = 3.6 \%$ ,  $s = 3.2 \%$ ), indicating high reproducibility within replicate samples. There was no consistent trend in the magnitude or variability of Li/Ca ratios between different preparative methods, suggesting all methods are equally suitable to generate Li/Ca ratios. As with phosphorus and barium, Bulk 1 did give higher Li/Ca ratios than Bulk 2 and Bulk 3 (Bulk 1 all preparative methods:  $\bar{x} = 92.2 \mu\text{mol mol}^{-1}$ ,  $s = 17.4 \mu\text{mol mol}^{-1}$ ,  $n = 27$ ; Bulk 2 and Bulk 3 all preparative methods:  $\bar{x} = 16.5 \mu\text{mol mol}^{-1}$ ,  $s = 3.1$ ,  $n = 36$ ) due to potentially higher concentrations of lithium containing minerals, mainly clays and other aluminosilicates in the infilled phragmocone region and a lower concentration of  $\text{CaCO}_3$  in the contaminated material. As with barium, the variability within individual belemnites and within stratigraphic levels was much higher ( $CV_{\text{ind}}: \bar{x}_{\text{CV}} = 40 \%$ ,  $s = 24 \%$ ; Penny Nab:  $CV_{\text{I}} = 33 \%$ ,  $n = 77$ ; Wine Haven  $CV_{\text{I}} = 62 \%$ ,  $n = 52$ ). A t test demonstrated that differences in Li/Ca ratios do not correlate with differences in species and that there were no statistically significant differences between Li/Ca values in samples from *Parapassaloteuthis* sp. ( $\bar{x} = 31.2 \mu\text{mol mol}^{-1}$ ,  $s = 10.1 \mu\text{mol mol}^{-1}$ ) and samples from *Passaloteuthis pessula* ( $\bar{x} = 32.0 \mu\text{mol mol}^{-1}$ ,  $s = 8.32 \mu\text{mol mol}^{-1}$ ) in samples from the *Amaltheus gibbosus* subzone);  $t(62) = 1.999$ ,  $p = 0.720$ . Unlike Ba/Ca ratios an additional t test demonstrated statistically significant differences in Li/Ca ratios between the two stratigraphic levels studied with samples from the *Amaltheus gibbosus* subzone ( $\bar{x} = 32.3 \mu\text{mol mol}^{-1}$ ,  $s = 10.5 \mu\text{mol mol}^{-1}$ ) having mean Li/Ca ratios a factor of two higher than Li/Ca ratios from the *Phricodoceras taylori* subzone ( $\bar{x} = 14.9 \mu\text{mol mol}^{-1}$ ,  $s = 9.2 \mu\text{mol mol}^{-1}$ );  $t(118) = 1.980$ ,  $p = 5.5E-17$ . The statistical differences in Li/Ca between stratigraphic levels but not between species within the same zone suggests that producing profiles of Li/Ca through time is possible, though as with Ba/Ca the elevated levels of variability within individuals and stratigraphic levels means that ensuring these profiles are robust and reliable may be challenging.

### 3.3.1.2. Iodine

During sample preparation, separate solutions were generated to ensure iodine was stabilised using ammonium hydroxide to prevent evaporation of the iodine and reduce matrix effects using variable dilutions based on the calcium concentration of the sample (He *et al.*, 2022). Issues occurred during the analysis of iodine for Bulk Samples and Variability Samples, as well as stratigraphic samples described in 4.2. For many of the samples the concentration of iodine in the calcite fell below the LOD or LOQ, though this is potentially due to the stratigraphic levels being selected for the Variability Samples both representing low-oxygen water-columns. There were also analytical issues where the internal standard recovery, which for some samples was as low as 20 % – far outside the normal range of 85-115 %. These internal standard recoveries are outside the bounds of what can be corrected for after analysis, and it was unknown whether the suppression of the signal was specific to the Te internal standard peak or if the iodine peak was also being suppressed.

For the stratigraphic samples, these issues appeared to be run or site specific, with analyses of some sections resulting in poorer internal standard recovery than others. We investigated these analysis issues to determine if the issues were related to signal suppression due to matrix effects, and if the suppression also affected measurements of iodine as well as the internal standard peak. To investigate this, six samples which had been previously analysed were prepared again from previously cleaned and dried powders. They were re analysed on the ICP-MS using two internal standards – Te which had been used in previous runs and Rh (2ppm) as an additional standard. Of the six rerun samples, two had internal standard recovery between 85-115 % and four had poor internal standard recovery. Repeat analysis found only one sample demonstrated low internal standard recovery on repeat analysis – one of the four samples with previously poor internal standard recovery. In all samples including the sample with poor recovery, both internal standards were giving ‘suppressed’ peaks, suggesting that the signal suppression was not specific to Te measurements, and the iodine signal was likely also suppressed.

Further investigations were conducted including measuring the pH of samples with good internal standard recovery and samples with poor internal standard recovery using litmus paper. It was found that samples with poor internal standard recovery were more acidic than those with good internal standard recovery. It is likely that the lower pH of the dissolved samples caused issues with the analysis leading to the signal suppression of the Te internal standard and likely the iodine signal too. The method used here was adapted from a previous method which used 3 % HNO<sub>3</sub> acid instead of 30 % acetic acid for dissolution of the carbonate samples (He *et al.*, 2022). In the previous study, the ammonium hydroxide content of the

matrix was enough to raise the pH enough to eliminate or reduce matrix effects. It is likely that in choosing a higher concentration of a different acid, even a weak acid, the ammonium hydroxide content of the matrix was no longer sufficient to raise the pH enough to eliminate the signal suppression. It is suggested that in order to negate this, extra ammonium hydroxide should be added to the matrix prior to dilution of the sample to ensure the pH is high enough to prevent the signal suppression. Even if the signal suppression effects are negated, it is still possible that this is not a suitable method to measure I/Ca concentrations as so many samples fell below the LOD/LOQ for iodine. This may just reflect the low concentrations of iodine in samples from deoxygenated water-columns, and a stratigraphic redox profile may still be creatable.

### 3.3.2. Impact of cleaning method

#### 3.3.2.1. Magnitude

For Bulk Samples, the magnitudes of the E/Ca ratios were compared to investigate the impact of different cleaning methods.

For magnesium, there was found to be statistically significant but small differences in Mg/Ca ratios between different cleaning methods for Bulk 1 samples with samples cleaned by H<sub>2</sub>O<sub>2</sub> giving slightly lower Mg/Ca values than samples cleaned by NaOCl or water (Table 13). For Bulk 2 samples, when values are averaged across all dissolution methods, there was also a small but statistically significant differences in Mg/Ca between samples cleaned with water and samples cleaned with hydrogen peroxide – with water cleaned samples giving 2 % higher Mg/Ca values (Table 13). For Bulk 3 there were no statistically significant differences between different cleaning methods. In each case where a statistically significant difference between different cleaning methods was identified, the percentage difference in the average values was low – below 5.5 % - suggesting that even where differences can be statistically considered significant, they are small in magnitude.

Differences in Sr/Ca ratios with different sample cleaning methods showed similar patterns to Mg/Ca ratios. In Sr/Ca ratios, there were statistically significant differences between Bulk 2 samples cleaned with water and Bulk 2 samples cleaned with hydrogen peroxide averaged over all dissolution methods, with samples cleaned using water giving 3 % higher Sr/Ca values. For Bulk 2 samples cleaned with acetic acid, there was no statistically significant difference between different cleaning methods. There were also statistically significant differences between Bulk 3 samples cleaned with hydrogen peroxide and samples cleaned with water, both for samples dissolved with acetic acid and for averaged samples across different dissolution methods. In contrast to samples from Bulk 2, the samples cleaned with hydrogen peroxide gave slightly higher Sr/Ca values for Bulk 3 – by 3 % for samples dissolved in acetic

acid and 5 % for averaged samples dissolved by any dissolution method. For Bulk 1, there was no statistically significant difference between any of the different cleaning methods. As with magnesium, where there were statistically significant differences, the magnitude of these differences was very low, still no more than 5.5 %.

For Na/Ca ratios, the only statistically significant difference between cleaning methods which was determined was that Bulk 2 samples for all averaged dissolution methods gave slightly higher Na/Ca values for samples cleaned with water than samples cleaned with hydrogen peroxide by 8 %. Statistically significant differences in Na/Ca ratios between cleaning methods were not identified for any other set of samples.

Table 11 - T-test results demonstrating the differences in Mg/Ca and Sr/Ca between samples cleaned with water and samples cleaned with hydrogen peroxide for two *Passaloteuthis Pessula belemnites* from the Variability Samples, one from each stratigraphic level. Average El/Ca ratios ( $\bar{x}$ ) in  $\mu\text{mol mol}^{-1}$ , standard deviation ( $s$ ) in  $\mu\text{mol mol}^{-1}$ , and coefficient of variation values (CV) in % are reported for each sample and cleaning method combination. The degrees of freedom ( $df$ ),  $P$  and  $t$  values are reported for each  $t$  test. Statistically significant results have  $P$  values highlighted in pale green. For statistically significant differences, the % difference in the El/Ca ratios is also given.

Place	Water				Hydrogen peroxide				Water and hydrogen peroxide t test			
	$\bar{x}$	$s$	CV	$n$	$\bar{x}$	$s$	CV	$n$	$df$	$P$	$t$	% diff.
<b>Magnesium (Mg/Ca)</b>												
<b>Wine Haven</b>	8,409	694	8.3	18	6,899	390	5.7	5	11	1.09E-04	2.20	18.0
<b>Penny Nab</b>	11,594	330	2.8	15	9,877	941	9.5	7	7	3.33E-03	2.36	14.8
<b>Strontium (Sr/Ca)</b>												
<b>Wine Haven</b>	1,603	116	7.2	18	1,342	80	6.0	5	8	7.08E-04	2.31	16.2
<b>Penny Nab</b>	1,822	23	1.3	15	1,560	41	2.6	7	8	4.69E-07	2.3	14.4

Modern Analogue Samples were also prepared by two different cleaning methods. As with the Variability Samples, there were not enough replicates to compare El/Ca values between replicate samples so instead multiple samples from different sites on the same individual were used to compare El/Ca differences between different cleaning methods. Both *S. officinalis* and one *S. spirula* had enough replicate samples to compare El/Ca ratios for different cleaning methods. To identify statistically significant differences between the different cleaning methods,  $t$  tests were conducted, and the results are presented in Table 12. For both Na/Ca and Sr/Ca there were no statistically significant differences in the El/Ca ratios between samples cleaned with water and samples cleaned with hydrogen peroxide for any samples

(Table 12). Cleaning method did impact Mg/Ca ratios in all Modern Analogue Samples, with higher Mg/Ca ratios in all modern analogue cleaned with water by 21-36 % (Table 12).

Table 12 - T test results demonstrating the differences in Mg/Ca and Sr/Ca in Modern Analogue (*Spirula spirula* and *Sepia officinalis*) Samples cleaned with different methods (water and H<sub>2</sub>O<sub>2</sub>). Results are from three individuals – two cuttlefish (Cuttlefish A is biologically younger, Cuttlefish B is older) and one *Spirula spirula*. Average El/Ca ratios ( $\bar{x}$ ) in  $\mu\text{mol mol}^{-1}$ , standard deviation (s) in  $\mu\text{mol mol}^{-1}$ , number of replicate analyses (n) and coefficient of variation values (CV) in % are reported for each sample and cleaning method combination. The degrees of freedom (df), P and t values are reported for each t test. Statistically significant results have P values highlighted in pale green. For statistically significant differences, the % difference in the El/Ca ratios is also given.

Sample	Water				Hydrogen peroxide				Water and hydrogen peroxide t test			
	$\bar{x}$	s	CV	n	$\bar{x}$	s	CV	n	df	P	t	% diff.
<b>Magnesium (Mg/Ca)</b>												
<b>Cuttlefish A</b>	1,756	31	1.8	3	1,375	39	2.9	3	4	4.17E-04	2.78	21.7
<b>Cuttlefish B</b>	2,452	235	9.6	9	1,581	59	3.7	6	10	1.58E-06	2.23	35.5
<b><i>S. spirula</i></b>	647	50	7.7	6	481	41	8.6	5	9	3.89E-04	2.26	25.7
<b>Strontium (Sr/Ca)</b>												
<b>Cuttlefish A</b>	3,936	144	3.7	3	3,911	191	4.9	3	4	0.892	2.78	-
<b>Cuttlefish B</b>	5,208	163	3.1	9	5,239	162	3.1	6	11	0.744	2.20	-
<b><i>S. spirula</i></b>	3,533	142	4.0	6	3,429	155	4.5	5	8	0.333	2.31	-
<b>Sodium (Na/Ca)</b>												
<b>Cuttlefish A</b>	22,851	1,751	7.7	3	26,826	7,048	26.3	3	2	0.520	4.30	-
<b>Cuttlefish B</b>	24,777	320	1.3	9	24,207	528	2.2	6	7	0.066	2.36	-
<b><i>S. spirula</i></b>	23,396	1,042	4.5	6	23,967	577	2.4	5	8	0.328	2.31	-

Table 13 - T-test results demonstrating the differences in Mg/Ca and Sr/Ca and Na/Ca between Bulk Samples cleaned with different methods (water, H<sub>2</sub>O<sub>2</sub> and NaOCl). For each combination of acid, cleaning method and sample n = 3. Where all acids (HNO<sub>3</sub>, HCl and acetic acid) are averaged, n = 9. Average El/Ca ratios ( $\bar{x}$ ) in  $\mu\text{mol mol}^{-1}$ , standard deviation (s) in  $\mu\text{mol mol}^{-1}$ , and coefficient of variation values (CV) in % are reported for each sample and cleaning method. The degrees of freedom (df), P and t values are reported for each t test. Statistically significant results have P values highlighted in pale green. For statistically significant differences, the % difference in the El/Ca ratios is also given.

Sample material	Acid	Water			H <sub>2</sub> O <sub>2</sub>			NaOCl			Water and H <sub>2</sub> O <sub>2</sub>				H <sub>2</sub> O <sub>2</sub> and NaOCl			
		$\bar{x}$	s	CV	$\bar{x}$	s	CV	$\bar{x}$	s	CV	df	P	t	% diff.	df	P	t	% diff.
<b>Magnesium (Mg/Ca)</b>																		
Bulk 1	All	22,580	225	1.0	21,720	149	0.7	22803	151	0.7	14	3.33E-07	2.14	3.81	16	1.33E-10	2.12	4.99
	Acetic	22,775	262	1.1	21,670	105	0.5	22791	65	0.3	3	1.16E-02	3.18	4.85	3	1.01E-03	3.18	5.17
Bulk 2	All	11,068	146	1.3	10,842	58	0.5	-	-	-	10	2.25E-03	2.23	2.04	-	-	-	-
	Acetic	10,932	33	0.3	10,877	38	0.3	-	-	-	4	1.99E-01	2.78		-	-	-	-
Bulk 3	All	12,915	136	1.1	12,955	145	1.1	-	-	-	16	5.85E-01	2.12		-	-	-	-
	Acetic	12,955	38	0.3	13,086	118	0.9	-	-	-	2	2.75E-01	4.30		-	-	-	-
<b>Strontium (Sr/Ca)</b>																		
Bulk 1	All	3,295	34	1.0	3,302	25	0.7	3278	54	1.6	15	6.41E-01	2.13		11	2.74E-01	2.20	
	Acetic	3,336	15	0.5	3,320	21	0.6	3345	13	0.4	4	4.46E-01	2.78		3	2.60E-01	3.18	
Bulk 2	All	1,691	26	1.5	1,645	23	1.4	-	-	-	16	1.47E-03	2.12	2.77	-	-	-	-
	Acetic	1,696	10	0.6	1,676	8	0.5	-	-	-	4	9.95E-02	2.78		-	-	-	-
Bulk 3	All	1,978	98	4.9	2,081	49	2.3	-	-	-	12	1.99E-02	2.18	5.24	-	-	-	-
	Acetic	2,094	6	0.3	2,146	8	0.4	-	-	-	4	1.80E-03	2.78	2.52	-	-	-	-
<b>Sodium (Na/Ca)</b>																		
Bulk 1	All	14,419	657	4.6	14,146	564	4.0	15691	3240	20.7	16	3.86E-01	2.12		8	2.21E-01	2.31	
	Acetic	14,708	708	4.8	14,254	69	0.5	18161	4648	25.6	2	4.62E-01	4.30		2	3.57E-01	4.30	
Bulk 2	All	8,521	318	3.7	7,822	711	9.1	-	-	-	11	2.74E-02	2.20	8.21	-	-	-	-
	Acetic	8,751	247	2.8	8,708	533	6.1	-	-	-	3	9.24E-01	3.18		-	-	-	-
Bulk 3	All	12,039	1,248	10.4	11,792	577	4.9	-	-	-	11	6.21E-01	2.20		-	-	-	-
	Acetic	13,601	833	6.1	12,570	3	0.0	-	-	-	2	2.22E-01	4.30		-	-	-	-

### 3.3.2.2. Variance

In Bulk Samples, the  $CV_{rep}$  values for Na/Ca, Sr/Ca and Mg/Ca ratios were all low (less than 10 %, mostly less than 1 %) indicating a high degree of reproducibility within replicate samples for all cleaning methods. The only exception to this was Na/Ca values for Bulk 1 samples cleaned with sodium hypochlorite – this is likely because sodium hypochlorite contains sodium which contaminated the sample, and variable amounts of remaining Na from the cleaning agent was analysed alongside sample sodium. This suggests that cleaning by NaOCl is not appropriate for methods to determine Na/Ca ratios.

CV values could also be investigated for the Variability Samples and Modern Analogue Samples. For samples cleaned with water, the  $CV_{rep}$  values for Na/Ca ( $\bar{x}_{CV} = 2.45$  %,  $s_{CV} = 1.31$  %,  $n = 33$ ), Sr/Ca ( $\bar{x}_{CV} = 0.67$  %,  $s_{CV} = 0.54$  %,  $n = 33$ ) and Mg/Ca ( $\bar{x}_{CV} = 0.89$  %,  $s_{CV} = 0.92$  %,  $n = 33$ ) were all low indicating a high degree of reproducibility in the measurements. There was not enough material for any of the modern analogue or Variability Samples cleaned with hydrogen peroxide to be analysed in triplicate, so  $CV_{rep}$  values for hydrogen peroxide cleaned samples could not be determined.  $CV_{ind}$  values could be calculated for hydrogen peroxide cleaned samples from Variability Samples for two *Passaloteuthis pessula* belemnites, one from each stratigraphic level, as well as two *S. officinalis* and one *S. spirula* from the Modern Analogue Samples. For almost all combinations of sample and cleaning method, the  $CV_{ind}$  values for Variability Samples and modern analogue fell below 10 % indicating high reproducibility of the Sr/Ca, Mg/Ca and Na/Ca ratios within the belemnites, *S. officinalis* and *S. spirula*.

### 3.3.3. Impact of dissolution method

#### 3.3.3.1. Magnitude

Multiple dissolution methods were trialled on the Bulk Samples, with three acids being used for dissolution of samples – two strong acids (nitric and hydrochloric acid) and one weak acid (acetic acid). T tests were used to investigate differences in El/Ca values between the different dissolution methods. For each combination of sample material and cleaning method, t tests were used to determine statistically significant differences in Na/Ca, Sr/Ca, and Mg/Ca ratios between the different acids (Table 14). In all but one instance there was found to be no statistically significant difference in any of the El/Ca ratios between samples dissolved in hydrochloric acid and samples dissolved in nitric acid. The only exception to this is there was a statistically significant difference in Na/Ca in Bulk 1 cleaned with NaOCl between samples dissolved in hydrochloric acid ( $\bar{x} = 13,892$   $\mu\text{mol mol}^{-1}$ ,  $s = 274$   $\mu\text{mol mol}^{-1}$ ,  $n = 3$ ) and samples dissolved in nitric acid ( $\bar{x} = 15,020$   $\mu\text{mol mol}^{-1}$ ,  $s = 174$   $\mu\text{mol mol}^{-1}$ ,  $n = 3$ ) (Table 14). This is likely a result of contaminant sodium introduced from NaOCl in the cleaning step affecting Na/Ca ratios, rather than as a result of differences in the dissolution method.

There were more statistically significant differences in El/Ca ratios between samples dissolved in nitric acid and samples dissolved in acetic acid (Table 14). For Mg/Ca there was one sample and cleaning method combination where a statistically significant difference between dissolution methods was determined, and this difference was small (Table 14). In Bulk 2 samples cleaned with H<sub>2</sub>O<sub>2</sub>, samples dissolved in nitric acid gave average Mg/Ca values 1 % higher than samples dissolved in acetic acid (Table 14). For Na/Ca there were statistically significant differences between nitric and acetic acid only in samples from Bulk 3, for both cleaning methods (Table 14). In this case samples dissolved in acetic acid gave Na/Ca ratios 9 % and 18 % higher compared to samples dissolved in nitric acid for water cleaned and hydrogen peroxide cleaned samples respectively (Table 14). For Sr/Ca, samples dissolved with acetic acid gave slightly higher Sr/Ca values for all Bulk Samples compared to samples dissolved in nitric acid by about 3 % (Table 14). For Bulk 1, samples cleaned with NaOCl also gave higher Sr/Ca values when dissolved in acetic acid than when dissolved in nitric acid by about 2 % (Table 14). For samples cleaned with hydrogen peroxide there were no statistically significant differences between the dissolution methods (Table 14). A comparison between hydrochloric acid and acetic acid was also conducted but is not reported here. This is because there were no statistical differences between nitric and hydrochloric acid dissolutions, and the results of hydrochloric-acetic comparison were remarkably similar to the results of the nitric-acetic acid comparison reported. As with t tests comparing cleaning methods, it is possible that some statistically significant t test results with P values close to 0.05 may be false positives, and these are indicated with dark green bordered P values (Table 14).

Table 14 - T-test results demonstrating the differences in Mg/Ca and Sr/Ca values between Bulk Samples dissolved in different acids, (HCl, HNO<sub>3</sub> and acetic). For each combination of acid, cleaning method and sample n = 3. Average El/Ca ratios ( $\bar{x}$ ) in  $\mu\text{mol mol}^{-1}$ , standard deviation (s) in  $\mu\text{mol mol}^{-1}$ , and coefficient of variation values (CV) in % are reported for each combination of sample and preparative method. The degrees of freedom (df), P and t values are reported for each t test. Statistically significant results have P values highlighted in pale green. For statistically significant differences, the % difference in the El/Ca ratios is also given.

Sample Material	Cleaning method	Hydrochloric			Nitric			Acetic			Hydrochloric and nitric				Nitric and acetic			
		$\bar{x}$	s	CV	$\bar{x}$	s	CV	$\bar{x}$	s	CV	df	P	t	% diff.	df	P	t	% diff.
<b>Magnesium (Mg/Ca)</b>																		
Bulk 1	Water	22,384	79	0.4	22,580	24	0.1	22,775	262	1.1	2	7.82E-02	4.30		2	4.04E-01	4.30	
	NaOCl	22,702	100	0.4	22,917	175	0.8	22,791	65	0.3	3	2.29E-01	3.18		3	4.12E-01	3.18	
	H <sub>2</sub> O <sub>2</sub>	21,608	47	0.2	21,881	112	0.5	21,670	105	0.5	3	5.05E-02	3.18		4	1.24E-01	2.78	
Bulk 2	Water	10,782	53	0.5	10,867	20	0.2	10,877	38	0.3	3	1.25E-01	3.18		3	7.52E-01	3.18	
	H <sub>2</sub> O <sub>2</sub>	11,221	140	1.2	11,051	29	0.3	10,932	33	0.3	2	2.33E-01	4.30		4	1.86E-02	2.78	1.08
Bulk 3	Water	12,837	95	0.7	12,941	94	0.7	13,086	118	0.9	4	3.32E-01	2.78		4	2.47E-01	2.78	
	H <sub>2</sub> O <sub>2</sub>	12,898	136	1.1	12,893	183	1.4	12,955	38	0.3	4	9.73E-01	2.78		2	6.82E-01	4.30	
<b>Strontium (Sr/Ca)</b>																		
Bulk 1	Water	3,282	13	0.4	3,267	19	0.6	3,336	15	0.5	4	4.21E-01	2.78		4	1.64E-02	2.78	2.11
	NaOCl	3,222	12	0.4	3,267	24	0.7	3,345	13	0.4	3	9.81E-02	3.18		3	2.76E-02	3.18	2.39
	H <sub>2</sub> O <sub>2</sub>	3,304	22	0.7	3,281	10	0.3	3,320	21	0.6	3	2.77E-01	3.18		3	1.01E-01	3.18	
Bulk 2	Water	1,634	5	0.3	1,624	3	0.2	1,676	8	0.5	3	1.24E-01	3.18		3	3.93E-03	3.18	3.16
	H <sub>2</sub> O <sub>2</sub>	1,706	34	2.0	1,672	12	0.7	1,696	10	0.6	2	3.11E-01	4.30		4	9.95E-02	2.78	
Bulk 3	Water	2,041	17	0.8	2,056	17	0.8	2,146	8	0.4	4	4.32E-01	2.78		3	6.74E-03	3.18	4.38
	H <sub>2</sub> O <sub>2</sub>	1,873	27	1.5	1,967	58	2.9	2,094	6	0.3	3	1.30E-01	3.18		2	9.07E-02	4.30	
<b>Sodium (Na/Ca)</b>																		
Bulk 1	Water	14,310	718	5.0	14,238	174	1.2	14,708	708	4.8	3	9.08E-01	3.18		3	4.70E-01	3.18	
	NaOCl	13,892	274	2.0	15,020	174	1.2	18,161	4648	25.6	2	1.62E-02	3.18	8.12	3	4.40E-01	4.30	
	H <sub>2</sub> O <sub>2</sub>	13,535	468	3.5	14,648	302	2.1	14,254	69	0.5	3	6.64E-02	3.18		2	2.14E-01	4.30	

Sample Material	Cleaning method	Hydrochloric			Nitric			Acetic			Hydrochloric and nitric				Nitric and acetic			
		$\bar{x}$	s	CV	$\bar{x}$	s	CV	$\bar{x}$	s	CV	df	P	t	% diff.	df	P	t	% diff.
Bulk 2	Water	7,243	64	0.9	7,514	105	1.4	8,708	533	6.1	3	5.26E-02	3.18		2	8.99E-02	4.30	
	H <sub>2</sub> O <sub>2</sub>	8,568	173	2.0	8,245	283	3.4	8,751	247	2.8	3	2.63E-01	3.18		4	1.30E-01	2.78	
Bulk 3	Water	11,301	194	1.7	11,504	184	1.6	12,570	3	0.0	4	3.42E-01	2.78		2	1.45E-02	4.30	9.26
	H <sub>2</sub> O <sub>2</sub>	11,037	237	2.2	11,479	408	3.6	13,601	833	6.1	3	2.77E-01	3.18		3	4.81E-02	3.18	18.48

### 3.3.3.2. Variance

In each combination of sample and cleaning method, the  $CV_{rep}$  values for each  $El/Ca$  ratio was low indicating low variability and high reproducibility between replicate samples. For  $Mg/Ca$  and  $Sr/Ca$  with all dissolution methods, the  $CV_{rep}$  values are below 1 %. For  $Na/Ca$   $CV$  values are slightly higher, with average  $CV$  values of 2.5 %, 2.2 % and 3.4 % for samples dissolved in hydrochloric, nitric, and acetic acid respectively (when results for samples cleaned with  $NaOCl$  are excluded due to contamination with variable amounts of  $Na$ ). The higher  $CV$  values for  $Na/Ca$  are still very low and indicate high reproducibility of  $Na/Ca$  values between replicate samples.

### 3.3.4. Impact of sample size

Three sample sizes were assessed for Bulk Samples 1, 2 and 3 – 2 mg, 5 mg, and 10 mg. For 2 mg and 10 mg samples were cleaned with  $H_2O_2$  and dissolved in acetic acid. These were compared to 5 mg samples prepared the same way. For all sample sizes evaluated,  $Na$ ,  $Sr$  and  $Mg$  did not fall below the  $LOD/LOQ$  for any samples. The  $CV_{rep}$  values calculated for each sample at each sample mass were all below 20 % indicating a good level of reproducibility. For the low abundance trace elements  $Ba$  and  $S$  were below  $Lod$  or  $LOQ$  in many of the measured 2 mg samples, so if trace element measurements are required then smaller sample sizes are not suitable.

### 3.3.5. Investigating variability

#### 3.3.5.1. Evaluating the impact of diagenesis

The variability and modern analogue were investigated to determine the variability of  $El/Ca$  ratios within and between individuals. For Variability Samples, there was potential for  $El/Ca$  ratios to be affected by diagenetic alteration and contamination. As with  $P/Ca$  ratios, to attempt to negate the impact of diagenesis,  $Mn$  and  $Fe$  were used to screen out altered and contaminated samples. The same  $Mn/Ca$  and  $Fe/Ca$  limits ( $Mn/Ca > 300 \mu mol mol^{-1}$ ;  $Fe/Ca < 600 \mu mol mol^{-1}$ ) were used for the  $El/Ca$  ratios as were used for  $P/Ca$  ratios (2.5.5.1). For the screened samples,  $Mn/Ca$  and  $Fe/Ca$  values were compared to  $El/Ca$  ratios to determine if  $Na/Ca$ ,  $Sr/Ca$ , or  $Mg/Ca$  values varied with the diagenetic indicators (Table 15).

Table 15 -  $R^2$  values for the correlation between  $Fe/Ca$  and  $Mn/Ca$  and other  $El/Ca$  ratios for samples from the *Amaltheus gibbosus ammonite subzone* in the Penny Nab section and the *Phricodoceras taylori ammonite subzone* in the Wine Haven section.

El ratio	Wine Haven		Penny Nab	
	Fe/Ca	Mn/Ca	Fe/Ca	Mn/Ca
<b>Mg/Ca</b>	0.01	0.05	0.33	0.31
<b>Sr/Ca</b>	0.15	0.08	0.20	0.26
<b>Na/Ca</b>	0.24	0.17	0.15	0.20

$R^2$  values were calculated to examine potential correlations between El/Ca and Mn/Ca and Fe/Ca for samples from the Wine Haven section and samples from the Penny Nab section (Table 15). The  $R^2$  values ranged from 0.01 to 0.33, with an average of 0.18 (Table 15). All of the values were low which indicated poor correlation between Mn/Ca and Fe/Ca and the other El/Ca ratios (Table 15). This suggests that in the screened samples, diagenetic alteration and contamination does not influence the El/Ca ratios included here (Table 15).

Alternatively, the relationship between Mn and Fe may be highly sample-specific and complicated by availability of Mn and Fe in the diagenetic fluid causing differential uptake even on the scale of millimetres. This can cause complications in the use of Mn and Fe as diagenesis markers, as the El/Ca ratios may still be affected by the impacts of diagenesis.

#### 3.3.5.2. Variability within a belemnite

The Variability Samples were used to investigate El/Ca variations within individual belemnites. As discussed previously, for all preparative methods studied there were low  $CV_{ind}$  values for Na/Ca, Mg/Ca, and Sr/Ca – which indicates low variability and high reproducibility within individuals (3.3.3.2).

Trends in El/Ca along the length of the rostra were examined for Na/Ca, Sr/Ca, and Mg/Ca for samples from Penny Nab and Wine Haven. In samples from Wine Haven, it was found that for Na, Mg and Sr there were higher El/Ca concentrations towards the apex of the belemnite rostrum (Figure 18). For all elements, the correlation between El/Ca and proximity to the apex was strongest for the *Nannobelus delicatus* belemnites compared to the *Bairstowius* sp. individual (Figure 18). The sampling was not controlled for position of the samples between the apical line of the belemnite and the outer rim, unaltered samples close to the apical line may demonstrate elevated El/Ca ratios which would account for the enrichment of El/Ca away from the apex in some samples.

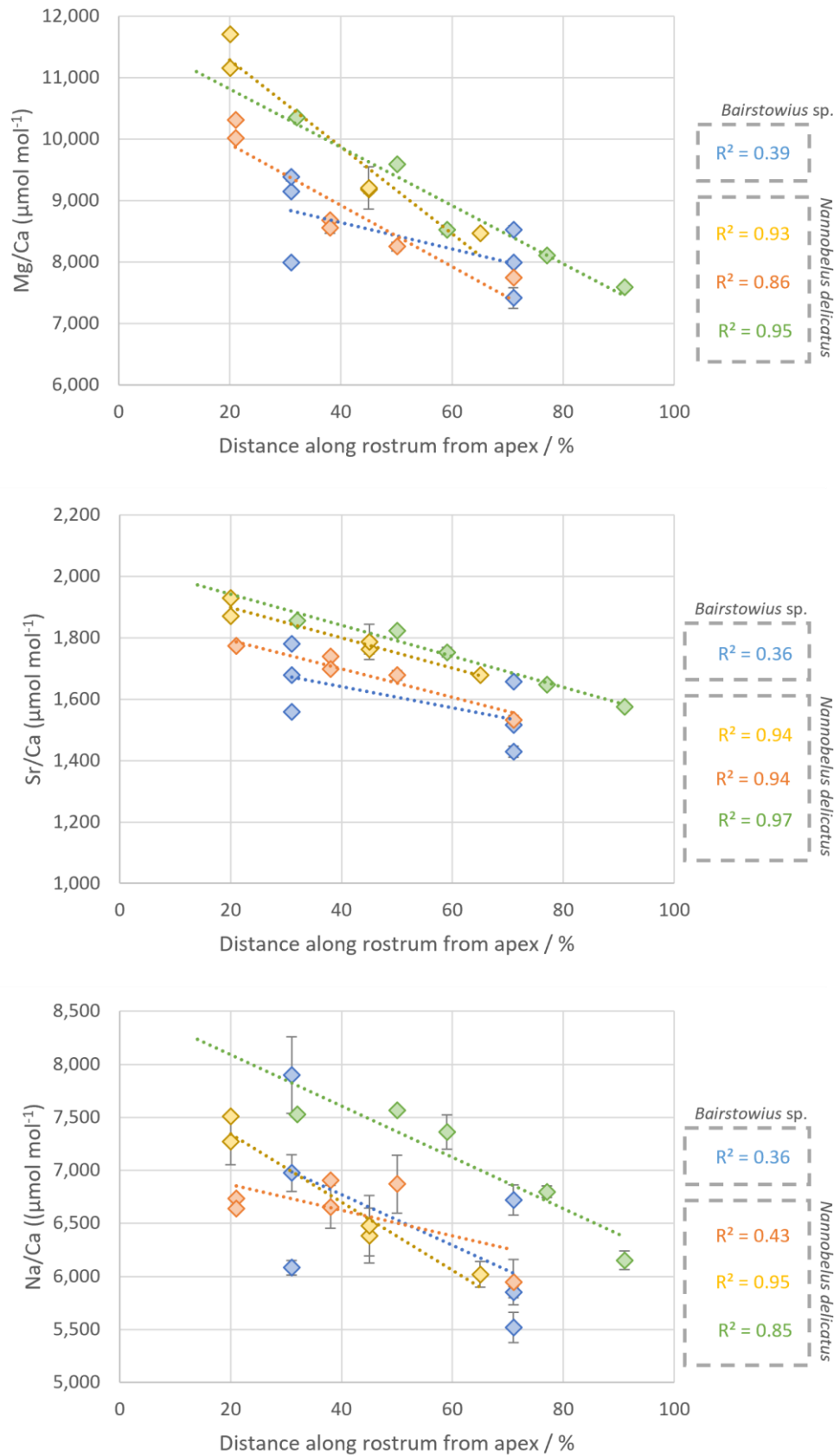


Figure 18 -  $\text{El}/\text{Ca}$  against the distance along the belemnite rostrum from the apex in percent for four individual belemnites collected from Wine Haven, Yorkshire (Phricodoceras taylori zone). The sample in blue is *Passaloteuthis sp.* and the other three samples are *Nannobelus delicatus*. Each data point is the average of triplicate sample analysis and error bars included give one standard deviation where  $n=3$ .

For Samples from Penny Nab, some belemnites showed the same trend where El/Ca ratios were enriched near the apex, whereas some showed no trend or opposing trends where El/Ca ratios were enriched further from the apex (Table 16). There did not appear to be any trend in individual, species, or element between which El/Ca ratios were enriched closer to the apex in the Penny Nab samples (Table 16). Overall, El/Ca ratios were more often enriched towards the apex (10 instances) in individual belemnites than depleted (3 instances) though there were also 10 instances where no trend could be determined (Table 16).

Table 16 -  $R^2$  values for relationships between distance from the apex and El/Ca ratios for individual belemnites from three distinct species collected from the *Amaltheus gibbosus ammonite* subzone at Penny Nab. Where El/Ca correlated negatively with distance to the apex (elements enriched nearer apex) cells are shaded green, with darker green for stronger correlations. Where El/Ca correlates positively with distance from the apex (elements depleted nearer apex) cells are shaded orange with darker orange for stronger correlation.

El ratio	<i>Bairstowius</i> sp.		<i>Parapassaloteuthis</i> sp.		<i>Passaloteuthis pessula</i>	
	1	1	2	3	1	2
Mg/Ca	0.10	0.35	0.52	0.02	0.34	0.45
P/Ca	0.32	0.05	0.43	0.56	4E-05	1.00
Sr/Ca	0.64	0.34	0.95	0.03	0.13	0.91
Na/Ca	0.17	0.99	0.97	5E-04	9E-04	0.84

### 3.3.5.3. Between belemnites

Differences in El/Ca ratios between species, between stratigraphic level and between different sizes of belemnite were studied. To investigate the impact of species, El/Ca results from all *Passaloteuthis pessula* and all *Parapassaloteuthis* sp. belemnites from the same stratigraphic level (*Amaltheus gibbosus* level from the Penny Nab section) were compared using t tests.

For Na/Ca there were shown to be no statistically significant differences between the *Passaloteuthis pessula* samples ( $\bar{x} = 8,384 \mu\text{mol mol}^{-1}$ ,  $s = 828 \mu\text{mol mol}^{-1}$ ,  $n = 27$ ) and the *Parapassaloteuthis* sp. belemnites ( $\bar{x} = 8,713 \mu\text{mol mol}^{-1}$ ,  $s = 730 \mu\text{mol mol}^{-1}$ ,  $n = 42$ );  $t(50) = 2.01$ ,  $p = 0.104$  (Figure 19). For both Sr/Ca and Mg/Ca there were statistically significant differences between *Passaloteuthis pessula* (Sr:  $\bar{x} = 1,876 \mu\text{mol mol}^{-1}$ ,  $s = 182 \mu\text{mol mol}^{-1}$ ,  $n = 27$ ; Mg:  $\bar{x} = 12,121 \mu\text{mol mol}^{-1}$ ,  $s = 1,019 \mu\text{mol mol}^{-1}$ ,  $n = 27$ ) and *Parapassaloteuthis* (Sr:  $\bar{x} = 1,715 \mu\text{mol mol}^{-1}$ ,  $s = 184 \mu\text{mol mol}^{-1}$ ,  $n = 43$ ; Mg:  $\bar{x} = 10,579 \mu\text{mol mol}^{-1}$ ,  $s = 777 \mu\text{mol mol}^{-1}$ ,  $n = 43$ ); Sr:  $t(56) = 2.00$ ,  $p = 8.00\text{E-}04$ ; Mg:  $t(66) = 2.00$ ,  $p = 9.88\text{E-}05$  (Figure 19). This suggests that differences in species is one factor which can affect Sr/Ca and Mg/Ca ratios but is not a factor which affects Na/Ca ratios (Figure 19). Despite the variability within and between individuals of the same and different species, for each El/Ca ratio there was low variability within each stratigraphic level. For each El/Ca ratio,  $\text{CV}_{\text{M}}$  values were calculated using each El/Ca ratio

measured from each stratigraphic level (Table 17). In each case, the  $CV_{VI}$  calculated was less than 20 % indicating a high degree of reproducibility within samples from the same stratigraphic level (based on 77 samples from 6 individuals in the *Amaltheus gibbosus* ammonite subzone at Penny Nab and 52 samples from four individuals in the *Phricodoceras taylori* ammonite subzone in the Wine Haven section) (Table 17).

*Table 17 -  $CV_{VI}$  values indicating the variability of El/Ca values for samples collected from two stratigraphic levels on the Yorkshire coast, calculated from El/Ca values from Modern Analogue Samples from each stratigraphic level. Penny Nab samples were collected from the Penny Nab section in Staithes from the *Amaltheus gibbosus* ammonite subzone in the Upper Pliensbachian. Wine Haven samples are from the *Phricodoceras taylori* ammonite subzone in the Lower Pliensbachian. For samples from Wine Haven,  $n = 52$ . For samples from Penny Nab  $n = 78$  except in the case of sodium, where  $n = 77$ .*

<b>El ratio</b>	<b>Penny Nab</b>	<b>Wine Haven</b>
<b>Mg/Ca</b>	17.8	11.4
<b>Sr/Ca</b>	12.0	7.1
<b>Na/Ca</b>	9.1	9.7

For Na, Mg and Sr there were statistically significant differences in the El/Ca ratios between the stratigraphic levels studied, with higher El/Ca ratios for samples from Penny Nab (Sr:  $\bar{x} = 1,748 \mu\text{mol mol}^{-1}$ ,  $s = 210 \mu\text{mol mol}^{-1}$ ,  $n = 78$ ; Mg:  $\bar{x} = 10,908 \mu\text{mol mol}^{-1}$ ,  $s = 1,943 \mu\text{mol mol}^{-1}$ ,  $n = 78$ ; Na:  $\bar{x} = 8,656 \mu\text{mol mol}^{-1}$ ,  $s = 787 \mu\text{mol mol}^{-1}$ ,  $n = 77$ ) than from Wine Haven (Sr:  $\bar{x} = 1,685 \mu\text{mol mol}^{-1}$ ,  $s = 119 \mu\text{mol mol}^{-1}$ ,  $n = 52$ ; Mg:  $\bar{x} = 8,800 \mu\text{mol mol}^{-1}$ ,  $s = 1,004 \mu\text{mol mol}^{-1}$ ,  $n = 52$ ; Na:  $\bar{x} = 6,655 \mu\text{mol mol}^{-1}$ ,  $s = 649$ ,  $n = 52$ ); Sr:  $t(125) = 1.98$ ,  $p = 0.036$ ; Mg:  $t(122) = 1.98$ ,  $p = 6.58E-13$ ; Na:  $t(122) = 1.98$ ,  $p = 6.98E-31$  (Figure 19).

The impact of belemnite size on El/Ca ratios was also investigated. Belemnite sizes included in the Variability Samples ranged from 3.5-6.8 cm in length. As with P/Ca, for all El/Ca ratios studied, there was no significant correlation between belemnite length and El/Ca – though as with P/Ca this may have been affected by the selection criteria for the variability test where larger samples which could be sampled multiple times were selected in preference to smaller samples.

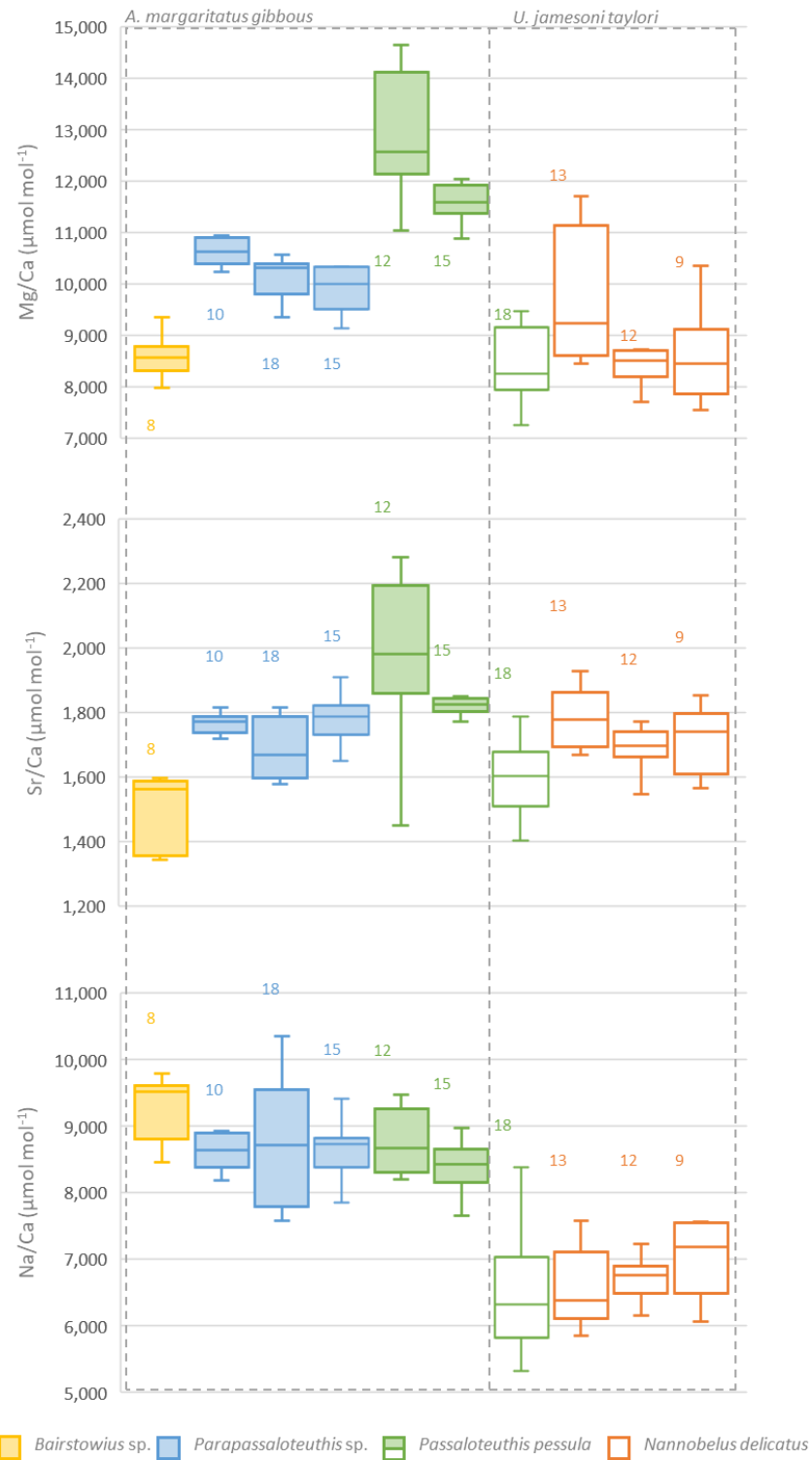


Figure 19 -  $El/Ca$  values for 10 belemnites from two different stratigraphic heights collected from the Yorkshire coast. Each box represents  $El/Ca$  values for one individual belemnite. Each colour represents a belemnite species. Each individual was sampled six times along the length of the rostrum, and where material was available each sample was analysed in triplicate. Filled boxes indicate samples collected from Penny Nab in Staithes from the *Amaltheus gibbous* ammonite subzone in the Upper Pliensbachian. Unfilled boxes indicate samples collected from Wine Haven in Robin Hood's Bay from the *Phricodoceras taylori* ammonite subzone in the Lower Pliensbachian. The  $n$  number for the number of samples included in each box is displayed.

### 3.3.5.4. Variability in modern analogues

#### 3.3.5.4.1. *Within individuals*

CV<sub>ind</sub> values were calculated for variability within individual cuttlebones and *S. spirula* shells, as described in Section 3.3.2.2. CV<sub>ind</sub> values for both cleaning methods were consistently low, all below 10 % indicating high reproducibility of Na/Ca, Sr/Ca and Mg/Ca ratios within *S. officinalis* and *S. spirula* regardless of preparative method.

For Na/Ca it was found that there were no statistically significant differences between individuals for either *S. officinalis* or *S. spirula* (Table 18). For strontium, there were statistically significant differences in Sr/Ca ratios between both *S. officinalis* and *S. spirula* – with one individual giving 23 – 24 % higher Sr/Ca values in both cases). In *S. officinalis*, the highest Sr/Ca value was from Cuttlefish bulk – which was the older cuttlefish who lived in higher average water temperatures (Table 18). For magnesium, there was only a statistically significant difference in Mg/Ca between *S. officinalis*, no difference was seen in Mg/Ca ratios between the *S. spirula* (Table 18). The concentration of Mg in the cuttlebones was considerably higher than the concentration in the *S. spirula* shells. This may suggest the presence of magnesium in a contaminant phase, such as organic matter, which may be more concentrated in cuttlebones than *S. spirula* shells. Both are likely to have higher primary magnesium concentrations than calcite biominerals, such as belemnites are made of, as aragonitic carbonates have higher magnesium concentrations than calcitic carbonates (e.g., Taft, 1967; Katz, 1973; Berner, 1975; Mucci and Morse, 1983; Davis *et al.*, 2000; Astilleros *et al.*, 2010). Again, the *S. officinalis* with the highest Mg/Ca ratio is Cuttlefish B, which lived in water with higher average temperatures than Cuttlefish A (Table 18). It should be noted however, that Cuttlefish A died of predation, whereas Cuttlefish bulk was euthanised after illness by injection of magnesium chloride hexahydrate, so the elevated Mg/Ca ratios may be accounted for by this injection.

Table 18 - T-test results to examine the differences in El/Ca ratios between two *Sepia officinalis* and two *Spirula spirula* individuals. All samples were cleaned with water and dissolved in acetic acid. For each individual, average El/Ca ratios ( $\bar{x}$ ) in  $\mu\text{mol mol}^{-1}$ , one standard deviation ( $s$ ) in  $\mu\text{mol mol}^{-1}$ , and coefficient of variation values (CV) in % were calculated. For each t test performed the degrees of freedom (df) and P and t values are reported. Where the t test results demonstrate a statistically significant difference between cleaning methods, the P values are highlighted in pale green. For statistically significant differences, the % difference in the El/Ca ratios is also given.

El ratio	<i>Sepia officinalis</i> A				<i>Sepia officinalis</i> B				t-test Results			
	$\bar{x}$	s	CV	n	$\bar{x}$	s	CV	n	df	P	t	% diff
Mg / Ca	1,756	31	1.8	3	2,452	235	9.6	9	9	2E-05	2.26	28
Sr / Ca	3,936	144	3.7	3	5,208	163	3.1	9	3	0.0017	3.18	24
Na / Ca	22,851	1,751	7.7	3	24,777	320	1.3	9	2	0.26	4.30	-
El ratio	<i>Spirula spirula</i> A				<i>Spirula spirula</i> B				t-test Results			
	x	s	CV	n	x	s	CV	n	df	P	t	% diff
Mg / Ca	647	50	7.7	6	635	16	2.6	4	7	0.63	2.36	-
Sr / Ca	3,533	142	4.0	6	2,873	41	1.4	4	6	6.9E-05	2.45	23
Na / Ca	2,3396	1,042	4.5	6	23,853	566	2.4	4	8	0.44	2.31	-

### 3.4. Discussion

#### 3.4.1. Impact of a cleaning method

For all cleaning methods, the reproducibility of El/Ca ratios was high, with CV<sub>rep</sub> values below 10. The only exception to this was in the determination of Na/Ca ratios in samples cleaned with NaOCl, likely due to the inclusion of variable amounts of sodium from the cleaning agent in the final sample analysis. As all the cleaning methods gave consistently reproducible results, the main differences between cleaning methods were the magnitudes of the El/Ca ratios (Table 19).

*Table 19 - Summary of the differences in El/Ca ratios between different cleaning methods for different sample materials and dissolution methods.*

<b>Sample</b>	<b>Magnesium (Mg/Ca)</b>	<b>Strontium (Sr/Ca)</b>	<b>Sodium (Na/Ca)</b>
<b>Bulk 1</b>	H <sub>2</sub> O <sub>2</sub> cleaned samples gave 2-5 % higher Mg/Ca values than water cleaned samples	No difference between cleaning methods	No difference between cleaning methods
<b>Bulk 2</b>	Water cleaned samples gave 2 % higher Mg/Ca values than H <sub>2</sub> O <sub>2</sub> cleaned samples when averaged across all dissolution methods, for acetic acid dissolved samples only no difference between cleaning methods was seen	Water cleaned samples gave 3 % higher Sr/Ca values than H <sub>2</sub> O <sub>2</sub> cleaned samples when averaged across all dissolution methods, for acetic acid dissolved samples only no difference between cleaning methods was seen	No difference between cleaning methods
<b>Bulk 3</b>	No difference between cleaning methods	H <sub>2</sub> O <sub>2</sub> cleaned samples gave 3-5 % higher Mg/Ca values than water cleaned samples	No difference between cleaning methods
<b>Variability Samples</b>	Water cleaned samples gave 20 % higher Mg/Ca values than H <sub>2</sub> O <sub>2</sub> cleaned samples	Water cleaned samples gave 17 % higher Sr/Ca values than H <sub>2</sub> O <sub>2</sub> cleaned samples	No data for H <sub>2</sub> O <sub>2</sub> cleaned samples (below LOD/LOQ)

<b>Modern Analogue Samples</b>	Water cleaned samples gave 20-40 % higher Mg/Ca values than H <sub>2</sub> O <sub>2</sub> cleaned samples	No difference between cleaning methods	No difference between cleaning methods
--------------------------------	---	--	--

After correcting for the difference in calcium concentration by using a ratio to sample mass, Bulk 1 contained lower quantities of acid soluble Sr, Mg and Na than Bulk 2 and Bulk 3. This suggests that diagenetic and infilled sediment material from the phragmocone is not a significant source of Mg, Sr, or Na, or that the forms of Mg, Na and Sr found in the phragmocone material are easily removed during cleaning steps or that they are insoluble during dissolution.

Different cleaning methods impacted Bulk Samples and Variability Samples in different ways (Table 10). Variability Samples gave higher Sr/Ca and Mg/Ca ratios in samples cleaned with water compared to samples cleaned with hydrogen peroxide, whereas Bulk Samples gave mixed results for different combinations of El/Ca ratios, sample, and cleaning methods. This is likely because the H<sub>2</sub>O<sub>2</sub> used to prepare the Bulk Samples was older and had potentially been incorrectly stored, so had degraded in comparison to the H<sub>2</sub>O<sub>2</sub> used to prepare the variability and Modern Analogue Samples. Degraded hydrogen peroxide may have affected the dissolution of some forms of contaminant phases in the samples, for example being less able to effectively oxidise and remove organic matter and creating more variable results. This suggests the Variability Samples cleaned with hydrogen peroxide are more representative of a true oxidative cleaning method than the Bulk Samples cleaned with H<sub>2</sub>O<sub>2</sub>. Based on the Variability Samples data, Both Mg/Ca and Sr/Ca ratios were lower in oxidatively cleaned samples than in water cleaned samples – with Mg/Ca 20 % lower in H<sub>2</sub>O<sub>2</sub> cleaned samples and Sr/Ca 17 % lower. Previous work on belemnites has shown two phases of calcite in the rostra, a high-Mg, high-P, low-S phase and a low-Mg-low-P, high-S phase (Hoffmann *et al.*, 2016). Further work has indicated that it is likely both phases of calcite have similar concentrations of Sr (Hoffmann *et al.*, 2021). This suggests that hydrogen peroxide may be preferentially dissolving high Mg calcite, which would remove both Mg and Sr, though proportionally slightly more Mg.

Mg/Ca gave significantly higher values (30-40 %) in modern analogue cleaned with water than samples cleaned with H<sub>2</sub>O<sub>2</sub> (Table 11; Table 19). This is likely to be due to magnesium associated with organic matter in the rostra, which is removed by the oxidative cleaning. This is consistent with the results for phosphorus, which gave substantially higher P/Ca ratio with

oxidative cleaning, as P is likely to reabsorb to the surface of the powder and magnesium is not (Table 9). For Sr/Ca, there was no difference between the cleaning methods for modern analogue – likely due to lower amount of strontium associated with organic matter in the samples, compared to magnesium and phosphorus.

For sodium, measurements for the Variability Samples were below the limit of detection and cannot be examined. In the Bulk Samples there were no statistically significant differences in Na/Ca between different cleaning methods, though it is possible that this is also an artefact of weaker H<sub>2</sub>O<sub>2</sub> used for the Bulk Samples. In Modern Analogue Samples, there no statistically significant differences between cleaning methods, likely because there was no organic-associated sodium. Overall, the lack of impact of cleaning methods on Na/Ca is likely because there is little sodium present in contamination (such as in the infilled sediment and diagenetic material in Bulk 1), or that the sodium present is in a form which is easily soluble such as NaCl or other simple salts, feldspars, or clays, which are easily removed by either cleaning method. Alternatively, it is possible that the sodium in contaminant sediment or diagenetic material is in an insoluble form which is not removed by cleaning method or dissolved in any of the acids. This is possible as sodium is likely to be bound to aluminosilicate frameworks which are resistant to leaching, meaning Na released would be from surface sites but not the lattice interior (e.g., Buckley and Cranston, 1971).

### 3.4.2. Impact of dissolution method

As with the different cleaning methods, for each dissolution method El/Ca ratios were shown to have high reproducibility, with CV values for each dissolution method all below 10 % (Table 14). As all the dissolution methods gave consistently reproducible results, the main differences between dissolution methods were the magnitudes of the El/Ca ratios (Table 14). Three different acids were assessed for sample dissolution on Bulk Samples – two strong acids (hydrochloric and nitric acid) and one weak acid (acetic acid). T tests showed that there were no statistically significant differences in El/Ca ratios for Na, Sr, and Mg between the two strong acids tested (Table 14). There were statistically significant differences between the strong acids and acetic acid, for some sample and cleaning method combinations (Table 14). T tests showed that samples where there were statistically significant differences between nitric and acetic acid, also had statistically significant differences between hydrochloric and acetic acid, and vice versa, so differences can be described as being between strong acids and acetic acid as opposed to nitric acid or hydrochloric acid specifically (Table 20).

Table 20 - Summary of the differences in *El/Ca* ratios between different dissolution methods for different sample materials and cleaning methods. Percentage differences are based on the differences between nitric acid and acetic acid dissolution (Table 14).

Sample	Magnesium (Mg/Ca)	Strontium (Sr/Ca)	Sodium (Na/Ca)
<b>Bulk 1</b>	No difference between strong acids and acetic acid dissolution for all samples regardless of cleaning method	Acetic acid dissolution gave 2 % higher Sr/Ca values compared to strong acids in samples cleaned with water and NaOCl; no difference between dissolution methods in samples cleaned with H <sub>2</sub> O <sub>2</sub>	No difference between strong acids and acetic acid dissolution for all samples regardless of cleaning method
<b>Bulk 2</b>	Strong acids acid gave 1 % higher Mg/Ca values compared to acetic acid in samples cleaned with H <sub>2</sub> O <sub>2</sub> ; no difference between dissolution methods in samples cleaned with water	Acetic acid dissolution gave 3 % higher Sr/Ca values compared to strong acids in samples cleaned with water; no difference between dissolution methods in samples cleaned with H <sub>2</sub> O <sub>2</sub>	No difference between strong acids and acetic acid dissolution for all samples regardless of cleaning method
<b>Bulk 3</b>	No difference between strong acids and acetic acid dissolution for all samples regardless of cleaning method	Acetic acid dissolution gave 4 % higher Sr/Ca values compared to strong acids in samples cleaned with water; no difference between dissolution methods in samples cleaned with H <sub>2</sub> O <sub>2</sub>	Acetic acid dissolution gave higher Na/Ca values by 9 % in samples cleaned with water and 18 % in samples cleaned with H <sub>2</sub> O <sub>2</sub> compared to samples dissolved in strong acids

Dissolution method did not appear to have a strong effect on Mg/Ca ratios (Table 14; Table 20). Between dissolution methods there was either no difference in Mg/Ca values or a difference of only 1 % (Table 14; Table 20). This suggests that in belemnite calcite the form in which magnesium is found is soluble in both weak and strong acids. In modern biogenic

carbonates, even in organisms with very high Mg calcite, such as is found in modern sea-urchin *Paracentrotus lividus* (which is 11 % MgCO<sub>3</sub>), the vast majority of Mg is substituted into the Ca lattice position (Politi *et al.*, 2010). It is therefore likely that the magnesium found in belemnite calcite is substituted into the Ca lattice positions. Magnesium carbonate is highly soluble in acids, including weak acid, so this would explain why there is no difference in Mg/Ca value between dissolution methods.

For Sr/Ca ratios, samples cleaned with water and dissolved in acetic acid showed slightly higher Sr/Ca values than samples dissolved in strong acids by 2-4 %. The same trend was not seen in samples cleaned with H<sub>2</sub>O<sub>2</sub>. This may be due to differences in the quantity of organic matter remaining in the samples after application of the different cleaning methods, with even a weaker H<sub>2</sub>O<sub>2</sub> having removed more organic matter than cleaning with water.

For Na/Ca ratios there was no difference in Na/Ca ratios between dissolution methods for samples from Bulk 1 and 2. For samples from Bulk 3, samples dissolved in acetic acid have higher Na/Ca ratios than samples dissolved in strong acids by 9 % for samples cleaned with water and 18 % for samples cleaned with H<sub>2</sub>O<sub>2</sub>. This is surprising due to the similarity between Bulk 2 and Bulk 3 in other tests, so may be a result of a contamination of samples or reagents in the lab in this case. This highlights the importance of avoiding contamination in samples for sodium analysis, as sodium is a common contaminant in laboratories and everyday life.

### 3.4.3. Impact of sample size

Sampling size did not appear to have an impact on analysis of Na, Sr or Mg with no samples falling below the LOD/LOQ and all the CV<sub>rep</sub> values falling below 20 % for each El/Ca ratio, sample, preparative method, and sample size combination, indicating sample size differences did not negatively impact reproducibility. This is unexpected as we may anticipate a negative correlation of CV with sample size, though this is not observed here – potentially as the number of replicates at each sample size analysed was fairly small (3 replicates).

For trace elements, Ba and S fell below the LOD/LOQ in 2 mg samples, suggesting that for these elements smaller sample sizes are not appropriate.

### 3.4.4. Variability

#### 3.4.4.1. Sampling technique

Na, Sr, and Mg did not fall below the LOD or LOQ for analysis at any of the sample sizes trialled (2 mg, 5 mg, 10 mg) and all analyses gave CV<sub>rep</sub> values indicating good reproducibility of results (< 20 %). This suggests that, while 5 mg was determined to be the preferred sample size for analysis of phosphorus, should limited sample material mean that smaller samples are required, Na, Sr and Mg can still be measured reliably.

#### 3.4.4.2. Within belemnites

For each El/Ca ratio, the  $CV_{ind}$  value indicating variability and reproducibility within individual belemnites were all low, with average  $CV_{ind}$  values below 10 % indicating high reproducibility. For each Na, Sr and Mg, there were trends in each El/Ca ratio within individual belemnites for some individuals. In individuals where these trends were observed, El/Ca ratios were enriched closer to the apex of the rostrum and depleted further down the rostrum. This was not observed for all individuals but was observed for all belemnites from the Wine Haven section – with particularly strong trends (with  $R^2$  values generally greater than 0.8) for *Nannobelus delicatus*. In belemnites from the Penny Nab section, some belemnites showed the trend for some elements, but there was no consistent pattern of which species or individuals demonstrated the trend. Wine Haven samples also exhibited better preservation than Penny Nab samples, with lower  $R^2$  values indicating reduced correlation between Mn and Fe with Mg, Sr, and Na (Table 15). This suggests that it is possible that preservation issues have masked the trend in El/Ca ratios within belemnites from the Penny Nab sections, though species differences cannot be ruled out. Alternatively, the lack of an evident trend in El/Ca along the length of the rostra may be a result of not controlling for the positioning of the sampling between the apical line of the rostra and the rostra's rim. In unaltered samples close to the apical line, an enrichment in El/Ca similar to the enrichment seen at the rostra is also found (Ullmann *et al.*, 2017). This may be responsible for the lack of trend in El/Ca ratios along the rostra seen in the majority of individuals from the Penny Nab section – though it is curious that the effect appears to be section specific (Table 16). For a more thorough investigation of the variation of El/Ca variation along the length of the rostra, a better attempt should be made to control the sampling distance from the apical line, though for the purposes of identifying natural levels of variability of El/Ca in belemnites the results obtained here are sufficient.

The variability within belemnites is mirrored by variability in Mg/Ca ratios in biogenic carbonates of other organisms. Magnesium is also vitally important for biogenic carbonate formation – though the mechanisms behind this are poorly understood. In the modern ocean, magnesium is five times more abundant than calcium, and Mg concentrations in biogenic calcite can vary from 0-30 mol % (Chave, 1954a). In many organisms Mg concentrations can vary across the carbonate skeletons, suggesting an element of biological control on Mg incorporation (e.g., Wang *et al.*, 1997; McArthur *et al.*, 2007a; Ullmann *et al.*, 2015). Previous studies in belemnites have also demonstrated variability in El/Ca ratios within belemnite rostra, including identifying the same trends of enrichment in Sr/Ca and Mg/Ca towards the apex of the belemnite as was observed in some individuals in this study. Some researchers have suggested that Mg/Ca and Sr/Ca are controlled in part by growth rate effects, which would cause this variation along the rostra due to differences in the distance between the

concentric growth rings at the apex compared to the distances between them in the rest of the rostrum. At the apex it may be expected that there will be fewer concentric growth rings with proportionally larger distances between them (Ullmann *et al.*, 2015). In addition, sampling close to the apex of the belemnite often means sampling closer to the apical line, which has compounding effects on the crystal morphology and El/Ca ratios – which have been shown to be enriched closer to the apical line in unaltered samples (e.g., Ullmann *et al.*, 2015). Other studies have shown differences in El/Ca ratios within different phases of calcite within the rostrum. A study by Hoffmann *et al.* (2016) used electron microprobe data to show two phases of calcite: tetrahedral regions of calcite with higher concentrations of Mg and P and lower levels of S, and surrounding calcite outside the tetrahedral regions with lower P and Mg and higher S. Hoffmann *et al.* (2016) suggested that the high-Mg calcite phase in the tetrahedral regions, which also contained higher levels of organic material, were more likely to be primary calcite, with the low-Mg surrounding phase likely to result from pores in the belemnite structure being infilled with calcite during early diagenetic processes – though it is possible that both phases were formed during the belemnite's lifetime (Hoffmann *et al.*, 2016). If the two calcite phases are representative of pre- and post-mortem calcite growth, then the two phases would have formed at different depths in the water column, with primary calcite growth in the top 100-200 modern analogue of the water column (where belemnites are likely to have lived) and the infilled calcite formed after death on the seafloor or in the upper sediment (Hoffmann *et al.*, 2021). It is possible that both phases of the calcite contain a temperature signal, but due to the differences in depths of formation, and the delay in forming the infilled calcite, the temperatures recorded are offset and not in phase. The average concentration of magnesium in the rostrum calcite may then be determined by the ratio between the two phases of calcite, which may in turn be affected by other factors such as differences in species, age, sex. It may also be expected that different regions of the same belemnite may have different ratios of these two phases, leading to the observed trends in El/Ca within individuals. The differences in proportions of the two phases of calcite may explain why Mg is a poor temperature proxy in belemnites, and the different times and depths of calcite formation may also explain the relative unreliability of oxygen isotopes in belemnites compared to other carbonates.

A further study by Hoffmann *et al.* (2021) demonstrates that Sr concentrations are very similar between the two phases of calcite, suggesting that differences between the relative proportions of the two phases are unlikely to be a control for average Sr concentration in the rostra. This is further supported by work conducted by McArthur *et al.* (2007a), which found little to no radial variation of Sr concentrations, while Mg concentrations varied across the

radial profiles studied. This is interesting as the data produced in this study shows that Sr/Ca and Mg/Ca exhibit similar trends along the length of the belemnite rostra, with enrichment in El/Ca ratios near the apex of the rostra. Previous work has demonstrated that the magnitudes of variation in El/Ca ratios are different across radial transects compared to along the rostra, with larger variations in Mg/Ca and Sr/Ca from the rim to the apical line of a rostra compared to along the length of the rostra, when distance from the apical line is controlled for (e.g., Sørensen *et al.*, 2015; Ullmann *et al.*, 2015). When distance from the apical line is not controlled for as in this study, elevated values of Mg/Ca and Sr/Ca are more likely to be recorded close to the apex as the cross sections become much shorter (Sørensen *et al.*, 2015; Ullmann *et al.*, 2015). Due to this it is possible that the variations in Mg/Ca and Sr/Ca recorded along the length of the belemnite reflect the variability across a radial transect (Sørensen *et al.*, 2015; Ullmann *et al.*, 2015).

For sodium, there has yet to be a study examining the distribution of Na between different calcite phases in belemnites, it is possible that the different phases of calcite also have different concentrations of other elements— also potentially contributing to the changes in El/Ca along the rostrum which are seen for Na. McArthur *et al.* (2007a) examined radial profiles of Na in Toarcian belemnites, and found that – similar to Sr – there was no or limited variation in Na between the apical line and the exterior of the rostra, which adds weight to a more consistent Na distribution between the different calcite phases.

#### 3.4.4.3. Between individual belemnites

Both Mg/Ca and Sr/Ca are suggested to be temperature proxies in carbonates, including belemnites. The extent to which they are reliable temperature proxies in belemnites is disputed, with some suggesting that palaeotemperature is faithfully recorded by Mg/Ca (Rosales *et al.*, 2004; McArthur *et al.*, 2007a; b; Armendáriz *et al.*, 2008) or Sr/Ca (McArthur *et al.*, 2007a; Li *et al.*, 2012) and some suggesting that Mg/Ca does not record palaeotemperature at all (Wierzbowski and Rogov, 2011; Li *et al.*, 2013; Stevens *et al.*, 2014). The discrepancies in the results of these previous studies show that Mg/Ca is influenced by a range of factors, including biological controls on Mg incorporation which are species specific or even related to sexual dimorphism in some species (McArthur *et al.*, 2007a). McArthur *et al.* (2007a) suggested that significantly less biological control was exerted on Sr/Ca ratios in belemnites, making Sr/Ca ratios a more suitable palaeo-temperature proxy.

In the data for the Variability Samples, there were statistically significant differences in El/Ca ratios between different species of belemnite for Sr/Ca and Mg/Ca, but not Na/Ca (3.4.4.3). McArthur *et al.* (2007a) suggested that strontium is subject to limited biological control, with little variation between species in Sr/Ca ratios. However, this was not seen in the data from

this study, where there were statistically significant differences in Sr/Ca between species (3.4.4.3). This may be due to the different species studied by McArthur *et al.* (2007a), which compared *Acrocoelites (Odontobelus) vulgaris* and *(Acrocoelites) subtenuis* – species from the Toarcian which were not included in this study. Alternatively, it is possible that the differences in Sr/Ca between the species studied here were not different due to biotic effects of individuals, but due to differences in the modes of life of the species. This may include small differences in habitat (such as water depth) or differences in the lifecycle of each species such as breeding-seasons and lifespan meaning that some individuals lived in warmer waters on average (e.g., Hewitt, 2000; Wierzbowski, 2013; Hoffmann and Stevens, 2020).

For magnesium, differences in Mg/Ca may also be related to the same differences in temperature, considering that both Mg/Ca and Sr/Ca had higher values in the same species, and lower values in the other species tested (3.4.4.3). Alternatively, differences in Mg/Ca may be a result of species-specific biological or morphological effects. Additionally, differences in the ratios between the high-Mg and low-Mg phases of calcite (as described by Hoffmann *et al.*, 2016) may be affected by the morphological features of the rostrum which differ between species, also leading to species differences in Mg. Hoffmann *et al.* (2021) showed that Sr values were similar between the two phases of calcite – the primary calcite from the belemnite's growth and the infilled calcite during early diagenetic processes. Studies of Na between the two phases have not been completed, however McArthur *et al.* (2007a) examined the radial distribution of Na, Sr and Mg and found that Sr and Na concentrations did not vary along transverse sections, while Mg did. Considering the overlap in Na and Sr results it is possible that both Na and Sr are distributed similarly throughout the rostra, – though this would need further investigation to confirm.

For sodium, only limited research has been conducted into its variability in belemnites and between species (e.g., McArthur *et al.*, 2000; Bailey *et al.*, 2003; McArthur *et al.*, 2007a). McArthur *et al.* (2007a) suggested that, like Sr/Ca, they are subject to only limited biological control, which is consistent with this study, where no differences in Na/Ca values were observed between species (Figure 19). The differences in Na/Ca between species could therefore be related to environmental effects, or morphological species-specific controls in the same way as magnesium. What is clear, is that Na/Ca ratios are consistent and reproducible, within replicate samples and individuals suggesting that it is not a result of contamination from salt water or sediment. Previous studies have demonstrated a correlation between Na/Ca, Mg/Ca, Sr/Ca, and oxygen isotopes, and suggested that Na/Ca may covary with palaeotemperature in a similar way as Mg/Ca and Sr/Ca, though the correlation between  $\text{EI/Ca}$  and oxygen isotopes was weaker for Na than Mg and Sr (McArthur *et al.*, 2000; Bailey *et al.*,

2003). These previous studies have measured Na/Ca in belemnites from Yorkshire and Germany across the Toarcian to investigate stratigraphic changes and have observed shifts in Na/Ca values by a factor between 1.7 and 2 from the mid-*tenuicostatum* zone until the lower *falciferum* zone. In other carbonates, previous studies have suggested Na/Ca incorporation is controlled by temperature (Bertlich *et al.*, 2018; Schleinkofer *et al.*, 2019), Na/Ca ratios in the surrounding water (Evans *et al.*, 2018; Hauzer *et al.*, 2018; Evans *et al.*, 2020; Zhou *et al.*, 2021; Nambiar *et al.*, 2023), salinity (Gordon *et al.*, 1970; Veizer *et al.*, 1977; White, 1978; Ishikawa and Ichikuni, 1984) or growth rate related effects (Mitsuguchi *et al.*, 2010). Investigating changes in Na/Ca ratios in belemnites with time and examining any relationships between Na and other proxies may go some way to clarifying the relationship between Na and environmental factors in belemnites.

For each El/Ca ratio, the  $CV_M$  value indicating low variability and high reproducibility within stratigraphic levels (amalgamating all analyses using the same method from all individuals within each stratigraphic level) for both stratigraphic levels. For Mg/Ca, Sr/Ca, and Na/Ca ratios, the  $CV_M$  values were all below 20 %, 12 % and 10 % respectively – all of which are low enough to indicate a high degree of reproducibility within stratigraphic levels. These values are extremely useful in placing bounds on the interpretation of stratigraphic records where replicates at each level are much less abundant, and multiple samples from the same belemnite may be limited by fragmented or small samples. There were statistically significant differences between stratigraphic levels for Mg, Sr, and Na. All of this indicates that this method could be used to produce stratigraphic records for all of these El/Ca ratios.

#### 3.4.4.4. Between modern analogues

For the Modern Analogue Samples, differences in El/Ca ratios between individuals were investigated (Table 18). For strontium, there were statistically significant differences of about 23-24 % in Sr/Ca ratios between individual *S. officinalis* and individual *S. spirula* (Table 18). There were no differences between individuals for Na/Ca ratios (Table 18). For Mg/Ca there was a statistically significant difference of 28 % between the individual *S. officinalis*, but no difference between *S. spirula* individuals (Table 18).

The differences in Sr/Ca and Mg/Ca may be due to differences in average water temperature the individuals lived in. For Mg/Ca, the *S. officinalis* with the highest ratios of Mg/Ca and Sr/Ca was older than the other *S. officinalis* individual studied and had lived in water of a higher average temperature. For Mg/Ca ratios, the interpretation must also consider that the older *S. officinalis* (with higher Mg/Ca ratios) was euthanised by injection of magnesium chloride hexahydrate, which may have led to the elevated Mg/Ca levels. For Sr/Ca, studied on *S. officinalis* have shown that Sr/Ca is not affected by salinity or temperature, and can vary even

in individuals reared in the same conditions (Ikeda *et al.*, 2002a; b). Other studies have demonstrated that Sr/Ca in some regions of the cuttlebone are affected by diet – with differences of up to 10 % in the lateral dome, though not in other regions of the cuttlebone (Zumholz *et al.*, 2007). Sr/Ca ratios in *S. spirula* are not as understood, and their responses to temperature, salinity, diet, and other environmental factors have not been studied (Immenhauser *et al.*, 2016). Overall, it seems unlikely that differences in Mg/Ca and Sr/Ca between these individual *S. spirula* and *S. officinalis* are related to temperature changes in their environment. It seems more likely the differences can be attributed to slight differences in diet, or contamination with magnesium in the older *S. officinalis* during euthanasia.

#### 3.4.5. Effect of P/Ca protocol

For determining P/Ca ratios, the selected method was to clean samples in ultrapure water, then dissolve in acetic acid (2.6). This method gave low variability and high reproducibility in Mg/Ca, Sr/Ca, and Na/Ca for replicate samples ( $CV_{rep}$  values below 10 %). This shows that this method is suitable to measure not just P/Ca, but other EI/Ca ratios as well.

The variability of some elements with this method was higher, such as Ba, Li, B and S, and this method is not as good at determining concentrations of these elements. For B and S this is due to low concentrations of these elements in the analyte used for the ICP analysis, causing them to frequently fall below the LOD/LOQ and creating additional variability (3.3.1). To combat this, solutions with lower dilution factors could be used, or higher masses of dissolved sample to ensure these trace elements could be analysed. For sulfur, using ion chromatography to quantify the amount of  $SO_4^{2-}$  ions in the calcite is likely to be a more effective method which will reduce variability.

Ba and Li gave variable  $CV_{rep}$  values (between 3-30 %) indicating the potential for the method to quantify these elements reproducibility, though further work is needed. For both Ba and Li, the  $CV_{ind}$  and  $CV_{lv}$  values were higher (over 20 %) suggesting that these elements are highly variable within and between individuals- which would make stratigraphic trends difficult to determine. Characterising these elements in individual samples and belemnites is still important, as the concentrations and distribution of these elements can give indications of the mineralogical and biological controls on their incorporation – such as their distribution between the two phases of calcite (primary growth and infilled). Quantifying these elements and examining their distribution can also be useful to identify links between incorporation of these elements and other ions, which may indicate co-incorporation or lattice replacements. Once the mineralogy and distribution of these elements is understood, it may be possible to refine sampling and analytical techniques to mitigate variability and biological effects and develop stratigraphic profiles of them, enabling new proxies to be explored.

Overall, the calculation of  $CV_{rep}$ ,  $CV_{ind}$  and  $CV_{IV}$  values is valuable to determining the limits of interpretation of stratigraphic records by providing an illustration of the variability at each level. This will allow trends in Mg/Ca, Sr/Ca, and Na/a to be examined through time, and these can be compared to records of P/Ca to investigate potential mechanisms for P incorporation and the potential of P/Ca to be used as a water column P proxy. Quantifying other elements and examining their distribution is also important when investigating mineralogy and determine the mechanisms for elemental incorporation which is vital to fully interpret existing proxies and develop new ones.

### 3.5. Conclusion

The results indicated high reproducibility in El/Ca ratios with all of the methods studied. For the method which was chosen for P/Ca analysis,  $CV_{rep}$  values (for replicate analysis of the same samples using the same method) were all less than 10 % and mostly lower than 1 % for Mg/Ca, Sr/Ca, and Na/Ca, respectively. There was also evidence that Mg, Sr, and Na values were not a result of contamination based on the consistent analytical results, and the lower El/Ca ratios given by the contaminated bulk (Bulk 1) compared to the other samples.

Different preparative methods did impact the El/Ca ratios. In the modern samples, oxidative cleaning removed organic matter, which reduced Mg/Ca ratios due to the removal of Mg associated with the organics. For Sr and Na, there were no statistically significant differences between cleaning methods in the Modern Analogue Samples, as Na and Sr are not as associated with organic matter as magnesium. There were also differences between cleaning methods, with 20 % Mg/Ca and 17 % higher Sr/Ca ratios for Variability Samples cleaned with water than samples cleaned with hydrogen peroxide, suggesting hydrogen peroxide may be preferentially removing high Mg calcite. Much larger differences between cleaning methods were seen in Mg/Ca ratios in the Modern Analogue Samples, though there was little to no difference in Sr/Ca and Na/Ca for the same samples. In modern samples, 30-40 % higher Mg/Ca ratios were obtained with water than hydrogen peroxide, which is attributed to the removal of magnesium associated with organic matter in Modern Analogue Samples. This suggests that organic matter associated contamination creates the largest differences between the cleaning methods for magnesium but has minimal impact on Sr/Ca and Na/Ca ratios, though other forms of contamination cannot be assessed as easily. Different dissolution methods did not have large effects on any of the El/Ca ratios in Bulk Samples, which suggests that the forms in which Mg, Sr and Na are in are either resistant to dissolution by all acids or easily dissolved even by the weaker acetic acid.

There were variations in all El/Ca ratios within individuals, with apparent enrichment in Na, Mg and Sr towards the apex of each belemnite from Wine Haven samples, and some of the Penny Nab samples. This may be because the trend appears in some species and not others, or a result of preservational differences. Na/Ca ratios were very consistent between individuals from the same stratigraphic level (For both belemnites and modern analogues) indicating little to no biological control on Na incorporation. Species specific differences were found in Mg/Ca (in both belemnites and modern analogues) which is consistent with McArthur *et al.* (2007a) which found that Mg is subject to strong biological control and varies between species and even between sexes in some species. Sr/Ca was consistent between modern analogues but there were differences between species in belemnite samples, which is different to the previous studies which have found Sr varies little between species (McArthur *et al.*, 2007a). This may be due to the different species included in this study compared those included in McArthur *et al.* (2007a), or due to different modes of life between the species which meant they lived in slightly different habitats and experienced different palaeoenvironmental conditions. Despite being affected by biological controls, both Sr/Ca and Mg/Ca have potential promise as palaeotemperature proxies as the reproducibility within stratigraphic levels was high. Whether Sr/Ca or Mg/Ca is a more appropriate temperature proxy has been considered by a number of previous studies (e.g., McArthur *et al.*, 2000; Bailey *et al.*, 2003; McArthur *et al.*, 2007a; b) – this cannot be determined by the variability studies presented. Comparing Mg/Ca and Sr/Ca records to oxygen isotope records may indicate which record is most reliable in this case, though previous studies have indicated that  $\delta^{18}\text{O}$  records have the same issues with variability and partitioning between the different phases of calcite as magnesium does (Hoffmann *et al.*, 2021). Na/Ca may be a better temperature proxy than Sr/Ca and Mg/Ca as it is not subject to the same biological controls as the other El/Ca ratios (McArthur *et al.*, 2000), though previous studies indicate it may also represent a salinity (White, 1978; Ishikawa and Ichikuni, 1984; McArthur *et al.*, 2007a; Wit *et al.*, 2013; Mezger *et al.*, 2016; Bertlich *et al.*, 2018; Gray *et al.*, 2023), oceanic  $\text{Ca}^{2+}$  concentration (Evans *et al.*, 2018; Hauzer *et al.*, 2018; Evans *et al.*, 2020; Zhou *et al.*, 2021; Nambiar *et al.*, 2023) record, or vary based on growth rate and mineralogical parameters - this will be investigated further in Chapter 5.

Overall, there was a high degree of reproducibility within stratigraphic levels, which shows that, even where there is variation within and between individual belemnites, this method may still be used to determine stratigraphic trends in El/Ca ratios. For both stratigraphic levels,  $\text{CV}_{\text{M}}$  values fell below 20 %, 12 % and 10 % for Mg/Ca, Sr/Ca and Na/Ca which places bounds on the magnitudes of changes which may be significant when observed over stratigraphic time, where replicate samples to determine  $\text{CV}_{\text{M}}$  values may not be available.

## 4. Early Jurassic P/Ca records in a stratigraphic context

### 4.1. Introduction

Having determined a method to extract and quantify phosphorus from belemnite calcite and quantified the variability in CAP within and between individuals and stratigraphic levels, this chapter will focus on investigating changes in CAP through time (Figure 29). Samples from the Early Jurassic were analysed from multiple sections across three locations in the Laurasian Seaway including the Cleveland Basin in modern day Yorkshire, the Cardigan Bay Basin in North Wales, and the Moesian Basin in Bulgaria (Figure 21). This chapter will present P/Ca records generated for each location, so that stratigraphic changes in CAP can be examined, and compared between. The magnitude of changes in CAP values will be compared to the variance within stratigraphic levels determined by the analysis of the Variability Samples. This will help determine if the changes in P/Ca through time are greater than those which can be accounted for by natural variability in P/Ca within and between individuals.

The samples analysed span a time interval of almost 30 million years, from the end of the Sinemurian to the end of the Aalenian (Figure 29). This is a time of significant environmental change, with perturbations in the carbon isotope record, palaeotemperature, ocean redox state, the intensity of the hydrological cycle, and biodiversity. The time period also includes several significant events, such as the Early Toarcian Negative Carbon Isotope Excursion (ETNCIE) which is coincident with widespread ocean dysoxia in the Laurasian Seaway (the Toarcian Ocean Anoxic Event [TOAE]) and a second order mass extinction responsible for the loss of 5 % of marine invertebrate families, with shallow marine molluscs particularly affected (the Early Toarcian Mass Extinction [ETME] (Little and Benton, 1995). It may be expected that palaeoenvironmental changes will impact water-column phosphorus concentrations. As CAP in carbonates has been suggested as a method of investigating changes in water-column phosphorus concentrations (e.g., Dodge *et al.*, 1984; Shotyk *et al.*, 1995; Kumarsingh *et al.*, 1998; Montagna *et al.*, 2006; LaVigne *et al.*, 2008; 2010; Anagnostou *et al.*, 2011; Mallela *et al.*, 2013; Chen *et al.*, 2013; Ingalls *et al.*, 2020; 2022; Dodd *et al.*, 2021; 2023), then P/Ca in belemnites may covary with some existing palaeoenvironmental proxies, such as proxies for redox and temperature. To investigate the factors affecting CAP in belemnites, the P/Ca records generated are compared to records of temperature and redox to investigate the potential for CAP to record water column phosphorus changes.

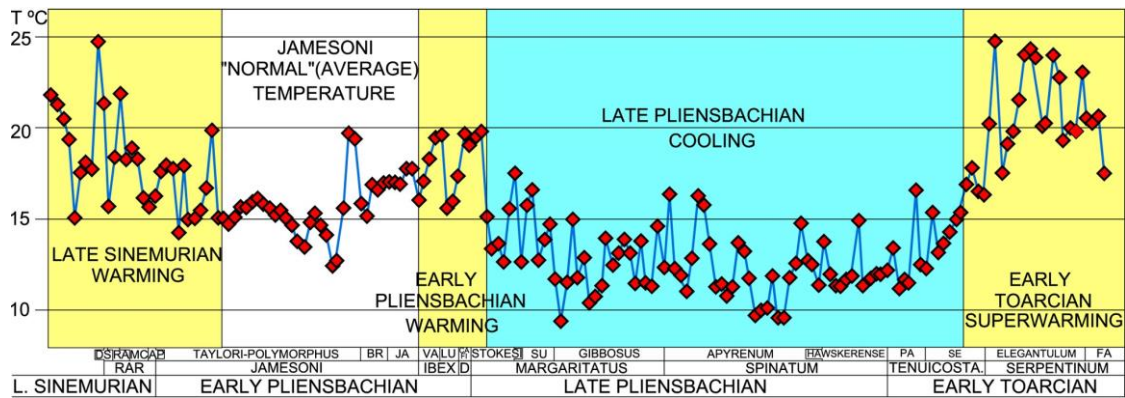


Figure 20 - Seawater palaeotemperatures of the Late Sinemurian, Pliensbachian and Early Toarcian based on oxygen isotope measurements of belemnite calcite in the Rodiles section of Northern Spain, taken from Gomez et al. (2016). Chronozone abbreviations: RAR: raricostatum. D: davoei. TENUICOSTA.: tenuicostatum. Subchronozones abbreviations: DS: densinodulum. RA: raricostatum. MC: macdonnelli. AP: aplanatum. BR: brevispina. JA: jamesoni. VA: valdani. LU: luridum. CA: capricornus. FI: figulinum. SU: subnodosus. PA: paltum. SE: semicelatum. FA: falciferum.

Palaeotemperature varies throughout the time interval studied with global palaeotemperatures alternating between suspected ice-house and greenhouse conditions (e.g., Sælen et al., 1996; McArthur et al., 2000; Röhl et al., 2001; Schmidt-Röhl et al., 2002; Bailey et al., 2003; Jenkyns, 2003; Rosales et al., 2004; Gómez et al., 2008; Metodiev and Koleva-Rekalova, 2008; Suan et al., 2008; 2010; Dera et al., 2009a; b; 2010; 2011; Gómez and Arias, 2010; García Joral et al., 2011; Gómez and Goy, 2011; Fraguas et al., 2012; Gomez et al., 2016). Gomez et al. (2016) generated a temperature record covering the majority of the interval studied using oxygen isotope values obtained from belemnite calcite in the Rodiles section of Northern Spain. This record demonstrated that relatively warm palaeotemperatures at the end of the Sinemurian are followed by lower temperatures during the Early Pliensbachian (Gomez et al., 2016; Figure 20). A brief interval of warming at the end of the Early Pliensbachian is followed by sustained cooling, with temperatures remaining low into the Early Toarcian (Gomez et al., 2016; Figure 20). In the *serpentinum* zone of the Early Toarcian, there was a 'super warming' event, with palaeotemperatures increasing to 20-25 °C (Gomez et al., 2016; Figure 20). This warming has been linked to the eruption of the Karroo-Ferrar LIP as they occur near-simultaneously (McElwain et al., 2005; Hesselbo et al., 2007; Moulin et al., 2017; Fantasia et al., 2019). The changes in palaeotemperature have been linked to changes in the hydrological cycle throughout the same period. In particular, the shift to high temperatures in the Early Toarcian is believed to have caused a period of intense weathering due to increased precipitation (McArthur et al., 2000; Cohen et al., 2004; Percival et al., 2016). This increased weathering is likely to have increased the flux of phosphorus to the ocean, increasing oceanic phosphorus concentrations (McArthur et al., 2000; Cohen et al., 2004; Percival et al., 2016). Some authors have even suggested that this increased flux of nutrients to the ocean may be responsible for the development of dysoxia in the restricted basins of the

Laurasian Seaway via a eutrophication mechanism (e.g., Zempolich, 1993; Tremolada *et al.*, 2005). It is therefore reasonable to assume that if CAP is representative of water-column phosphorus concentrations, there may be a correlation between palaeotemperature and CAP. In order to investigate this, oxygen isotope ratios were determined for the same samples as P/Ca values in all of the studied locations. The  $\delta^{18}\text{O}$  record was then compared to the P/Ca record to investigate any correlation between palaeotemperature and CAP.

There were also significant changes in oceanic redox throughout the interval studied. Most notable is the TOAE in the Early Toarcian, which is coincident with the high palaeotemperatures, ETNCIE and ETME. The TOAE is characterised by the presence of organic-rich black shales deposited in various epicontinental basins (Jenkyns, 1988). The TOAE is poorly defined as an interval, as not all basins show evidence of anoxia, and the basins show evidence of anoxia were likely anoxic asynchronously (e.g., Them *et al.*, 2018). The best measure of an integrated global signature of anoxia is provided by the thallium isotope record of Them *et al.* (2018), which indicates anoxia is began expanding roughly around the Pliensbachian-Toarcian boundary. In this study the TOAE is defined as the period of wide-spread anoxia in the Laurasian Seaway, though other studies may have differing definitions. There is no general consensus regarding the causes of the TOAE, though potential causes which have been discussed include the release of methane and carbon dioxide from the eruption of the Karroo-Ferrar LIP or the destabilisation of methane hydrates (Hesselbo *et al.*, 2000; Kemp *et al.*, 2005; McElwain *et al.*, 2005; Hesselbo *et al.*, 2007; Moulin *et al.*, 2017; Fantasia *et al.*, 2019). There is also no consensus on the mechanism by which ocean anoxia developed, though there were several major environmental changes concomitant with the TOAE which may have been related. For example, the TOAE coincides with a significant increase in global temperatures (e.g., Sælen *et al.*, 1996; McArthur *et al.*, 2000; Röhl *et al.*, 2001; Schmidt-Röhl *et al.*, 2002; Bailey *et al.*, 2003; Jenkyns, 2003; Rosales *et al.*, 2004; Gómez *et al.*, 2008; Metodiev and Koleva-Rekalova, 2008; Suan *et al.*, 2008; 2010; Dera *et al.*, 2009a; b; 2010; 2011; Gómez and Arias, 2010; García Joral *et al.*, 2011; Gómez and Goy, 2011; Fraguas *et al.*, 2012; Gomez *et al.*, 2016), rising sea-levels (Hallam, 1987; de Graciansky *et al.*, 1998; Pittet *et al.*, 2014; Haq, 2018), and potential increased ocean stratification (e.g., Mattioli *et al.*, 2009). Also debated is the geographic extent of the TOAE (e.g., Rodríguez-Tovar and Reolid, 2013): originally believed to represent a global event due to the simultaneous deposition of black shales in basins around the world (though predominantly in the Laurasian Seaway), recent work has indicated geographical variation in the extent or even presence of evidence for the TOAE (McArthur *et al.* 2008; Rodríguez-Tovar and Uchman 2010; Rodríguez-Tovar and Reolid, 2013).

Redox may be expected to influence water-column phosphorus concentrations (and hence potentially belemnite CAP) as different redox conditions influence the fluxes of phosphorus to and from the sediment. In an oxic environment, much of the phosphorus which reaches the sediment remains in the sediment, with a portion being trapped by authigenesis or adsorption (e.g., onto clay minerals and Mn/Fe oxyhydroxides) (Sundby *et al.*, 1992; Faul *et al.*, 2005). Some is still removed from the sediment by bacterial mining of the detrital organic matter, though this fraction is relatively small, and often phosphorus binds to minerals such as iron (oxy)hydroxides before it can be recycled into the water column (Slomp *et al.*, 1996; Algeo and Ingall, 2007). In ferruginous water columns, there is a greater proportion of reactive iron in detrital particles which bind to dissolved phosphorus, enriching Fe-bound phosphorus in the sediment and decreasing the water column phosphorus concentration. In contrast, in euxinic conditions, dissolved hydrogen sulphide in the water column reduces reactive iron and in doing so removes a sink for dissolved phosphorus. This reduces the amount of Fe-bound phosphorus in the sediment and increases water column phosphorus concentrations in the water column. Additionally, in anoxic environments, anaerobic bacterial communities on the seabed preferentially mine sedimentary organic matter for nutrients such as phosphorus and releasing them from the sediment. Where sulfidic pore-waters are present close to the sediment-water interface, the released phosphorus is predominantly released back into the water column, as free hydrogen sulfide removes phosphorus sinks such as iron (oxy)hydroxides (e.g., Alcott *et al.*, 2022). Sulfidic bottom waters are most commonly associated with euxinic environments, though ferruginous conditions with small amounts of added sulfide can have the same effect (e.g., Alcott *et al.*, 2022). This means that different redox conditions impact not only the cycling of phosphorus, but also phosphorus signals which could be preserved by both sediments and water column proxies.

To investigate variations in P/Ca with redox, the P/Ca record was compared to various redox proxies including iron speciation and trace metal ratios in the sediments. These sediment samples were taken directly adjacent to belemnite samples from the Dove's Nest core in Yorkshire, in order to create a paired carbonate and sediment record. Attempts were also made to compare the P/Ca ratio to I/Ca ratios from the same belemnites across all locations studied, as this has been suggested as a method of determining water column redox state, but analysis issues made the data unreliable (3.3.1.2). This assumes that belemnites would be able to survive in water-columns of variable redox levels. As actively swimming cephalopods, belemnites (and other cephalopods such as ammonites), require high levels of dissolved oxygen. Where belemnites coexist with sedimentological evidence of dysoxia, this likely indicates a stratified water-column with bottom-water dysoxia or anoxia, and oxic conditions

further up the water-column providing a 'refuge' for biota such as belemnites (Rexfort and Mutterlose, 2009; Malkoč *et al.*, 2010). Changes in bottom-water redox conditions may still alter the nutrient concentrations in the shallower, oxic water column, which may be recorded in belemnite CAP.

Mineralogical factors affecting P/Ca incorporation into belemnites are also investigated. Research into the formation of carbonates has suggested that the incorporation of phosphate is controlled by a number of factors such as temperature, salinity, and the presence of other ions (particularly calcium and magnesium) on the growing surface (Millero *et al.*, 2001). While little work has been done investigating the incorporation of phosphate into carbonates in modern cephalopods such as *S. spirula* or *S. officinalis*, there is some evidence that Mg and P may be related in belemnites (e.g., Hoffmann *et al.*, 2016). Existing research has demonstrated that belemnites contain two phases of calcite – one phase with a tetrahedral crystal structure which is high in Mg, P, and organic matter but low in sulphate and a surrounding phase which is low in Mg, P, and organic matter but high in S (Hoffmann *et al.*, 2016). It has been suggested that the tetrahedral phase is primary and grew during the belemnite's lifetime, and the surrounding phase is formed during early diagenetic alteration (Hoffmann *et al.*, 2016). In order to investigate the potential impact on P incorporation of mineralogical factors – such as the concentration of magnesium, Mg/Ca and P/Ca records were compared for all samples from each location studied (Figure 37). Additionally, a subset of samples from North Wales were analysed using XRD to investigate the changes in the calcite unit cell parameters and cell volume with increasing concentrations of Mg.

By examining changes in P/Ca through time across multiple locations, the aim is to establish if there are changes in P/Ca which are greater than the variability within and between individuals already established. By comparing the P/Ca record to proxies for temperature and redox and investigating the mineralogical factors affecting the incorporation of phosphorus into calcite, the aim is to determine the factors affecting CAP in belemnites.

## 4.2. Materials

Stratigraphic samples were analysed from three different locations. Samples were analysed from the Llanbedr core in the Cardigan Bay Basin, North Wales, UK; coastal outcrops and the Dove's Nest core in North Yorkshire, UK; and inland outcrops in the Moesian Basin, Bulgaria.

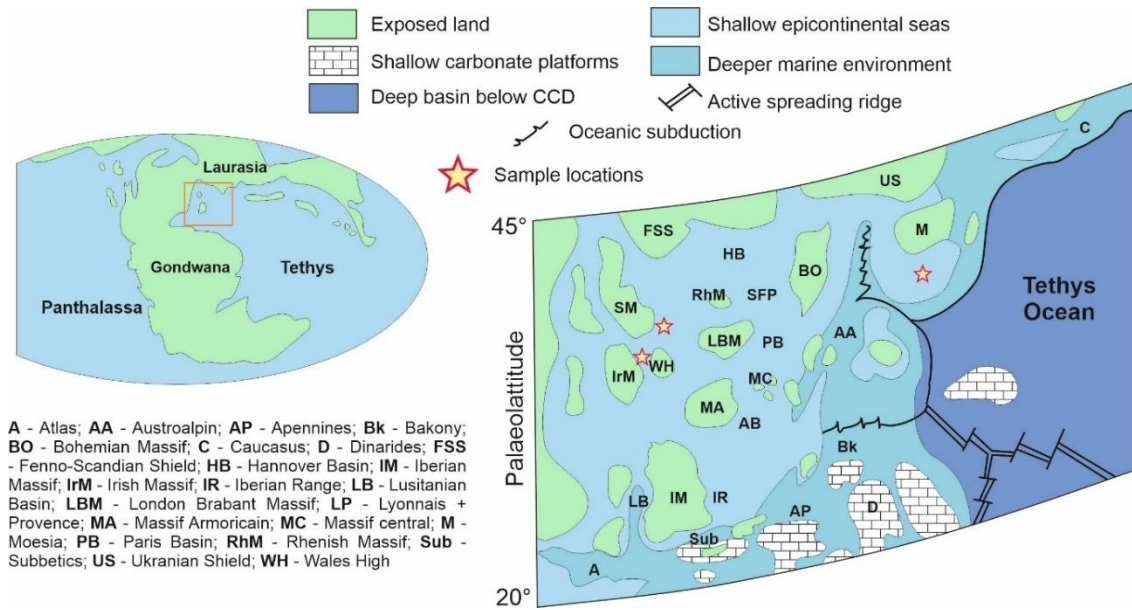


Figure 21 - Palaeogeographic map of the Western Tethys and Laurasian Seaway during the mid-Toarcian (Early Jurassic) and locations of the sites from which specimens have been collected and analysed. Map is redrawn from Metodiev and Koleva-Rekalova (2008) and was originally simplified from Bassoulet et al. (1993) and Fourcade et al. (1995).

#### 4.2.1. North Wales

Specimens from North Wales were collected from the Llanbedr (Mochras Farm) borehole which was drilled onshore near the coast of Wales between 1967 and 1969. The core consists of an extremely expanded (1300 m thick) Early Jurassic succession – approximately three times the peak thickness in other UK sections. The sediment was deposited in the Cardigan Bay Basin, and the depositional environment was fully marine, with close proximity to relatively low relief islands which formed the Welsh Massif (Cope *et al.* 1992; Tappin *et al.* 1994; Deconick *et al.*, 2019). The core lithology is relatively uniform, mudstone, with sections of siltier mudstone and limestone, and a short interval of laminations in the ibex zone of the Pliensbachian (e.g., Pieńkowski *et al.*, 2021).

The Llanbedr core has been extensively studied, so ammonite, foraminifera, and trace fossil biostratigraphy (Copestake and Johnson, 2013; Pieńkowski *et al.*, 2021), low resolution carbon isotope curves (Jenkyns *et al.*, 2002; Katz *et al.*, 2005; van de Schootbrugge *et al.*, 2005), high-resolution carbon isotope curves (Xu *et al.*, 2018) and a magnetostratigraphy for the Toarcian (Xu *et al.*, 2018) have already been established. The most up to date isotope records of this core are Storm *et al.* (2020) for organic carbon and Ullmann *et al.* (2022) which updates the carbonate curve, (macrofossils and vein calcite) and summarises the organic carbon isotope data. These existing records have been used to correlate the Llanbedr core with other contemporaneous sections in the UK and globally and create an age model for the core which can be used to investigate changes over time. All Early Jurassic zones were found to be

present, except the Hettangian *tilmanni* zone (Woodland 1971; Copestake and Johnson 2014), suggesting that major sedimentation breaks are not present.

The core and associated specimens are stored at the British Geological Survey (BGS) National Geological Repository in Keyworth, along with a Registered Specimen collection of nearly 8000 fossil specimens with depths recorded with one-inch precision. For this work, belemnite rostra from the Early Jurassic were loaned from the registered specimen collection at BGS. In total 126 belemnite rostra were sampled, spanning from the Lower Pliensbachian to the Upper Toarcian (Figure 22). There were gaps in the belemnite record at several points in the core, including around the TOAE.

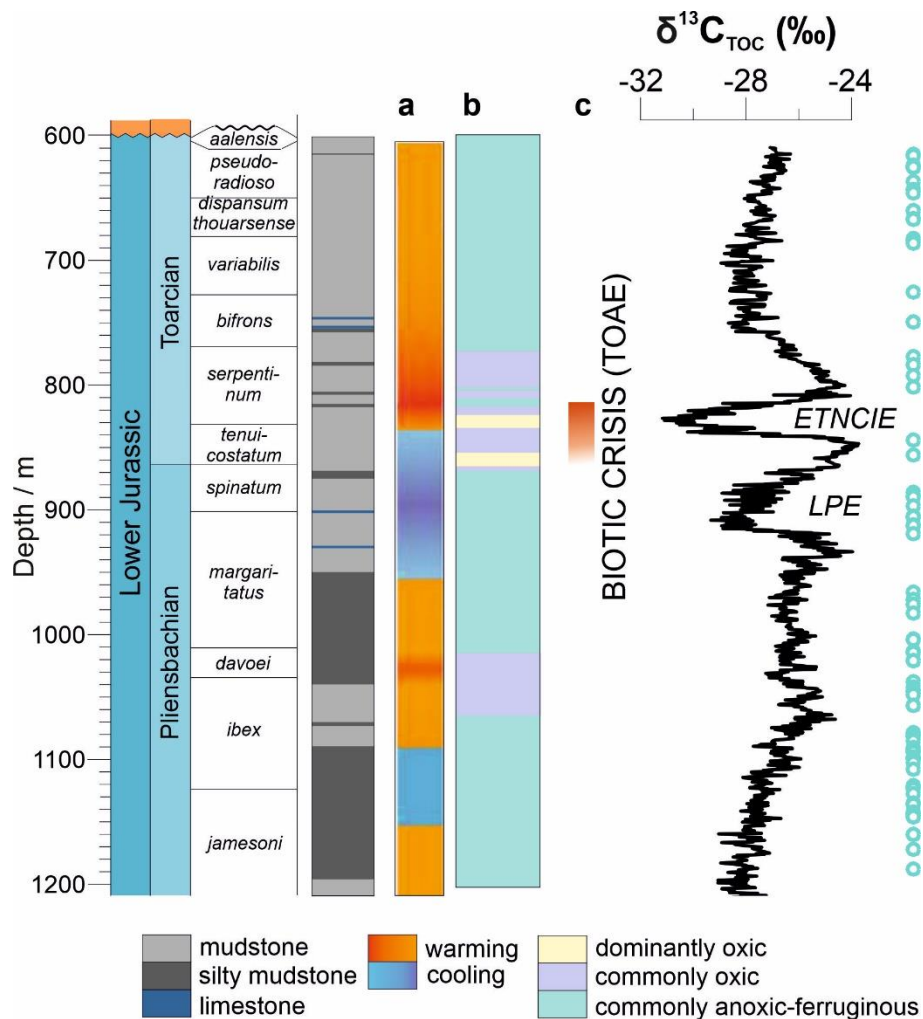


Figure 22 - Log of the Llanbedr borehole adapted from He et al. (in prep). Core depth and lithological log presented alongside the global stages and regional biostratigraphy (O'Sullivan et al., 1971; Ivimey-Cook, 1971; Xu et al., 2018; Storm et al., 2020). **a** temperature record adapted from Storm et al., 2020 where orange = warming, blue = cooling and red = short-lived hypothermals **b** Variation in water column redox conditions in the Cardigan Bay Basin (determined from a combination of Fe speciation, trace metal and pyrite sulfur isotope data). Based on work completed by He et al. (in prep) **c**  $\delta^{13}\text{C}$  trend of total organic carbon (TOC) (Xu et al., 2018; Storm et al., 2020); ETNCIE: early Toarcian negative  $\delta^{13}\text{C}$  excursion; LPE: Late Pliensbachian event; TOAE: Toarcian oceanic anoxic event; The interval of foraminiferal biotic turnover was determined based on analyses of benthic foraminiferal assemblages from the Llanbedr (Mochras Farm) core (Reolid et al., 2019).

#### 4.2.2. North Yorkshire

The Lower Jurassic exposures on the North Yorkshire coast are one of the most well studied Jurassic marine successions (e.g., Bailey *et al.*, 2003; Kemp *et al.*, 2011; French *et al.*, 2014; Thibault *et al.*, 2018; Rawson and Wright, 2018; Lord, 2019). The successions are formed from sediment accumulation in the Cleveland Basin in the Laurasian Seaway. Several boreholes have also been drilled in North Yorkshire, including the Felixkirk borehole which provides an additional succession through the Lower Jurassic, but is much more condensed when compared to the succession exposed on the coast. For this work, samples were taken from several exposed coastal sections, as well as a new borehole drilled by Sirius Minerals (now Anglo American) at Dove's Nest, near Whitby, the site of the new polyhalite mine now being developed by Anglo American.

The North Yorkshire Lower Jurassic lithology is dominated by transitions between mudstones and sandstones, with the Redcar Mudstone Formation at the base, overlain by the Staithes Sandstone Formation, Cleveland Ironstone Formation, Whitby Mudstone Formation and Blea Wyke Sandstone Formation. The successions also contain other features, such as calcite and siderite nodules, ooids, bioturbation, bituminous shales, and lamination, all of which have been well documented (Bailey *et al.*, 2003; Kemp *et al.*, 2011; French *et al.*, 2014; Thibault *et al.*, 2018; Rawson and Wright, 2018; Lord, 2019). Sedimentary evidence from the Lower Toarcian mudstones suggests that the seafloor was above the storm-wave base during deposition of the Gray Shale Member and that storm-driven bottom currents were responsible for much of the sediment deposition, erosion, and transport during this time. The biozones relating to each of these lithological members/formations are shown in Figure 23.

Early Jurassic exposures on the Yorkshire coast have been extensively studied (e.g., Howarth, 1962; Powell, 1984; Young, 1997; Van Buchem *et al.*, 1998; 2007; Powell, 2010). Detailed composite logs have been produced for coastal sections using multiple exposures along the coast (e.g., Rawson and Wright (2018) and Lord (2019)). These have included lithological and biostratigraphic logs, and composite carbon isotope curves have also been produced. Due to the Cleveland Basin's proximity to the Cardigan Bay Basin, the same ammonite biostratigraphy framework can be applied in both locations allowing easy correlation between different time periods. Correlations between the two can also be made using lithology and carbon isotope curves at each location.

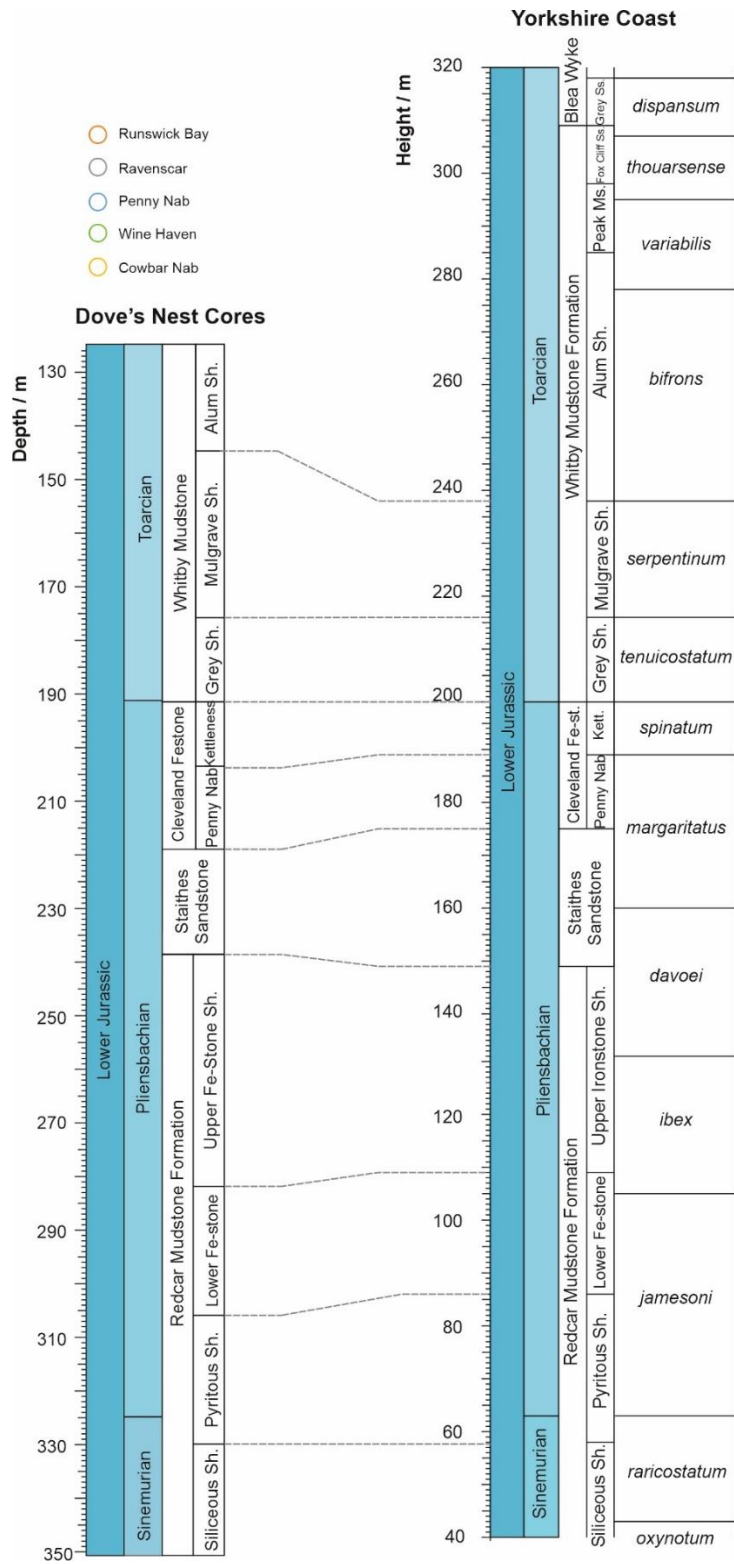


Figure 23 - The distribution of Yorkshire coast (right) samples included in this study against the bio- and litho-stratigraphy of the Yorkshire coast. Also shown is how the coastal sections correlate with the Dove's Nest cores (left). The lithology and biostratigraphy of the coastal log is adapted from Rawson and Wright (2018) and Lord (2019). The depth for the Dove's Nest Core is in m below surface; lithology for Dove's Nest is adapted from Trabucho-Alexandre et al. (2022) for depths up to 200 m and based on observations of the core for depths up to 350 m. Where abbreviations for lithological units are used due to limited space: Fe-stone = ironstone; Ms. = mudstone, Sh. = Shale; Ss. = sandstone.

Core samples were collected from the Dove's Nest borehole, about 5.5 km south of Whitby, North Yorkshire. The cores were drilled in 2013 for Sirius Minerals (now Anglo American) as an exploration borehole targeting Permian evaporites for use as fertiliser. The drilling site of the boreholes is now the site of Anglo American's Woodsmith Mine.

The samples used in this study were from two different boreholes – the north shaft borehole (NS1) and the borehole SM14. Both boreholes were drilled in the same location. NS1 covers depth from 0 - 250.55 m below ground level (which was +205.20 mOD at the time) (Figure 24). SM14 was drilled with a 5 m elevated rotary table at a total elevation of +208.70 mOD (Figure 24).

Trabucho-Alexandre *et al.* (2022) provided a lithological description of 125-220 m of the NS1 core, alongside carbon isotope and TOC records for the borehole. Trabucho-Alexandre *et al.* (2022) observed that the thickness of the lithological units in the Dove's Nest cores are approximately the same as the coastal exposures of the same members, which was corroborated by our own observations of NS1. Our observations also showed the same was true of the deeper SM14 core, with similar thicknesses for each lithological unit in the core to the successions exposed on the coast. Samples from Dove's Nest were compared to samples from the coastal sections by comparing the similar lithology and scaling the thicknesses of each lithological unit in the core to allow a combined Yorkshire core and coast record to be created. This method was chosen due to the absence of a bio-stratigraphic framework for the Dove's Nest core but is likely to be sufficient due to the close proximity (5.5 km) of the Dove's Nest core to the coast.

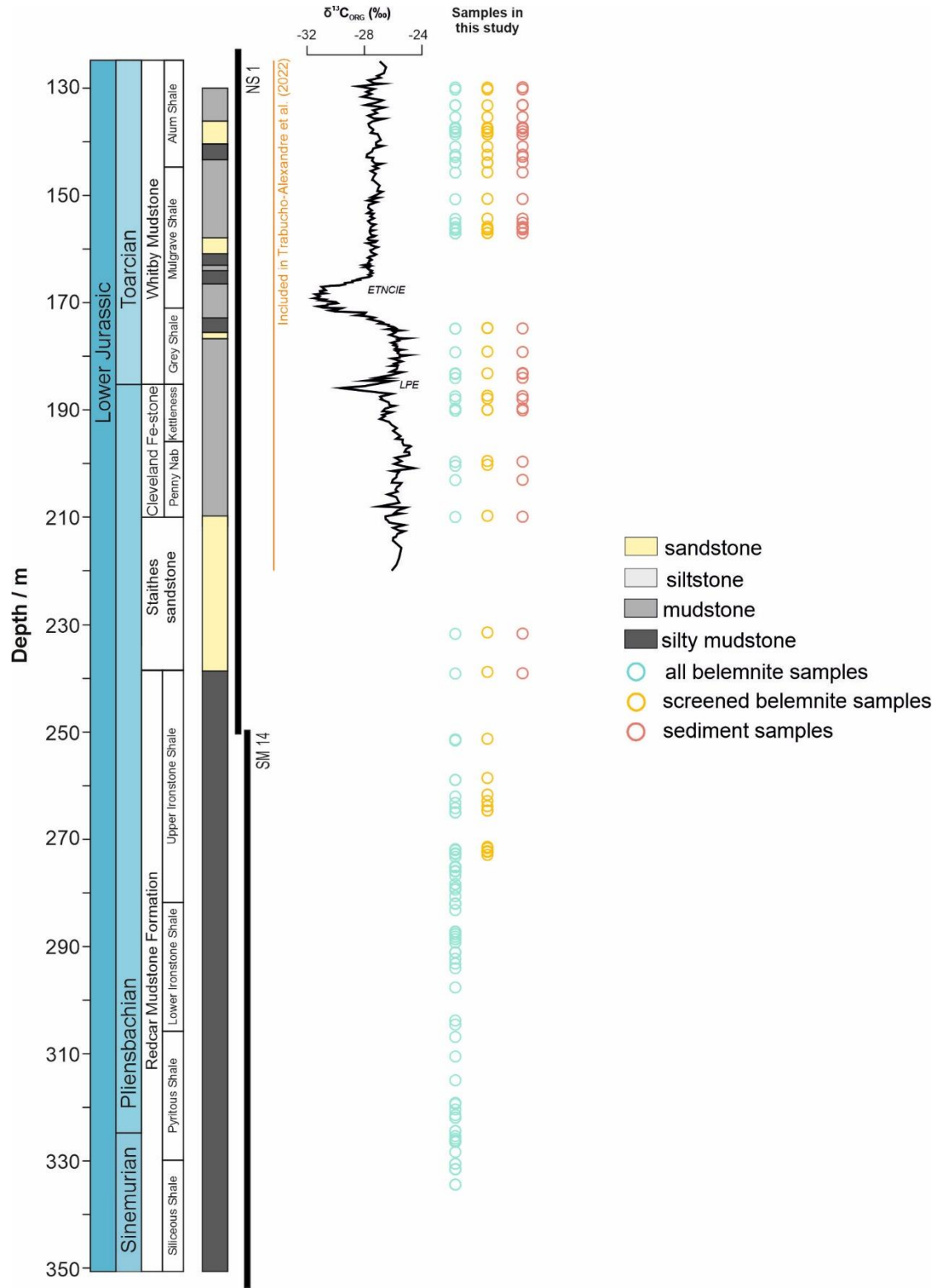


Figure 24 - Log of the Dove's Nest borehole adapted from Trabucho-Alexandre et al. (2022) and observations of the core made during sampling. Core depth and lithological log presented alongside the depths of the Anglo-American cores sampled, the organic carbon isotope curve from Trabucho-Alexandre et al. (2022) and sample heights for belemnite samples (turquoise circles) and sediment samples (red). Also included are sample heights for belemnite samples after screening protocol (4.4.1.1) was applied (yellow) as many of the samples from the lower SM14 core were extensively diagenetically altered.; ETNCIE: early Toarcian negative  $\delta^{13}C$  excursion; LPE: Late Pliensbachian event.

The similarities between the core and coastal sections means that the successions can be easily correlated with each other (Trabucho-Alexandre *et al.*, 2022). As with the coastal exposures, the dominant lithology is dark grey mudstones separated by sandstone sections, with occasional oolitic ironstone bands and cross-stratified sandstones (Trabucho-Alexandre *et al.*, 2022) (Figure 24).

For coastal material, 75 belemnites were reanalysed from previously studied material collected in 2011 from Ravenscar and Runswick Bay (described in Newton *et al.* (2011)). Seventy-one additional belemnites were collected in 2020 from Penny Nab and Cowbar Nab near Staithes, and Wine Haven in Robin Hood's Bay. For core material, 128 belemnite specimens were collected from the NS1 and SM14 cores. These specimens cover the latest Sinemurian to the Toarcian. For a subset of 40 specimens, ranging from the *A. margaritatus stokesi* ammonite subzone in the Pliensbachian to the *H. bifrons commune* ammonite subzone, sediment samples were taken from the rounds of core material, with an aim to take samples of sediment directly next to the belemnites to best compare sediment and carbonate records (Figure 24).

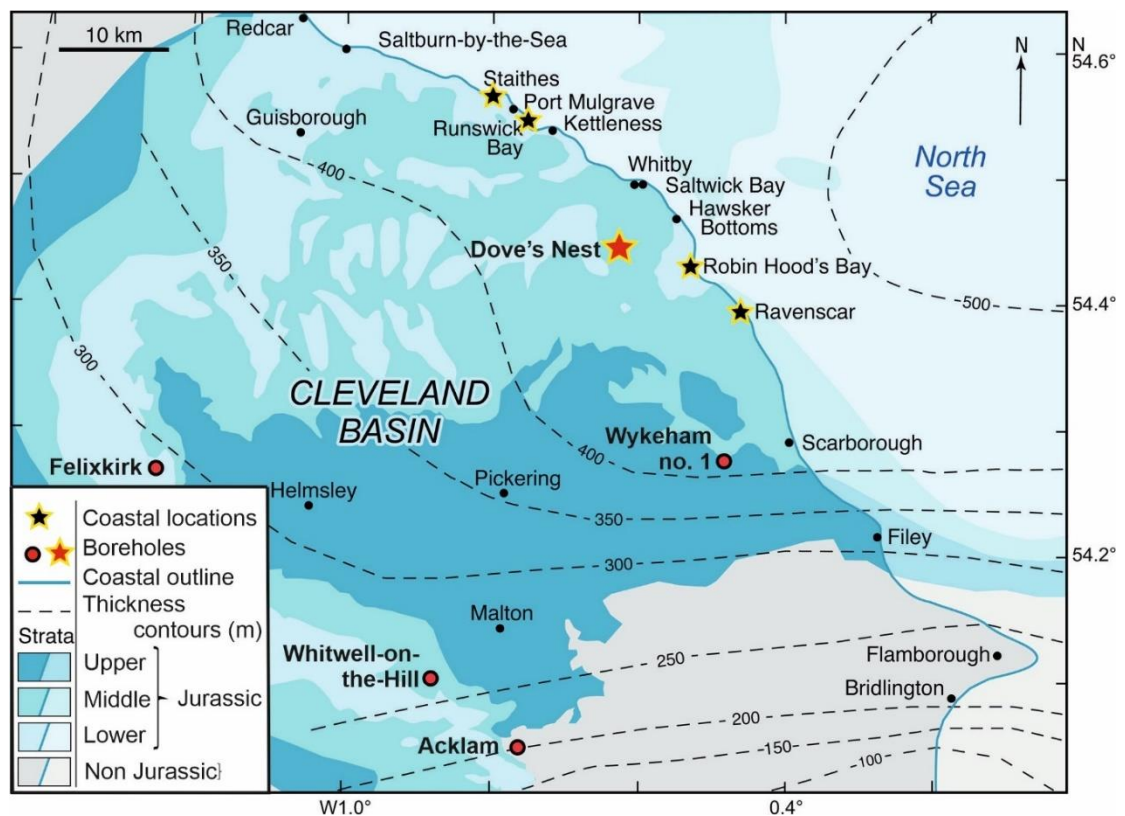


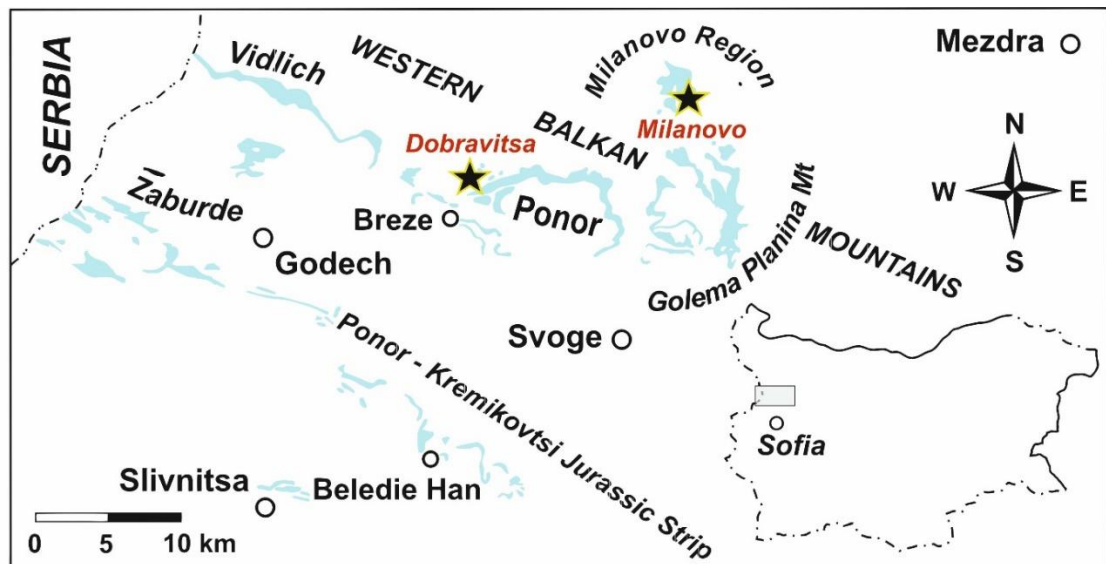
Figure 25 - Map of the locations of Yorkshire samples, adapted from Trabucho-Alexandre *et al.* (2022). Sample locations are indicated by stars filled red for core samples and black for coastal exposures. Also indicated are the geographic locations of Jurassic sediments in the Cleveland Basin, isopachs for the Lias Group (dashed black lines) and the location of other nearby boreholes (indicated by red circles with black borders).

### 4.2.3. Bulgaria

Specimens from Bulgaria were collected from three different sections: Dobravitsa-1, Dobravitsa-2 and Milanovo. All of the sections are located in the Western Balkan Mountains, where sediments were deposited in a fragmented epicontinental seaway, on the border of the Moesian Early-Middle Jurassic Platform. Palaeogeographic reconstructions show that the successions demonstrate a transition during the Lower Jurassic from an isolated lacustrine setting in Early Hettangian, to a rapidly expanding shallow marine basin, which by the beginning of the Toarcian was part of a broad epeiric sea (Metodiev, 2008; Metodiev and Koleva-Rekalova, 2008) (Figure 21).

Compared to the sections in North Wales and Yorkshire, the Bulgarian sections are proximal to the open Tethys Ocean. Different biostratigraphic frameworks are applied in the Bulgarian sections compared to the other sites studied, due to the different location and palaeogeography of the sites. The ammonite biostratigraphy for Bulgaria is well developed, and correlated with the North-Western standard zones and sub-zones which are used in Wales and Yorkshire (Metodiev, 2008). This allows comparison between the sections in Bulgaria and the other sites in this study (Metodiev, 2008).

The Bulgarian Lower Jurassic record is considerably more condensed than the equivalent records at either of the UK sites studied, and only around 2-7 m of Lower Jurassic sediments are exposed in each section. There are also gaps in the exposure and hiatuses in some of the studied sections, particularly Milanovo and Dobravitsa-1, which are both missing the Pliensbachian-Toarcian boundary. The condensed nature of the sections precludes the production of high-resolution carbon isotope curves for the Lower Jurassic from these sections, but carbon and oxygen isotope curves from belemnite calcite have previously been produced for all three sections studied here, using the same samples as are included in this study (Metodiev and Koleva-Rekalova, 2008; Pugh, 2018).



★ - locations of the studied sections      ■ - Lower - Middle Jurassic outcrops

Figure 26 - Map of modern locations of sections studied in Bulgaria, with Dobravitsa sections and Milanovo sections marked with stars. Also included are the locations of other Early-Middle Jurassic exposures in Bulgaria. Map redrawn from Metodiev and Koleva-Rekalova (2008).

The Dobravitsa-1 section is around 7 m thick; previously described by Metodiev and Koleva-Rekalova (2008) (Figure 27). The section comprises the Bukorovtsi Member of the Ozirovo Formation, overlain by the Etropole Member (Figure 27). The exposure spans from the *spinatum* zone of the upper Pliensbachian to the *discites* zone of the Bajocian in the Middle Jurassic, though there is no exposure of the Pliensbachian-Toarcian boundary (Figure 27). The lithology is predominantly pink-brown and grey marls and grey silty marls interspersed with layers of limestones and siltstone (Figure 27). Phosphate nodules and ooids are also found at several levels throughout the section. Sixty-seven belemnite specimens from Dobravitsa-1 were analysed, ranging from the *spinatum* zone in the Upper Pliensbachian to the Bajocian *discites* zone (Figure 27). The majority of the Dobravitsa-1 specimens are distributed throughout the Middle Jurassic, with only a few specimens from the Lower Jurassic (Figure 27). Previous carbon and oxygen isotope analysis of the belemnites in this section, as well as El/Ca measurements was conducted by Metodiev and Koleva-Rekalova (2008), and the  $\delta^{13}\text{C}$  isotope record, OAE placements and palaeotemperature estimates for this section are included in Figure 27.

The Dobravitsa-2 section is around 2 m thick and formed of the Bukorovtsi Member of the Ozirovo Formation. It preserves a mid-Toarcian section, which is not present in to Dobravitsa-1 due to the presence of hyper-condensed beds (Figure 26; Figure 27). Dobravitsa-2 section is predominantly shale, with some interspersed limestone beds (Figure 27). and ranges from the *bifrons* to the *fallaciosum* zone in the Toarcian (Figure 27). Fourteen belemnite specimens were analysed from Dobravitsa-2 and are predominantly distributed from the *bifrons* to the

*thouarsense* zones of the Toarcian, with one specimen from the *fallaciosum* zone (Figure 27). Previous carbon and oxygen isotope analysis of the belemnites in this section, as well as EI/Ca measurements was conducted by Metodiev and Koleva-Rekalova (2008), and the  $\delta^{18}\text{O}$  and  $\delta^{13}\text{C}$  isotope records, OAE placement and palaeotemperature estimates for this section are included in Figure 27.

The Milanovo section is 4.3 m thick section of the Bukorovtsi Member, comprising dark marls likely deposited in a deeper water than the Dobravitsa sections (Metodiev *et al.*, 2014) (Figure 26; Figure 27). The section spans from the *spinatum* to the *aalensis* Zone, and there is likely a hiatus around the Pliensbachian-Toarcian boundary (Metodiev *et al.*, 2014; Pugh, 2018) (Figure 27). Thirty-six belemnite specimens from this section were analysed, ranging from the Mid-upper Toarcian (*variabilis-aalensis* zones) (Figure 27). Specimens were also analysed from the *spinatum* zone in the Upper Pliensbachian and beds above it, but temporal placing of these specimens is difficult due to the hiatus in the stratigraphy (Figure 27).

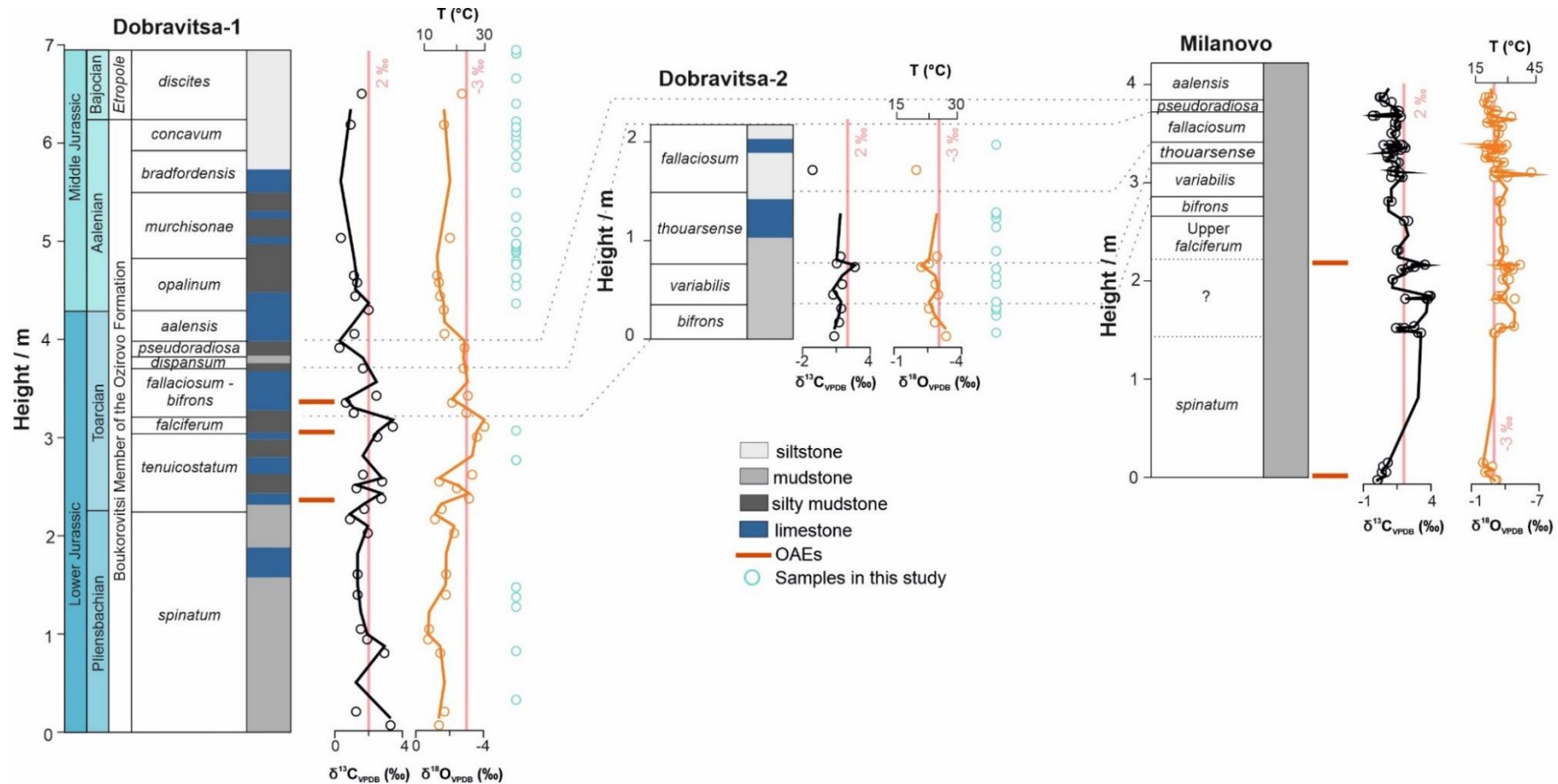


Figure 27 - Simplified lithological columns of the Bulgarian sections studied (Dobravitsa-1, Dobravitsa-2, and Milano) plotted against OAE occurrences, belemnite C isotopes and palaeotemperature estimations based on belemnite oxygen isotopes for each section. For C isotopes (black circles) and O isotopes (orange circles) 2-point moving average lines are shown (black and orange respectively) alongside comparison lines (pink) at  $\delta^{13}C = 2\text{‰}$  and  $\delta^{18}O = -3\text{‰}$  for each location. Dobravitsa-1 and Dobravitsa-2 lithologies, OAE occurrences [based on isotopes], belemnite  $\delta^{13}C$  and  $\delta^{18}O$  isotope curves and palaeotemperature estimates are adapted from Metodiev and Koleva-Rekalova (2008). Milano lithology,  $\delta^{13}C$  and  $\delta^{18}O$  isotope curves, OAE occurrences [based on framboid analysis] and palaeotemperature estimates are taken from Pugh (2018), and temperature estimates are based on  $\delta^{18}O$  values using the equation of Anderson and Arthur (1983), and assuming an original  $\delta^{18}O$  of non-glacial seawater of  $-1\text{‰}$  SMOW. Stratigraphic placement of samples included in this study are shown in pale blue for each section.

## 4.3. Methods

### 4.3.1. Sampling

All of the Bulgarian samples analysed were from powders previously produced by A. Pugh or L. Metodiev. Most Bulgarian belemnites used in this study were previously analysed by either Metodiev and Koleva-Rekalova (2008) (for samples from Dobravitsa-1 and 2) or Pugh (2018) (samples from Milanovo) with multiple techniques applied by these studies including  $\delta^{13}\text{C}$  isotope,  $\delta^{18}\text{O}$  isotope, cathode luminescence studies to indicate preservation, elemental analysis and in some cases strontium isotope analysis. For samples included in this study, a summary of the isotope results is included in the appendix (8.4.4). Samples were re-analysed to determine El/Ca ratios using the method described in Chapters 2 and 3, though the isotope and preservation data was not replicated.

For samples from North Wales and Yorkshire – including samples previously analysed by Newton *et al.* (2011) – fresh samples were prepared by drilling belemnite rostra. For these specimens, each belemnite was sampled by carefully removing the exterior of the rostrum using an abrasive diamond tipped drill bit with a handheld Dremel drill. A fresh abrasive drill bit was then used to sample the interior of the rostrum, avoiding the exterior, apical line and phragmocone region. Attempts were made to sample belemnites at the same point on each rostrum, though in some cases, particularly in core material (North Wales and Dove's Nest), fragmented and broken rostra made this more difficult. Belemnites were sampled in duplicate or triplicate where there was sufficient material, though not all replicate samples were analysed to streamline analytical time and leave material for potential future studies. For belemnite samples which were not powdered using a drill (that often still felt gritty between fingers or had visible larger lumps), samples were powdered using an agate pestle and mortar.

For Dove's Nest specimens, belemnites were extracted from the core as part of whole 'rounds' of sediment. As well as taking belemnite specimens from these rounds, 40 sediment samples were also collected. The whole rounds were cleaned with water to remove any remaining drilling fluid from the coring process, and then air dried. Belemnites were extracted from these rounds, then sediment samples were taken using a chisel from positions adjacent to the belemnites' positions to allow for the best comparison between sediment and carbonate records. These sediment samples were pre-crushed using a steel pestle and mortar and then ground to a fine powder which felt smooth to the touch using a Retsch vibratory disc mill with an agate grinding set, using a 15-minute milling cycle for each sample or until the powder felt smooth to the touch.

## 4.3.2. Carbonate analyses

### 4.3.2.1. El/Ca determination

Replicate samples from the same site on the same specimen were analysed approximately every five samples, depending on sufficient material being available. Samples were analysed from multiple specimens at the same stratigraphic level where available.

Powdered samples were analysed using the methods described in 2.4. Briefly, samples were weighed into 10-20 mg aliquots, rinsed with ultrapure water (2 mL, five rinses), air dried, and then accurately weighed into subsamples in the range of 5-6 mg. In some cases, particularly the Bulgarian samples which had been previously analysed, there was not sufficient remaining material to allow for 10-20 mg samples for cleaning or 5-6 mg samples for dissolution so smaller sample masses were required. As the results are presented as ratios to Ca, smaller sample masses are unlikely to impact results, and this is supported by the method development work (2.6.3). These samples were dissolved in acetic acid (1 mL, 30 %). Then, 0.3 mL of dissolved sample was added to nitric acid (8.6 mL, 0.5 %) and Y standard (0.1 mL, 10 ppb). The samples were analysed for Li, B, Na, Al, K, Mn, Ba and U by ICP-MS and Ca, Mg, P, Fe, Mn, S and Sr by ICP-OES. The LOD/LOQ and precisions for each elemental analysis are described in section 2.4.3. Using the ICP-OES and ICP-MS results, El/Ca ratios, including P/Ca ratios were calculated. The same diagenetic screening protocol was applied to these samples, as the Variability Samples (described in 2.4.6). Full elemental results for the stratigraphic samples can be found in the appendix (8.4).

### 4.3.2.2. Isotope ratios

Carbon and oxygen isotope ratios were measured using the methods described in 3.2.1. Carbon and oxygen isotopes were measured for most samples from North Wales and Dove's Nest cores where there was remaining sample material after El/Ca analysis. Carbon and oxygen isotope measurements were also made for a subset of samples with remaining material for analysis, from all sections studied on the Yorkshire coast (70 samples total, 36 % of the Yorkshire coast samples).

Carbon and oxygen isotopes for the Bulgarian sections were taken from previously published results. Carbon and oxygen isotope measurements for a subset of the samples used in this study were published for Milanovo (in Pugh (2018)) and for Dobravitsa-1 and Dobravitsa-2 (in Metodiev and Koleva-Rekalova (2008)). As these measurements used the same samples in the determination of  $\delta^{13}\text{C}$  and  $\delta^{18}\text{O}$  as were used in this study to determine El/Ca ratios direct comparisons between isotope ratios and El/Ca ratios can be made. Full isotopic results for the stratigraphic samples can be found in the appendix (8.4).

For all oxygen isotope measurements, temperature estimates are based on  $\delta^{18}\text{O}$  values using the equation of Anderson and Arthur (1983), and assuming an original  $\delta^{18}\text{O}$  of non-glacial seawater of -1 ‰ SMOW.

#### 4.3.2.3. XRD analysis

Unit cell parameters were determined for a subset of 11 belemnite carbonate samples from North Wales. Samples for X-ray diffraction (XRD) analysis were selected from uncleaned samples with sufficient remaining material after isotope and El/Ca analyses. El/Ca results were used to ensure that the samples selected for XRD represented a range of P, Mg and Na values.

XRD samples were prepared and analysed by L. Neve at the University of Leeds. Sample preparation was limited to finely powdering the samples with an agate pestle and mortar to avoid grain-size effects distorting the results and mixing with a silicon standard. The unit cell parameters for each sample were determined by performing a Rietveld analysis using Topas 4-2 (Bruker AXS, 2009). Unit cell parameters and volumes were identified using Bruker Eva. A table of the XRD results and a set of example scans are included in the appendix (8.5).

Where XRD identified a contaminant phase (such as chlorite) which is a clay mineral that is not well quantified in TOPAS, calcite values were also discarded as they appeared significantly different to other results. This was attributed to the presence of other mineral phases and may be avoided by using samples cleaned with water which would remove clays. Calcite unit cell parameters were compared to literature values for calcite lattice parameters to ensure the reliability of the measurements. Calcite has a true rhombohedral unit cell with a trigonal 167 space group (Redfern and Angel, 1999). In this structure, unit cell parameters  $a$  and  $b$  are the same and in pure calcite have a length of 4.98 Å; angles  $\alpha$  and  $\beta$  are also the same at 90 ° (Redfern and Angel, 1999). In pure calcite, unit cell parameter  $c$  is 17.192 Å, and angle  $\gamma$  is 120 ° (Redfern and Angel, 1999). The unit cell volume in pure calcite is 369.246 Å<sup>3</sup> (Redfern and Angel, 1999).

#### 4.3.3. Sediment analyses

The 40 Dove's Nest core samples were analysed for major and minor elemental concentrations. In addition, iron speciation and phosphorus speciation techniques were applied. Full sediment analysis results can be found in the appendix (8.6).

##### 4.3.3.1. Iron speciation

Iron speciation is used to distinguish between different ocean redox states, from oxic to anoxic conditions (including ferruginous and euxinic) (Poulton and Canfield, 2011; Poulton, 2021). Redox conditions are determined by evaluating the amount of highly reactive iron ( $\text{Fe}_{\text{HR}}$ ) compared to the total amount of iron ( $\text{Fe}_{\text{TOT}}$ ), as well as the amount of pyrite ( $\text{Fe}_{\text{Py}}$ ) relative to

$Fe_{HR}$ .  $Fe_{HR}$  is comprised of carbonate-associated iron ( $Fe_{Carb}$ ), pyrite ( $Fe_{Py}$ ), ferric oxides ( $Fe_{Ox}$ ) and magnetite ( $Fe_{Mag}$ ). Sequential extraction was performed using the protocol described by Poulton and Canfield (2005).  $Fe_{Carb}$  was extracted in sodium acetate solution;  $Fe_{Ox}$  was then extracted using sodium dithionite solution;  $Fe_{Mag}$  was then extracted in a final leach using ammonium oxalate (room temperature, 6 hr). The iron concentrations of the resultant solutions from these extractions were measured using a ThermoFisher iCE 3300 atomic absorption spectrometer (AAS) in the Cohen Geochemistry Laboratory, University of Leeds.  $Fe_{Py}$  was determined following a chromous chloride distillation protocol (Canfield *et al.*, 1986) and the concentration of pyrite was calculated from the weight of precipitated silver sulfide produced by the extraction. Replicate extractions of samples and reference material WHIT (Alcott *et al.*, 2020) yielded relative standard deviations (RSDs) of < 5 % for all  $Fe_{HR}$  phases.

$Fe_{HR}/Fe_{TOT}$  ratios > 0.38 suggest deposition in anoxic bottom waters, and values < 0.22 suggest deposition in oxic waters, with values in between being more ambiguous (Poulton and Canfield, 2011; Raiswell and Canfield, 2012; Poulton, 2021).  $Fe_{Py}/Fe_{HR}$  > 0.8 suggests deposition in euxinic waters, and values < 0.6 suggest deposition in ferruginous waters with intermediate values once again being considered equivocal (Poulton and Canfield, 2011; Raiswell and Canfield, 2012; Poulton, 2021). Iron speciation data is considered alongside sediment trace metal systematics to give a fuller understanding of the redox environment of sediment deposition.

#### 4.3.3.2. Major and minor elements

For analysis of major and trace elements, the powdered sediment samples (100 mg) were digested using a multi-acid ( $HNO_3$ – $HF$ – $HCl$ ) treatment. Major and trace elements were analysed using an Agilent 7700X quadrupole inductively coupled plasma mass spectrometer (ICP-MS) and Agilent 710 inductively coupled plasma-optical emission spectrometer (ICP-OES) at the State Key Laboratory of Palaeobiology and Stratigraphy, Nanjing Institute of Geology and Palaeontology, Chinese Academy of Sciences (NIGPAS). Accuracy was monitored by analysing certified reference materials USGS Eocene Green River Shale (SGR-1) and GSR-1. Repeated measurement of samples yielded RSDs for all elements of less than 3-5 %.

#### 4.3.3.3. Phosphorus speciation

A sequential extraction protocol for Fe-rich rocks was applied to identify and quantify the pools of phosphorus present in the samples, using the method described in Thompson *et al.* (2019). This method targets four different pools of phosphorus: iron-bound phosphorus ( $P_{Fe}$ ), authigenic phosphorus ( $P_{Aut}$ ), organic bound phosphorus ( $P_{Org}$ ), crystalline apatite-bound phosphorus (predominantly detrital;  $P_{Apt}$ ) (Thompson *et al.*, 2019).

$P_{Fe}$  was extracted in a solution of sodium citrate/sodium dithionate/sodium bicarbonate (room temperature, 8 hrs);  $P_{Aut}$  was extracted in sodium acetate solution (room temperature, 6 hrs);  $P_{Apt}$  was extracted in HCl (1 M, room temperature, 16 hrs); To determine  $P_{Org}$ , remaining sample material was dried (100 °C, several hours) then ashed in a furnace (550 °C, 2 hours) to ensure dry oxidation was complete. Samples were then extracted in HCl (1M, room temperature, 16 hrs) to determine  $P_{Org}$ . The resultant solutions from all extractions were analysed to determine the concentration of P using either a spectrophotometric method at 880 nm (particularly for  $MgCl_2$  washes of samples to remove readsorbed phosphorus after extraction) or ICP-OES (particularly for solutions from primary extractions and those which contain chemicals which interfere with colour development in the molybdate blue method) (Strickland and Parsons, 1972; Thompson *et al.*, 2019). Reactive phosphorus ( $P_{Reac}$ ) was calculated as the sum of  $P_{Fe}$ ,  $P_{Aut}$  and  $P_{Org}$  (Ingall and Jahnke, 1994).

To fully interpret phosphorus speciation results, different forms of phosphorus are compared to the organic carbon content of the samples. At the time of writing, organic carbon concentrations have yet to be analysed, so description and analysis of the phosphorus speciation samples is not included here pending completion of organic carbon quantification.

## 4.4. Results

### 4.4.1. Screening

#### 4.4.1.1. Diagenesis

The belemnite samples from all sections were screened using Fe/Ca and Mn/Ca values in the same way as described in sections 2.5.5.1 and 3.3.5.1. A plot of Fe/Ca and Mn/Ca with the screening criteria indicated is shown in Figure 28.

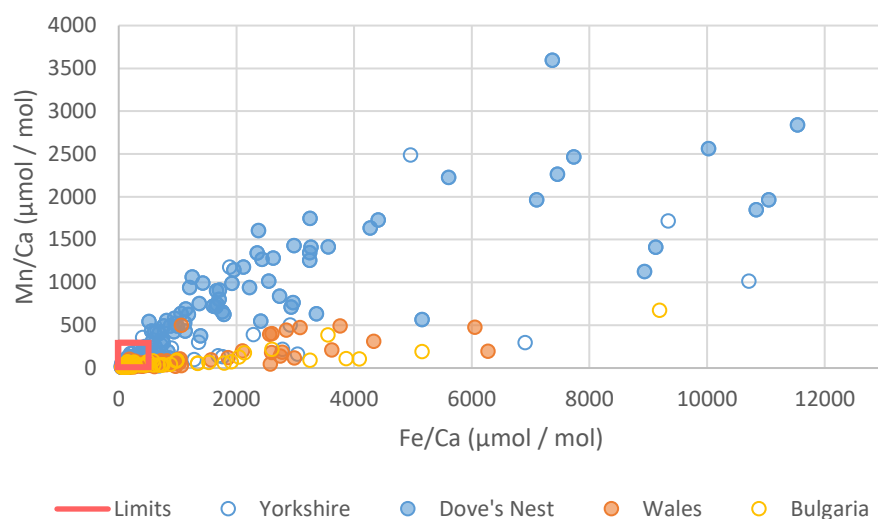


Figure 28 - Plot of Fe/Ca and Mn/Ca for samples from all sites with the screening limits indicated in red. Core samples are indicated with filled in circles, outcrop samples with unfilled circles.

Samples were screened using the limits of Fe/Ca < 600  $\mu\text{mol mol}^{-1}$  and Mn/Ca < 300  $\mu\text{mol mol}^{-1}$ . After screening, 30 % of samples were excluded from subsequent assessment of other elements across all sites (Figure 28). To determine if the screening limits were suitable to negate the impact of diagenesis on P/Ca values,  $R^2$  values were calculated using El/Ca ratios for Fe vs Mn, Fe vs P and Mn vs P (Table 21). Good correlation between Fe and Mn ratios to Ca indicate the presence of diagenetic alteration or contamination with diagenetic minerals. Correlation between Fe/Ca or Mn/Ca and P/Ca indicates that the diagenetic alteration or contamination may be impacting P/Ca ratios.

Table 21 -  $R^2$  values indicating correlation between El/Ca ratios for samples in different locations.  $R^2$  values are given for Fe/Ca and Mn/Ca; Fe/Ca and P/Ca and Mn/Ca and P/Ca. Cells are shaded green to denote correlation, with darker green indicating strong correlation ( $R^2 > 0.8$ ) and light green denoting weaker correlation ( $R^2 > 0.3$ ). The  $R^2$  values for each location are calculated before and after sample screening criteria were applied and the results are given for both.  $R^2$  values for Dobravitsa-2 could not be calculated due to the Fe and Mn measurements falling below the LOD/LOQ for most samples.

Sample location	Unscreened samples				Screened samples			
	n	Mn and Fe	P and Fe	P and Mn	n	Mn and Fe	P and Fe	P and Mn
<b>Yorkshire coast</b>	162	0.52	0.60	0.36	136	0.60	5E-02	6E-03
Ravenscar	34	0.48	0.95	0.86	27	0.53	1E-02	1E-03
Runswick Bay	86	0.48	0.30	0.14	73	0.55	0.17	3E-03
Cowbar Nab	16	0.91	5E-02	4E-02	14	0.93	3E-02	9E-02
Penny Nab	11	0.83	0.46	0.68	10	0.53	0.25	0.49
Wine Haven	15	0.95	6E-03	9E-02	12	0.94	0.13	2E-03
<b>Yorkshire core</b>	124	0.67	0.12	0.18	52	0.28	8E-02	9E-02
<b>Wales</b>	148	0.79	4E-02	0.04	102	0.32	1E-02	3E-02
<b>Bulgaria</b>	101	0.77	0.20	0.28	82	0.40	5E-02	0.20
Dobravitsa-1	60	0.83	0.29	0.55	41	0.76	4E-02	2E-02
Dobravitsa-2	7	-	-	-	7	-	-	-
Milanovo	34	9E-02	6E-03	0.17	34	9E-02	6E-03	0.17

All	541	0.67	0.10	0.73	375	0.17	4E-02	5E-03
-----	-----	------	------	------	-----	------	-------	-------

In the unscreened samples there was a correlation between Fe/Ca and Mn/Ca for almost all sites studied, indicating the samples contained diagenetic material from contamination or alteration (Table 21). There was also correlation between P/Ca and either Fe/Ca or Mn/Ca in samples from several sites in the unscreened samples (Table 21). After screening criteria were applied, there were still good correlations between Fe/Ca and Mn/Ca in the majority of sites studied, however in almost all sites the correlation was lower in the screened samples than in the unscreened samples (Table 21). For R<sup>2</sup> values for correlation between P/Ca and either Fe/Ca or Mn/Ca, the R<sup>2</sup> values decreased for every site studied except Milanovo where there was no change (Table 21). For screened samples there was no or very low correlation between P/Ca and either Fe/Ca or Mn/Ca in almost all sites studied except in the case of Penny Nab, where there was an R<sup>2</sup> value of 0.49 between P/Ca and Mn/Ca – but no significant correlation between P/Ca and Fe/Ca (Table 21).

For the majority of sections studied the distribution of the samples through the stratigraphy was very similar between all the samples studied and the screened samples and covered similar stratigraphic ranges. This was not the case in the samples from the Dove's Nest cores, where the majority of samples from the lower SM14 core (and all samples below the base of the Upper-Ironstone Shale Member in the Redcar Mudstone Formation) had iron and manganese values well above the limits used for other samples Fe/Ca < 600  $\mu\text{mol mol}^{-1}$  and Mn/Ca < 300  $\mu\text{mol mol}^{-1}$  (Figure 24; Figure 28). The samples which exceeded the limits in Dove's Nest were examined to determine if higher limits may be appropriate, to include more samples across a greater stratigraphic range, without increasing the influence of diagenetic alteration and contamination. It was found that in the excluded samples, there was a correlation between P/Ca ratios and both Fe/Ca and Mn/Ca ratios, demonstrating that the degree of diagenetic alteration and contamination in these samples was affecting the P/Ca ratios. This meant that the existing limits of Fe/Ca < 600  $\mu\text{mol mol}^{-1}$  and Mn/Ca < 300  $\mu\text{mol mol}^{-1}$  were determined to be appropriate limits for iron and manganese in these samples, and the samples which fell outside of these limits were excluded. Due to this, the range of samples covered by the samples in the Dove's Nest cores is significantly lower after screening criteria were applied (Figure 24).

#### 4.4.2. Carbonate-associated phosphorus ratios

P/Ca values were calculated for each belemnite sample from Wales, Yorkshire, and Bulgaria (Figure 29). For each location, sections were combined to produce a single stratigraphic record using the correlations shown in Figure 23 (Yorkshire) and Figure 27 (Bulgaria). Ammonite zones

and lithological markers were then used to correlate the records between each location (Figure 29). This enabled P/Ca records to be compared for three different locations in the Laurasian Seaway (Figure 29).



the Penny Nab section taken from the 'Variability samples' (2.3.2) to indicate the magnitude of changes compared to the natural levels of variability at each stratigraphic level. For Bulgaria and Yorkshire, stratigraphic plots combine samples from multiple sections, using correlations previously presented (Yorkshire (Rawson and Wright (2018); Lord (2019); Trabucho-Alexandre et al. (2022) (Figure 23); Bulgaria (Metodiev and Koleva-Rekalova (2008); Pugh (2018) (Figure 27)). Where samples in each location are from different sections the data points are indicated with different symbols. Where abbreviations for lithological units are used due to limited space: Fe-stone = ironstone; Ms. = mudstone, Sh. = Shale; Ss. = sandstone. Hashed areas indicate either stratigraphic gaps in the sampling, or where samples were below the limit of detection.

The magnitude of the P/Ca ratios in each section were similar, with values ranging from around 100 to 2,200  $\mu\text{mol mol}^{-1}$  in all three locations. T tests conducted using the methods described in 2.4.5 showed that there were no statistically significant differences in P/Ca values between Bulgaria ( $\bar{x} = 865 \mu\text{mol mol}^{-1}$ ;  $s = 397 \mu\text{mol mol}^{-1}$ ) and North Wales ( $\bar{x} = 961 \mu\text{mol mol}^{-1}$ ;  $s = 289 \mu\text{mol mol}^{-1}$ ) ( $t(150) = 1.65$ ;  $p = 0.067$ ), though there were statistically significant differences between Bulgaria and Yorkshire ( $\bar{x} = 719 \mu\text{mol mol}^{-1}$ ;  $s = 305 \mu\text{mol mol}^{-1}$ ) ( $t(130) = 1.66$ ;  $p = 0.003$ ) and North Wales and Yorkshire ( $t(216) = 1.65$ ;  $p = 2.32\text{E-}10$ ).

The P/Ca records for all locations have relatively high levels of variability, though some of this variability can be explained by the differences within and between individual belemnites (Figure 15). Based on the Variability Samples, standard deviations were calculated for all samples from the Penny Nab section from the variability section which included 77 samples from six belemnites from four different species from the same stratigraphic level. The standard deviation of P/Ca in the Penny Nab Variability Samples was determined to be 107  $\mu\text{mol mol}^{-1}$ . A bar indicating two standard deviations (214  $\mu\text{mol mol}^{-1}$ ) is shown for each plot on Figure 29 to demonstrate the magnitude of changes which can be deemed to be attributable to something other than the natural variability in P/Ca values within and between belemnites.

For the locations studied, there are changes greater than those which can be explained by natural variability in P/Ca ratios between and within individuals (Figure 29). There are also similarities between the stratigraphic trends observed in P/Ca between each section.

Most notably in Yorkshire there was a decrease in P/Ca in the lower *tenuicostatum* zone, with values of P/Ca falling from around 800 to around 200  $\mu\text{mol mol}^{-1}$  (Figure 29). The P/Ca decrease occurs between two previously described pulses of extinction – one at the Pliensbachian-Toarcian boundary (mostly affecting ammonoids), and a later pulse at the top of the *tenuicostatum* affecting many other marine invertebrates (including belemnites) (Jenkyns, 1988; Arias et al., 1992; Bassoullet and Baudin, 1994; Little and Benton, 1995; Wignall et al., 2006; Mailliot et al., 2006; Mattioli et al., 2009; Caswell et al., 2009). In the samples from North Wales and Bulgaria, there are limited samples in the *tenuicostatum* zone, so it is difficult to determine if there is a similar fall in P/Ca values in these sections (Figure 29). In Yorkshire, the P/Ca values remain low until the lower *serpentinum* zone where there is an increase in

P/Ca values to 1,200-1,800  $\mu\text{mol mol}^{-1}$  (Figure 29). This rise is also seen in the samples from North Wales, where the P/Ca values rise from around 800 to around 1,600  $\mu\text{mol mol}^{-1}$  in the mid-late *serpentinum* zone. An increase in P/Ca values also occurs in the samples from Bulgaria, though slightly earlier than the rise seen in both Yorkshire and North Wales, with a change from around 500  $\mu\text{mol mol}^{-1}$  to around 1,300  $\mu\text{mol mol}^{-1}$  in the latest *tenuicostatum* zone (Figure 29). In North Wales, limited samples above the *tenuicostatum* zone make determining the duration of the peak in P/Ca values in the North Wales core difficult, although from the few data points present it appears that P/Ca ratios decrease again somewhere in the *bifrons* zone. In Bulgaria, elevated P/Ca values remain for a longer period of time, and do not return to the values of around 500  $\mu\text{mol mol}^{-1}$  until the late Toarcian – possibly the *fallaciosum* zone – though as with North Wales, limited numbers of samples make this difficult to determine.

#### 4.4.3. CAP variation with redox

Iron speciation and trace metal analysis results were used to determine the redox state during sediment deposition throughout time using the sediment samples from the Dove's Nest core. These results were compared to the P/Ca values from belemnite calcite which were located directly adjacent to sampled sediment to create a paired carbonate-sediment record (Figure 30). The sediment analysis showed a general trend from likely oxic depositional conditions at the base of the core, towards dysoxic-anoxic depositional conditions at the top (Figure 30).

In the lower part of the NS1 core (below 190 m; corresponding to samples from the Staithes Sandstone Formation and Cleveland Ironstone Member (ranging from the upper *davoei* to *spinatum* zones of the late Pliensbachian) the  $\text{Fe}_{\text{HR}}/\text{Fe}_{\text{TOT}}$  values for the sediment samples were around 0.3 (g; Figure 30). This corresponds to low  $\text{Fe}_{\text{PY}}/\text{Fe}_{\text{HR}}$  values (below 0.6) and low ratios for trace elements. For Mo/Al, U/Al, and Mo/U the ratios in the samples below 220 mbs are all similar to the average upper continental crustal (UCC) values (c, d, e; Figure 30). For  $\text{Fe}_{\text{TOT}}/\text{Al}$  ratios, the value fell above the average oxic threshold, with most values falling in the range of 0.8-1.1 wt%/wt%, with one elevated value of 1.7 at 210 m depth (corresponding to the Penny Nab Member) (f; Figure 30). Below 190 m, P/Ca values were also fairly low, though showed a gradual increase, with values below 220 m of around 400  $\mu\text{mol mol}^{-1}$  rising to around 1000 from 190-220 m (j; Figure 30).

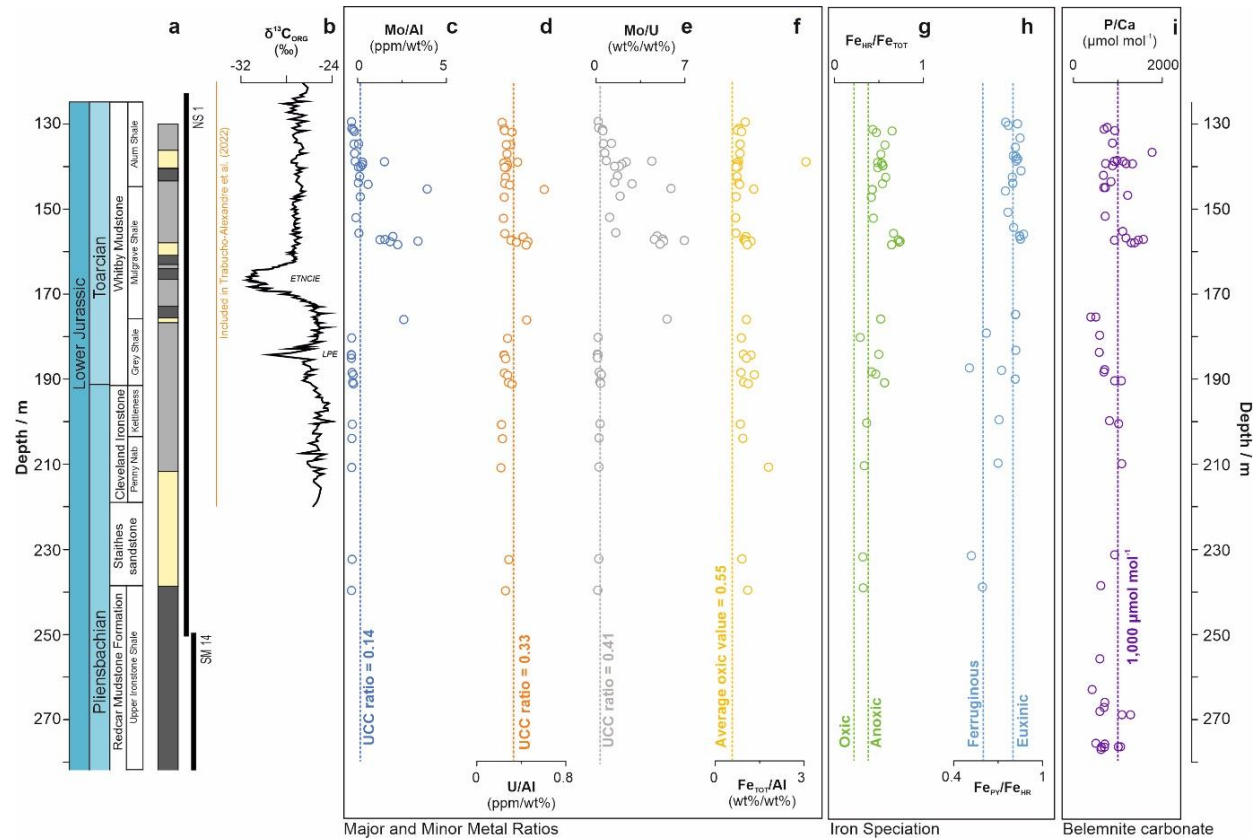


Figure 30 - Core depths, global geochronological stages, and lithological log (a, Trabuco-Alexandre et al. (2022) above 220 m and observations of the core below 220 m); the carbon isotope curve for the same core from Trabuco-Alexandre et al. (2022) (b); trace metal element ratios (c-f) are calculated from elemental concentrations element/element; for c-e, upper continental crust (UCC) values (calculated from Rudrick and Gao (2003)) used for comparison (dashed lines), for f the average oxidic value for Fe/Al is indicated (from Clarkson et al. (2014)). Iron speciation ratios (g-h) highly reactive iron to total iron ratio ( $\text{Fe}_{\text{HR}}/\text{Fe}_{\text{TOT}}$ ; g) shown alongside the reported thresholds for anoxic ( $\text{Fe}_{\text{HR}}/\text{Fe}_{\text{TOT}} > 0.38$ ) and oxidic ( $\text{Fe}_{\text{HR}}/\text{Fe}_{\text{TOT}} < 0.22$ ) conditions (pale grey dashed lines) (Poulton and Canfield, 2011; Raiswell and Canfield, 2012; Poulton, 2021); pyrite to highly reactive iron ratios ( $\text{Fe}_{\text{PY}}/\text{Fe}_{\text{HR}}$ ; h) are shown with reported thresholds for ferruginous ( $\text{Fe}_{\text{PY}}/\text{Fe}_{\text{HR}} < 0.6$ ) and euxinic ( $\text{Fe}_{\text{PY}}/\text{Fe}_{\text{HR}} > 0.8$ ) conditions, where  $\text{Fe}_{\text{PY}}/\text{Fe}_{\text{HR}}$  values of 0.6-0.8 and  $\text{Fe}_{\text{HR}}/\text{Fe}_{\text{TOT}}$  values of 0.22-0.38 are equivocal (Poulton and Canfield, 2011; Raiswell and Canfield, 2012; Poulton, 2021); P/Ca records from belemnite calcite (i) from belemnites directly adjacent to the sampled sediment plotted against a line of  $\text{P}/\text{Ca} = 1,000 \mu\text{mol mol}^{-1}$  to allow for better comparison of trends throughout the section.

From 175-190 m (corresponding to the Grey Shale Member of the Whitby Mudstone Formation; *tenuicostatum* zone)  $Fe_{HR}/Fe_{TOT}$  values are predominantly over 0.38 between 170-190 m and  $Fe_{PY}/Fe_{HR}$  varies from values above 0.8 to values below 0.6 (g, h; Figure 30). Mo/Al, U/Al and Mo/U ratios still fall close to the UCC values (c, d, e; Figure 30). Values for  $Fe_{TOT}/Al$  continue to be enriched compared to the average oxic value, however they also show little change from the samples below 190m depth (f; Figure 30). At 175 m there is an increase in Mo/Al, U/Al and Mo/U values – which corresponds with values of  $Fe_{HR}/Fe_{TOT} > 0.38$  and  $Fe_{PY}/Fe_{HR} > 0.8$  which indicate potential anoxic/euxinic bottom water conditions – though the Fe speciation ratios are very similar to the values in the 175-190 m interval (c, d, e, g, h; Figure 30).  $Fe_{TOT}/Al$  is also unchanged at 175 m depth compared to samples from 175-190 m (f; Figure 30). Due to limited belemnite recovery from the core, these changes are based on the elevated values of a single sample – ideally more sediment samples would be collected above and below this depth to confirm (Figure 30). There is a gradual decrease in P/Ca from values of around  $1,050 \mu\text{mol mol}^{-1}$  at 190 m depth to values of around  $350 \mu\text{mol mol}^{-1}$  at 170 m depth (i; Figure 30).

There is a gap in the record from around 160-174 m where no belemnites were recovered (Figure 24; Figure 30). This interval is coincident with the TOAE, ETNCIE and ETME in the coastal sections (Figure 23) and is a period of laminated black shale deposition (Figure 23; Figure 30). Sediment samples were taken directly adjacent to belemnites in the core so there is also no sediment analysis for this interval.

From 160 m to 120 m (corresponding to Mulgrave and Alum Shale Members of the Whitby Mudstone Formation; *serpentinum* and *bifrons* zones) the trace element and iron speciation proxies appear to indicate a dominantly euxinic interval (Figure 30). Throughout this interval  $Fe_{HR}/Fe_{TOT}$  remains above 0.38 and  $Fe_{PY}/Fe_{HR}$  also remains high, with values predominantly above 0.8 with the exception of an excursion to around 0.78 at 143 m depth (g, h; Figure 30). Just above 160 m there are elevated values in Mo/Al, U/Al, Mo/U, which correspond to elevations in  $Fe_{HR}/Fe_{TOT}$  and  $Fe_{PY}/Fe_{HR}$  as well as an increase in P/Ca as well as potentially elevated  $Fe_{TOT}/Al$ , though these values are similar to values lower in the core (c-i; Figure 30). These elevated trace element ratios are not sustained, with values returning to near-UCC ratios from 155 m depth for Mo/Al, U/Al, and  $Fe_{TOT}/Al$  – though Mo/U values remain elevated until near the top of the Alum Shales (Figure 30). There are two further peaks in Mo/Al and U/Al and – the first of which is at 144 m and the second at 138 m (c, e; Figure 30). The peak at 144 m corresponds to increases in  $Fe_{TOT}/Al$  values, as well as small increases in  $Fe_{HR}/Fe_{TOT}$  and  $Fe_{PY}/Fe_{HR}$  (d, f, g, h; Figure 30). The second peak at 138 m corresponds with an increase in

$Fe_{TOT}/Al$  and a peak in  $P/Ca$  values, but there is no change in the iron speciation ratios (f, g, h, i; Figure 30).

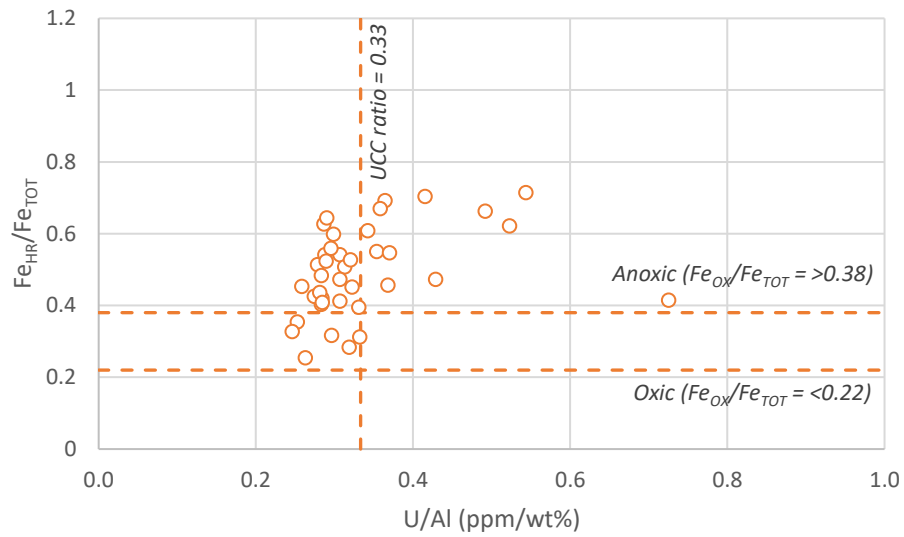


Figure 31 - Cross-plot of  $U/Al$  values against  $Fe_{HR}/Fe_{TOT}$  values for sediment samples from the Dove's Nest NS1 core) shown alongside the reported thresholds for anoxic ( $Fe_{HR}/Fe_{TOT} > 0.38$ ) and oxic ( $Fe_{HR}/Fe_{TOT} < 0.22$ ) conditions (Poulton and Canfield, 2011; Raiswell and Canfield, 2012; Poulton, 2021), and the UCC ratio for  $U/Al$  ratios (in ppm/wt%, calculated from Rudrick and Gao, 2003).

To investigate the possible presence of anoxic depositional environments in the upper part of the core, cross-plots of  $Fe_{HR}/Fe_{TOT}$  vs  $U/Al$  and  $Fe_{PY}/Fe_{HR}$  vs  $Mo/Al$  were created for samples in the 160-120 m interval (Figure 30; Figure 31; Figure 32). Both  $Fe_{HR}/Fe_{TOT}$  and  $U/Al$  are proxies for anoxia, so coenrichments of both proxies two would indicate the presence of an anoxic depositional environment in this interval of the section, supported by two different sedimentological proxies. For the samples from Dove's Nest, there was a co-enrichment between of  $Fe_{HR}/Fe_{TOT}$  and  $U/Al$ , with only the samples with high values of  $U/Al$  having values of  $Fe_{HR}/Fe_{TOT} > 0.38$ .

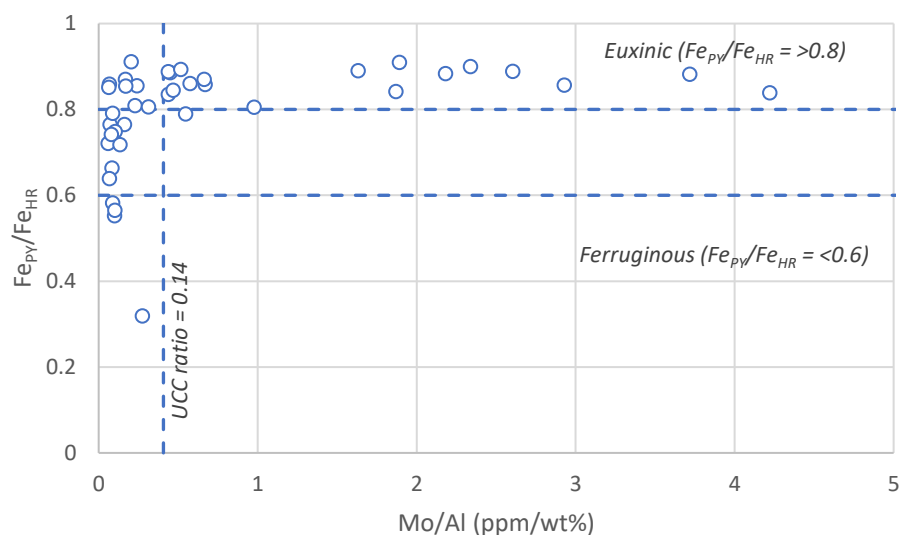


Figure 32 - Cross-plot of Mo/Al values against  $Fe_{py}/Fe_{hr}$  values for sediment samples from the Dove's Nest NS1 core) shown alongside the reported thresholds for euxinic ( $Fe_{py}/Fe_{hr} > 0.80$ ) and ferruginous ( $Fe_{py}/Fe_{hr} < 0.60$ ) conditions (Poulton and Canfield, 2011; Raiswell and Canfield, 2012; Poulton, 2021), and the UCC ratio for Mo/Al ratios (in ppm/wt%, calculated from Rudrick and Gao, 2003).

$Fe_{py}/Fe_{hr}$  and Mo/Al are both indicators of euxinia so co-enrichment between the two would indicate the presence of an euxinic depositional environment. There was an observable co-enrichment between the  $Fe_{py}/Fe_{hr}$  and Mo/Al, with the samples giving the highest Mo/Al values (over the UCC ratio) all also having elevated  $Fe_{py}/Fe_{hr}$  ratios (predominantly over 0.8) (Figure 32).

The relationship between P/Ca and iron speciation ratios was further investigated to determine if there was correlation between them (Figure 30; Figure 33; Figure 34). P/Ca values were compared to iron speciation ratios  $Fe_{hr}/Fe_{tot}$  and  $Fe_{py}/Fe_{hr}$  using cross-plots (Figure 33; Figure 34). For both  $Fe_{hr}/Fe_{tot}$  and  $Fe_{py}/Fe_{hr}$ , there was evidence of some covariance between P/Ca and both  $Fe_{hr}/Fe_{tot}$  and  $Fe_{py}/Fe_{hr}$  (Figure 33; Figure 34). All the samples with the highest P/Ca values fell above  $Fe_{hr}/Fe_{tot} > 0.38$  and  $Fe_{py}/Fe_{hr} > 0.8$  (Figure 33; Figure 34). This suggests that there is a possibility that P/Ca varies with redox, and so it is possible the results here are consistent with P recycling under euxinic conditions. Redox is also variable with many other factors including temperature, so it is possible that the covariation of P/Ca and redox proxies is due to P/Ca covarying with other environmental factors.

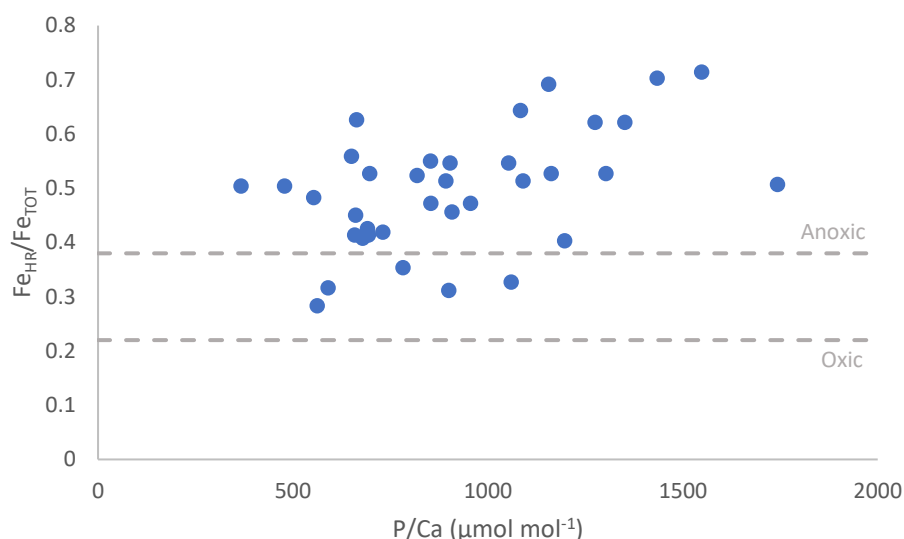


Figure 33 – Cross-plot of iron speciation ratio  $Fe_{HR}/Fe_{TOT}$  against  $P/Ca$  from analysis of belemnite carbonate for the analysis of paired sediment and belemnite samples from the Dove's Nest NS1 core. Iron speciation thresholds for oxic ( $Fe_{HR}/Fe_{TOT} < 0.22$ ) and anoxic ( $Fe_{HR}/Fe_{TOT} > 0.38$ ) conditions are indicated with (pale grey dashed lines) (Poulton and Canfield, 2011; Raiswell and Canfield, 2012; Poulton, 2021).

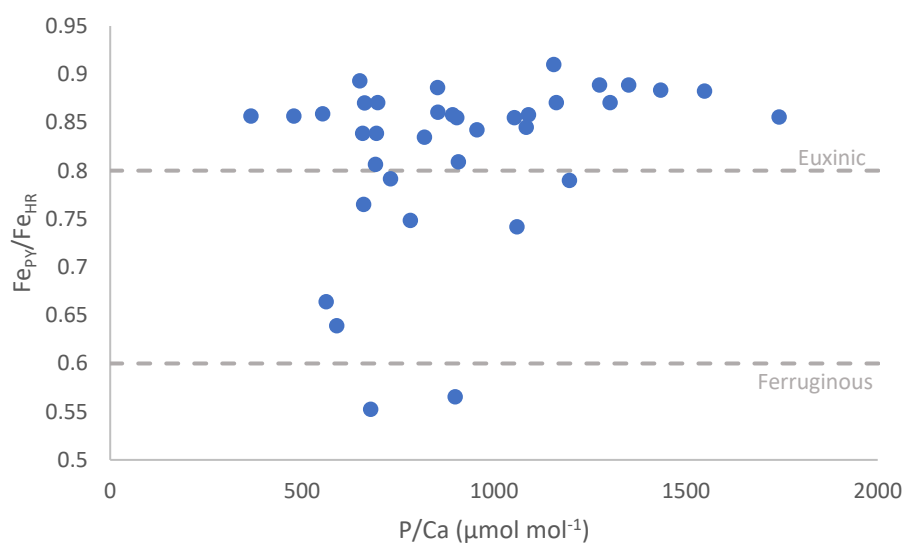


Figure 34 - Cross-plot of iron speciation ratio  $Fe_{Py}/Fe_{HR}$  against  $P/Ca$  from analysis of belemnite carbonate for the analysis of paired sediment and belemnite samples from the Dove's Nest NS1 core. Iron speciation thresholds for ferruginous ( $Fe_{Py}/Fe_{HR} < 0.6$ ) and euxinic ( $Fe_{Py}/Fe_{HR} > 0.8$ ) conditions are indicated with (pale grey dashed lines) (Poulton and Canfield, 2011; Raiswell and Canfield, 2012; Poulton, 2021).

#### 4.4.4. CAP variation with temperature

Oxygen isotope measurements were used as an indication of temperature and compared to  $P/Ca$  records across all sections studied.  $\delta^{18}O$  values were collected from the same belemnite calcite samples as  $El/Ca$  ratios to ensure a paired isotope and  $P/Ca$  record. This meant that oxygen isotope records could be generated for all locations and sections studied. The

resolution of the oxygen isotope data is lower than the resolution of the EI/Ca data, due to limited sample material for some samples, and only a subset of samples for Bulgaria (Figure 35). Nevertheless, the spreads of isotope data and EI/Ca data cover similar time ranges in each study location which allows for comparison between EI/Ca ratios  $\delta^{18}\text{O}$  values (Figure 35).

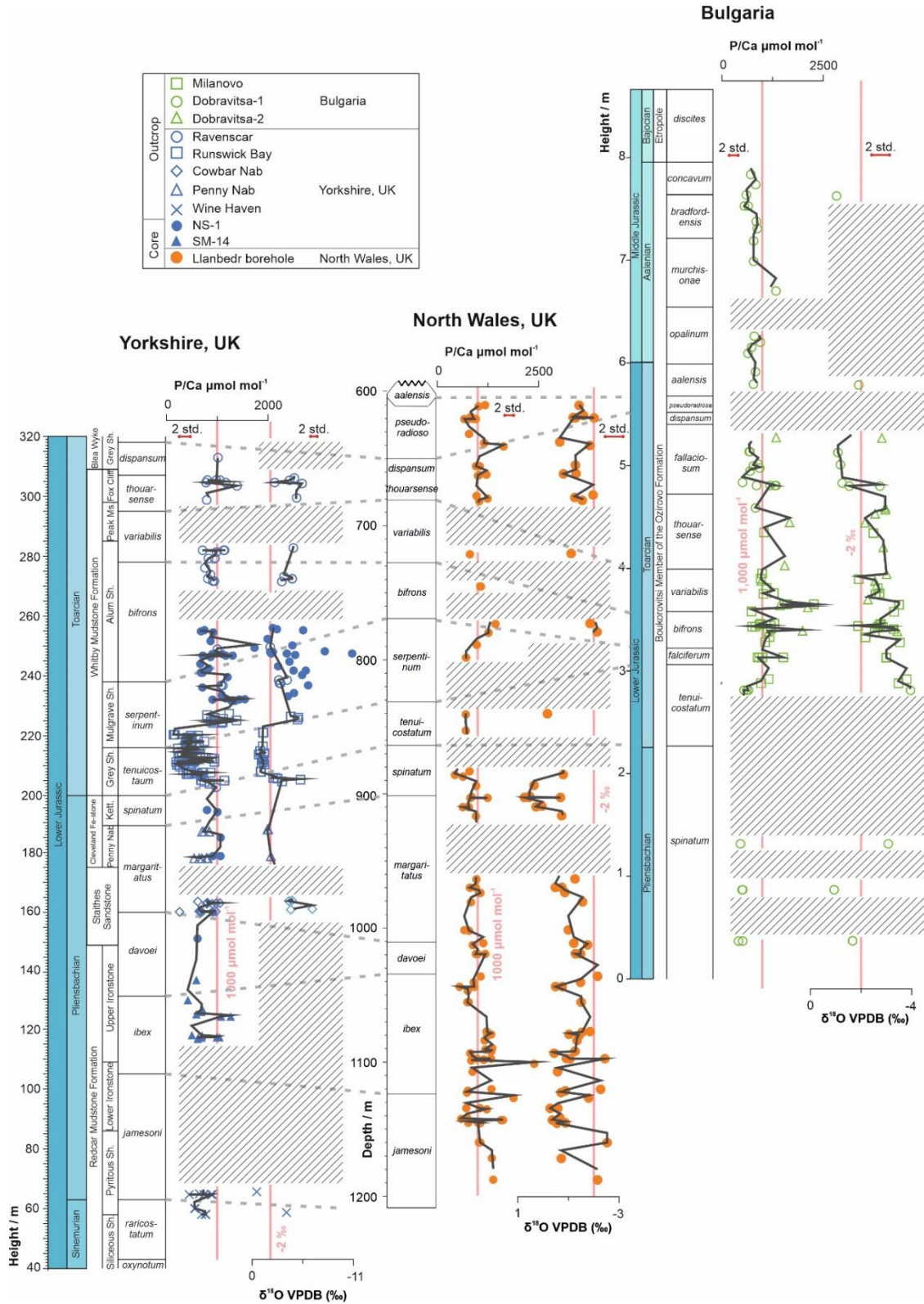


Figure 35 - P/Ca ratios alongside  $\delta^{18}\text{O}$  values compared to the Vienna Pee Dee Belemnite (VPDB) for screened samples from multiple sections across three locations (North Yorkshire, UK; North Wales, UK;

Bulgaria).  $\delta^{18}\text{O}$  plots use a reversed x axis scale so warmer temperatures are on the right, and cooler temperatures to the left.  $\delta^{18}\text{O}$  and P/Ca values were collected from the same samples from the same individual belemnites.  $\delta^{18}\text{O}$  values for Bulgarian samples are taken from Metodiev and Koleva-Rekalova (2008) and Pugh (2018). In each location a 2-point moving average line (dark grey) is included to show the trends in P/Ca. For each record, values of P/Ca = 1,000  $\mu\text{mol mol}^{-1}$  and  $\delta^{18}\text{O}_{\text{VPDB}} = -2\text{‰}$  are indicated (pale red lines) for reference. Also included for each plot is a bar indicating two standard deviations (based on the variability of P/Ca and  $\delta^{18}\text{O}$  within a stratigraphic level calculated from the analysis of 77 samples from 6 individual belemnites from the Penny Nab section taken from the 'Variability samples' (2.3.2). Where abbreviations for lithological units are used due to limited space: Fe-stone = ironstone; Ms. = mudstone, Sh. = Shale; Ss. = sandstone. Hashed areas indicate either stratigraphic gaps in the sampling, or where samples were below the limit of detection.

The stratigraphic P/Ca and  $\delta^{18}\text{O}$  records for each section are broadly comparable, with excursions to high P/Ca values coinciding with excursions to low  $\delta^{18}\text{O}$  values within the same locations (Figure 35). In each location there were major and minor perturbations which could be seen in both the P/Ca and the oxygen isotope records (Figure 35). For example, in the samples from North Yorkshire there is a low point in P/Ca which coincides with high  $\delta^{18}\text{O}$  values from the mid-*tenuicostatum* zone to the mid-*serpentinum* zone, followed by an increased P/Ca and a decrease in  $\delta^{18}\text{O}$  values in both records until the upper *serpentinum*/lower *bifrons* zone (Figure 35). In samples from the North Wales record there were also broad similarities between the P/Ca and  $\delta^{18}\text{O}$  values including coincident excursions in both records at multiple stratigraphic heights (such as small excursions at the *margaritatus-spinatum* zone boundary in the late Pliensbachian, and the *serpentinum-bifrons* zone boundary in the Toarcian) (Figure 35). There was also an increase in P/Ca values in samples from Bulgaria with P/Ca values rising to above 1,000  $\mu\text{mol mol}^{-1}$  from the mid-*tenuicostatum* zone in the early Toarcian, with values not decreasing to be consistently below 1,000  $\mu\text{mol mol}^{-1}$  again until the *fallaciosum* zone in the late Toarcian (Figure 35). Coincident with this were low  $\delta^{18}\text{O}$  values of around -4 ‰ in the mid-*tenuicostatum* zone, followed a general trend of gradually increasing P/Ca with gradually increasing  $\delta^{18}\text{O}$  values until at least the mid-*fallaciosum* zone.

While there are several points where there are coincident excursions between P/Ca and  $\delta^{18}\text{O}$  values, which are suggestive of a negative correlation between CAP and  $\delta^{18}\text{O}$ , there are some regions of the curve where opposite behaviour is seen (excursions to more positive  $\delta^{18}\text{O}$  values coinciding with positive P/Ca values and vice versa) (Figure 35). The North Wales samples are the best sample to use to observe this, as they exhibit the most complete isotope record compared to the El/Ca record (Figure 35). For example, a peak in P/Ca ratios at 670 m depth in the *thouarsense/dispansum* zone of 1,166  $\mu\text{mol mol}^{-1}$  corresponded to a positive peak in  $\delta^{18}\text{O}$  of -1.05 ‰ (Figure 35). Similarly, at 889 m depth in the *spinatum* zone, a negative excursion of P/Ca to 382  $\mu\text{mol mol}^{-1}$  corresponded to a negative excursion in  $\delta^{18}\text{O}$  to -1.05 ‰ (Figure 35). Also, at 983 m depth in the *margaritatus* zone a negative excursion in  $\delta^{18}\text{O}$  to -1.74 ‰ corresponded to a P/Ca value of 782  $\mu\text{mol mol}^{-1}$ , with no obvious excursion in P/Ca values

(Figure 35). These were predominantly small changes in both P/Ca and  $\delta^{18}\text{O}$  values, compared to the scale of changes exhibited in the core as a whole – particularly the changes at the *thouarsense/dispansum* and *margaritatus* zones (Figure 35). Nevertheless, it is clear that the records of P/Ca and  $\delta^{18}\text{O}$  do not perfectly correlate through time in the locations studied (Figure 35).

To further investigate this, as with the sediment analysis, a cross-plot of P/Ca and  $\delta^{18}\text{O}$  for each location studied was created (Figure 36). Linear lines of best fit were applied to samples from each location: Yorkshire, Wales, and Bulgaria (Figure 36). An additional subset of the Yorkshire samples was included, comprising of core samples taken from the Dove's Nest site (Figure 36).  $R^2$  values for the lines of best fit were calculated and displayed alongside the key symbols for each sample set, in a colour matching the sample symbol (Figure 36).

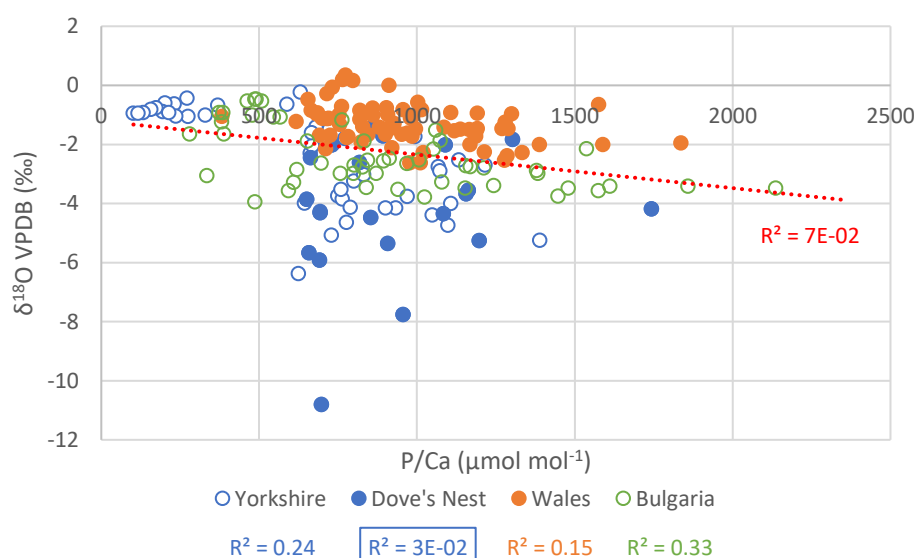


Figure 36 - Cross-plot of belemnite  $\delta^{18}\text{O}$  compared to the Vienna Pee Dee Belemnite (VPDB) against P/Ca values from the same belemnites. Samples are from three different locations (Yorkshire [dark blue], Wales [orange] and Bulgaria [green]). Core samples are shown with filled circles, outcrop samples with open circles. For Yorkshire samples, the Yorkshire dataset samples includes both coastal outcrops and core samples, Dove's Nest is a subset of these samples and is shown separately in addition to being included in the Yorkshire samples. For each sample set an  $R^2$  is calculated using a linear line of best fit (all of which had negative gradients, not shown) and  $R^2$  values are shown next to the key in the colour corresponding to the data points.

The correlation between  $\delta^{18}\text{O}$  and P/Ca was examined for each location studied (Figure 36). There was a negative correlation between  $\delta^{18}\text{O}$  and P/Ca for samples from Bulgaria, with an  $R^2$  value of 0.33 (Figure 36). In other sections, there was no relationship between  $\delta^{18}\text{O}$  and P/Ca with  $R^2$  values of 0.001, 0.029 and 0.043 for all samples from Yorkshire, samples from Dove's Nest and samples from North Wales respectively (Figure 36).

#### 4.4.5. CAP variation with magnesium

Correlation between Mg/Ca and P/Ca was investigated using the same methods as were used to investigate potential correlation between  $\delta^{18}\text{O}$  and P/Ca (Figure 35; Figure 37). Mg/Ca and P/Ca were obtained from analysis of the same samples by ICP-MS across all samples studied (Figure 37). This means that P/Ca and Mg/Ca can be investigated for all sections and locations studied (Figure 37). Also, as both Mg and P values were collected from the same analysis, both records have the same stratigraphic spread and the same resolution (Figure 37).

Similar to the relationship between  $\delta^{18}\text{O}$  and P/Ca, the stratigraphic records of P/Ca and Mg/Ca show strong covariation in all of the three locations studied, with excursions to high P/Ca values coinciding with excursions with high Mg/Ca values, and vice versa (Figure 37). In each of the locations studied there were major and minor perturbations which were visible in both the P/Ca and the Mg/Ca records (Figure 37). For example, in the samples from North Yorkshire there is a low point in P/Ca which coincides with low Mg/Ca values from the mid-*tenuicostatum* zone to the mid-*serpentinum* zone, followed by an increase in both P/Ca and Mg/Ca until the upper *serpentinum*/lower *bifrons* zone (Figure 37). In Yorkshire, both P/Ca and Mg/Ca values remain high at least until the mid-*bifrons* zone (Figure 37). In samples from North Wales, a similar increase in P/Ca ratios and Mg/Ca ratios is seen in the mid to late *serpentinum* zone, though sparse samples from just above this interval make it difficult to determine the duration of these elevated ratios (Figure 37). In Bulgaria, there is also a strong correlation between the Mg/Ca and P/Ca records through time. Values of both P/Ca and Mg/Ca are low in the lowermost part of the Bulgarian sections, corresponding to the *spinatum* zone in the Pliensbachian (Figure 37). After this, there is an increase in both Mg/Ca and P/Ca from the mid-*tenuicostatum* (or possibly earlier as there is a large sampling gap prior to the elevated values) (Figure 37). Both records are noisy, but it appears that elevated values of both Mg/Ca and P/Ca are sustained until at least the *fallaciosum* zone (Figure 37). After this point, Mg/Ca and P/Ca values are less variable and show lower values than the elevated portion of the record, but higher values than the base (Figure 37). In each section, aside from the broad trends, there appears to be covariation in Mg/Ca and P/Ca on a sample-by-sample basis, with even small trends in P/Ca matched by similar trends in Mg/Ca (Figure 37).

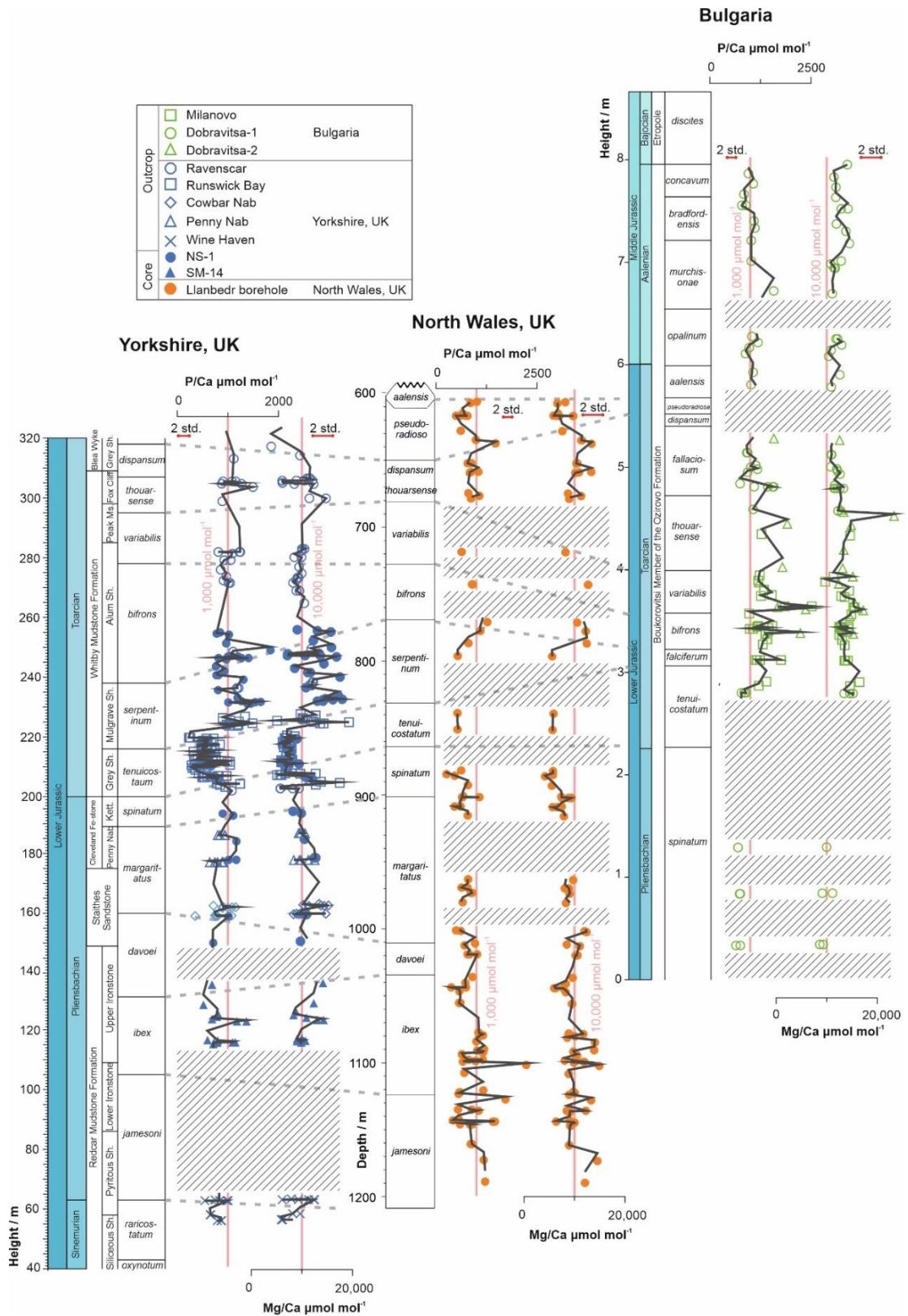


Figure 37 - P/Ca ratios alongside Mg/Ca values for screened samples from multiple sections across three locations (North Yorkshire, UK; North Wales, UK; Bulgaria). Mg/Ca and P/Ca values were collected from the same individuals. For each plot a 2-point moving average line (dark grey) is included to show the trends in P/Ca and Mg/Ca. For each record, values of P/Ca = 1,000  $\mu\text{mol mol}^{-1}$  and Mg/Ca = 10,000  $\mu\text{mol mol}^{-1}$  are indicated (pale red lines) to allow for easier determination of trends and comparison between each location. For each plot, a bar indicating two standard deviations (based on the variability within a stratigraphic level calculated from the analysis of 77 samples from 6 individual belemnites from the Penny Nab section taken from the 'Variability Samples' (2.3.2) is included to indicate the magnitude of

changes compared to the natural levels of variability at each stratigraphic level. Where abbreviations for lithological units are used due to limited space: Fe-stone = ironstone; Ms. = mudstone, Sh. = Shale; Ss. = sandstone. Hashed areas indicate either stratigraphic gaps in the sampling, or where samples were below the limit of detection.

By examination of the stratigraphic plots for each location, it appears that P/Ca records correlate more closely with the records for Mg/Ca than the records of  $\delta^{18}\text{O}$  (Figure 35; Figure 37). To further investigate the relationship between Mg/Ca and P/Ca, a cross-plot to examine the correlation between them was created to compare the values, using the same method as was used to compare  $\delta^{18}\text{O}$  and P/Ca (Figure 35; Figure 38). It would be useful to determine if the apparent stronger correlation between P/Ca and Mg/Ca, compared to P/Ca and  $\delta^{18}\text{O}$ , was related to the greater resolution in the Mg/Ca record compared to the  $\delta^{18}\text{O}$  record for most locations (Figure 35; Figure 37).

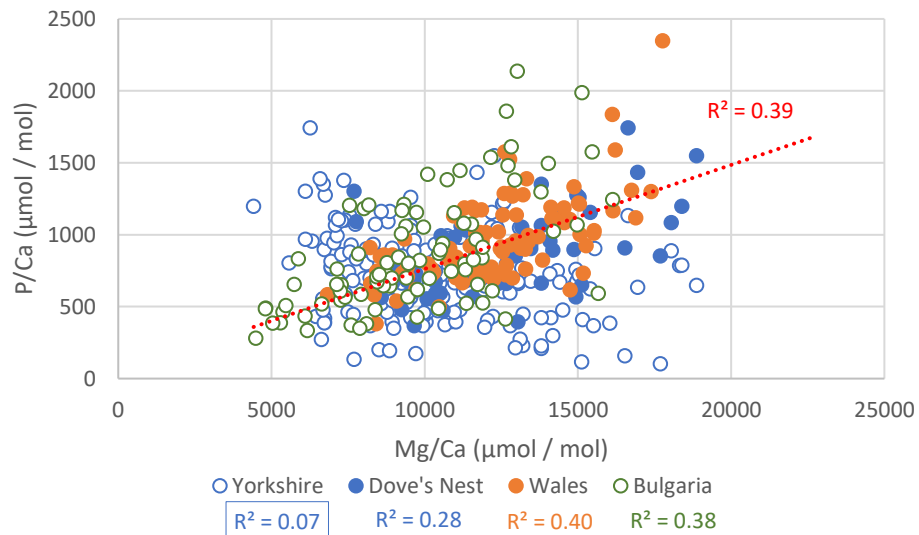


Figure 38 - Cross-plot of P/Ca values and Mg/Ca values for belemnite calcite. Samples are from three different locations (Yorkshire [dark blue], Wales [orange] and Bulgaria [green]). Core samples are shown with filled circles, outcrop samples with open circles. For Yorkshire samples, the Yorkshire dataset samples includes both coastal outcrops and core samples, Dove's Nest is a subset of these samples and is shown separately in addition to being included in the Yorkshire samples. For each sample set, an  $R^2$  is calculated using a linear line of best fit (not shown) and  $R^2$  values are shown next to the key in the colour corresponding to the data points; where lines of best fit had a negative gradient (Yorkshire) the  $R^2$  value is shown with a border. An overall linear line of best fit and corresponding  $R^2$  value are shown on the chart (red).

There was positive correlation between Mg/Ca and P/Ca in samples from Wales ( $R^2 = 0.40$ ) and Bulgaria ( $R^2 = 0.38$ ) (Figure 38). In samples from Yorkshire there was a positive correlation between Mg/Ca and P/Ca in samples from the Dove's Nest cores ( $R^2 = 0.28$ ), but not when all the samples from Yorkshire were taken together ( $R^2 = 0.06$  and negative slope). The correlation between Mg/Ca and P/Ca was stronger than the correlation between P/Ca and  $\delta^{18}\text{O}$  that was seen for the Bulgarian samples, and there was correlation between Mg/Ca and

P/Ca in samples from Wales and Doves Nest which was not seen between P/Ca and  $\delta^{18}\text{O}$  for the same samples (Figure 35; Figure 38)

#### 4.4.5.1. Factors affecting the incorporation of magnesium

To investigate the correlation between Mg/Ca and P/Ca, factors affecting the incorporation of Mg/Ca were investigated (Figure 39). To investigate the relationship between Mg and temperature, correlation between Mg/Ca and  $\delta^{18}\text{O}$  was investigated using a cross-plot (Figure 35; Figure 39).

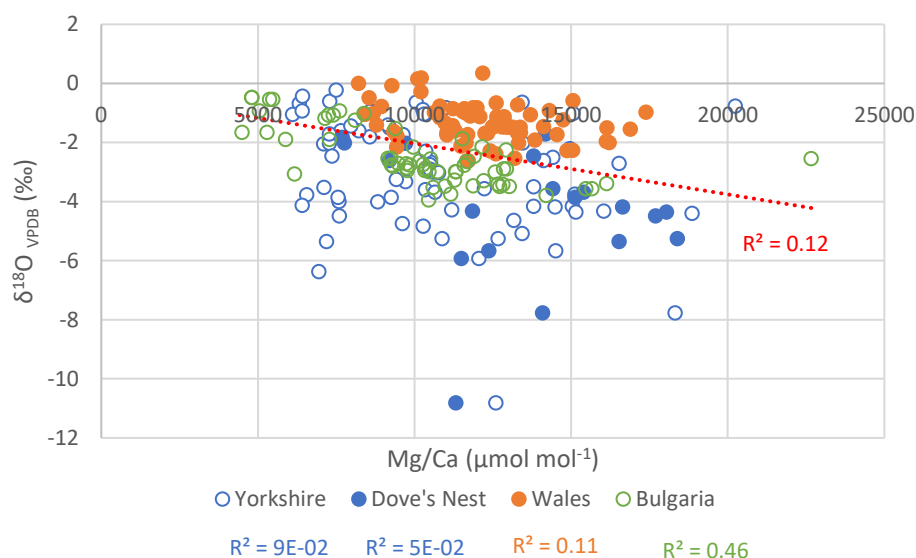


Figure 39 - Cross-plot of belemnite  $\delta^{18}\text{O}$  compared to the Vienna Pee Dee Belemnite (VPDB) against Mg/Ca values from the same belemnites. Samples are from three different locations (Yorkshire [dark blue], Wales [orange] and Bulgaria [green]). Core samples are shown with filled circles, outcrop samples with open circles. For Yorkshire samples, the Yorkshire dataset samples includes both coastal outcrops and core samples, Dove's Nest is a subset of these samples and is shown separately in addition to being included in the Yorkshire samples. For each sample set an  $R^2$  is calculated using a linear line of best fit (all of which had negative gradients, not shown) and  $R^2$  values are shown next to the key in the colour corresponding to the data points. An overall linear line of best fit and corresponding  $R^2$  value are shown on the chart (red).

Mg/Ca and  $\delta^{18}\text{O}$  were negatively correlated for samples from the Bulgarian sections ( $R^2 = 0.46$ ) (Figure 39). There was no significant correlation between Mg/Ca and  $\delta^{18}\text{O}$  in samples from Wales ( $R^2 = 0.01$ ), Dove's Nest cores ( $R^2 = 0.05$ ) or Yorkshire as a whole ( $R^2 = 0.02$ ; positive slope) (Figure 39). Overall, the relationship between Mg/Ca and  $\delta^{18}\text{O}$  showed similar trends to the relationship between  $\delta^{18}\text{O}$  and P/Ca (Figure 35; Figure 39). This is unsurprising based on the strong correlations between P/Ca and Mg/Ca (Figure 37; Figure 38).

As well as investigating the relationship between temperature and Mg/Ca, the relationship between Mg/Ca and carbonate mineralogical properties were also investigated. Magnesium was shown to be the dominant substituted ion in belemnite carbonate, accounting for an average of about 2 % of the measured  $2^+$  ions (Ca, Mg, Sr, Mn, Ba) present in the carbonate

across all of the samples analysed in this study – more than twice as much as the average Mn, Ba and Sr concentrations combined (Figure 40). Out of all the substituted ions measured (all ions measured excluding Ca), Mg accounted for 38 % – the largest amount of any substituted ion (Figure 41).

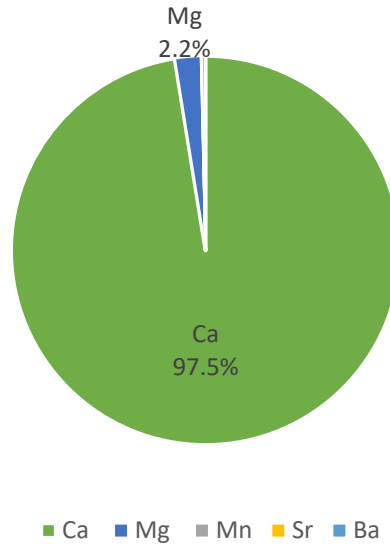


Figure 40 - Pie chart showing the relative proportions of measured  $2^+$  ions (Ca, Mg, Mn, Sr, Ba) in moles across all screened samples used for the building of stratigraphic records across all sections and locations (North Yorkshire, North Wales, and Bulgaria).

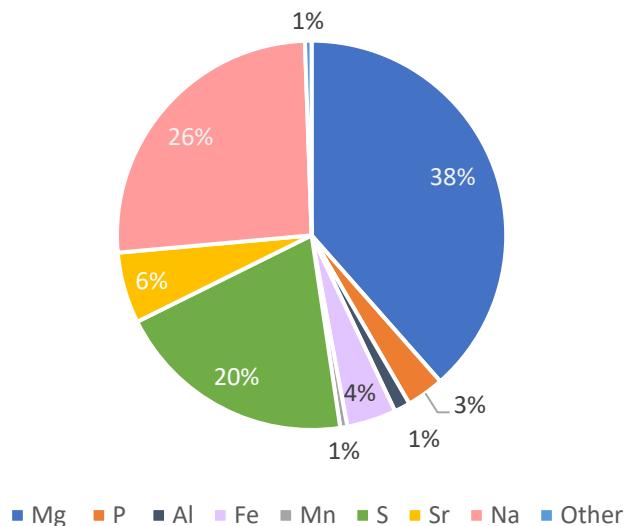


Figure 41 - Pie chart showing the relative proportions of substituted ions (all measured ions except Ca) in moles across all screened samples used for the building of stratigraphic records across all sections and locations (North Yorkshire, North Wales, and Bulgaria). The category 'other' is the sum of averaged measured values of K, Li, B, Ba, U, and I.

As Mg is the dominant substituted ion, it is reasonable to expect that incorporation of Mg may alter the structure of the calcite mineral. Other components, including those not covered by this study, such as anions and organic matter may also affect the crystal morphology – but Mg

is focused on here due to being such a major component of belemnite calcite and the observed relationship between Mg and P. To investigate the impact of magnesium incorporation on the lattice cell parameters ( $a$ ,  $c$ , and unit volume [Figure 42]), XRD analysis was performed on a subset of samples from North Wales which represented a range of Mg/Ca values (Figure 43; Figure 44; Figure 45).

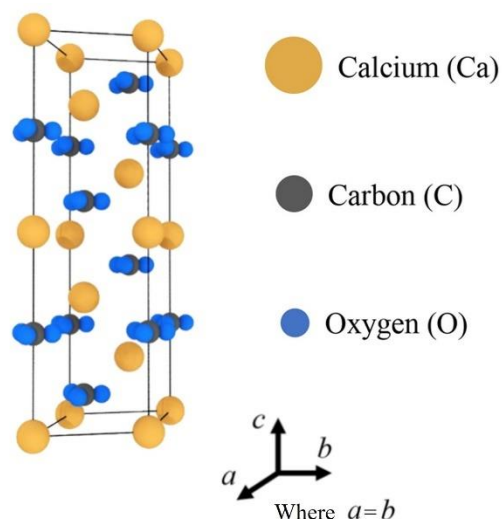


Figure 42 – Diagram of a pure calcite unit cell with the directions of each unit parameter indicated, adapted from Sáenz-Ezquerro et al. (2022).

Cross-plotting unit cell parameters and Mg/Ca ratios was used to investigate the relationship between Mg/Ca and each unit cell parameter ( $a$ ,  $c$  and unit cell volume) (Figure 43; Figure 44; Figure 45). There was a strong, negative correlation between Mg/Ca and lattice parameter  $a$  ( $R^2 = 0.62$ ); there was also a good correlation between unit cell parameter  $c$  and Mg/Ca ( $R^2 = 0.37$ ); there was a strong correlation between unit cell volume and Mg/Ca values ( $R^2 = 0.53$ ) (Figure 43; Figure 44; Figure 45). This demonstrates that higher proportions of magnesium in belemnite calcite correlates with smaller unit cell parameters and lower unit cell volumes (Figure 43; Figure 44; Figure 45).

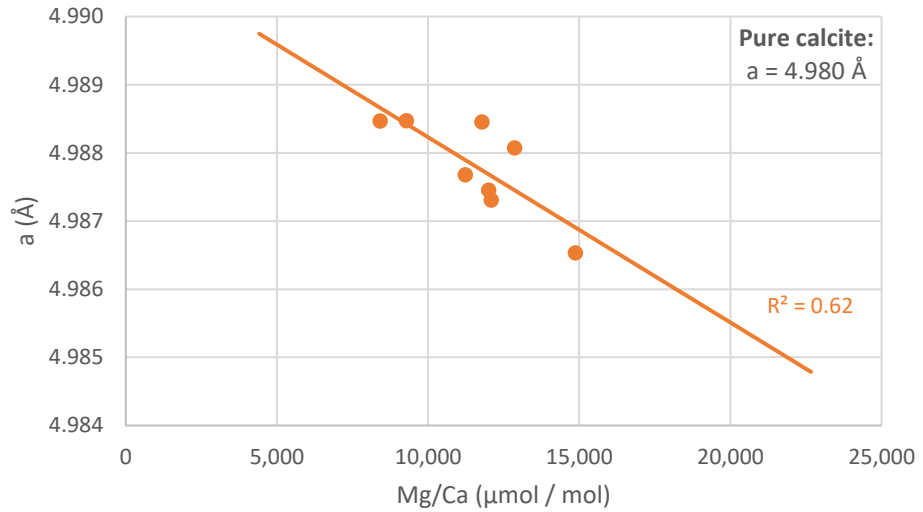


Figure 43 - Cross-plot of belemnite Mg/Ca values and unit cell parameter  $a$  in angstroms from XRD analysis of the same samples. Samples are a subset of the belemnite carbonate samples from North Wales. A linear line of best fit is shown along with the corresponding  $R^2$  value (orange).

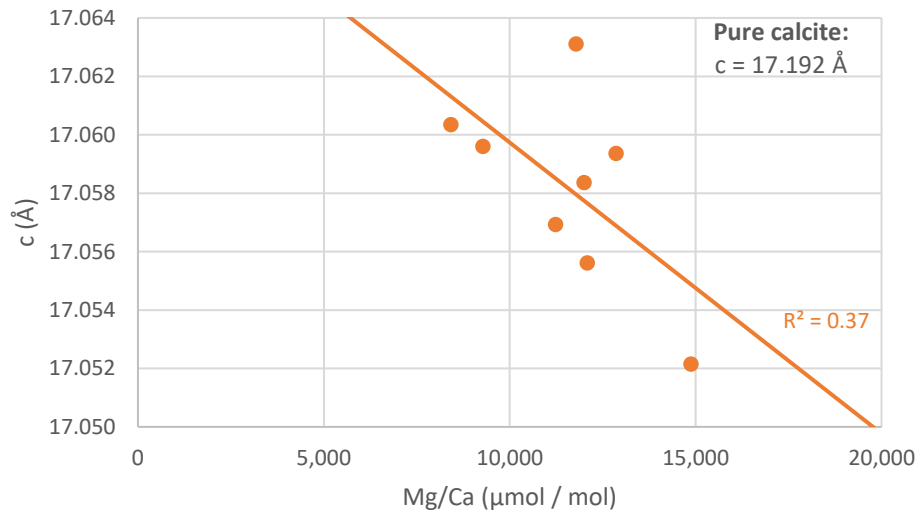


Figure 44 - Cross-plot of belemnite Mg/Ca values and unit cell parameter  $c$  in angstroms from XRD analysis of the same samples. Samples are a subset of the belemnite carbonate samples from North Wales. A linear line of best fit is shown along with the corresponding  $R^2$  value (orange).

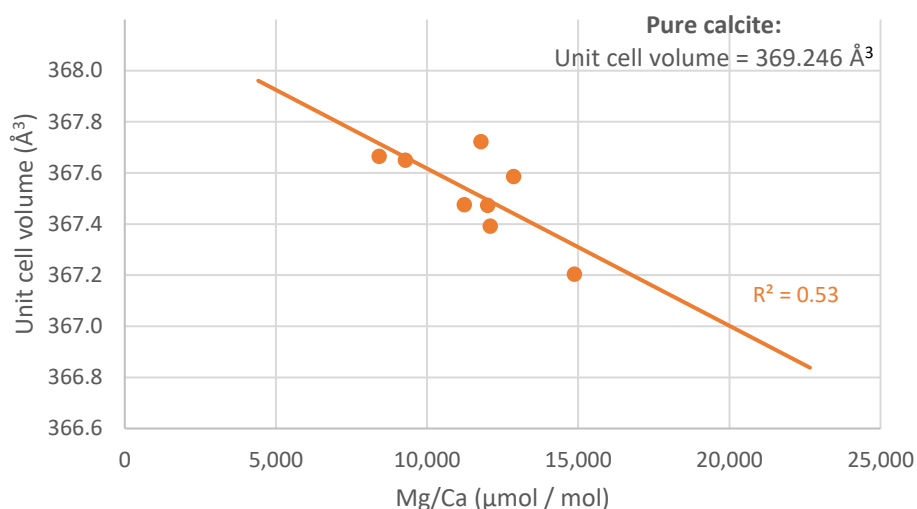


Figure 45 – Cross-plot of belemnite Mg/Ca values and unit cell volume in cubic angstroms from XRD analysis of the same samples. Samples are a subset of the belemnite carbonate samples from North Wales. A linear line of best fit is shown along with the corresponding R<sup>2</sup> value (orange).

The measured unit cell parameters and unit cell volume were also compared to literature values of pure calcite unit cells (Redfern and Angel, 1999). A percentage difference between literature and averaged measured values for unit cell parameters a and c and unit cell volume was calculated using Equation 3.

$$\% \text{ Difference} = 100 \times \frac{\text{Pure calcite} - \text{Average measured value}}{\text{Literature value}} \quad \text{Equation 3}$$

Table 22 - Average, maximum and minimum and the standard deviation of measured values of unit cell parameters a and c and unit cell volume. Also included are values for a, c and unit cell volume for pure calcite and the calculated percentage difference between the average measured value and the literature values (Redfern and Angel, 1999).

Quantity	a (Å)	c (Å)	Unit cell volume (Å <sup>3</sup> )
<b>Average</b>	4.988	17.058	367.521
<b>Standard deviation</b>	0.001	0.003	0.171
<b>Maximum value</b>	4.988	17.063	367.723
<b>Minimum value</b>	4.987	17.052	367.204
<b>Pure calcite</b>	4.980	17.192	369.246
<b>% Difference</b>	-0.157	0.778	0.467

It was shown that in the measured samples, unit cell parameter a was larger than the reported value for pure calcite (Table 22). Unit cell parameter c and the unit cell volume were smaller than the reported value for pure calcite (Table 22). This shows that the unit cell is distorted by the addition of magnesium and is overall smaller in belemnite calcite than in pure calcite for all the samples measured (Table 22).

## 4.5. Discussion

### 4.5.1. Impact of diagenesis

After screening criteria were applied, there were still good correlations between Fe/Ca and Mn/Ca in most sites studied, however in almost all sites the correlation was lower in the screened samples than in the unscreened samples (Table 21). For  $R^2$  values for correlation between P/Ca and either Fe/Ca or Mn/Ca also decreased in most of the studied sites, and in screened samples there was no significant or very low correlation between P/Ca and either Fe/Ca or Mn/Ca in almost all sites studied. In Penny Nab, there was still a correlation with an  $R^2$  value of 0.49 between P/Ca and Mn/Ca – but no significant correlation between P/Ca and Fe/Ca (Table 21).

Overall, this suggests that the screening criteria does not eliminate the impact of diagenetic alteration or contamination (hence the correlation between Mn/Ca and Fe/Ca). It appears that in the screened samples the levels of diagenetic alteration and contamination present are sufficiently low that they are not affecting the P/Ca ratios, so it may be assumed that variations in the P/Ca ratios in the screened samples are not a result of differences in diagenetic alteration or contamination. This method assumes that diagenetic alteration is the only (or primary) source of iron and manganese in belemnite calcite, and other factors may affect the incorporation of Fe or Mn into primary calcite and the correlations between them and other El/Ca ratios.

### 4.5.2. CAP records

P/Ca records were generated for three different locations in the Laurasian Seaway – North Yorkshire, and North Wales in the UK and Bulgaria (Figure 29). The P/Ca records showed coherent stratigraphic change, with shifts in P/Ca values larger than could be accounted for by the natural variability in P/Ca records examined previously (Figure 29). There were coincident excursions in the P/Ca records from multiple locations, with records from Yorkshire demonstrating a decrease in P/Ca values in the early Toarcian coincided with the well-studied negative carbon isotope excursion and ocean anoxic event (Figure 29). All of this suggests that P/Ca in belemnite calcite is potentially recording some kind of environmental change, such as water column phosphorus concentration, or other environmental factor, rather than varying randomly or according to natural levels of variation between and within individuals (Figure 29). To investigate the potential of P/Ca to act as a proxy for environmental changes, the P/Ca record was compared to existing palaeoenvironmental proxies in order to establish the factors around the incorporation of phosphorus into belemnite calcite (4.5.3; 4.5.4; 4.5.5).

### 4.5.3. Redox

Redox was investigated as water column phosphorus may be expected to vary with redox, therefore if P/Ca in carbonates records water column phosphorus then P/Ca in belemnites may be expected to vary with redox.

In the data from the Dove's Nest core, there were co-enrichments in trace element (Mo/Al; U/Al; Mo/U;  $Fe_{TOT}/Al$ ) and iron speciation ratios ( $Fe_{HR}/Fe_{TOT}$ ;  $Fe_{PY}/Fe_{HR}$ ) in the upper half of the core (120-160 m), in contrast to the lower half (170-240 m) (Figure 30). Co-enrichment of trace element and iron speciation proxies were investigated, as co-enrichments with multiple sedimentological proxies indicating changes in redox conditions would provide strong evidence of changes in ocean oxygenation. When cross-plotted, it was shown that there were co-enrichments in  $Fe_{HR}/Fe_{TOT}$  and U/Al, both proxies which indicate dysoxic-anoxic conditions in samples from the upper part of the core, indicating this interval likely represents reduced oxygen conditions (Figure 31). It was also shown that there were co-enrichments between  $Fe_{PY}/Fe_{HR}$  and Mo/Al, both of which are proxies which can indicate euxinic conditions – demonstrating the interval in the upper core was likely represented by dominantly euxinic conditions (Figure 32). Mo records for samples from the Cleveland basin can be considered to be complicated by debates around the degree of restriction the basin experienced during the Early Jurassic, potentially making  $Fe_{PY}/Fe_{HR}$  the best proxy for euxinia for this section (e.g., McArthur *et al.*, 2008). Despite this, there is good agreement in the Mo records for the samples from the Dove's Nest core and the samples described in McArthur *et al.* (2008), which suggested water mass restriction during the jet rock, followed by an interval of greater circulation above this point, albeit still with euxinic conditions (Figure 30). Sediment samples were only taken directly adjacent to belemnites, indicating that the water-column was not strongly euxinic/anoxic throughout, as belemnites (alongside the other nektonic fauna present in the Cleveland Basin in this interval such as ammonoids and marine reptiles) require oxic conditions (e.g., O'Dor and Webber, 1986; Seibel *et al.*, 1997; Jereb and Roper, 2005; Neil and Askew, 2018; Hoffmann and Stevens, 2020). This suggests that the euxinic conditions were transient, or the water column was stratified to provide a 'refuge depth' with oxic conditions for fauna to reside in (e.g., Rexfort and Mutterlose, 2009; Malkoč *et al.*, 2010).

Alongside the changes in redox proxies, there were changes in the P/Ca records which, for some intervals, corresponded changes in the redox state (Figure 30). The upper section of the core had higher P/Ca values, which corresponded with the interval which was likely euxinic (Figure 30). When P/Ca values were cross-plotted against the iron-speciation ratios, the samples with the highest P/Ca values corresponded to  $Fe_{HR}/Fe_{TOT} > 0.38$  and  $Fe_{PY}/Fe_{HR} > 0.8$  values, indicating the highest P/Ca values likely corresponded to a euxinic interval (Figure 33;

Figure 34). In euxinic environments, anaerobic bacterial communities preferentially mine organic matter for nutrients such as phosphorus and releasing them from the sediment. If P/Ca in belemnites reflects water-column phosphorus, this implies that the interval of euxinia in Dove's Nest corresponded with increased water-column phosphorus concentrations (Figure 30). This is consistent with recycling of phosphorus via the preferential release of organic phosphorus by bacteria mining organic matter (e.g., Sinkko *et al.*, 2013). Recycling of phosphorus from the sediment occurs in several different conditions but required sulfidic pore-waters to prevent re-absorption of phosphorus to iron-containing minerals (e.g., Allcott *et al.*, 2022). A portion of the released phosphorus may be retained in the sediment through 'sink switching' to authigenic phases such as carbonate fluorapatite or vivianite, though a significant proportion is likely to be released to the water-column in euxinic/sulfidic conditions (e.g., Ruttenger and Berner, 1993; Dijkstra *et al.*, 2014; Xiong *et al.*, 2019; Alcott *et al.*, 2022). Euxinic environments also reduce the flux of phosphate to the sediment, by removing reactive iron from the water-column as iron sulfide, preventing the loss of phosphorus bound to iron (oxy)hydroxides, which sink to the sediment interface (e.g., Ruttenger and Berner, 1993).

Overall, the redox conditions in the Cleveland Basin during the upper Toarcian (represented by 125-160 m depth in the Dove's Nest core) is likely representative of euxinic conditions. This may have contributed to higher concentrations of bio-available phosphorus in the water column, potentially even increasing water column P in oxic zones (which could support fauna) above the euxinic/sulfidic bottom waters (Ruttenger and Berner, 1993; Dijkstra *et al.*, 2014; Xiong *et al.*, 2019; Alcott *et al.*, 2022). The higher P/Ca ratios in belemnites during this interval may reflect belemnites recording the elevated concentrations of phosphorus in the water they lived in. Alternatively, it may be that the apparent covariance of P/Ca and redox proxies is an artefact of covariance between P/Ca and another environmental factor, such as temperature or weathering, which also impacts redox – or a combination of multiple factors. A combination of factors is considered the most likely explanation, based on the clear variability of P/Ca values in the Dove's Nest samples, but also the similarities between the P/Ca records for different locations with different redox states. The P/Ca records for North Wales and Yorkshire are very similar, but the redox record for North Wales indicates less sustained and widespread anoxic conditions compared to the conditions in Yorkshire (Figure 22). This suggests that the reasons behind the changes in P/Ca are more complicated, potentially as the dominant control on water-column phosphorus differs by location and time interval.

#### 4.5.4. Temperature

Change in P/Ca with palaeotemperature was investigated as water column phosphorus may be expected to vary with temperature (e.g., McArthur *et al.*, 2000). Generally, warmer

temperatures can lead to an increasingly active hydrological cycle which increases weathering, bringing more phosphate into the ocean. These are factors which may impact ocean redox conditions or affect water column phosphorus concentrations in their own right. As with P/Ca, the variability of  $\delta^{18}\text{O}$  through time was greater than the variability within a stratigraphic level (determined from 16 samples from 6 belemnites of four different species taken from Penny Nab; 2.3.2) (Figure 35). This suggested that the natural variability of  $\delta^{18}\text{O}$  within and between individuals was small enough when compared to the changes in  $\delta^{18}\text{O}$  through time to enable perturbations in the record to be examined and compared to the P/Ca record (Figure 35). This is supported by the broad correlation of  $\delta^{18}\text{O}$  records from belemnites and other calcifying organisms, which are considered to give more reliable isotope values (e.g., Korte *et al.*, 2015).

To investigate the link between palaeotemperature and CAP in our data we compared the P/Ca records for each location with oxygen isotope records, where the oxygen isotope and El/Ca measurements were taken from the same samples (Figure 35). It was shown in this study that, while there appeared to be stratigraphic covariation between  $\delta^{18}\text{O}$  and P/Ca, there was no significant correlation between them in samples from Yorkshire or North Wales, though there was correlation in samples from Bulgaria. The stratigraphic profiles of P/Ca and  $\delta^{18}\text{O}$  in each of the locations studied had broad visual similarities, with excursions to higher P/Ca values coincident with excursions to lower  $\delta^{18}\text{O}$  values and vice versa (Figure 35). For example, the low point in P/Ca values in the Yorkshire record from the mid-*tenuicostatum* to mid-*serpentinum* zones in the Early Toarcian coincides with elevated  $\delta^{18}\text{O}$  values (Figure 35). After the low P/Ca values, when P/Ca values rise in the mid-*serpentinum* until the late-*serpentinum*/mid-*bifrons* zone there is a coincident decrease in  $\delta^{18}\text{O}$  values (Figure 35). Similar coincident excursions are observed in the P/Ca and  $\delta^{18}\text{O}$  records for North Wales and Bulgaria – suggesting a negative correlation between  $\delta^{18}\text{O}$  and P/Ca values (Figure 35). There are some points in the P/Ca records where the opposite trend is observed, for example in the record from North Wales at 890 m depth in the *spinatum* zone, a negative excursion of P/Ca to  $382 \mu\text{mol mol}^{-1}$  corresponded to a negative excursion in  $\delta^{18}\text{O}$  to  $-1.05 \text{‰}$ , suggesting a positive correlation between P/Ca and  $\delta^{18}\text{O}$  (Figure 35). The relationship was investigated for each location using a cross plot (Figure 36). This demonstrated that there was a negative correlation between P/Ca and  $\delta^{18}\text{O}$  in samples from Bulgaria ( $R^2 = 0.33$ ) (Figure 36). No significant correlation between  $\delta^{18}\text{O}$  and P/Ca was observed in Yorkshire or Wales ( $R^2 = 0.001$  and  $0.03$  respectively) (Figure 36). This suggests that while there is apparent negative correlation between P/Ca and  $\delta^{18}\text{O}$  in the stratigraphic record, there is not a strong relationship between them when the values are compared (Figure 35; Figure 36). This indicates that temperature is not a strong control on P/Ca values during this time period. The only exception to this is in the

samples from Bulgaria – though it's possible that this was related to Mg concentrations affecting phosphorus concentration (see 4.5.5).

One explanation for the correlation between P/Ca and  $\delta^{18}\text{O}$  being limited, is that temperature was not a dominant control on water-column phosphorus during this time period. In samples from Dove's Nest, it was demonstrated that P/Ca values vary with redox (Figure 30). Where there are multiple environmental factors affecting water column P/Ca concentrations (redox, temperature changes, salinity changes, weathering, restriction), it is reasonable to expect that, even if P/Ca in belemnites faithfully records water column phosphorus, belemnite CAP would not vary with any single environmental factor. This is particularly the case for samples from the Cleveland and Cardigan Bay basins, which had more variable redox than the Moesian basin, which was closer to the open ocean (Figure 21; Figure 22, Figure 24, Figure 27). Additionally, it's suggested that there were variable levels of restriction in the Cardigan Bay and Cleveland Basins throughout the Early Jurassic, restricting the exchange of nutrients with the open ocean (Sælen *et al.*, 1996; 2000; van de Schootbrugge *et al.*, 2005; McArthur *et al.*, 2008). There are also thought to have been changes in salinity and sea-level – which also would have impacted the more restricted basins more than the Moesian Basin proximal to the open Tethys. This may explain why it is that P/Ca in Bulgarian samples varies with  $\delta^{18}\text{O}$ , as temperature was a dominant control on water-column phosphorus in the Moesian Basin, while in the other basins studied, more complex and variable ocean chemistry meant that multiple factors-controlled water-column phosphorus.

Alternatively, it is possible that the disparity between Bulgaria and the other sites studied is due to temperature being the dominant control on the incorporation of magnesium in samples Bulgaria. In other locations, the incorporation of magnesium may have been affected by the other environmental factors which contribute to the more complex ocean chemistry of the other basins. Magnesium may then directly affect the incorporation of phosphorus into the calcite – this is considered the most likely explanation and is discussed further in 4.5.5.

Alternatively, it is possible that temperature is a dominant control on carbonate associated phosphorus in all locations studied, but that oxygen isotopes are not a faithful measure of temperature in all the locations studied. Oxygen isotopes are a well-established method of investigating variations in palaeotemperature, which has been applied to biogenic and abiogenic carbonates and phosphates for samples from time periods throughout Earth's history. Interpretation of oxygen isotope records is complicated by a range of other factors which have also been shown to impact oxygen isotopes in carbonates, such as the sample preservation state, salinity, sea-level, bathymetry and water circulation changes (Wierzbowski, 2021 and references therein). Several studies have suggested that during the time interval

studied, alongside changes in temperature there were changes in sea-level (e.g., Graciansky *et al.*, 1993; Hallam, 1997; Hesselbo and Jenkyns, 1999; Krencker *et al.*, 2019), changes in the circulation of water to the restricted basins in the Lurasian Seaway (e.g., Sælen *et al.*, 1996; 2000; Schwark and Frimmel, 2004; Frimmel *et al.*, 2004; van de Schootbrugge *et al.*, 2005; McArthur *et al.*, 2008), and even potential changes in salinity (e.g., Prauss *et al.*, 1991; Sælen *et al.*, 1996; Bailey *et al.*, 2003; McArthur *et al.*, 2008; Remírez and Algeo, 2020). Consequently, it is possible that changes in oxygen isotope values during the Early Jurassic are not representative of only changes in temperature – particularly for samples from the restricted basins of the Lurasian Seaway. This would potentially explain the observation that P/Ca does not vary with oxygen isotopes in the basins which are thought to have more complicated and variable ocean chemistry (Mochras and Yorkshire, which both experienced periods of anoxia (though to different extents) as well as restriction, salinity, and sea level changes). This is considered less likely, based on the observations of Mg/Ca and P/Ca – discussed further in 4.5.5.

In biogenic carbonates, further factors can affect oxygen isotope ratios, including vital effects which may be species specific, as well as different habitats occupied by different species or even individuals, including different depths, or even changes in habitats during different life stages or during migrations (e.g., McArthur *et al.*, 2002; Li *et al.*, 2012; Hoffmann *et al.*, 2016; Stevens *et al.*, 2017; Hoffmann and Stevens, 2020 and references therein). Species specific differences in oxygen isotope measurements from belemnites have been reported, possibly related to differences in species habitats or to species-specific vital effects (e.g., McArthur *et al.*, 2002; 2007; Li *et al.*, 2012; Stevens *et al.*, 2017) In belemnites, this is further complicated by the possibility that the rostra were originally porous, with one phase of calcite representing the calcite grown during the belemnite's life in the surface waters of the ocean, and the other phase representing calcite formed during early diagenesis on the ocean-floor or in the upper sediment after the belemnite's death (Hoffmann *et al.*, 2016; 2021). As the two phases would have formed at different depths representing different temperatures, and potentially giving different oxygen isotope values (Hoffmann *et al.*, 2016; 2021). Despite the issues with oxygen isotopes in belemnites as a temperature proxy, they are the best available record of palaeotemperature for comparison with the P/Ca record generated, though it is important to keep in mind the other factors which may impact oxygen isotopes for this time period. In samples from this study, we can see that correlation between P/Ca and  $\delta^{18}\text{O}$  is site specific, suggesting vital effects and species differences do not have a significant impact, as the largest differences seem to be between locations and are likely related to different palaeoenvironments.

#### 4.5.4.1. Potential concatenated temperature and ocean pH impact

Dodd *et al.* (2021) suggested that changes in both temperature and pH may alter CAP values, based on the response of CAP in synthetic carbonates. The temperature and pH changes investigated in Dodd *et al.* (2021) to induce changes in CAP values are large compared to the changes which would normally be expected in a natural system. For example, CAP increased less than two-fold over a temperature change of 20 °C and increased around five-fold with a pH decrease of 2; both of which would be very large environmental changes in a natural ocean system (Dodd *et al.*, 2021). Nevertheless, as the Early Toarcian is a time period encompassing both a warming climate and ocean acidification, it is possible that the observed changes in CAP may be attributable to the concatenated effects of pH and temperature change. Dodd *et al.* (2021) suggested linear relationships between CAP and both temperature and pH, so these results can be used to estimate theoretical changes in CAP with combined temperature and pH shifts.

Gomez *et al.* (2016) used oxygen isotopes to suggest a temperature increase of around 10 °C from the late Pliensbachian to the Early Toarcian (Figure 20). Müller *et al.* (2020) used boron isotopes to suggest a change in ocean pH from around 7.7 in the late Pliensbachian to around 7.2 at the peak of the ETNCIE. Based on the relationships determined by Dodd *et al.*, 2021, a change of 10 °C would correspond to an increase in CAP of around 20 %, and a decrease in pH of 0.5 would correspond to an increase in CAP of 37 %. This relates to a 64% increase if the two effects are combined, though this does not consider the relationship between ocean pH and temperature. For each study location, the measured high P/Ca values recorded in the Early Toarcian were compared to predicted high P/Ca values based on the average Late Pliensbachian P/Ca, and the predicted change with the changing temperature and pH determined using the data from Dodd *et al.* (2021) (Table 23).

*Table 23 - Comparison between high measured P/Ca values in the Early Toarcian and predicted high values of P/Ca based on the relationships between CAP and temperature/pH established in Dodd et al. (2021). Predicted values are calculated using a percentage change calculated using the linear relationships established by Dodd et al. (2021) and initial P/Ca values for each location from the approximate P/Ca value in the Late Pliensbachian.*

Location	Measured Late Pliensbachian P/Ca ( $\mu\text{mol mol}^{-1}$ )	Predicted Early Toarcian P/Ca $\mu\text{mol mol}^{-1}$			High Early Toarcian high P/Ca values ( $\mu\text{mol mol}^{-1}$ )
		Temperature ( $\Delta T = 10\text{ }^{\circ}\text{C}$ )	pH ( $\Delta\text{pH} = 0.5$ )	Temperature and pH change	
Yorkshire	800	960	1,100	1,320	1,200-1,800
North Wales	800	960	1,100	1,320	1,600

<b>Bulgaria</b>	500	600	690	820	1,300
-----------------	-----	-----	-----	-----	-------

It was shown that based on the relationships established in Dodd *et al.* (2021), the combined impact of changing temperature and pH could account for a significant portion of the measured change in P/Ca between the Late Pliensbachian and the Early Toarcian in each location, though the change in CAP was not fully accounted for at any location (Table 23).

This rough calculation is used to illustrate the potential impacts of pH and temperature on CAP; however, it is based on a number of assumptions which mean it is unlikely to reflect the true impact of changing temperature and pH changes during this time period. For example, this calculation treats pH and temperature as separate conditions, and does not account for the interconnected relationship between temperature and pH, where increasing temperature would have led to increased ocean acidification, due to increased dissolution of CO<sub>2</sub> (Figure 29). This calculation is also based on results from Dodd *et al.* (2021) which were conducted on synthetic carbonates precipitated from solutions with set solution phosphate concentration. Across the Pliensbachian-Toarcian boundary, disruption to the nutrient cycling caused by changing environmental conditions, mean it is unlikely that ocean phosphorus concentrations would have remained unchanged during this period. The relationships determined by Dodd *et al.* (2021) were also determined using aragonite, whereas belemnite rostra are comprised on calcite, and it is likely that there would be mineralogical differences in the response of CAP to changes in pH and temperature. The calculations conducted here also do not account for regional differences in pH and temperature change between the locations studied, despite each location likely representing different ocean environments.

There are also features of the CAP record which are not accounted for based on the changes in pH and temperature during this time period, such as the decrease in CAP values in Yorkshire during the *tenuicostatum* zone, prior to the increase in the *seppentinum* zone (Figure 29). Temperature and pH changes also do not explain the different timings of the increases in P/Ca for each location, though this could be due to regional responses to changing climate and ocean chemistry (Figure 29). It also does not explain the lack of correlation between P/Ca and  $\delta^{18}\text{O}$ . If CAP varied with temperature and pH, it would be expected that some correlation between P/Ca and  $\delta^{18}\text{O}$  would be present in each study location – which is not the case in the data from this study.

Overall, it is possible that temperature and pH changes do contribute to the measured change in CAP between the Late Pliensbachian and the Early Toarcian, but further work is required to fully investigate this. This may include investigating the impact of temperature and pH on CAP

in synthetic calcites, and at variable phosphorus concentrations, as well as the impact of altering multiple conditions (pH, temperature, solution phosphate concentrations) simultaneously. It would also require investigation to account for the timings of the CAP excursions comparative to the changes in temperature and pH, and to account for the decrease in CAP observed in the *tenuicostatum* zone in Yorkshire. This would be helped by developing regional records of ocean acidification and climate, for each of the locations included in this study.

#### 4.5.5. Magnesium

To further investigate the potential relationship between P/Ca and temperature, correlation between P/Ca and Mg/Ca was investigated. Mg/Ca is known to vary with temperature in biogenic carbonates and some studies have shown this trend in belemnite calcite as well (McArthur *et al.*, 2000; Bailey *et al.*, 2003; Rosales *et al.*, 2004; McArthur *et al.*, 2007a; b; Armendáriz *et al.*, 2008). Other studies have demonstrated that Mg/Ca in belemnites does not correlate with  $\delta^{18}\text{O}$  and so is unlikely to be a record of temperature (Wierzbowski and Rogov, 2011; Li *et al.*, 2013; Stevens *et al.*, 2014).

Other factors such as salinity, mineralogy and biological factors that are specific to species or even different between sexes have been posited as controls on Mg/Ca incorporation into belemnites (e.g., McArthur *et al.*, 2007a). As with P/Ca, the variability of Mg/Ca through time was greater than the variability within a stratigraphic level. This suggests that the natural variability of Mg/Ca within and between individuals was small enough, when compared to the changes in Mg/Ca through time, to enable perturbations in the record to be examined and compared to the P/Ca record.

P/Ca and Mg/Ca showed generally strong stratigraphic correlation, which was also reflected in the correlation between Mg/Ca and P/Ca. A positive correlation between Mg/Ca and P/Ca was observed in samples from Bulgaria ( $R^2 = 0.38$ ), Wales ( $R^2 = 0.40$ ), and in samples from the Dove's Nest cores in Yorkshire ( $R^2 = 0.28$ ), though not in samples from the Yorkshire coast as a whole ( $R^2 = 0.07$ ) (Figure 39). The correlation observed between P/Ca with Mg/Ca is greater than the correlation of P/Ca with  $\delta^{18}\text{O}$  in Bulgaria, and Mg/Ca and P/Ca correlate in multiple locations where P/Ca does not correlate with  $\delta^{18}\text{O}$  (Figure 35; Figure 38). Rather than being related to environmental factors, this may be related to Mg exerting a mineralogical control on the incorporation of phosphate into the calcite.

Magnesium is the most abundant substituted ion in belemnite calcite, accounting for 38.5 % of the ions measured in this study when Ca was excluded – more than any other element (Figure 41).  $\text{Mg}^{2+}$  also accounts for 2.2 % of all the 2+ ions measured ( $\text{Ca}^{2+}$ ,  $\text{Mg}^{2+}$ ,  $\text{Mn}^{2+}$ ,  $\text{Ba}^{2+}$ ,  $\text{Sr}^{2+}$ ),

more than twice the amount accounted for by Mn, Ba and Sr combined (Figure 40). As previously discussed in section 3.3.5.2, concentrations of Mg can vary greatly across carbonate skeletons, suggesting biological control on Mg incorporation (e.g., Wang *et al.*, 1997; McArthur *et al.*, 2007a; Ullmann *et al.*, 2017). In lab-based studies of synthetically grown carbonates, magnesium is a control on the formation, growth, and structure of carbonate minerals. For example, in saturated solutions with ratios of Mg:Ca or 2:1, Mg is incorporated into the Ca lattice position in low concentrations (1-3 mol %) (Albeck *et al.*, 1993). This alters the unit cell structure due to  $Mg^{2+}$  having a comparatively smaller ionic radius, so decreases the size of the unit cell (Albeck *et al.*, 1993). At  $Mg > 4$  mol %, calcite nucleation is kinetically inhibited and aragonite or amorphous calcium carbonate (ACC) precipitates in preference (Kitano and Hood, 1962; Raz *et al.*, 2000; Loste *et al.*, 2003). In biogenic carbonates, it's likely that magnesium also fulfils a role in the formation, growth, and stabilisation of carbonates however the exact mechanisms for this role have yet to be identified (Politi *et al.*, 2010).

Previous work on the adsorption of phosphate into calcite has focussed on the adsorption of phosphate onto the calcite surface (e.g., Stumm and Leckie, 1970; de Kanel and Morse, 1978; Millero *et al.*, 2001). This has demonstrated that the uptake of phosphate is a multi-stage process, with different steps taking different lengths of time to occur (Millero *et al.*, 2001). It is possible the impact of Mg on phosphate incorporation could be occurring at any of these stages, though it is most likely to be an important factor in the initial adsorption of phosphate. There is very little research on the influence of Mg concentration on the incorporation of phosphate, but some studies have suggested that increased Mg concentrations increase phosphate adsorption (e.g., Millero *et al.*, 2001). Millero *et al.* (2001) investigated the adsorption and desorption of phosphate by both calcite and aragonite as a function of temperature (5–45 °C) and salinity (0–40 ‰) in carbonate equilibrated seawater. They found that increasing temperature increased the 'adsorption equilibrium' resulting in increased phosphate being adsorbed, while increased salinity reduced the amount of phosphate adsorbed. They also found that adsorption values were higher in seawater than in a NaCl solution due to the presence of Mg and Ca ions. They suggest that adsorbed  $Ca^{2+}$  and  $Mg^{2+}$  at carbonate sites may act as carbonate bridges to  $PO_4^{3-}$  ions, though also suggest this relationship is strongest with  $Ca^{2+}$  ions (by a factor of 5) due to stronger interactions between calcium and phosphate than calcium and magnesium (Millero *et al.*, 2001). Other studies have suggested that increased Mg concentration in calcite can inhibit or promote the incorporation of phosphate, depending on the ionic strength of the solution from which the calcite precipitates in (Morse, 1985; Millero *et al.*, 2001; Xu *et al.*, 2013;). DeKanel and Morse (1978) suggested that phosphate uptake by calcite and aragonite was not impacted by solution

concentration of Mg between zero and modern seawater concentrations, though the impact of more concentrated solutions was not studied.

Studies of Mg and P distribution in belemnite calcite have shown that P and Mg are concentrated in the same phase of calcite in the rostra, a tetrahedral phase high in P, Mg and organic matter which has been attributed as the primary calcite phase which formed during the belemnite's life (Hoffmann *et al.*, 2016). The calcite surrounding the tetrahedral phases, attributed as a secondary calcite formed early in the diagenetic processes after the belemnite's death, is low in both phosphorus and magnesium (Hoffmann *et al.*, 2016). Whilst far from conclusive, the close spatial distribution of P and Mg in belemnite calcite lends weight to the idea that P and Mg are linked by mineralogical factors.

To investigate the impact of Mg concentration on the structure of the unit cells in belemnite calcite, XRD was used to provide measurements for unit parameters *a* and *c*, and the unit cell volume for samples covering a range of Mg concentrations (Figure 43; Figure 44; Figure 45; Table 22). It was found that in belemnite calcite the average value for lattice parameter *a* was larger than the reported value for pure calcite (by 0.16 %), while lattice parameter *c* and the unit cell volume were smaller than for pure calcite (by 0.78 and 0.47 % respectively) (Table 22). This is consistent with previous findings for synthetic calcite or 1-3 mol % Mg, which had a smaller unit cell volumes than pure calcite due to the higher charge density of magnesium ions compared to calcium (Albeck *et al.*, 1993). The average belemnite included in this study had Mg concentrations around 2 mol %, falling well within the range studied by Albeck *et al.* (1993).

It was also found that there was a negative correlation between unit cell parameters *a* and *c* and unit cell volume ( $R^2$  values of 0.62, 0.37 and 0.53 respectively) (Figure 43; Figure 44; Figure 45). This demonstrates that higher concentrations of magnesium lead to reductions in both unit cell parameter *a* and *c* and the overall unit cell volume (Figure 43; Figure 44; Figure 45). A possible explanation for the correlation between P/Ca and Mg/Ca, is that the distortions to the lattice structure caused by higher Mg concentrations allow greater concentrations of phosphate to be incorporated. The mechanism by which this takes place is unclear, as phosphate ions have a larger ionic radius ( $r = 238$  pm) than carbonate ions ( $r = 178$  pm), which seems to suggest that increased Mg concentrations would make phosphate ions harder to incorporate due to the smaller unit cell volumes (Jenkins and Thakur, 1979). It is possible that the increased concentrations of Mg increase disorder or defects in the lattice structure as a whole, resulting in gaps suitable for phosphate incorporation elsewhere in the structure. This could be further investigated using lab-based synthetic calcite growth experiments for a range of different Mg, Ca, and P concentrations as well as solution saturation states. Alternatively,

using a technique such as EDX imaging to gain a closer insight into the spatial distribution of Mg and P in the calcite to determine their distribution relative to each other may be useful.

As Mg appears to be a dominant control on P incorporation into belemnite calcite, the factors affecting Mg incorporation into calcite were also investigated. Studies in both synthetic and natural calcites (biogenic and abiogenic) have demonstrated that temperature is one of the most significant factors affecting Mg incorporation into calcite (e.g., Katz, 1973; Micci, 1987). At higher temperatures, greater amounts of Mg are incorporated into the lattice due to thermodynamic effects (e.g., Katz, 1973; Micci, 1987; Burton and Walter, 1991; Alkhatib *et al.*, 2022). Other mineralogical factors have been demonstrated to impact Mg incorporation into calcites, such as Mg/Ca fluid ratios,  $P_{CO_2}$ , precipitation rates and the presence of other ions (such as sulfate which inhibits Mg incorporation) (e.g., Lahann and Siebert, 1982; Mucci and Morse, 1983; Mucci *et al.*, 1989; Zhong and Mucci, 1989; Burton and Walter, 1991; Hartley and Mucci, 1996; De Choudens-Sánchez and González, 2009). Despite the multiple factors which can affect Mg incorporation, Mg/Ca in calcite is generally considered a reliable proxy for seawater temperature (e.g., Chave, 1954a; b; Rosenthal *et al.*, 1997; Stanley and Hardie, 1998; Elderfield and Ganssen, 2000; Dekens *et al.*, 2002; Dickson, 2002; and Bryan and Marchitto, 2008). This is not always the case for belemnites, with some studies suggesting Mg/Ca in belemnites does not accurately reflect palaeotemperatures due to a lack of correlation with  $\delta^{18}O$  (e.g., Wierzbowski and Rogov, 2011; Li *et al.*, 2013; Stevens *et al.*, 2014).

The impact of temperature on Mg/Ca ratios in this study was investigated using correlations between  $\delta^{18}O$  and Mg/Ca (Figure 39). This demonstrated that there was a negative correlation between  $\delta^{18}O$  and Mg/Ca in samples from Bulgaria ( $R^2 = 0.46$ ), but not in samples from Yorkshire or Wales (0.02 and 0.05 respectively) (Figure 39). This is very similar to the results obtained for the correlations between P/Ca and  $\delta^{18}O$  – which is unsurprising based on the observed correlation between P/Ca and Mg/Ca (Figure 35; Figure 38). This suggests that the incorporation of Mg into the calcite is related to temperature in samples from Bulgaria, but not in samples from the other sites studied. In the samples from Yorkshire and Wales, other factors may have influenced the incorporation of magnesium which were not as impactful or not present in samples from Bulgaria.

The relationship between temperature and Mg/Ca in Bulgaria, but not in Yorkshire or Wales may be related to differing palaeoenvironmental conditions between Bulgaria and the other sites studied. For example, during the Early Jurassic, the Moesian basin (where the Bulgarian samples were deposited) was much more proximal to the open Tethys Ocean than the Cleveland Basin or Cardigan Bay Basin (where the Yorkshire samples and Welsh samples are from respectively) (Figure 21). This meant that the Bulgarian sections would have had greater

water-mass exchange with the open ocean and has an ocean chemistry much more similar to the open ocean than the other study sites. By comparison, the Cleveland Basin and Cardigan Bay Basin were much further away from the open ocean, and much more restricted basins with limited water-mass exchange to the open ocean (e.g., Sælen *et al.*, 1996; 2000; van de Schootbrugge *et al.*, 2005; McArthur *et al.*, 2008). The Moesian Basin also shows less evidence of sustained low-oxygen conditions, whereas the other basins have shown evidence of dysoxic conditions – particularly Yorkshire where there is evidence of widespread and sustained dysoxic to anoxic conditions during the TOAE (e.g., Jenkyns, 1988; Hesselbo *et al.*, 2007; Metodiev and Koleva-Rekalova, 2008; Gröcke *et al.*, 2011; Pugh, 2018; Reolid *et al.*, 2021). Several studies have suggested the possibility of changes in salinity during the ETNCIE and TOAE in the more restricted basins of the Laurasian Seaway, including Yorkshire (e.g., Prauss *et al.*, 1991; Sælen *et al.*, 1996; Bailey *et al.*, 2003; McArthur *et al.*, 2008; Hesselbo *et al.*, 2020; Remírez and Algeo, 2020). Most authors suggest the development of a stratified water-column with a less-saline surface layer and more saline deeper water (e.g., Prauss *et al.*, 1991; Sælen *et al.*, 1996; Bailey *et al.*, 2003; McArthur *et al.*, 2008). Some recent studies have suggested the possibility of an entirely brackish water-column, though this is controversial (Hesselbo *et al.*, 2020; Remírez and Algeo, 2020). Overall, this demonstrates that the water chemistry in the Cardigan Bay Basin and the Cleveland Basin is likely to be more complicated and more varied through time than in the Moesian Basin for the Early Jurassic. The changes in ocean chemistry, water mass exchange and potentially salinity in the Cardigan Bay and Cleveland Basins may explain why Mg/Ca or  $\delta^{18}\text{O}$  values have been impacted in belemnites from these locations, thus explaining why they do not correlate well in these locations. In the samples from the Moesian Basin in Bulgaria where the ocean chemistry is comparatively more straightforward, there is a correlation between Mg/Ca and  $\delta^{18}\text{O}$  (Figure 39). Alternatively, it may be that the differences between Mg/Ca and  $\delta^{18}\text{O}$  are caused by species specific biologic effects, and there is less overlap in the species studied between Bulgaria and the other sites than there was between Yorkshire and Wales, due to the greater distance between them and different palaeogeography (e.g., McArthur *et al.*, 2002; McArthur *et al.*, 2007a; b; Li *et al.*, 2012; Hoffmann *et al.*, 2016; Stevens *et al.*, 2017; Hoffmann and Stevens, 2020 and references therein).

To further investigate regional differences in the relationship between  $\delta^{18}\text{O}$  and Mg/Ca, previous studies of the correlation between Mg/Ca and  $\delta^{18}\text{O}$  can be investigated. Several studies have shown a negative correlation between  $\delta^{18}\text{O}$  and Mg/Ca, suggesting Mg/Ca may correlate positively with temperature (e.g., McArthur *et al.*, 2000; Bailey *et al.*, 2003; Rosales *et al.*, 2004; Armendáriz *et al.*, 2008), while others have shown no significant correlation

between Mg/Ca and  $\delta^{18}\text{O}$  (e.g., Wierzbowski and Rogov, 2011; Li *et al.*, 2013; Stevens *et al.*, 2014). The locations and basic palaeogeographic/palaeoenvironmental information for several previous studies was examined to determine if Mg/Ca and  $\delta^{18}\text{O}$  were found to covary more strongly in sections with similar conditions (e.g., in more open ocean locations) (Table 24). Studies which found  $\delta^{18}\text{O}$  and Mg/Ca covaried in Early Jurassic samples used samples from multiple locations, though the majority were from basins which were closer to the open Tethys (e.g., South German Basin: Bailey *et al.*, 2003; basins in Northern Spain: Rosales *et al.*, 2004; Armendáriz *et al.*, 2008). However, some studies also used samples from Yorkshire and also found covariation in Mg/Ca and  $\delta^{18}\text{O}$  (e.g., McArthur *et al.*, 2000; Bailey *et al.*, 2003). The finding of covariation between Mg/Ca and  $\delta^{18}\text{O}$  in samples from multiple sites in Yorkshire contradicts the findings of the samples in this study, where no covariation was observed – to identify the reasons behind this discrepancy, further investigation is required.

In studies where no covariation was observed between Mg/Ca and  $\delta^{18}\text{O}$ , samples were from a range of sampling locations. Whilst many of these had environmental factors which may complicate the relationship between Mg/Ca and  $\delta^{18}\text{O}$  (e.g., lagoonal settings (Stevens *et al.*, 2014), changes in ocean circulation (Wierzbowski and Rogov, 2011)), this was not the case in all of the study locations (e.g., Li *et al.*, 2013). It is clear that more research is needed to identify factors affecting both Mg/Ca and  $\delta^{18}\text{O}$ , to determine why some studies find they covary while other studies do not, even in studies conducted on samples from in similar palaeoenvironments (Table 24).

Table 24 - Summary of the locations, time periods and important palaeoenvironmental factors in a subset of previous studies which have compared Mg/Ca and  $\delta^{18}\text{O}$ , broken down into samples which found covariation between  $\delta^{18}\text{O}$  (McArthur *et al.*, 2000; Bailey *et al.*, 2003; Rosales *et al.*, 2004; Armendáriz *et al.*, 2008), and studies which did not (Wierzbowski and Rogov, 2011; Li *et al.*, 2013; Stevens *et al.*, 2014).

Study	Time Period	Location	Palaeoenvironment Notes
<b>Negative correlation between Mg/Ca and <math>\delta^{18}\text{O}</math></b>			
McArthur <i>et al.</i> (2000)	Upper Pliensbachian-Lower Toarcian, Early Jurassic	Cleveland Basin, Yorkshire (UK)	Samples collected from the Yorkshire Coast, similar locations to samples used in this study (4.2.2).
Bailey <i>et al.</i> (2003)	Upper Pliensbachian-Lower Toarcian, Early Jurassic	Cleveland Basin, Yorkshire (UK); South German	German sections are more proximal to the open ocean, than the Yorkshire sections

Study	Time Period	Location	Palaeoenvironment Notes
<b>Negative correlation between Mg/Ca and <math>\delta^{18}\text{O}</math></b>			
		Basin, SE Germany	
Rosales <i>et al.</i> (2004)	Pliensbachian-Lower Toarcian, Early Jurassic	Basque– Cantabrian basin of northern Spain	Hemipelagic basin with likely dysoxic-anoxic bottom water conditions
Armendáriz <i>et al.</i> (2008)	Lower Pliensbachian, Early Jurassic	Asturian basin, northern Spain	Through the study interval, the palaeogeography of the sampling location changes from shallow restricted lagoons to shallow partially restricted nearshore/epicontinental shelf due to continental uplift.
<b>No correlation between Mg/Ca and <math>\delta^{18}\text{O}</math></b>			
Wierzbowski and Rogov (2011)	Upper Callovian – Lower Oxfordian, Mid-Late Jurassic	Middle Russian Sea, near Saratov (Russia)	The sediments were deposited in a deeper basin, a significant distance from land and freshwater influx, though there is evidence of a shallowing and an influx of warm currents in the <i>lamberti</i> zone of the Upper Callovian.
Li <i>et al.</i> (2013)	Pliensbachian, Early Jurassic	Dorset, UK	Various palaeoenvironmental conditions, but in each location only a brief interval was studied.
	Callovian, Mid- Jurassic	Cambridgeshire, UK	
	Valangian, Early Cretaceous	Vocontian Basin, SE France	
Stevens <i>et al.</i> (2014)	Upper Kimmeridgian, Late Jurassic	near the village of Nusplingen in SW Germany	Lagoonal setting

Regardless of the factors behind Mg incorporation, the covariation of Mg and P in samples from multiple locations suggests that care needs to be taken in the interpretation of CAP data. If phosphorus incorporation is controlled, at least in part, by mineralogical factors relating to the incorporation of magnesium, care needs to be taken to quantify the concentrations of magnesium to aid interpretation of phosphorus data. Some previous studies of CAP in carbonates have presented CAP ratios as  $P/(Ca+Mg)$ , rather than  $P/Ca$  as is discussed here (e.g., Dodd *et al.*, 2021; 2023). The grouping of Mg and Ca potentially hinders the comparison of P and Mg records in these datasets, making links between ion incorporations more difficult to identify. It is our suggestion that  $P/Ca$  ratios be used in preference, to allow for better comparison between P and Mg records.

It is also likely that other components of calcite which are not studied here (such as anions, organic matter, and others) have impacts on P incorporation, Mg incorporation or both. For example, it has been shown that the presence of sulfate ions inhibits magnesium incorporation – given the relationship between Mg and P, this may also reduce the incorporation of phosphorus, which could be further studied (Mucci *et al.*, 1989; Zhong and Mucci, 1989). Data from this study has also provided evidence for links between other cations, such as Na and Ca, which is further discussed in Chapter 5.

## 4.6. Conclusions

$P/Ca$  records were produced for three different locations in the Laurasian Seaway, which demonstrated clear and coherent changes through time, including a negative excursion in  $P/Ca$  in samples from Yorkshire in the Grey Shales, prior to the ETNCIE and TOAE (Figure 29). Similar trends were seen in  $P/Ca$  in all of the study locations, including an increase in  $P/Ca$  in all locations in the upper *serpentinum* zone of Yorkshire and Wales and the upper *tenuicostatum* of Bulgaria (Figure 29). Determining the exact timings of excursions within each record and making comparisons between locations was made more difficult by stratigraphic gaps in samples for all locations, particularly in the mid-Pliensbachian (Figure 29). Further work should focus on filling in these stratigraphic gaps and increasing the resolution, to enable more robust comparisons within and between study sites (Figure 29).

$P/Ca$  records were compared to a range of proxies to determine the factors affecting P incorporation. It was shown that  $P/Ca$  likely partially reflects water column phosphorus concentrations, with different environmental factors controlling the water column phosphorus concentrations in different locations. In samples from Dove's Nest, higher CAP was found

during intervals of euxinia, suggesting that enhanced recycling of phosphorus from the sediment was controlling water-column phosphorus (Figure 30; Figure 33; Figure 34). When the P/Ca values were compared to  $\delta^{18}\text{O}$  values to investigate the influence of temperature, they were found to only covary in samples from Bulgaria. This may be explained based on the different palaeoenvironments between Bulgaria and the other study locations, with Bulgarian samples representing an environment more similar to the open ocean, and the samples from elsewhere having more complex and variable conditions due to changing salinity, levels of water mass exchange, sea level and oxygenation.

P/Ca records were also compared to Mg/Ca records, which correlated more strongly with P/Ca records in Bulgaria (compared to  $\delta^{18}\text{O}$ ), and also correlated with P/Ca in samples from Dove's Nest and Wales (Figure 37; Figure 38). I suggest that Mg concentrations may exert a mineralogical control on the incorporation of phosphorus into calcite in belemnites, perhaps by affecting the rate of adsorption of phosphate into the calcite's surface. Magnesium was also shown to be altering the structure of the calcite, with higher-Mg samples demonstrating smaller unit cell volumes (Figure 45). It is possible that this may also have an impact on the incorporation of phosphorus into calcite, but the mechanism of this effect would require more research.

Magnesium was then compared to  $\delta^{18}\text{O}$  to determine if magnesium incorporation was controlled by temperature. There was a negative correlation between Mg/Ca and  $\delta^{18}\text{O}$  in samples from Bulgaria, but not any of the other sites studied (Figure 39). This suggests that in Bulgaria, the incorporation of Mg is temperature controlled, whilst in other areas of the Laurasian Seaway, the incorporation of Mg is controlled by a range of factors potentially related to changes in sea-level, salinity, water-circulation and redox. When the relationship between Mg/Ca and  $\delta^{18}\text{O}$  was examined for samples from previous studies, there was no consistent trend in types of palaeoenvironment which gave rise to covariation between them (Table 24). Alternatively, it is possible that the oxygen isotope values for North Wales and Yorkshire are overly influenced by the changes in salinity, ocean circulation and bathymetry, and do not reflect changes in palaeotemperature which may still be a control on Mg incorporation, though this is considered less likely.

Further work is clearly needed to disentangle the relative contributions of different palaeoenvironmental factors to P/Ca ratios, and it is likely that the influence of many of these factors (such as redox and temperature) will be specific to a location and time interval. Nevertheless, the apparent control on P incorporation by Mg concentration across samples from a range of species across a large time interval and geographical spread, suggests that the potential of a mineralogical control on P incorporation by magnesium is not necessarily limited

to belemnites. It is possible that the control is the inverse, with P exerting a control on Mg incorporation – but this is less likely as P is much less abundant both in the ocean and belemnite calcite, and there is an understood mechanism for magnesium incorporation being dependant on temperature, which isn't established for phosphorus (e.g., Katz, 1973; Micci, 1987; Burton and Walter, 1991; Alkhatib *et al.*, 2022). This raises important considerations for existing studies using P/Ca in other biogenic and abiogenic carbonates to investigate the mineralogical relationships between P and Mg, as well as other major ionic components of the carbonates being studied. In particular, studies which use P/(Ca+Mg) as a measure of CAP may need to consider the relationships between P and Mg which are contained within that ratio (e.g., Dodd *et al.* 2021; 2023).

Future work would benefit from examining the apparent mineralogical relationships within carbonates more closely, comparing relationships in concentration for as many elements as possible in both natural and synthetic carbonates, and using techniques such as EDX imaging to produce elemental maps. Additionally, this work emphasises the importance of understanding the relationships between the incorporation of multiple different components into carbonates (both biogenic and abiogenic). This demonstrates the importance of characterising samples as fully as possible (including anions, organic matter, etc.) in order to ensure that mineralogical relationships are understood, and environmental information – such as the variation of CAP with water column phosphorus can be examined.

## 5. Na/Ca records in a stratigraphic context

### 5.1. Introduction

Alongside measuring values of P, Ca, and Mg, several other major, minor and trace elements in belemnite rostra were analysed in each of the specimens from North Yorkshire, Bulgaria, and North Wales (4.2). Several elements were analysed including Li, B, Na, Al, K, Mn, Ba, U, Sr, and S (4.3). This resulted in a large dataset, with the potential to investigate many proxies across multiple locations in the Laurasian Seaway (Figure 21). One of the most complete records generated was for Na. It has already been demonstrated that Na had low variability within stratigraphic levels; statistically significant differences between stratigraphic levels and was not affected by differences between species in this study or previous work (McArthur *et al.*, 2007a).

Despite being one of the most abundant elements in belemnite calcite, Na in belemnites is little studied. A small number of previous authors have recorded Na values as an additional element in a multi-elemental study (McArthur *et al.*, 2000; 2004; Wierzbowski, 2004; McArthur *et al.*, 2007a; Wierzbowski and Rogov, 2011; Li *et al.*, 2012; 2013; Wierzbowski *et al.*, 2013; Wierzbowski, 2015; Wierzbowski *et al.*, 2017; 2018). The Na results in each of these previous studies have rarely been discussed at length, and only limited attempts have been made to interpret them. Several factors have been suggested as potentially impacting Na concentrations in belemnites and biogenic carbonates more widely (McArthur *et al.*, 2000; 2004; Wierzbowski, 2004; 2015). For example, some studies have demonstrated a covariance between Na/Ca and Mg/Ca, Sr/Ca, and  $\delta^{18}\text{O}$  and suggested that Na incorporation may be controlled by temperature, making Na/Ca a potential palaeotemperature proxy (e.g., McArthur *et al.*, 2000; 2004). Other studies have Na concentrations as an indication of preservation (e.g., McArthur *et al.*, 2007a; Wierzbowski and Rogov, 2011; Li *et al.*, 2012; 2013; Wierzbowski *et al.*, 2013; 2017; 2018). Na/Ca and Sr/Ca covariance in these studies has been attributed to both elements being lost through diagenetic alteration of the carbonate mineral (Wierzbowski, 2004; 2015). It has been demonstrated that Na is lost from marine carbonates during freshwater diagenesis (Brand and Veizer, 1980; Veizer, 1983), so some studies have investigated sample diagenesis using Na/Ca values – even going as far as to put limits on Na/Ca values for sample screening (e.g., Wierzbowski, 2004; 2015).

Other work on different biogenic and abiogenic carbonates has tentatively suggested that Na/Ca may have potential utility as a palaeosalinity proxy (e.g., White, 1978; Ishikawa and Ichikuni, 1984; McArthur *et al.*, 2007a; Wit *et al.*, 2013; Mezger *et al.*, 2016; Bertlich *et al.*,

2018; Gray *et al.*, 2023). More convincingly, recent work on foraminifera has demonstrated the potential of Na/Ca ratios to record changes in water-column Ca concentrations (Evans *et al.*, 2018; Hauzer *et al.*, 2018; Evans *et al.*, 2020; Zhou *et al.*, 2021; Gray *et al.*, 2023; Nambiar *et al.*, 2023). Gray *et al.* (2023) demonstrated that the Na/Ca ratios of foraminifera were weakly affected by other factors such as temperature, carbonate ion concentration, bottom water saturation state, and salinity, but is dominantly controlled by the calcium ion concentration. If belemnite Na/Ca values also had the potential to record ocean Ca concentrations, this would give an opportunity to investigate variations in major ion ocean chemistry through a large portion of Earth's history – which is an exciting prospect.

In this chapter, a Na/Ca record for each study location will be presented and discussed. To investigate each of the factors potentially affecting Na concentrations in belemnite calcite, results from this study are presented and discussed in context with Na measurements from existing published datasets (McArthur *et al.*, 2000; 2004; 2007; Wierzbowski and Rogov, 2011; Li *et al.*, 2012; 2013; Wierzbowski *et al.*, 2013; 2017; 2018). Na/Ca will be compared to known temperature and salinity proxies ( $\delta^{18}\text{O}$ , Mg/Ca, Sr/Ca) and to proxies for diagenesis (Mn/Ca, Fe/Ca, Sr/Ca, results of visual inspection) and the potential of Na/Ca in carbonates to record Ca concentrations will be discussed.

## 5.2. Materials and methods

The same specimens were used to generate the Na/Ca records as were used to form the P/Ca records in 3.2. Belemnite specimens from all studied locations in the Laurasian Seaway (the Moesian Basin in Bulgaria, the Cleveland Basin in Yorkshire, and the Cardigan Bay Basin in North Wales) were analysed according to the method described in 2.4. Full elemental, isotopic and sediment analysis results can be found in the appendix (8.4; 8.5; 8.6). The same diagenetic screening protocol was applied to these samples, as the Variability Samples (described in 2.4.6).

## 5.3. Results

### 5.3.1. Screening for Diagenesis

#### 5.3.1.1. Iron and manganese

Diagenetic screening of samples is described in sections 2.5.5.1, 3.3.5.1 and 4.4.1.1. The same screening criteria ( $\text{Fe/Ca} < 600 \mu\text{mol mol}^{-1}$  and  $\text{Mn/Ca} < 300 \mu\text{mol mol}^{-1}$ ) was used for other El/Ca ratios. To ensure that this screening protocol was suitable for examining sodium in belemnites, the correlation between Fe/Mn with each other and with Na was investigated in the unscreened and screened sample sets for each section studied (Table 25).

The same screening criteria was used on samples for investigating other  $\text{El}/\text{Ca}$  ratios as was used with  $\text{P}/\text{Ca}$ , so the same samples were excluded. The  $\text{Na}/\text{Ca}$  ratios were compared to  $\text{Fe}/\text{Ca}$  and  $\text{Mn}/\text{Ca}$  ratios. As the same screening criteria was used, the same reduction in the strength of correlation between  $\text{Fe}/\text{Ca}$  and  $\text{Mn}/\text{Ca}$  was observed. Before screening criteria was applied, there was a positive correlation between  $\text{Na}/\text{Ca}$  and  $\text{Fe}/\text{Ca}$  in the samples from the Yorkshire Coast ( $R^2 = 0.36$ ), the Dove's Nest core in Yorkshire ( $R^2 = 0.71$ ) and in the samples overall ( $R^2 = 0.71$ ) (Table 25). There was also weak correlation between  $\text{Na}/\text{Ca}$  and  $\text{Mn}/\text{Ca}$  in samples from North Wales ( $R^2 = 0.35$ ) (Table 25). After screening criteria was applied there was no significant correlation between  $\text{Na}/\text{Ca}$  and  $\text{Fe}/\text{Ca}$  in any of the sections studied (Table 25). There was a weak positive correlation between  $\text{Na}/\text{Ca}$  and  $\text{Mn}/\text{Ca}$  in samples from Penny Nab ( $R^2 = 0.30$ ) and Dobravitsa-1 ( $R^2 = 0.78$ ) – though both of these locations only represented a small number of samples ( $n \leq 11$ ) (Table 25). There was no significant correlation between  $\text{Mn}/\text{Ca}$  and  $\text{Na}/\text{Ca}$  in Bulgaria or Yorkshire overall (Table 25).

Table 25 -  $R^2$  values indicating correlation between  $El/Ca$  ratios for samples in different locations.  $R^2$  values are given for  $Fe/Ca$  and  $Mn/Ca$ ;  $Fe/Ca$  and  $Na/Ca$  and  $Mn/Ca$  and  $Na/Ca$ . Cells are shaded green to denote correlation, with darker green indicating strong correlation ( $R^2 > 0.8$ ) and light green denoting weaker correlation ( $R^2 > 0.3$ ). The  $R^2$  values for each location are calculated before and after sample screening criteria were applied and the results are given for both.  $R^2$  values for Dobravitsa-2 could not be calculated due to the  $Fe$  and  $Mn$  measurements falling below the LOD/LOQ for most samples.  $n$  is also indicated for each set of samples (both screened and unscreened) to indicate the quantity of samples retained after screening criteria is applied, where  $n$  is the number of  $Na/Ca$  measurements.

Sample location	Unscreened samples				Screened samples			
	n	Mn and Fe	Na and Fe	Na and Mn	n	Mn and Fe	Na and Fe	Na and Mn
<b>Yorkshire coast</b>	192	0.52	0.36	2.5E-02	163	0.60	1.4E-02	1.3E-03
Ravenscar	65	0.48	0.14	1.8E-02	55	0.53	6.4E-02	2.2E-03
Runswick Bay	84	0.48	0.11	1.4E-02	72	0.55	3.1E-03	8.4E-04
Cowbar Nab	16	0.91	0.14	0.15	14	0.93	3.2E-05	6.3E-04
Penny Nab	11	0.83	0.20	2.8E-02	10	0.53	2.0E-03	0.30
Wine Haven	16	0.95	2.0E-02	4.3E-04	12	0.94	6.5E-02	0.20
<b>Yorkshire core</b>	109	0.67	0.71	0.22	38	0.28	1.1E-03	5.2E-03
<b>Wales</b>	148	0.79	0.20	0.35	102	0.32	0.14	5.2E-02
<b>Bulgaria</b>	41	0.77	2.4E-02	1.2E-02	39	0.40	3.5E-03	5.8E-05
Dobravitsa-1	8	0.83	6.6E-02	8.6E-02	7	0.76	3.3E-04	0.78
Dobravitsa-2	11	-	-	-	10	-	-	-
Milanovo	22	0.09	2.4E-02	3.5E-02	22	0.09	2.4E-02	3.5E-02
<b>All</b>	490	0.67	0.71	0.23	342	0.17	2.3E-02	1.3E-03

Overall, the screening criteria reduced the strength of the correlation between Fe/Ca and Na/Ca in all sections studied except Wine Haven (where the  $R^2$  value increased slightly but was still very low) and Milanovo (where the  $R^2$  value was unchanged as no samples were excluded).

As with P/Ca, while the screening criteria did not eliminate the impact of diagenetic alteration (hence the strength of the correlation between Fe/Ca and Mn/Ca) the degree of diagenetic alteration in the remaining samples did not have a strong effect on Na/Ca in the majority of sections studied, nor in any of the study locations overall (Table 25). This suggests that this screening criteria is suitable for examining changes in Na/Ca in the locations included in this study, though future work could apply different screening criteria to each section or location rather than applying one set of criteria to all sections.

### 5.3.1.2. Strontium

Positive correlation between Sr/Ca and Na/Ca has been reported previously by a few studies, some of which suggested it may indicate a temperature relationship (McArthur *et al.*, 2000; 2004), and others which suggested it may be controlled by diagenesis (e.g., Wierzbowski, 2004; 2015). Sr/Ca and Na/Ca values were compared for samples in our screened dataset from each location. Sr/Ca has also been suggested as a palaeotemperature indicator in belemnite calcite, so any positive correlation may also indicate temperature dependence of one or both elements.

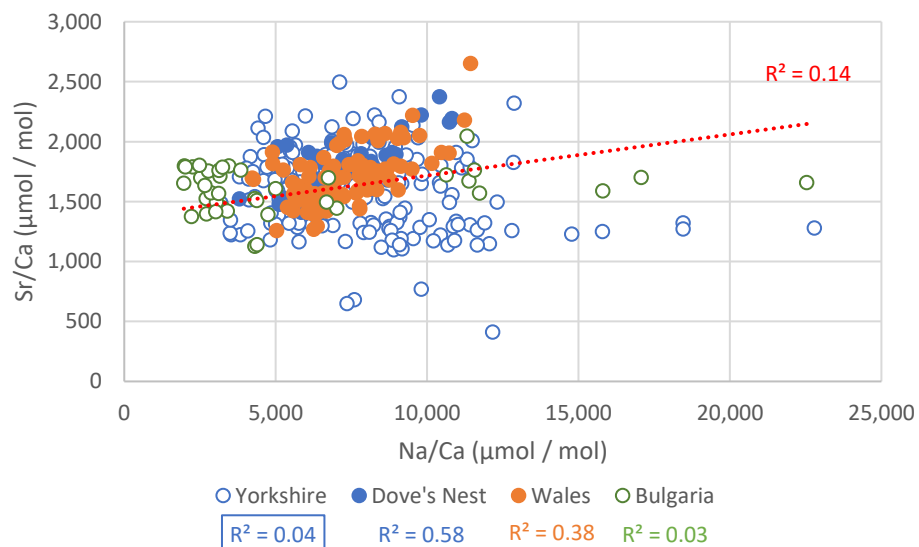


Figure 46 - Cross-plot of belemnite Sr/Ca against Na/Ca values. Samples are from three different locations (Yorkshire [dark blue], Wales [orange] and Bulgaria [green]). Core samples are shown with filled circles, outcrop samples with open circles. For each sample set an  $R^2$  is calculated using a linear line of best fit (not shown) and  $R^2$  values are shown next to the key in the colour corresponding to the data points; where lines of best fit had a negative gradient (Yorkshire) the  $R^2$  value is shown with a border. A linear line of best fit for all samples is shown (dashed red line) along with the corresponding  $R^2$  value (red).

There was shown to be a positive correlation between Sr/Ca and Na/Ca in two of the sample sets studied: Dove's Nest ( $R^2 = 0.58$ ) and Wales ( $R^2 = 0.38$ ). Both of these sets of samples were obtained from core material. In the other locations, containing samples from outcrops, no significant correlation was seen between Na/Ca and Sr/Ca (Bulgaria ( $R^2 = 0.03$ ) and Yorkshire ( $R^2 = 0.04$ )).

### 5.3.2. Sodium in belemnites through time

Na/Ca values were calculated for each belemnite sample from Wales, Yorkshire, and Bulgaria (Figure 47). For each location, sections were combined to produce a single stratigraphic record using the correlations shown in Figure 23 (Yorkshire) and Figure 27 (Bulgaria). Ammonite zones and lithological markers were then used to correlate the records between each location (Figure 47). This enabled Na/Ca records to be compared for three different locations in the Laurasian Seaway (Figure 47).



calculated from the analysis of 77 samples from 6 specimens of 4 different species from the Penny Nab section taken from the 'Variability Samples' (2.3.2) to indicate the magnitude of changes compared to the natural levels of variability at each stratigraphic level. For Bulgaria and Yorkshire, stratigraphic plots combine samples from multiple sections, using correlations previously presented (Yorkshire (Rawson and Wright (2018); Lord (2019); Trabucho-Alexandre et al. (2022) (Figure 23); Bulgaria (Metodiev and Koleva-Rekalova (2008); Pugh (2018) (Figure 27)). Where samples in each location are from different sections the data points are indicated with different symbols. Where abbreviations for lithological units are used due to limited space: Fe-stone = ironstone; Ms. = mudstone, Sh. = Shale; Ss. = sandstone.

The magnitude of the Na/Ca ratios in each section were similar, with values ranging from around 2,500 to 25,000  $\mu\text{mol mol}^{-1}$  in all three locations. T tests conducted using the methods described in 2.4.5 showed that there were no statistically significant differences in P/Ca values between Bulgaria ( $\bar{x} = 5,573 \mu\text{mol mol}^{-1}$ ;  $s = 4,708 \mu\text{mol mol}^{-1}$ ) and North Wales ( $\bar{x} = 7,209 \mu\text{mol mol}^{-1}$ ;  $s = 1,457 \mu\text{mol mol}^{-1}$ ) ( $t(43) = 2.02$ ;  $p = 0.035$ ); or between Bulgaria and Yorkshire ( $\bar{x} = 7,773 \mu\text{mol mol}^{-1}$ ;  $s = 2,828 \mu\text{mol mol}^{-1}$ ) ( $t(46) = 2.01$ ;  $p = 0.006$ ), or between Yorkshire and North Wales ( $t(301) = 1.97$ ;  $p = 0.022$ ).

As with P/Ca, the Na/Ca records for all locations have relatively high levels of variability, though some of this variability can be explained by the differences within and between individual belemnites (Figure 19). Based on the Variability Samples, standard deviations were calculated for all samples from the Penny Nab section from the variability section which included 77 samples from 6 belemnites from 4 different species from the same stratigraphic level (3.4.4). The standard deviation of Na/Ca in the Penny Nab Variability Samples was determined to be 792  $\mu\text{mol mol}^{-1}$  (Figure 19). A bar indicating two standard deviations (1585  $\mu\text{mol mol}^{-1}$ ) is shown for each plot on Figure 47 to demonstrate the magnitude of changes which can be deemed to be attributable to something other than the natural variability in P/Ca values within and between belemnites.

In all locations studied there are changes greater than those which can be explained by natural variability in Na/Ca ratios between and within individuals (Figure 47). There are also similarities between the stratigraphic trends observed in P/Ca between each section. There were coherent changes in Na/Ca within each location studied, but unlike P/Ca there are no significant covariations in Na/Ca which are visible in multiple locations.

In Yorkshire, the Na/Ca ratios in the end Sinemurian to end-Pliensbachian are relatively stable at around 10,000  $\mu\text{mol mol}^{-1}$ , though there is a large stratigraphic gap in the sample set for the *jamesoni* and early *ibex* ammonite zones (Figure 47). At the Pliensbachian-Toarcian boundary, there is an increase in Na/Ca to values of 14,800  $\mu\text{mol mol}^{-1}$ , followed by a sharp decline to 3,200  $\mu\text{mol mol}^{-1}$  in the mid-*tenuicostatum* ammonite zone (Figure 47). Na/Ca values then gradually increase throughout the remainder of the Toarcian reaching values of 8,800-12,900  $\mu\text{mol mol}^{-1}$  in the *thouarsense* and *variabilis* ammonite zones (Figure 47). In samples from

North Wales, the Na/Ca values from the Pliensbachian ( $\bar{x} = 7,568 \mu\text{mol mol}^{-1}$ ;  $s = 1,558 \mu\text{mol mol}^{-1}$ ) were higher than the values from the Toarcian ( $\bar{x} = 6,385 \mu\text{mol mol}^{-1}$ ;  $s = 692 \mu\text{mol mol}^{-1}$ ) and more variable (Figure 47). The Na/Ca values decrease in the *spinatum* ammonite in the latest Pliensbachian (Figure 47). In Bulgaria, there are no samples below the *tenuicostatum* ammonite zone, and a further gap occurs from the upper *fallaciosum* ammonite zone until the mid-*bradfordensis* ammonite zone (Figure 47). The majority of samples from the *tenuicostatum* to the upper *variabilis* ammonite zones have Na/Ca values around 2,000-3,500  $\mu\text{mol mol}^{-1}$ , except for a brief excursion to higher Na/Ca values (to values of around 15,000  $\mu\text{mol mol}^{-1}$ ) in the mid-*bifrons* ammonite zone (Figure 47). In the *thouarsense* and *fallaciosum* ammonite zones the Na/Ca values are more variable, changing between high values (11,300-22,500  $\mu\text{mol mol}^{-1}$ ) and low values (3,200-7,000  $\mu\text{mol mol}^{-1}$ ) (Figure 47).

While there were no observable major coincident excursions, there were similarities between the records for North Wales and Yorkshire, with Pliensbachian belemnites giving values of around 6,000-12,000  $\mu\text{mol mol}^{-1}$  in the *ibex*, *davoei* and *margaritatus* ammonite zones, with lower values in the early Toarcian – particularly the *tenuicostatum*, and *serpentinum* ammonite zones (Figure 47). The Bulgarian samples also showed generally low Na/Ca values in the early Toarcian, particularly the *tenuicostatum* – though the magnitude of these values was much lower than the values for North Wales or Yorkshire (with the exception of the previously described excursions) (Figure 47).

### 5.3.3. Sodium and temperature

To investigate the potential variation of sodium in belemnite calcite with temperature, Na/Ca ratios were compared to oxygen isotopes in each of the locations studied (Figure 48). As with P/Ca, this was done by creating a cross-plot of Na/Ca and  $\delta^{18}\text{O}$  for each location studied (Figure 48). Linear lines of best fit were applied to samples from each location: Yorkshire, Wales, and Bulgaria (Figure 48). An additional subset of the Yorkshire samples was included, comprising core samples taken from the Dove's Nest site (Figure 48).  $R^2$  values for the lines of best fit were calculated and displayed alongside the key symbols for each sample set, in a colour matching the sample symbol (Figure 48). It was found that there was no significant correlation between Na/Ca and  $\delta^{18}\text{O}$  in any of the locations studied, with an  $R^2$  across all locations of 0.01 (in each location: Yorkshire  $R^2 = 0.01$ ; Wales  $R^2 = 0.0003$ ; Bulgaria  $R^2 = 0.01$ ) (Figure 48).

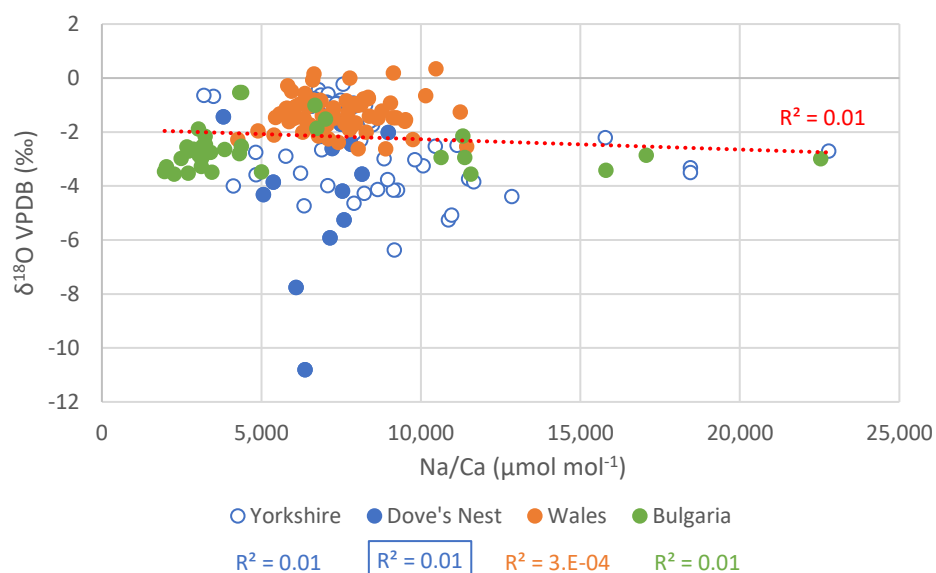


Figure 48 - Cross-plot of belemnite  $\delta^{18}\text{O}$  compared to the Vienna Pee Dee Belemnite (VPDB) against Na/Ca values from the same belemnites. Samples are from three different locations (Yorkshire [dark blue], Wales [orange] and Bulgaria [green]). Core samples are shown with filled circles, outcrop samples with open circles. For Yorkshire samples, the Yorkshire dataset includes both coastal outcrops and core samples, Dove's Nest is a subset of these samples and is shown separately in addition to being included in the Yorkshire samples. For each sample set an  $R^2$  is calculated using a linear line of best fit (not shown) and  $R^2$  values are shown next to the key in the colour corresponding to the data points; where lines of best fit had a positive gradient (Dove's Nest) the  $R^2$  value is shown with a border. A linear line of best fit for all samples is shown (dashed red line) along with the corresponding  $R^2$  value (red).

It has already been demonstrated that in samples from Bulgaria, Mg/Ca is related to temperature (Figure 39). This indicates that in samples from Bulgaria, Mg/Ca can be used as a temperature proxy alongside  $\delta^{18}\text{O}$ . This relationship was used to further investigate the potential for Na/Ca to vary with temperature, by comparing Na/Ca values with Mg/Ca values for Bulgarian sections (Figure 49). Again, this comparison was made using a cross-plot of Mg/Ca and Na/Ca values for samples from Bulgaria. It was found that there was no significant correlation between Mg/Ca and Na/Ca for samples from Bulgaria, with an  $R^2$  value of 0.04 (Figure 49).

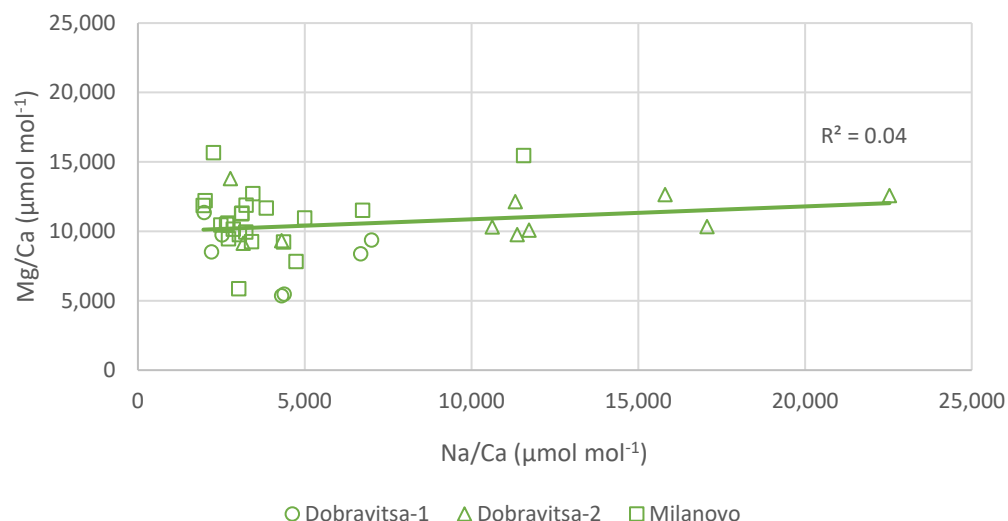


Figure 49 - Cross-plot of belemnite Mg/Ca against Na/Ca values from the same belemnites. Samples are from three different sections in Bulgaria (Dobravitsa-1 [circles]; Dobravitsa-2 [triangles]; Milanovo [squares]). A linear line of best fit for all samples is shown (green line) along with the corresponding  $R^2$  value.

#### 5.3.4. Observations from El/Na ratios

While comparing Na/Ca and Mg/Ca values, it was observed that the strength of correlations between elements included in this study were increased when the elements were given as ratios to sodium rather than calcium (i.e., El/Na rather than El/Ca). For example, it was found that across most locations studied there was a positive correlation between Sr/Ca and Mg/Ca, with an  $R^2$  value 0.41 across all samples (in specific locations: Yorkshire  $R^2 = 0.48$ ; Wales  $R^2 = 0.09$ ; Bulgaria  $R^2 = 0.53$ ) (Figure 50). This is unsurprising as both Mg/Ca and Sr/Ca have been suggested as palaeotemperature proxies in belemnite calcite and have been demonstrated to covary (e.g., McArthur *et al.*, 2000; 2004; 2007). However, it was found that the strength of the correlation between Sr and Mg was greater in every study location when they were given as ratios to sodium instead of calcium, with an overall  $R^2$  value of 0.84 (in each location: Yorkshire  $R^2 = 0.68$ ; Wales  $R^2 = 0.58$ ; Bulgaria  $R^2 = 0.93$ ) (Figure 51). Sr/Na and Mg/Na also demonstrated a correlation in Wales which was not seen between Sr/Ca and Mg/Ca (Figure 50; Figure 51).

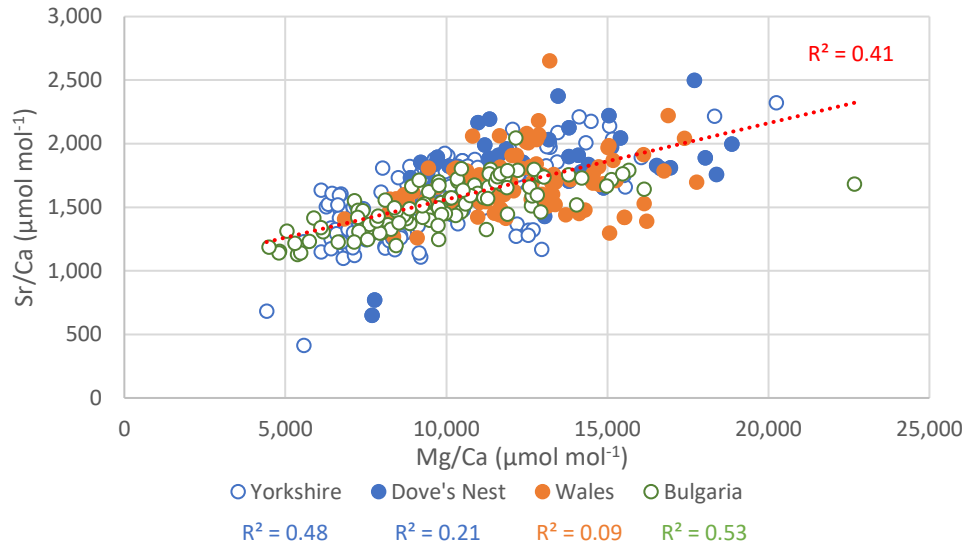


Figure 50 - Cross-plot of belemnite Mg/Ca against Sr/Ca ratios from the same belemnites. Samples are from three different locations (Yorkshire [dark blue], Wales [orange] and Bulgaria [green]). Core samples are shown with filled circles, outcrop samples with open circles. For Yorkshire samples, the Yorkshire dataset samples includes both coastal outcrops and core samples, Dove's Nest is a subset of these samples and is shown separately in addition to being included in the Yorkshire samples. For each sample set an  $R^2$  is calculated using a linear line of best fit (all with positive gradients; not shown) and  $R^2$  values are shown next to the key in the colour corresponding to the data points. A linear line of best fit for all samples is shown (dashed red line) along with the corresponding  $R^2$  value (red).

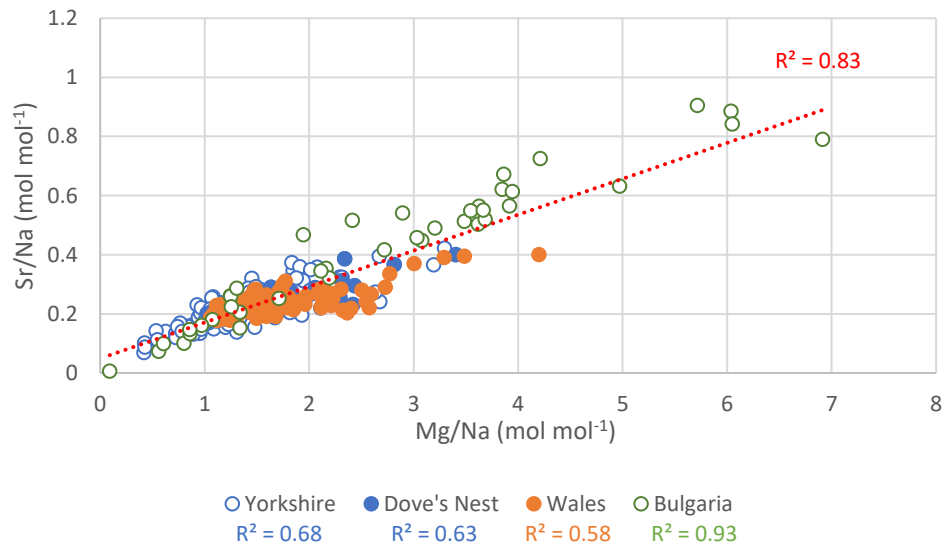


Figure 51 - Cross-plot of belemnite Mg/Na against Sr/Na ratios from the same belemnites. Samples are from three different locations (Yorkshire [dark blue], Wales [orange] and Bulgaria [green]). Core samples are shown with filled circles, outcrop samples with open circles. For Yorkshire samples, the Yorkshire dataset samples includes both coastal outcrops and core samples, Dove's Nest is a subset of these samples and is shown separately in addition to being included in the Yorkshire samples. For each sample set an  $R^2$  is calculated using a linear line of best fit (all with positive gradients; not shown) and  $R^2$  values are shown next to the key in the colour corresponding to the data points. A linear line of best fit for all samples is shown (dashed red line) along with the corresponding  $R^2$  value (red).

The relationship between Mg and P (as described in 4.5.5) was also investigated using ratios to Na rather than Ca to determine if the strength of the correlation increased (Figure 37; Figure

52). A cross-plot of P/Na vs Mg/Na was created and  $R^2$  values were calculated for each location studied (Figure 52).

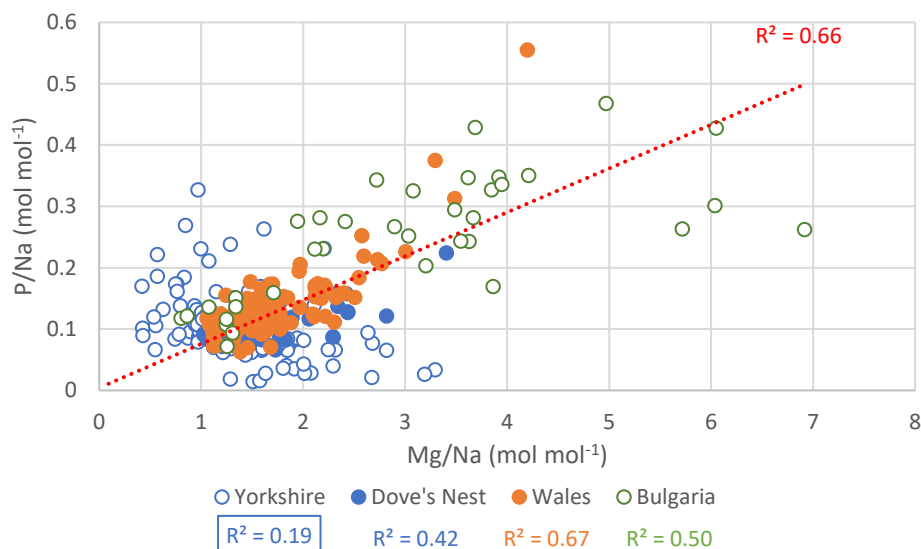


Figure 52 - Cross-plot of belemnite Mg/Na against P/Na ratios from the same belemnites. Samples are from three different locations (Yorkshire [dark blue], Wales [orange] and Bulgaria [green]). Core samples are shown with filled circles, outcrop samples with open circles. For Yorkshire samples, the Yorkshire dataset samples includes both coastal outcrops and core samples, Dove's Nest is a subset of these samples and is shown separately in addition to being included in the Yorkshire samples. For each sample set an  $R^2$  is calculated using a linear line of best fit (not shown) and  $R^2$  values are shown next to the key in the colour corresponding to the data points; where lines of best fit had a negative gradient (Yorkshire) the  $R^2$  value is shown with a border. A linear line of best fit for all samples is shown (dashed red line) along with the corresponding  $R^2$  value (red).

It was shown that there was a positive correlation between P/Na and Mg/Na in samples from Dove's Nest, Wales, and Bulgaria (with  $R^2$  values of 0.42, 0.62 and 0.50 respectively) (Figure 52). There was a weak negative correlation between P/Na and Mg/Na for samples from Yorkshire, with an  $R^2$  value of 0.19 (Figure 52). The  $R^2$  values for this plot were compared to the  $R^2$  values for each location for the relationship between Mg/Ca and P/Ca (Table 26).

Table 26 -  $R^2$  values for the correlation between Mg and P as ratios to Na or to Ca in the different locations included in this study.

Sample location	$R^2$ value	
	Mg/Ca vs P/Ca	Mg/Na vs P/Na
Yorkshire	0.07 (negative gradient)	0.19 (negative gradient)
Dove's Nest	0.28	0.42
Wales	0.40	0.67
Bulgaria	0.38	0.50
<b>All samples</b>	<b>0.39</b>	<b>0.66</b>

In every location there was a stronger correlation between Mg/Na and P/Na than between Mg/Ca and P/Ca (Figure 37; Figure 52; Table 26). This was true even in Yorkshire, where there was no significant correlation between Mg and P when given as ratios to calcium ( $R^2 = 0.07$ ) and a weak, albeit negative, correlation between Mg/Na and P/Na ( $R^2 = 0.19$ ) (Figure 37; Figure 52; Table 26). In every other location there was a positive correlation between P and Mg when given as a ratio to both calcium and sodium, though the strength of the correlation when given as a ratio to sodium was greater in every case (Figure 37; Figure 52; Table 26).

The relationship between oxygen isotopes and Mg was also reinvestigated, using Mg values as ratios to Na (Figure 53). There was no significant correlation between Mg/Na and  $\delta^{18}\text{O}$  in samples from Yorkshire, Dove's Nest or Wales (with  $R^2$  value of 0.01, 0.002 and 0.06 respectively) (Figure 53). There was a weak negative correlation between Mg/Na and  $\delta^{18}\text{O}$  with an  $R^2$  value of 0.18 (Figure 53) for samples from Bulgaria. This was similar to the results previously obtained examining the correlation between Mg/Ca and  $\delta^{18}\text{O}$ , where no significant correlation between Mg/Ca and  $\delta^{18}\text{O}$  was found in samples from Yorkshire, Dove's Nest or Wales – though there was a negative correlation between Mg/Ca and  $\delta^{18}\text{O}$  in samples from Bulgaria with an  $R^2$  value of 0.46 (Figure 39). This demonstrates that ratios of Mg to Na rather than Ca does not improve the correlation of Mg with temperature, and in fact reduces the correlation in samples from Bulgaria (Figure 39; Figure 53).

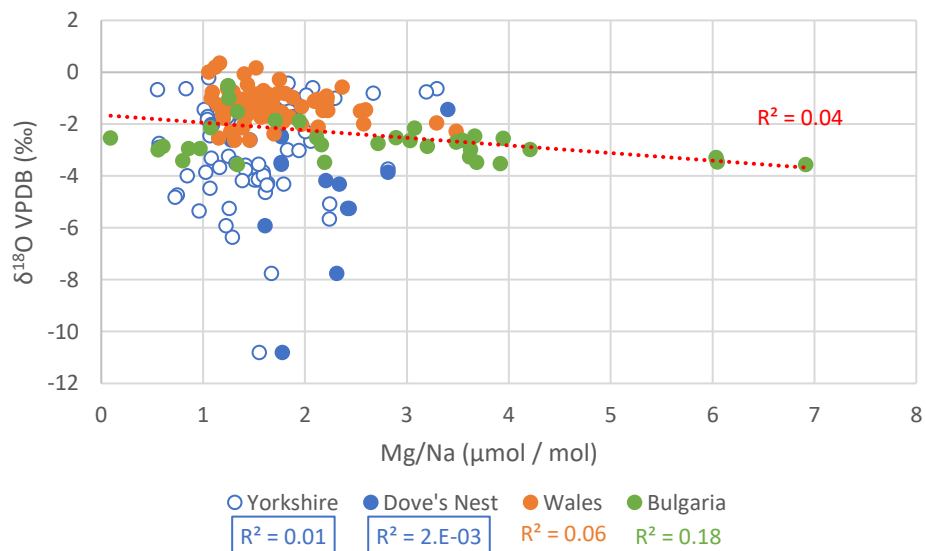


Figure 53 - Cross-plot of belemnite  $\delta^{18}\text{O}$  compared to the Vienna Pee Dee Belemnite (VPDB) against Mg/Na values from the same belemnites. Samples are from three different locations (Yorkshire [dark blue], Wales [orange] and Bulgaria [green]). Core samples are shown with filled circles, outcrop samples with open circles. For Yorkshire samples, the Yorkshire dataset samples includes both coastal outcrops and core samples, Dove's Nest is a subset of these samples and is shown separately in addition to being included in the Yorkshire samples. For each sample set an  $R^2$  is calculated using a linear line of best fit (not shown) and  $R^2$  values are shown next to the key in the colour corresponding to the data points; where lines of best fit had a positive gradient (Yorkshire and Dove's Nest) the  $R^2$  value is shown with a

*border. A linear line of best fit for all samples is shown (dashed red line) along with the corresponding  $R^2$  value (red).*

## 5.4. Discussion

### 5.4.1. Factors affecting Na concentrations

This section will address each the potential factors affecting Na concentrations in calcite (diagenesis, temperature, salinity, calcium concentration and mineralogy) in turn, using data from this study as well as data from some previous studies which have measured Na in belemnites. Studies which have previously measured Na in belemnites have done so for a diverse range of belemnite species and time periods from the Early Jurassic to the Early Cretaceous (Table 27). Previous studies have also used a variety of methods for screening, preparing, and analysing belemnites to produce Na data, all of which may have an impact on measured Na concentrations (Table 27). A summary of the sample locations, time periods and methodologies used in these studies is included in Table 27. Alongside the previous studies, data from this study will be examined including both the screened and altered datasets. When the altered dataset was investigated, it was found that some altered samples from this study were had Sr/Ca values higher than would be expected in carbonates, even in aragonite, and also had high values for Mn/Ca, Fe/Ca, and El/Ca ratios. It was determined this was likely due to analytical issues resulting in lower-than-expected Ca measurements. These samples were excluded, using a criterion of Sr/Ca > 3,000  $\mu\text{mol mol}^{-1}$ . Samples with extremely elevated Fe/Ca values (Fe/Ca < 5,000  $\mu\text{mol mol}^{-1}$ ) and Mn/Ca values (Mn/Ca > 1,000  $\mu\text{mol mol}^{-1}$ ) were also removed for the same reason.

This section contains a large number of plots as it draws on data from multiple studies and compares many elemental and isotopic ratios to attempt to unravel the factors affecting Na incorporation. For simplicity, a table containing a summary of the correlations between different ratios in each dataset is included at the end of the discussion section (Table 28).

Table 27 – Summary of samples and methodologies used by this study and some previous studied which measured Na concentrations in belemnite calcite.

Study	Location	Stage	Sediment	Screening	Cleaning	Dissolution	Na notes
This study	Yorkshire, UK	Sinemurian-Toarcian (Early Jurassic)	Mixed, mostly mudstones and some sandstones	Samples screened using concentrations of Mn ( $\leq 411$ ppm) and Fe ( $\leq 828$ ppm), which correspond to Mn/Ca $\leq 300$ $\mu\text{mol mol}^{-1}$ and Fe/Ca $\leq 600$ $\mu\text{mol mol}^{-1}$ .	Powders cleaned by washing 5 x with ultra-pure water.	30 % acetic acid	See 2.4.3 and 3.3.2.2.
	Bulgaria	Pliensbachian-Bajocian (Early-Middle Jurassic)	Mixed, mostly mudstones and limestones				
	North Wales, UK	Pliensbachian-Toarcian (Early Jurassic)	Mixed, mostly mudstone				
Li <i>et al.</i> (2012)	Yorkshire, UK	Toarcian (Early Jurassic)	Mixed, mostly shales	Samples were assigned a visual preservation index (VPI) based on visual inspection, with 1 = best preserved; 5 = complete alteration. Included samples had VPI values of 1-4.	Fragments were cleaned using 1.2 M HCl then washed and dried.	0.32 M HNO <sub>3</sub>	Precision for Na better than $\pm 4$ %

Study	Location	Stage	Sediment	Screening	Cleaning	Dissolution	Na notes
Li <i>et al.</i> (2013)	Dorset, UK	Pliensbachian (Early Jurassic)	Marls	Screened samples were visually well preserved under binocular microscope.	Fragments were cleaned using 1.2 M HCl then washed and dried.	0.32 M HNO <sub>3</sub>	Precision for Na exceeded the limit of $\pm 4$ %
	Cambridge, UK	Calloviaian (Middle Jurassic)	Clays				
	Vocontian Basin, SE France	Valanginian (Early Cretaceous)	Interbedded marls and limestones				
McArthur <i>et al.</i> (2000)	Yorkshire, UK	Pliensbachian-Toarcian (Early Jurassic)	Mixed	Screened samples were visually well-preserved (based on appearance under plane/polarised light and cathode luminescence), had replicable trace element concentrations and low quantities of Mn ( $\leq 88$ ppm) and Fe ( $\leq 251$ ppm).	Fragments were cleaned with 1.2 M HCl and ultra-pure water.	1.8 M acetic acid	Precision for Na exceeded the limit of $\pm 5$ %
McArthur <i>et al.</i> (2004)	Yorkshire, UK	Valangian-Hauterivian (Early Cretaceous)	Predominantly clays with calcareous mudstones	Screened samples were visually well preserved under binocular microscope, had replicable trace element concentrations and low	Fragments were cleaned with 1.2 M HCl and ultra-pure water.	1.2 M HCl	Precision for Na better than $\pm 5$ %

Study	Location	Stage	Sediment	Screening	Cleaning	Dissolution	Na notes
				quantities of Mn ( $\leq 20$ ppm) and Fe ( $\leq 193$ ppm).			
McArthur <i>et al.</i> (2007a)	Yorkshire, UK	Toarcian (Lower Jurassic)	Mudstone	Screened samples were visually well preserved under binocular microscope, altered samples were also analysed.	Fragments were cleaned with 1.2 M HCl and ultra-pure water.	1.2 M HCl	
Wierzbowski <i>et al.</i> (2018)	Kostroma Region, Russia	Callovia-Kimmeridgian (Middle-Late Jurassic)	Mixture of clays, calcareous clays, and marls	Screened samples were visually well preserved under binocular microscope, and cathode luminescence, had replicable trace element concentrations and low quantities of Mn ( $\leq 20$ ppm) and Fe ( $\leq 33$ ppm) and high concentrations of Sr ( $\geq 824$ ppm).	-	1.4 M HCl	Na concentrations in the standards used too low to determine precision of measurements.

#### 5.4.1.1. Diagenetic alteration

Some previous studies which have measured Na in belemnite calcite have suggested that Na concentrations can be used to assess levels of diagenetic alteration (e.g., McArthur *et al.*, 2007a; Li *et al.*, 2012; 2013; Wierzbowski, 2004; 2015). A limited number of studies have measured Na concentrations in well preserved and poorly preserved belemnites, allowing for potential comparison between the two (e.g., McArthur *et al.*, 2007a; Li *et al.*, 2012). Some further studies have used these values of Na measured in 'well-preserved samples' to compare to values obtained in subsequent datasets (e.g., McArthur *et al.*, 2007a; Wierzbowski and Rogov, 2011; Li *et al.*, 2012; 2013; Wierzbowski *et al.*, 2013; 2017; 2018). Wierzbowski (2015) even set limits for Na, in a similar way to Sr, Mn and Fe to screen for alteration and identify well preserved samples – identifying altered samples as samples containing  $\text{Na/Ca} \leq 4,790 \mu\text{mol mol}^{-1}$  or  $\text{Na} \leq 1100 \text{ ppm}$  in pure calcite. The loss of Na from calcite has previously been suggested as an impact of freshwater diagenesis of marine carbonates (Brand and Veizer, 1980; Veizer, 1983). Hence it is possible that the concentration of Na in belemnite calcite is determined by the degree of diagenetic alteration the sample has undergone. This was investigated using data from this study, and a number of previous studies.

In this study, only iron ( $\text{Fe/Ca} \geq 600 \mu\text{mol mol}^{-1}$ ) and manganese ( $\text{Mn/Ca} \geq 300 \mu\text{mol mol}^{-1}$ ) were used to identify and exclude samples with altered calcite (2.5.5.1; 3.3.5.1; 4.4.1.1; 5.3.1). This was deemed sufficient for analysis of P/Ca, as in each section studied there was no significant correlation between P/Ca and either Mn/Ca or Fe/Ca (Table 21). There was also no significant correlation between Na/Ca and either Mn/Ca or Fe/Ca for the majority of sections studied (Table 25). This suggests that diagenesis is not, or not wholly, responsible for the variations in Na/Ca seen in this study. Nevertheless, as diagenesis has been demonstrated to decrease sodium concentrations in carbonates, the potential for diagenetic changes to alter sodium concentrations is worthy of further consideration.

Previous studies have used a range of screening techniques to identify diagenetic alteration, but the majority of studies have included visual assessment of diagenetic alteration (Table 27). The majority of studies do not analyse samples which are determined visually to be altered, so most of the data described in previous publications is considered to be screened (Table 27). This discussion will focus on datasets from this study and a range of previous publications, as well as both screened and altered samples from this study.

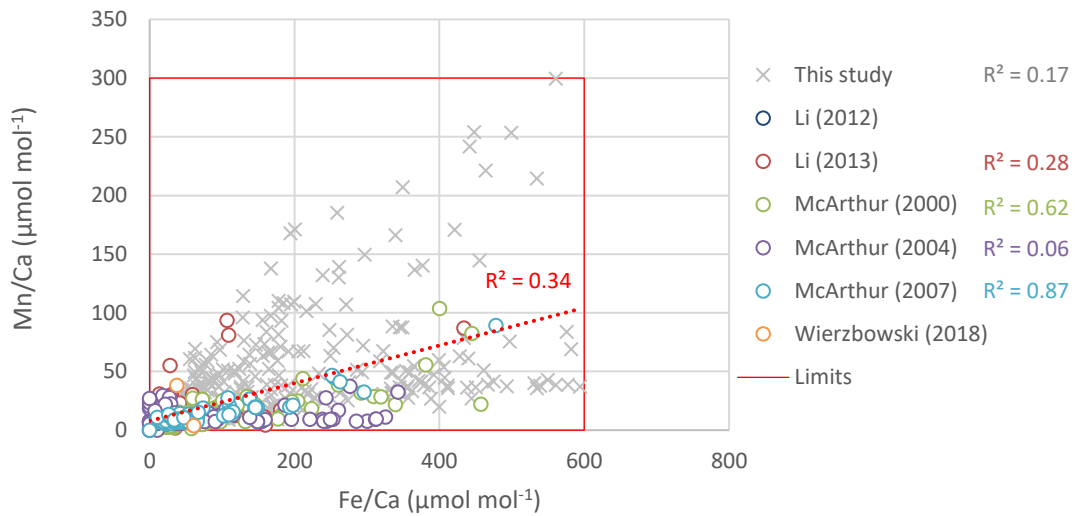


Figure 54 - Fe/Ca and Mn/Ca values for samples from this study (screened [crosses; pale grey] and altered [plusses, dark grey]) and some previous studies (circles: Li *et al.* (2012) [dark blue]; Li *et al.* (2013) [dark red]; McArthur *et al.* (2000) [pale green]; McArthur *et al.* (2004) [purple]; McArthur *et al.* (2007a) [pale blue] and Wierzbowski *et al.* (2018) and references therein [orange]). An  $R^2$  value (assuming a linear line of best fit, not shown) for each set of samples is displayed in a colour corresponding to the sample marker; for Li *et al.* (2012) and Wierzbowski *et al.* (2018) there were insufficient Fe and Mn values to calculate an  $R^2$  value. An overall linear line of best fit and corresponding  $R^2$  value is also shown (red). The limits used in this study are indicated in red.

Studies which determine the degree of alteration of samples partially using Na values are excluded so as not to reinforce circular logic (e.g., Wierzbowski, 2015). In order to compare between the different diagenetic screening methods, Fe/Ca and Mn/Ca values for all studies were compared (Figure 54). It was demonstrated that for the studies included here, samples had iron and manganese values which fell inside the limits set by this study (Mn/Ca < 300  $\mu\text{mol mol}^{-1}$ ; Fe/Ca < 600  $\mu\text{mol mol}^{-1}$ ) (Figure 54). In fact, for most studies, samples fell below Mn/Ca = 50  $\mu\text{mol mol}^{-1}$ , with the exception of four samples from Li *et al.* (2013); three from McArthur *et al.* (2000) and one from McArthur *et al.* (2007a) – though these still fell within the limits used in this study (Figure 54). Samples also fell below the prescribed limit for Fe/Ca used by this study (Fe/Ca < 600  $\mu\text{mol mol}^{-1}$ ), with the majority of samples falling below Fe/Ca = 300  $\mu\text{mol mol}^{-1}$  (Figure 54). It appears that the screening criteria used by this study and previous studies are broadly comparable, though it appears previous studies criteria may have resulted in a narrower range of Mn/Ca values, even when Mn concentrations were not used for screening (Figure 54).

The Na/Ca values were then compared to Fe/Ca and Mn/Ca values for samples from each of the studies investigated – in order to determine if there was a significant correlation between the diagenetic markers used in this study (Fe/Ca, Mn/Ca) and Na (Figure 55; Figure 56). As Na

concentrations in carbonates are suggested to be decreased during diagenesis, and both Fe and Mn are thought to increase, a negative correlation may be expected.

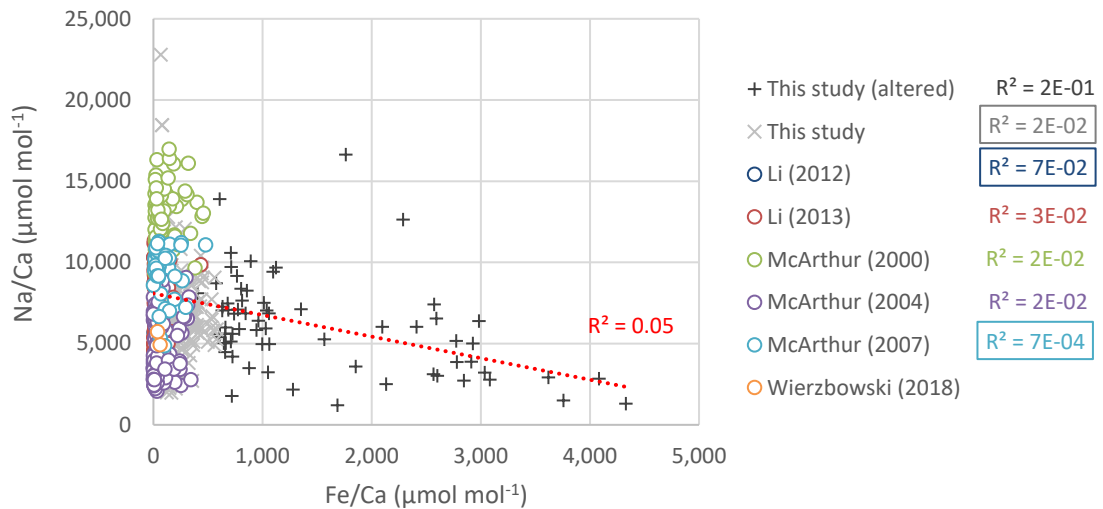


Figure 55 - Fe/Ca and Na/Ca values for samples from this study (screened [crosses; pale grey] and altered [plusses, dark grey]) and some previous studies (circles). An  $R^2$  value (assuming a linear line of best fit, not shown) for each set of samples is displayed in a colour corresponding to the sample marker. An overall linear line of best fit and corresponding  $R^2$  value is also shown (red); where there is a negative correlation between Fe/Ca and Na/Ca (This study, Li et al. (2012); McArthur et al. (2007a)) the  $R^2$  value is shown with a border.

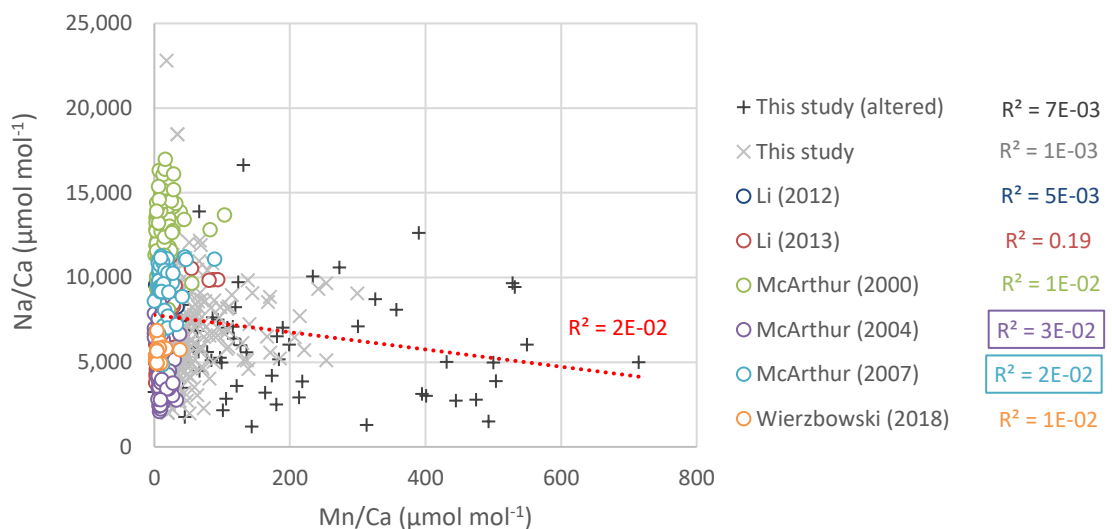


Figure 56 - Mn/Ca and Na/Ca values for samples from this study (screened [crosses; pale grey] and altered [plusses, dark grey]) and some previous studies (circles). An  $R^2$  value (assuming a linear line of best fit, not shown) for each set of samples is displayed in a colour corresponding to the sample marker. An overall linear line of best fit and corresponding  $R^2$  value is also shown (red); where there is a negative correlation between Mn/Ca and Na/Ca (McArthur et al. (2004); McArthur et al. (2007a)) the  $R^2$  value is shown with a border.

In all samples from the previous studies investigated, and both the screened and altered samples from this study, there was no significant correlation between Fe/Ca and Na/Ca or Mn/Ca and Na/Ca (Figure 55; Figure 56). For the majority of samples, visual screening was

used prior to analysis to estimate the level of diagenetic alteration, which means fewer samples with high levels of diagenetic alteration are analysed (Table 27). This was not true for samples from this study, where all samples were analysed, regardless of appearance, and chemical screening criteria were applied (Table 27). Samples from previous studies, and screened samples from this study, all had similar values of Mn/Ca ( $< 350 \mu\text{mol mol}^{-1}$ ), Fe/Ca ( $< 2,000 \mu\text{mol mol}^{-1}$ ) and Na/Ca ( $< 25,000 \mu\text{mol mol}^{-1}$ ) (Figure 55; Figure 56). There was no indication in any of the datasets from previous studies or the screened samples from this study that samples with high Fe or Mn values had lower or higher Na values (Figure 55; Figure 56). This is surprising as a negative correlation between Na and Fe, and Na and Mn would have been expected, as Mn and Fe are generally enriched during diagenesis whereas some studies have suggested that Na is depleted (e.g., Brand and Veizer, 1980; Veizer, 1983; Wierzbowski, 2004; 2015).

Several authors have previously observed a positive correlation between Sr and Na in belemnite calcite (e.g., Mc Arthur *et al.*, 2000; 2004; 2007; Wierzbowski 2004; 2015). This was observed in the data produced in this study (Figure 46), and in data from other studies of sodium in carbonates – plotted together in Figure 57. Generally, the data from previous studies plotted in the same region as data from this study and showed similar trends. Some studies have suggested that Sr/Ca and Na/Ca covary as both are lost from carbonates during diagenetic processes (e.g., Brand and Veizer, 1980; Veizer, 1983; Wierzbowski, 2004; 2015).

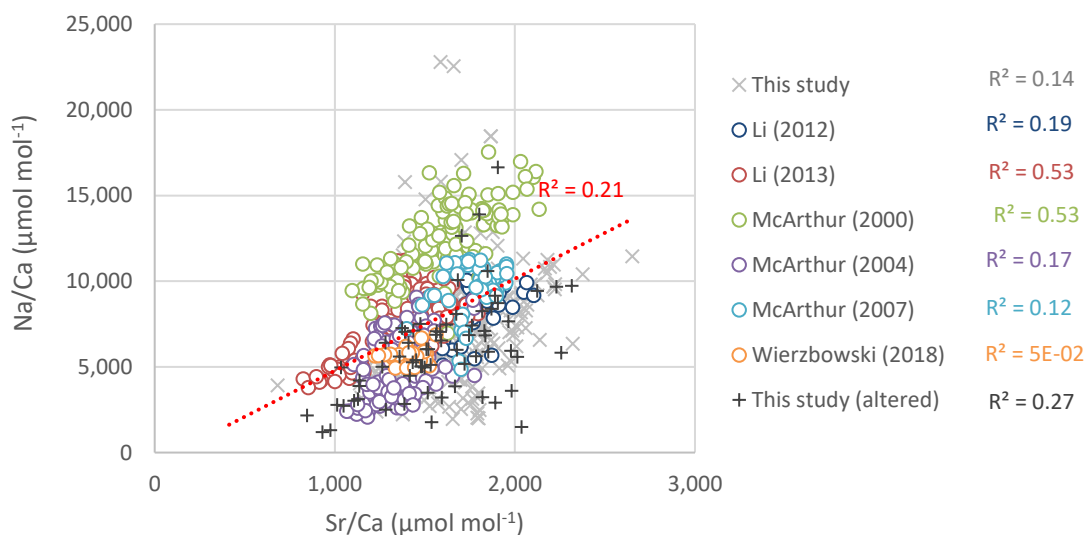


Figure 57 - Sr/Ca and Na/Ca values for samples from this study (screened [crosses; pale grey]) and some previous studies (circles). An  $R^2$  value (assuming a linear line of best fit, not shown) for each set of samples is displayed in a colour corresponding to the sample marker. An overall linear line of best fit and corresponding  $R^2$  value is also shown (red).

To investigate the idea that Sr and Na covary as a result of diagenetic alteration Sr and Na values were investigated for three datasets containing samples with differing levels of diagenetic alteration – i.e., screened and altered samples. These datasets were:

1. The screened and altered data from this study (which was determined to be altered based on Fe/Ca and Mn/Ca values). Some altered samples from this study were found to have Sr/Ca values higher than would be expected in carbonates, even in aragonite, and had high values for Mn/Ca, Fe/Ca, and others. It was determined this was likely due to analytical issues resulting in lower-than-expected Ca measurements. These samples were excluded, using a criterion of  $\text{Sr/Ca} < 3,000 \mu\text{mol mol}^{-1}$ .
2. Altered and unaltered sample sets from McArthur *et al.* (2007a) (which were identified based on visual inspection)
3. Samples from Li *et al.* (2012) which were assigned a visual preservation index (VPI) of 1-5 (1 = best preserved; 5 = completely altered; samples in the study had VPI values 1-4).

Both Li *et al.* (2012) and McArthur *et al.* (2007a) focus on Toarcian belemnite specimens from Yorkshire, so would be expected to give similar results as they cover similar time intervals and environmental conditions. McArthur *et al.* (2007a) takes specimens from a single belemnite bed in the *falciferum* ammonite zone, representing a 'snapshot' in time, whereas Li *et al.* (2012) uses samples from the *falciferum* to the *commune* ammonite zones. Both studies use similar species of belemnites, with McArthur *et al.* (2007a) focussing on *Acrocoelites* (*Acrocoelites*) *subtenuis* and *Acrocoelites* *vulgaris*, both of which were also analysed by Li *et al.* (2012) alongside *Simpsonibelus dorsalis* and *Youngibelus simpsoni*.

In the altered samples from this study, there was a positive correlation between Na/Ca and Sr/Ca ( $R^2 = 0.27$ ) which was stronger than the correlation in the screened samples from this study ( $R^2 = 0.14$ ) (Figure 57). A t test conducted using the methods described in 2.4.5, demonstrated that there were statistically significant differences between the screened samples from this study ( $\bar{x} = 7,343 \mu\text{mol mol}^{-1}$ ;  $s = 2,892 \mu\text{mol mol}^{-1}$ ), and the altered samples ( $\bar{x} = 6,026 \mu\text{mol mol}^{-1}$ ;  $s = 2,929 \mu\text{mol mol}^{-1}$ ), with altered samples having lower Na/Ca values by nearly 20 %;  $t(93) = 1.99$ ;  $p = 0.001$  (Figure 57).

The same trend was observed in the altered and unaltered samples from McArthur *et al.* (2007a) (Figure 58). McArthur *et al.* (2007a) analysed altered and unaltered samples of belemnite calcite, based on visual inspection of the calcite prior to analysis (Table 27). These values were given for multiple individuals of two different species, *Acrocoelites* (*Odontobelus*) *vulgaris* and *Acrocoelites* (*Acrocoelites*) *subtenuis* (McArthur *et al.*, 2007a). The individuals in this study are from the same 'belemnite bed' so are believed to be contemporaneous, hence

there should be no changes in temperature or other environmental conditions (McArthur *et al.*, 2007a). When Sr/Ca and Na/Ca values for altered and unaltered examples of the same belemnite species were compared, altered individuals gave lower values for Na and marginally lower average values for Sr for both species of belemnite (Figure 58). Values of Mn/Ca and Fe/Ca were compared for the same samples, and there were no changes in Mn/Ca or Fe/Ca between the altered and unaltered samples for either species (Figure 59). This suggests that, if Na is representative of diagenetic alteration, Na may be more sensitive to diagenesis than Sr, while both may be more sensitive than Fe or Mn.

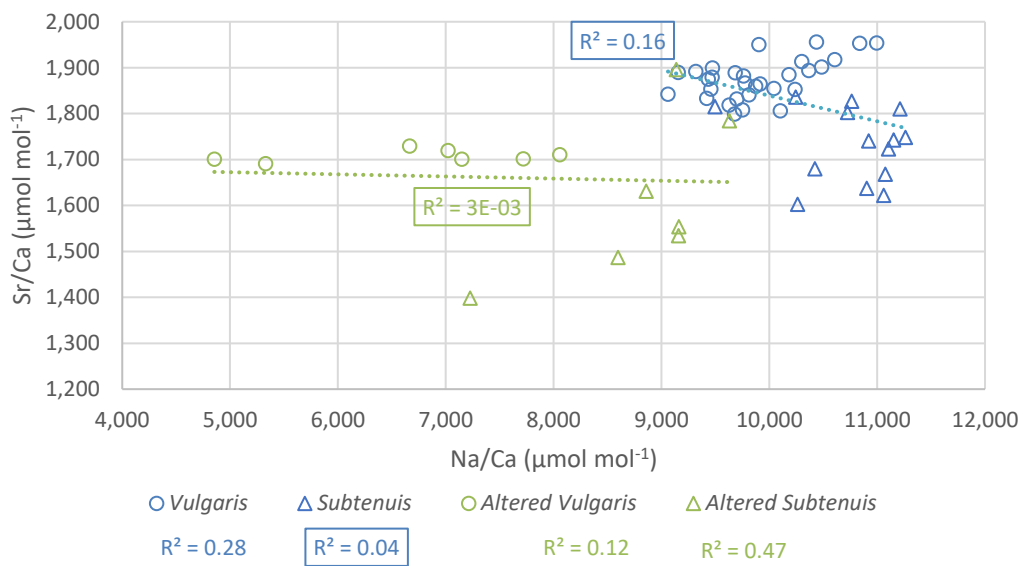


Figure 58 - Sr/Ca against Na/Ca for belemnite samples from McArthur *et al.* (2007a), comprising of altered (pale green) and unaltered (blue) samples (as identified by visual inspection) for two different species (*Acrocoelites* (*Odontobelus*) *vulgaris* [*'Vulgaris'*; circles] and *Acrocoelites* (*Acrocoelites*) *subtenuis* [*'Subtenuis'*; triangles]). For each set of samples an  $R^2$  value assuming a linear line of best fit (not shown) is given adjacent to the sample marker in the figure legend in the same colour as the marker; overall lines of best fit and corresponding  $R^2$  values for all altered (green) and unaltered (blue); Where lines of best fit showed a negative trend (*'Subtenuis'*; all altered, all unaltered),  $R^2$  values are shown with a border.

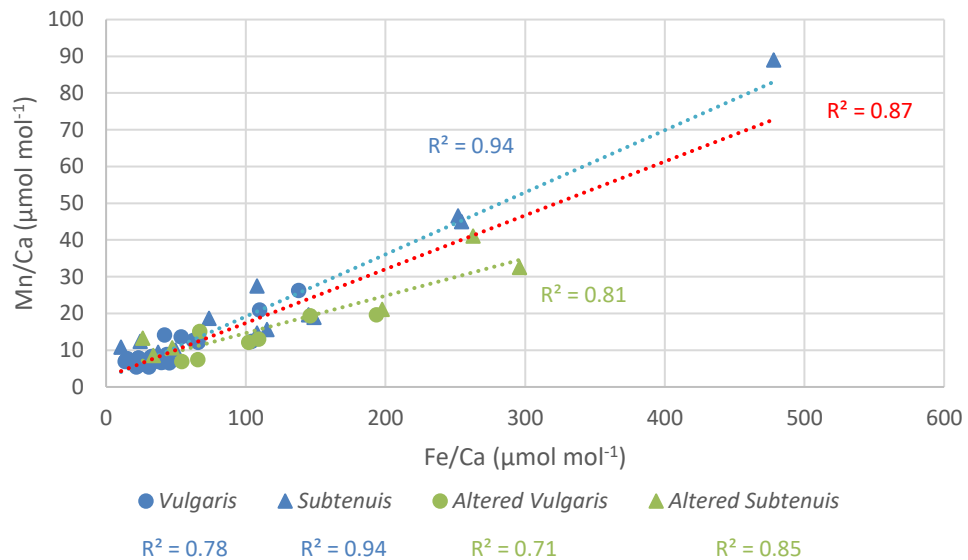


Figure 59 - Fe/Ca against Mn/Ca for belemnite samples from McArthur *et al.* (2007a), comprising of altered (pale green) and unaltered (blue) samples (as identified by visual inspection) for two different species (*Acrocoelites* (*Odontobelus*) *vulgaris* [*'Vulgaris'*; circles] and *Acrocoelites* (*Acrocoelites*) *subtenuis* [*'Subtenuis'*; triangles]). For each set of samples an  $R^2$  value assuming a linear line of best fit (not shown) is given adjacent to the sample marker in the figure legend in the same colour as the marker; overall lines of best fit and corresponding  $R^2$  values for all altered (green), unaltered (blue) and overall (red).

Values of Na/Ca and Sr/Ca were also examined for samples from Li *et al.* (2012) and compared to the assigned visual preservation index (VPI) values (where 1 = best preserved; 5 = completely altered) (Table 27; Figure 60; Figure 61; Figure 62). Most samples in Li *et al.* (2012) had Fe and Mn values below the LOD/LOQ so Na and Sr values couldn't be compared to Fe/Ca or Mn/Ca ratios. When Na/Ca values were compared for each of the assigned VPI values, samples with higher VPI values had lower average Na/Ca values (Figure 60). When the same method was used to investigate Sr/Ca values, there was no consistent trend in Sr/Ca with VPI value (Figure 61). Within each VPI value bracket, there was a range of Na/Ca and Sr/Ca values, and there was correlation between Sr/Ca and Na/Ca within most VPI brackets, particularly 1 and 4 (1:  $R^2 = 0.49$ ; 2:  $R^2 = 0.24$ ; 3:  $R^2 = 0.09$ ; 4:  $R^2 = 0.43$ ) (Figure 60; Figure 61; Figure 62). This was different from the altered and unaltered samples from McArthur *et al.* (2007a), where there was no significant correlation between Sr/Ca and Na/Ca within the altered samples group and the 'unaltered' sample group (Figure 58). This may be because the samples from Li *et al.* (2012) are spread through time in the Early Jurassic, whereas the samples from McArthur *et al.* (2007a) represent a snapshot in time, and the variation in Sr/Ca and Na/Ca within the each VPI bracket in Li *et al.* (2012) may relate to changes in environmental conditions through the time period studied.

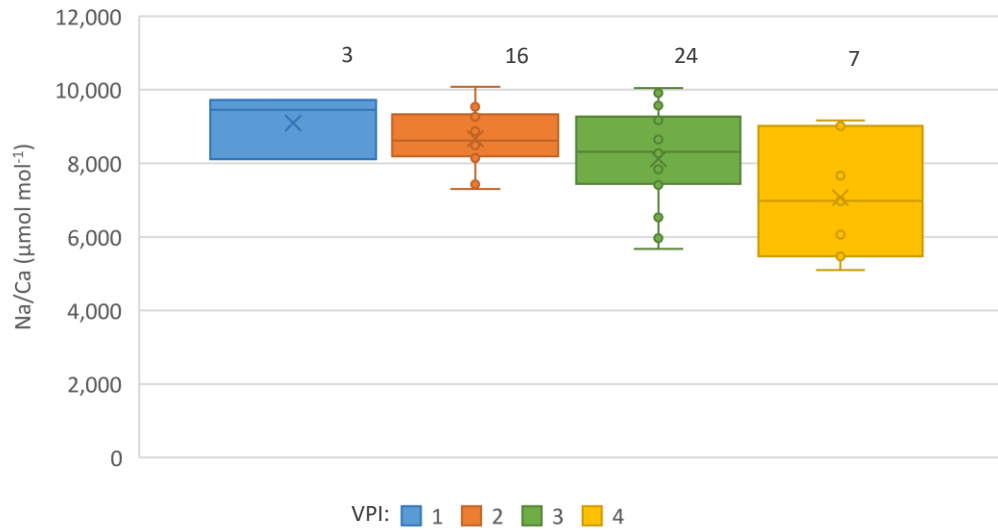


Figure 60 – Box plot of Na/Ca values for samples of different visual preservation index (VPI) values for samples taken from Li et al. (2012), where 1 = best preserved and 5 = completely altered. For each box plot, the number of samples (n) is indicated next to each box.

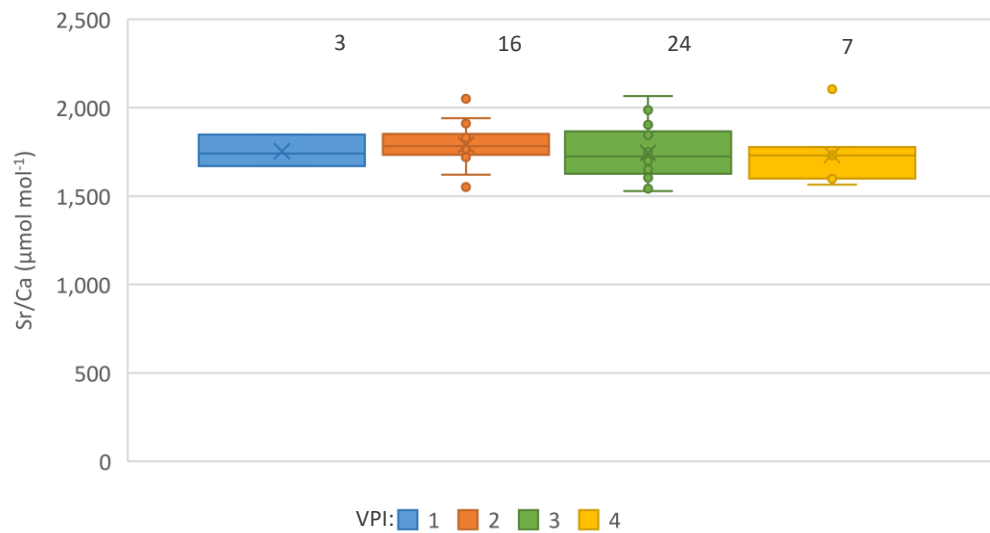


Figure 61 - Box plot of Sr/Ca values for samples of different visual preservation index (VPI) values for samples taken from Li et al. (2012), where 1 = best preserved and 5 = completely altered. For each box plot, the number of samples (n) is indicated next to each box.

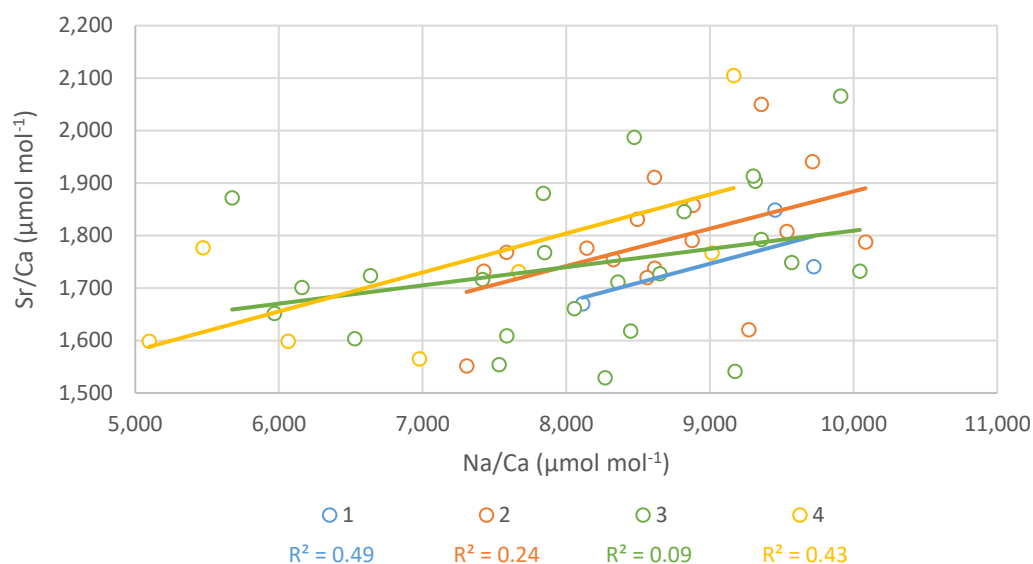


Figure 62 - Na/Ca against Sr/Ca for belemnite samples from Li et al. (2012), for different visual preservation index (VPI) values (where 1 = best preserved and 5 = completely altered). For each VPI value, a linear line of best fit was applied and a corresponding  $R^2$  value is shown adjacent to the legend in a colour corresponding to the marker colour for each VPI.

#### 5.4.1.2. Temperature and salinity

A few studies suggested that Na/Ca values in belemnites may be related to palaeotemperature, due to some observed covariance between Mg/Ca,  $\delta^{18}\text{O}$  and Sr/Ca (e.g., McArthur *et al.*, 2000; 2004; 2007). As discussed in 4.5.4, despite several issues,  $\delta^{18}\text{O}$  is considered the most reliable temperature indicator in belemnite calcite and has been widely used in a number of studies to create palaeotemperature records (e.g., Wierzbowski, 2021 and references therein).  $\delta^{18}\text{O}$  is also considered to vary with salinity, so examining changes in oxygen isotopes can allow us to investigate if El/Ca values can be expected to vary with both temperature and salinity. Also, as previously discussed (section 4.5.5), Mg/Ca is related to temperature in many biogenic carbonates, though in belemnites this is not always the case (e.g., Rosales *et al.*, 2004; McArthur *et al.*, 2007a; Armendáriz *et al.*, 2008; Wierzbowski and Rogov, 2011; Li *et al.*, 2013; Stevens *et al.*, 2014). In samples from this study, comparison to  $\delta^{18}\text{O}$  showed that Mg/Ca was a reasonable temperature proxy for samples from Bulgaria, but not in any of the other locations studied (Figure 39). Sr/Ca in biogenic carbonates is also considered to vary with temperature (e.g., Villiers *et al.*, 1994; Rosenthal *et al.*, 1997; Ingram *et al.*, 1998; Sinclair *et al.*, 1998; Freitas *et al.*, 2005; Irie and Suzuki, 2020) and several studies have demonstrated the use of Sr/Ca ratios as a palaeotemperature proxy in belemnites (e.g., McArthur *et al.*, 2000; 2004; Rosales *et al.*, 2004; Wierzbowski and Joachimski (2009); Ullmann *et al.* (2014)). McArthur *et al.* (2007a) even suggested that Sr/Ca is a more reliable temperature proxy than Mg/Ca as it was not shown to vary between individuals or species – though it did vary between individuals and species in the data in this study (Figure 19).

Sr/Ca and Na/Ca have already been demonstrated to covary in samples from this study and previous belemnite analyses (Figure 46; Figure 57). Sr/Ca has also been demonstrated to give lower values in altered samples from this study and McArthur *et al.* (2007a) (Figure 58), though this was not seen in samples from Li *et al.* (2012) (Figure 61) or in altered samples from this study (Figure 57). There was also positive correlation between Sr/Ca and Na/Ca within samples of the same preservation bracket (VPI values) in samples from Li *et al.* (2012) (Figure 62), which suggests that an additional factor, other than diagenetic alteration, is controlling the correlation between Na/Ca and Sr/Ca. To investigate the potential link between Na/Ca and temperature or salinity, Na/Ca values were compared to Mg/Ca and  $\delta^{18}\text{O}$  values for samples from this study (Figure 48; Figure 49) and previous studied (Figure 63; Figure 65).

There was no significant correlation between  $\delta^{18}\text{O}$  and Na/Ca in samples from this study for any of the locations (Figure 48). In samples from previous studies, there was a weak positive correlation between  $\delta^{18}\text{O}$  and Na/Ca in samples from McArthur *et al.* (2007a) ( $R^2 = 0.29$ ); but there was no significant correlation between  $\delta^{18}\text{O}$  and Na/Ca in samples from other studies, or in the samples overall (Figure 63).

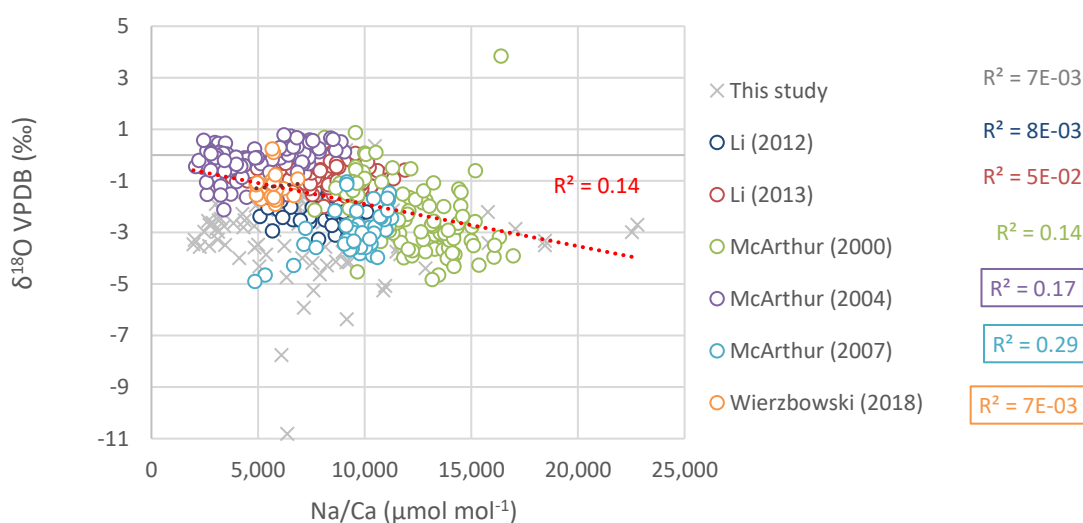


Figure 63 - Na/Ca against  $\delta^{18}\text{O}$  values compared to the Vienna Pee Dee Belemnite (VPDB) for screened samples from this study [crosses; pale grey] and some previous studies (circles). An  $R^2$  value (assuming a linear line of best fit, not shown) for each set of samples is displayed in a colour corresponding to the sample marker. An overall linear line of best fit and corresponding  $R^2$  value is also shown (red); where there is a positive correlation between Na/Ca and  $\delta^{18}\text{O}$  (McArthur *et al.* (2004); McArthur *et al.* (2007a); Wierzbowski *et al.* (2018)) the  $R^2$  value is shown with a border.

Mg/Ca was then compared to  $\delta^{18}\text{O}$  to determine if magnesium in each study was likely to vary with temperature or salinity (Figure 64). There was a weak negative correlation between  $\delta^{18}\text{O}$  and Mg/Ca in the data overall ( $R^2 = 0.29$ ), and in samples from McArthur *et al.* (2000) ( $R^2 = 0.30$ ); there was a weak positive correlation between  $\delta^{18}\text{O}$  and Mg/Ca in samples from

McArthur *et al.* (2007a) ( $R^2 = 0.27$ ) (Figure 64). This suggests that, as with data from this study (Figure 39), Mg/Ca was related to temperature and/or salinity in some time-periods and regions, but not all.

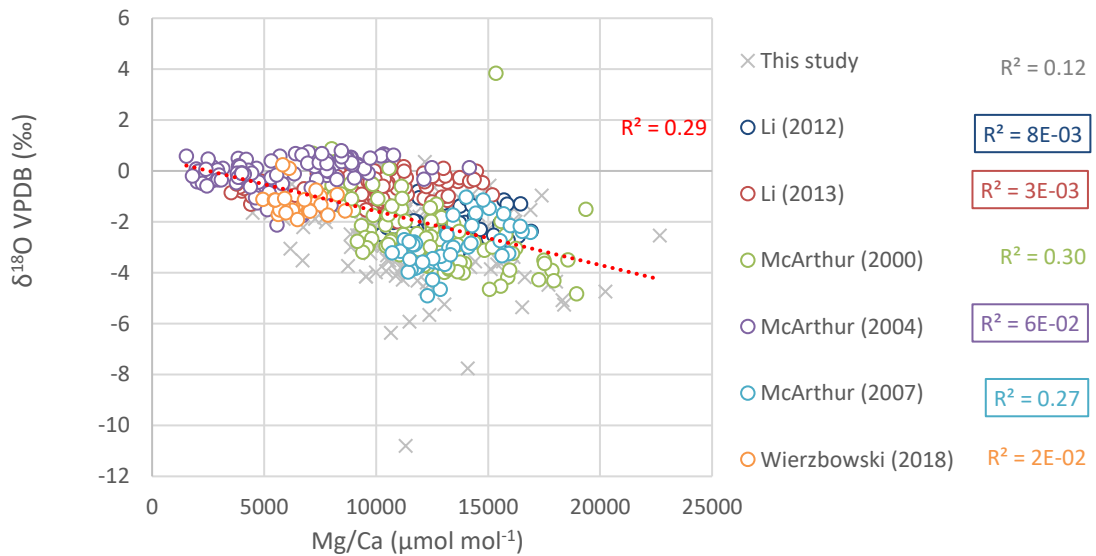


Figure 64 - Mg/Ca against  $\delta^{18}O$  values compared to the Vienna Pee Dee Belemnite (VPDB) for screened samples from this study [crosses; pale grey] and some previous studies (circles). An  $R^2$  value (assuming a linear line of best fit, not shown) for each set of samples is displayed in a colour corresponding to the sample marker. An overall linear line of best fit and corresponding  $R^2$  value is also shown (red); where there is a positive correlation between Mg/Ca and  $\delta^{18}O$  (Li *et al.* (2012); Li *et al.* (2013); McArthur *et al.* (2004); McArthur *et al.* (2007a)) the  $R^2$  value is shown with a border.

Mg/Ca values were then compared to Na/Ca values, and there was positive correlation between Na/Ca and Mg/Ca in Li *et al.* (2013) ( $R^2 = 0.47$ ), McArthur *et al.* (2000) ( $R^2 = 0.25$ , very weak correlation), McArthur *et al.* (2004) ( $R^2 = 0.72$ ), Wierzbowski *et al.* (2018) ( $R^2 = 0.57$ ) and a very weak correlation in the data overall ( $R^2 = 0.27$ ) (Figure 65). There was no significant correlation between Na/Ca and Mg/Ca in samples from this study ( $R^2 = 2E-02$ ), Li *et al.* (2012) ( $R^2 = 2E-02$ ) or McArthur *et al.* (2007a) ( $R^2 = 2E-02$ ) (Figure 65). This correlation was present even in samples from studies which had demonstrated no variation between  $\delta^{18}O$  and Mg/Ca, suggesting that the reason behind the covariation of Na/Ca and Mg/Ca was unrelated to changes in temperature and salinity. This indicates that it is possible that Mg and Na incorporation are linked by a mineralogical effect, similar to the effect described for the incorporation of phosphorus (4.5.5). Alternatively, as Na/Ca varied with Sr/Ca – potentially due to diagenesis – it is possible that Mg/Ca is also variable with diagenetic alteration. It is almost certainly the case that diagenetic alteration does affect Mg concentrations in some way, but the recrystallisation pathways of Mg are complex and the endmember Mg/Ca is often

intermediate to low-Mg calcite composition, so altered levels of Mg can be difficult to interpret.

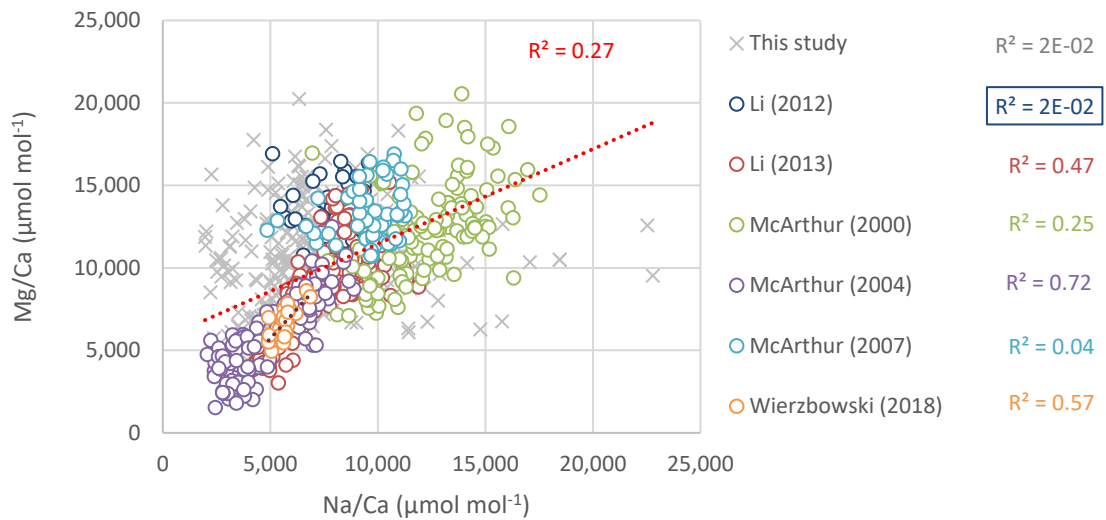


Figure 65 - Mg/Ca against Na/Ca values for screened samples from this study [crosses; pale grey] and some previous studies (circles). An  $R^2$  value (assuming a linear line of best fit, not shown) for each set of samples is displayed in a colour corresponding to the sample marker. An overall linear line of best fit and corresponding  $R^2$  value is also shown (red); where there is a negative correlation between Mg/Ca and Na/Ca (Li et al. (2012)) the  $R^2$  value is shown with a border.

To investigate if Mg/Ca shows variance with diagenetic alteration in the samples studied here, Mg/Ca values for altered and unaltered samples from McArthur *et al.* (2007a) were compared for both species studied (*Acrocoelites (Odontobelus) vulgaris* and *Acrocoelites (Acrocoelites) subtenuis*) (Figure 66). McArthur *et al.* (2007a) was used as the samples represent a 'snapshot' in time so should not include temperature variations. This showed that there was no difference in Mg/Ca between altered and 'unaltered' samples, indicating that diagenesis was not affecting Mg/Ca ratios in this case (Figure 66).

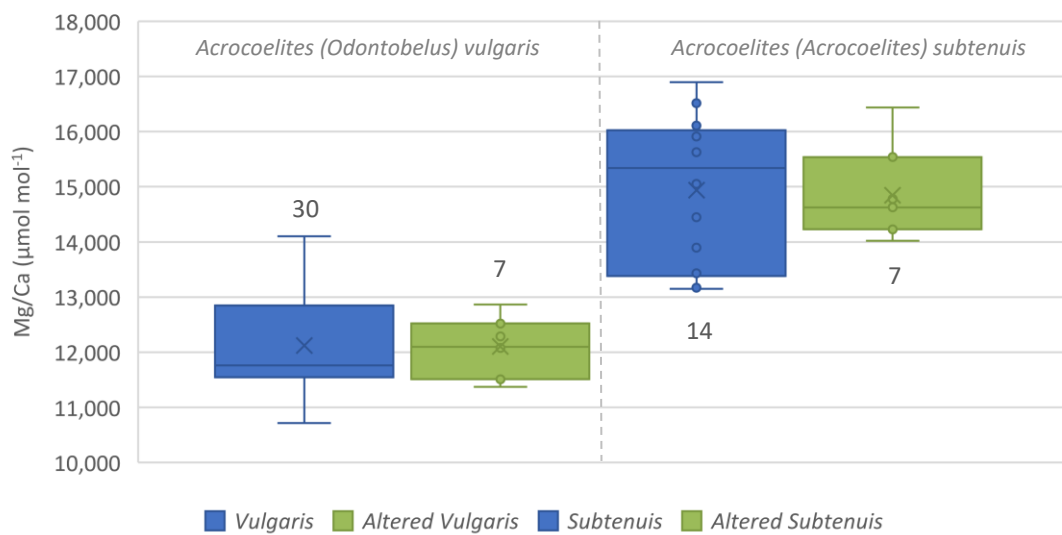


Figure 66 - Box plot of Mg/Ca for values for altered and 'unaltered' samples from McArthur *et al.* (2007). Samples are of two different species, shown separately ('Vulgaris' = *Acrocoelites (Odontobelus) vulgaris*; 'Subtenuis' = *Acrocoelites (Acrocoelites) subtenuis*). For each box plot, the number of samples (n) is indicated next to each box.

#### 5.4.2. Ratio to sodium

It was also observed that in sample from this study, in some cases elements given as ratios to Na rather than to Ca (i.e., El/Na rather than El/Ca), improved the correlation between some elements – in particular Sr and Mg, and Mg and P (Figure 51; Figure 52). There was also a correlation between Mg/Na and Sr/Na in data from several previous studies, in the data overall ( $R^2 = 0.49$ ) and in individual studies, particularly Li *et al.* (2012) ( $R^2 = 0.54$ ); McArthur *et al.* (2000) ( $R^2 = 0.47$ ) and McArthur *et al.* (2007a) ( $R^2 = 0.48$ ) (Figure 67).

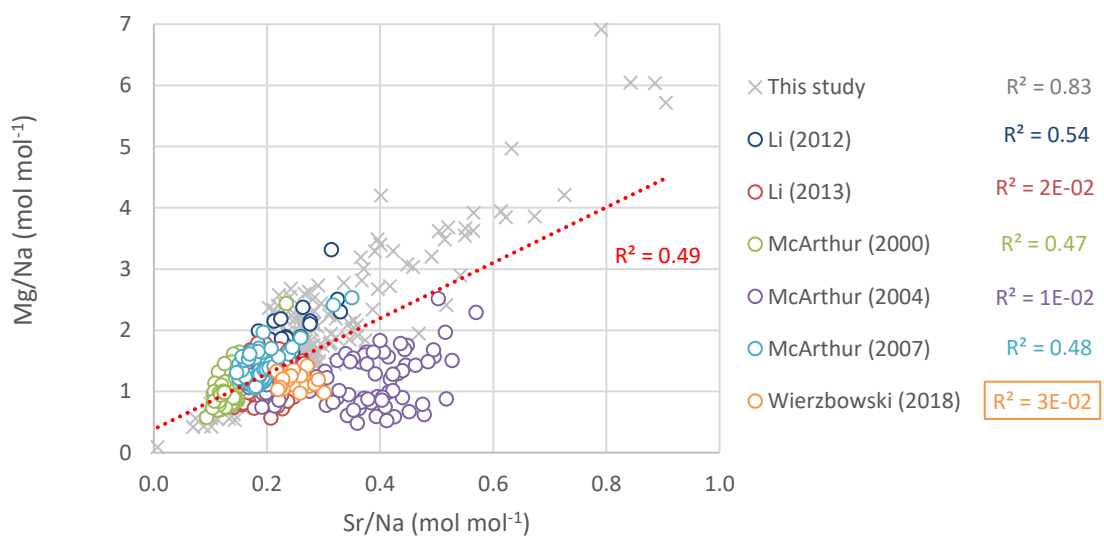


Figure 67 - Mg/Na against Sr/Na values for screened samples from this study [crosses; pale grey] and some previous studies (circles). An  $R^2$  value (assuming a linear line of best fit, not shown) for each set of samples is displayed in a colour corresponding to the sample marker. An overall linear line of best fit and

corresponding  $R^2$  value is also shown (red); where there is a negative correlation between Mg/Na against Sr/Na (Wierzbowski et al. (2018)) the  $R^2$  value is shown with a border.

This was compared to the strength of the correlation between Mg/Ca and Sr/Ca (Figure 68; Table 28). It was shown that Mg and Sr values given as ratios to Na increased the strength of the correlation compared to when they were given as ratios to Ca for the majority of studies, including samples from this study (El/Ca:  $R^2 = 0.41$ ; El/Na:  $R^2 = 0.83$ ), altered samples from this study (El/Ca:  $R^2 = 0.23$ ; El/Na:  $R^2 = 0.75$ ), Li et al. (2012) (El/Ca:  $R^2 = 0.02$ ; El/Na:  $R^2 = 0.54$ ), McArthur et al. (2007a) (El/Ca:  $R^2 = 0.14$ ; El/Na:  $R^2 = 0.48$ ) and in the data overall (El/Ca:  $R^2 = 0.45$ ; El/Na:  $R^2 = 0.49$ ) (Figure 67; Figure 68; Table 28).

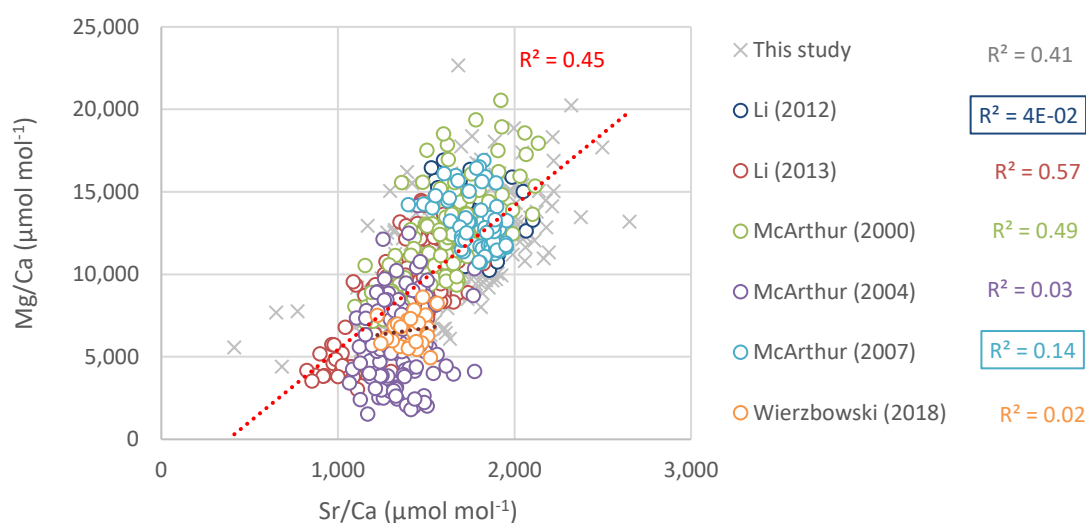


Figure 68 - Mg/Ca against Sr/Ca values for screened samples from this study [crosses; pale grey] and some previous studies (circles). An  $R^2$  value (assuming a linear line of best fit, not shown) for each set of samples is displayed in a colour corresponding to the sample marker. An overall linear line of best fit and corresponding  $R^2$  value is also shown (red); where there is a negative correlation between Mg/Ca against Sr/Ca (Li et al (2012); McArthur et al. (2007a)) the  $R^2$  value is shown with a border.

As there is a positive correlation between Mg/Ca and Sr/Ca in the majority of studies, albeit a weaker one than the correlation between Mg/Na and Sr/Na (Figure 67; Figure 68; Table 28), this suggests that the correlation between Mg/Na and Sr/Na is partially controlled by the relationship between Mg and Sr in belemnite calcite. Giving elements as ratios to Na rather than Ca appears to reduce the scatter of the data and increase the strength correlation in most datasets available (Figure 67; Figure 68; Table 28). There is no pattern in the studies which show this behaviour and those that don't (i.e., they aren't the studies which show Mg varying with  $\delta^{18}\text{O}$ , or studies which use samples from the same time periods), so more work needs to be done to try and establish why this doesn't happen in some datasets (Table 27; Figure 67; Figure 68; Table 28).

The reason why giving elements as ratios to Na rather than Ca improves the strength of the correlation between element ratios remains unclear, particularly as Sr has been shown to vary with the level of diagenetic alteration (Figure 58; Figure 61), but Mg has not (Figure 66). It seems likely that there is a mineralogical control which is exerted across multiple ions, Mg, Sr, Na and Ca and affects the incorporation of each of these elements in turn. This is similar to the mechanism which was determined for phosphorus, where the incorporation of phosphorus appeared to be dominantly controlled by the incorporation of magnesium (4.5.5). In the dataset from this study, it was observed that giving P and Mg values as a ratio to Na also increased the strength of the correlation between P and Mg compared with ratios to Ca (Figure 52). This suggests that if there is a multi-element system control on the ratios of incorporation of different elements, phosphate may form part of the system too. Unfortunately, phosphorus has not been measured in any of the previous studies which have reported Na values, so these cannot be used to interrogate this relationship. Other elements are likely needed to be studied to fully characterise this system, particularly other anions which are commonly substituted into calcite, such as sulfate and chloride.

#### 5.4.3. What information might Na values contain?

In this study, Na/Ca records were generated for three different locations in the Laurasian Seaway – North Yorkshire, North Wales, and Bulgaria (Figure 47). The Na/Ca records in each location were similar, with values ranging from around 2,500 to 25,000  $\mu\text{mol mol}^{-1}$ , and t tests showed there were no statistically significant differences between any of the locations studied (Figure 47). As with P/Ca, the records were noisy but did show coherent stratigraphic trends in Na/Ca within each location, though trends differed between locations (Figure 47). When the magnitudes of the stratigraphic changes in Na/Ca were compared to two standard deviations of Na/Ca values within a stratigraphic level (taken from 77 samples from 6 belemnites of four different species from Penny Nab, taken from the Variability Samples (2.3.2) it was shown that the stratigraphic changes in Na/Ca were greater than could be explained by the natural variability of Na/Ca within and between individuals (Figure 47).

There were similarities in the records between locations, for example in Yorkshire and North Wales there were similar Na/Ca values for samples in both locations during the Pliensbachian, which were higher than the baseline values in the samples from Bulgaria in the lowermost Toarcian (Figure 47). There were then lower Na/Ca values in both Yorkshire and North Wales in the lower Toarcian, though in Yorkshire these values gradually increased for the remainder of the Toarcian while in North Wales they remained constant. The similarities between the Yorkshire and North Wales Na/Ca records, and coherent changes in Na/Ca suggest that Na/Ca

may be suitable for use as a proxy, though there is debate about the factors which affect Na concentrations in belemnites and biogenic carbonates more widely.

Though there are apparent mineralogical factors which affect the incorporation of Na, alongside Mg, Sr, Ca, and possibly other ions, it is possible that Na concentrations in calcite also vary according to further environmental factors. If this is the case, Na concentrations may contain information which, when the mineralogical relationships are understood, could be used to investigate environmental changes. This would also explain why there appear to be coherent changes in Na/Ca ratios through time (Figure 47). It may also help explain the similarities in the Na/Ca ratios between North Wales and Yorkshire (Figure 47). If this is the case, the differences between Bulgaria and the other sites studied may be a result of differences in regional environmental conditions (Figure 47).

It has already been demonstrated that Na/Ca ratios do not vary with  $\delta^{18}\text{O}$ , suggesting that there is no relationship between Na incorporation and either salinity or temperature (Figure 48; Figure 63). Recent work on sodium in foraminifera has suggested that Na/Ca ratios are related to water column calcium concentration (e.g., Evans *et al.*, 2018; Hauzer *et al.*, 2018; Evans *et al.*, 2020; Zhou *et al.*, 2021; Gray *et al.*, 2023; Nambiar *et al.*, 2023). Na/Ca in foraminifera has also been shown to vary weakly with other factors such as salinity, temperature, and carbonate ion concentration – though by far the strongest relationship was with calcium ion concentration, suggesting that changes in other environmental factors would not complicate seawater [Ca] reconstructions (Gray *et al.*, 2023).

The potential relationship between seawater [Ca] and carbonate Na/Ca has yet to be investigated in other carbonates such as belemnites, and cannot be investigated within the bounds of this study due to the lack of seawater [Ca] data to compare to the belemnite Na/Ca. Nevertheless, the prospect of generating a long-term seawater [Ca] record using belemnites is exciting, as there are very few proxies to investigate major ion seawater chemistry throughout time. If Na/Ca values in belemnite did record seawater calcium concentrations, then the datasets generated by this study and past studies would already form the basis of a significant record of major ocean ion chemistry across a large timescale (Figure 47; Table 27). Though more work would need to be done to unravel the influences of mineralogical relationships on the incorporations of different ions, if the data produced in this study is examined for potential evidence of changes in calcium concentrations, the coherent changes in the records, particularly in Yorkshire, could contain exciting information. The sharp increase in Na/Ca values at the Pliensbachian-Toarcian boundaries, followed by a decrease would be likely to represent a sudden fall in Ca concentrations at the boundary, followed immediately by an increase (Figure 47). The gradual increase in Na/Ca concentrations throughout the remainder

of the Toarcian would then be representative of a gradual decline in Ca concentrations through the same time period (Figure 47). The differences between the different study basins, particularly the Bulgarian samples, could potentially be explained by Na/Ca responding to regional variations in Ca concentrations. There are several factors which could affect ocean Ca concentrations independent of Na, including inducing regional variations. For example, increased weathering – especially of carbonates – can deposit greater quantities of Ca into the ocean. Deposition of calcium carbonates or calcium sulfate would remove Ca from the water column. The TOAE is understood to be a time of ocean acidification, which would likely increase ocean calcium concentration, though concurrent evaporite formation would decrease oceanic Ca (e.g., Trecalli *et al.*, 2012; Müller *et al.*, 2020). Examining the potential contributions of these processes across the time interval and locations studied, as well as other factors, such as the positioning of carbonate platforms in the Laurasian Seaway, may lead to insight into the factors affecting belemnite Na/Ca ratios in the samples studied here, and potentially lead to the extraction of environmental information related to early Jurassic seawater chemistry.

While this initial interpretation of the Na/Ca data as a proxy for [Ca] is exciting, to have any confidence in any potential interpretations of the Na concentrations, it would be necessary to understand the mineralogical relationships affecting the incorporations across multiple elements. This study has demonstrated that there are likely to be inter-connected relationships between the incorporation of multiple elements, including Na, Sr, Mg, Ca, and other ions such as P. Not included here, is an investigation of the impacts of other major substituted anions such as sulfate, as well as chloride which has been shown to spatially covary with Na in electron-microprobe element mapping studies (Florek *et al.*, 2004). Further work to understand the mineralogical relationships across the full range of major, minor and trace element incorporations, likely including the production of synthetic carbonates in a range of conditions, is needed to allow confident interpretations of a range of proxies in belemnite calcite, and other biogenic and abiogenic carbonates. Further work investigating modern and ancient biogenic carbonates of different species may also be useful to determine if the co-variations of elements described here is purely mineralogical, or also influenced by an organism's biology and biotic controls.

Table 28 - Summary of  $R^2$  values for relationships between key elemental and isotopic ratios relating to the factors behind the incorporation of sodium in each of the studies (mainly diagenesis, temperature, strontium and magnesium and factors affecting strontium and magnesium incorporation) where the data has been reinterpreted here. Colours are used to denote the direction of correlation; cells with an orange border (and orange fill) denote negative correlation; samples with no border (and green fill) denote positive correlations. The darkness of colours is used to represent the strength of correlation: dark green/orange =  $R^2 > 0.8$ ; mid-green/orange =  $R^2 > 0.5$ ; pale green/orange  $R^2 > 0.3$ .

Study	Mn/Ca vs Fe/Ca	Mn/Ca vs Na/Ca	Fe/Ca vs Na/Ca	Mg/Ca vs $\delta^{18}\text{O}$	Sr/Ca vs $\delta^{18}\text{O}$	Na/Ca vs $\delta^{18}\text{O}$	Sr/Ca vs Na/Ca	Mg/Ca vs Na/Ca	Sr/Ca vs Mg/Ca	Sr/Na vs Mg/Na
<b>This study</b>	0.17	1E-03	2E-02	0.12	0.41	7E-03	0.14	2E-02	0.41	0.83
<b>This study (altered)</b>	0.17	1E-02	0.18	4E-02	8E-02	0.27	0.89	3E-02	0.23	0.75
<b>Li (2012)</b>	-	5E-03	7E-02	8E-03	0.31	8E-03	0.19	2E-02	4E-02	0.54
<b>Li (2013)</b>	0.28	0.19	3E-02	3E-03	5E-02	5E-02	0.53	0.47	0.57	2E-02
<b>McArthur (2000)</b>	0.62	1E-02	2E-02	0.30	0.25	0.14	0.53	0.25	0.49	0.47
<b>McArthur (2004)</b>	0.06	3E-02	2E-02	6E-02	2E-03	0.17	0.17	0.72	3E-02	1E-02
<b>McArthur (2007)</b>	0.87	2E-02	7E-04	0.27	0.18	0.29	0.15	0.04	0.14	0.48
<b>Wierzbowski (2013)</b>	-	1E-02	-	2E-02	0.15	7E-03	5E-02	0.57	2E-02	3E-02
<b>Overall (excluding this study altered)</b>	0.34	7E-04	4E-03	0.29	0.29	0.14	0.22	0.27	0.45	0.49

## 5.5. Conclusions

In each of the locations studied in the Laurasian Seaway, there were coherent changes in Na/Ca (Figure 47). There were also observable similarities between Na/Ca records in different locations – which indicate the potential utility of Na/Ca as a palaeoproxy.

The factors affecting Na/Ca values in belemnite calcite were investigated, and it was shown that temperature or salinity does not appear to be a dominant control on Na incorporation into calcite, as Na/Ca has no significant correlation with  $\delta^{18}\text{O}$ . Na/Ca was compared to common proxies for diagenetic alteration such as Mn/Ca, Fe/Ca, Sr/Ca and visual markers of alteration (McArthur *et al.*, 2007a; Li *et al.*, 2012) to investigate the impact of diagenesis on Na/Ca. It was shown that, in general, visually altered samples had lower Na/Ca values (Figure 58; Figure 60). There was no significant correlation between Mn/Ca and Fe/Ca in screened samples – suggesting that Na may be a more sensitive diagenetic proxy than the commonly used Fe and Mn (Figure 55; Figure 56). Sr correlated with Na in screened samples, and comparison of altered and ‘unaltered’ sample groups showed that Sr/Ca was lost in a similar way to Na, though proportionally the loss was smaller (Figure 50; Figure 57; Figure 58; Figure 60; Figure 61). This indicates that it is possible that Na/Ca is a much more sensitive proxy for freshwater diagenetic alteration of calcite than Mn or Fe, and Sr falls somewhere in the middle. Overall, the impact of diagenesis on minor and trace elements has been understudied, and there is little understanding of the impact of different mechanisms or forms of diagenesis on calcite’s elemental composition. Examining concentrations of Mn, Fe, Ca, Sr, and Na in previous studies has also demonstrated that there are inconsistencies in the application of purely visual screening techniques, and that a more thorough review of the impacts of different methods of screening on results would be beneficial. It is possible that geochemical screening methods, potentially applying Na/Ca and/or Sr/Ca screening limits, may be an important feature of any future standardised sample screening method.

A positive relationship was also found between Na/Ca and Mg/Ca – which was unrelated to diagenetic alteration (Figure 49; Figure 65; Figure 66). Mg/Ca and Sr/Ca were also both found to be unrelated to changes in palaeotemperature (Figure 64; Table 28). Sr/Ca and Mg/Ca were positively correlated with each other though, a correlation which was strengthened across multiple datasets by ratios to Na (El/Na rather than El/Ca) (Figure 50; Figure 51; Figure 67; Figure 68). In samples from this study, ratios to Na rather than Ca, also improved the relationship between Mg and P (Figure 52). All of this indicates potential co-relationships between the incorporation of multiple elements into belemnite calcite. These relationships may be purely mineralogical, may rely on biotic effects, or which could be at least partially

organism specific. Further research into potential co-relationships for the incorporation of different ions into biogenic and abiogenic carbonates is a priority to fully understand or interpret any proxy data based on them. This may involve production and analysis of laboratory grown carbonates under different conditions, and element mapping studies of abiogenic and modern and ancient biogenic carbonates. It would also be important to consider possible impact of the dominant substituted anions, such as phosphate, sulfate, and also more minor anions such as chloride – which has been shown to vary spatially with Na (Florek *et al.*, 2004).

The strength of the correlation between Na and Mg indicates that it is likely that Na varies with factors other than diagenetic alteration (Figure 49; Figure 65; Figure 67). This is supported by the presence of coherent trends in Na/Ca through time in multiple locations, as well as the similarities between Na/Ca records for Yorkshire and North Wales (Figure 47). One exciting possibility is that Na/Ca in belemnites varies with water-column calcium ion concentration, as has been observed in recent work on foraminifera (Evans *et al.*, 2018; Hauzer *et al.*, 2018; Evans *et al.*, 2020; Zhou *et al.*, 2021; Gray *et al.*, 2023; Nambiar *et al.*, 2023). This would open up the possibility of investigating long-term changes in major-ion seawater chemistry, for which there are few existing proxies. To ensure the validity of the interpretation, further work would be required to explain the timing, direction and magnitude of the trends observed in the Na/Ca records, and the lower baseline Na/Ca values (implied higher Ca values) which were recorded in samples from Bulgaria (Figure 47). It would also be important to gain a more complete understanding of the inter-connected relationships of Na and other ions in the calcite, to determine the bounds of interpretation which are likely to be possible and valid.

## 6. Conclusions and further work

This section summarises the broad findings of this project and identifies opportunities for further study based on the results presented.

### 6.1. Impacts of preparative methods

Different preparative methods were tested on belemnite calcite, including oxidative and non-oxidative cleaning methods, and weak and strong acids for dissolution. Different preparative methods were found to affect the measured values of phosphorus, as well as other elements from the samples due to the interactions of different preparative methods with 'contaminant' phases in the samples.

For phosphorus, oxidative cleaning methods released phosphate from organic matter and caused it to re-adsorb to the surface of the powder, particularly where higher concentrations of iron-containing minerals were present. Different dissolution methods also impacted measured phosphorus concentrations, with strong acids dissolving more 'contaminant' phases of phosphorus -such as phosphorus in apatite and iron-bound phosphorus. For other elements, in samples with high organic matter content (Modern Analogue Samples) oxidative cleaning methods gave lower measured concentrations of Mg but did not affect measurements of Sr or Na values. The samples which were most affected by differences in preparative method were samples with high levels of 'contaminant' phases. In this study these were Modern Analogue Samples which contained high levels of organic matter, or samples which contained non-carbonate phases or sediment with high levels of iron in it.

This has implications for studies focussing on elemental concentrations across all carbonates, particularly for samples which are likely to have higher concentrations of non-carbonate phases. This may be of particular importance for studies on bulk-rock carbonates (e.g., CAP studies on bulk rock [Dodd *et al.*, 2021; 2023]), which are likely to have higher levels of apatite and iron-bound phosphorus than are present in biogenic carbonates. It is also important in the study of modern biogenic carbonates, which are likely to have higher levels of organic matter which may be broken down by oxidative treatments. In order to ensure carbonate EI/Ca ratios are representative of only carbonate-associated signals, care should be taken to characterise any 'contaminant' phases and identify suitable preparative methods to reduce their impact on the final EI/Ca values.

To ensure that future studies investigating CAP, as well as other EI/Ca ratios in carbonates are reflective of the carbonate-associated pools of the target element, care should be taken to characterise and quantify the 'contaminants' in the sample. This includes quantifying the

different forms of the target element in the sample, but also other minerals which could interact with the target element. For example, to determine the impact of contaminant phases on CAP measurements, quantifying the different pools of phosphorus in the sample (for example by phosphorus speciation (Thompson *et al.*, 2019) would be helpful, but it would also be helpful to quantify iron-containing minerals which free phosphate may adhere to. Once contaminant phases have been identified and quantified, steps can be taken to determine the most appropriate preparative method to minimise the impact of the contaminant phases on the El/Ca measurements. For organic matter, this may include using oxidative cleaning methods to remove organic matter from samples, possibly followed by high salinity washes (such as  $\text{MgCl}_2$  or NaCl) to remove readsorbed ions (which is particularly an issue for phosphorus (e.g., Thompson *et al.*, 2019; Dodd *et al.*, 2021). For other forms of contamination, it may include using a weak acid to avoid breaking down non-carbonate minerals in the sample.

## 6.2. Natural variability of elements

Data from this study indicates that there is significant variability of El/Ca ratios within belemnites, including for phosphorus, magnesium, and sodium. This indicates the importance of consistent sampling practice which target the same region of the belemnite rostra. This study focussed on variations in P/Ca along the belemnite rostra, while several previous studies have demonstrated differences in El/Ca values based on radial distance from the apical line (e.g., McArthur *et al.*, 2007a; Sørensen *et al.*, 2015; Ullmann *et al.*, 2015; Hoffmann *et al.*, 2019) or between growth bands (Dutton *et al.*, 2007; Hoffmann *et al.*, 2016; Hoffmann and Stevens, 2020). Completing similar studies for phosphorus, and other elements of interest such as sodium, would help to develop ideas around where these elements sit in the rostra. A wider variety of element mapping studies, focussing on a wider range of elements, including phosphorus and sodium, would be useful to examine the distribution and develop ideas around their incorporation. For example, some trace elements may be found to be associated with cracks in the crystal structure, suggesting later addition as contaminants, or defects which may increase primary incorporation of ions such as sulfate, or may be closely spatially associated with higher concentrations of organic matter in the darker growth bands, suggesting a potentially organic-associated phase.

There were determined to be differences in phosphorus concentrations between individual belemnites, which were unrelated to species differences, and potentially related to small differences in the habitats and habits of individuals. Species differences were found to be significant for other elements, such as Mg and Sr, while no differences between individuals was found for sodium. As this study indicated that P incorporation is likely to be linked to

magnesium concentrations, it is curious that Mg should show species-specific differences while P does not. Further investigation into the factors affecting differences between individuals could be conducted using modern carbonates, including the potential to use organisms raised in specific controlled conditions. Differences between belemnites and other bio-calcifying organisms should also be investigated. While some studies have conducted preliminary investigations on CAP in foraminifera and brachiopods, no attempt has been made to identify species-specific vital effects in CAP for these groups (e.g., Dodd *et al.*, 2021). Developing an understanding of the potential vital effects in these groups, particularly in brachiopods, may extend the applicability carbonate proxy records, such as CAP and Na/Ca, to significant portions of Earth's history, from the earliest emergence of brachiopods in the early Cambrian to the present day.

### 6.3. Stratigraphic variation of El/Ca and relationships between elements

This study investigated the variation of El/Ca through time across the Early Jurassic. For both Na/Ca and P/Ca, coherent changes were identified through time, with similarities between different study locations identified. This indicates the potential of both P and Na in belemnite calcite to act as proxies which reflect changing environmental conditions. For phosphorus, covariation of P with redox state in some regions, and temperature in others, suggested that belemnite CAP may be a suitable proxy for water column phosphorus, in a time period with differing regional controls on water-column phosphorus. Sodium varied with Sr/Ca ratios in both altered and screened samples, indicating its potential as a sensitive proxy for diagenetic alteration. Within diagenetically screened samples, coherent changes in Na/Ca were unrelated to changing temperature or salinity, so may represent another changing environmental factor such as Ca concentration (which Na/Ca has been shown to represent in foraminifera (Evans *et al.*, 2018; Hauzer *et al.*, 2018; Evans *et al.*, 2020; Zhou *et al.*, 2021; Gray *et al.*, 2023; Nambiar *et al.*, 2023)).

For both P and Na, this study indicated interconnected relationships in the concentrations of multiple elements in belemnite calcite, including Mg, Sr, P, Na, Ca. There are also likely to be relationships with other components, including components not measured here such as organic matter and anions including sulfate and chlorine (which has been shown to vary spatially with Na in belemnites). Further work is required to investigate the factors affecting these interconnected relationships, in order for environmental signals contained within the carbonate to be extracted and interpreted. I suggest the first step to understanding the relationships between the different components is to fully characterise belemnite calcite for specimens with a range of compositions. This includes the quantification of the ions discussed here, as well as other cations (such as barium potassium, lithium [though these are trace

elements and less likely to have an influence on the calcite charge], anions (such as carbonate, sulfate, and chlorine) and organic matter. Once data has been obtained for belemnites with a range of compositions, examining covariance between different components can begin to unravel the relationships between the components. This can be paired with element mapping studies, which can demonstrate spatial links between elements, and XRD which can be used to investigate the impacts of different ions on the calcite unit cell parameters and unit cell strain.

The cause of the apparent covariations between elements in belemnite carbonate could not be established using the data in this study, but it is possible that the relationships are based on mineralogical effects, biotic effects, or the effects of diagenetic alteration which are not picked up by conventional screening methods. If the observed covariations of elements are based on mineralogical factors which affect the incorporation of elements into calcite, then it is likely that these effects will be observed in other carbonates as well as belemnites. To investigate the factors controlling the relationships between the incorporation of different elements in belemnites and carbonates more widely, a number of different techniques could be applied:

1. Mapping of the spatial distribution of different components in belemnites (similar to that conducted for P, Mg, Sr, organic matter, and Mg (Hoffmann *et al.*, 2016; Hoffmann and Stephens, 2021)) may help to develop ideas around which elements are associated with other elements, and more likely be exerting influence on their concentration. Florek *et al.* (2004) found that Na and Cl, which was not measured in this study, had similar distribution in belemnite calcite so extending these element mapping techniques to trace elements and anions would help to determine which elements are likely to affect the incorporation of other elements.
2. Interconnected elemental relationships could also be examined in other biogenic carbonates, such as foraminifera, corals, and brachiopods to determine if any biological control on the relationships between elements is specific to belemnites, or present in calcifying organisms more widely.
3. The relationships between element concentrations in natural abiotic carbonates could be investigated, including samples with variable degrees of diagenetic alteration, to determine if the interconnected relationships between elements in belemnites is related to vital effects or diagenesis.
4. Synthetic carbonates could be grown under a variety of condition and solution concentrations, to determine if the interconnected relationships between the incorporation of different elements are present in samples which are abiotic and have not undergone any transformative processes during diagenesis.

5. XRD analysis of synthetic carbonates with a range of concentrations of major, minor and trace components could be conducted to determine levels of strain and distortion in the unit cell. These factors affect the production of defects, which may be important for trace element incorporation.
6. Investigations could be conducted to investigate where the substituted ions are situated in the carbonate lattice (e.g., substituted for  $\text{Ca}^{2+}$ ,  $\text{CO}_3^{2-}$  or interstitial). This has impacts on the interconnected relationships if ions are competing for substitution into the same sites. This is particularly important for ions which have significantly different size or charge to the ion they are replacing, as this will impact unit cell strain and defect formation which impacts the incorporation of other elements.
7. XANES (X-ray Absorption Near-Edge Structure) or EXAFS (Extended X-ray Absorption Fine Structure) studies could be conducted on synthetic, abiotic, or biogenic carbonates (including belemnite calcite) to examine specific elements of interest, which would give information about the local environment for the elements selected (potentially including determining the oxidation state, coordination environment and bonding characteristics).

Once the apparent interconnected relationships affecting  $\text{El}/\text{Ca}$  ratios in belemnites and other carbonates are better understood, it may be possible to better interpret the environmental information within those ratios. This would allow the production of  $\text{CAP}$  and  $\text{Na}/\text{Ca}$  records in belemnites from the Jurassic and Cretaceous, and potentially from other carbonate records for much longer periods of time. If  $\text{P}/\text{Ca}$  could be shown to reflect water-column phosphorus concentrations, this would enable the development of a long-term record of water-column phosphorus concentrations throughout Earth's history, which could be used to enhance interpretation of past events of climate change, weathering, ocean anoxia and biotic change. Similarly,  $\text{Na}/\text{Ca}$  could be used to develop a record potentially representing ocean calcium concentrations, giving a long-term record of major ion seawater chemistry – though much more work would be required to refine both proxies and ensure their validity.

## 7. References

1. Ainsworth, N. (2015) 'Lower Jurassic foraminifera from the Llanbedr (Mochras Farm) borehole, North Wales, UK by Philip Copestake and Ben Johnson. Monograph of the Palaeontological Society', *Geological Journal*, 50(3), pp. 398-398.
2. Albeck, S., Aizenberg, J., Addadi, L. and Weiner, S. (1993) 'Interactions of Various Skeletal Intracrystalline Components with Calcite Crystals', *Journal of the American Chemical Society*, 115(25), pp. 11691-11697.
3. Alcott, L. J., Mills, B. J. W., Bekker, A. and Poulton, S. W. (2022) 'Earth's Great Oxidation Event facilitated by the rise of sedimentary phosphorus recycling', *Nature Geoscience*, 15(3), pp. 210-215.
4. Algeo, T. J. and Ingall, E. (2007) 'Sedimentary Corg:P ratios, paleocean ventilation, and Phanerozoic atmospheric pO<sub>2</sub>', *Palaeogeography, Palaeoclimatology, Palaeoecology*, 256(3-4), pp. 130-155.
5. Alkhatib, M., Qutob, M., Alkhatib, S. and Eisenhauer, A. (2022) 'Influence of precipitation rate and temperature on the partitioning of magnesium and strontium in calcite overgrowths', *Chemical Geology*, 599, pp. 120841-120841.
6. Anagnostou, E., Sherrell, R. M., Gagnon, A., Lavigne, M., Field, M. P. and McDonough, W. F. (2011) 'Seawater nutrient and carbonate ion concentrations recorded as P/Ca, Ba/Ca, and U/Ca in the deep-sea coral *Desmophyllum dianthus*', *Geochimica et Cosmochimica Acta*, 75, pp. 2529-2543.
7. Anderson, T. F. and Arthur, M. A. (1983) 'Stable Isotopes of Oxygen and Carbon and their Application to Sedimentologic and Paleoenvironmental Problems', *Stable Isotopes in Sedimentary Geology*, 10.
8. Anderson, T. F., Popp, B. N., Williams, A. C., Ho, L. Z. and Hudson, J. D. (1994) 'The stable isotopic records of fossils from the Peterborough Member, Oxford Clay Formation (Jurassic), UK: palaeoenvironmental implications', *Journal of the Geological Society*, 151(1), pp. 125-138.
9. Arend, K. K., Beletsky, D., DePinto, J. V., Ludsin, S. A., Roberts, J. J., Rucinski, D. K., Scavia, D., Schwab, D. J. and Höök, T. O. (2011) 'Seasonal and interannual effects of hypoxia on fish habitat quality in central Lake Erie', *Freshwater Biology*, 56(2), pp. 366-383.
10. Armendáriz, M., Rosales, I. and Quesada, C. (2008) 'Oxygen isotope and Mg/Ca composition of Late Viséan (Mississippian) brachiopod shells from SW Iberia:

Palaeoclimatic and palaeogeographic implications in northern Gondwana', *Palaeogeography, Palaeoclimatology, Palaeoecology*, 268(1-2), pp. 65-79.

11. Armendáriz, M., Rosales, I., Bádenas, B., Aurell, M., García-Ramos, J. C. and Piñuela, L. (2012) 'High-resolution chemostratigraphic records from Lower Pliensbachian belemnites: Palaeoclimatic perturbations, organic facies and water mass exchange (Asturian basin, northern Spain)', *Palaeogeography, Palaeoclimatology, Palaeoecology*, 333-334, pp. 178-191.
12. Astilleros, J. M., Fernández-Díaz, L. and Putnis, A. (2010) 'The role of magnesium in the growth of calcite: An AFM study', *Chemical Geology*, 271(1-2), pp. 52-58.
13. Bailey, T. R., Rosenthal, Y., McArthur, J. M., van de Schootbrugge, B. and Thirlwall, M. F. (2003) 'Paleoceanographic changes of the Late Pliensbachian–Early Toarcian interval: a possible link to the genesis of an Oceanic Anoxic Event', *Earth and Planetary Science Letters*, 212(3-4), pp. 307-320.
14. Bassoulet, J. P. and Baudin, F. (1994) 'Le toarcien inférieur: Une période de crise dans les bassins et sur les plate-formes carbonatées de l'Europe du Nord-Ouest et de la Téthys', *Geobios*, 27(SUPPL. 3), pp. 645-654.
15. Baturin, G. N. (2003) 'Phosphorus Cycle in the Ocean', *Lithology and Mineral Resources* 38:2, 38(2), pp. 101-119.
16. Berner, R. A. (1975) 'The role of magnesium in the crystal growth of calcite and aragonite from sea water', *Geochimica et Cosmochimica Acta*, 39(4), pp. 489-504.
17. Bertlich, J., Nürnberg, D., Hathorne, E. C., De Nooijer, L. J., Mezger, E. M., Kienast, M., Nordhausen, S., Reichart, G. J., Schönfeld, J. and Bijma, J. (2018) 'Salinity control on Na incorporation into calcite tests of the planktonic foraminifera *Trilobatus sacculifer* - Evidence from culture experiments and surface sediments', *Biogeosciences*, 15(20), pp. 5991-6018.
18. Bettencourt, V. and Guerra, A. (2000) 'Growth increments and biomineralization process in cephalopod statoliths', *Journal of Experimental Marine Biology and Ecology*, 248, pp. 191–205.
19. Birchall, J. D. and Thomas, N. L. (1983) 'On the architecture and function of cuttlefish bone.', *Journal of Material Science*, 18, pp.2081-2086.
20. Bjerrum, C. J. and Canfield, D. E. (2002) 'Ocean productivity before about 1.9 Gyr ago limited by phosphorus adsorption onto iron oxides', *Nature*, 417(6885), pp. 159-162.

21. Boyle, E. A. (1981) 'Cadmium, zinc, copper, and barium in foraminifera tests', *Earth and Planetary Science Letters*, 53(1), pp. 11-35.
22. Brand, U. and Veizer, J. (1980) 'Chemical diagenesis of a multicomponent carbonate system', *SEPM Society for Sedimentary Geology*.
23. Brazier, J. M., Suan, G., Tacail, T., Simon, L., Martin, J. E., Mattioli, E. and Balter, V. (2015) 'Calcium isotope evidence for dramatic increase of continental weathering during the Toarcian oceanic anoxic event (Early Jurassic)', *Earth and Planetary Science Letters*, 411, pp. 164-176.
24. Broecker, W. S. and Peng, T. H. (1982) 'Tracers in the Sea' *Radiocarbon*, 24(3), b1-2.
25. Bryan, S. P. and Marchitto, T. M. (2008) 'Mg/Ca-temperature proxy in benthic foraminifera: New calibrations from the Florida Straits and a hypothesis regarding Mg/Li', *Paleoceanography*, 23(2).
26. Buchem, F. S. P. v. and Knox, R. W. O. B. (1998) 'Lower and Middle Liassic Depositional Sequences of Yorkshire (U.K.)', *Society for Sedimentary Geology*, 60.
27. Buckley, D. E. and Cranston, R. E. (1971) 'Atomic absorption analyses of 18 elements from a single decomposition of aluminosilicate', *Chemical Geology*, 7(4), pp. 273-284.
28. Burton, E. A. and Walter, L. M. (1991) 'The effects of pCO<sub>2</sub> and temperature on magnesium incorporation in calcite in seawater and MgCl<sub>2</sub>-CaCl<sub>2</sub> solutions', *Geochimica et Cosmochimica Acta*, 55(3), pp. 777-785.
29. Busenberg, E. and Plummer, L. (1989) 'Thermodynamics of magnesian calcite solid-solutions at 25°C and 1 atm total pressure', *Geochimica et Cosmochimica Acta*, 53(6), pp. 1189-1208.
30. Canfield, D. E., Raiswell, R., Westrich, J. T., Reaves, C. M. and Berner, R. A. (1986) 'The Use of Chromium Reduction in the Analysis of Reduced Inorganic Sulfur in Sediments and Shales Redox proxies', *Chemical Geology*, 54, pp. 149-155.
31. Carroll, J., Falkner, K., Brown, E. T. and Moore, W. S. (1993) 'The role of the Ganges-Brahmaputra mixing zone in supplying barium and <sup>226</sup>Ra to the Bay of Bengal', *Geochimica et Cosmochimica Acta*, 57(13), pp. 2981-2990.
32. Case, D. H., Robinson, L. F., Auro, M. E. and Gagnon, A. C. (2010) 'Environmental and biological controls on Mg and Li in deep-sea scleractinian corals', *Earth and Planetary Science Letters*, 300(3-4), pp. 215-225.

33. Caswell, B. A., Coe, A. L. and Cohen, A. S. (2009) 'New range data for marine invertebrate species across the early Toarcian (Early Jurassic) mass extinction', *Journal of the Geological Society*, 166(5), pp. 859-872.
34. Chan, L. H., Edmond, J. M., Thompson, G. and Gillis, K. (1992) 'Lithium isotopic composition of submarine basalts: implications for the lithium cycle in the oceans', *Earth and Planetary Science Letters*, 108(1-3), pp. 151-160.
35. Chan, L.H., Leeman, W. P., Plank, T., Chan, L. H., Leeman, W. P. and Plank, T. (2006) 'Lithium isotopic composition of marine sediments', *Geochemistry, Geophysics, Geosystems*, 7(6), pp. 6005-6005.
36. Chave, K. E. (1954a) 'Aspects of the Biogeochemistry of Magnesium 1. Calcareous Marine Organisms', *The Journal of Geology*, 62(3), pp. 266-283.
37. Chave, K. E. (1954b) 'Aspects of the Biogeochemistry of Magnesium 2. Calcareous Sediments and Rocks', *The Journal of Geology*, 62(6), pp. 587-599.
38. Checa, A. G., Cartwright, J. H. E., Sánchez-Almazo, I., Andrade, J. P., Ruiz-Raya, F. (2015) 'The cuttlefish *Sepia officinalis* (Sepiidae, Cephalopoda) constructs cuttlebone from a liquid-crystal precursor.', *Scientific Reports*, 5, 11513.
39. Checa, A. G., Grenier, C., Griesshaber, E., Schmahl, W. W., Cartwright, J. H. E., Salas, C. and Oudot, M. (2022) 'The shell structure and chamber production cycle of the cephalopod *Spirula* (Coleoidea, Decabrachia)', *Marine Biology*, 169, pp. 132-132.
40. Chen, M., Martin, P., Goodkin, N. F., Tanzil, J., Murty, S. and Wiguna, A. A. (2019) 'An assessment of P speciation and P:Ca proxy calibration in coral cores from Singapore and Bali', *Geochimica et Cosmochimica Acta*, 267, pp. 113-123.
41. Chislock, M. F., Doster, E., Zitomer, R. A. and Wilson, A. E. (2013) 'Eutrophication: Causes, Consequences, and Controls in Aquatic Ecosystems', *Nature Education Knowledge*, 4(4):10.
42. Christensen, W. K. (1976) 'Palaeobiogeography of late Cretaceous belemnites of Europe', *Paläontologische Zeitschrift*, 50, pp. 113-129.
43. Chung, M.T., Huang, K.F., You, C.F., Chiao, C.C. and Wang, C.H. (2020) 'Elemental Ratios in Cuttlebone Indicate Growth Rates in the Cuttlefish *Sepia pharaonis*', *Frontiers in Marine Science*, 6.
44. Cohen, A. S., Coe, A. L., Harding, S. M. and Schwark, L. (2004) 'Osmium isotope evidence for the regulation of atmospheric CO<sub>2</sub> by continental weathering', *Geology*, 32(2), pp. 157-160.

45. Cope, J. C. W. (1980) 'A correlation of Jurassic rocks in British: Introduction and Lower Jurassic'. United Kingdom: Blackwell Scientific Publications.
46. Crisp, M., Demarchi, B., Collins, M., Morgan-Williams, M., Pilgrim, E. and Penkman, K. (2013) 'Isolation of the intra-crystalline proteins and kinetic studies in *Struthio camelus* (ostrich) eggshell for amino acid geochronology', *Quaternary Geochronology*, 16, pp. 110-128.
47. Davis, K. J., Dove, P. M. and De Yoreo, J. J. (2000) 'Resolving the Control of Magnesium on Calcite Growth: Thermodynamic and Kinetic Consequences of Impurity Incorporation for Biomineral Formation', *MRS Online Proceedings Library (OPL)*, 620, pp. M9.5.1-M9.5.1.
48. Davis, K. J., Dove, P. M. and De Yoreo, J. J. (2001) 'Understanding the Molecular-Scale Processes of Biomineralization: The Role of Mg<sup>2+</sup> and Sr<sup>2+</sup> in Calcite Growth', *AGUFM*, pp. B21C-06.
49. De Choudens-Sánchez, V. and Gonzalez, L. A. (2009) 'Calcite and Aragonite Precipitation Under Controlled Instantaneous Supersaturation: Elucidating the Role of CaCO<sub>3</sub> Saturation State and Mg/Ca Ratio on Calcium Carbonate Polymorphism', *Journal of Sedimentary Research*, 79(6), pp. 363-376.
50. de Kanel, J. and Morse, J. W. (1978) 'The chemistry of orthophosphate uptake from seawater on to calcite and aragonite', *Geochimica et Cosmochimica Acta*, 42(9), pp. 1335-1340.
51. de Villiers, S., Shen, G. T. and Nelson, B. K. (1994) 'The Sr/Ca-temperature relationship in coralline aragonite: Influence of variability in (Sr/Ca)seawater and skeletal growth parameters', *Geochimica et Cosmochimica Acta*, 58(1), pp. 197-208.
52. Deconinck, J. F., Hesselbo, S. P. and Pellenard, P. (2019) 'Climatic and sea-level control of Jurassic (Pliensbachian) clay mineral sedimentation in the Cardigan Bay Basin, Llanbedr (Mochras Farm) borehole, Wales', *Sedimentology*, 66(7), pp. 2769-2783.
53. Dekens, P. S., Lea, D. W., Pak, D. K., Spero, H. J., Dekens, P. S., Lea, D. W., Pak, D. K. and Spero, H. J. (2002) 'Core top calibration of Mg/Ca in tropical foraminifera: Refining paleotemperature estimation', *Geochemistry, Geophysics, Geosystems*, 3(4), pp. 1-29.
54. Delaney, M. L. (1998) 'Phosphorus accumulation in marine sediments and the oceanic phosphorus cycle', *Global Biogeochemical Cycles*, 12(4), pp. 563-572.

55. Delaney, M. L., Popp, B. N., Lepzelter, C. G. and Anderson, T. F. (1989) 'Lithium-to-calcium ratios in Modern, Cenozoic, and Paleozoic articulate brachiopod shells', *Paleoceanography*, 4(6), pp. 681-691.
56. Delaney, M. L., W.H.Bé, A. and Boyle, E. A. (1985) 'Li, Sr, Mg, and Na in foraminiferal calcite shells from laboratory culture, sediment traps, and sediment cores', *Geochimica et Cosmochimica Acta*, 49(6), pp. 1327-1341.
57. Dellinger, M., West, A. J., Paris, G., Adkins, J. F., Pogge Von Strandmann, P. A. E., Ullmann, C. V., Eagle, R. A., Freitas, P., Bagard, M.-L., Ries, J. B., Corsetti, F. A., Perez-Huerta, A., Kampf, A. R. and Dellinger, M. (2018) 'The Li isotope composition of marine biogenic carbonates: Patterns and mechanisms', *Geochimica et Cosmochimica Acta*, 236, pp. 315-335.
58. Dera, G., Neige, P., Dommergues, J. L., Fara, E., Laffont, R. and Pellenard, P. (2010) 'High-resolution dynamics of early Jurassic marine extinctions: The case of Pliensbachian-Toarcian ammonites (Cephalopoda)', *Journal of the Geological Society*, 167(1), pp. 21-33.
59. Dera, G., Pellenard, P., Neige, P., Deconinck, J. F., Pucéat, E. and Dommergues, J. L. (2009a) 'Distribution of clay minerals in Early Jurassic Peritethyan seas: Palaeoclimatic significance inferred from multiproxy comparisons', *Palaeogeography, Palaeoclimatology, Palaeoecology*, 271(1-2), pp. 39-51.
60. Dera, G., Pucéat, E., Pellenard, P., Neige, P., Delsate, D., Joachimski, M. M., Reisberg, L. and Martinez, M. (2009b) 'Water mass exchange and variations in seawater temperature in the NW Tethys during the Early Jurassic: Evidence from neodymium and oxygen isotopes of fish teeth and belemnites', *Earth and Planetary Science Letters*, 286(1-2), pp. 198-207.
61. Dickson, J. A. D. (2002) 'Fossil echinoderms as monitor of the Mg/Ca ratio of Phanerozoic oceans', *Science*, 298(5596), pp. 1222-1224.
62. Dodd, M. S., Shi, W., Li, C., Zhang, Z., Cheng, M., Gu, H., Hardisty, D. S., Loyd, S. J., Wallace, M. W., vS. Hood, A., Lamothe, K., Mills, B. J. W., Poulton, S. W. and Lyons, T. W. (2023) 'Uncovering the Ediacaran phosphorus cycle', *Nature*, 618(7967), pp. 974-980.
63. Dodd, M. S., Zhang, Z., Li, C., Algeo, T. J., Lyons, T. W., Hardisty, D. S., Loyd, S. J., Meyer, D. L., Gill, B. C., Shi, W. and Wang, W. (2021) 'Development of carbonate-associated phosphate (CAP) as a proxy for reconstructing ancient ocean phosphate levels', *Geochimica et Cosmochimica Acta*, 301, pp. 48-69.

64. Dodge, R. E., Jickells, T. D., Knap, A. H., Boyd, S. and Bak, R. P. M. (1984) 'Reef-building coral skeletons as chemical pollution (phosphorus) indicators', *Marine Pollution Bulletin*, 15(5), pp. 178-187.
65. Doguzhaeva, L. A., Weis, R., Delsate, D. and Mariotti, N. (2013) 'Embryonic shell structure of Early-Middle Jurassic belemnites, and its significance for belemnite expansion and diversification in the Jurassic', *Jurassic. Lethaia*, 47, pp. 49-65.
66. Doyle, P. 1990. The British Toarcian (Lower Jurassic) Belemnites - Part 1. *Monograph of the Palaeontographical Society*.
67. Doyle, P. and Bennett, M. R. (1995). Belemnites in biostratigraphy. *Palaeontology* 38, 815–829.
68. Drozdova, T. V. (1969) 'Organic matter of belemnites', *Geokhimiya*, 10, pp. 1281-1285.
69. Dunca, E., Doguzhaeva, L., Schöne, B. R., van de Schootbrugge, B. (2006) 'Growth patterns in rostra of the Middle Jurassic belemnite *Megateuthis giganteus*: controlled by the moon', *Acta Universitatis Carolinae – Geologic*, 49, pp. 107-117.
70. Dutton, A., Huber, B. T., Lohmann, K. C. and Zinsmeister, W. J. (2007) 'High-resolution stable isotope profiles of a dimitobelid belemnite: implications for paleodepth habitat and late Maastrichtian climate seasonality', *Palaaios*, 22(6), pp. 642-650.
71. Elderfield, H. and Ganssen, G. (2000) 'Past temperature and  $\delta^{18}\text{O}$  of surface ocean waters inferred from foraminiferal Mg/Ca ratios', *Nature*, 405(6785), pp. 442-445.
72. Elemental Microanalysis (EMA) (2016) 'Carrara Marble Powder IRMS Standards', *Elemental Microanalysis*.
73. Evans, D., Erez, J., Oron, S. and Müller, W. (2015) 'Mg/Ca-temperature and seawater-test chemistry relationships in the shallow-dwelling large benthic foraminifera *Operculina ammonoides*', *Geochimica et Cosmochimica Acta*, 148, pp. 325-342.
74. Evans, D., Gray, W. R., Rae, J. W. B., Greenop, R., Webb, P. B., Penkman, K., Kröger, R. and Allison, N. (2020) 'Trace and major element incorporation into amorphous calcium carbonate (ACC) precipitated from seawater', *Geochimica et Cosmochimica Acta*, 290, pp. 293-311.
75. Evans, D., Müller, W. and Erez, J. (2018) 'Assessing foraminifera biomineralisation models through trace element data of cultures under variable seawater chemistry', *Geochimica et Cosmochimica Acta*, 236, pp. 198-217.

76. Fantasia, A., Föllmi, K. B., Adatte, T., Bernárdez, E., Spangenberg, J. E. and Mattioli, E. (2018a) 'The Toarcian Oceanic Anoxic Event in southwestern Gondwana: an example from the Andean Basin, northern Chile', *Journal of the Geological Society*, 175(6), pp. 883-902.
77. Faul, K. L., Paytan, A. and Delaney, M. L. (2005) 'Phosphorus distribution in sinking oceanic particulate matter', *Marine Chemistry*, 97(3-4), pp. 307-333.
78. Filippelli, G. M. (2008) 'The Global Phosphorus Cycle: Past, Present, and Future', *Elements*, 4(2), pp. 89-95.
79. Florek, M., Fornal, E., Gómez-Romero, P., Zieba, E., Paszkowicz, W., Lekki, J., Nowak, J. and Kuczumow, A. (2009) 'Complementary microstructural and chemical analyses of *Sepia officinalis* endoskeleton', *Materials Science and Engineering: C*, 29(4), pp. 1220-1226.
80. Fowell, S. E., Sandford, K., Stewart, J. A., Castillo, K. D., Ries, J. B. and Foster, G. L. (2016) 'Intrareef variations in Li/Mg and Sr/Ca sea surface temperature proxies in the Caribbean reef-building coral *Siderastrea siderea*', *Paleoceanography*, 31(10), pp. 1315-1329.
81. Fraguas, Á., Comas-Rengifo, M. J., Gómez, J. J. and Goy, A. (2012) 'The calcareous nanofossil crisis in Northern Spain (Asturias province) linked to the Early Toarcian warming-driven mass extinction', *Marine Micropaleontology*, 94-95, pp. 58-71.
82. Freitas, P., Clarke, L. J., Kennedy, H., Richardson, C., Freitas, P., Clarke, L. J., Kennedy, H., Richardson, C. and Abrantes, F. (2005) 'Mg/Ca, Sr/Ca, and stable-isotope ( $\delta^{18}\text{O}$  and  $\delta^{13}\text{C}$ ) ratio profiles from the fan mussel *Pinna nobilis*: Seasonal records and temperature relationships', *Geochemistry, Geophysics, Geosystems*, 6(4), pp. 4-14.
83. French, K. L., Sepúlveda, J., Trabucho-Alexandre, J., Gröcke, D. R. and Summons, R. E. (2014) 'Organic geochemistry of the early Toarcian oceanic anoxic event in Hawsker Bottoms, Yorkshire, England', *Earth and Planetary Science Letters*, 390, pp. 116-127.
84. Frimmel, A., Oschmann, W. and Schwark, L. (2004) 'Chemostratigraphy of the Posidonia Black Shale, SW Germany: I. Influence of sea-level variation on organic facies evolution', *Chemical Geology*, 206(3-4), pp. 199-230.
85. Fu, X., Wang, J., Zeng, S., Feng, X., Wang, D. and Song, C. (2017) 'Continental weathering and palaeoclimatic changes through the onset of the Early Toarcian oceanic anoxic event in the Qiangtang Basin, eastern Tethys', *Palaeogeography, Palaeoclimatology, Palaeoecology*, 487, pp. 241-250.

86. Gabitov, R. I., Schmitt, A. K., Rosner, M., McKeegan, K. D., Gaetani, G. A., Cohen, A. L., Watson, E. B. and Harrison, T. M. (2011) 'In situ  $\delta^7\text{Li}$ , Li/Ca, and Mg/Ca analyses of synthetic aragonites', *Geochemistry, Geophysics, Geosystems*, 12(3), pp. 3001-3001.
87. García Joral, F., Gómez, J. J. and Goy, A. (2011) 'Mass extinction and recovery of the Early Toarcian (Early Jurassic) brachiopods linked to climate change in Northern and Central Spain', *Palaeogeography, Palaeoclimatology, Palaeoecology*, 302(3-4), pp. 367-380.
88. Gill, B. C., Lyons, T. W., Young, S. A., Kump, L. R., Knoll, A. H. and Saltzman, M. R. (2011) 'Geochemical evidence for widespread euxinia in the Later Cambrian ocean', *Nature*, 469(7328), pp. 80-83.
89. Gillikin, D. P., Dehairs, F., Lorrain, A., Steenmans, D., Baeyens, W. and André, L. (2006) 'Barium uptake into the shells of the common mussel (*Mytilus edulis*) and the potential for estuarine paleo-chemistry reconstruction', *Geochimica et Cosmochimica Acta*, 70(2), pp. 395-407.
90. Gillikin, D. P., Lorrain, A., Paulet, Y. M., André, L. and Dehairs, F. (2008) 'Synchronous barium peaks in high-resolution profiles of calcite and aragonite marine bivalve shells', *Geo-Marine Letters*, 28(5-6), pp. 351-358.
91. Golonka, J. (2007) 'Late Triassic and Early Jurassic palaeogeography of the world', *Palaeogeography, Palaeoclimatology, Palaeoecology*, 244(1-4), pp. 297-307.
92. Golonka, J. and Ford, D. (2000) 'Pangean (Late Carboniferous-Middle Jurassic) Palaeoenvironment and Lithofacies', *Palaeogeography, Palaeoclimatology, Palaeoecology*, 161, pp. 1-34.
93. Gómez, J. J. and Arias, C. (2010) 'Rapid warming and ostracods mass extinction at the Lower Toarcian (Jurassic) of central Spain', *Marine Micropaleontology*, 74(3-4), pp. 119-135.
94. Gómez, J. J. and Goy, A. (2011) 'Warming-driven mass extinction in the Early Toarcian (Early Jurassic) of northern and central Spain. Correlation with other time-equivalent European sections', *Palaeogeography, Palaeoclimatology, Palaeoecology*, 306(3-4), pp. 176-195.
95. Gómez, J. J., Goy, A. and Canales, M. L. (2008) 'Seawater temperature and carbon isotope variations in belemnites linked to mass extinction during the Toarcian (Early Jurassic) in Central and Northern Spain. Comparison with other European sections', *Palaeogeography, Palaeoclimatology, Palaeoecology*, 258(1-2), pp. 28-58.

96. Gordon, C. M., Carr, R. A. and Larson, R. E. (1970) 'The influence of environmental factors on the sodium and manganese content of barnacle shells', *Limnology and Oceanography*, 15(3), pp. 461-466.
97. Graciansky, P. C. D., Dardeau, G., Dumont, T., Jacquin, T., Marchand, D., Mouterde, R. and Vail, P. R. (1993) 'Depositional sequence cycles, transgressive-regressive facies cycles, and extensional tectonics : Example from the southern Subalpine Jurassic basin, France', *Bulletin de la Société géologique de France*, 164(5), pp. 709-718.
98. Graciansky, P. C. d., Jacquin, T. and Hesselbo, S. P. (1998) 'The Ligurian Cycle: An Overview of Lower Jurassic 2nd-Order Transgressive/Regressive Facies Cycles in Western Europe', *Society for Sedimentary Geology*, 60.
99. Gray, W. R., Evans, D., Henehan, M., Weldeab, S., Lea, D. W., Müller, W. and Rosenthal, Y. (2023) 'Sodium incorporation in foraminiferal calcite: An evaluation of the Na/Ca salinity proxy and evidence for multiple Na-bearing phases', *Geochimica et Cosmochimica Acta*, 348, pp. 152-164.
100. Gröcke, D. R., Hori, R. S., Trabucho-Alexandre, J., Kemp, D. B. and Schwark, L. (2011) 'An open ocean record of the Toarcian oceanic anoxic event', *Solid Earth*, 2(2), pp. 245-257.
101. Guay, C. K. and Falkner, K. K. (1997) 'Barium as a tracer of Arctic halocline and river waters', *Deep Sea Research Part II: Topical Studies in Oceanography*, 44(8), pp. 1543-1569.
102. Guay, C. K. and Falkner, K. K. (1998) 'A survey of dissolved barium in the estuaries of major Arctic rivers and adjacent seas', *Continental Shelf Research*, 18(8), pp. 859-882.
103. Hallam, A. (1987) 'Radiations and extinctions in relation to environmental change in the marine Lower Jurassic of northwest Europe', *Paleobiology*, 13(2), pp. 152-168.
104. Hallam, A. (1997) 'Estimates of the amount and rate of sea-level change across the Rhaetian-Hettangian and Pliensbachian-Toarcian boundaries (latest Triassic to early Jurassic)', *Journal of the Geological Society*, 154(5), pp. 773-779.
105. Hallam, A. and Wignall, P. B. (1997) *Mass extinctions and their aftermath*. United Kingdom: Oxford University Press.
106. Haq, B. U. (2017) 'Jurassic Sea-Level Variations: A Reappraisal', *GSA Today*, 28(1), pp. 4-10.
107. Hardenbol, J., Thierry, J., Farley, M. B., Jacquin, T., Graciansky, P.-C. d. and Vail, P. R. (2010) *Mesozoic and Cenozoic Sequence Chronostratigraphic Framework of European*

*Basins. Mesozoic and Cenozoic Sequence Stratigraphy of European Basins* Tulsa: SEPM Society for Sedimentary Geology.

108. Hartley, G. and Mucci, A. (1996) 'The influence of pCO<sub>2</sub> on the partitioning of magnesium in calcite overgrowths precipitated from artificial seawater at 25° and 1 atm total pressure', *Geochimica et Cosmochimica Acta*, 60(2), pp. 315-324.
109. Hathorne, E. C. and James, R. H. (2006) 'Temporal record of lithium in seawater: A tracer for silicate weathering?', *Earth and Planetary Science Letters*, 246(3-4), pp. 393-406.
110. Hauzer, H., Evans, D., Müller, W., Rosenthal, Y. and Erez, J. (2018) 'Calibration of Na partitioning in the calcitic foraminifer *Operculina ammonoides* under variable Ca concentration: Toward reconstructing past seawater composition', *Earth and Planetary Science Letters*, 497, pp. 80-91.
111. Hauzer, H., Evans, D., Müller, W., Rosenthal, Y. and Erez, J. (2021) 'Salinity Effect on Trace Element Incorporation in Cultured Shells of the Large Benthic Foraminifer *Operculina ammonoides*', *Paleoceanography and Paleoclimatology*, 36(6).
112. He, T., Wignall, P. B., Newton, R. J., Atkinson, J. W., Keeling, J. F. J., Xiong, Y. and Poulton, S. W. (2022) 'Extensive marine anoxia in the European epicontinental sea during the end-Triassic mass extinction', *Global and Planetary Change*, 210.
113. Hemming, N. G. and Hanson, G. N. (1992) 'Boron isotopic composition and concentration in modern marine carbonates', *Geochimica et Cosmochimica Acta*, 56(1), pp. 537-543.
114. Hermoso, M. and Pellenard, P. (2014) 'Continental weathering and climatic changes inferred from clay mineralogy and paired carbon isotopes across the early to middle Toarcian in the Paris Basin', *Palaeogeography, Palaeoclimatology, Palaeoecology*, 399, pp. 385-393.
115. Hermoso, M., Minoletti, F., Rickaby, R. E. M., Hesselbo, S. P., Baudin, F. and Jenkyns, H. C. (2012) 'Dynamics of a stepped carbon-isotope excursion: Ultra high-resolution study of Early Toarcian environmental change', *Earth and Planetary Science Letters*, 319-320, pp. 45-54.
116. Hesselbo, S. P., Bjerrum, C. J., Hinnov, L. A., Macniocail, C., Miller, K. G., Riding, J. B., Van De Schootbrugge, B., Revisited, M. and Team, S. (2013) 'Scientific Drilling Mochras borehole revisited: a new global standard for Early Jurassic earth history', *Scientific Drilling*, 16, pp. 81-91.

117. Hesselbo, S. P., Gröcke, D. R., Jenkyns, H. C., Bjerrum, C. J., Farrimond, P., Morgans Bell, H. S. and Green, O. R. (2000) 'Massive dissociation of gas hydrate during a Jurassic oceanic anoxic event', *Nature*, 406(6794), pp. 392-395.
118. Hesselbo, S. P., Jenkyns, H. C., Duarte, L. V. and Oliveira, L. C. V. (2007) 'Carbon-isotope record of the Early Jurassic (Toarcian) Oceanic Anoxic Event from fossil wood and marine carbonate (Lusitanian Basin, Portugal)', *Earth and Planetary Science Letters*, 253(3-4), pp. 455-470.
119. Hewitt, R. A. (2000) 'Geological interpretations from cephalopod habitat and implosion depth limits', *Revue de paléobiologie*, 8 pp.95-107.
120. Hoffmann, R. and Stevens, K. (2020) 'The palaeobiology of belemnites – foundation for the interpretation of rostrum geochemistry', *Biological Reviews*, 95(1), pp. 94-123.
121. Hoffmann, R., Linzmeier, B. J., Kitajima, K., Nehrke, G., Dietzel, M., Jöns, N., Stevens, K. and Immenhauser, A. (2021) 'Complex biomineralization pathways of the belemnite rostrum cause biased paleotemperature estimates', *Minerals*, 11(12), pp. 1406-1406.
122. Hoffmann, R., Richter, D. K., Neuser, R. D., Jöns, N., Linzmeier, B. J., Lemanis, R. E., Füsseis, F., Xiao, X. and Immenhauser, A. (2016) 'Evidence for a composite organic–inorganic fabric of belemnite rostra: Implications for palaeoceanography and palaeoecology', *Sedimentary Geology*, 341, pp. 203-215.
123. House, W. A. and Donaldson, L. (1986) 'Adsorption and coprecipitation of phosphate on calcite', *Journal of Colloid And Interface Science*, 112(2), pp. 309-324.
124. Howarth, M. K. (1962) 'The Jet rock series and the Alum Shale series of the Yorkshire Coast', *Proceedings of the Yorkshire Geological Society*, 33(4), pp. 381-422.
125. Huh, Y., Chan, L. H., Zhang, L. and Edmond, J. M. (1998) 'Lithium and its isotopes in major world rivers: implications for weathering and the oceanic budget', *Geochimica et Cosmochimica Acta*, 62(12), pp. 2039-2051.
126. Hülse, D., Lau, K. V., van de Velde, S. J., Arndt, S., Meyer, K. M. and Ridgwell, A. (2021) 'End-Permian marine extinction due to temperature-driven nutrient recycling and euxinia', *Nature Geoscience*, 14(11), pp. 862-867.
127. Iba, Y., Mutterlose, J., Tanabe, K., Sano, S. I., Misaki, A. and Terabe, K. (2011) 'Belemnite extinction and the origin of modern cephalopods 35 m.y. prior to the Cretaceous–Paleogene event', *Geology*, 39(5), pp. 483-486.

128. Iba, Y., Sano, S. I., Mutterlose, J. and Kondo, Y. (2012) 'Belemnites originated in the Triassic—A new look at an old group', *Geology*, 40(10), pp. 911-914.
129. Ichikuni, M. (1981) 'Coprecipitation of phosphate with calcite', *Geochemical Journal*, 15, pp. 283-283.
130. Ikeda, Y., Arai, N., Sakamoto, W., Kidokoro, H. and Yoshida, K. (1998) 'Microchemistry of the Statoliths of the Japanese Common Squid *Todarodes pacificus* with Special Reference to its Relation to the Vertical Temperature Profiles of Squid Habitat', *Fisheries Science*, 64(2), pp. 179-184.
131. Ikeda, Y., Okazaki, J., Sakurai, Y. and Sakamoto, W. (2002a) 'Periodic variation in Sr/Ca ratios in statoliths of the Japanese common squid *todarodes pacificus* steenstrup, 1880 (cephalopoda: Ommastrephidae) maintained under constant water temperature', *Journal of Experimental Marine Biology and Ecology*, 273(2), pp. 161-170.
132. Ikeda, Y., Yatsu, A., Arai, N. and Sakamoto, W. (2002b) 'Concentration of statolith trace elements in the jumbo flying squid during El Niño and non-El Niño years in the eastern Pacific', *Journal of the Marine Biological Association of the United Kingdom*, 82(5), pp. 863-866.
133. Immenhauser, A., Schöne, B. R., Hoffmann, R. and Niedermayr, A. (2016) 'Mollusc and brachiopod skeletal hard parts: Intricate archives of their marine environment', *Sedimentology*, 63(1), pp. 1-59.
134. Ingall, E. and Jahnke, R. (1997) 'Influence of water-column anoxia on the elemental fractionation of carbon and phosphorus during sediment diagenesis', *Marine Geology*, 139(1-4), pp. 219-229.
135. Ingall, E. D., Bustin, R. M. and Van Cappellen, P. (1993) 'Influence of water column anoxia on the burial and preservation of carbon and phosphorus in marine shales', *Geochimica et Cosmochimica Acta*, 57(2), pp. 303-316.
136. Ingalls, M., Blättler, C. L., Higgins, J. A., Magyar, J. S., Eiler, J. M. and Fischer, W. W. (2020) 'P/Ca in Carbonates as a Proxy for Alkalinity and Phosphate Levels', *Geophysical Research Letters*, 47(21).
137. Ingalls, M., Grotzinger, J. P., Present, T., Rasmussen, B. and Fischer, W. W. (2022) 'Carbonate-Associated Phosphate (CAP) Indicates Elevated Phosphate Availability in Neoproterozoic Shallow Marine Environments', *Geophysical Research Letters*, 49(6).

138. Ingram, B. L., De Deckker, P., Chivas, A. R., Conrad, M. E. and Byrne, A. R. (1998) 'Stable isotopes, Sr/Ca, and Mg/Ca in biogenic carbonates from Petaluma Marsh, northern California, USA', *Geochimica et Cosmochimica Acta*, 62(19-20), pp. 3229-3237.
139. Irie, T. and Suzuki, A. (2020) 'High temperature stress does not distort the geochemical thermometers based on biogenic calcium carbonate: Stable oxygen isotope values and Sr/Ca ratios of gastropod shells in response to rearing temperature', *Geochimica et Cosmochimica Acta*, 288, pp. 1-15.
140. Ishikawa, M. and Ichikuni, M. (1984) 'Uptake of sodium and potassium by calcite', *Chemical Geology*, 42(1-4), pp. 137-146.
141. Ivanova, D. and Koleva, E. (2007) 'Documentation and correlation of transgressive-regressive cycles from three Lower-Middle Jurassic successions of the Western Balkan Mts, Bulgaria.' *Geologica Balcanica*, 36(3-4), pp. 91-96.
142. Ivimey-Cook, H. C. and Powell, J. H. (1991) 'Late Triassic and early Jurassic biostratigraphy of the Felixkirk Borehole, North Yorkshire', *Proceedings - Yorkshire Geological Society*, 48(4), pp. 367-374.
143. Jarvis, I. (1980). Palaeobiology of upper cretaceous Belemnites from the phosphatic chalk of the Anglo-Paris basin. *Palaeontology* 23, pp. 889–914.
144. Jenkins, H. D. B. and Thakur, K. P. (1979) 'Reappraisal of thermochemical radii for complex ions', *Journal of Chemical Education*, 56(9), pp. 576-576.
145. Jenkyns, H. C. (1988) 'The early Toarcian ( Jurassic) anoxic event: stratigraphic, sedimentary, and geochemical evidence', *American Journal of Science*, 288(2), pp. 101-151.
146. Jenkyns, H. C. (2010) 'Geochemistry of oceanic anoxic events', *Geochemistry Geophysics Geosystems*, 11(3).
147. Jenkyns, H. C. and Clayton, C. J. (1986) 'Black shales and carbon isotopes in pelagic sediments from the Tethyan Lower Jurassic', *Sedimentology*, 33(1), pp. 87-106.
148. Jenkyns, H. C. and Weedon, G. P. (2003) 'Evidence for rapid climate change in the Mesozoic Palaeogene greenhouse world', *Philosophical Transactions of the Royal Society of London. Series A: Mathematical, Physical and Engineering Sciences*, 361(1810), pp. 1885-1916.

149. Jenkyns, H. C., Jones, C. E., Gröcke, D. R., Hesselbo, S. P. and Parkinson, D. N. (2002) 'Chemostratigraphy of the Jurassic System: Applications, limitations and implications for palaeoceanography', *Journal of the Geological Society*, 159(4), pp. 351-378.
150. Jereb, P. and Roper, C. F. E. (2005) 'Cephalopods of the World – An Annotated and Illustrated Catalogue of Cephalopod Species Known to Date Volume 1 – Chambered Nautilus and Sepioids (Nautilidae, Sepiidae, Sepiolidae, Sepiadariidae, Idiosepiidae and Spirulidae)', *Food and Agriculture Organization of the United Nations, Rome*.
151. Joachimski, M. M., Simon, L., van Geldern, R. and Lécuyer, C. (2005) 'Boron isotope geochemistry of Paleozoic brachiopod calcite: Implications for a secular change in the boron isotope geochemistry of seawater over the Phanerozoic', *Geochimica et Cosmochimica Acta*, 69(16), pp. 4035-4044.
152. Katz, A. (1973) 'The interaction of magnesium with calcite during crystal growth at 25–90°C and one atmosphere', *Geochimica et Cosmochimica Acta*, 37(6), pp. 1563-1586.
153. Katz, M. E., Wright, J. D., Miller, K. G., Cramer, B. S., Fennel, K. and Falkowski, P. G. (2005) 'Biological overprint of the geological carbon cycle', *Marine Geology*, 217(3-4), pp. 323-338.
154. Kemp, D. B., Coe, A. L., Cohen, A. S. and Schwark, L. (2005) 'Astronomical pacing of methane release in the Early Jurassic period', *Nature*, 437(7057), pp. 396-399.
155. Kemp, D. B., Coe, A. L., Cohen, A. S. and Weedon, G. P. (2011) 'Astronomical forcing and chronology of the early Toarcian (Early Jurassic) oceanic anoxic event in Yorkshire, UK', *Paleoceanography*, 26(4), pp. 4210-4210.
156. Kennard, J. M., Jackson, M. J., Romine, K. K., Shaw, R. D., Southgate, P. N., Van Cappellen, P., Ingall, E. D., Van Cappellen, P. and Ingall, E. D. (1996) 'Redox Stabilization of the Atmosphere and Oceans by Phosphorus-Limited Marine Productivity', *Science*, 271(5248), pp. 493-496.
157. Kitano, Y. and Hood, D. W. (1962) 'Calcium Carbonate Crystal Forms Formed from Sea Water by Inorganic Processes', *Journal of the Oceanographical Society of Japan*, 18(3), pp. 141-145.
158. Klochko, K., Kaufman, A. J., Yao, W., Byrne, R. H. and Tossell, J. A. (2006) 'Experimental measurement of boron isotope fractionation in seawater', *Earth and Planetary Science Letters*, 248(1-2), pp. 276-285.

159. Kolowitz, L. C., Ingall, E. D. and Benner, R. (2001) 'Composition and cycling of marine organic phosphorus', *Limnology and Oceanography*, 46(2), pp. 309-320.
160. Korte C. and Hesselbo S. P. (2011) 'Shallow marine carbon and oxygen isotope and elemental records indicate icehouse-greenhouse cycles during the Early Jurassic', *Paleoceanography*, 26.
161. Krencker, F. N., Lindström, S. and Bodin, S. (2019) 'A major sea-level drop briefly precedes the Toarcian oceanic anoxic event: implication for Early Jurassic climate and carbon cycle', *Scientific Reports*, 9(1), pp. 1-12.
162. Krief, S., Hendy, E. J., Fine, M., Yam, R., Meibom, A., Foster, G. L. and Shemesh, A. (2010) 'Physiological and isotopic responses of scleractinian corals to ocean acidification', *Geochimica et Cosmochimica Acta*, 74(17), pp. 4988-5001.
163. Kumarsingh, K., Laydoo, R., Chen, J. K. and Siung-Chang, A. M. (1998) 'Historic records of phosphorus levels in the reef-building coral *Montastrea annularis* from Tobago, West Indies', *Marine Pollution Bulletin*, 36(12), pp. 1012-1018.
164. Lahann, R. W. and Siebert, R. M. (1982) 'A kinetic model for distribution coefficients and application to Mg-calcites', *Geochimica et Cosmochimica Acta*, 46(11), pp. 2229-2237.
165. LaVigne, M., Field, M. P., Anagnostou, E., Grottoli, A. G., Wellington, G. M. and Sherrell, R. M. (2008) 'Skeletal P/Ca tracks upwelling in Gulf of Panamá coral: Evidence for a new seawater phosphate proxy', *Geophysical Research Letters*, 35(5).
166. LaVigne, M., Matthews, K. A., Grottoli, A. G., Cobb, K. M., Anagnostou, E., Cabioch, G. and Sherrell, R. M. (2010) 'Coral skeleton P/Ca proxy for seawater phosphate: Multi-colony calibration with a contemporaneous seawater phosphate record', *Geochimica et Cosmochimica Acta*, 74, pp. 1282-1293.
167. Lea, D. W. and Boyle, E. A. (1989) 'Barium content of benthic foraminifera controlled by bottom-water composition', *Nature*, 338(6218), pp. 751-753.
168. Lea, D. W. and Boyle, E. A. (1990) 'A 210,000-year record of barium variability in the deep northwest Atlantic Ocean', *Nature*, pp. 269-272.
169. Lea, D. W. and Boyle, E. A. (1991) 'Barium in planktonic foraminifera', *Geochimica et Cosmochimica Acta*, 55(11), pp. 3321-3331.

170. Lea, D. W. and Boyle, E. A. (1993) 'Determination of carbonate-bound barium in foraminifera and corals by isotope dilution plasma-mass spectrometry', *Chemical Geology*, 103(1-4), pp. 73-84.
171. Lechler, M., Pogge von Strandmann, P. A. E., Jenkyns, H. C., Prosser, G. and Parente, M. (2015) 'Lithium-isotope evidence for enhanced silicate weathering during OAE 1a (Early Aptian Selli event)', *Earth and Planetary Science Letters*, 432, pp. 210-222.
172. Lécuyer, C., Grandjean, P., Reynard, B., Albarède, F. and Telouk, P. (2002) '<sup>11</sup>B/<sup>10</sup>B analysis of geological materials by ICP–MS Plasma 54: Application to the boron fractionation between brachiopod calcite and seawater', *Chemical Geology*, 186(1-2), pp. 45-55.
173. Lenton, T. M. and Watson, A. J. (2000) 'Redfield revisited: 2. What regulates the oxygen content of the atmosphere?', *Global Biogeochemical Cycles*, 14(1), pp. 249-268.
174. Lenton, T. M., Crouch, M., Johnson, M., Pires, N. and Dolan, L. (2012) 'First plants cooled the Ordovician', *Nature Geoscience*, 5(2), pp. 86-89.
175. Lenton, T. M., Daines, S. J. and Mills, B. J. W. (2018) 'COPSE reloaded: An improved model of biogeochemical cycling over Phanerozoic time', *Earth-Science Reviews*, 178, pp. 1-28.
176. Li, Q., McArthur, J. M. and Atkinson, T. C. (2012) 'Lower Jurassic belemnites as indicators of palaeo-temperature', *Palaeogeography, Palaeoclimatology, Palaeoecology*, 315-316, pp. 38-45.
177. Li, Q., McArthur, J. M., Doyle, P., Janssen, N., Leng, M. J., Müller, W. and Reboulet, S. (2013) 'Evaluating Mg/Ca in belemnite calcite as a palaeo-proxy', *Palaeogeography, Palaeoclimatology, Palaeoecology*, 388, pp. 98-108.
178. Lippmann, F. (1973) 'Sedimentary Carbonate Minerals', *Springer Verlag: Berlin*.
179. Little, C. T. S. and Benton, M. J. (1995) 'Early Jurassic mass extinction: A global long-term event', *Geology*, 25(6), 495-498.
180. Longinelli, A., Wierzbowski, H. and Di Matteo, A. (2003) ' $\delta^{18}\text{O}(\text{PO}_4^{3-})$  and  $\delta^{18}\text{O}(\text{CO}_3^{2-})$  from belemnite guards from Eastern Europe: implications for palaeoceanographic reconstructions and for the preservation of pristine isotopic values', *Earth and Planetary Science Letters*, 209(3-4), pp. 337-350.

181. Lord, G. S., Mørk, M. B. E., Mørk, A., Olausson, S. (2019) 'Sedimentology and petrography of the Svenskøya Formation on Hopen, Svalbard: an analogue to sandstone reservoirs in the Realgrunnen Subgroup', *Polar Research*, 38.
182. Loste, E., Wilson, R. M., Seshadri, R. and Meldrum, F. C. (2003) 'The role of magnesium in stabilising amorphous calcium carbonate and controlling calcite morphologies', *Journal of Crystal Growth*, 254(1-2), pp. 206-218.
183. Lowenstam, H. A. and Epstein, S. (1954) 'Paleotemperatures of the Post-Aptian Cretaceous as Determined by the Oxygen Isotope Method', *The Journal of Geology*, 62(3), pp. 207-248.
184. Lu, Z., Jenkyns, H. C. and Rickaby, R. E. M. (2010) 'Iodine to calcium ratios in marine carbonate as a paleo-redox proxy during oceanic anoxic events', *Geology*, 38(12), pp. 1107-1110.
185. Lyons, T. W., Droser, M. L., Lau, K. V., Porter, S. M., Li, C., Cheng, M. and Zhu, M. (2018) 'Heterogeneous and dynamic marine shelf oxygenation and coupled early animal evolution', *Emerging Topics in Life Sciences*, 2(2), pp. 279-288.
186. Mailliot, S., Mattioli, E., Bartolini, A., Baudin, F., Pittet, B. and Guex, J. (2009) 'Late Pliensbachian–Early Toarcian (Early Jurassic) environmental changes in an epicontinental basin of NW Europe (Causses area, central France): A micropaleontological and geochemical approach', *Palaeogeography, Palaeoclimatology, Palaeoecology*, 273(3-4), pp. 346-364.
187. Mailliot, S., Mattioli, E., Guex, J. and Pittet, B. (2006) 'The Early Toarcian anoxia, a synchronous event in the Western Tethys? An approach by quantitative biochronology (Unitary Associations), applied on calcareous nannofossils', *Palaeogeography, Palaeoclimatology, Palaeoecology*, 240(3-4), pp. 562-586.
188. Malkoč, M., Mutterlose, J. and Pauly, S. (2010a) 'Timing of the Early Aptian  $\delta^{13}\text{C}$  excursion in the Boreal Realm', *Newsletters on Stratigraphy*, 43(3), pp. 251-273.
189. Mallela, J., Lewis, S. E. and Croke, B. (2013) 'Coral Skeletons Provide Historical Evidence of Phosphorus Runoff on the Great Barrier Reef', *PLOS ONE*, 8(9).
190. Marriott, C. S., Henderson, G. M., Crompton, R., Staubwasser, M. and Shaw, S. (2004) 'Effect of mineralogy, salinity, and temperature on Li/Ca and Li isotope composition of calcium carbonate', *Chemical Geology*, 212(1-2), pp. 5-15.

191. Mason, H. E., Montagna, P., Kubista, L., Taviani, M., McCulloch, M. and Phillips, B. L. (2011) 'Phosphate defects and apatite inclusions in coral skeletal aragonite revealed by solid-state NMR spectroscopy', *Geochimica et Cosmochimica Acta*, 75(23), pp. 7446-7457.
192. McArthur, J. M., Algeo, T. J., Van De Schootbrugge, B., Li, Q. and Howarth, R. J. (2008) 'Basinal restriction, black shales, Re-Os dating, and the Early Toarcian (Jurassic) oceanic anoxic event', *Paleoceanography*, 23(4), pp. 4217-4217.
193. McArthur, J. M., Donovan, D. T., Thirlwall, M. F., Fouke, B. W. and Matthey, D. (2000) 'Strontium isotope profile of the early Toarcian (Jurassic) oceanic anoxic event, the duration of ammonite biozones, and belemnite palaeotemperatures', *Earth and Planetary Science Letters*, 179(2), pp. 269-285.
194. McArthur, J. M., Doyle, P., Leng, M. J., Reeves, K., Williams, C. T., Garcia-Sanchez, R. and Howarth, R. J. (2007a) 'Testing palaeo-environmental proxies in Jurassic belemnites: Mg/Ca, Sr/Ca, Na/Ca,  $\delta^{18}\text{O}$  and  $\delta^{13}\text{C}$ ', *Palaeogeography, Palaeoclimatology, Palaeoecology*, 252(3-4), pp. 464-480.
195. McArthur, J. M., Janssen, N. M. M., Reboulet, S., Leng, M. J., Thirlwall, M. F. and van de Schootbrugge, B. (2007b) 'Palaeotemperatures, polar ice-volume, and isotope stratigraphy (Mg/Ca,  $\delta^{18}\text{O}$ ,  $\delta^{13}\text{C}$ ,  $^{87}\text{Sr}/^{86}\text{Sr}$ ): The Early Cretaceous (Berriasian, Valanginian, Hauterivian)', *Palaeogeography, Palaeoclimatology, Palaeoecology*, 248(3-4), pp. 391-430.
196. McCulloch, M., Fallon, S., Wyndham, T., Hendy, E., Lough, J. and Barnes, D. (2003) 'Coral record of increased sediment flux to the inner Great Barrier Reef since European settlement', 421(6924), pp. 727-730.
197. McElwain, J. C., Wade-Murphy, J. and Hesselbo, S. P. (2005) 'Changes in carbon dioxide during an oceanic anoxic event linked to intrusion into Gondwana coals', *Nature*, 435(7041), pp. 479-482.
198. Metodiev, L. (2008) 'The ammonite zones of the Toarcian in Bulgaria: new evidence, subzonation and correlation with the standard zones and subzones in north-western Europe', *Proceedings of the Bulgarian Academy of Sciences*, 61(1), pp. 87-132.
199. Metodiev, L. and Koleva-Rekalova, E. (2008) 'Stable isotope records ( $\delta^{18}\text{O}$  and  $\delta^{13}\text{C}$ ) of Lower-Middle Jurassic belemnites from the Western Balkan mountains (Bulgaria): Palaeoenvironmental application', *Applied Geochemistry*, 23(10), pp. 2845-2856.

200. Mezger, E. M., de Nooijer, L. J., Boer, W., Brummer, G. J. A. and Reichart, G. J. (2016) 'Salinity controls on Na incorporation in Red Sea planktonic foraminifera', *Paleoceanography*, 31(12), pp. 1562-1582.
201. Millero, F., Huang, F., Zhu, X., Liu, X. and Zhang, J. Z. (2001) 'Adsorption and desorption of phosphate on calcite and aragonite in seawater', *Aquatic Geochemistry*, 7(1), pp. 33-56.
202. Mills, B. J. W., Donnadieu, Y. and Godd ris, Y. (2021) 'Spatial continuous integration of Phanerozoic global biogeochemistry and climate', *Gondwana Research*, 100, pp. 73-86.
203. Misra, S. and Froelich, P. N. (2012) 'Lithium isotope history of cenozoic seawater: Changes in silicate weathering and reverse weathering', *Science*, 335(6070), pp. 818-823.
204. Montagna, P., McCulloch, M., Douville, E., L pez Correa, M., Trotter, J., Rodolfo-Metalpa, R., Dissard, D., Ferrier-Pag s, C., Frank, N., Freiwald, A., Goldstein, S., Mazzoli, C., Reynaud, S., R ggeberg, A., Russo, S. and Taviani, M. (2014) 'Li/Mg systematics in scleractinian corals: Calibration of the thermometer', *Geochimica et Cosmochimica Acta*, 132, pp. 288-310.
205. Montagna, P., McCulloch, M., Taviani, M., Mazzoli, C. and Vendrell, B. (2006) 'Phosphorus in cold-water corals as a proxy for seawater nutrient chemistry', *Science*, 312(5781), pp. 1788-1791.
206. Monteiro, F. M., Pancost, R. D., Ridgwell, A. and Donnadieu, Y. (2012) 'Nutrients as the dominant control on the spread of anoxia and euxinia across the Cenomanian-Turonian oceanic anoxic event (OAE2): Model-data comparison', *Paleoceanography*, 27(4).
207. Moulin, M., Fluteau, F., Courtillot, V., Marsh, J., Delpech, G., Quidelleur, X. and G rard, M. (2017) 'Eruptive history of the Karoo lava flows and their impact on early Jurassic environmental change', *Journal of Geophysical Research: Solid Earth*, 122(2), pp. 738-772.
208. Mucci, A. (1987) 'Influence of temperature on the composition of magnesian calcite overgrowths precipitated from seawater', *Geochimica et Cosmochimica Acta*, 51(7), pp. 1977-1984.
209. Mucci, A. and Morse, J. W. (1983) 'The incorporation of Mg<sup>2+</sup> and Sr<sup>2+</sup> into calcite overgrowths: influences of growth rate and solution composition', *Geochimica et Cosmochimica Acta*, 47(2), pp. 217-233.
210. Mucci, A., Canuel, R. and Zhong, S. (1989) 'The solubility of calcite and aragonite in sulfate-free seawater and the seeded growth kinetics and composition of the precipitates at 25 C', *Chemical Geology*, 74(3-4), pp. 309-320.

211. Müller, T., Tomašových, A., Milovský, R., Jurikova, H., Gutjahr, M., Liebetrau, V., Eisenhauer, A., Schlögl, J., Duarte, L. v., Suan, G., Mattioli, E. and Pittet, B. (2020) 'Ocean acidification during the early Toarcian extinction event: Evidence from boron isotopes in brachiopods', *Geology*, 48(12), pp. 1184-1188.
212. Mutvei, H. (1964) 'On the shell of *Nautilus* and *Spirula* with notes on the shell secretion in non-cephalopod molluscs', Sweden: Almqvist and Wiksell
213. Nambiar, R., Evans, D., Gray, W., Raddatz, J., Henehan, M., Müller, W., Kniest, J., Cotton, L., Hauzer, H., Renema, W. and Erez, J. (2021) 'Evaluating the utility of K/Ca in marine carbonates as a recorder of seawater chemistry'. *Goldschmidt 2021 Abstracts*.
214. Neil, T. R. and Askew, G. N. (2018) 'Swimming mechanics and propulsive efficiency in the chambered Nautilus', *Royal Society Open Science*, 5, pp. 1–9.
215. Newton, R. J., Reeves, E. P., Kafousia, N., Wignall, P. B., Bottrell, S. H. and Sha, J. G. (2011) 'Low marine sulfate concentrations and the isolation of the European epicontinental sea during the Early Jurassic', *Geology*, 39(1), pp. 7-10.
216. O'Dor, R. K. and Webber, D. M. (1986) 'The constraints on cephalopods: why squids aren't fish', *Canadian Journal of Zoology*, 64, pp. 1591–1604.
217. Okumura, M. and Kitano, Y. (1986) 'Coprecipitation of alkali metal ions with calcium carbonate', *Geochimica et Cosmochimica Acta*, 50(1), pp. 49-58.
218. Pancost, R. D., Boot, C. S. (2004) 'The palaeoclimatic utility of terrestrial biomarkers in marine sediments', *Marine Chemistry*, 92(1-4), pp. 239-261.
219. Papineau, D. (2010) 'Global Biogeochemical Changes at Both Ends of the Proterozoic: Insights from Phosphorites', *Astrobiology*, 10(2), pp. 165-181.
220. Paris, G., Fehrenbacher, J. S., Sessions, A. L., Spero, H. J. and Adkins, J. F. (2014) 'Experimental determination of carbonate-associated sulfate  $\delta^{34}\text{S}$  in planktonic foraminifera shells', *Geochemistry, Geophysics, Geosystems*, 15(4), pp. 1452-1461.
221. Paytan, A. and McLaughlin, K. (2007) 'The oceanic phosphorus cycle', *Chemical Reviews*, 107(2), pp. 563-576.
222. Penkman, K. E. H., Kaufman, D. S., Maddy, D. and Collins, M. J. (2008) 'Closed-system behaviour of the intra-crystalline fraction of amino acids in mollusc shells', *Quaternary Geochronology*, 3(1-2), pp. 2-25.

223. Penman, D. E., Hönisch, B., Rasbury, E. T., Hemming, N. G. and Spero, H. J. (2013) 'Boron, carbon, and oxygen isotopic composition of brachiopod shells: Intra-shell variability, controls, and potential as a paleo-pH recorder', *Chemical Geology*, 340, pp. 32-39.
224. Percival, L. M. E., Cohen, A. S., Davies, M. K., Dickson, A. J., Hesselbo, S. P., Jenkyns, H. C., Leng, M. J., Mather, T. A., Storm, M. S. and Xu, W. (2016) 'Osmium isotope evidence for two pulses of increased continental weathering linked to Early Jurassic volcanism and climate change', *Geology*, 44(9), pp. 759-762.
225. Petrochenkov, D. A., Veligzhanin, A. A., Frey, D. I. and Chernyshov, A. A. (2018) 'Riddle of the Nautilus: Specific Structural Features of Its Shell', *Oceanology*, 58(1), pp. 45-52.
226. Pieńkowski, G., Uchman, A., Ninard, K. and Hesselbo, S. P. (2021) 'Ichnology, sedimentology, and orbital cycles in the hemipelagic Early Jurassic Laurusian Seaway (Pliensbachian, Cardigan Bay Basin, UK)', *Global and Planetary Change*, 207, pp. 103648-103648.
227. Pistiner, J. S. and Henderson, G. M. (2003) 'Lithium-isotope fractionation during continental weathering processes', *Earth and Planetary Science Letters*, 214(1-2), pp. 327-339.
228. Pittet, B., Suan, G., Lenoir, F., Duarte, L. V. and Mattioli, E. (2014) 'Carbon isotope evidence for sedimentary discontinuities in the lower Toarcian of the Lusitanian Basin (Portugal): Sea level change at the onset of the Oceanic Anoxic Event', *Sedimentary Geology*, 303, pp. 1-14.
229. Planavsky, N. J., Rouxel, O. J., Bekker, A., Lalonde, S. V., Konhauser, K. O., Reinhard, C. T. and Lyons, T. W. (2010) 'The evolution of the marine phosphate reservoir', *Nature*, 467(7319), pp. 1088-1090.
230. Podlaha, O. G., Mutterlose, J. and Veizer, J. (1998) 'Preservation of delta 18 O and delta 13 C in belemnite rostra from the Jurassic/Early Cretaceous successions', *American Journal of Science*, 298(4), pp. 324-347.
231. Pogge von Strandmann, P. A. E. and Henderson, G. M. (2015) 'The Li isotope response to mountain uplift', *Geology*, 43(1), pp. 67-70.
232. Pogge Von Strandmann, P. A. E., Jenkyns, H. C. and Woodfine, R. G. (2013) 'Lithium isotope evidence for enhanced weathering during Oceanic Anoxic Event 2', *Nature Geoscience*, 6(8), pp. 668-672.

233. Pogge von Strandmann, P. A. E., Vaks, A., Bar-Matthews, M., Ayalon, A., Jacob, E. and Henderson, G. M. (2017) 'Lithium isotopes in speleothems: Temperature-controlled variation in silicate weathering during glacial cycles', *Earth and Planetary Science Letters*, 469, pp. 64-74.
234. Politi, Y., Batchelor, D. R., Zaslansky, P., Chmelka, B. F., Weaver, J. C., Sagi, I., Weiner, S. and Addadi, L. (2010) 'Role of magnesium ion in the stabilization of biogenic amorphous calcium carbonate: A structure-function investigation', *Chemistry of Materials*, 22(1), pp. 161-166.
235. Poulain, C., Gillikin, D. P., Thébault, J., Munaron, J. M., Bohn, M., Robert, R., Paulet, Y. M. and Lorrain, A. (2015) 'An evaluation of Mg/Ca, Sr/Ca, and Ba/Ca ratios as environmental proxies in aragonite bivalve shells', *Chemical Geology*, 396, pp. 42-50.
236. Poulton, S. W. (2021) 'The Iron Speciation Paleoredox Proxy.' United Kingdom: Cambridge University Press.
237. Poulton, S. W. and Canfeld, D. E. (2011) 'Ferruginous Conditions: A Dominant Feature of the Ocean through Earth's History', *Elements*, 7(2), pp. 107-112.
238. Poulton, S. W. and Canfield, D. E. (2005) 'Development of a sequential extraction procedure for iron: Implications for iron partitioning in continentally derived particulates', *Chemical Geology*, 214(3-4), pp. 209-221.
239. Powell, J. H. (1984) 'Lithostratigraphical nomenclature of the Lias Group in the Yorkshire Basin', *Proceedings of the Yorkshire Geological Society*, 45(1-2), pp. 51-57.
240. Powell, J. H. (2010) 'Jurassic sedimentation in the Cleveland Basin: a review', *Proceedings of the Yorkshire Geological Society*, 58(1), pp. 21-72.
241. Price, G. D., Twitchett, R. J., Smale, C. and Marks, V. (2009) 'Isotopic analysis of the life history of the enigmatic squid *Spirula spirula*, with implications for studies of fossil cephalopods', *Palaios*, 24(5-6), pp. 273-279.
242. Pugh, A. (2018) 'Palaeoenvironmental and biotic change through the Lower Jurassic in Bulgaria', *University of Leeds*.
243. Qiu, Z., Zou, C., Mills, B. J. W., Xiong, Y., Tao, H., Lu, B., Liu, H., Xiao, W. and Poulton, S. W. (2022) 'A nutrient control on expanded anoxia and global cooling during the Late Ordovician mass extinction', *Communications Earth and Environment* 2022 3:1, 3(1), pp. 1-9.

244. Raiswell, R. and Canfield, D. E. (2012) 'The iron biogeochemical cycle past and present', *Geochemical Perspectives*, 1(1), pp. 1-232.
245. Raz, S., Weiner, S. and Addadi, L. (2000) 'Formation of High-Magnesian Calcites via an Amorphous Precursor Phase: Possible Biological Implications', *Advanced Materials*, 12(1).
246. Redfern, S. A. T. and Angel, R. J. (1999) 'High-pressure behaviour and equation of state of calcite, CaCO<sub>3</sub>', *Contributions to Mineralogy and Petrology*, 134(1), pp. 102-106.
247. Reinhard, C. T., Planavsky, N. J., Gill, B. C., Ozaki, K., Robbins, L. J., Lyons, T. W., Fischer, W. W., Wang, C., Cole, D. B. and Konhauser, K. O. (2016) 'Evolution of the global phosphorus cycle', 541(7637), pp. 386-389.
248. Reolid, M., Mattioli, E., Duarte, L. V. and Ruebsam, W. (2021) 'The Toarcian oceanic anoxic event: Where do we stand?', *Geological Society Special Publication*, 514(1), pp. 1-11.
249. Rexfort, A. and Mutterlose, J. (2006) 'Stable isotope records from *Sepia officinalis*—a key to understanding the ecology of belemnites?', *Earth and Planetary Science Letters*, 247(3-4), pp. 212-221.
250. Rexfort, A. and Mutterlose, J. (2009) 'The role of biogeography and ecology on the isotope signature of cuttlefishes (Cephalopoda, Sepiidae) and the impact on belemnite studies', *Palaeogeography, Palaeoclimatology, Palaeoecology*, 284(3-4), pp. 153-163.
251. Riding, J. B. (2021) 'A guide to preparation protocols in palynology', *Palynology*, 45(1), pp. 1-110.
252. Rodriguez-Tovar, F. J. and Uchman, A. (2010) 'Ichnofabric evidence for the lack of bottom anoxia during the lower Toarcian oceanic anoxic event in the Fuente de la Vidriera section, Betic Cordillera, Spain', *Palaios*, 25(9), pp. 576-587.
253. Röhl, H. J., Schmid-Röhl, A., Oschmann, W., Frimmel, A. and Schwark, L. (2001) 'The Posidonia Shale (Lower Toarcian) of SW-Germany: an oxygen-depleted ecosystem controlled by sea level and palaeoclimate', *Palaeogeography, Palaeoclimatology, Palaeoecology*, 165(1-2), pp. 27-52.
254. Rollion-Bard, C. and Blamart, D. (2015) 'Possible controls on Li, Na, and Mg incorporation into aragonite coral skeletons', *Chemical Geology*, 396, pp. 98-111.
255. Rosales, I., Robles, S. and Quesada, S. (2004) 'Elemental and Oxygen Isotope Composition of Early Jurassic Belemnites: Salinity vs. Temperature Signals', *Journal of Sedimentary Research*, 74(3), pp. 342-354.

256. Rosenthal, Y., Boyle, E. A. and Slowey, N. (1997) 'Temperature control on the incorporation of magnesium, strontium, fluorine, and cadmium into benthic foraminiferal shells from Little Bahama Bank: Prospects for thermocline paleoceanography', *Geochimica et Cosmochimica Acta*, 61(17), pp. 3633-3643.
257. Rue, E. L., Smith, G. J., Cutter, G. A. and Bruland, K. W. (1997) 'The response of trace element redox couples to suboxic conditions in the water column', *Deep Sea Research Part I: Oceanographic Research Papers*, 44(1), pp. 113-134.
258. Ruebsam, W. and Al-Husseini, M. (2020) 'Calibrating the Early Toarcian (Early Jurassic) with stratigraphic black holes (SBH)', *Gondwana Research*, 82, pp. 317-336.
259. Ruebsam, W., Mayer, B. and Schwark, L. (2019) 'Cryosphere carbon dynamics control early Toarcian global warming and sea level evolution', *Global and Planetary Change*, 172, pp. 440-453.
260. Ruttenberg, K. C. (1992) 'Development of a sequential extraction method for different forms of phosphorus in marine sediments', *Limnology and Oceanography*, 37(7), pp. 1460-1482.
261. Ruttenberg, K. C. (1993) 'Reassessment of the oceanic residence time of phosphorus', *Chemical Geology*, 107(3-4), pp. 405-409.
262. Ruttenberg, K. C. (2001) 'Phosphorus Cycle', *Encyclopedia of Ocean Sciences*, pp. 2149-2162.
263. Ruttenberg, K. C. (2003) 'The Global Phosphorus Cycle', *Treatise on Geochemistry*, 8-9, pp. 585-643.
264. Ruttenberg, K. C. and Berner, R. A. (1993) 'Authigenic apatite formation and burial in sediments from non-upwelling, continental margin environments', *Geochimica et Cosmochimica Acta*, 57(5), pp. 991-1007.
265. Sælen, G. (1989) 'Diagenesis and construction of the belemnite rostrum', *Palaeontology*, 32(4), pp. 765-797.
266. Sælen, G., Doyle, P. and Talbot, M. R. (1996) 'Stable-isotope analyses of belemnite rostra from the Whitby Mudstone Fm., England: Surface water conditions during deposition of a marine black shale', *Palaios*, 11(2), pp. 97-117.
267. Sælen, G., Tyson, R. V., Telnæs, N. and Talbot, M. R. (2000) 'Contrasting watermass conditions during deposition of the Whitby Mudstone (Lower Jurassic) and Kimmeridge

- Clay (Upper Jurassic) formations, UK', *Palaeogeography, Palaeoclimatology, Palaeoecology*, 163(3-4), pp. 163-196.
268. Sáenz Ezquerro, C., Laspalas, M., García Aznar, J. M. and Crespo Miñana, C. (2023) 'Monitoring interactions through molecular dynamics simulations: effect of calcium carbonate on the mechanical properties of cellulose composites', *Cellulose*, 30(2), pp. 705-726.
269. Sanyal, A., Bijma, J., Spero, H. and Lea, D. W. (2001) 'Empirical relationship between pH and the boron isotopic composition of Globigerinoides sacculifer: Implications for the boron isotope paleo-pH proxy', *Paleoceanography*, 16(5), pp. 515-519.
270. Sanyal, A., Hemming, N. G., Broecker, W. S., Lea, D. W., Spero, H. J. and Hanson, G. N. (1996) 'Oceanic pH control on the boron isotopic composition of foraminifera: Evidence from culture experiments', *Paleoceanography*, 11(5), pp. 513-517.
271. Sanyal, A., Nugent, M., Reeder, R. J. and Bijma, J. (2000) 'Seawater pH control on the boron isotopic composition of calcite: evidence from inorganic calcite precipitation experiments', *Geochimica et Cosmochimica Acta*, 64(9), pp. 1551-1555.
272. Savenko, A. V. (2010) 'Hydrochemical structure of mouth areas of the small rivers discharging into Kandalaksha Bay of the White Sea', Translated from *Okeanologiya*, 1999, 41(6), pp. 835-843, *Oceanology*, 41(6), pp. 799-807.
273. Schindler, D. W. (1974) 'Eutrophication and recovery in experimental lakes: implications for lake management', *Science*, 184(4139), pp. 897-899.
274. Schindler, D. W. (2006) 'Recent advances in the understanding and management of eutrophication', *Limnology and Oceanography*, 51(1part2), pp. 356-363.
275. Schlanger, S. and Jenkyns, H. C. (1976) 'Cretaceous Oceanic Anoxic Events: Causes and Consequences', *Geologie en Mijnbouw*, 55(3-4), pp. 179-184.
276. Schleinkofer, N., Raddatz, J., Freiwald, A., Evans, D., Beuck, L., Rüggeberg, A. and Liebetrau, V. (2019) 'Environmental and biological controls on Na/Ca ratios in scleractinian cold-water corals', *Biogeosciences*, 16(18), pp. 3565-3582.
277. Schobben, M., Foster, W. J., Sleveland, A. R. N., Zuchuat, V., Svensen, H. H., Planke, S., Bond, D. P. G., Marcelis, F., Newton, R. J., Wignall, P. B. and Poulton, S. W. (2020) 'A nutrient control on marine anoxia during the end-Permian mass extinction', *Nature Geosciences*, 13(9), pp. 640-646.

278. Schwark, L. and Frimmel, A. (2004) 'Chemostratigraphy of the Posidonia Black Shale, SW-Germany: II. Assessment of extent and persistence of photic-zone anoxia using aryl isoprenoid distributions', *Chemical Geology*, 206(3-4), pp. 231-248.
279. Seibel, B. A., Thuesen, E. V., Childress, J. J. and Gorodezky, L. A. (1997) 'Decline in pelagic cephalopod metabolism with habitat depth reflects differences in locomotory efficiency', *The Biological Bulletin*, 192, pp.262–278.
280. Serrano, O., Serrano, L. and Mateo, M. A. (2008) 'Effects of sample pre-treatment on the  $\delta^{13}\text{C}$  and  $\delta^{18}\text{O}$  values of living benthic foraminifera', *Chemical Geology*, 257(3-4), pp. 218-220.
281. Shaw, T. J., Moore, W. S., Kloepfer, J. and Sochaski, M. A. (1998) 'The flux of barium to the coastal waters of the southeastern USA: the importance of submarine groundwater discharge', *Geochimica et Cosmochimica Acta*, 62(18), pp. 3047-3054.
282. Shen, G. T. and Sanford, C. L. (1990) 'Trace Element Indicators of Climate Variability in Reef-Building Corals', *Elsevier Oceanography Series*, 52(C), pp. 255-283.
283. Shotyk, W., Immenhauser-Potthast, I. and Vogel, H. A. (1995) 'Determination of nitrate, phosphate and organically bound phosphorus in coral skeletons by ion chromatography', *Journal of Chromatography A*, 706(1-2), pp. 209-213.
284. Simon, L., Lécuyer, C., Maréchal, C. and Coltice, N. (2006) 'Modelling the geochemical cycle of boron: Implications for the long-term  $\delta^{11}\text{B}$  evolution of seawater and oceanic crust', *Chemical Geology*, 225(1-2), pp. 61-76.
285. Sinclair, D. J. and McCulloch, M. T. (2004) 'Corals record low mobile barium concentrations in the Burdekin River during the 1974 flood: evidence for limited Ba supply to rivers?', *Palaeogeography, Palaeoclimatology, Palaeoecology*, 214(1-2), pp. 155-174.
286. Sinclair, D. J., Kinsley, L. P. J. and McCulloch, M. T. (1998) 'High resolution analysis of trace elements in corals by laser ablation ICP-MS', *Geochimica et Cosmochimica Acta*, 62(11), pp. 1889-1901.
287. Sinkko, H., Lukkari, K., Sihvonen, L. M., Sivonen, K., Leivuori, M., Rantanen, M., Paulin, L. and Lyra, C. (2013) 'Bacteria Contribute to Sediment Nutrient Release and Reflect Progressed Eutrophication-Driven Hypoxia in an Organic-Rich Continental Sea', *PLoS ONE*, 8(6).

288. Slomp, C. P., Epping, E. H. G., Helder, W. and Van Raaphorst, W. (1996) 'A key role for iron-bound phosphorus in authigenic apatite formation in North Atlantic continental platform sediments', *Journal of Marine Research*, 54(6), pp. 1179-1205.
289. Sørensen, A. M., Ullmann, C. V., Thibault, N. and Korte, C. (2015) 'Geochemical signatures of the early Campanian belemnite *Belemnellocamax mammillatus* from the Kristianstad Basin in Scania, Sweden', *Palaeogeography, Palaeoclimatology, Palaeoecology*, 433, pp. 191-200.
290. Stanley, S. M. and Hardie, L. A. (1998) 'Secular oscillations in the carbonate mineralogy of reef-building and sediment-producing organisms driven by tectonically forced shifts in seawater chemistry', *Palaeogeography, Palaeoclimatology, Palaeoecology*, 144(1-2), pp. 3-19.
291. Stevens, G. R. (1965) 'The Jurassic and cretaceous belemnites of New Zealand, and a review of the Jurassic and cretaceous belemnites of the indo-Pacific region', *Geological Survey of New Zealand Palaeontological Bulletin*, pp. 36, 1–233.
292. Stevens, G. R. and Clayton, R. N. (1971) 'Oxygen isotope studies on Jurassic and cretaceous belemnites from New Zealand and their biogeographic significance', *New Zealand Journal of Geology and Geophysics*, 14, pp. 829–897.
293. Stevens, G. R. and Clayton, R. N. (1971) 'Oxygen isotope studies on jurassic and cretaceous belemnites from New Zealand and their biogeographic significance', *New Zealand Journal of Geology and Geophysics*, 14(4), pp. 829-897.
294. Stevens, K., Griesshaber, E., Schmahl, W., Casella, L. A., Iba, Y. and Mutterlose, J. r. (2017) 'Belemnite biomineralization, development, and geochemistry: The complex rostrum of *Neohibolites minimus*', *Palaeogeography, Palaeoclimatology, Palaeoecology*, 468, pp. 388-402.
295. Stevens, K., Mutterlose, J. and Schweigert, G. (2014) 'Belemnite ecology and the environment of the Nusplingen Plattenkalk (late Jurassic, southern Germany): evidence from stable isotope data', *Lethaia*, 47, pp. 512–523.
296. Stevens, K., Mutterlose, J., Ohnemus, B., Idakieva, V. and Ivanov, M. (2022) 'Microstructures of Early Cretaceous belemnite rostra and their diagenesis', *Cretaceous Research*, 137.
297. Storm, M. S., Hesselbo, S. P., Jenkyns, H. C., Ruhl, M., Ullmann, C. V., Xu, W., Leng, M. J., Riding, J. B. and Gorbanenko, O. (2020) 'Orbital pacing and secular evolution of the Early

- Jurassic carbon cycle', *Proceedings of the National Academy of Sciences of the United States of America*, 117(8), pp. 3974-3982.
298. Strickland, J. D. H. and Parsons, T. R. (1968) 'A practical handbook of seawater analysis.', *Bulletin of Fisheries Research Board of Canada*, 167, pp. 1-311.
299. Suan, G., Mattioli, E., Pittet, B., Lécuyer, C., Suchéras-Marx, B., Duarte, L. V., Philippe, M., Reggiani, L. and Martineau, F. (2010) 'Secular environmental precursors to Early Toarcian (Jurassic) extreme climate changes', *Earth and Planetary Science Letters*, 290(3-4), pp. 448-458.
300. Suan, G., Nikitenko, B. L., Rogov, M. A., Baudin, F., Spangenberg, J. E., Knyazev, V. G., Glinskikh, L. A., Goryacheva, A. A., Adatte, T., Riding, J. B., Föllmi, K. B., Pittet, B., Mattioli, E. and Lécuyer, C. (2011) 'Polar record of Early Jurassic massive carbon injection', *Earth and Planetary Science Letters*, 312(1-2), pp. 102-113.
301. Suan, G., Pittet, B., Bour, I., Mattioli, E., Duarte, L. V. and Mailliot, S. (2008) 'Duration of the Early Toarcian carbon isotope excursion deduced from spectral analysis: Consequence for its possible causes', *Earth and Planetary Science Letters*, 267(3-4), pp. 666-679.
302. Sugiura, Y., Ishikawa, K., Onuma, K. and Makita, Y. (2019) 'PO<sub>4</sub> adsorption on the calcite surface modulates calcite formation and crystal size', *American Mineralogist*, 104(10), pp. 1381-1388.
303. Sundby, B. r., Gobeil, C., Silverberg, N. and Alfonso, M. (1992) 'The phosphorus cycle in coastal marine sediments', *Limnology and Oceanography*, 37(6), pp. 1129-1145.
304. Svensen, H., Planke, S., Chevallier, L., Malthe-Sørensen, A., Corfu, F. and Jamtveit, B. (2007) 'Hydrothermal venting of greenhouse gases triggering Early Jurassic global warming', *Earth and Planetary Science Letters*, 256(3-4), pp. 554-566.
305. Sykes, G. A., Collins, M. J. and Walton, D. I. (1995) 'The significance of a geochemically isolated intracrystalline organic fraction within biominerals', *Organic Geochemistry*, 23(11-12), pp. 1059-1065.
306. Taft, W. H. (1967) 'Chapter 3 Physical Chemistry of Formation of Carbonates', *Developments in Sedimentology*, 9(PART B), pp. 151-167.
307. Thaler, C., Paris, G., Dellinger, M., Dissard, D., Berland, S., Marie, A., Labat, A. and Bartolini, A. (pre-print) 'Impact of seawater sulfate concentration on sulfur concentration and isotopic composition in calcite of two cultured benthic foraminifera'. *EGUsphere* [preprint].

308. Thibault, N., Ruhl, M., Ullmann, C. V., Korte, C., Kemp, D. B., Gröcke, D. R. and Hesselbo, S. P. (2018) 'The wider context of the Lower Jurassic Toarcian oceanic anoxic event in Yorkshire coastal outcrops, UK', *Proceedings of the Geologists' Association*, 129(3), pp. 372-391.
309. Thompson, J., Poulton, S. W., Guilbaud, R., Doyle, K. A., Reid, S. and Krom, M. D. (2019) 'Development of a modified SEDEX phosphorus speciation method for ancient rocks and modern iron-rich sediments', *Chemical Geology*, 524, pp. 383-393.
310. Torres, M. E., Barry, J. P., Hubbard, D. A. and Suess, E. (2001) 'Reconstructing the history of fluid flow at cold seep sites from Ba/Ca ratios in vesicomid clam shells', *Limnology and Oceanography*, 46(7), pp. 1701-1708.
311. Trabucho-Alexandre, J. P., Gröcke, D. R., Atar, E., Herringshaw, L. and Jarvis, I. (2022) 'A new subsurface record of the Pliensbachian–Toarcian, Lower Jurassic, of Yorkshire', *Proceedings of the Yorkshire Geological Society*, 64(2).
312. Trecalli, A., Spangenberg, J., Adatte, T., Föllmi, K. B. and Parente, M. (2012) 'Carbonate platform evidence of ocean acidification at the onset of the early Toarcian oceanic anoxic event', *Earth and Planetary Science Letters*, 357-358, pp. 214-225.
313. Tremolada, F., Van de Schootbrugge, B. and Erba, E. (2005) 'Early Jurassic schizosphaerellid crisis in Cantabria, Spain: Implications for calcification rates and phytoplankton evolution across the Toarcian oceanic anoxic event', *Paleoceanography*, 20(2), pp. 1-11.
314. Trotter, J., Montagna, P., McCulloch, M., Silenzi, S., Reynaud, S., Mortimer, G., Martin, S., Ferrier-Pagès, C., Gattuso, J. P. and Rodolfo-Metalpa, R. (2011) 'Quantifying the pH 'vital effect' in the temperate zooxanthellate coral *Cladocora caespitosa*: Validation of the boron seawater pH proxy', *Earth and Planetary Science Letters*, 303(3-4), pp. 163-173.
315. Tudhope, A. W., Lea, D. W., Shimmield, G. B., Chilcott, C. P. and Head, S. (1996) 'Monsoon climate and Arabian Sea coastal upwelling recorded in massive corals from southern Oman', *Palaeos*, 11(4), pp. 347-361.
316. Turan, C., Yaglioglu, D., Turan, C. and Yaglioglu, D. (2010) 'Population identification of common cuttlefish (*Sepia officinalis*) inferred from genetic, morphometric and cuttlebone chemistry data in the NE Mediterranean Sea', *Scientia Marina*, 74(1), pp. 77-86.
317. Tyrrell, T. (1999) 'The relative influences of nitrogen and phosphorus on oceanic primary production', *Nature*, 400(6744), pp. 525-531.

318. Ullmann, C. V. and Korte, C. (2015) 'Diagenetic alteration in low-Mg calcite from macrofossils: A review', *Geological Quarterly*, 59(1), pp. 3-20.
319. Ullmann, C. V. and Pogge Von Strandmann, P. A. E. (2017) 'The effect of shell secretion rate on Mg / Ca and Sr / Ca ratios in biogenic calcite as observed in a belemnite rostrum', *Biogeosciences*, 14(1), pp. 89-97.
320. Ullmann, C. V., Campbell, H. J., Frei, R., Hesselbo, S. P., Pogge von Strandmann, P. A. E. and Korte, C. (2013) 'Partial diagenetic overprint of Late Jurassic belemnites from New Zealand: Implications for the preservation potential of  $\delta^7\text{Li}$  values in calcite fossils', *Geochimica et Cosmochimica Acta*, 120, pp. 80-96.
321. Ullmann, C. V., Frei, R., Korte, C. and Hesselbo, S. P. (2015) 'Chemical and isotopic architecture of the belemnite rostrum', *Geochimica et Cosmochimica Acta*, 159, pp. 231-243.
322. Ullmann, C. V., Szűcs, D., Jiang, M., Hudson, A. J. L. and Hesselbo, S. P. (2022) 'Geochemistry of macrofossil, bulk rock and secondary calcite in the Early Jurassic strata of the Llanbedr (Mochras Farm) drill core, Cardigan Bay Basin, Wales, UK', *Journal of the Geological Society*, 179(1).
323. Urey, H. C. (1948) 'Oxygen isotopes in nature and in the laboratory', *Science*, 108(2810), pp. 489-496.
324. Urey, H. C., Lowenstam, H. A., Epstein, S. and McKinny, C. R. (1951) 'measurement of paleotemperatures and temperatures of the upper cretaceous of England, Denmark, and the southeastern United States', *Bulletin of the Geological Society of America*, 62, pp. 399-416.
325. Van Buchem, F. S. P., Melnyk, D. H. and McCave, I. N. (1992) 'Chemical cyclicity and correlation of Lower Lias mudstones using gamma ray logs, Yorkshire, UK', *Journal - Geological Society (London)*, 149(6), pp. 991-1002.
326. Van Cappellen, P. and Ingall, E. D. (1996) 'Redox Stabilization of the Atmosphere and Oceans by Phosphorus-Limited Marine Productivity', *Science*, 271(5248), pp. 493-496.
327. van de Schootbrugge, B., McArthur, J. M., Bailey, T. R., Rosenthal, Y., Wright, J. D. and Miller, K. G. (2005) 'Toarcian oceanic anoxic event: An assessment of global causes using belemnite C isotope records', *Paleoceanography*, 20(3), pp. 1-10.

328. Veizer, J. (1974) 'Chemical diagenesis of belemnite shells and possible consequences for paleotemperature determinations', *Neues Jahrbuch für Geologie und Paläontologie Abhandlungen*, 147 (1), pp. 91-111.
329. Veizer, J., Lemieux, J., Jones, B., Gibling, M. and Savelle, J. M. (1977) 'Sodium: paleosalinity indicator in ancient carbonate rocks', *Geology*, 5(3), pp. 177-179.
330. Vigier, N., Rollion-Bard, C., Levenson, Y. and Erez, J. (2015) 'Lithium isotopes in foraminifera shells as a novel proxy for the ocean dissolved inorganic carbon (DIC)', *Comptes Rendus Geoscience*, 347(1), pp. 43-51.
331. Wallmann, K. (2010) 'Phosphorus imbalance in the global ocean?', *Global Biogeochemical Cycles*, 24(4), pp. 4030-4030.
332. Wang, R. Z., Addadi, L. and Weiner, S. (1997) 'Design strategies of sea urchin teeth: structure, composition and micromechanical relations to function', *Philosophical transactions of the Royal Society of London. Series B, Biological sciences*, 352(1352), pp. 469-480.
333. Wang, Y., Ossa, F. O., Spangenberg, J. E., Wille, M. and Schoenberg, R. (2021) 'Restricted Oxygen-Deficient Basins on the Northern European Epicontinental Shelf Across the Toarcian Carbon Isotope Excursion Interval', *Paleoceanography and Paleoclimatology*, 36(6).
334. Westbroek, P., van der Meide, P. H., van der Wey-Kloppers, J. S., van der Sluis, R. J., De Leeuw, J. W. and De Jong, E. W. (1979) 'Fossil macromolecules from cephalopod shells: characterization, immunological response and diagenesis', *Paleobiology*, 5(2), pp. 151-167.
335. White, A. F. (1977) 'Sodium and potassium coprecipitation in aragonite', *Geochimica et Cosmochimica Acta*, 41(5), pp. 613-625.
336. White, A. F. (1978) 'Sodium coprecipitation in calcite and dolomite', *Chemical Geology*, 23(1-4), pp. 65-72.
337. Wierzbowski, H. (2013) 'Life span and growth rate of Middle Jurassic mesohibolitid belemnites deduced from rostrum microincrements', *Volumina Jurassica*, 11, pp. 1-18.
338. Wierzbowski, H. (2021) 'Advances and challenges in palaeoenvironmental studies based on oxygen isotope composition of skeletal carbonates and phosphates', *Geosciences (Switzerland)*, 11(10), pp. 419-419.

339. Wierzbowski, H. and Joachimski, M. M. (2009) 'Stable isotopes, elemental distribution, and growth rings of belemnite rostra: proxies for belemnite life habitat', *Palaios*, 24(6), pp. 377-386.
340. Wierzbowski, H., Rogov, M. A., Matyja, B. A., Kiselev, D. and Ippolitov, A. (2013) 'Middle-upper Jurassic (upper Callovian-lower Kimmeridgian) stable isotope and elemental records of the Russian platform: Indices of oceanographic and climatic changes', *Global and Planetary Change*, 107, pp. 196-212.
341. Wignall, P. B., Hallam, A., Newton, R. J., Sha, J. G., Reeves, E., Mattioli, E. and Crowley, S. (2006) 'An eastern Tethyan (Tibetan) record of the Early Jurassic (Toarcian) mass extinction event', *Geobiology*, 4(3), pp. 179-190.
342. Wit, J. C., De Nooijer, L. J., Wolthers, M. and Reichart, G. J. (2013) 'A novel salinity proxy based on Na incorporation into foraminiferal calcite', *Biogeosciences*, 10(10), pp. 6375-6387.
343. Wong, G. T. F. and Brewer, P. G. (1977) 'The marine chemistry of iodine in anoxic basins', *Geochimica et Cosmochimica Acta*, 41(1), pp. 151-159.
344. Wood, A. and Woodland, A. W. (1968) 'Borehole at Mochras, West of Llanbedr, Merionethshire', *Nature*, 219(5161), pp. 1352-1354.
345. Xu, W., Ruhl, M., Jenkyns, H. C., Leng, M. J., Huggett, J. M., Minisini, D., Ullmann, C. V., Riding, J. B., Weijers, J. W. H., Storm, M. S., Percival, L. M. E., Tosca, N. J., Idiz, E. F., Tegelaar, E. W. and Hesselbo, S. P. (2018) 'Evolution of the Toarcian (Early Jurassic) carbon-cycle and global climatic controls on local sedimentary processes (Cardigan Bay Basin, UK)', *Earth and Planetary Science Letters*, 484, pp. 396-411.
346. Zeebe, R. E. and Wolf-Gladrow, D. (2001) 'CO<sub>2</sub> in seawater: Equilibrium, kinetics, isotopes', *Elsevier Oceanography Series*, pp. 1-346.
347. Zempolich, W. G. (1993) 'The Drowning Succession in Jurassic Carbonates of the Venetian Alps, Italy: A Record of Supercontinent Breakup, Gradual Eustatic Rise, and Eutrophication of Shallow-Water Environments: Chapter 3', 168, pp. 63-105.
348. Zhang, N., Lin, M., Yamada, K., Kano, A., Liu, Q., Yoshida, N. and Matsumoto, R. (2020) 'The effect of H<sub>2</sub>O<sub>2</sub> treatment on stable isotope analysis ( $\delta^{13}\text{C}$ ,  $\delta^{18}\text{O}$  and  $\Delta_{47}$ ) of various carbonate minerals', *Chemical Geology*, 532.

349. Zhong, S. and Mucci, A. (1989) 'Calcite and aragonite precipitation from seawater solutions of various salinities: Precipitation rates and overgrowth compositions', *Chemical Geology*, 78(3-4), pp. 283-299.
350. Zhou, X., Rosenthal, Y., Haynes, L., Si, W., Evans, D., Huang, K.-F., Hö Nisch G, B. and Erez, J. (2021) 'Planktic foraminiferal Na/Ca: A potential proxy for seawater calcium concentration', *Geochimica et Cosmochimica Acta*, 305, pp. 306-322.

## 8. Appendix

### 8.1. Bulk Samples analysis

Table 29 – Main elemental results for analysis of Bulk Samples including Ca values (mol), and Mg/Ca, P/Ca, Sr/Ca, Na/Ca, Fe/Ca, and Mn/Ca values ( $\mu\text{mol mol}^{-1}$ ).

Sample number	Cleaning method	Mass / mg	Acid	Ca (mol)	Mg/Ca ( $\mu\text{mol mol}^{-1}$ )	P/Ca ( $\mu\text{mol mol}^{-1}$ )	Sr/Ca ( $\mu\text{mol mol}^{-1}$ )	Na/Ca ( $\mu\text{mol mol}^{-1}$ )	Fe/Ca ( $\mu\text{mol mol}^{-1}$ )	Mn/Ca ( $\mu\text{mol mol}^{-1}$ )
<b>Bulk 1 (approximately 5 mg mass)</b>										
B1-PER-C-001	H <sub>2</sub> O <sub>2</sub>	5.19	HCl	2.00E-05	21,542	4,481	3,335	14,190	9,402	760
B1-PER-C-002	H <sub>2</sub> O <sub>2</sub>	6.26	HCl	2.20E-05	21,650	4,071	3,285	13,290	9,049	774
B1-PER-C-003	H <sub>2</sub> O <sub>2</sub>	4.88	HCl	1.90E-05	21,632	4,109	3,292	13,125	8,901	740
B1-PER-N-004	H <sub>2</sub> O <sub>2</sub>	5.96	HNO <sub>3</sub>	2.26E-05	21,879	4,741	3,292	14,368	10,161	766
B1-PER-N-005	H <sub>2</sub> O <sub>2</sub>	4.74	HNO <sub>3</sub>	1.99E-05	21,745	3,907	3,284	15,068	8,780	708
B1-PER-N-006	H <sub>2</sub> O <sub>2</sub>	4.40	HNO <sub>3</sub>	1.66E-05	22,019	4,806	3,268	14,508	10,499	778
B1-PER-A-007	H <sub>2</sub> O <sub>2</sub>	6.59	Acetic	2.71E-05	21,815	1,798	3,350	14,352	6,656	784
B1-PER-A-008	H <sub>2</sub> O <sub>2</sub>	6.00	Acetic	2.40E-05	21,626	2,176	3,301	14,216	6,642	754
B1-PER-A-009	H <sub>2</sub> O <sub>2</sub>	6.04	Acetic	2.40E-05	21,570	2,111	3,310	14,195	6,871	747
B1-SOD-C-010	NaOCl	5.47	HCl	2.09E-05	22,661	4,722	3,210	14,277	8,863	755
B1-SOD-C-011	NaOCl	5.23	HCl	1.86E-05	22,839	4,666	3,238	13,743	9,073	812
B1-SOD-C-012	NaOCl	6.20	HCl	2.37E-05	22,604	4,993	3,217	13,656	8,994	791
B1-SOD-N-013	NaOCl	5.37	HNO <sub>3</sub>	1.88E-05	23,018	5,132	3,237	15,209	7,181	821
B1-SOD-N-014	NaOCl	6.52	HNO <sub>3</sub>	2.42E-05	22,670	4,920	3,268	14,790	6,912	778
B1-SOD-N-015	NaOCl	5.68	HNO <sub>3</sub>	2.62E-05	23,062	5,063	3,296	15,060	7,157	802
B1-SOD-A-016	NaOCl	6.03	Acetic	1.99E-05	22,708	2,867	3,363	14,811	5,666	757
B1-SOD-A-017	NaOCl	4.89	Acetic	1.66E-05	22,799	3,479	3,331	24,735	5,457	749
B1-SOD-A-018	NaOCl	5.67	Acetic	1.59E-05	22,866	3,748	3,341	14,938	5,680	793

Sample number	Cleaning method	Mass / mg	Acid	Ca (mol)	Mg/Ca ( $\mu\text{mol mol}^{-1}$ )	P/Ca ( $\mu\text{mol mol}^{-1}$ )	Sr/Ca ( $\mu\text{mol mol}^{-1}$ )	Na/Ca ( $\mu\text{mol mol}^{-1}$ )	Fe/Ca ( $\mu\text{mol mol}^{-1}$ )	Mn/Ca ( $\mu\text{mol mol}^{-1}$ )
B1-WAT-C-019	Water	5.16	HCl	1.67E-05	22,470	4,991	3,279	13,621	5,984	892
B1-WAT-C-020	Water	4.88	HCl	1.71E-05	22,279	5,083	3,267	15,300	5,904	833
B1-WAT-C-021	Water	5.42	HCl	2.70E-05	22,403	5,099	3,299	14,010	6,039	907
B1-WAT-N-022	Water	6.33	HNO <sub>3</sub>	1.51E-05	22,593	5,262	3,294	13,690	5,790	836
B1-WAT-N-023	Water	6.18	HNO <sub>3</sub>	1.91E-05	22,601	5,315	3,251	14,478	6,298	889
B1-WAT-N-024	Water	6.86	HNO <sub>3</sub>	1.63E-05	22,547	5,132	3,255	14,545	5,979	851
B1-WAT-A-025	Water	5.56	Acetic	1.90E-05	23,108	3,766	3,357	13,931	5,881	894
B1-WAT-A-026	Water	6.27	Acetic	1.96E-05	22,468	3,676	3,322	15,643	5,264	818
B1-WAT-A-027	Water	5.00	Acetic	1.50E-05	22,750	3,627	3,329	14,549	5,257	824
<b>Bulk 2 (approximately 5 mg mass)</b>										
B2-PER-C-019	H <sub>2</sub> O <sub>2</sub>	5.80	HCl	5.70E-05	11,334	797	1,729	8,346	132	27
B2-PER-C-020	H <sub>2</sub> O <sub>2</sub>	4.60	HCl	4.54E-05	11,306	808	1,732	8,769	166	22
B2-PER-C-021	H <sub>2</sub> O <sub>2</sub>	3.50	HCl	3.62E-05	11,025	817	1,659	8,589	152	32
B2-PER-N-022	H <sub>2</sub> O <sub>2</sub>	5.20	HNO <sub>3</sub>	5.12E-05	11,087	801	1,689	8,639	126	22
B2-PER-N-023	H <sub>2</sub> O <sub>2</sub>	6.30	HNO <sub>3</sub>	6.29E-05	11,015	811	1,667	8,108	116	22
B2-PER-N-024	H <sub>2</sub> O <sub>2</sub>	5.70	HNO <sub>3</sub>	5.63E-05	11,052	762	1,662	7,987	103	23
B2-PER-A-025	H <sub>2</sub> O <sub>2</sub>	5.10	Acetic	5.21E-05	10,972	796	1,709	8,942	143	20
B2-PER-A-026	H <sub>2</sub> O <sub>2</sub>	5.50	Acetic	5.43E-05	10,892	746	1,685	8,909	100	21
B2-PER-A-027	H <sub>2</sub> O <sub>2</sub>	5.70	Acetic	5.78E-05	10,931	776	1,693	8,402	92	21
B2-WAT-C-028	Water	5.70	HCl	5.56E-05	10,853	793	1,641	7,289	99	18
B2-WAT-C-029	Water	6.10	HCl	5.84E-05	10,770	787	1,631	7,153	142	20
B2-WAT-C-030	Water	5.50	HCl	5.41E-05	10,724	769	1,629	7,286	75	18
B2-WAT-N-031	Water	5.40	HNO <sub>3</sub>	5.53E-05	10,888	792	1,626	7,522	74	19
B2-WAT-N-032	Water	5.90	HNO <sub>3</sub>	6.07E-05	10,872	803	1,627	7,382	93	17

Sample number	Cleaning method	Mass / mg	Acid	Ca (mol)	Mg/Ca ( $\mu\text{mol mol}^{-1}$ )	P/Ca ( $\mu\text{mol mol}^{-1}$ )	Sr/Ca ( $\mu\text{mol mol}^{-1}$ )	Na/Ca ( $\mu\text{mol mol}^{-1}$ )	Fe/Ca ( $\mu\text{mol mol}^{-1}$ )	Mn/Ca ( $\mu\text{mol mol}^{-1}$ )
B2-WAT-N-033	Water	5.60	HNO <sub>3</sub>	5.38E-05	10,840	802	1,620	7,640	92	18
B2-WAT-A-034	Water	5.60	Acetic	5.86E-05	10,838	766	1,681	8,393	90	20
B2-WAT-A-035	Water	5.90	Acetic	6.16E-05	10,928	755	1,682	8,273	89	19
B2-WAT-A-036	Water	4.80	Acetic	5.07E-05	10,866	796	1,664	9,459	97	26
<b>Bulk 3 (approximately 5 mg mass)</b>										
B3-PER-C-037	H <sub>2</sub> O <sub>2</sub>	5.50	HCl	5.39E-05	12,711	1,136	1,835	10,735	581	205
B3-PER-C-038	H <sub>2</sub> O <sub>2</sub>	5.50	HCl	5.43E-05	12,955	1,128	1,885	11,060	560	164
B3-PER-C-039	H <sub>2</sub> O <sub>2</sub>	5.20	HCl	5.00E-05	13,029	1,150	1,899	11,315	566	183
B3-PER-N-040	H <sub>2</sub> O <sub>2</sub>	5.50	HNO <sub>3</sub>	5.17E-05	12,970	1,106	1,899	11,339	652	176
B3-PER-N-041	H <sub>2</sub> O <sub>2</sub>	5.40	HNO <sub>3</sub>	5.34E-05	12,640	1,144	1,961	11,065	535	182
B3-PER-N-042	H <sub>2</sub> O <sub>2</sub>	4.80	HNO <sub>3</sub>	4.81E-05	13,068	1,220	2,040	12,034	504	180
B3-PER-A-043	H <sub>2</sub> O <sub>2</sub>	5.50	Acetic	5.48E-05	12,969	1,065	2,088	14,750	415	171
B3-PER-A-044	H <sub>2</sub> O <sub>2</sub>	5.00	Acetic	5.09E-05	12,993	1,075	2,102	12,800	427	196
B3-PER-A-045	H <sub>2</sub> O <sub>2</sub>	6.40	Acetic	6.39E-05	12,903	1,051	2,091	13,252	431	184
B3-WAT-C-046	Water	5.00	HCl	5.00E-05	12,853	1,125	2,037	11,047	392	177
B3-WAT-C-047	Water	5.40	HCl	5.33E-05	12,944	1,132	2,064	11,516	332	169
B3-WAT-C-048	Water	5.90	HCl	6.04E-05	12,714	1,114	2,023	11,340	360	172
B3-WAT-N-049	Water	6.00	HNO <sub>3</sub>	5.79E-05	12,821	1,114	2,040	11,251	336	168
B3-WAT-N-050	Water	4.90	HNO <sub>3</sub>	4.97E-05	13,052	1,120	2,080	11,581	352	173
B3-WAT-N-051	Water	5.40	HNO <sub>3</sub>	5.26E-05	12,950	1,101	2,049	11,681	344	190
B3-WAT-A-052	Water	6.10	Acetic	5.96E-05	13,197	1,085	2,158	12,568	307	197
B3-WAT-A-053	Water	4.70	Acetic	3.80E-05	13,138	1,099	2,139	12,574	303	185
B3-WAT-A-054	Water	6.10	Acetic	6.41E-05	12,922	1,048	2,142	12,568	273	171
<b>Bulk 2 (approximately 2 mg mass)</b>										
B2-PER-A-055	H <sub>2</sub> O <sub>2</sub>	1.90	Acetic	2.00E-05	11,464		1,904	9,648		17

Sample number	Cleaning method	Mass / mg	Acid	Ca (mol)	Mg/Ca ( $\mu\text{mol mol}^{-1}$ )	P/Ca ( $\mu\text{mol mol}^{-1}$ )	Sr/Ca ( $\mu\text{mol mol}^{-1}$ )	Na/Ca ( $\mu\text{mol mol}^{-1}$ )	Fe/Ca ( $\mu\text{mol mol}^{-1}$ )	Mn/Ca ( $\mu\text{mol mol}^{-1}$ )
B2-PER-A-056	H <sub>2</sub> O <sub>2</sub>	2.10	Acetic	2.17E-05	11,391		1,894	9,888	116	24
B2-PER-A-057	H <sub>2</sub> O <sub>2</sub>	2.30	Acetic	2.59E-05	11,415	763	1,890	9,427	184	23
<b>Bulk 2 (approximately 10 mg mass)</b>										
B2-PER-A-058	H <sub>2</sub> O <sub>2</sub>	7.20	Acetic	7.24E-05	11,107	720	1,873	8,619	114	18
B2-PER-A-059	H <sub>2</sub> O <sub>2</sub>	6.70	Acetic	6.90E-05	10,996	941	1,832	12,997	125	20
B2-PER-A-060	H <sub>2</sub> O <sub>2</sub>	8.40	Acetic	8.69E-05	10,931	716	1,839	8,263	104	18
<b>Bulk 3 (approximately 2 mg mass)</b>										
B3-PER-A-061	H <sub>2</sub> O <sub>2</sub>	2.20	Acetic	2.20E-05	13,196	1,103	2,162	13,935	408	197
B3-PER-A-062	H <sub>2</sub> O <sub>2</sub>	2.20	Acetic	2.36E-05	13,571	1,082	2,146	15,731	751	193
B3-PER-A-063	H <sub>2</sub> O <sub>2</sub>	1.70	Acetic	1.76E-05	13,511	1,129	2,213	14,158	455	611
<b>Bulk 3 (approximately 10 mg mass)</b>										
B3-PER-A-064	H <sub>2</sub> O <sub>2</sub>	12.70	Acetic	1.31E-04	12,710	1,004	2,134	15,630	428	170
B3-PER-A-065	H <sub>2</sub> O <sub>2</sub>	8.30	Acetic	8.33E-05	12,987	1,048	2,157	12,582	365	165
B3-PER-A-066	H <sub>2</sub> O <sub>2</sub>	10.30	Acetic	1.04E-04	12,753	1,023	2,149	12,680	366	167
<b>Bulk 1 (approximately 2 mg mass)</b>										
B1-PER-A-067	H <sub>2</sub> O <sub>2</sub>	2.10	Acetic	2.01E-05	8,680	1,321	1,492	9,311	3,653	456
B1-PER-A-068	H <sub>2</sub> O <sub>2</sub>	2.20	Acetic	2.01E-05	8,722	1,170	1,495	9,528	3,342	2,852
B1-PER-A-069	H <sub>2</sub> O <sub>2</sub>	1.80	Acetic	1.64E-05	8,894	1,589	1,504	13,497	3,663	551
<b>Bulk 1 (approximately 10 mg mass)</b>										
B1-PER-A-070	H <sub>2</sub> O <sub>2</sub>	7.80	Acetic	7.66E-05	8,496	652	1,469	7,858	3,595	317
B1-PER-A-071	H <sub>2</sub> O <sub>2</sub>	9.10	Acetic	8.87E-05	8,379	621	1,460	7,731	3,404	300
B1-PER-A-072	H <sub>2</sub> O <sub>2</sub>	7.30	Acetic	7.17E-05	8,480	660	1,473	8,631	3,244	309

Table 30 - Supplemental elemental results for analysis of Bulk Samples including Ca values (mol), and Al/Ca, S/Ca, K/Ca, Li/Ca, B/Ca, Ba/Ca, and I/Ca values  $\mu\text{mol mol}^{-1}$ .

Sample number	Cleaning method	Mass / mg	Acid	Ca (mol)	Al/Ca ( $\mu\text{mol mol}^{-1}$ )	S/Ca ( $\mu\text{mol mol}^{-1}$ )	K/Ca ( $\mu\text{mol mol}^{-1}$ )	Li/Ca ( $\mu\text{mol mol}^{-1}$ )	B/Ca ( $\mu\text{mol mol}^{-1}$ )	Ba/Ca ( $\mu\text{mol mol}^{-1}$ )	U/Ca ( $\mu\text{mol mol}^{-1}$ )	I/Ca ( $\mu\text{mol mol}^{-1}$ )
<b>Bulk 1 (approximately 5 mg mass)</b>												
B1-PER-C-001	H <sub>2</sub> O <sub>2</sub>	5.19	HCl	2.00E-05	409	20,216	661	145.83		35.39	2.3E+00	
B1-PER-C-002	H <sub>2</sub> O <sub>2</sub>	6.26	HCl	2.20E-05	201	19,958	558	91.17		23.97		
B1-PER-C-003	H <sub>2</sub> O <sub>2</sub>	4.88	HCl	1.90E-05	145	19,596	353	88.76		22.04		
B1-PER-N-004	H <sub>2</sub> O <sub>2</sub>	5.96	HNO <sub>3</sub>	2.26E-05	1,400	19,498	733	82.85		33.06		
B1-PER-N-005	H <sub>2</sub> O <sub>2</sub>	4.74	HNO <sub>3</sub>	1.99E-05	487	19,619	827	83.12		27.01		
B1-PER-N-006	H <sub>2</sub> O <sub>2</sub>	4.40	HNO <sub>3</sub>	1.66E-05	588	19,420	847	80.53		37.94		
B1-PER-A-007	H <sub>2</sub> O <sub>2</sub>	6.59	Acetic	2.71E-05	212	19,473	442	85.72		14.25		
B1-PER-A-008	H <sub>2</sub> O <sub>2</sub>	6.00	Acetic	2.40E-05	1,113	19,171	441	82.06		14.34		
B1-PER-A-009	H <sub>2</sub> O <sub>2</sub>	6.04	Acetic	2.40E-05	1,650	19,039	469	81.44		13.74		
B1-SOD-C-010	NaOCl	5.47	HCl	2.09E-05	261	19,443	525	55.12		33.99		
B1-SOD-C-011	NaOCl	5.23	HCl	1.86E-05	556	19,437	579	108.42		25.52		
B1-SOD-C-012	NaOCl	6.20	HCl	2.37E-05	270	19,438	362	68.89		25.38		
B1-SOD-N-013	NaOCl	5.37	HNO <sub>3</sub>	1.88E-05	611	19,749	916	99.10		29.71		
B1-SOD-N-014	NaOCl	6.52	HNO <sub>3</sub>	2.42E-05	498	19,441	788	97.02		20.46		
B1-SOD-N-015	NaOCl	5.68	HNO <sub>3</sub>	2.62E-05	612	19,545	717	102.99		21.45		
B1-SOD-A-016	NaOCl	6.03	Acetic	1.99E-05	64	19,712	585	95.76		12.22		
B1-SOD-A-017	NaOCl	4.89	Acetic	1.66E-05	0	19,210	605	93.32		19.17		
B1-SOD-A-018	NaOCl	5.67	Acetic	1.59E-05	14	19,490	644	94.04		14.28		
B1-WAT-C-019	Water	5.16	HCl	1.67E-05	773	20,175	716	84.83		33.02		
B1-WAT-C-020	Water	4.88	HCl	1.71E-05	1,170	19,806	673	78.22		42.73		
B1-WAT-C-021	Water	5.42	HCl	2.70E-05	571	19,259	430	136.94		30.62	1.6E+00	
B1-WAT-N-022	Water	6.33	HNO <sub>3</sub>	1.51E-05	807	19,169	619	94.76		69.07		

Sample number	Cleaning method	Mass / mg	Acid	Ca (mol)	Al/Ca ( $\mu\text{mol mol}^{-1}$ )	S/Ca ( $\mu\text{mol mol}^{-1}$ )	K/Ca ( $\mu\text{mol mol}^{-1}$ )	Li/Ca ( $\mu\text{mol mol}^{-1}$ )	B/Ca ( $\mu\text{mol mol}^{-1}$ )	Ba/Ca ( $\mu\text{mol mol}^{-1}$ )	U/Ca ( $\mu\text{mol mol}^{-1}$ )	I/Ca ( $\mu\text{mol mol}^{-1}$ )
B1-WAT-N-023	Water	6.18	HNO <sub>3</sub>	1.91E-05	858	19,095	849	95.30		32.75		
B1-WAT-N-024	Water	6.86	HNO <sub>3</sub>	1.63E-05	795	19,224	575	93.71		24.44		
B1-WAT-A-025	Water	5.56	Acetic	1.90E-05	519	19,286	434	90.00		17.97		
B1-WAT-A-026	Water	6.27	Acetic	1.96E-05	523	19,086	422	91.70		20.53		
B1-WAT-A-027	Water	5.00	Acetic	1.50E-05	371	19,063	511	87.13		15.77		
<b>Bulk 2 (approximately 5 mg mass)</b>												
B2-PER-C-019	H <sub>2</sub> O <sub>2</sub>	5.80	HCl	5.70E-05				14.28	17.43	4.97	5.6E-03	
B2-PER-C-020	H <sub>2</sub> O <sub>2</sub>	4.60	HCl	4.54E-05				14.37	36.55	5.64	3.2E-03	
B2-PER-C-021	H <sub>2</sub> O <sub>2</sub>	3.50	HCl	3.62E-05	132			13.92	81.86	5.55	1.4E-02	
B2-PER-N-022	H <sub>2</sub> O <sub>2</sub>	5.20	HNO <sub>3</sub>	5.12E-05				13.86	39.89			
B2-PER-N-023	H <sub>2</sub> O <sub>2</sub>	6.30	HNO <sub>3</sub>	6.29E-05				13.18	32.93			3.45
B2-PER-N-024	H <sub>2</sub> O <sub>2</sub>	5.70	HNO <sub>3</sub>	5.63E-05				13.57	26.52			
B2-PER-A-025	H <sub>2</sub> O <sub>2</sub>	5.10	Acetic	5.21E-05				12.78	37.92			6.90
B2-PER-A-026	H <sub>2</sub> O <sub>2</sub>	5.50	Acetic	5.43E-05				13.27	36.86	1.48		6.62
B2-PER-A-027	H <sub>2</sub> O <sub>2</sub>	5.70	Acetic	5.78E-05				13.17		0.22		7.49
B2-WAT-C-028	Water	5.70	HCl	5.56E-05				14.28		17.45	1.1E-02	
B2-WAT-C-029	Water	6.10	HCl	5.84E-05				14.18		18.19	2.4E-03	
B2-WAT-C-030	Water	5.50	HCl	5.41E-05				13.63		10.69	1.5E-03	
B2-WAT-N-031	Water	5.40	HNO <sub>3</sub>	5.53E-05				12.94		10.37	1.5E-03	
B2-WAT-N-032	Water	5.90	HNO <sub>3</sub>	6.07E-05	404			13.06		11.56	1.6E-03	
B2-WAT-N-033	Water	5.60	HNO <sub>3</sub>	5.38E-05			39	12.30		11.61	1.9E-03	
B2-WAT-A-034	Water	5.60	Acetic	5.86E-05			23	12.87		2.78	2.7E-03	3.98
B2-WAT-A-035	Water	5.90	Acetic	6.16E-05				13.43		3.53	1.6E-03	2.59
B2-WAT-A-036	Water	4.80	Acetic	5.07E-05				12.84		4.84	2.6E-03	3.10

Sample number	Cleaning method	Mass / mg	Acid	Ca (mol)	Al/Ca ( $\mu\text{mol mol}^{-1}$ )	S/Ca ( $\mu\text{mol mol}^{-1}$ )	K/Ca ( $\mu\text{mol mol}^{-1}$ )	Li/Ca ( $\mu\text{mol mol}^{-1}$ )	B/Ca ( $\mu\text{mol mol}^{-1}$ )	Ba/Ca ( $\mu\text{mol mol}^{-1}$ )	U/Ca ( $\mu\text{mol mol}^{-1}$ )	I/Ca ( $\mu\text{mol mol}^{-1}$ )
<b>Bulk 3 (approximately 5 mg mass)</b>												
B3-PER-C-037	H <sub>2</sub> O <sub>2</sub>	5.50	HCl	5.39E-05		796		21.65		8.84	1.7E-03	
B3-PER-C-038	H <sub>2</sub> O <sub>2</sub>	5.50	HCl	5.43E-05		967		21.13		5.56	1.4E-03	
B3-PER-C-039	H <sub>2</sub> O <sub>2</sub>	5.20	HCl	5.00E-05		1,040		21.65		8.03	1.5E-03	
B3-PER-N-040	H <sub>2</sub> O <sub>2</sub>	5.50	HNO <sub>3</sub>	5.17E-05		851		20.05				
B3-PER-N-041	H <sub>2</sub> O <sub>2</sub>	5.40	HNO <sub>3</sub>	5.34E-05		1,105		19.11	30.66	0.98		
B3-PER-N-042	H <sub>2</sub> O <sub>2</sub>	4.80	HNO <sub>3</sub>	4.81E-05		1,055		19.30	18.02	6.18		
B3-PER-A-043	H <sub>2</sub> O <sub>2</sub>	5.50	Acetic	5.48E-05		1,125		18.77	14.59	7.76		3.91
B3-PER-A-044	H <sub>2</sub> O <sub>2</sub>	5.00	Acetic	5.09E-05		810		18.78	17.87	2.57		12.65
B3-PER-A-045	H <sub>2</sub> O <sub>2</sub>	6.40	Acetic	6.39E-05		1,234		19.05	11.55	4.86		
B3-WAT-C-046	Water	5.00	HCl	5.00E-05	381	853		18.74	30.77	16.66	5.6E-03	
B3-WAT-C-047	Water	5.40	HCl	5.33E-05		974		18.94	16.63	16.57	3.3E-03	
B3-WAT-C-048	Water	5.90	HCl	6.04E-05		1,108		18.24	25.43	13.28	1.9E-03	
B3-WAT-N-049	Water	6.00	HNO <sub>3</sub>	5.79E-05		1,076		19.32	31.14	13.50	1.2E-03	
B3-WAT-N-050	Water	4.90	HNO <sub>3</sub>	4.97E-05	120	890		19.20	24.23	14.43	1.4E-03	
B3-WAT-N-051	Water	5.40	HNO <sub>3</sub>	5.26E-05		937		19.09	5.07	11.84	1.7E-03	
B3-WAT-A-052	Water	6.10	Acetic	5.96E-05		717		19.28	0.86	4.66	1.6E-03	2.20
B3-WAT-A-053	Water	4.70	Acetic	3.80E-05				19.06		4.26	1.9E-03	4.58
B3-WAT-A-054	Water	6.10	Acetic	6.41E-05		850		19.01	2.19	4.28	1.7E-03	2.94
<b>Bulk 2 (approximately 2 mg mass)</b>												
B2-PER-A-055	H <sub>2</sub> O <sub>2</sub>	1.90	Acetic	2.00E-05				13.56	12.99			6.56
B2-PER-A-056	H <sub>2</sub> O <sub>2</sub>	2.10	Acetic	2.17E-05				13.12	11.96			6.21
B2-PER-A-057	H <sub>2</sub> O <sub>2</sub>	2.30	Acetic	2.59E-05				12.56	2.45			4.10
<b>Bulk 2 (approximately 10 mg mass)</b>												

Sample number	Cleaning method	Mass / mg	Acid	Ca (mol)	Al/Ca ( $\mu\text{mol mol}^{-1}$ )	S/Ca ( $\mu\text{mol mol}^{-1}$ )	K/Ca ( $\mu\text{mol mol}^{-1}$ )	Li/Ca ( $\mu\text{mol mol}^{-1}$ )	B/Ca ( $\mu\text{mol mol}^{-1}$ )	Ba/Ca ( $\mu\text{mol mol}^{-1}$ )	U/Ca ( $\mu\text{mol mol}^{-1}$ )	I/Ca ( $\mu\text{mol mol}^{-1}$ )
B2-PER-A-058	H <sub>2</sub> O <sub>2</sub>	7.20	Acetic	7.24E-05				12.88	0.86	0.67		0.97
B2-PER-A-059	H <sub>2</sub> O <sub>2</sub>	6.70	Acetic	6.90E-05			2,606	11.58	3.54	1.90		1.05
B2-PER-A-060	H <sub>2</sub> O <sub>2</sub>	8.40	Acetic	8.69E-05				12.15	0.56	1.42		0.46
<b>Bulk 3 (approximately 2 mg mass)</b>												
B3-PER-A-061	H <sub>2</sub> O <sub>2</sub>	2.20	Acetic	2.20E-05				22.47	81.72	1.77		
B3-PER-A-062	H <sub>2</sub> O <sub>2</sub>	2.20	Acetic	2.36E-05				20.01	40.42	1.17		3.24
B3-PER-A-063	H <sub>2</sub> O <sub>2</sub>	1.70	Acetic	1.76E-05				21.19	35.04			5.08
<b>Bulk 3 (approximately 10 mg mass)</b>												
B3-PER-A-064	H <sub>2</sub> O <sub>2</sub>	12.7 0	Acetic	1.31E-04		1,405		18.51	5.83	2.54	3.4E-02	0.51
B3-PER-A-065	H <sub>2</sub> O <sub>2</sub>	8.30	Acetic	8.33E-05		1,127		19.71	7.02	1.83	8.3E-02	0.69
B3-PER-A-066	H <sub>2</sub> O <sub>2</sub>	10.3 0	Acetic	1.04E-04		1,264		19.54	6.71	1.80		0.01
<b>Bulk 1 (approximately 2 mg mass)</b>												
B1-PER-A-067	H <sub>2</sub> O <sub>2</sub>	2.10	Acetic	2.01E-05				36.53	24.20	0.42		4.23
B1-PER-A-068	H <sub>2</sub> O <sub>2</sub>	2.20	Acetic	2.01E-05				37.08	30.02	0.52	6.5E-02	1.91
B1-PER-A-069	H <sub>2</sub> O <sub>2</sub>	1.80	Acetic	1.64E-05				38.64	45.40	21.98	1.6E-03	3.80
<b>Bulk 1 (approximately 10 mg mass)</b>												
B1-PER-A-070	H <sub>2</sub> O <sub>2</sub>	7.80	Acetic	7.66E-05				36.85	11.62	4.16	3.6E-04	0.91
B1-PER-A-071	H <sub>2</sub> O <sub>2</sub>	9.10	Acetic	8.87E-05				36.74	10.70	3.62	8.1E-04	
B1-PER-A-072	H <sub>2</sub> O <sub>2</sub>	7.30	Acetic	7.17E-05				38.16	19.75	3.59	2.4E-03	0.39

## 8.2. Variability Samples analysis

Table 31 - Main elemental and isotopic results for analysis of Variability Samples including carbon and oxygen isotope analysis results, Ca values (mol), and Mg/Ca, P/Ca, Sr/Ca, Na/Ca, Fe/Ca, and Mn/Ca values ( $\mu\text{mol mol}^{-1}$ ).

Sample number	Rostrum Length / cm	Distance from apex / cm	Ca (mol)	Mg/Ca ( $\mu\text{mol mol}^{-1}$ )	P/Ca ( $\mu\text{mol mol}^{-1}$ )	Sr/Ca ( $\mu\text{mol mol}^{-1}$ )	Na/Ca ( $\mu\text{mol mol}^{-1}$ )	Fe/Ca ( $\mu\text{mol mol}^{-1}$ )	Mn/Ca ( $\mu\text{mol mol}^{-1}$ )	$\delta^{13}\text{C}_{\text{VPDB}}$ (‰)	$\delta^{18}\text{O}_{\text{VPDB}}$ (‰)
<b>Variability samples cleaned with water</b>											
Samples from Penny Nab											
<i>Bairstowius</i>											
PN008 A (1)	4	0.8	2.3E-05	8,671	983	1,593	9,540	335	96	2.15	0.96
PN008 A (2)	4	0.8									
PN008 A (3)	4	0.8									
PN008 B (1)	4	0.8	4.4E-05	8,467	903	1,597	9,508	187	90		
PN008 B (2)	4	0.8									
PN008 B (3)	4	0.8									
PN008 C (1)	4	1.7	2.2E-05	8,287	978	1,570	9,790	344	129		
PN008 C (2)	4	1.7									
PN008 C (3)	4	1.7									
PN008 D (1)	4	1.7	5.7E-05	8,423	877	1,560	8,769	176	98		
PN008 D (2)	4	1.7									
PN008 D (3)	4	1.7									
PN008 E (1)	4	2.7	4.7E-05	9,354	691	1,567	8,463	420	168		
PN008 E (2)	4	2.7									
PN008 E (3)	4	2.7									
PN008 F (1)	4	3.3	5.1E-05	7,984	850	1,347	8,944	247	83		
PN008 F (2)	4	3.3	4.7E-05	8,722	913	1,355	9,563	351	95		
PN008 F (3)	4	3.3	4.2E-05	8,805	872	1,362	9,623	288	79		
<i>Parapassaloteuthis</i>											

Sample number	Rostrum Length / cm	Distance from apex / cm	Ca (mol)	Mg/Ca ( $\mu\text{mol mol}^{-1}$ )	P/Ca ( $\mu\text{mol mol}^{-1}$ )	Sr/Ca ( $\mu\text{mol mol}^{-1}$ )	Na/Ca ( $\mu\text{mol mol}^{-1}$ )	Fe/Ca ( $\mu\text{mol mol}^{-1}$ )	Mn/Ca ( $\mu\text{mol mol}^{-1}$ )	$\delta^{13}\text{C}_{\text{VPDB}}$ (‰)	$\delta^{18}\text{O}_{\text{VPDB}}$ (‰)
PN009 A (1)	3.5	1.1	4.2E-05	10,232	969	1,776	8,925	188	66		
PN009 A (2)	3.5	1.1	6.8E-05	10,413	931	1,818	9,713	200	69		
PN009 A (3)	3.5	1.1									
PN009 B (1)	3.5	1.1	4.6E+07	22,936		664					
PN009 B (2)	3.5	1.1	8.8E-05	10,440	959	1,865	10,484	629	279		
PN009 B (3)	3.5	1.1									
PN009 C (1)	3.5	1.1	6.7E+06	10,639	1,504	1,777	8,363	1,118	508		
PN009 C (2)	3.5	1.1	5.8E-05	10,773	1,026	1,832	9,282	862	403		
PN009 C (3)	3.5	1.1	3.0E-05	10,682	1,107	1,786	9,215	866	406		
PN009 D (1)	3.5	2.4	5.8E-05	10,618	899	1,744	8,869	129	75		
PN009 D (2)	3.5	2.4	5.6E-05	10,366	908	1,721	8,180	129	74		
PN009 D (3)	3.5	2.4									
PN009 E (1)	3.5	2.4	4.2E+08							2.97	2.43
PN009 E (2)	3.5	2.4	4.1E-05	10,454	1,007	1,750	8,241	379	209	2.93	2.53
PN009 E (3)	3.5	2.4	5.0E-05	10,633	1,009	1,787	8,783	369	200		
PN009 F (1)	3.5	2.4	6.3E-05	10,944	998	1,782	8,579	328	197	2.87	2.13
PN009 F (2)	3.5	2.4	5.7E-05	10,878	1,002	1,774	8,514	312	187		
PN009 F (3)	3.5	2.4	3.9E-05	10,868	1,029	1,788	8,645	335	200		
PN015 A (1)	4.9	1.7	4.4E-05	10,342	1,074	1,810	9,319	111	44	3.29	1.60
PN015 A (2)	4.9	1.7	5.3E-05	10,379	1,045	1,815	10,124	161	58		
PN015 A (3)	4.9	1.7	7.6E-05	10,296	993	1,818	10,348	215	84		
PN015 B (1)	4.9	1.7	4.9E-05	10,328	979	1,785	10,339	145	52		
PN015 B (2)	4.9	1.7	4.8E-05	10,529	1,052	1,804	9,337	143	56		
PN015 B (3)	4.9	1.7	5.6E-05	10,506	998	1,783	9,204	178	72		
PN015 C (1)	4.9	1.7	4.4E-05	10,358	1,036	1,756	9,438	156	54	3.20	1.94
PN015 C (2)	4.9	1.7	5.8E-05	10,379	1,006	1,761	9,875	160	55	3.20	2.00

Sample number	Rostrum Length / cm	Distance from apex / cm	Ca (mol)	Mg/Ca ( $\mu\text{mol mol}^{-1}$ )	P/Ca ( $\mu\text{mol mol}^{-1}$ )	Sr/Ca ( $\mu\text{mol mol}^{-1}$ )	Na/Ca ( $\mu\text{mol mol}^{-1}$ )	Fe/Ca ( $\mu\text{mol mol}^{-1}$ )	Mn/Ca ( $\mu\text{mol mol}^{-1}$ )	$\delta^{13}\text{C}_{\text{VPDB}}$ (‰)	$\delta^{18}\text{O}_{\text{VPDB}}$ (‰)
PN015 C (3)	4.9	1.7	4.4E-05	10,407	980	1,726	9,045	464	145		
PN015 D (1)	4.9	3.3	4.8E-05	9,461	985	1,613	8,387	116	57		
PN015 D (2)	4.9	3.3	5.8E-05	9,361	976	1,607	7,804	71	46		
PN015 D (3)	4.9	3.3	5.4E-05	9,373	980	1,599	7,761	96	47		
PN015 E (1)	4.9	3.3	4.5E-05	9,817	1,006	1,589	7,867	105	53		
PN015 E (2)	4.9	3.3	5.1E-05	9,806	982	1,579	7,670	103	56		
PN015 E (3)	4.9	3.3	5.6E-05	9,886	965	1,595	7,579	98	54		
PN015 F (1)	4.9	3.3	5.6E-05	10,152	1,024	1,598	7,865	142	60	2.62	1.82
PN015 F (2)	4.9	3.3	4.7E-05	10,198	1,009	1,609	7,750	136	61	2.66	1.87
PN015 F (3)	4.9	3.3	4.9E-05	10,562	1,011	1,590	8,284	281	93		
PN021 A (1)	4.2	2.5	5.5E-05	9,324	1,112	1,685	7,728	68	45		
PN021 A (2)	4.2	2.5	5.9E-05	9,234	1,098	1,668	7,847	71	45		
PN021 A (3)	4.2	2.5	3.8E-05	9,136	1,099	1,650	7,919	86	45		
PN021 B (1)	4.2	2.5	6.0E-05	9,564	1,150	1,733	8,513	211	79		
PN021 B (2)	4.2	2.5	5.0E-05	9,517	1,151	1,764	9,382	176	78		
PN021 B (3)	4.2	2.5									
PN021 C (1)	4.2	2.5	4.6E-05	12,219	1,167	1,873	9,147	288	138	3.20	2.12
PN021 C (2)	4.2	2.5	5.5E-05	12,412	1,159	1,910	9,414	284	142		
PN021 C (3)	4.2	2.5	5.5E-05	12,228	1,160	1,867	8,822	276	136		
PN021 D (1)	4.2	1.2	5.5E-05	10,004	1,174	1,802	8,642	71	42		
PN021 D (2)	4.2	1.2	5.3E-05	10,150	1,155	1,792	8,385	144	48		
PN021 D (3)	4.2	1.2									
PN021 E (1)	4.2	1.2	4.6E-05	9,870	1,167	1,750	8,569	464	106	3.00	1.87
PN021 E (2)	4.2	1.2	4.8E-05	9,865	1,226	1,775	8,744	231	101		
PN021 E (3)	4.2	1.2									
PN021 F (1)	4.2	1.2	5.5E-05	10,317	1,208	1,824	8,811	355	151		

Sample number	Rostrum Length / cm	Distance from apex / cm	Ca (mol)	Mg/Ca ( $\mu\text{mol mol}^{-1}$ )	P/Ca ( $\mu\text{mol mol}^{-1}$ )	Sr/Ca ( $\mu\text{mol mol}^{-1}$ )	Na/Ca ( $\mu\text{mol mol}^{-1}$ )	Fe/Ca ( $\mu\text{mol mol}^{-1}$ )	Mn/Ca ( $\mu\text{mol mol}^{-1}$ )	$\delta^{13}\text{C}_{\text{VPDB}}$ (‰)	$\delta^{18}\text{O}_{\text{VPDB}}$ (‰)
PN021 F (2)	4.2	1.2	5.3E-05	10,340	1,207	1,809	8,739	308	170		
PN021 F (3)	4.2	1.2	4.7E-05	10,237	1,192	1,790	8,818	255	151		
<i>Passaloteuthis pessula</i>											
PN010 A (1)	6.8	1.0	3.8E-05	15,838	1,257	2,292	10,881	1,052	495		
PN010 A (2)	6.8	1.0	5.4E-05	16,041	1,251	2,343	11,081	1,099	515		
PN010 A (3)	6.8	1.0	5.8E-05	16,371	1,275	2,344	10,870	1,111	516		
PN010 B (1)	6.8	1.0	4.6E-05	14,523	1,151	2,284	9,473	286	109		
PN010 B (2)	6.8	1.0	4.9E-05	14,622	1,130	2,259	9,346	293	119		
PN010 B (3)	6.8	1.0	4.8E-05	14,658	1,149	2,253	9,335	264	109		
PN010 C (1)	6.8	3.7	7.1E-05	12,626	1,085	2,003	8,625	193	99		
PN010 C (2)	6.8	3.7	4.9E-05	12,929	1,106	2,026	8,675	183	93		
PN010 C (3)	6.8	3.7	4.8E-05	12,724	1,152	1,994	8,208	157	83		
PN010 D (1)	6.8	3.7	5.0E-05	11,070	1,174	1,451	5,619	250	100		
PN010 D (2)	6.8	3.7	5.1E-05	11,039	1,175	1,498	6,126	254	98		
PN010 D (3)	6.8	3.7	5.2E-05	11,229	1,136	1,490	5,945	806	107		
PN010 E (1)	6.8	5.3	4.8E-05	12,118	1,135	1,867	9,059	318	163		
PN010 E (2)	6.8	5.3	4.8E-05	12,199	1,177	1,857	8,673	240	129		
PN010 E (3)	6.8	5.3	5.6E-05	12,322	1,118	1,869	8,594	252	138		
PN010 F (1)	6.8	6.8	4.4E-05	12,825	1,124	1,946	8,424	612	256		
PN010 F (2)	6.8	6.8	4.5E-05	12,531	1,144	1,969	8,924	517	237		
PN010 F (3)	6.8	6.8	5.0E-05	12,750	1,097	1,985	9,005	620	258		
PN022 A (1)	6.6	0.7	5.7E-05	14,135	1,085	2,044	10,418	1,441	368		
PN022 A (2)	6.6	0.7	5.2E-05	14,130	1,074	2,040	10,206	1,363	361		
PN022 A (3)	6.6	0.7	4.5E-05	14,226	1,082	2,035	9,820	1,527	382		
PN022 B (1)	6.6	1.8	4.9E-05	10,888	914	1,804	8,331	183	47		
PN022 B (2)	6.6	1.8	6.2E-05	11,200	887	1,851	8,662	213	49		

Sample number	Rostrum Length / cm	Distance from apex / cm	Ca (mol)	Mg/Ca ( $\mu\text{mol mol}^{-1}$ )	P/Ca ( $\mu\text{mol mol}^{-1}$ )	Sr/Ca ( $\mu\text{mol mol}^{-1}$ )	Na/Ca ( $\mu\text{mol mol}^{-1}$ )	Fe/Ca ( $\mu\text{mol mol}^{-1}$ )	Mn/Ca ( $\mu\text{mol mol}^{-1}$ )	$\delta^{13}\text{C}_{\text{VPDB}}$ (‰)	$\delta^{18}\text{O}_{\text{VPDB}}$ (‰)
PN022 B (3)	6.6	1.8	4.7E-05	11,261	882	1,851	8,545	184	49	3.65	1.72
PN022 C (1)	6.6	1.8	5.9E-05	11,565	914	1,844	8,968	431	66		
PN022 C (2)	6.6	1.8	6.1E-05	11,584	915	1,844	8,570	447	66		
PN022 C (3)	6.6	1.8	5.5E-05	11,594	914	1,838	8,587	536	64	3.49	2.11
PN022 D (1)	6.6	2.9	5.8E-05	12,028	1,051	1,824	8,279	370	77		
PN022 D (2)	6.6	2.9	5.7E-05	11,964	1,046	1,825	8,437	340	78		
PN022 D (3)	6.6	2.9	5.8E-05	11,930	1,038	1,832	8,268	310	77	3.72	2.13
PN022 E (1)	6.6	2.9	5.3E-05	11,409	1,069	1,821	8,694	497	172		
PN022 E (2)	6.6	2.9	5.1E-05	11,408	1,077	1,812	8,163	392	110		
PN022 E (3)	6.6	2.9	6.0E-05	11,376	1,047	1,828	8,681	403	100	3.24	2.22
PN022 F (1)	6.6	4.2	5.5E-05	11,819	1,157	1,773	7,964	363	69		
PN022 F (2)	6.6	4.2	4.9E-05	12,037	1,133	1,798	7,900	352	74		
PN022 F (3)	6.6	4.2	4.9E-05	11,854	1,148	1,781	7,657	317	70	3.29	2.13
Samples from Wine Haven											
<i>Passaloteuthis pessula</i>											
WH014 A (1)	6.5	2.0	5.0E-05	9,096	600	1,671	7,177	74	99	0.92	1.00
WH014 A (2)	6.5	2.0	4.8E-05	9,194	582	1,687	6,754	68	93		
WH014 A (3)	6.5	2.0	5.0E-05	9,146	620	1,677	6,993	65	95		
WH014 B (1)	6.5	2.0	5.5E-05	9,304	673	1,785	8,383	61	73	1.04	0.86
WH014 B (2)	6.5	2.0	4.7E-05	9,463	654	1,787	7,509	56	73		
WH014 B (3)	6.5	2.0	5.6E-05	9,386	654	1,767	7,804	110	106		
WH014 C (1)	6.5	2.0	5.0E-05	8,048	505	1,563	6,137		71	1.04	0.86
WH014 C (2)	6.5	2.0	6.4E-05	7,980	516	1,561	5,984		66		
WH014 C (3)	6.5	2.0	5.3E-05	7,947	524	1,552	6,125		67		
WH014 D (1)	6.5	4.6	5.6E-05	8,601	529	1,670	6,854		71	1.04	0.86
WH014 D (2)	6.5	4.6	5.7E-05	8,526	513	1,657	6,781		66		

Sample number	Rostrum Length / cm	Distance from apex / cm	Ca (mol)	Mg/Ca ( $\mu\text{mol mol}^{-1}$ )	P/Ca ( $\mu\text{mol mol}^{-1}$ )	Sr/Ca ( $\mu\text{mol mol}^{-1}$ )	Na/Ca ( $\mu\text{mol mol}^{-1}$ )	Fe/Ca ( $\mu\text{mol mol}^{-1}$ )	Mn/Ca ( $\mu\text{mol mol}^{-1}$ )	$\delta^{13}\text{C}_{\text{VPDB}}$ (‰)	$\delta^{18}\text{O}_{\text{VPDB}}$ (‰)
WH014 D (3)	6.5	4.6	5.1E-05	8,450	531	1,643	6,525		68	0.85	0.75
WH014 E (1)	6.5	4.6	5.1E-05	8,056	608	1,512	5,833	76	88		
WH014 E (2)	6.5	4.6	4.8E-05	7,998	601	1,521	5,920		76		
WH014 E (3)	6.5	4.6	5.6E-05	7,920	576	1,512	5,799		74	0.89	1.00
WH014 F (1)	6.5	4.6	5.5E-05	7,256	690	1,433	5,598	265	186		
WH014 F (2)	6.5	4.6	5.9E-05	7,336	673	1,447	5,641	155	141		
WH014 F (3)	6.5	4.6	6.6E-05	7,652	665	1,405	5,320	470	280		
<i>Nannobelus delicatus</i>											
WH016 A (1)	5	1.0	4.5E-05	11,704	865	1,929	7,511	220	119		
WH016 A (2)	5	1.0									
WH016 A (3)	5	1.0									
WH016 B (1)	5	1.0	6.6E-05	11,132	866	1,880	7,118	486	275		
WH016 B (2)	5	1.0	5.0E-05	11,197	916	1,874	7,576	488	278		
WH016 B (3)	5	1.0	5.0E-05	11,135	888	1,854	7,115	494	284		
WH016 C (1)	5	2.3	2.6E-05	9,236	654	1,781	6,066	235	156		
WH016 C (2)	5	2.3	5.3E-05	9,216	720	1,760	6,385	222	150		
WH016 C (3)	5	2.3	5.2E-05	9,088	723	1,744	6,699	224	161		
WH016 D (1)	5	2.3	5.1E-05	8,720	712	1,706	6,186	204	175		
WH016 D (2)	5	2.3	5.2E-05	9,417	702	1,819	6,385	264	186		
WH016 D (3)	5	2.3	5.1E-05	9,476	702	1,835	6,863	248	178		
WH016 E (1)	5	3.3	5.3E-05	8,482	735	1,686	6,148	128	103	0.50	0.48
WH016 E (2)	5	3.3	4.6E-05	8,446	743	1,670	6,048	127	100		
WH016 E (3)	5	3.3	5.2E-05	8,466	756	1,681	5,857	132	107		
WH016 F (1)	5	3.3	4.9E-05	9,122	720	1,486	5,167	6,281	1,776	1.25	2.89
WH016 F (2)	5	3.3	5.6E-05	8,979	717	1,466	5,089	6,399	1,804		
WH016 F (3)	5	3.3	4.9E-05	9,116	719	1,481	5,092	6,349	1,779		

Sample number	Rostrum Length / cm	Distance from apex / cm	Ca (mol)	Mg/Ca ( $\mu\text{mol mol}^{-1}$ )	P/Ca ( $\mu\text{mol mol}^{-1}$ )	Sr/Ca ( $\mu\text{mol mol}^{-1}$ )	Na/Ca ( $\mu\text{mol mol}^{-1}$ )	Fe/Ca ( $\mu\text{mol mol}^{-1}$ )	Mn/Ca ( $\mu\text{mol mol}^{-1}$ )	$\delta^{13}\text{C}_{\text{VPDB}}$ (‰)	$\delta^{18}\text{O}_{\text{VPDB}}$ (‰)
WH020 A (1)	5.5	1.2	6.1E-05	10,312	776	1,773	6,736	400	219	0.70	0.33
WH020 A (2)	5.5	1.2									
WH020 A (3)	5.5	1.2									
WH020 B (1)	5.5	1.2	5.6E-05	10,020	743	1,773	6,640	307	192		
WH020 B (2)	5.5	1.2									
WH020 B (3)	5.5	1.2									
WH020 C (1)	5.5	2.1	5.3E-05	8,728	729	1,732	6,856	66	56		
WH020 C (2)	5.5	2.1	2.4E-05	8,627	635	1,745	6,454		59		
WH020 C (3)	5.5	2.1									
WH020 D (1)	5.5	2.1	5.1E-05	8,634	728	1,706	6,904	174	116		
WH020 D (2)	5.5	2.1	4.8E-05	8,431	738	1,684	6,929	205	126		
WH020 D (3)	5.5	2.1	4.9E-05	8,601	704	1,703	6,882	192	118		
WH020 E (1)	5.5	2.8	4.4E-05	8,331	730	1,696	7,234	69	65		
WH020 E (2)	5.5	2.8	5.1E-05	8,165	729	1,658	6,573	70	62		
WH020 E (3)	5.5	2.8	5.8E-05	8,258	732	1,680	6,804	73	64		
WH020 F (1)	5.5	3.9	5.5E-05	7,697	613	1,517	5,731	48	45		
WH020 F (2)	5.5	3.9	5.6E-05	7,797	610	1,548	6,157	49	49		
WH020 F (3)	5.5	3.9									
WH022 A (1)	4.5	0.6	4.5E-05	12,049	744	1,797	7,530	1,498	818		
WH022 A (2)	4.5	0.6									
WH022 A (3)	4.5	0.6									
WH022 B (1)	4.5	1.4	6.4E-05	10,352	780	1,856	7,529	429	210		
WH022 B (2)	4.5	1.4									
WH022 B (3)	4.5	1.4									
WH022 C (1)	4.5	2.3	5.5E-05	9,592	747	1,823	7,567	319	163		
WH022 C (2)	4.5	2.3									

Sample number	Rostrum Length / cm	Distance from apex / cm	Ca (mol)	Mg/Ca ( $\mu\text{mol mol}^{-1}$ )	P/Ca ( $\mu\text{mol mol}^{-1}$ )	Sr/Ca ( $\mu\text{mol mol}^{-1}$ )	Na/Ca ( $\mu\text{mol mol}^{-1}$ )	Fe/Ca ( $\mu\text{mol mol}^{-1}$ )	Mn/Ca ( $\mu\text{mol mol}^{-1}$ )	$\delta^{13}\text{C}_{\text{VPDB}}$ (‰)	$\delta^{18}\text{O}_{\text{VPDB}}$ (‰)
WH022 C (3)	4.5	2.3									
WH022 D (1)	4.5	2.7	5.1E-05	8,459	676	1,742	7,572	203	121		
WH022 D (2)	4.5	2.7	4.9E-05	8,625	705	1,774	7,326	196	120		
WH022 D (3)	4.5	2.7	5.5E-05	8,487	677	1,741	7,182	217	122		
WH022 E (1)	4.5	3.5	4.5E-05	8,130	704	1,657	6,743	253	137	1.85	0.93
WH022 E (2)	4.5	3.5	4.7E-05	8,086	699	1,639	6,854	235	140		
WH022 E (3)	4.5	3.5									
WH022 F (1)	4.5	4.1	5.4E-05	7,650	729	1,583	6,241	141	97		
WH022 F (2)	4.5	4.1	5.5E-05	7,538	688	1,566	6,064	133	95		
WH022 F (3)	4.5	4.1									
<b>Variability samples cleaned with hydrogen peroxide</b>											
Samples from Penny Nab											
<i>Parapassaloteuthis</i>											
PN015 B (1)	4.9	1.7	5.8E-05	9,331	1,208	1,549		236	90		
PN015 C (1)	4.9	1.7	5.9E-05	8,788	1,191	1,495		279	77		
PN015 F (1)	4.9	3.4	5.0E-05	8,153	1,244	1,346		185	82	2.62	1.82
PN021 C (1)	4.2	2.5	5.4E-05	7,619	1,342	1,410			26	3.20	2.12
PN021 C (2)	4.2	2.5	5.2E-05	7,627	1,322	1,382			25		
<i>Passaloteuthis pessula</i>											
PN010 C (1)	6.8	3.7	4.2E-05	11,030	1,301	1,735		188	95		
PN010 D (1)	6.8	3.7	5.1E-05	9,416	1,289	1,202		315	107		
PN010 E (1)	6.8	5.3	4.7E-05	10,244	1,322	1,597		258	132	2.97	2.43
PN010 E (2)	6.8	5.3	5.7E-05	10,571	1,278	1,637		290	140	2.93	2.53
PN010 F (1)	6.8	6.8	5.2E-05	11,017	1,215	1,681		601	264	2.87	2.13
PN022 B (1)	6.6	1.8	5.4E-05	12,122	1,000	1,503	298,549	210	50		
PN022 C (1)	6.6	1.8	4.1E-05	9,147	1,142	1,544		174	49	3.65	1.72

Sample number	Rostrum Length / cm	Distance from apex / cm	Ca (mol)	Mg/Ca ( $\mu\text{mol mol}^{-1}$ )	P/Ca ( $\mu\text{mol mol}^{-1}$ )	Sr/Ca ( $\mu\text{mol mol}^{-1}$ )	Na/Ca ( $\mu\text{mol mol}^{-1}$ )	Fe/Ca ( $\mu\text{mol mol}^{-1}$ )	Mn/Ca ( $\mu\text{mol mol}^{-1}$ )	$\delta^{13}\text{C}_{\text{VPDB}}$ (‰)	$\delta^{18}\text{O}_{\text{VPDB}}$ (‰)
PN022 D (1)	6.6	2.9	4.4E-05	9,463	1,127	1,553		254	63	3.49	2.11
PN022 D (2)	6.6	2.9	5.8E-05	9,314	1,018	1,533		254	60		
PN022 E (1)	6.6	2.9	5.1E-05	9,741	1,180	1,633		347	106	3.72	2.13
PN022 E (2)	6.6	2.9	5.9E-05	9,532	1,103	1,605		338	104		
PN022 F (1)	6.6	4.2	5.6E-05	9,820	1,126	1,547		254	68	3.24	2.22
Samples from Wine Haven											
<i>Passaloteuthis pessula</i>											
WH014 B (1)	6.5	2.0	4.2E-05	7,656	832	1,501			94		
WH014 C (1)	6.5	2.0	4.6E-05	6,649	721	1,316			73		
WH014 E (1)	6.5	4.6	4.0E-05	6,849	821	1,313			85		
WH014 E (2)	6.5	4.6	5.3E-05	6,764	733	1,285			80	0.85	0.75
WH014 F (1)	6.5	4.6	6.1E-05	6,575	859	1,297		286	187	0.89	1.00
<i>Nannobelus delicatus</i>											
WH016 D (1)	5	2.3	4.1E-05	7,754	963	1,501		276	204		

Table 32 - Supplemental elemental results for analysis of Variability Samples including Ca values (mol), and Al/Ca, S/Ca, K/Ca, Li/Ca, B/Ca, Ba/Ca, and I/Ca values ( $\mu\text{mol mol}^{-1}$ ).

Sample number	Rostrum Length / cm	Distance from apex / cm	Ca (mol)	Al/Ca ( $\mu\text{mol mol}^{-1}$ )	S/Ca ( $\mu\text{mol mol}^{-1}$ )	Li/Ca ( $\mu\text{mol mol}^{-1}$ )	B/Ca ( $\mu\text{mol mol}^{-1}$ )	Ba/Ca ( $\mu\text{mol mol}^{-1}$ )	U/Ca ( $\mu\text{mol mol}^{-1}$ )	I/Ca ( $\mu\text{mol mol}^{-1}$ )
<b>Variability samples cleaned with water</b>										
Samples from Penny Nab										
<i>Bairstowius</i>										
PN008-A (1)	4	0.8	2.31E-05			22.7		59.1		4.14
PN008-A (2)	4	0.8	-							
PN008-A (3)	4	0.8	-							
PN008-B (1)	4	0.8	4.40E-05			22.3		9.1		0.94
PN008-B (2)	4	0.8	-							
PN008-B (3)	4	0.8	-							
PN008-C (1)	4	1.7	2.21E-05			26.2		29.8		3.93
PN008-C (2)	4	1.7	-							
PN008-C (3)	4	1.7	-							
PN008-D (1)	4	1.7	5.70E-05			32.7		16.7		0.39
PN008-D (2)	4	1.7	-							
PN008-D (3)	4	1.7	-							
PN008-E (1)	4	2.7	4.72E-05			30.4		25.9		0.62
PN008-E (2)	4	2.7	-							
PN008-E (3)	4	2.7	-							
PN008-F (1)	4	3.3	5.06E-05			56.8		44.0		0.53
PN008-F (2)	4	3.3	4.69E-05		2,003	56.0		45.4		0.65
PN008-F (3)	4	3.3	4.23E-05		1,989	64.1		51.3		1.00
<i>Parapassaloteuthis</i>										
PN009-A (1)	3.5	1.1	4.17E-05			23.0		23.8		0.41
PN009-A (2)	3.5	1.1	6.75E-05		1,439	24.6		20.8		0.05
PN009-A (3)	3.5	1.1	-							

Sample number	Rostrum Length / cm	Distance from apex / cm	Ca (mol)	Al/Ca ( $\mu\text{mol mol}^{-1}$ )	S/Ca ( $\mu\text{mol mol}^{-1}$ )	Li/Ca ( $\mu\text{mol mol}^{-1}$ )	B/Ca ( $\mu\text{mol mol}^{-1}$ )	Ba/Ca ( $\mu\text{mol mol}^{-1}$ )	U/Ca ( $\mu\text{mol mol}^{-1}$ )	I/Ca ( $\mu\text{mol mol}^{-1}$ )
PN009-B (1)	3.5	1.1	4.64E-07	15,394				522.1		251.84
PN009-B (2)	3.5	1.1	8.76E-05		1,540	14.7		24.9		0.23
PN009-B (3)	3.5	1.1	-							
PN009-C (1)	3.5	1.1	6.68E-06			10.8		53.5		18.72
PN009-C (2)	3.5	1.1	5.82E-05			11.0		37.7		0.60
PN009-C (3)	3.5	1.1	3.03E-05			11.0		39.9		2.18
PN009-D (1)	3.5	2.4	5.80E-05		1,295	21.3		11.6		0.29
PN009-D (2)	3.5	2.4	5.62E-05			20.1		12.0		0.28
PN009-D (3)	3.5	2.4	-							
PN009-E (1)	3.5	2.4	4.21E-08					485.9		3361.71
PN009-E (2)	3.5	2.4	4.10E-05			15.4		11.1		1.71
PN009-E (3)	3.5	2.4	5.00E-05			16.9		11.1		0.63
PN009-F (1)	3.5	2.4	6.31E-05			17.1		9.8		0.18
PN009-F (2)	3.5	2.4	5.69E-05			17.6		8.3		0.33
PN009-F (3)	3.5	2.4	3.86E-05			17.1		8.8		1.97
PN015-A (1)	4.9	1.7	4.41E-05			22.1		2.4		0.28
PN015-A (2)	4.9	1.7	5.30E-05			23.6		2.8		0.12
PN015-A (3)	4.9	1.7	7.64E-05		1,377	26.0		3.1	3.1E-03	
PN015-B (1)	4.9	1.7	4.93E-05		1,560	31.1		23.7		
PN015-B (2)	4.9	1.7	4.76E-05			24.1		3.3		
PN015-B (3)	4.9	1.7	5.58E-05			27.3		3.8		
PN015-C (1)	4.9	1.7	4.43E-05			24.2		3.0		0.29
PN015-C (2)	4.9	1.7	5.82E-05			23.3		3.4		0.01
PN015-C (3)	4.9	1.7	4.41E-05			32.0		4.7	3.7E-03	0.17
PN015-D (1)	4.9	3.3	4.77E-05		1,735	37.8		5.1		0.35
PN015-D (2)	4.9	3.3	5.76E-05		1,520	37.9		4.7		

Sample number	Rostrum Length / cm	Distance from apex / cm	Ca (mol)	Al/Ca ( $\mu\text{mol mol}^{-1}$ )	S/Ca ( $\mu\text{mol mol}^{-1}$ )	Li/Ca ( $\mu\text{mol mol}^{-1}$ )	B/Ca ( $\mu\text{mol mol}^{-1}$ )	Ba/Ca ( $\mu\text{mol mol}^{-1}$ )	U/Ca ( $\mu\text{mol mol}^{-1}$ )	I/Ca ( $\mu\text{mol mol}^{-1}$ )
PN015-D (3)	4.9	3.3	5.41E-05		1,558	38.1		4.4		
PN015-E (1)	4.9	3.3	4.53E-05		1,411	43.7		9.2		
PN015-E (2)	4.9	3.3	5.12E-05		1,343	43.6		10.0		
PN015-E (3)	4.9	3.3	5.56E-05		1,472	45.1		9.6		
PN015-F (1)	4.9	3.3	5.63E-05		1,933	52.9		10.2		
PN015-F (2)	4.9	3.3	4.68E-05		1,912	49.2		11.5		
PN015-F (3)	4.9	3.3	4.90E-05	72	1,949	57.9		7.2		
PN021-A (1)	4.2	2.5	5.48E-05			35.9		13.3		
PN021-A (2)	4.2	2.5	5.91E-05		1,178	35.1		11.3		
PN021-A (3)	4.2	2.5	3.76E-05			32.2		15.8		
PN021-B (1)	4.2	2.5	5.97E-05		1,215	36.5		80.8		
PN021-B (2)	4.2	2.5	4.95E-05		1,380	38.0		92.6		
PN021-B (3)	4.2	2.5	-							
PN021-C (1)	4.2	2.5	4.64E-05	68	1,771	39.1		80.4		
PN021-C (2)	4.2	2.5	5.51E-05	40	1,795	41.4		71.4		0.25
PN021-C (3)	4.2	2.5	5.46E-05	47	1,575	38.3		77.3		0.06
PN021-D (1)	4.2	1.2	5.48E-05		1,397	29.9		6.3		
PN021-D (2)	4.2	1.2	5.29E-05	77	1,436	30.3		16.8		
PN021-D (3)	4.2	1.2	-							
PN021-E (1)	4.2	1.2	4.63E-05	270	1,917	29.7		701.3		
PN021-E (2)	4.2	1.2	4.82E-05	100	1,675	28.2		177.2		0.10
PN021-E (3)	4.2	1.2	-							
PN021-F (1)	4.2	1.2	5.45E-05	126	1,646	28.5		79.4		0.04
PN021-F (2)	4.2	1.2	5.35E-05	55	1,748	27.7		85.3		
PN021-F (3)	4.2	1.2	4.69E-05	52	1,689	26.7		60.3		

*Passaloteuthis pessula*

Sample number	Rostrum Length / cm	Distance from apex / cm	Ca (mol)	Al/Ca ( $\mu\text{mol mol}^{-1}$ )	S/Ca ( $\mu\text{mol mol}^{-1}$ )	Li/Ca ( $\mu\text{mol mol}^{-1}$ )	B/Ca ( $\mu\text{mol mol}^{-1}$ )	Ba/Ca ( $\mu\text{mol mol}^{-1}$ )	U/Ca ( $\mu\text{mol mol}^{-1}$ )	I/Ca ( $\mu\text{mol mol}^{-1}$ )
PN010-A (1)	6.8	1.0	3.82E-05		3,794	26.6		21.4		3.14
PN010-A (2)	6.8	1.0	5.41E-05		3,642	26.6		23.8	3.1E-03	0.09
PN010-A (3)	6.8	1.0	5.75E-05		3,671	26.9		23.6	2.9E-03	0.03
PN010-B (1)	6.8	1.0	4.59E-05		2,381	28.5		61.4		0.12
PN010-B (2)	6.8	1.0	4.87E-05		2,355	28.7		46.4		0.26
PN010-B (3)	6.8	1.0	4.77E-05		2,325	29.1		48.8		0.38
PN010-C (1)	6.8	3.7	7.07E-05		1,701	34.4		11.2		
PN010-C (2)	6.8	3.7	4.89E-05		1,644	38.1		12.8		
PN010-C (3)	6.8	3.7	4.77E-05		1,791	34.3		12.5		0.07
PN010-D (1)	6.8	3.7	5.02E-05		1,646	48.2		53.6		
PN010-D (2)	6.8	3.7	5.05E-05		1,940	51.6		47.2		
PN010-D (3)	6.8	3.7	5.23E-05		1,869	50.2		52.5		0.01
PN010-E (1)	6.8	5.3	4.84E-05		2,284	40.9		27.9		0.12
PN010-E (2)	6.8	5.3	4.80E-05		1,878	40.5		21.7		0.05
PN010-E (3)	6.8	5.3	5.57E-05		1,921	38.7		24.2		
PN010-F (1)	6.8	6.8	4.45E-05		1,785	35.3		72.5	3.9E-03	
PN010-F (2)	6.8	6.8	4.48E-05		1,752	34.9		35.6		0.22
PN010-F (3)	6.8	6.8	5.03E-05		2,271	32.8		59.5		0.02
PN022-A (1)	6.6	0.7	5.72E-05	222				38.9	1.3E-01	0.11
PN022-A (2)	6.6	0.7	5.19E-05	200				57.3	1.3E-01	
PN022-A (3)	6.6	0.7	4.55E-05	261				168.1	1.3E-01	
PN022-B (1)	6.6	1.8	4.87E-05	40		18.0		56.9		
PN022-B (2)	6.6	1.8	6.18E-05	41		19.7		68.5		
PN022-B (3)	6.6	1.8	4.73E-05			18.8		43.7		
PN022-C (1)	6.6	1.8	5.87E-05	224		23.6		25.8		
PN022-C (2)	6.6	1.8	6.05E-05	251	1,047	23.8		18.5		0.86

Sample number	Rostrum Length / cm	Distance from apex / cm	Ca (mol)	Al/Ca ( $\mu\text{mol mol}^{-1}$ )	S/Ca ( $\mu\text{mol mol}^{-1}$ )	Li/Ca ( $\mu\text{mol mol}^{-1}$ )	B/Ca ( $\mu\text{mol mol}^{-1}$ )	Ba/Ca ( $\mu\text{mol mol}^{-1}$ )	U/Ca ( $\mu\text{mol mol}^{-1}$ )	I/Ca ( $\mu\text{mol mol}^{-1}$ )
PN022-C (3)	6.6	1.8	5.47E-05	340		24.3		15.9		
PN022-D (1)	6.6	2.9	5.81E-05		1,465	31.3		42.7		
PN022-D (2)	6.6	2.9	5.74E-05	47	1,368	30.4		44.9		
PN022-D (3)	6.6	2.9	5.82E-05		1,330	30.9		20.3		
PN022-E (1)	6.6	2.9	5.35E-05	232		27.7		17.6		
PN022-E (2)	6.6	2.9	5.14E-05	235		26.7		8.3		
PN022-E (3)	6.6	2.9	5.97E-05	252		27.7		12.3		
PN022-F (1)	6.6	4.2	5.51E-05	61	1,890	43.2		44.3		
PN022-F (2)	6.6	4.2	4.88E-05	50	1,780	35.2		41.2		0.06
PN022-F (3)	6.6	4.2	4.93E-05		1,815	35.4		40.0		
Samples from Wine Haven										
<i>Passaloteuthis pessleri</i>										
WH014-A (1)	6.5	2.0	5.05E-05			8.7		2.6		
WH014-A (2)	6.5	2.0	4.75E-05			8.1		10.9		
WH014-A (3)	6.5	2.0	5.05E-05			8.2		2.5		0.05
WH014-B (1)	6.5	2.0	5.45E-05			8.4		3.2		
WH014-B (2)	6.5	2.0	4.66E-05			8.3		2.9		
WH014-B (3)	6.5	2.0	5.57E-05			8.8		4.5		
WH014-C (1)	6.5	2.0	5.00E-05			17.1		3.3		0.86
WH014-C (2)	6.5	2.0	6.42E-05	3		17.6		3.3		0.03
WH014-C (3)	6.5	2.0	5.29E-05			17.8		2.9		
WH014-D (1)	6.5	4.6	5.63E-05			7.5		2.2		
WH014-D (2)	6.5	4.6	5.65E-05			7.5		2.2		0.07
WH014-D (3)	6.5	4.6	5.09E-05			7.7		2.1		0.53
WH014-E (1)	6.5	4.6	5.06E-05			23.3		6.5		0.06
WH014-E (2)	6.5	4.6	4.78E-05			24.3		4.6		0.18

Sample number	Rostrum Length / cm	Distance from apex / cm	Ca (mol)	Al/Ca ( $\mu\text{mol mol}^{-1}$ )	S/Ca ( $\mu\text{mol mol}^{-1}$ )	Li/Ca ( $\mu\text{mol mol}^{-1}$ )	B/Ca ( $\mu\text{mol mol}^{-1}$ )	Ba/Ca ( $\mu\text{mol mol}^{-1}$ )	U/Ca ( $\mu\text{mol mol}^{-1}$ )	I/Ca ( $\mu\text{mol mol}^{-1}$ )
WH014-E (3)	6.5	4.6	5.56E-05			22.7		3.8		0.01
WH014-F (1)	6.5	4.6	5.52E-05	3		30.9		18.2		0.07
WH014-F (2)	6.5	4.6	5.90E-05			31.6		19.8		0.02
WH014-F (3)	6.5	4.6	6.63E-05			32.7		41.5		0.10
<i>Nannobelus delicatus</i>										
WH016-A (1)	5	1.0	4.48E-05			6.4		9.1		0.55
WH016-A (2)	5	1.0	-							
WH016-A (3)	5	1.0	-							
WH016-B (1)	5	1.0	6.58E-05	2		3.1		9.1		0.12
WH016-B (2)	5	1.0	5.02E-05			3.2		8.6		0.06
WH016-B (3)	5	1.0	5.01E-05			3.1		8.2		0.29
WH016-C (1)	5	2.3	2.60E-05			8.6		29.9		2.18
WH016-C (2)	5	2.3	5.31E-05	11		8.6		27.0		0.22
WH016-C (3)	5	2.3	5.16E-05			8.6		19.2		0.28
WH016-D (1)	5	2.3	5.11E-05			10.5		15.6		0.22
WH016-D (2)	5	2.3	5.23E-05	10		10.8		16.6		0.15
WH016-D (3)	5	2.3	5.14E-05	10		11.9		18.4		0.22
WH016-E (1)	5	3.3	5.26E-05	18		30.9		153.7		0.26
WH016-E (2)	5	3.3	4.60E-05	25		30.0		135.4		0.53
WH016-E (3)	5	3.3	5.18E-05			30.6		250.9		0.10
WH016-F (1)	5	3.3	4.85E-05	1,243		37.4		50.2	4.1E-02	
WH016-F (2)	5	3.3	5.59E-05	1,318		36.8		21.0	4.0E-02	
WH016-F (3)	5	3.3	4.88E-05	1,266		36.4		15.8	4.2E-02	
WH020-A (1)	5.5	1.2	6.09E-05	23		8.8		10.2		
WH020-A (2)	5.5	1.2	-							
WH020-A (3)	5.5	1.2	-							

Sample number	Rostrum Length / cm	Distance from apex / cm	Ca (mol)	Al/Ca ( $\mu\text{mol mol}^{-1}$ )	S/Ca ( $\mu\text{mol mol}^{-1}$ )	Li/Ca ( $\mu\text{mol mol}^{-1}$ )	B/Ca ( $\mu\text{mol mol}^{-1}$ )	Ba/Ca ( $\mu\text{mol mol}^{-1}$ )	U/Ca ( $\mu\text{mol mol}^{-1}$ )	I/Ca ( $\mu\text{mol mol}^{-1}$ )
WH020-B (1)	5.5	1.2	5.63E-05	5		8.7		109.1		
WH020-B (2)	5.5	1.2	-							
WH020-B (3)	5.5	1.2	-							
WH020-C (1)	5.5	2.1	5.34E-05			18.6		4.6		0.11
WH020-C (2)	5.5	2.1	2.36E-05			18.6		3.0		0.24
WH020-C (3)	5.5	2.1	-							
WH020-D (1)	5.5	2.1	5.13E-05			18.1		24.8		
WH020-D (2)	5.5	2.1	4.82E-05			17.5		26.4		0.16
WH020-D (3)	5.5	2.1	4.91E-05			17.7		29.7		
WH020-E (1)	5.5	2.8	4.45E-05			20.4		40.6		0.08
WH020-E (2)	5.5	2.8	5.12E-05			19.9		44.9		0.10
WH020-E (3)	5.5	2.8	5.77E-05			19.9		89.8		
WH020-F (1)	5.5	3.9	5.45E-05	4		31.5		3.6		
WH020-F (2)	5.5	3.9	5.56E-05			30.2		2.4		
WH020-F (3)	5.5	3.9	-							
WH022-A (1)	4.5	0.6	4.52E-05			2.6		8.5	2.3E-02	0.03
WH022-A (2)	4.5	0.6	-							
WH022-A (3)	4.5	0.6	-							
WH022-B (1)	4.5	1.4	6.41E-05	8		1.5		48.0		
WH022-B (2)	4.5	1.4	-							
WH022-B (3)	4.5	1.4	-							
WH022-C (1)	4.5	2.3	5.45E-05	3		2.7		16.2		0.03
WH022-C (2)	4.5	2.3	-							
WH022-C (3)	4.5	2.3	-							
WH022-D (1)	4.5	2.7	5.13E-05			3.7		29.7		
WH022-D (2)	4.5	2.7	4.90E-05			3.8		33.7		

Sample number	Rostrum Length / cm	Distance from apex / cm	Ca (mol)	Al/Ca ( $\mu\text{mol mol}^{-1}$ )	S/Ca ( $\mu\text{mol mol}^{-1}$ )	Li/Ca ( $\mu\text{mol mol}^{-1}$ )	B/Ca ( $\mu\text{mol mol}^{-1}$ )	Ba/Ca ( $\mu\text{mol mol}^{-1}$ )	U/Ca ( $\mu\text{mol mol}^{-1}$ )	I/Ca ( $\mu\text{mol mol}^{-1}$ )
WH022-D (3)	4.5	2.7	5.51E-05	12		4.1		28.5		
WH022-E (1)	4.5	3.5	4.50E-05			13.1		110.0		0.25
WH022-E (2)	4.5	3.5	4.65E-05			13.0		75.9		
WH022-E (3)	4.5	3.5	-							
WH022-F (1)	4.5	4.1	5.38E-05	10		23.1		17.4		
WH022-F (2)	4.5	4.1	5.51E-05	5		22.5		10.5		
WH022-F (3)	4.5	4.1	-							
<b>Variability samples cleaned with hydrogen peroxide</b>										
Samples from Penny Nab										
<i>Parapassaloteuthis</i>										
PN015-B (1)	4.9	1.7	5.81E-05							
PN015-C (1)	4.9	1.7	5.95E-05							
PN015-F (1)	4.9	3.4	5.02E-05							
PN021-C (1)	4.2	2.5	5.45E-05							
PN021-C (2)	4.2	2.5	5.25E-05							
<i>Passaloteuthis pessula</i>										
PN010-C (1)	6.8	3.7	4.22E-05							
PN010-D (1)	6.8	3.7	5.13E-05							
PN010-E (1)	6.8	5.3	4.69E-05							
PN010-E (2)	6.8	5.3	5.67E-05							
PN010-F (1)	6.8	6.8	5.18E-05							
PN022-B (1)	6.6	1.8	5.41E-05							
PN022-C (1)	6.6	1.8	4.11E-05							
PN022-D (1)	6.6	2.9	4.39E-05							
PN022-D (2)	6.6	2.9	5.80E-05							
PN022-E (1)	6.6	2.9	5.08E-05							

Sample number	Rostrum Length / cm	Distance from apex / cm	Ca (mol)	Al/Ca ( $\mu\text{mol mol}^{-1}$ )	S/Ca ( $\mu\text{mol mol}^{-1}$ )	Li/Ca ( $\mu\text{mol mol}^{-1}$ )	B/Ca ( $\mu\text{mol mol}^{-1}$ )	Ba/Ca ( $\mu\text{mol mol}^{-1}$ )	U/Ca ( $\mu\text{mol mol}^{-1}$ )	I/Ca ( $\mu\text{mol mol}^{-1}$ )
PN022-E (2)	6.6	2.9	5.93E-05							
PN022-F (1)	6.6	4.2	5.63E-05							
Samples from Wine Haven										
<i>Passaloteuthis pessula</i>										
WH014-B (1)	6.5	2.0	4.22E-05							
WH014-C (1)	6.5	2.0	4.58E-05							
WH014-E (1)	6.5	4.6	3.99E-05							
WH014-E (2)	6.5	4.6	5.33E-05							
WH014-F (1)	6.5	4.6	6.10E-05							
<i>Nannobelus delicatus</i>										
WH016-D (1)	5	2.3	4.15E-05							

### 8.3. Modern Analogue Samples analysis

Table 33 - Elemental results for analysis of Modern Analogue Samples including Ca values (mol), and Mg/Ca, P/Ca, Sr/Ca, Na/Ca, Fe/Ca, Mn/Ca, Li/Ca, and Ba/Ca values ( $\mu\text{mol mol}^{-1}$ ).

Sample number	Cleaning method	Ca (mol)	Mg/Ca ( $\mu\text{mol mol}^{-1}$ )	P/Ca ( $\mu\text{mol mol}^{-1}$ )	Sr/Ca ( $\mu\text{mol mol}^{-1}$ )	Na/Ca ( $\mu\text{mol mol}^{-1}$ )	Fe/Ca ( $\mu\text{mol mol}^{-1}$ )	Mn/Ca ( $\mu\text{mol mol}^{-1}$ )	Li/Ca ( $\mu\text{mol mol}^{-1}$ )	Ba/Ca ( $\mu\text{mol mol}^{-1}$ )
<b>Cuttlefish (<i>Sepia officinalis</i>)</b>										
Specimen A (biological age 8 months)										
706 Cu-A-A(2) - Bl	H <sub>2</sub> O <sub>2</sub>	4.33E-05	1,384	6,360	3,957	20,354			8.77	3.19
708 Cu-A-B(2) - Bl	H <sub>2</sub> O <sub>2</sub>	4.41E-05	1,323	7,505	3,658	23,496			10.44	4.90
710 Cu-A-C(2) - Bl	H <sub>2</sub> O <sub>2</sub>	4.83E-05	1,418	8,822	4,120	36,626			12.49	6.56
705 Cu-A-A(1) - Wa	Water	4.27E-05	1,765	1,092	3,968	20,400			9.15	3.03
707 Cu-A-B(1) - Wa	Water	4.62E-05	1,789	584	3,745	23,771			11.18	4.46
709 Cu-A-C(1) - Wa	Water	4.17E-05	1,715	524	4,094	24,383			12.52	5.95
Specimen B (biological age 13 months)										
712 Cu-B-A(2) - Bl	H <sub>2</sub> O <sub>2</sub>	2.70E-05	1,621	10,060	5,377	23,555		943.98	14.27	6.56
715 Cu-B-B(2) - Bl	H <sub>2</sub> O <sub>2</sub>	5.05E-05	1,601	8,076	5,167	23,953		102.33	14.29	7.68
718 Cu-B-C(2) - Bl	H <sub>2</sub> O <sub>2</sub>	4.33E-05	1,654	8,181	5,047	24,947		244.72	13.06	8.38
720 Cu-B-C(4) - Bl	H <sub>2</sub> O <sub>2</sub>	5.50E-05	1,593	7,669	5,039	24,216		96.08	13.64	7.82
722 Cu-B-D(2) - Bl	H <sub>2</sub> O <sub>2</sub>	4.62E-05	1,472	9,192	5,377	24,844		61.79	13.2	8.83
725 Cu-B-E(2) - Bl	H <sub>2</sub> O <sub>2</sub>	4.46E-05	1,542	8,752	5,430	23,728		46.50	14.52	8.68
711 Cu-B-A(1) - Wa	Water	4.73E-05	2,287	328	5,201	24,771		277.89	14.32	7.31
713 Cu-B-A(3) - Wa	Water	4.20E-05	2,010	291	5,341	24,297		256.67	14.47	7.34
714 Cu-B-B(1) - Wa	Water	4.80E-05	2,320	339	5,114	24,764		113.46	15.39	7.32
716 Cu-B-B(3) - Wa	Water	5.23E-05	2,869	345	4,988	24,615		116.86	14.74	7.00
717 Cu-B-C(1) - Wa	Water	5.03E-05	2,430	342	5,031	25,194		66.40	14.82	7.17
719 Cu-B-C(3) - Wa	Water	5.18E-05	2,442	355	5,036	25,034		60.27	13.26	7.58

Sample number	Cleaning method	Ca (mol)	Mg/Ca ( $\mu\text{mol mol}^{-1}$ )	P/Ca ( $\mu\text{mol mol}^{-1}$ )	Sr/Ca ( $\mu\text{mol mol}^{-1}$ )	Na/Ca ( $\mu\text{mol mol}^{-1}$ )	Fe/Ca ( $\mu\text{mol mol}^{-1}$ )	Mn/Ca ( $\mu\text{mol mol}^{-1}$ )	Li/Ca ( $\mu\text{mol mol}^{-1}$ )	Ba/Ca ( $\mu\text{mol mol}^{-1}$ )
721 Cu-B-D(1) - Wa	Water	4.81E-05	2,408	499	5,338	24,826		44.47	12.88	8.06
723 Cu-B-D(3) - Wa	Water	4.86E-05	2,621	529	5,383	25,207		46.41	13.98	8.28
724 Cu-B-E(1) - Wa	Water	5.05E-05	2,677	734	5,443	24,288		34.39	14.26	8.08
<b>Spirula (<i>Spirula spirula</i>)</b>										
Specimen A										
727 Sp-A-A(2) - Bl	H <sub>2</sub> O <sub>2</sub>	4.20E-05	479	3,550	3,540	23,483		22.11	11.13	2.70
729 Sp-A-A(4) - Bl	H <sub>2</sub> O <sub>2</sub>	4.98E-05	485	3,676	3,527	24,145		18.74	10.9	3.08
731 Sp-A-B(2) - Bl	H <sub>2</sub> O <sub>2</sub>	4.68E-05	448	3,957	3,274	24,264		22.52	11.76	2.94
733 Sp-A-B(4) - Bl	H <sub>2</sub> O <sub>2</sub>	4.68E-05	438	2,743	3,211	24,781		19.72	10.97	2.94
735 Sp-A-C(2) - Bl	H <sub>2</sub> O <sub>2</sub>	4.27E-05	555	4,122	3,594	23,163		29.57	10.98	3.32
726 Sp-A-A(1) - Wa	Water	4.37E-05	602	772	3,702	23,649		15.50	12.22	2.79
728 Sp-A-A(3) - Wa	Water	4.28E-05	594	729	3,584	23,432			12.66	2.63
730 Sp-A-B(1) - Wa	Water	4.68E-05	606	764	3,359	24,675		14.00	11.6	3.18
732 Sp-A-B(3) - Wa	Water	4.44E-05	692	760	3,321	24,404		15.75	11.66	2.83
734 Sp-A-C(1) - Wa	Water	5.59E-05	667	794	3,584	22,596		18.67	11.76	2.96
736 Sp-A-C(3) - Wa	Water	4.55E-05	724	787	3,645	21,618		19.81	11.29	2.55
Specimen B										
738 Sp-B-A(2) - Bl	H <sub>2</sub> O <sub>2</sub>	4.63E-05	521	3,543	3,347	22,640		15.45	12.57	2.95
737 Sp-B-A(1) - Wa	Water	4.89E-05	701	615	3,344	22,948			11.69	2.74
739 Sp-B-A(3) - Wa	Water	4.71E-05	771	721	3,440	22,628			13.35	3.04
Specimen C										
741 Sp-C-A(2) - Bl	H <sub>2</sub> O <sub>2</sub>	5.18E-05	371	2,937	2,693	23,686			9.59	2.44
744 Sp-C-B(2) - Bl	H <sub>2</sub> O <sub>2</sub>	4.55E-05	438	2,933	2,829	23,540		16.08	8	2.96
740 Sp-C-A(1) - Wa	Water	4.71E-05	610	715	2,855	22,997		14.26	10.76	2.29
742 Sp-C-A(3) - Wa	Water	4.66E-05	646	596	2,815	23,937			8.08	2.56

Sample number	Cleaning method	Ca (mol)	Mg/Ca ( $\mu\text{mol mol}^{-1}$ )	P/Ca ( $\mu\text{mol mol}^{-1}$ )	Sr/Ca ( $\mu\text{mol mol}^{-1}$ )	Na/Ca ( $\mu\text{mol mol}^{-1}$ )	Fe/Ca ( $\mu\text{mol mol}^{-1}$ )	Mn/Ca ( $\mu\text{mol mol}^{-1}$ )	Li/Ca ( $\mu\text{mol mol}^{-1}$ )	Ba/Ca ( $\mu\text{mol mol}^{-1}$ )
743 Sp-C-B(1) - Wa	Water	4.49E-05	652	656	2,903	23,891			8.47	2.95
745 Sp-C-B(3) - Wa	Water	4.68E-05	633	594	2,919	24,588		14.25	10.64	2.92
Specimen D										
747 Sp-D-A(1) - Bl	H <sub>2</sub> O <sub>2</sub>	3.74E-05	568	594	3,757	24,148			20.92	4.76
749 Sp-D-A(3) - Bl	H <sub>2</sub> O <sub>2</sub>	5.02E-05	442	3,036	3,406	22,907		15.03	17.45	3.53
748 Sp-D-A(2) - Wa	Water	4.48E-05	559	674	2,979	24,982			12.66	3.09
Specimen E										
751 Sp-E-A(2) - Bl	H <sub>2</sub> O <sub>2</sub>	4.72E-05	594	3,400	3,272	21,921		15.28	17.49	2.42
753 Sp-E-B(2) - Bl	H <sub>2</sub> O <sub>2</sub>	4.90E-05	372	3,490	3,242	21,075		15.38	9.12	3.05
750 Sp-E-A(1) - Wa	Water	4.63E-05	521	537	3,301	21,952			15.8	2.33
752 Sp-E-B(1) - Wa	Water	5.00E-05	379	514	3,130	21,895			9.08	2.57

## 8.4. Stratigraphic Samples

### 8.4.1. Yorkshire coast

Table 34 - Main elemental and isotopic results for analysis of stratigraphic samples from the Yorkshire Coast, including oxygen and carbon isotope values, Ca values (mol), and Mg/Ca, P/Ca, Sr/Ca, Na/Ca, Fe/Ca, and Mn/Ca values in  $\mu\text{mol mol}^{-1}$ . Sample heights are the calculated height above the base of the Sinemurian. In the notes column 1 = sample which was defined as altered ( $\text{Fe} > 600$  and/or  $\text{Mn} > 300$ ), 2 = sample not included in the discussion in Chapter 5 due to extremely elevated Na, Sr, Fe or Mn values ( $\text{Sr/Ca} > 3,000$ ;  $\text{Fe/Ca} > 5,000$ ;  $\text{Mn/Ca} > 1000$ ), 5 = sample previously included in Newton et al. (2011).

Sample number	Height (m)	Ca (mol)	Mg/Ca ( $\mu\text{mol mol}^{-1}$ )	P/Ca ( $\mu\text{mol mol}^{-1}$ )	Sr/Ca ( $\mu\text{mol mol}^{-1}$ )	Na/Ca ( $\mu\text{mol mol}^{-1}$ )	Fe/Ca ( $\mu\text{mol mol}^{-1}$ )	Mn/Ca ( $\mu\text{mol mol}^{-1}$ )	$\delta^{13}\text{C}_{\text{VPDB}}$ (‰)	$\delta^{18}\text{O}_{\text{VPDB}}$ (‰)	Notes
<b>Ravenscar</b>											
RS001(A) - 1	336.0	4.99E-05	10,495		1,865	18,454	80	34	2.66	-3.32	5
RS001(A) - 1	336.0	4.99E-05	10,495		1,865	18,454	80	34	3.18	-3.49	5
RS001b(A) - 1	336.0	6.10E-05	8,893		1,515	16,151	1,885	1,182	3.23	-4.49	1, 2, 5
RS001c(A) - 1	336.0	4.79E-05	9,526	1,216	1,588	22,786	68	18	1.94	-2.70	5
RS002(A) - 1	338.1	5.51E-05	8,012	2,620	1,803	13,885	607	66	1.40	-3.95	1, 5
RS002a(A) - 1	338.1	6.71E-05	9,023	3,580	1,868	14,781	244	20	1.95	-3.90	5
RS002a(B) - 1	338.1	5.73E-05	9,979	15,019	1,905	16,639	1,762	131			1, 5
RS002b(A) - 1	338.1	2.79E-05	14,864	75,568	2,095	22,371	10,709	1,014	1.21	-4.02	1, 2, 5
RS003(A) - 1	335.9	1.04E-04	9,943	1,172	1,747	12,537	365	69			5
RS003a(A) - 1	335.9	6.28E-05	9,253		1,708	10,438	68	18			5
RS004(A) - 1	200.0	5.21E-05	6,263		1,504	14,771	104	22			5
RS004(A) - 2	200.0	6.45E-05	6,327		1,524	11,416	106	23			5
RS004(B) - 1	200.0	5.73E-05	8,799		1,309	8,175	67	21			5
RS004a(A) - 1	200.0	5.95E-05	10,048	968	1,904	12,060	286	51			5
RS005(A) - 1	331.5	6.27E-05	11,232	783	1,704	12,635	2,288	390			1, 5
RS005a(A) - 1	331.5	5.70E-05	11,495	981	1,803	15,670	64				5
RS005b(A) - 1	331.5	6.39E-05	8,020		1,810	12,795	135	33			5
RS005c(A) - 1	331.5	6.27E-05	8,868		1,327	11,135	146	46	1.58	-2.49	5

Sample number	Height (m)	Ca (mol)	Mg/Ca ( $\mu\text{mol mol}^{-1}$ )	P/Ca ( $\mu\text{mol mol}^{-1}$ )	Sr/Ca ( $\mu\text{mol mol}^{-1}$ )	Na/Ca ( $\mu\text{mol mol}^{-1}$ )	Fe/Ca ( $\mu\text{mol mol}^{-1}$ )	Mn/Ca ( $\mu\text{mol mol}^{-1}$ )	$\delta^{13}\text{C}_{\text{VPDB}}$ (‰)	$\delta^{18}\text{O}_{\text{VPDB}}$ (‰)	Notes
RS005c(B) - 1	331.5	6.08E-05	6,104		1,634	11,425	98	19			5
RS007(A) - 1	332.6	5.37E-05	7,523		1,166	8,573	4,959	2,490			1, 2, 5
RS008(A) - 1	324.3	5.90E-05	8,901		1,399	9,533		17			5
RS008(A) - 2	324.3	6.27E-05	8,753	749	1,377	11,492	46	18	2.42	-3.74	5
RS009(A) - 1	323.3	6.64E-05	9,617		1,876	12,869					5
RS010(A) - 1	322.7	6.20E-05	8,788	804	1,634	12,164	205	67			5
RS010(B) - 1	322.7	6.30E-05	8,827		1,641	10,440	103	32			5
RS011(A) - 1	314.2	5.46E-05	4,415		683	3,916					5
RS012(A) - 1	311.2	5.37E-05	10,280	1,006	1,708	14,159					5
RS014(A) - 1	303.6	5.52E-05	12,308		1,699	11,322	99	27			5
RS014a(A) - 1	303.6	5.71E-05	12,187	974	1,368	7,294	428	63			5
RS014b(A) - 1	303.6	6.18E-05	12,265	1,048	1,722	12,851		14	2.94	-4.39	5
RS014b(B) - 1	303.6	5.72E-05	11,703	792	1,634	9,101	94	28			5
RS015(A) - 1	302.1	6.08E-05	6,726		1,385	12,313					5
RS015(A) - 2	302.1	5.27E-05	6,751		1,389	15,785			2.77	-2.21	5
RS015a(A) - 1	302.1	5.93E-05	6,695		1,479	8,762					5
RS016(A) - 1	302.8	5.78E-05	12,788	1,162	1,784	8,743					5
RS016a(A) - 1	302.8	6.46E-05	11,151	763	1,792	11,658			3.74	-3.85	5
RS016b(A) - 1	302.8	5.96E-05	9,544		1,466	10,956	50	26			5
RS016b(B) - 1	302.8	5.78E-05	6,673		1,416	9,008	57	35			5
RS017(A) - 1	301.7	6.31E-05	9,119		1,356	10,209	88	15			5
RS017a(A) - 1	301.7	5.77E-05	13,048	1,389	1,681	10,864	135	36	2.02	-5.25	5
RS018(A) - 1	296.9	6.06E-05	12,188	777	1,700	7,902	44	14	3.32	-4.63	5
RS018a(A) - 1	296.9	3.69E-05	15,553		1,659	11,904	97	68			5
RS019(A) - 1	280.0	5.94E-05	10,654	1,119	1,799	10,682					5
RS019(A) - 2	280.0	6.19E-05	10,736	1,136	1,831	11,024					5

Sample number	Height (m)	Ca (mol)	Mg/Ca ( $\mu\text{mol mol}^{-1}$ )	P/Ca ( $\mu\text{mol mol}^{-1}$ )	Sr/Ca ( $\mu\text{mol mol}^{-1}$ )	Na/Ca ( $\mu\text{mol mol}^{-1}$ )	Fe/Ca ( $\mu\text{mol mol}^{-1}$ )	Mn/Ca ( $\mu\text{mol mol}^{-1}$ )	$\delta^{13}\text{C}_{\text{VPDB}}$ (‰)	$\delta^{18}\text{O}_{\text{VPDB}}$ (‰)	Notes
RS019(B) - 1	280.0	6.34E-05	11,197	693	1,695	8,228			3.25	-4.27	5
RS020(A) - 1	279.4	6.30E-05	10,694	975	1,762	10,902	41				5
RS021(A) - 1	277.2	6.08E-05	9,126	945	1,639	11,655					5
RS021a(A) - 1	277.2	5.44E-05	10,575	815	1,685	9,539					5
RS022(A) - 1	274.0	6.00E-05	10,046	742	1,671	9,762					5
RS023(A) - 1	270.4	6.49E-05	9,744	800	1,498	10,071			2.64	-3.24	5
RS023(B) - 1	270.4	5.83E-05	9,975		1,573	8,903					5
RS023a(A) - 1	270.4	6.00E-05	10,888		1,683	10,066	893	234	2.39	-2.71	1, 5
RS024(A) - 1	271.8	5.74E-05	10,593	856	1,700	8,800					5
RS025(A) - 1	269.6	5.99E-05	9,543	932	1,651	9,273			3.66	-4.15	5
RS025(A) - 2	269.6	6.11E-05	9,545	900	1,653	9,141			3.66	-4.15	5
RS026(A) - 1	268.7	6.00E-05	8,870		1,540	8,845			3.26	-2.99	5
RS027(A) - 1	266.1	6.10E-05	10,153		1,443	8,091	120	32			5
RS027(B) - 1	266.1	6.17E-05	9,545		1,558	9,172					5
RS028(A) - 1	261.9	6.05E-05	11,154		1,495	9,084	322	67			5
RS031(A) - 1	246.6	6.04E-05	12,547	993	1,320	8,484		20	2.04	-1.73	5
RS032(A) - 1	235.5	5.83E-05	12,953		1,169	4,837	168	30	1.64	-3.59	5
RS032a(A) - 1	235.5	5.34E-05	12,785		1,525	6,887	57	17	2.42	-2.66	5
RS033(A) - 1	234.4	6.47E-05	12,691	1,067	1,323	4,819	106	25	1.67	-2.75	5
RS033(C) - 1	234.4	5.68E-05	12,162	1,073	1,272	5,768	191	38	1.76	-2.90	5
RS033(C) - 2	234.4	5.46E-05	12,543	1,102	1,280	6,505	211	37			5
<b>Runswick Bay</b>											
RW001a(A) - 1	204.5	5.55E-05	6,510	418	1,221	3,529		19			5
RW001b(A) - 1	204.5	5.63E-05	5,569	389	1,230	3,839		14			5
RW001c(A) - 1	204.5	5.28E-05	6,420	368	1,308	3,499		20	1.99	-0.68	5
RW002(A) - 1	205.0	4.63E-05	13,433	859	1,724	4,077	69	54			5

Sample number	Height (m)	Ca (mol)	Mg/Ca ( $\mu\text{mol mol}^{-1}$ )	P/Ca ( $\mu\text{mol mol}^{-1}$ )	Sr/Ca ( $\mu\text{mol mol}^{-1}$ )	Na/Ca ( $\mu\text{mol mol}^{-1}$ )	Fe/Ca ( $\mu\text{mol mol}^{-1}$ )	Mn/Ca ( $\mu\text{mol mol}^{-1}$ )	$\delta^{13}\text{C}_{\text{VPDB}}$ (‰)	$\delta^{18}\text{O}_{\text{VPDB}}$ (‰)	Notes
RW002a(A) - 1	205.0	5.10E-05	10,610	637	1,667	3,862	2,781	218			1, 5
RW002a(B) - 1	205.0	6.22E-05	10,785	611	1,594	3,205	3,035	164	0.04	-5.57	1, 5
RW002b(A) - 1	205.0	5.34E-05	12,648	1,106	1,678	5,986	659	127	1.41	-2.33	1, 5
RW004(A) - 1	204.6	4.93E-05	6,106	588	1,149	3,194	86	44	1.74	-0.64	5
RW005(A) - 1	205.1	4.62E-05	7,295	463	1,259	3,513	177	59			5
RW006(A) - 1	205.0	5.14E-05	10,269	701	1,784	5,097	499	253			5
RW006(A) - 2	205.0	5.74E-05	10,306	682	1,787	5,713	464	221			5
RW007(A) - 1	221.8	4.46E-05	15,060	906	2,138	6,568		12			5
RW007(B) - 1	221.8	4.20E-05	14,325	1,073	2,009	6,190	162	39			5
RW007a(A) - 1	221.8	5.17E-05	13,145	1,012	1,366	843	690	95	-0.15	-7.94	1, 5
RW010(A) - 1	222.2	5.36E-05	17,497	1,320	2,014	5,571	611	136	-0.39	-6.14	1, 5
RW010a(A) - 1	222.2	4.95E-05	20,239	1,098	2,321	6,341		11	1.47	-4.74	5
RW011a(A) - 1	222.7	5.34E-05	5,576	1,378	413		380	52			5
RW013(A) - 1	223.2	5.91E-06	19,190	2,210	1,736		6,904	299	24.16	-0.02	1, 2, 5
RW013(B) - 1	223.2	4.82E-05	11,004	1,107	1,630	4,119	77	26	3.22	-4.00	5
RW014a(A) - 1	222.8	4.62E-05	14,991	1,076	1,732	1,952	249	45			5
RW014a(A) - 2	222.8	5.04E-05	14,563	1,078	1,720	1,864	237	45	3.16	-4.83	5
RW015a(A) - 1	224.4	5.61E-05	13,436	785	1,856	5,986		11			5
RW016a(A) - 1	223.5	5.46E-05	10,768	931	1,737	5,546	141	28			5
RW017(A) - 1	222.3	4.72E-05	13,098	860	1,827	6,533	333	49			5
RW018a(A) - 1	224.9	4.61E-05	7,544	1,181	847	2,165	1,279	101	0.58	-9.00	1, 5
RW018a(B) - 1	224.9	6.04E-05	10,357	1,230	1,372	5,167	336	32			5
RW018b(A) - 1	224.9	5.29E-05	10,270	855	931	1,190	1,688	143	1.32	-7.64	1, 5
RW020(A) - 1	209.4	5.81E-05	7,100	431	1,498	6,533		21			5
RW020b(A) - 1	209.4	5.01E-05	6,412	446	1,250	4,995		54			5
RW021a(A) - 1	209.7	5.53E-05	8,690	929	1,294	5,766	182	38			5

Sample number	Height (m)	Ca (mol)	Mg/Ca ( $\mu\text{mol mol}^{-1}$ )	P/Ca ( $\mu\text{mol mol}^{-1}$ )	Sr/Ca ( $\mu\text{mol mol}^{-1}$ )	Na/Ca ( $\mu\text{mol mol}^{-1}$ )	Fe/Ca ( $\mu\text{mol mol}^{-1}$ )	Mn/Ca ( $\mu\text{mol mol}^{-1}$ )	$\delta^{13}\text{C}_{\text{VPDB}}$ (‰)	$\delta^{18}\text{O}_{\text{VPDB}}$ (‰)	Notes
RW021a(A) - 2	209.7	4.75E-05	8,577	879	1,278	5,446	173	38			5
RW023a(A) - 1	208.9	5.18E-05	6,954	424	1,265	4,664	62	49			5
RW023a(B) - 1	208.9	5.98E-05	6,419	476	1,337	5,600		28			5
RW023b(A) - 1	208.9	5.09E-05	6,554	385	1,326	4,622	181	71			5
RW023c(A) - 1	208.9	5.45E-05	6,416	397	1,173	4,159	101	52			5
RW023d(A) - 1	208.9	5.10E-05	6,583	405	1,293	4,419		33			5
RW023e(A) - 1	208.9	4.90E-05	8,115	1,251	1,136	3,883	2,912	504	1.02	-2.51	1, 5
RW023f(A) - 1	208.9	5.17E-05	6,943	410	1,243	4,595	54	36			5
RW023f(B) - 1	208.9	6.33E-05	6,942	374	1,324	5,384		23			5
RW024(A) - 1	208.7	5.41E-05	7,087	932	1,139	4,036	178	81			5
RW024a(A) - 1	208.7	5.49E-05	7,550	424	1,311	4,853		28			5
RW024a(A) - 2	208.7	5.53E-05	7,593	439	1,305	4,767		28			5
RW024b(A) - 1	208.7	5.32E-05	6,820	394	1,175	4,110	66	37			5
RW025(A) - 1	208.6	5.91E-05	8,763	1,160	1,137	4,199	724	173	1.62	-1.19	1, 5
RW026a(A) - 1	213.8	4.91E-05	7,039	394	1,138	4,315	73	34			5
RW026a(B) - 1	213.8	5.73E-05	6,941	367	1,193	4,246	117	48			5
RW027(A) - 1	214.8	4.85E-05	7,515	461	1,287	5,018	346	87			5
RW028(A) - 1	214.9	5.41E-05	8,105	447	1,349	5,654	129	42			5
RW028a(A) - 1	214.9	5.59E-05	6,794	350	1,099	5,014		15			5
RW029(A) - 1	213.4	5.07E-05	8,574	620	1,259	6,217		20			5
RW030(A) - 1	211.3	4.95E-05	8,323	644	1,447	5,893	200	109			5
RW030(B) - 1	211.3	4.74E-05	8,086	494	1,192	5,108	239	132			5
RW030(B) - 2	211.3	5.11E-05	8,092	582	1,178	4,599	261	139			5
RW030b(A) - 1	211.3	5.43E-05	7,500	466	1,246	5,806	51	27			5
RW031(A) - 1	217.5	5.80E-05	9,200	600	1,108	4,980	96	47			5
RW031a(A) - 1	217.5	4.72E-05	9,154	457	1,141	5,394	84	45			5

Sample number	Height (m)	Ca (mol)	Mg/Ca ( $\mu\text{mol mol}^{-1}$ )	P/Ca ( $\mu\text{mol mol}^{-1}$ )	Sr/Ca ( $\mu\text{mol mol}^{-1}$ )	Na/Ca ( $\mu\text{mol mol}^{-1}$ )	Fe/Ca ( $\mu\text{mol mol}^{-1}$ )	Mn/Ca ( $\mu\text{mol mol}^{-1}$ )	$\delta^{13}\text{C}_{\text{VPDB}}$ (‰)	$\delta^{18}\text{O}_{\text{VPDB}}$ (‰)	Notes
RW032a(A) - 1	216.9	5.12E-05	7,142	472	1,121	4,708	69	39			5
RW032b(A) - 1	216.9	5.89E-05	7,419	433	1,320	5,646	192	67			5
RW032b(B) - 1	216.9	5.00E-05	7,108	388	1,302	5,368		21			5
RW033(A) - 1	215.5	5.34E-05	7,093	476	1,182	5,061	92	44			5
RW033b(A) - 1	215.5	5.74E-05	8,394	727	1,166	5,235	53	23			5
RW034(A) - 1	215.6	5.60E-05	7,400	460	1,318	5,548		23			5
RW034a(A) - 1	215.6	4.63E-05	6,728	357	1,226	5,470		20			5
RW034a(A) - 2	215.6	5.23E-05	6,734	368	1,224	5,471		21			5
RW035a(A) - 1	210.4	5.48E-05	8,227	272	1,238	6,791	76	32	2.69	-0.43	5
RW035a(B) - 1	210.4	5.26E-05	8,327	231	1,257	6,861	83	40	2.63	-0.63	5
RW036a(A) - 1	210.8	5.55E-05	7,417	274	1,488	7,885			2.18	-1.05	5
RW037(A) - 1	211.6	5.21E-05	7,493	201	1,346	7,086	59	31	1.93	-0.59	5
RW038(A) - 1	213.1	4.85E-05	9,067	289	1,435	7,110	1,354	300			1, 5
RW039(A) - 1	213.1	4.74E-05	8,222	195	1,388	7,051	64	43	2.03	-0.89	5
RW040a(A) - 1	207.0	4.45E-05	7,649	236	1,287	6,581	156	94	1.53	-1.04	5
RW040b(A) - 1	208.0	4.72E-05	8,938	329	1,757	8,265	58		2.08	-1.01	5
RW041a(A) - 1	208.0	5.68E-05	7,731	426	1,309	6,484	159	73			5
RW042(A) - 1	207.6	5.12E-05	7,282	173	1,378	6,656			1.85	-0.76	5
RW042(A) - 2	207.6	5.44E-05	7,363	210	1,389	6,900					5
RW042a(A) - 1	208.6	4.17E-05	7,188	157	1,517	7,484			1.86	-0.81	5
RW042a(B) - 1	208.6	5.33E-05	7,967	214	1,621	7,880			2.15	-0.92	5
RW043(A) - 1	202.3	4.80E-05	14,487	1,132	2,178	10,453	156	63	1.31	-2.53	5
RW044a(A) - 1	201.9	4.90E-05	18,320	729	2,216	10,961	163	66	1.09	-5.08	5
RW045(A) - 1	201.3	5.25E-05	13,459	832	2,089	9,806	72		1.88	-3.02	5
RW046(A) - 1	205.8	5.78E-05	7,288	299	1,299	6,966	65				5
RW047a(A) - 1	202.5	4.46E-05	12,599	662	1,801	8,116	87		0.85	-2.29	5

Sample number	Height (m)	Ca (mol)	Mg/Ca ( $\mu\text{mol mol}^{-1}$ )	P/Ca ( $\mu\text{mol mol}^{-1}$ )	Sr/Ca ( $\mu\text{mol mol}^{-1}$ )	Na/Ca ( $\mu\text{mol mol}^{-1}$ )	Fe/Ca ( $\mu\text{mol mol}^{-1}$ )	Mn/Ca ( $\mu\text{mol mol}^{-1}$ )	$\delta^{13}\text{C}_{\text{VPDB}}$ (‰)	$\delta^{18}\text{O}_{\text{VPDB}}$ (‰)	Notes
RW047a(B) - 1	202.5	4.97E-05	12,232	669	1,755	7,912	178	47	0.86	-2.04	5
RW048(A) - 1	217.8	4.13E-05	7,673	133	1,314	7,356			3.00	-0.92	5
RW048(B) - 1	217.8	3.95E-05	7,597	102	1,321	7,108			3.01	-0.95	5
RW048(B) - 2	217.8	4.11E-05	7,557	117	1,322	7,346			3.01	-0.95	5
<b>Cowbar Nab</b>											
CN001(A) - 1	161.5	3.85E-05	14,119	597	2,212	9,665	448	254			
CN002(A) - 1	161.0	3.44E-05	14,503	1,042	1,708	6,475	349	207			
CN003(A) - 1	161.0	3.77E-05	16,045	969	1,892	8,956	129	114	1.08	-3.76	
CN005(A) - 1	161.2	5.37E-05	10,877	788	1,876	8,650	61	46	1.29	-4.13	
CN006(A) - 1	160.8	4.11E-05	12,052	779	2,114	9,835	167	138			
CN006(B) - 1	160.8	4.13E-05	15,150	887	2,036	9,316	442	242			
CN008(A) - 1	161.2	5.87E-05	11,782	362	1,673	8,088	403	357			1
CN010(A) - 1	161.2	4.57E-05	12,549	1,060	1,480	5,016	646	431	1.72	-2.52	1
CN013(A) - 1	158.3	4.13E-05	10,658	624	1,823	9,164			-0.02	-6.37	
CN014(A) - 1	158.3	4.62E-05	10,339	648	1,780	8,412		36			
CN014(B) - 1	158.3	4.90E-05	9,544	633	1,406	5,221	259	185			
CN016(A) - 1	158.1	4.93E-05	9,986	644	1,688	7,077	130	76	1.33	-3.99	
CN016(B) - 1	158.1	4.08E-05	8,934	676	1,688	8,689	63	69			
CN017(A) - 1	158.1	4.71E-05	11,013	227	1,541	8,235	167	97			
CN018(A) - 1	158.2	4.82E-05	15,511	960	1,751	8,543	194	168			
CN019(A) - 1	158.1	4.87E-05	10,966	663	1,814	8,603	93	75			
<b>Penny Nab</b>											
PN001(A) - 1	176.1	4.31E-05	13,213	521	1,973	9,112	70				
PN002(A) - 1	176.1	4.29E-05	8,990	623	1,593	8,947	72	49			
PN002(B) - 1	176.1	5.37E-05	11,930	771	1,764	7,704	56	60	2.61	-1.80	
PN003(A) - 1	176.1	5.19E-05	11,972	798	1,750	7,972	63	62			





## 8.4.2. Yorkshire core

Table 35 - Main elemental and isotopic results for analysis of stratigraphic samples from the Dove's Nest core, including oxygen and carbon isotope values, Ca values (mol), and Mg/Ca, P/Ca, Sr/Ca, Na/Ca, Fe/Ca, and Mn/Ca values in  $\mu\text{mol mol}^{-1}$ . In the notes column 1 = sample which was defined as altered (Fe > 600 and/or Mn > 300), 2 = sample not included in the discussion in Chapter 5 due to extremely elevated Na, Sr, Fe or Mn values (Sr/Ca > 3,000; Fe/Ca > 5,000; Mn/Ca > 1000), 7 = selected for paired sediment analysis.

Sample number	Depth (m)	Ca (mol)	Mg/Ca ( $\mu\text{mol mol}^{-1}$ )	P/Ca ( $\mu\text{mol mol}^{-1}$ )	Sr/Ca ( $\mu\text{mol mol}^{-1}$ )	Na/Ca ( $\mu\text{mol mol}^{-1}$ )	Fe/Ca ( $\mu\text{mol mol}^{-1}$ )	Mn/Ca ( $\mu\text{mol mol}^{-1}$ )	$\delta^{13}\text{C}$ VPDB (‰)	$\delta^{18}\text{O}$ VPDB (‰)	Notes
NS1-85-129.97 B(1A)	130.0	5.57E-05	9,714	731	1,895	8,977	73	13	-2.02	28.78	7
NS1-85-130.35 B(1A)	130.4	5.34E-05	13,806	663	1,899	7,818	129	28	-2.45	28.33	7
NS1-85-130.71 B(1A)	130.7	5.58E-05	16,528	908	1,828		193	23	-5.35	25.34	7
NS1-86-133.69 B(1A)	133.7	4.95E-05	13,529	1,077	841		684	28	-13.15	17.31	1
NS1-87-133.65 B(1A)	133.7	5.73E-05	12,958	853	1,525	3,808	321	30	-4.74	25.97	7
NS1-87-135.88 B(1A)	135.9	3.93E-05	16,640	1,743	1,805	7,547	406	54	-1.44	29.38	7
NS1-88-137.75 B(1A)	137.8	5.99E-05	11,941	981	930		671	32	-4.18	26.55	1
NS1-88-137.84 B(1A)	137.8	5.24E-05	14,087	956	1,910	6,090	264	33	-7.76	22.86	7
NS1-88-138.01 B(1A)	138.0	4.82E-05	7,763	1,090	771		467	39			7
NS1-88-138.01 B(1A)	138.0	5.27E-05	14,184	892	1,778	7,495			-7.76	22.86	7
NS1-88-138.55-64 B(1A)	138.6	4.46E-05	11,318	697	1,880	6,366					7
NS1-88-138.55-64 B(2A)	138.6	5.87E-05	14,413	1,162	1,837	8,151	46	11	3.90	-2.01	7
NS1-88-138.55-64 B(3A)	138.6	4.86E-05	15,328	1,220	2,316	9,719	713	124	2.55	-1.71	7
NS1-88-138.55-64 B(4A)	138.6	5.83E-05	7,693	1,303	651		493	37	2.24	-2.62	
NS1-88-139.05 B(1A)	139.1	6.20E-05	17,696	854	2,498		72	14	-0.18	-10.81	7
NS1-89-141.34 B(1A)	141.3	5.55E-05	15,123	650	1,974	5,372	163	19	3.44	-4.00	7
NS1-90-142.87 B(1A)	142.9	4.86E-05	9,199	818	1,853	7,219	70	13	4.56	-1.83	7
NS1-90-143.22 B(1A)	143.2	5.39E-05	17,995	2,214	1,819	8,251	856	119	2.76	-2.63	1
NS1-90-144.31 B(1A)	144.3	5.67E-05	12,374	658	1,854		87	17	4.36	-4.48	7
NS1-90-144.31 B(1B)	144.3	4.92E-05	11,852	694	1,960	5,067	115	26	4.55	-3.85	7
NS1-91-146.13 B(1A)	146.1	5.18E-05	18,387	1,197	1,759	7,598	131	24	3.41	-2.61	7

Sample number	Depth (m)	Ca (mol)	Mg/Ca ( $\mu\text{mol mol}^{-1}$ )	P/Ca ( $\mu\text{mol mol}^{-1}$ )	Sr/Ca ( $\mu\text{mol mol}^{-1}$ )	Na/Ca ( $\mu\text{mol mol}^{-1}$ )	Fe/Ca ( $\mu\text{mol mol}^{-1}$ )	Mn/Ca ( $\mu\text{mol mol}^{-1}$ )	$\delta^{13}\text{C}$ VPDB (‰)	$\delta^{18}\text{O}$ VPDB (‰)	Notes
NS1-92-151.1 B(1A)	151.1	5.42E-05	11,494	691	1,730	7,149	49	10	4.33	-1.05	7
NS1-93-154.75 B(1A)	154.8	5.13E-05	18,041	1,084	1,889		318	59	2.75	-5.66	7
NS1-94-155.52 B(1A)	155.5	5.47E-05	12,973	1,017	1,831	7,099	776	116	1.62	-2.07	1
NS1-94-156.27 B(1A)	156.3	4.83E-05	15,400	1,156	2,046		118	18	3.83	-4.31	7
NS1-94-156.61 B(1A)	156.6	4.57E-05	18,866	1,549	1,997		347	41	3.08	-5.25	7
NS1-94-156.78 B(1A)	156.8	4.70E-05	16,954	1,434	1,811		227	28	2.95	-5.92	7
NS1-94-156.83 B(1A)	156.8	5.33E-05	14,872	896	1,653		223	35	4.27	-4.35	
NS1-94-157.45 B(1A)	157.5	5.69E-05	14,961	1,275	1,682		345	37	1.42	-5.22	7
NS1-94-157.45 B(1B)	157.5	5.67E-05	13,804	1,351	1,705		228	27	1.37	-3.67	7
NS1-100-175.16 B(1A)	175.2	4.67E-05	9,660	367	1,526	5,587	45	34			7
NS1-100-175.16 B(2A)	175.2	4.36E-05	9,250	479	1,544	5,813	79	13			7
NS1-102-179.52 B(1A)	179.5	5.73E-05	8,583	562	1,412	5,843	212	67			7
NS1-103-183.44 B(1A)	183.4	4.69E-05	9,179	611	1,263	5,001	2,928	714			1
NS1-103-183.58 B(1A)	183.6	4.38E-05	10,073	553	1,823	6,587	349	88			7
NS1-103-184.32 B(1A)	184.3	4.17E-05	13,402	1,826	1,519	6,023	2,410	550			1
NS1-104-187.73 B(1A)	187.7	4.94E-05	11,326	678	1,886	8,644	335	88			7
NS1-105-188.26 B(1A)	188.3	4.48E-05	12,665	661	1,537	5,200	68	35			7
NS1-105-190 B(1A)	190.0	5.54E-05	14,859	807	1,220		833	192			1
NS1-105-190.36 B(1A)	190.4	5.27E-05	13,171	1,053	2,034	8,175	229	107			7
NS1-105-190.36 B(1B)	190.4	5.56E-05	13,460	903	2,376	10,407	434	78			7
NS1-109-199.91 B(1A)	199.9	4.73E-05	8,881	782	1,733	8,214	161	84			7
NS1-110-200.63 B(1A)	200.6	3.97E-05	10,531	993	1,765	7,234	377	140			
NS1-111-203.28 B(1A)	203.3	7.61E-08	508,134		9,853		869,993				1, 2
NS1-113-210.13 B(1A)	210.1	4.72E-05	11,192	1,060	1,991	6,843	81	40			7
NS1-120-231.84 B(1A)	231.8	4.29E-05	11,619	899	1,911	8,851	421	171			7
NS1-123-239.22 B(1A)	239.2	4.45E-05	10,351	590	1,780	7,629	129	96			7

Sample number	Depth (m)	Ca (mol)	Mg/Ca ( $\mu\text{mol mol}^{-1}$ )	P/Ca ( $\mu\text{mol mol}^{-1}$ )	Sr/Ca ( $\mu\text{mol mol}^{-1}$ )	Na/Ca ( $\mu\text{mol mol}^{-1}$ )	Fe/Ca ( $\mu\text{mol mol}^{-1}$ )	Mn/Ca ( $\mu\text{mol mol}^{-1}$ )	$\delta^{13}\text{C}$ VPDB (‰)	$\delta^{18}\text{O}$ VPDB (‰)	Notes
SM14-4-256.44 B(1A)	253.4	4.20E-05	21,192	395	2,790	7,700	10,020	2,562			1, 2
SM14-4-256.44 B(1B)	253.4	4.62E-05	24,672	612	2,938	8,463	20,856	2,658			1, 2
SM14-4-256.66 B(1A)	253.7	4.97E-05	12,359	366	1,624		1,124	433			1
SM14-4-256.66 B(1B)	253.7	4.62E-05	14,933	567	1,675	6,511	339	166			
SM14-7-263.99 B(1A)	261.0	4.71E-05	14,330	530	1,289		613	252			1
SM14-7-263.99 B(1B)	261.0	5.29E-05	13,043	394	1,428		297	149			
SM14-9-267.09 B(1A)	264.1	4.73E-05	9,423	681	1,781	7,532	168	66			
SM14-10-268.28 B(1A)	265.3	5.38E-05	8,943	663	1,689	7,035	182	93			
SM14-10-269.22 B(1A)	266.2	4.22E-05	11,546	569	1,656		216	101			
SM14-10-270.03 B(1A)	267.0	5.48E-05	15,041	1,261	2,223	9,810	55	28			
SM14-10-270.03 B(1B)	267.0	5.25E-05	13,803	1,065	2,125	9,164		22			
SM14-14-276.83 B(1A)	273.8	5.17E-05	10,597	475	1,604	5,794	271	107			
SM14-14-277.03 B(1A)	274.0	4.51E-05	9,734	706	1,585	7,034	629	189			1
SM14-14-277.03 B(2A)	274.0	4.30E-05	9,644	681	1,696	6,281	124	52			
SM14-14-277.64 B(1A)	274.6	5.33E-05	11,337	1,033	2,195	10,822	248	85			
SM14-14-277.64 B(1B)	274.6	5.08E-05	10,975	982	2,166	10,734	102	41			
SM14-14-277.74 B(1A)	274.7	5.70E-05	9,636	604	1,840	7,789	130	59			
SM14-14-277.74 B(1B)	274.7	5.53E-05	10,349	672	1,821	7,303	295	72			
SM14-14-278.28 B(1A)	275.3	4.75E-05	10,513	594	1,478	5,111	366	137			
SM14-15-280.05 B(1A)	277.1	5.98E-05	104,324	6,523	17,937	69,344	937	424			1, 2
SM14-15-280.05 B(2A)	277.1	5.49E-05	137,053	11,502	20,701	89,487	4,409	1,731			1, 2
SM14-15-280.14 B(1A)	277.1	5.63E-05	97,287	6,204	15,304	66,635	678	404			1, 2
SM14-15-280.23 B(1A)	277.2	5.80E-05	114,257	6,768	16,175	48,065	2,220	939			1, 2
SM14-15-280.23 B(2A)	277.2	5.18E-05	118,164	9,282	13,727	41,250	3,557	1,417			1, 2
SM14-16-280.87 B(1A)	277.9	5.17E-05	108,213	5,144	15,305	22,236	3,264	1,412			1, 2
SM14-16-280.97 B(1A)	278.0	5.65E-05	100,246	6,538	15,649	56,539	761	493			1, 2

Sample number	Depth (m)	Ca (mol)	Mg/Ca ( $\mu\text{mol mol}^{-1}$ )	P/Ca ( $\mu\text{mol mol}^{-1}$ )	Sr/Ca ( $\mu\text{mol mol}^{-1}$ )	Na/Ca ( $\mu\text{mol mol}^{-1}$ )	Fe/Ca ( $\mu\text{mol mol}^{-1}$ )	Mn/Ca ( $\mu\text{mol mol}^{-1}$ )	$\delta^{13}\text{C}$ VPDB (‰)	$\delta^{18}\text{O}$ VPDB (‰)	Notes
SM14-16-280.97 B(2 A)	278.0	4.96E-05	113,389	6,430	15,362	48,429	2,116	1,181			1, 2
SM14-16-281.76 B(1A)	278.8	5.50E-05	106,899	8,351	15,896	70,118	3,250	1,749			1, 2
SM14-17-283.37 B(1A)	280.4	5.43E-05	121,307	9,187	19,708	87,570	1,202	940			1, 2
SM14-17-283.37 B(2A)	280.4	5.91E-05	86,820	8,144	16,715	66,973	2,731	841			1, 2
SM14-17-283.99B(1A)	281.0	5.51E-05	105,861	4,333	15,584	21,568	2,432	1,270			1, 2
SM14-17-284.33 B(1A)	281.3	5.91E-05	148,947	7,749	17,288	75,638	4,273	1,635			1, 2
SM14-18-285.57 B(1A)	282.6	5.07E-05	105,582	10,528	17,422	68,585	2,371	1,607			1, 2
SM14-19-286.91 B(1A)	283.9	5.71E-05	121,136	8,161	18,952	74,636	514	546			1, 2
SM14-19-286.95 B(1A)	284.0	5.66E-05	109,903	6,558	16,705	64,661	813	556			1, 2
SM14-19-286.95 B(2A)	284.0	5.65E-05	89,534	9,086	15,466	75,952	1,657	904			1, 2
SM14-19-286.95 B(3A)	284.0	5.31E-05	136,290	9,373	21,537	96,444	1,954	1,146			1, 2
SM14-19-288.14 B(1A)	285.1	5.51E-05	104,753	8,438	18,302	76,128	754	295			1, 2
SM14-21-292.16 B(1A)	289.2	5.31E-05	106,918	4,901	15,737	26,797	2,549	1,016			1, 2
SM14-21-292.2 B(1A)	289.2	5.29E-05	99,705	3,834	14,427	23,617	1,428	992			1, 2
SM14-21-292.2 B(2A)	289.2	5.35E-05	108,645	6,544	15,860	53,948	1,248	1,065			1, 2
SM14-21-292.64 B(1A)	289.6	5.74E-05	108,705	6,586	16,697	56,420	2,352	1,346			1, 2
SM14-21-292.64 B(2A)	289.6	5.04E-05	113,220	8,280	15,514	48,116	11,533	2,841			1, 2
SM14-21-292.64 B(3A)	289.6	5.45E-05	125,708	5,538	17,165	60,885	1,136	690			1, 2
SM14-22-293.12 B(1A)	290.1	5.41E-05	105,990	7,258	17,540	58,324	957	521			1, 2
SM14-22-293.57 B(1A)	290.6	5.18E-05	92,450	8,666	16,325	60,491	879	493			1, 2
SM14-22-293.57 B(1B)	290.6	5.12E-05	101,169	9,128	17,443	57,063	1,650	718			1, 2
SM14-22-294.21 B(1A)	291.2	6.17E-05	145,821	9,654	19,351	65,595	1,390	377			1, 2
SM14-23-296 B(1A)	293.0	6.28E-05	99,898	9,145	18,426	68,336	606	422			1, 2
SM14-23-296 B(2A)	293.0	6.15E-05	105,972	8,308	19,359	61,870	1,921	991			1, 2
SM14-23-296 B(3A)	293.0	5.73E-05	120,828	6,451	18,318	59,061	3,245	1,258			1, 2
SM14-24-297.21 B(1A)	294.2	5.96E-05	118,078	9,751	19,428	63,832	7,731	2,466			1, 2

Sample number	Depth (m)	Ca (mol)	Mg/Ca ( $\mu\text{mol mol}^{-1}$ )	P/Ca ( $\mu\text{mol mol}^{-1}$ )	Sr/Ca ( $\mu\text{mol mol}^{-1}$ )	Na/Ca ( $\mu\text{mol mol}^{-1}$ )	Fe/Ca ( $\mu\text{mol mol}^{-1}$ )	Mn/Ca ( $\mu\text{mol mol}^{-1}$ )	$\delta^{13}\text{C}$ VPDB (‰)	$\delta^{18}\text{O}$ VPDB (‰)	Notes
SM14-24-298.1 B(1A)	295.1	4.75E-05	132,998	7,669	21,349	83,679	7,452	2,263			1, 2
SM14-25-298.97 B(1A)	296.0	5.18E-05	95,965	4,651	13,223	40,253	1,179	625			1, 2
SM14-26-302.54 B(1A)	299.5	5.78E-05	110,962	5,813	18,491	62,794	1,668	743			1, 2
SM14-29-308.70 B(1A)	305.7	5.33E-05	96,590	7,418	15,573	65,317	2,979	1,431			1, 2
SM14-30-309.44 B(1A)	306.4	5.26E-05	91,147	4,408	12,596	33,117	1,703	804			1, 2
SM14-31-311.71 B(1A)	308.7	5.16E-05	66,389	6,644	12,157	55,642	741	329			1, 2
SM14-32-315.32 B(1A)	312.3	5.42E-05	80,585	6,563	13,739	56,759	3,243	1,349			1, 2
SM14-35-319.75 B(1A)	316.8	5.02E-05	87,960	5,352	16,006	68,035	556	433			1, 2
SM14-37-323.94 B(1A)	320.9	5.52E-05	87,728	5,146	16,322	66,341	1,785	626			1, 2
SM14-37-324.19 B(1A)	321.2	4.86E-05	96,268	4,057	15,934	17,790	2,623	1,286			1, 2
SM14-37-325.2 B(1A)	322.2	5.51E-05	72,555	4,154	13,229	56,731	1,708	913			1, 2
SM14-38-326.26 B(1A)	323.3	5.71E-05	104,783	7,527	16,542	67,180	1,606	725			1, 2
SM14-38-326.71 B(1A)	323.7	5.05E-05	88,706	6,190	16,168	66,078	1,368	755			1, 2
SM14-38-326.71 B(1B)	323.7	5.22E-05	87,139	6,298	16,337	62,354	992	493			1, 2
SM14-39-329.2 B(1A)	326.2	5.88E-05	91,515	7,872	17,144	43,518	944	581			1, 2
SM14-39-329.2 B(1B)	326.2	5.65E-05	106,374	7,819	16,039	67,186	23,596	13,108			1, 2
SM14-40-330.17 B(1A)	327.2	8.43E-08	1,738,308		18,852	1,849,369	122,000,000	540,104			1, 2
SM14-40-330.61 B(1A)	327.6	5.96E-05	90,498	9,585	17,828	56,939	1,758	658			1, 2
SM14-40-331.00 B(1A)	328.0	5.85E-05	70,474	5,379	13,737	54,865	10,834	1,849			1, 2
SM14-40-331.00B(2A)	328.0	5.46E-05	73,387	5,280	15,881	58,185	3,360	636			1, 2
SM14-40-331.00- (3A)	328.0	5.67E-05	64,418	6,164	14,685	54,595	7,101	1,964			1, 2
SM14-40-331.22 B(1A)	328.2	6.00E-05	106,992	8,163	19,273	78,167	9,124	1,412			1, 2
SM14-41-333.08 B(1A)	330.1	4.46E-08	5,005,597		25,966	4,798,313	91,784,938	105,249			1, 2
SM14-42-335.29 B(1A)	332.3	5.40E-05	87,844	8,035	17,368	59,622	5,156	566			1, 2
SM14-42-335.29 B(1B)	332.3	5.31E-05	121,573	8,317	18,516	64,651	7,368	3,594			1, 2

Sample number	Depth (m)	Ca (mol)	Mg/Ca ( $\mu\text{mol mol}^{-1}$ )	P/Ca ( $\mu\text{mol mol}^{-1}$ )	Sr/Ca ( $\mu\text{mol mol}^{-1}$ )	Na/Ca ( $\mu\text{mol mol}^{-1}$ )	Fe/Ca ( $\mu\text{mol mol}^{-1}$ )	Mn/Ca ( $\mu\text{mol mol}^{-1}$ )	$\delta^{13}\text{C}$ VPDB (‰)	$\delta^{18}\text{O}$ VPDB (‰)	Notes
SM14-43-336.31 B(1A)	333.3	4.81E-05	87,268	6,083	17,694	59,691	11,043	1,965			1, 2
SM14-43-336.33 B(2A)	333.3	1.50E-06	2,223,694		6,381	103,193	2,706,521	205,186			1, 2
SM14-43-336.32 B(3A)	333.3	6.18E-06	1,199,255		6,499	77,604	1,487,627	161,723			1, 2
SM14-44-339.16 B(1A)	336.2	4.97E-05	95,887	5,968	16,702	25,659	8,935	1,128			1, 2
SM14-44-339.16 B(1B)	336.2	5.17E-05	89,354	6,308	16,227	34,298	5,603	2,226			1, 2

## 8.4.3. North Wales core

Table 36 - Main elemental and isotopic results for analysis of stratigraphic samples from the Llanbedr core in North Wales, including oxygen and carbon isotope values, Ca values (mol), and Mg/Ca, P/Ca, Sr/Ca, Na/Ca, Fe/Ca, and Mn/Ca values in  $\mu\text{mol mol}^{-1}$ . In the notes column 1 = sample which was defined as altered (Fe > 600 and/or Mn > 300), 2 = sample not included in the discussion in Chapter 5 due to extremely elevated Na, Sr, Fe or Mn values (Sr/Ca > 3,000; Fe/Ca > 5,000; Mn/Ca > 1000), 6 = sample analysed using XRD.

Sample number	BGS Identifier	Depth (m)	Ca (mol)	Mg/Ca ( $\mu\text{mol mol}^{-1}$ )	P/Ca ( $\mu\text{mol mol}^{-1}$ )	Sr/Ca ( $\mu\text{mol mol}^{-1}$ )	Na/Ca ( $\mu\text{mol mol}^{-1}$ )	Fe/Ca ( $\mu\text{mol mol}^{-1}$ )	Mn/Ca ( $\mu\text{mol mol}^{-1}$ )	$\delta^{13}\text{C}$ VPDB (‰)	$\delta^{18}\text{O}$ VPDB (‰)	Notes
MO001(A) - 1	BLC9192	615.6	1.55E-05	10,943	1,131	1,572	6,553	273	81			
MO002(A) - 1	BLC9195	616.0	2.51E-05	10,625	1,428	1,498	4,964	1,063	500			1
MO003(A) - 1	BLC9201	616.5	5.30E-05	10,241	1,022	1,509	6,029	2,098	199	2.01	-1.87	1
MO003(B) - 1	BLC9201	616.5	5.16E-05	9,340	971	1,552	5,869	582	69	1.94	-1.61	1
MO004(A) - 1	BLC9271	624.0	5.11E-05	11,208	1,219	1,964	7,644	814	86	2.68	-2.06	1
MO005(A) - 1	BLC9272	624.0	4.77E-05	9,438	778	1,808	7,852	100	17	2.61	-1.77	
MO005(B) - 1	BLC9272	624.0	5.15E-05	9,496	804	1,746	6,847	1,059	27	1.87	-1.78	1
MO006(A) - 1	BLC9311	625.5	5.00E-05	8,784	828	1,545	6,915	345	32	1.13	-1.40	
MO006(A) - 2	BLC9311	625.5	5.07E-05	8,554	846	1,541	6,343	334	32			
MO007(A) - 1	BLC9314	625.8	4.83E-05	9,434	711	1,536	6,787	375	41	1.10	-2.15	
MO008(A) - 1	BLC9315	625.8	5.27E-05	12,473	900	2,014	7,290	115	19	1.94	-1.48	
MO008(A) - 2	BLC9315	625.8	5.55E-05	12,544	881	2,008	8,381	101	19	1.64	-1.41	
MO008(B) - 1	BLC9315	625.8	4.89E-05	9,712	619	1,660	5,562	93	13			
MO009(A) - 1	BLC9335	626.9	4.79E-05	10,071	851	1,453	5,400	603	18	2.36	-2.31	1
MO010(A) - 1	BLC9375	631.5	4.02E-05	9,168	2,409	977	1,294	4,330	313	0.44	-5.28	1
MO011(A) - 1	BLC9406	636.8	5.50E-05	10,300	737	1,808	5,812	115	11			
MO012(A) - 1	BLC9459	641.4	3.41E-05	14,050	2,146	1,360	5,590	725	78	-0.75	-5.00	1
MO013(A) - 1	BLC9468	641.9	5.61E-05	15,852	1,475	1,281	6,391	2,983	117	-0.21	-1.61	1
MO014(A) - 1	BLC9497	643.5	4.94E-05	14,302	1,107	1,479	6,469	141	11	0.85	-0.92	
MO014(A) - 1	BLC9497	643.5	4.48E-05	14,147	1,113	1,477	6,688	162				
MO015(A) - 1	BLC9505	645.1	4.19E-05	11,308	1,162	1,837	6,837	741	63	1.22	-1.54	1

Sample number	BGS Identifier	Depth (m)	Ca (mol)	Mg/Ca ( $\mu\text{mol mol}^{-1}$ )	P/Ca ( $\mu\text{mol mol}^{-1}$ )	Sr/Ca ( $\mu\text{mol mol}^{-1}$ )	Na/Ca ( $\mu\text{mol mol}^{-1}$ )	Fe/Ca ( $\mu\text{mol mol}^{-1}$ )	Mn/Ca ( $\mu\text{mol mol}^{-1}$ )	$\delta^{13}\text{C}$ VPDB (‰)	$\delta^{18}\text{O}$ VPDB (‰)	Notes
MO016(A) - 1	BLC9515	646.1	4.65E-05	16,214	1,588	1,391	6,296	333	35	0.15	-2.00	6
MO017(A) - 1	BLC9581	652.9	4.33E-05	11,736	887	1,532	5,112	711	84	0.74	-1.06	1
MO018(A) - 1	BLC9614	655.9	3.11E-05	18,245	1,934	1,581	5,997	6,049	477	0.01	-3.04	1, 2
MO019(A) - 1	BLC9647	660.5	5.06E-05	13,376	995	1,522	6,012	438	36	0.75	-1.48	
MO019(A) - 2	BLC9647	660.5	5.60E-05	13,136	905	1,509	6,035	412	36	0.75	-1.48	
MO020(A) - 1	BLC9649	661.8	3.43E-05	19,732	2,465	1,590	6,529	2,593	181	-0.93	-1.66	1
MO021(A) - 1	BLC9669	666.8	4.79E-05	16,143	1,166	1,529	6,341	275	41	-0.63	-1.50	
MO022(A) - 1	BLC9670	667.1	5.22E-05	13,702	987	1,442	6,474	175	22	0.31	-1.05	
MO023(A) - 1	BLC9672	667.6	4.60E-05	12,966	956	1,602	5,991	392	47			
MO024(A) - 1	BLC9674	667.9	3.56E-05	16,127	1,418	1,475	7,504	1,011	94	-0.12	-1.20	1
MO025(A) - 1	BLC9789	680.1	4.75E-05	12,362	928	1,433	5,257	1,568	97			1
MO026(A) - 1	BLC9822	682.6	4.06E-05	11,483	920	1,454	5,392	293	49	0.45	-2.11	
MO027(A) - 1	BLC9827	683.0	4.18E-05	9,743	2,270	2,036	1,496	3,758	493	0.89	-5.55	1
MO028(A) - 1	BLC9839	684.5	4.61E-05	14,123	1,191	1,451	5,444	323	31	1.12	-1.46	
MO029(A) - 1	BLC9871	686.6	4.74E-05	11,696	984	1,481	6,517	155	24	0.73	-1.73	
MO033(A) - 1	BLD0042	716.5	4.59E-05	11,231	2,077	1,261	3,959	6,274	195	1.42	-3.33	1, 2
MO034(A) - 1	BLD0079	725.8	5.76E-05	10,968	755	1,424	5,577	211	17	0.93	-1.33	
MO036(A) - 1	BLD0274	749.5	5.70E-05	15,520	1,010	1,422	6,683	539	38			1
MO036(A) - 2	BLD0274	749.5	4.53E-05	15,530	1,028	1,420	6,471	535	36			1
MO037(A) - 1	BLD0279	749.6	5.85E-05	14,022	1,250	1,409	6,404	961	22	1.12	-1.05	1
MO038(A) - 1	BLD0372	759.4	4.48E-05	17,956	2,935	1,721	5,161	2,776	184			1
MO039(A) - 1	BLD0529	771.5	5.77E-05	10,055	1,775	1,537	1,766	720	45	2.67	-6.09	1
MO040(A) - 1	BLD0572	777.3	5.05E-05	13,327	1,388	1,758	6,772	173	12	2.24	-2.01	
MO041(A) - 1	BLD0656	783.6	5.00E-05	15,046	1,214	1,986	7,104	99	13	2.94	-2.26	
MO041(A) - 1	BLD0656	783.6	5.47E-05	15,018	1,219	1,970	7,012	101	12			6
MO042(A) - 1	BLD0711	790.3	5.28E-05	15,567	1,369	1,761	7,411	2,573	48	3.47	-1.48	1

Sample number	BGS Identifier	Depth (m)	Ca (mol)	Mg/Ca ( $\mu\text{mol mol}^{-1}$ )	P/Ca ( $\mu\text{mol mol}^{-1}$ )	Sr/Ca ( $\mu\text{mol mol}^{-1}$ )	Na/Ca ( $\mu\text{mol mol}^{-1}$ )	Fe/Ca ( $\mu\text{mol mol}^{-1}$ )	Mn/Ca ( $\mu\text{mol mol}^{-1}$ )	$\delta^{13}\text{C}$ VPDB (‰)	$\delta^{18}\text{O}$ VPDB (‰)	Notes
MO043(A) - 1	BLD0731	792.6	5.41E-05	15,266	924	1,711	6,094	362	33			
MO043(A) - 2	BLD0731	792.6	2.76E-05	23,660	1,485	915	1,611	26,226	1,077			1, 2
MO044(A) - 1	BLD0781	802.1	3.19E-05	24,015	1,424	943	1,683	25,965	1,061	2.24	-5.84	1, 2, 6
MO044(A) - 2	BLD0781	802.1	4.83E-05	8,242	661	1,565	5,592	67		2.24	-5.84	
MO045(A) - 1	BLD1492	844.1	4.60E-05	8,555	655	1,543	5,952	371	42	2.10	-0.48	
MO047(A) - 1	BLD1508	856.0	3.05E-05	8,334	654	1,497	5,655	407	45			
MO048(A) - 1	BLD1530	865.3	1.31E-05	13,436	2,288	1,390	7,039	1,037	108			1
MO049(A) - 1	BLD1537	868.6	4.81E-05	9,016	567	1,484	5,015	662	42	1.07	0.05	1
MO050(A) - 1	BLD1570	879.5	5.56E-05	6,109	275	1,013	2,775	3,083	475	0.24	-2.91	1
MO050(A) - 2	BLD1570	879.5	6.08E-05	6,156	276	1,049	2,719	2,844	445	0.24	-2.91	1
MO050(B) - 1	BLD1570	879.5	5.66E-05	6,191	301	1,129	3,114	2,566	395	0.34	-2.78	1
MO050(B) - 2	BLD1570	879.5	5.49E-05	6,121	301	1,108	3,016	2,601	401	0.34	-2.78	1
MO051(A) - 1	BLD1601	886.1	5.21E-05	8,432	746	1,567	6,298	219	21	2.48	-2.92	
MO052(A) - 1	BLD1618	888.9	4.91E-05	8,414	382	1,476	6,092	354	50	2.19	-1.05	6
MO053(A) - 1	BLD1626	890.0	4.79E-05	6,830	583	1,407	6,138					
MO055(A) - 1	BLD1652	896.8	5.70E-05	8,215	911	1,462	7,772	80	19	1.42	0.00	
MO056(A) - 1	BLD1674	899.9	2.45E-05	6,436	1,382	1,034	4,964	999	99			1
MO057(A) - 1	BLD1717	904.9	4.72E-05	10,108	796	1,478	6,653	178	104	0.85	0.16	
MO058(A) - 1	BLD1722	905.8	5.22E-05	10,221	764	1,797	9,136	77		1.70	0.19	
MO058(B) - 1	BLD1722	905.8	4.72E-05	11,545	1,192	1,636	7,948		11	1.57	-0.95	
MO059(A) - 1	BLD1723	905.8	5.00E-05	12,176	774	1,910	10,477			1.31	0.35	6
MO059(A) - 2	BLD1723	905.8	4.81E-05	12,028	771	1,906	10,727					
MO060(A) - 1	BLD1739	912.2	4.73E-05	10,201	714	1,547	5,828	110	26	2.15	-0.28	
MO061(A) - 1	BLD1740	912.6	4.47E-05	9,277	732	1,473	6,608	193	32	1.63	-0.07	
MO061(B) - 1	BLD1740	912.6	4.75E-05	8,354	580	1,269	6,257	136	21			
MO062(A) - 1	BLD1763	919.3	4.97E-05	10,635	907	1,786	8,128		12	1.36	-0.98	

Sample number	BGS Identifier	Depth (m)	Ca (mol)	Mg/Ca ( $\mu\text{mol mol}^{-1}$ )	P/Ca ( $\mu\text{mol mol}^{-1}$ )	Sr/Ca ( $\mu\text{mol mol}^{-1}$ )	Na/Ca ( $\mu\text{mol mol}^{-1}$ )	Fe/Ca ( $\mu\text{mol mol}^{-1}$ )	Mn/Ca ( $\mu\text{mol mol}^{-1}$ )	$\delta^{13}\text{C}$ VPDB (‰)	$\delta^{18}\text{O}$ VPDB (‰)	Notes
MO064(A) - 1	BLD1797	944.6	1.53E-05	13,746	608	1,417	4,473	657	67			1
MO066(A) - 1	BLD2137	965.9	4.79E-05	12,494	916	2,080	9,128	139	56	1.41	-1.47	6
MO066(B) - 1	BLD2137	965.9	5.10E-05	10,903	984	6,387	7,575	177	40	0.80	-1.36	2
MO066(B) - 2	BLD2137	965.9	4.19E-05	11,039	1,019	7,115	7,537	162	41	0.80	-1.36	2
MO067(A) - 1	BLD2140	969.1	1.76E-05	14,157	1,761	1,563	6,863	845	51			1
MO068(A) - 1	BLD2143	969.6	-									
MO069(A) - 1	BLD2152	972.1	4.86E-05	10,813	903	1,712	8,352	38		0.79	-0.76	
MO069(B) - 1	BLD2152	972.1	4.33E-05	11,647	753	1,441	7,774	174	17	1.32	-1.00	
MO070(A) - 1	BLD2168	975.9	4.08E-05	11,775	979	1,706	7,258	48	11	0.37	-1.10	6
MO070(A) - 2	BLD2168	975.9	4.92E-05	11,805	1,015	1,697	7,050	53	9			
MO071(A) - 1	BLD2191	982.8	4.29E-05	11,038	782	1,538	7,046	261	21	0.89	-1.74	6
MO072(A) - 1	BLD2264	1003.6	4.55E-05	14,745	618	1,681	8,772	445	27	0.98	-1.22	
MO073(A) - 1	BLD2268	1004.1	4.09E-05	15,173	733	1,868	6,580	388	27			
MO074(A) - 1	BLD2337	1013.2	4.87E-05	11,214	1,085	1,544	7,252	400	20	1.39	-1.42	
MO075(A) - 1	BLD2383	1014.5	4.59E-05	16,846	2,265	1,889	9,152	767	42	0.11	-2.45	1
MO075(B) - 1	BLD2383	1014.5	4.34E-05	13,847	823	1,719	7,761	136	22	1.26	-1.91	
MO076(A) - 1	BLD2479	1021.1	4.41E-05	13,388	952	1,699	7,846	178	20	0.24	-1.66	
MO076(A) - 2	BLD2479	1021.1	5.03E-05	13,278	900	1,685	7,954	171	21	0.24	-1.66	
MO076(B) - 1	BLD2479	1021.1	4.49E-05	12,990	1,137	1,757	8,652	142	20	0.43	-1.48	
MO077(A) - 1	BLD2628	1037.7	4.03E-05	12,409	1,020	2,052	9,753	95	37	2.46	-2.27	
MO078(A) - 1	BLD2654	1042.0	3.66E-05	11,035	845	1,593	7,718	107		0.96	-1.66	
MO079(A) - 1	BLD2662	1045.3	4.97E-05	8,678	860	1,599	8,019	101	10	2.15	-1.01	
MO080(A) - 1	BLD2663	1045.3	4.28E-05	8,951	859	1,620	8,209	77		2.26	-0.77	
MO081(A) - 1	BLD2664	1045.3	5.22E-05	10,468	498	1,562	7,193	106	17			
MO082(A) - 1	BLD2675	1048.3	4.08E-05	11,015	701	1,755	8,349	193	22			
MO083(A) - 1	BLD2696	1056.7	4.19E-05	12,330	725	1,806	7,617	329	28	1.21	-1.69	

Sample number	BGS Identifier	Depth (m)	Ca (mol)	Mg/Ca ( $\mu\text{mol mol}^{-1}$ )	P/Ca ( $\mu\text{mol mol}^{-1}$ )	Sr/Ca ( $\mu\text{mol mol}^{-1}$ )	Na/Ca ( $\mu\text{mol mol}^{-1}$ )	Fe/Ca ( $\mu\text{mol mol}^{-1}$ )	Mn/Ca ( $\mu\text{mol mol}^{-1}$ )	$\delta^{13}\text{C}$ VPDB (‰)	$\delta^{18}\text{O}$ VPDB (‰)	Notes
MO083(A) - 2	BLD2696	1056.7	3.98E-05	12,253	691	1,797	6,916	273	25	1.21	-1.69	
MO084(A) - 1	BLD2763	1075.2	5.66E-05	11,412	986	1,870	8,372	805	41	3.10	-2.04	1
MO085(A) - 1	BLD2807	1078.4	4.87E-05	11,649	1,167	2,062	8,288	240	25	2.79	-2.01	
MO086(A) - 1	BLD2810	1078.8	4.66E-05	14,216	1,989	1,374	7,268	634	61			1
MO087(A) - 1	BLD2811	1078.8	5.03E-05	14,549	1,186	1,691	7,871	359	49	-0.11	-1.72	
MO088(A) - 1	BLD2823	1080.5	4.32E-05	12,857	1,280	2,180	11,240	100	24	2.81	-1.25	6
MO089(A) - 1	BLD2832	1081.6	4.88E-05	11,301	1,186	1,771	9,498	168	35	1.97	-1.60	
MO090(A) - 1	BLD2845	1085.1	4.35E-05	16,886	1,118	2,222	9,521	256	15	1.01	-1.54	
MO091(A) - 1	BLD2866	1090.5	3.88E-05	23,909	1,491	5,993	10,195	2,744	140	1.95	-2.35	1
MO092(A) - 1	BLD2868	1090.7	3.49E-05	16,753	1,308	1,785	6,140	399	60			
MO093(A) - 1	BLD2870	1091.1	3.50E-05	15,269	959	1,891	2,907	3,619	213			1
MO094(A) - 1	BLD2872	1091.1	4.39E-05	18,723	1,268	1,982	3,590	1,855	121			1
MO095(A) - 1	BLD2875	1091.7	4.50E-05	12,554	1,137	2,029	9,023	168	20			
MO096(A) - 1	BLD2886	1093.0	3.94E-05	12,795	1,288	2,033	9,225	259	35	2.11	-1.47	
MO096(A) - 2	BLD2886	1093.0	4.86E-05	12,868	1,269	2,070	8,618	269	36	2.11	-1.47	
MO097(A) - 1	BLD2891	1094.4	5.40E-05	13,296	761	1,601	8,344	99	11	0.76	-0.71	
MO099(A) - 1	BLD2905	1098.3	6.06E-05	10,813	819	2,059	7,265	386	37	1.09	-1.15	
MO100(A) - 1	BLD2906	1098.5	4.05E-05	12,791	927	1,841	7,717	440	61	1.42	-1.28	6
MO100(B) - 1	BLD2906	1098.5	3.84E-05	13,205	1,277	2,652	11,435	190	20	3.84	-2.53	
MO101(A) - 1	BLD2909	1099.2	2.68E-05	14,559	1,085	1,765	5,255	577	39			1
MO102(A) - 1	BLD2910	1099.2	4.53E-05	14,730	1,106	1,818	4,902	561	38			1
MO103(A) - 1	BLD2914	1099.8	4.64E-05	12,668	787	1,699	7,113	140	15			
MO104(A) - 1	BLD2919	1102.2	1.46E-05	17,764	2,347	1,698	4,231	257				
MO105(A) - 1	BLD2917	1103.1	3.83E-05	15,897	1,312	1,853	5,883	787	48			1
MO106(A) - 1	BLD2939	1104.7	4.93E-05	17,804	1,513	2,257	5,830	945	58	0.73	-1.69	1
MO108(A) - 1	BLD2957	1107.2	4.61E-05	14,684	890	1,566	7,067	685	39	-0.11	-0.98	1

Sample number	BGS Identifier	Depth (m)	Ca (mol)	Mg/Ca ( $\mu\text{mol mol}^{-1}$ )	P/Ca ( $\mu\text{mol mol}^{-1}$ )	Sr/Ca ( $\mu\text{mol mol}^{-1}$ )	Na/Ca ( $\mu\text{mol mol}^{-1}$ )	Fe/Ca ( $\mu\text{mol mol}^{-1}$ )	Mn/Ca ( $\mu\text{mol mol}^{-1}$ )	$\delta^{13}\text{C}$ VPDB (‰)	$\delta^{18}\text{O}$ VPDB (‰)	Notes
MO108(A) - 2	BLD2957	1107.2	4.74E-05	14,544	875	1,619	7,469	681	40	-0.11	-0.98	1
MO109(A) - 1	BLD2963	1108.1	4.78E-05	11,599	819	1,572	7,665	82	11	0.41	-0.84	
MO110(A) - 1	BLD3014	1121.0	3.76E-05	12,592	1,286	1,808	7,414	379	38	1.27	-2.38	
MO111(A) - 1	BLD3023	1122.3	4.67E-05	12,631	721	1,563	5,992	531	40	-0.26	-1.12	1
MO111(A) - 2	BLD3023	1122.3	4.80E-05	12,867	700	1,560	5,804	550	43	-0.26	-1.12	1
MO112(A) - 1	BLD3025	1123.5	5.29E-05	11,666	682	1,491	6,204	52	18	-0.29	-0.96	
MO113(A) - 1	BLD3049	1127.5	4.21E-05	16,121	1,836	1,914	4,897	365	54	0.79	-1.95	
MO114(A) - 1	BLD3052	1128.4	4.41E-06	20,038	2,517	1,819	3,229	1,049		0.01	-2.05	1
MO115(A) - 1	BLD3060	1129.6	3.22E-05	18,774	1,823	1,784	5,609	657	65			1
MO116(A) - 1	BLD3121	1135.1	5.18E-05	11,226	665	1,611	6,873	125	11	-0.50	-0.85	6
MO116(B) - 1	BLD3121	1135.1	4.71E-05	15,064	1,003	1,296	6,369	83	12	-0.30	-0.57	
MO117(A) - 1	BLD3124	1136.0	4.34E-05	11,848	1,174	1,412	6,047	357	27			
MO118(A) - 1	BLD3141	1142.2	5.16E-05	11,781	685	1,599	9,052	88	19	-0.51	-0.93	
MO119(A) - 1	BLD3144	1143.1	4.37E-05	9,086	540	1,259	5,033	176	9			
MO120(A) - 1	BLD3146	1143.8	5.13E-05	12,611	1,575	1,820	10,153	56		0.41	-0.65	
MO120(B) - 1	BLD3146	1143.8	4.87E-05	12,769	1,524	1,772	8,611	355	36			
MO121(A) - 1	BLD3152	1145.9	4.47E-05	12,085	716	1,630	5,772	100	13	-0.70	-1.12	6
MO122(A) - 1	BLD3153	1146.0	4.43E-05	11,994	1,015	1,702	6,641	59		0.46	-0.82	6
MO122(A) - 2	BLD3153	1146.0	4.94E-05	11,871	956	1,667	6,841	55		0.46	-0.82	
MO123(A) - 1	BLD3155	1146.8	5.17E-05	13,456	819	1,978	5,928	1,029	65	1.10	-2.02	1, 6
MO124(A) - 1	BLD3282	1160.3	5.28E-05	11,715	977	1,777	8,034	99	18	0.54	-2.62	
MO124(A) - 2	BLD3282	1160.3	4.81E-05	11,664	1,011	1,815	8,894	95	16	0.54	-2.62	
MO125(A) - 1	BLD3311	1172.0	4.48E-05	17,390	1,299	2,044	7,839	188	27	-0.09	-0.97	
MO126(A) - 1	BLD3327	1187.9	4.91E-05	14,866	1,334	1,686	4,266	336	49	0.68	-2.27	6

## 8.4.4. Bulgarian outcrops

Table 37 - Main elemental and isotopic results for analysis of stratigraphic samples from the Bulgarian outcrops. including oxygen and carbon isotope values, Ca values (mol), and Mg/Ca, P/Ca, Sr/Ca, Na/Ca, Fe/Ca, and Mn/Ca values in  $\mu\text{mol mol}^{-1}$ . Sample heights are within each section are taken from Pugh (2018) for samples from Milanovo, and from Koleva and Metodiev (2008) for samples from Dobravitsa-1 and -2. In the notes column 1 = sample which was defined as altered (Fe > 600 and/or Mn > 300), 2 = sample not included in the discussion in Chapter 5 due to extremely elevated Na, Sr, Fe or Mn values (Sr/Ca > 3,000; Fe/Ca > 5,000; Mn/Ca > 1000), 3 = isotope data collected by Pugh (2018), 4 = isotope data collected by Koleva-Reklova and Metodiev (2008).

Sample number	Height (m)	Ca (mol)	Mg/Ca ( $\mu\text{mol mol}^{-1}$ )	P/Ca ( $\mu\text{mol mol}^{-1}$ )	Sr/Ca ( $\mu\text{mol mol}^{-1}$ )	Na/Ca ( $\mu\text{mol mol}^{-1}$ )	Fe/Ca ( $\mu\text{mol mol}^{-1}$ )	Mn/Ca ( $\mu\text{mol mol}^{-1}$ )	$\delta^{13}\text{C}$ VPDB (‰)	$\delta^{18}\text{O}$ VPDB (‰)	Notes
<b>Dobravitsa-1</b>											
Do1b - 1	-5.3	4.13E-05	4,813	490	1,153		141	15	1.74	-0.47	3
Do1b - 2	-5.3	4.66E-05	4,796	486	1,143		138	14	1.74	-0.47	3
Do1c - 1	-5.2	5.33E-05	5,374	462	1,128	4,317	63	13	1.36	-0.53	3
Do1c - 2	-5.2	4.82E-05	5,471	508	1,141	4,385	54	12	1.36	-0.53	3
Do1d - 1	-5.2	4.89E-05	8,862	644	1,374		25				
Do2a(1) - 1	-4.5	3.68E-05	5,291	388	1,218		26		1.18	-1.65	3
Do2a(2) - 1	-4.5	4.39E-05	4,489	280	1,186		136	19	1.18	-1.65	3
Do4a(1) - 1	-4.0	4.49E-05	5,042	385	1,312		52		0.74	-0.92	3
Do4a(2) - 1	-4.0	5.14E-05	7,605	373	1,365		497	75	0.74	-0.92	3
Do6 - 1	-3.5	4.74E-05	6,172	334	1,307		411	38	2.55	-3.06	3
Do6b - 1	-3.4	5.13E-05	7,243	328	1,365		975	83	2.59	-1.21	1, 3
Do7 - 1	-3.3	4.96E-05	10,897	443	1,637		984	90	1.49	-3.25	1, 3
Do7 - 2	-3.3	4.98E-05	11,387	478	1,632		987	92	1.49	-3.25	1, 3
Do10 - 1	-2.0	4.58E-05	10,450	487	1,463		199	20	3.21	-3.94	3
Do10a - 1	-2.0	5.00E-05	11,889	527	1,445		461	51			
Do10b - 1	-2.0	5.18E-05	12,634	415	1,513		450	36			
Do10c - 1	-2.0	5.17E-05	15,460	520	1,354		2,041	131			1
Do12a - 1	-1.7	4.60E-05	6,975	438	1,324		1,529	64	0.51	-2.02	1, 3
Do13c - 1		3.20E-06	10,281		1,437		592		1.49	-2.73	1, 4

Sample number	Height (m)	Ca (mol)	Mg/Ca ( $\mu\text{mol mol}^{-1}$ )	P/Ca ( $\mu\text{mol mol}^{-1}$ )	Sr/Ca ( $\mu\text{mol mol}^{-1}$ )	Na/Ca ( $\mu\text{mol mol}^{-1}$ )	Fe/Ca ( $\mu\text{mol mol}^{-1}$ )	Mn/Ca ( $\mu\text{mol mol}^{-1}$ )	$\delta^{13}\text{C}$ VPDB (‰)	$\delta^{18}\text{O}$ VPDB (‰)	Notes
Do13d - 1		1.04E-05	8,018	1,182	1,362		157				
Do13d - 2		7.17E-06	8,172	1,206	1,362		150				
Do13e - 1		2.22E-05	8,750	725	1,411						
Do14 - 1	-0.4	4.27E-05	11,290	451	1,634		2,599	220	1.00	-1.55	1, 3
Do15b - 1	-0.1	4.47E-05	8,616	720	1,562		714	36	1.82	-1.51	1, 3
Do15b - 2	-0.1	4.67E-05	8,585	677	1,590		733	35	1.82	-1.51	1, 3
Do15e - 1	-0.2	4.36E-05	8,924	699	1,665		63				
Do16 - 1	0.0	4.88E-05	8,099	381	1,556		594	37	1.05	-1.24	1, 3
Do16c - 1	0.1	4.17E-05	8,739	528	1,270		3,250	93			1,
Do16c - 2	0.1	4.79E-05	9,285	497	1,279		3,555	386			1
Do16f - 1	0.1	4.53E-05	9,446	568	1,623		108	9			
Do16g - 1	0.2	3.60E-05	8,775	806	1,464		50				
Do16h - 1	0.2	5.05E-05	8,660	646	1,433		75	8			
Do17 - 1	0.2	3.92E-05	10,337	595	1,496		1,340	55			1,
Do17a - 1	0.2	1.92E-05	7,138	762	1,551				1.15	-1.17	3
Do18 - 1	0.3	4.51E-05	7,255	545	1,475		104	11	0.97	-1.07	3
Do18 - 2	0.3	4.54E-05	7,404	566	1,474		109	9	0.97	-1.07	3
Do18a - 1	1.0	4.49E-05	7,282	653	1,311		121	10	0.22	-1.89	3
Do18c - 1	1.3	4.44E-05	6,638	519	1,226		136	9			
Do18d - 1	1.1	4.91E-05	9,397	700	1,446		225	14			
Do18d - 2	1.1	4.98E-05	9,614	529	1,452		1,340	58			1
Do18e - 1	0.7	5.12E-05	10,117	483	1,291		1,792	59			1
Do18f - 1	1.6	4.95E-05	9,944	414	1,107		5,151	192			1, 2
Do18g - 1	0.5	3.92E-05	11,976	472	1,294		3,862	112			1
Do18h - 1	1.5	4.08E-05	8,448	671	1,471		34				
Do18h - 2	1.5	3.87E-06	8,851		1,490						

Sample number	Height (m)	Ca (mol)	Mg/Ca ( $\mu\text{mol mol}^{-1}$ )	P/Ca ( $\mu\text{mol mol}^{-1}$ )	Sr/Ca ( $\mu\text{mol mol}^{-1}$ )	Na/Ca ( $\mu\text{mol mol}^{-1}$ )	Fe/Ca ( $\mu\text{mol mol}^{-1}$ )	Mn/Ca ( $\mu\text{mol mol}^{-1}$ )	$\delta^{13}\text{C}$ VPDB (‰)	$\delta^{18}\text{O}$ VPDB (‰)	Notes
Do18i - 1	1.9	7.35E-06	7,548	1,204	1,247		123				
Do18l - 1	1.2	8.93E-07	14,900		1,307		2,027				1
Do18m - 1	1.4	4.90E-05	7,245	607	1,421		36				
Do18n - 1	1.4	3.62E-05	9,840	820	1,537		38				
Do18o - 1	2.2	6.22E-06	7,987		1,300						
Do18o - 2	2.2	5.03E-06	8,277		1,327						
Do18p - 1	2.2	3.42E-05	12,309	3,298	1,059		9,189	674			1, 2
Do18q - 1	2.2	5.54E-05	7,128	655	1,226		75	10			
Do18r - 1	2.2	8.63E-07	9,756		1,246						
Do19b - 1	2.3	4.93E-05	8,981	516	1,410		671	37			1
Do19b - 2	2.3	4.11E-05	8,958	545	1,406		749	40			1
Do19c - 1	2.4	4.94E-05	11,723	654	1,677		576	84			1
Do19d - 1	2.5	4.77E-05	10,874	746	1,675		214	33			
Do19e - 1	2.9	4.83E-05	8,437	708	1,200		218	30			
Do19f - 1	3.0	4.78E-05	7,928	586	1,298		95	15			
Do19g - 1	3.2	1.26E-06	11,233		1,325						
Do19s - 1		2.14E-05	9,387	1,059	1,446	7,013	191		0.78	-1.52	3
Do20a - 1	2.8	3.71E-05	8,385	479	1,497	6,682			1.06	-1.01	3
Do20f - 1	2.6	5.21E-05	8,519	723	1,378	2,214	204	27			
Do20g - 1	2.7	5.11E-05	11,362	522	1,800	1,988	123	20			
Do20g - 2	2.7	5.37E-05	9,756	427	1,701	2,527	130	21			
Do20h - 1	2.9	4.41E-05	9,883	688	1,283	2,505	2,132	180			1
<b>Dobravitsa-2</b>											
D2-B1 - 1	0.1	4.87E-06	12,662	1,859	1,590	15,805			0.96	-3.41	3
D2-B3 - 1	0.2	2.16E-06	11,810		1,737						
D2-B4 - 1	0.3	7.99E-06	15,127	1,988	1,718						

Sample number	Height (m)	Ca (mol)	Mg/Ca ( $\mu\text{mol mol}^{-1}$ )	P/Ca ( $\mu\text{mol mol}^{-1}$ )	Sr/Ca ( $\mu\text{mol mol}^{-1}$ )	Na/Ca ( $\mu\text{mol mol}^{-1}$ )	Fe/Ca ( $\mu\text{mol mol}^{-1}$ )	Mn/Ca ( $\mu\text{mol mol}^{-1}$ )	$\delta^{13}\text{C}$ VPDB (‰)	$\delta^{18}\text{O}$ VPDB (‰)	Notes
D2-B4 - 2	0.3	2.62E-05	13,794	1,298	1,755	2,775		27			
D2-B5 - 1	0.4	3.81E-06	12,924		1,463				1.61	-2.25	3
D2-B6 - 1	0.6	3.59E-05	9,149	843	1,712	3,161	117		1.57	-2.53	3
D2-B7 - 1	0.6	3.36E-06	12,581		1,661	22,534			0.86	-2.99	3
D2-B8 - 1	0.7	6.51E-06	10,094	1,419	1,571	11,732			1.67	-2.86	3
D2-B9 - 1	0.9	4.16E-06	10,351		1,703	17,070			2.79	-2.14	3
D2-B10 - 1	1.1	7.26E-06	12,153	1,537	2,046	11,320					
D2-B11 - 1	1.2	3.03E-07	22,667		1,682	249,184					
D2-B12 - 1	1.3	7.63E-06	10,330		1,723	10,632			1.51	-2.94	3
D2-B12 - 2	1.3	6.15E-06	9,764		1,673	11,380			1.51	-2.94	3
D2-B12a - 1	2.0	2.01E-05	9,321	1,212	1,527	4,309			1.33	-2.80	3
<b>Milanovo</b>											
Mv-2.1 - 1	1.6	4.64E-05	10,968	1,153	1,610	4,999			1.67	-3.47	4
Mv-2.12(1) - 1	1.6	5.47E-05	15,663	593	1,792	2,265	147	73	2.13	-3.56	4
Mv-2.12(2) - 1	1.6	6.21E-06	15,471	1,575	1,764	11,565			2.13	-3.56	4
Mv-2.18 - 1	3.3	3.00E-05	10,591	940	1,527	2,703	356	38	1.46	-3.52	4
Mv-2.21 - 1	3.6	6.09E-05	12,209	609	1,792	2,023		20	1.17	-3.29	4
Mv-2.4 - 1	1.9	1.35E-05	12,820	1,611	1,597			105	2.94	-3.41	2, 4
Mv-2.5 - 1	1.5	4.90E-06	12,843		1,758				3.16	-2.89	4
Mv-2.5 - 2	1.5	8.89E-06	12,938	1,379	1,747				3.16	-2.89	4
Mv-2.6 - 1	2.1	9.70E-06	11,157	1,446	1,578			92	1.12	-3.75	4
Mv-2.72 - 1	2.2	2.01E-05	14,978	1,068	1,667			74			
Mv-2.73 - 1	2.2	1.62E-05	14,036	1,495	1,520			73			
Mv-2.9 - 1	2.9	4.02E-05	14,199	1,024	1,730		117	51	1.49	-3.78	4

Sample number	Height (m)	Ca (mol)	Mg/Ca ( $\mu\text{mol mol}^{-1}$ )	P/Ca ( $\mu\text{mol mol}^{-1}$ )	Sr/Ca ( $\mu\text{mol mol}^{-1}$ )	Na/Ca ( $\mu\text{mol mol}^{-1}$ )	Fe/Ca ( $\mu\text{mol mol}^{-1}$ )	Mn/Ca ( $\mu\text{mol mol}^{-1}$ )	$\delta^{13}\text{C}$ VPDB (‰)	$\delta^{18}\text{O}$ VPDB (‰)	Notes
Mv-3.85 - 1	2.2	1.82E-05	16,134	1,243	1,641			46	3.56	-3.39	4
Mv-4.5 - 1	2.9	3.86E-05	11,874	839	1,655	1,963	165	52	0.86	-3.46	4
Mv-5.1(1) - 1	3.1	4.67E-05	10,461	870	1,804	2,485		21	1.76	-2.98	4
Mv-5.1(1) - 2	3.1	1.02E-05	10,737	1,383	1,592				1.76	-2.98	4
Mv-5.1(2) - 1	3.1	3.31E-05	11,304	798	1,659				1.76	-2.98	4
Mv-5.1(3) - 1	3.1	4.76E-05	11,326	757	1,763	3,123			1.76	-2.98	4
Mv-5.3 - 1	3.3	2.44E-05	9,965	1,052	1,451	3,238			0.92	-2.15	4
Mv-5.4 - 1	3.4	4.94E-05	9,760	619	1,496	3,047	249	63	1.96	-2.85	4
Mv-5.42 - 1	3.4	3.06E-05	9,475	800	1,398	2,719	234	48	1.16	-2.70	4
Mv-5.43 - 1	3.4	2.21E-05	9,260	1,169	1,422	3,406		37	0.75	-2.75	4
Mv-5.43 - 2	3.4	3.49E-06	9,845		1,443				0.75	-2.75	4
Mv-6.1 - 1	3.4	4.79E-05	10,151	697	1,573	2,863		21	0.66	-2.63	4
Mv-6.11 - 1	3.4	1.26E-05	11,524	1,073	1,700	6,738			1.00	-1.86	4
Mv-6.13 - 1	3.4	4.39E-05	11,589	827	1,739				1.78	-2.77	4
Mv-6.5 - 1	3.4	3.49E-05	9,245	1,007	1,511	4,374			0.84	-2.52	4
Mv-6.8 - 1	3.4	3.89E-05	11,274	1,079	1,570	3,116		21	1.57	-3.27	4
Mv-7.1 - 1	3.6	2.71E-05	12,723	1,479	1,798	3,453		27	1.34	-3.48	4
Mv-7.1 - 2	3.6	7.53E-06	13,026	2,137	1,739				1.34	-3.48	4
Mv-7.2 - 1	3.7	4.69E-05	10,513	895	1,636	2,665		22	1.73	-2.55	4
Mv-7.21 - 1	3.7	1.34E-05	9,735	1,155	1,358				-0.30	-2.71	4
Mv-7.26 - 1	3.8	5.32E-05	11,676	968	1,764	3,850			1.46	-2.64	4
Mv-7.35 - 1	3.9	4.51E-05	5,878	833	1,416	3,023	126	35	0.77	-1.89	4
Mv-7.8 - 1	4.3	5.27E-05	11,897	913	1,789	3,245	70	16	1.20	-2.47	4
Mv-8.1 - 1	3.9	2.16E-05	7,836	866	1,394	4,743	254	70	0.23	-2.25	4

## 8.5. XRD analysis

Table 38 – XRD results for samples from the Llanbedr Borehole, North Wales, including Ca values (mol), and Mg/Ca, P/Ca, and unit cell parameters a and c and unit cell volume. In the notes column 1 = sample which was defined as altered (Fe > 600 and/or Mn > 300), 2 = sample not included in the discussion in Chapter 5 due to extremely elevated Na, Sr, Fe or Mn values (Sr/Ca > 3,000; Fe/Ca > 5,000; Mn/Ca > 1000), 8 = sample excluded from XRD results due to contamination with clays.

Sample number	BGS Identifier	Depth (m)	Ca (mol)	Mg/Ca ( $\mu\text{mol mol}^{-1}$ )	P/Ca ( $\mu\text{mol mol}^{-1}$ )	a (Å)	c (Å)	Unit cell volume (Å <sup>3</sup> )	Notes
MO041(A) - 1	BLD0656	783.6	5.47E-05	15,018	1,219	4.985898	17.0507	367.0791	8
MO044(A) - 1	BLD0781	802.1	3.19E-05	24,015	1,424	4.980063	17.0180	365.5185	1, 2
MO052(A) - 1	BLD1618	888.9	4.91E-05	8,414	382	4.988470	17.0603	367.6655	
MO061(A) - 1	BLD1740	912.6	4.47E-05	9,277	732	4.988472	17.0596	367.6499	
MO070(A) - 1	BLD2168	975.9	4.08E-05	11,775	979	4.988453	17.0631	367.7227	
MO088(A) - 1	BLD2823	1080.5	4.32E-05	12,857	1,280	4.988075	17.0594	367.5862	
MO116(A) - 1	BLD3121	1135.1	5.18E-05	11,226	665	4.987680	17.0569	367.4756	
MO121(A) - 1	BLD3152	1145.9	4.47E-05	12,085	716	4.987307	17.0556	367.3923	
MO122(A) - 1	BLD3153	1146.0	4.43E-05	11,994	1,015	4.987452	17.0584	367.4729	
MO123(A) - 1	BLD3155	1146.8	5.17E-05	13,456	819	4.987655	17.0550	367.4304	1
MO126(A) - 1	BLD3327	1187.9	4.91E-05	14,866	1,334	4.986533	17.0521	367.2037	

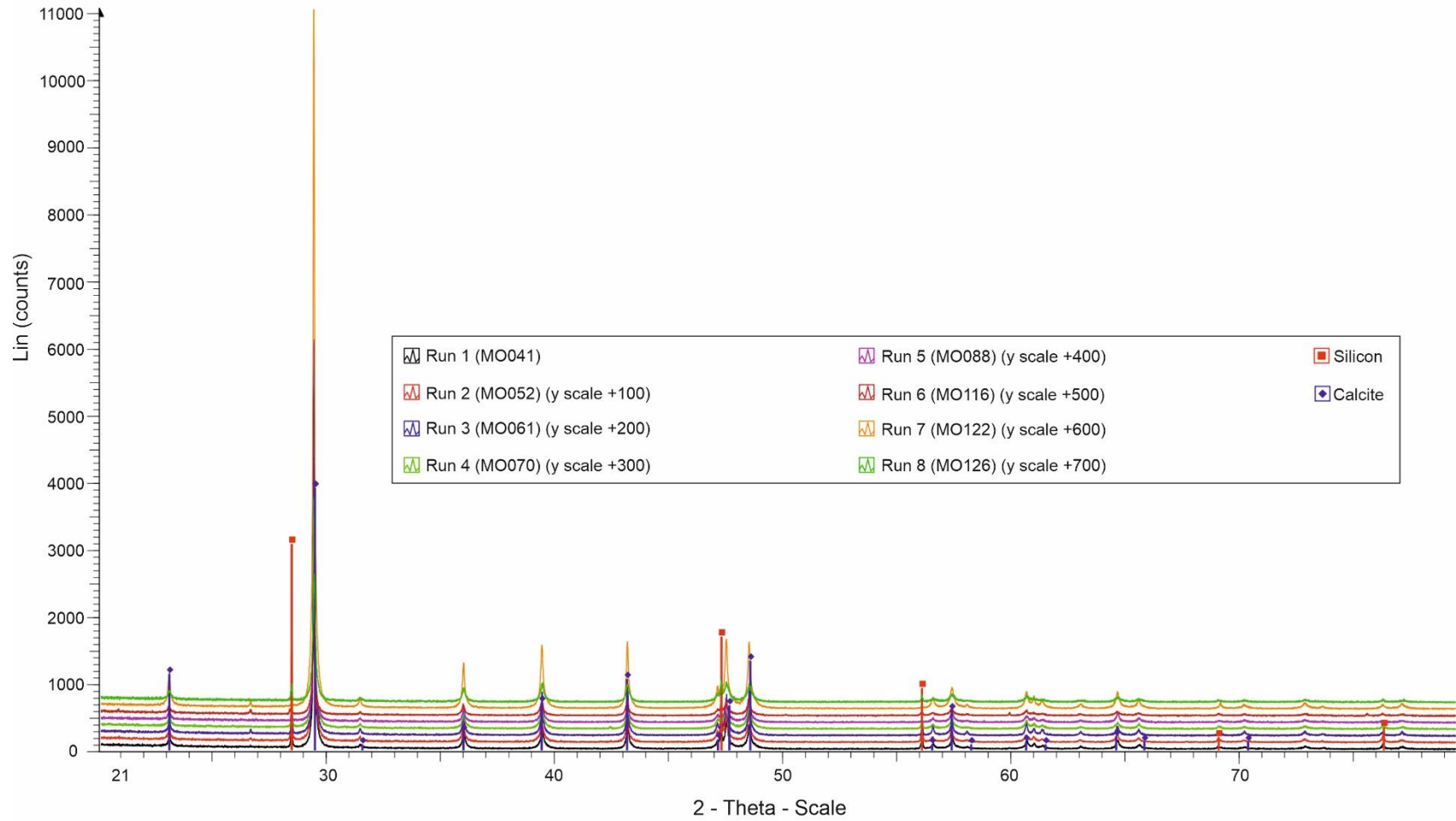


Figure 69 – Example plots for 8 samples run for XRD analysis. Each subsequent plot is shifted 100 counts in the y axis to allow for comparison between them on the same axis. Peaks corresponding to calcite and the silicone standard are labelled.

## 8.6. Sediment analysis

### 8.6.1. Major and minor element analysis

Table 39 – Results of the total digest sediment analysis. Included are the P/Ca values for paired belemnite calcite samples, as well as sediment concentrations of Al and Fe (wt%), Mo and U (ppm) and key redox sensitive element ratios (Mo/Al, U/Al, Mo/U, Fe/Al).

Sample number	Depth (m)	P/Ca ( $\mu\text{mol mol}^{-1}$ )	Al (wt%)	Fe (wt%)	Mo (ppm)	U (ppm)	Mo/Al (ppm/wt%)	U/Al (ppm/wt%)	Mo/U (ppm/ppm)	Fe <sub>TOT</sub> /Al (wt%/wt%)
NS1-85-129.97 B(1A)	130.0	731	12.01	9.20	1.06	3.41	0.09	0.28	0.31	0.77
NS1-85-130.35 B(1A)	130.4	663	11.95	8.62	2.02	3.43	0.17	0.29	0.59	0.72
NS1-85-130.71 B(1A)	130.7	908	10.93	9.36	2.50	4.03	0.23	0.37	0.62	0.86
NS1-86-133.69 B(1A)	133.7	1,077	11.43	9.20	5.15	4.04	0.45	0.35	1.27	0.81
NS1-87-133.65 B(1A)	133.7	853	11.84	9.57	2.42	3.64	0.20	0.31	0.67	0.81
NS1-87-135.88 B(1A)	135.9	1,743	11.49	9.19	2.78	3.60	0.24	0.31	0.77	0.80
NS1-88-137.75 B(1A)	137.8	981	11.54	8.73	3.17	3.54	0.27	0.31	0.90	0.76
NS1-88-137.84 B(1A)	137.8	956	8.00	23.65	14.96	3.43	1.87	0.43	4.36	2.96
NS1-88-138.01 B(1A)	138.0	1,090	12.24	8.65	8.19	3.41	0.67	0.28	2.40	0.71
NS1-88-138.55-64 B(1A)	138.6	697	11.71	8.43	7.77	3.75	0.66	0.32	2.07	0.72
NS1-88-139.05 B(1A)	139.1	854	11.84	8.36	5.99	3.52	0.51	0.30	1.70	0.71
NS1-89-141.34 B(1A)	141.3	650	12.25	8.64	6.33	3.62	0.52	0.30	1.75	0.71
NS1-90-142.87 B(1A)	142.9	818	12.10	9.20	5.30	3.50	0.44	0.29	1.51	0.76
NS1-90-143.22 B(1A)	143.2	2,214	11.79	9.33	11.53	4.04	0.98	0.34	2.85	0.79
NS1-90-144.31 B(1A)	144.3	658	10.31	12.88	43.50	7.47	4.22	0.73	5.82	1.25
NS1-91-146.13 B(1A)	146.1	1,197	11.86	7.99	6.49	3.36	0.55	0.28	1.93	0.67
NS1-92-151.1 B(1A)	151.1	691	12.14	8.02	3.80	3.33	0.31	0.27	1.14	0.66
NS1-93-154.75 B(1A)	154.8	1,084	11.98	8.00	5.62	3.48	0.47	0.29	1.61	0.67
NS1-94-155.52 B(1A)	155.5	1,017	11.12	11.07	26.02	5.47	2.34	0.49	4.75	0.99
NS1-94-156.27 B(1A)	156.3	1,156	11.29	10.75	19.90	4.08	1.76	0.36	4.87	0.95
NS1-94-156.61 B(1A)	156.6	1,549	10.35	12.00	38.47	5.63	3.72	0.54	6.84	1.16

Sample number	Depth (m)	P/Ca ( $\mu\text{mol mol}^{-1}$ )	Al (wt%)	Fe (wt%)	Mo (ppm)	U (ppm)	Mo/Al (ppm/wt%)	U/Al (ppm/wt%)	Mo/U (ppm/ppm)	Fe <sub>tot</sub> /Al (wt%/wt%)
NS1-94-156.78 B(1A)	156.8	1,434	11.13	11.06	24.28	4.63	2.18	0.42	5.25	0.99
NS1-94-157.45 B(1A)	157.5	1,275	10.65	11.10	27.74	5.57	2.60	0.52	4.98	1.04
NS1-100-175.16 B(1A)	175.2	367	10.86	11.03	31.82	5.76	2.93	0.53	5.53	1.02
NS1-102-179.52 B(1A)	179.5	562	10.45	8.84	0.87	3.33	0.08	0.32	0.26	0.85
NS1-103-183.44 B(1A)	183.4	611	10.85	9.88	0.65	3.05	0.06	0.28	0.21	0.91
NS1-103-183.58 B(1A)	183.6	553	10.38	12.08	0.71	2.94	0.07	0.28	0.24	1.16
NS1-103-184.32 B(1A)	184.3	1,826	10.23	10.39	0.66	3.06	0.06	0.30	0.22	1.02
NS1-104-187.73 B(1A)	187.7	678	8.85	7.39	0.89	2.52	0.10	0.28	0.35	0.84
NS1-105-188.26 B(1A)	188.3	661	7.57	9.62	1.24	2.44	0.16	0.32	0.51	1.27
NS1-105-190 B(1A)	190.0	807	8.18	7.58	1.09	2.71	0.13	0.33	0.40	0.93
NS1-105-190.36 B(1A)	190.4	1,053	7.30	7.82	1.24	2.70	0.17	0.37	0.46	1.07
NS1-109-199.91 B(1A)	199.9	782	11.04	9.00	1.16	2.79	0.10	0.25	0.41	0.82
NS1-111-203.28 B(1A)	203.3		10.44	9.35	0.93	2.74	0.09	0.26	0.34	0.90
NS1-113-210.13 B(1A)	210.1	1,060	5.47	9.49	0.44	1.35	0.08	0.25	0.33	1.74
NS1-120-231.84 B(1A)	231.8	899	9.00	7.78	0.91	2.99	0.10	0.33	0.30	0.87
NS1-123-239.22 B(1A)	239.2	590	9.98	10.49	0.68	2.96	0.07	0.30	0.23	1.05

## 8.6.2. Iron speciation

Table 40 - Results of the iron-speciation sediment analysis. Included are the P/Ca values for paired belemnite calcite samples, the concentrations of different pools of iron ( $Fe_{\text{Carb}}$ ,  $Fe_{\text{Ox}}$ ,  $Fe_{\text{Mag}}$ ,  $Fe_{\text{Py}}$ ), as well as key redox sensitive element ratios ( $Fe_{\text{Py}}/Fe_{\text{HR}}$ ,  $Fe_{\text{HR}}/Fe_{\text{TOT}}$ ).

Sample number	Depth (m)	P/Ca ( $\mu\text{mol mol}^{-1}$ )	$Fe_{\text{Carb}}$ (wt%)	$Fe_{\text{Ox}}$ (wt%)	$Fe_{\text{Mag}}$ (wt%)	$Fe_{\text{Py}}$ (wt%)	$Fe_{\text{HR}}/Fe_{\text{TOT}}$ (wt%/wt%)	$Fe_{\text{Py}}/Fe_{\text{HR}}$ (wt%/wt%)
NS1-85-129.97 B(1A)	130.0	731	0.75	0.09	0.13	3.18	0.42	0.79
NS1-85-130.35 B(1A)	130.4	663	0.42	0.23	0.10	2.86	0.63	0.87
NS1-85-130.71 B(1A)	130.7	908	0.46	0.21	0.09	5.10	0.46	0.81
NS1-86-133.69 B(1A)	133.7	1,077	0.43	0.28	0.09	3.40	0.55	0.89
NS1-87-133.65 B(1A)	133.7	853	0.34	0.04	0.08	4.72	0.54	0.91
NS1-87-135.88 B(1A)	135.9	1,743	0.38	0.11	0.09	4.48	0.51	0.86
NS1-88-137.75 B(1A)	137.8	981	0.40	0.13	0.11	3.79	0.41	0.32
NS1-88-137.84 B(1A)	137.8	956	2.68	0.21	3.75	3.11	0.47	0.84
NS1-88-138.01 B(1A)	138.0	1,090	0.44	0.11	0.10	3.44	0.51	0.86
NS1-88-138.55-64 B(1A)	138.6	697	0.42	0.12	0.08	3.72	0.53	0.87
NS1-88-139.05 B(1A)	139.1	854	0.42	0.05	0.09	3.62	0.51	0.87
NS1-89-141.34 B(1A)	141.3	650	0.40	0.05	0.08	4.15	0.56	0.89
NS1-90-142.87 B(1A)	142.9	818	0.43	0.04	0.08	4.59	0.52	0.83
NS1-90-143.22 B(1A)	143.2	2,214	0.57	0.09	0.15	4.08	0.61	0.81
NS1-90-144.31 B(1A)	144.3	658	0.62	0.24	0.66	6.31	0.41	0.84
NS1-91-146.13 B(1A)	146.1	1,197	0.37	0.07	0.09	2.77	0.40	0.79
NS1-92-151.1 B(1A)	151.1	691	0.49	0.05	0.13	2.55	0.43	0.81
NS1-93-154.75 B(1A)	154.8	1,084	0.53	0.05	0.08	2.75	0.64	0.84
NS1-94-155.52 B(1A)	155.5	1,017	0.81	0.09	0.21	6.02	0.66	0.90
NS1-94-156.27 B(1A)	156.3	1,156	0.60	0.04	0.05	6.59	0.68	0.90
NS1-94-156.61 B(1A)	156.6	1,549	0.65	0.09	0.13	7.15	0.71	0.88
NS1-94-156.78 B(1A)	156.8	1,434	0.81	0.07	0.05	6.97	0.70	0.88
NS1-94-157.45 B(1A)	157.5	1,275	0.76	0.08	0.07	6.89	0.62	0.89

Sample number	Depth (m)	P/Ca ( $\mu\text{mol mol}^{-1}$ )	Fe <sub>Carb</sub> (wt%)	Fe <sub>Ox</sub> (wt%)	Fe <sub>Mag</sub> (wt%)	Fe <sub>Py</sub> (wt%)	Fe <sub>HR</sub> /Fe <sub>TOT</sub> (wt%/wt%)	Fe <sub>Py</sub> /Fe <sub>HR</sub> (wt%/wt%)
NS1-100-175.16 B(1A)	175.2	367				3.73		0.86
NS1-102-179.52 B(1A)	179.5	562	1.27	0.04	0.07	3.73	0.28	0.66
NS1-103-183.44 B(1A)	183.4	611	0.64	0.08	0.23	1.86	0.44	0.72
NS1-103-183.58 B(1A)	183.6	553	0.46	0.20	0.17	5.01	0.48	0.86
NS1-103-184.32 B(1A)	184.3	1,826	0.68	0.15	0.10	5.29	0.60	0.85
NS1-104-187.73 B(1A)	187.7	678	1.05	0.16	0.14	1.67	0.41	0.55
NS1-105-188.26 B(1A)	188.3	661	0.59	0.14	0.30	3.32	0.45	0.76
NS1-105-190 B(1A)	190.0	807	0.64	0.07	0.14	2.15	0.39	0.72
NS1-105-190.36 B(1A)	190.4	1,053	0.42	0.07	0.13	3.66	0.55	0.85
NS1-109-199.91 B(1A)	199.9	782	0.38	0.11	0.32	2.38	0.35	0.75
NS1-111-203.28 B(1A)	203.3		0.46	0.18	0.36	1.38	0.25	0.58
NS1-113-210.13 B(1A)	210.1	1,060	0.34	0.18	0.28	2.30	0.33	0.74
NS1-120-231.84 B(1A)	231.8	899	0.65	0.14	0.27	1.37	0.31	0.57
NS1-123-239.22 B(1A)	239.2	590	0.61	0.28	0.30	2.12	0.32	0.64